THE UNIVERSITY OF CHICAGO

CYCLOADDITION REACTIONS OF 1,2-DIAZINES AND SILOXY ALKYNES; THE DEVELOPMENT AND APPLICATION OF CHIRAL DELTIC UREAS AND THIOSQUARAMIDES AS DUAL HYDROGEN-BOND DONOR CATALYSTS

A DISSERTATION SUBMITTED TO

THE FACULTY OF THE DIVISION OF THE PHYSICAL SCIENCES

IN CANDIDACY FOR THE DEGREE OF

DOCTOR OF PHILOSOPHY

DEPARTMENT OF CHEMISTRY

BY

CHINTAN SHANTILAL SUMARIA

CHICAGO, ILLINOIS

MARCH 2017

To my family

TABLE OF CONTENTS

LIST OF FIGURES

LIST OF SCHEMES

LIST OF TABLES

LIST OF CHARTS

LIST OF ABBREVIATIONS

°C	Degree Celsius
aq.	Aqueous
Ar	Aryl
binol	1,1′-binaphthalene-2,2′-diol
Bipy	2,2'-bipyridine
Bpy	2,2'-bipyridine
cod	Cyclooctadiene
Conc	concentration
Cy	Cyclohexyl
d	Day(s)
DA	Diels-Alder
DABCO	1,4-diazabicyclo[2.2.2]octane
DCE	1,2-dichloroethane
Deltamide	Deltic Urea; Amide of Deltic acid
DIPEA	*N*,*N*-Diisopropylethylamine
DMAP	4-dimethylaminopyridine
DMB	2,4-dimethoxybenzyl
DME	Dimethoxyethane
DMSO	Dimethylsulfoxide
d.r.	Diastereomeric ratio
ee	Enantiomeric excess

eq	Equivalents
equiv	Equivalents
e.r.	Enantiomeric ratio
Et	Ethyl
EWG	Electron-Withdrawing Groups
FDA	Food and Drug Administration
h	Hour(s)
HBD	Hydrogen-Bond Donor
HOMO	Highest Occupied Molecular Orbital
HRMS	High Resolution Mass Spectrometry
IEDDA	Inverse Electron-Demand Diels Alder
IR	Infrared
LUMO	Lowest Unoccupied Molecular Orbital
M	Molar
Me	Methyl
MeCN	Acetonitrile
MVK	Methyl Vinyl Ketone
NBS	*N*-Bromosuccinimide
NCS	*N*-Chlorosuccinimide
nd	Not detected (in significant quantities)
NMR	Nuclear Magnetic Resonance
Ph	Phenyl
pyr	Pyridine

quant	Quantitative
rt	Room temperature
t-Bu	*Tert*-butyl
TEA	Triethylamine
tert	Tertiary
Tf	Trifluoromethanesulfonyl
TFA	Trifluoroacetic acid
THF	Tetrahydrofuran
TIPS	Triisopropylsilyl
TLC	Thin Layer Chromatography

ABSTRACT

Over the past 15 years, there has been a profound interest in the asymmetric catalytic activation of reactants through hydrogen bonding interactions. The development of additional hydrogen-bond donor catalyst scaffolds is expected to greatly expand the classes of reactions that can be rendered enantioselective, and would also lead to improvements in the effectiveness and substrate-scope of other reactions. To this end, two design principles have been explored: 1) Larger H-H distances (via Deltic Ureas), and 2) Increased acidity and solubility (via Thiosquaramides). A detour was taken to explore cycloaddition reactions encountered while exploring another class of HBD scaffolds (bispyridiniums).

The first part of this dissertation (Chapter 1) describes the catalysis of formal [4+2] and [2+2+2] cycloaddition reactions of siloxy alkynes and 1,2-diazines, and of a formal [2+2] cycloaddition reaction of cyclohexenone and siloxy alkyne. While the use of copper(I) and nickel(0) complexes leads to the formal [4+2] cycloaddition product, the use of pyridinium salts provides access to the formal [2+2+2] cycloaddition adducts instead. Metal catalysts based on earth abundant metals are not only as competent as the previously reported Ag(I) salt, but the copper catalyst, in particular, promotes the formal [4+2] cycloadditions of pyrido[2,3-*d*]pyridazine and pyrido[3,4-*d*]pyridazine, enabling a new synthesis of quinoline and isoquinoline derivatives.

The second part of this dissertation (Chapter 2-3) elaborates upon the synthesis and application of chiral Deltic Urea and Thiosquaramide scaffolds as dual hydrogen-bond donor catalysts. Various approaches towards accessing the highly strained Deltic Ureas have been described, and we also report the first synthesis of, cross-substituted, chiral, bifunctional Deltic

Ureas. Their applicability towards the enantioselective catalysis of a Michael reaction is being demonstrated. More acidic than their oxosquaramide counterparts, and significantly more soluble in non-polar solvents, Thiosquaramides are also being demonstrated as excellent catalysts for the enantioselective conjugate addition reaction of barbituric acids to nitrostyrenes.

In the final chapter (Chapter 4), the use of Bordwell's method of overlapping indicators to determine the acidity of select Deltic Ureas and Thiosquaramides has been described.

ACKNOWLEDGEMENTS

First and foremost, I would like to thank Professor Viresh H. Rawal for giving me this opportunity. Dr. Rawal's style of work provides ample space to grow not only as a scientist, but also as a person. He is very patient, kind, forgiving and facilitates students to get the best out of themselves without imposing rigid expectations. I also thank Professor Krishna P. Kaliappan and Professor Pradeepkumar, P.I. for teaching me the basics of scientific research, and Dr. Devendar Vanga for teaching me basic laboratory techniques.

Special thanks to Professor Scott Snyder and Professor Guangbin Dong for accepting to be on my defense committee and to Professor Tristan H. Lambert, Professor Sergey A. Kozmin for fruitful collaborations.

I thank Ms. Melinda Moore and Dr. Vera Dragisich for their help. I also thank Dr. Antoni Jurkiewicz for patiently answering questions related to NMR spectroscopy, Dr. Jin Qin for enabling new LC-MS machines and to Dr. Alexander Filatov for their help in solving X-ray crystal structures.

Moving to the United States (from India) led to a non-negligible degree of culture shock. In that regard, I commend Alexander Schneider's Thanksgiving invitation (to an outright foreigner). I also thank Donglin Zhao and Frank Olechnowicz for their understanding. I also thank the research group of Prof. Luping Yu for letting me use their UV-Vis spectrophotometer.

Having spent over 10,000 hours working alongside Michael G. Rombola (Mike), I have enjoyed countless jokes and philosophical/cultural/historical/economic discussions with him. My ideas about American culture were shaped in no small measure by Mike, and I appreciate his humble approach to all concepts foreign. I've also enjoyed working with Dr. Julius R. Reyes, who often

gave me a different chemical perspective. While my yearning for knowledge often led me afield, I admire Julius' one-pointed dedication to organic chemistry. Special thanks to Ferdinand Taenzler, Dr. Lan Luo, Jiasu Xu, Dr. Yunus E. Türkmen, Dr. Aditya K. Unni, Pavel Elkin, Dr. Kin S. Yang, Dr. Antoinette E. Nibbs, Dr. Thomas D. Montgomery, Dr. Yen-Ku Wu and to members of the Snyder, Yamamoto, Kozmin and Dong groups for their company and discussions in chemistry.

I also enjoyed working with the cheerful Dr. Natsuko Kagawa during her short stint in the Rawal lab, and am fond of working alongside Chris Price, Christian Kissig and Hannah Zinky during their terms in the lab.

Life outside the department was fun because of my good friends from IIT Bombay: Aniket Joglekar and Romit Chakraborty. I appreciate the countless philosophical/historical discussions with Aniket. I thank my roommates (also from IIT): Piyush Arya and Vishnu Nair.

During the course of my studies, ancient Indian epics have allowed me to gaze onto an alternate world. Their consistency surprised me, and helped me derive meaning and context towards life in general.

Finally, I would like to express my gratitude to my parents (Shantilal Sumaria, Rupal Sumaria) and siblings (Mansi Sumaria, Mihin Sumaria). Without them, this endeavor would not have been possible.

CHAPTER I

CYCLOADDITION REACTIONS OF 1,2-DIAZINES AND SILOXY ALKYNES

I.1 Introduction

The efficacy and predictability of the Diels-Alder (DA) reaction has made it an indispensable part of synthetic organic chemist's toolbox. The use of Lewis acids as catalysts to lower the HOMO-LUMO gap between the diene and the dienophile facilitated the DA reaction under much milder reaction conditions, thus allowing it to be applicable enantioselectively over various substrate types and reaction conditions.[1] Nevertheless, efforts to harness Lewis acid, Brønsted Acid or Hydrogen-Bond Donor (HBD) catalysis of the reciprocal process, the Inverse-Electron Demand Diels-Alder (IEDDA) reaction have been less fruitful. Our lab's interest in dual hydrogen-bond donor catalysis motivated us to investigate pyridinium salts as catalysts towards IEDDA reactions, and led us to discover complementary reactivity between metal and Brønsted acid catalysis. While the [2+2+2], [4+2] and [2+2] cycloaddition reactions were developed *en route*, the formal IEDDA ([4+2]) developed herein paves the way towards accessing modified 1,1'-bi-2-naphthols in two steps from commercially available aldehydes.

I.2 The IEDDA Reaction of Heterocyclic Azadienes and Electron-rich Dienophiles

I.2.1 The IEDDA Reaction of heterocyclic azadienes

[1] Evans, D. A.; Johnson, J. S.; Jacobsen, E. N.; Pfaltz, A.; Yamamoto, H. *Comprehensive Asymmetric Catalysis*; Springer: New York, NY, 1999; Vol. 3, pp 1177 and references therein.

The IEDDA reaction of heterocyclic azadienes, including tetrazines, triazines and diazines provides access to a variety of carbocycles and heterocycles.[2,3,4,5] The utility of such IEDDA reactions is evident by the many total synthesis reports across literature. For example, in 2010, Boger and co-workers achieved an asymmetric total synthesis of (-)-vindoline based on the tandem [4+2]/[3+2] cycloaddition reaction of an oxadiazole moiety (Scheme 1).[6]

Scheme 1: Total Synthesis of (-)-Vindoline Mediated by a tandem [4+2]/[3+2] Cycloaddition Reaction of an Azadiene

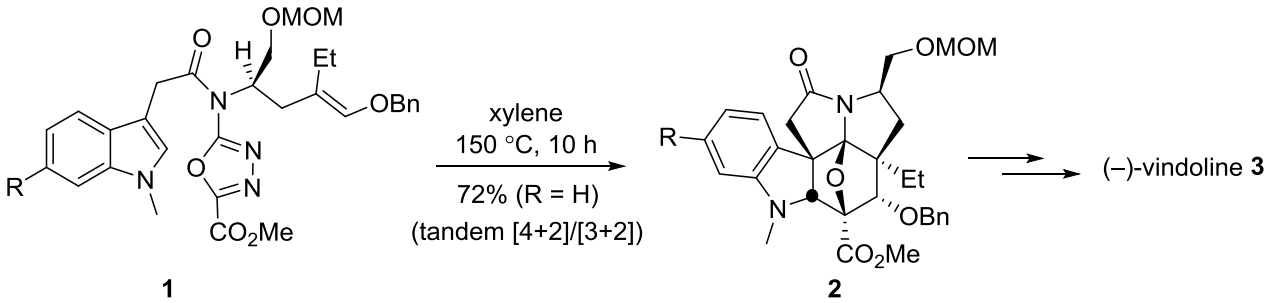

1 **2**

However, nearly all reported IEDDA reactions of heterocyclic azadienes are thermal processes,

[2] For selected reports on tetrazines, see: (a) Carboni, R. A.; Lindsey, R. V., Jr. *J. Am. Chem. Soc.* **1959**, *81*, 4342. (b) Boger, D. L.; Coleman, R. S.; Panek, J. S.; Yohannes, D. *J. Org. Chem.* **1984**, *49*, 4405. (c) Sauer, J.; Heldmann, D. K.; Hetzenegger, J.; Krauthan, J.; Sichert, H.; Schuster, J. *Eur. J. Org. Chem.* **1998**, 2885. For application of tetrazines in bioconjugation reactions, see: (d) Blackman, M. L.; Royzen, M.; Fox, J. M. *J. Am. Chem. Soc.* **2008**, *130*, 13518. (e) Taylor, M. T.; Blackman, M. L.; Dmitrenko, O.; Fox, J. M. *J. Am. Chem. Soc.* **2011**, *133*, 9646.

[3] For selected reports on 1,2,3-triazines, see: (a) Neunhoeffer, H.; Clausen, M.; Vötter, H. D.; Ohl, H.; Krüger, C.; Angermund, K. *Liebigs Ann. Chem.* **1985**, 1732. (b) Anderson, E. D.; Boger, D. L. *J. Am. Chem. Soc.* **2011**, *133*, 12285. For 1,2,4-Triazines, see: (c) Neunhoeffer, H.; Frühauf, H. W. *Tetrahedron Lett.* **1969**, *10*, 3151. (d) Dittmar, W.; Sauer, J.; Steigel, A. *Tetrahedron Lett.* **1969**, *10*, 5171. (e) Boger, D. L.; Panek, J. S. *J. Am. Chem. Soc.* **1985**, *107*, 5745.

[4] For selected reports on diazines, see: (a) Neunhoeffer, H.; Werner, G. *Tetrahedron Lett.* **1972**, *16*, 1517. (b) Neunhoeffer, H.; Werner, G. *Liebigs Ann. Chem.* **1973**, 437. (c) Gruseck, U.; Heuschmann, M. *Tetrahedron Lett.* **1987**, *28*, 6027. (d) Oishi, E.; Taido, N.; Iwamoto, K.; Miyashita, A.; Higashino, T. *Chem. Pharm. Bull.* **1990**, *38*, 3268.

[5] (a) Boger, D. L. *Tetrahedron* **1983**, *39*, 2869. (b) Boger, D. L. *Chem. Rev.* **1986**, 86, 781. (c) Fringuelli, F.; Taticchi, A. Dienes in the Diels-Alder Reaction; Wiley: New York, **1990**.

[6] Kato, D.; Sasaki, Y.; Boger, D. L. *J. Am. Chem. Soc.* **2010**, *132*, 3685.

typically requiring harsh conditions.[7] Catalytic activation of such IEDDA reactions in a manner similar to that for normal electron-demand Diels-Alder reactions would greatly expand the scope of IEDDA reactions of azadienes.

I.2.2 Catalyzing the IEDDA Reaction of Azadienes

Scheme 2: Lewis Acid Catalyzed IEDDA Reactions of Heterocyclic Azadienes

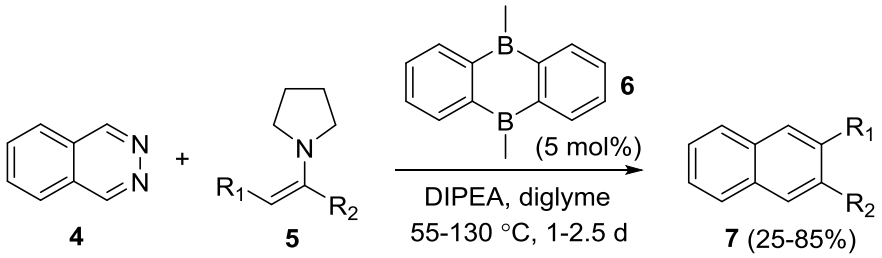

To the best of our knowledge, the only known example of Lewis acid catalyzed IEDDA reaction of azadienes is that reported by Wegner and co-workers (Scheme 2). Our interest in hydrogen bonding catalysis,[8] prompted us to explore pyridinium salts designed to form two hydrogen bonds to the phthalazine nitrogen atoms as catalysts for the IEDDA reaction between phthalazine and electron-rich alkynes.[9] As the Lewis acid catalysis of such a reaction had been reported, we wondered if similar catalysis could be achieved by hydrogen-bond donor catalysis (Scheme 3).

---

[7] For reviews on Diels-Alder reactions of azadienes, see: (a) Boger, D. L. *Tetrahedron* **1983**, *39*, 2869. (b) Boger, D. L. *Chem. Rev.* **1986**, *86*, 781. (c) Foster, R. A. A.; Willis, M. C. *Chem. Soc. Rev.* **2013**, *42*, 63. For selected examples of Diels-Alder reactions of 1,2-diazines, see: (d) Higashino, T.; Miyashita, A.; Iwamoto, K.; Taido, N.; Oishi, E. *Chem. Pharm. Bull.* **1990**, *38*, 3268. (e) Coleman, R. S.; Boger, D. L. *J. Am. Chem. Soc.* **1987**, *109*, 2717.

[8] (a) Huang, Y.; Unni, A. K.; Thadani, A. N.; Rawal, V. H. *Nature* **2003**, *424*, 146. (b) Malerich, J. P.; Hagihara, K.; Rawal, V. H., *J. Am. Chem. Soc.* **2008**, *130*, 14416. (c) Türkmen, Y. E.; Rawal, V. H. *J. Org. Chem.* **2013**, *78*, 8340.

[9] For bidentate Lewis acid activation of 1,2-diazines, see: (a) Kessler, S. N.; Wegner, H. A. *Org. Lett.* **2010**, *12*, 4052. (b) Kessler, S. N.; Neuburger, M.; Wegner, H. A. *Eur. J. Org. Chem.* **2011**, 3238. (c) Kessler, S. N.; Neuburger, M.; Wegner, H. A. *J. Am. Chem. Soc.* **2012**, *134*, 17885. (d) Kessler, S. N.; Wegner, H. A. *Synlett* **2012**, *5*, 699. (e) Schweighauser, L.; Bodoky, I.; Kessler, S. N.; Häussinger, D.; Wegner, H. A. *Synthesis* **2012**, *44*, 2195. (f) Bader, S. L.; Kessler, S. N.; Zampese, J. A.; Wegner, H. A. *Monatsh. Chem.* **2013**, *144*, 531.

Scheme 3: Potential Activation of 1,2-Diazines by a Dual Hydrogen-Bond Donor Catalyst

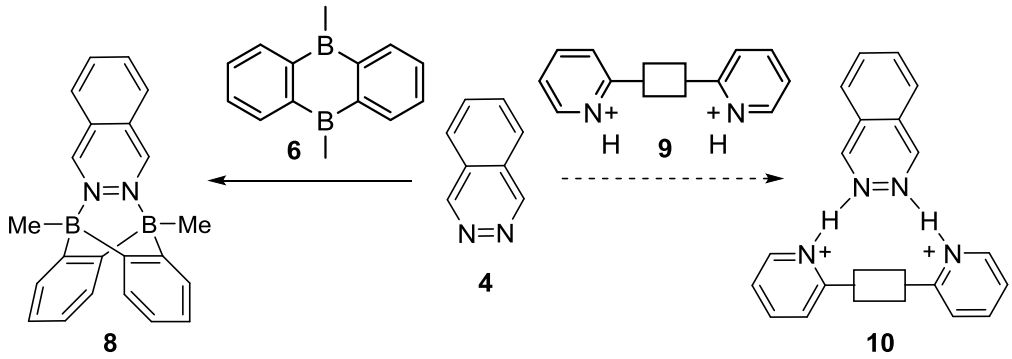

We found the reaction of phthalazine with siloxy alkynes,[10] while promoted by dual hydrogen bond donors, was catalyzed even by simple pyridinium salts and afforded, rather than the anticipated 2-naphthol derivative, an intriguing tetra-aza-pentacyclic compound, arising from a formal [2+2+2] cycloaddition between two phthalazines and a siloxy alkyne (Section I.3). Inspired by the ample precedent with normal electron demand Diels-Alder reactions, we evaluated various metals for promoting the desired IEDDA reaction and discovered that Ag(I) salts, especially when paired with bidentate *N*-donor ligands such as 2,2'-bipyridine and 1,10-phenanthroline, catalyzed the desired process to afford 3-substituted 2-naphthol silyl ethers in good yields.[11] To make this strategy more versatile and practical, we have examined complexes of earth abundant metals as catalysts for the IEDDA reaction and report here that Cu(I) and Ni(0) complexes can supplant Ag(I) salts for these (Section I.4)

---

[10] For other related reactions of siloxy alkynes, see: (a) Lal, G. S.; Kowalski, C. J. *J. Am. Chem. Soc.* **1988**, *110*, 3693. (b) Brisbois, R. G.; Kowalczyk, J. L.; Miller, R. F.; Danheiser, R. L. *J. Am. Chem. Soc.* **1990**, *112*, 3093. (c) Sweis, R. F.; Schramm, M. P.; Kozmin, S. A. *J. Am. Chem. Soc.* **2004**, *126*, 7442. (d) Zhang, L.; Kozmin, S. A. *J. Am. Chem. Soc.* **2004**, *126*, 10204. (e) Zhang, L.; Kozmin, S. A. *J. Am. Chem. Soc.* **2004**, *126*, 11806. (f) Austin, W. F.; Zhang, Y.; Danheiser, R. L. *Org. Lett.* **2005**, *7*, 3905. (g) Qi, X.; Ready, J. M. *Angew. Chem. Int. Ed.* **2008**, *47*, 7068. (h) Zhao, W.; Wang, Z.; Sun, J. *Angew. Chem. Int. Ed.* **2012**, *51*, 6209. (i) Cabrera-Pardo, J. R.; Chai, D. I.; Liu, S.; Mrksich, M.; Kozmin, S. A. *Nat. Chem.* **2013**, *5*, 423. (j) Zhao, W.; Li, Z.; Sun, J. *J. Am. Chem. Soc.* **2013**, *135*, 4680. (k) Cabrera-Pardo, J. R.; Chai, D. I.; Kozmin, S. A. *Adv. Synth. Catal.* **2013**, *355*, 2495.

[11] Türkmen, Y. E.; Montavon, T. J.; Kozmin, S. A.; Rawal, V. H. *J. Am. Chem. Soc.* **2012**, *134*, 9062.

I.3 The Formal [2+2+2] Cycloaddition Reaction of 1,2-Diazines and Siloxy Alkynes

I.3.1 Initial Findings for the Diastereoselective Formal [2+2+2] Cycloaddition Reaction

Our study began by examining the reaction of phthalazine **4** with siloxy alkyne **11** in the presence of common Brønsted acids. While no reaction between **4** and **11** was observed in the absence of such additives, even at elevated temperatures, it was found that addition of simple pyridinium salts promoted the formation of a new pentacyclic product **12** (Table 1). After examining a range of mono- and bispyridinium salts in various solvents, we determined the optimum protocol to entail the use of a stoichiometric amount of pyridinium trifluoromethanesulfonimide in CH_2Cl_2 at room temperature, which produced lactam **11** as a single diastereomer in 77% yield. Interestingly, the use of monopyridinium salt **13** and bispyridinium salt **14** produced no statistically relevant difference (Table 1). Note that the initial discovery was made by Dr. Yunus E. Türkmen, and the substrate scope was examined by Dr. Timothy J. Montavon (in collaboration with the research group of Prof. Sergey A. Kozmin). Further elaboration via a three-component reaction has been described below.[12] It was found that the reaction proceeds smoothly and in high diastereoselectivity with a variety of alkyl siloxy alkynes and with substituted phthalazines and benzo[*g*]phthalazine.[12]

Table 1: Catalysis by Monopyridinium and Bispyridinium Salts

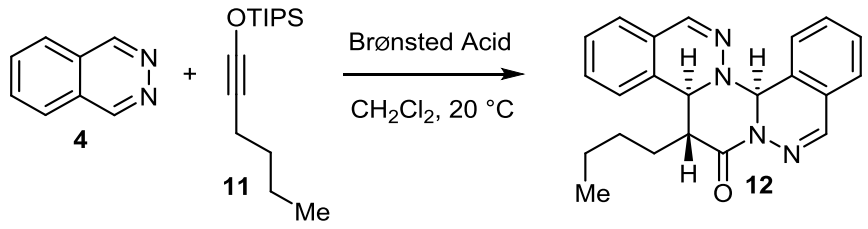

[12] Montavon, T. J.; Türkmen, Y. E.; Shamsi, N. A.; Miller, C.; Sumaria, C. S.; Rawal, V. H.; Kozmin, S. A. *Angew. Chem. Int. Ed.* **2013**,

Table 1, continued

Brønsted Acid	Yield (%)	d.r.
13 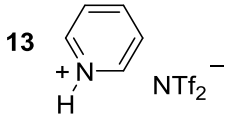	77	98:2
14 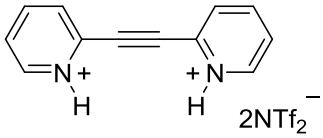	78	98:2

I.3.2 Significance of the Formal [2+2+2] Cycloaddition Reaction of Azadiene and Siloxy Alkyne

While most of the known [2+2+2] cycloadditions typically require the presence of a transition metal catalyst,[13] the above method promotes the condensation under remarkably mild reaction conditions, using only a simple, weak Brønsted acid. The excellent diastereoselectivity of this transformation was also highly noteworthy. Furthermore, the unique pentacyclic ring system of the product represents an addition to chemists' collection of nitrogen-containing heterocycles. As new nitrogen-containing heterocycles play a crucial role in chemical biology and medicinal chemistry,[14] a cellular screen of such structurally diverse products was carried out by Dr. Noumaan A. Shamsi. The study identified a lead compound towards inhibition of aerobic glycolysis.[12]

I.3.3 Proposed Reaction Mechanism

Two mechanistic pathways can explain the formation of pentacyclic lactams originating from [2+2+2] cycloadditions of phthalazines with siloxy alkynes (Figure 1). The reaction can proceed via initial formation of ketenium ion **19** via protonation of siloxy alkyne by the

[13] (a) Chopade, P. R.; Louie, J. *Adv. Synth. Catal.* **2006**, *348*, 2307 – 2327; (b) Shibata, T.; Tsuchikama, T. *Org. Biomol. Chem.* **2008**, *6*, 1317–1323; c) Dominguez, G.; Pérez-Castells, J. *Chem. Soc. Rev.* **2011**, *40*, 3430–3444

[14] Pozharskii, A. F.; Soldatenkov, A.; Katritzky, A. R. *Heterocycles in Life and Society*, John Wiley & Sons, Inc., Hoboken, **2011**.

pyridinium salt. This electrophilic intermediate can be intercepted by phthalazine **4** to give enol silane **20**, a heterodiene with nucleophilic and electrophilic carbons at opposite ends. Addition of a second phthalazine moiety to **20** would trigger cyclization of the central ring, to afford lactam **18** upon protodesilation.

Figure 1: Proposed Reaction Mechanism

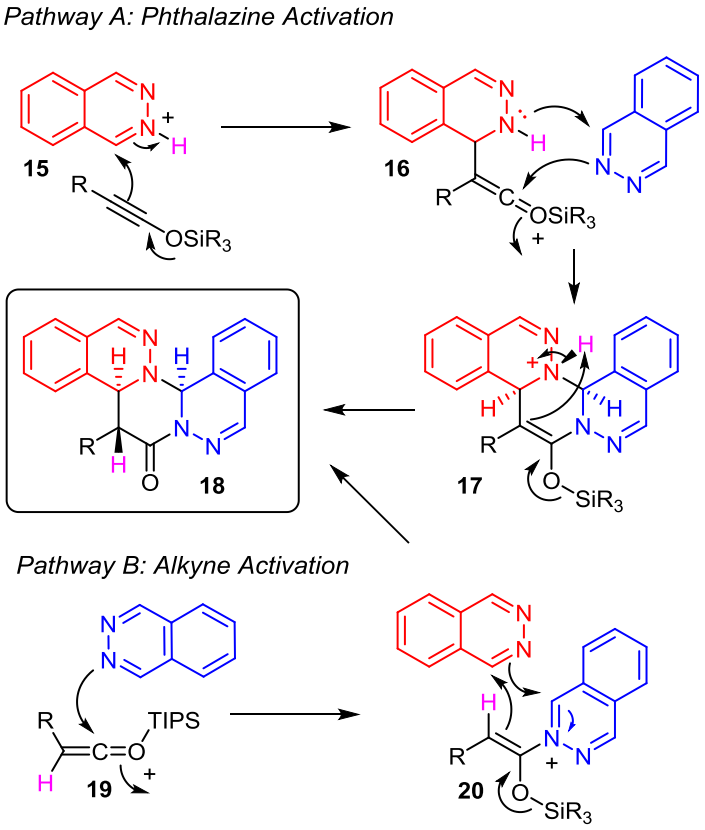

Alternatively, the process can begin with protonation of phthalazine by the pyridinium catalyst. The resulting phthalazinium ion **15** would then react with alkyne to give the ketenium ion **16**. Interception of this intermediate by another phthalazine **4** would give ammonium ion **17**, which can trigger protodesilation of the enol silane moiety to give the observed product **18.** Both mechanistic pathways were found to be consistent with deuterium labeling experiments.

Table 2: The Three-Component [2+2+2] Cycloaddition Reaction of Phthalazines and Siloxy Alkynes

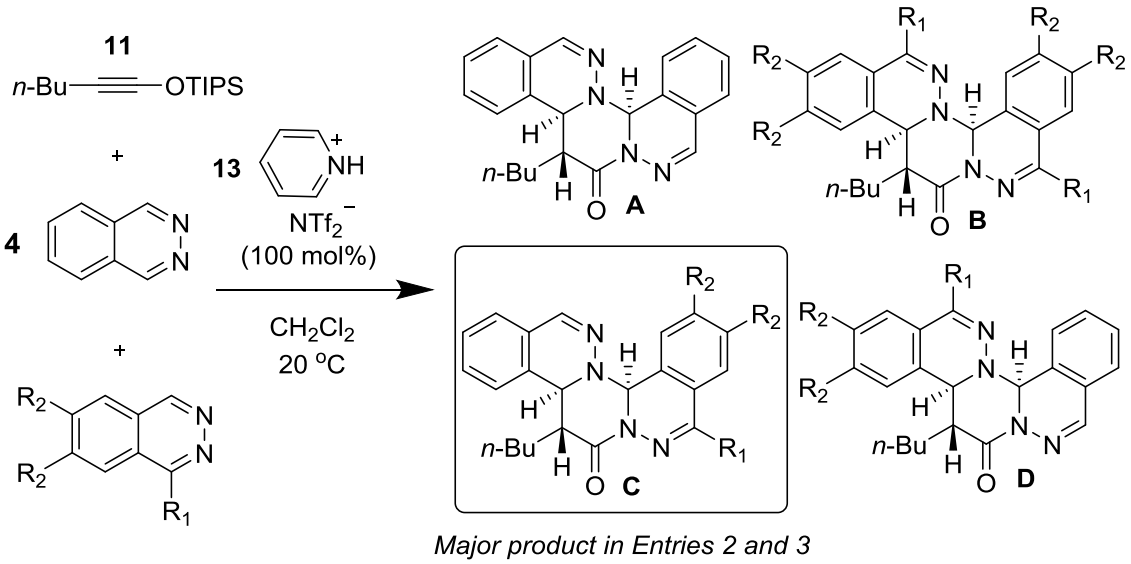

Major product in Entries 2 and 3

Entry	1,2-Diazine	Product Ratio: **A**:**B**:**C**:**D**[a]	Yield, %[b]
1	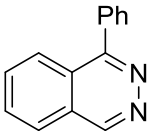 **21**	**24**:**25**:**26**:**27** = 29:21:23:27	56
2	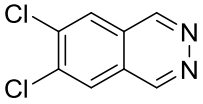 **22**	**24**:**28**:**29**:**30** = 5:19:48:28	43
3	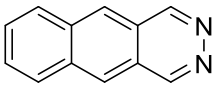 **23**	**24**:**31**:**32**:**33** = 0:33:67:0	68

[a]Yields refer to those of the major isolated diastereomer of each reaction. [b]Diastereomeric ratios were determined by 500 MHz ^{1}H NMR analysis of the crude reaction mixture prior to purification.

I.3.4 The Three-component [2+2+2] Cycloaddition Reaction

To gain further mechanistic insight, we next examined a possibility of conducting a three-component reaction using two different 1,2-diazines. Reaction of siloxy alkyne **11** with phthalazine **4** and 1-phenyl phthalazine **21** delivered roughly equal quantities of all four possible products (Table 2, Entry 1), as expected given the small electronic perturbation provided by the phenyl substituent C–2. However, treatment of siloxy alkyne **11** with phthalazine **4** and 6,7-dichlorophthalazine **22** with pyridinium trifluoromethane-sulfonimide afforded predominantly the hybrid product **29**, as well as smaller quantities of cycloadducts **28** and **30** (Table 2, entry 2). Finally, the use of benzo[*g*]phthalazine **23** in a similar three-component reaction with **4** and **11** resulted in the formation of only one of the hybrid products, **32**, as the major product along with the cycloadduct **31** (Table 2, entry 3). These results highlight the unique ability of this process to discriminate between two similar but electronically differentiated 1,3-diazine moieties.

I.4 The Formal [4+2] Cycloaddition Reaction of Siloxy Alkynes and 1,2-Diazines

I.4.1 Potential Application Towards Accessing 3-Substituted-2-hydroxy naphthols

The axially chiral 1,1′-binaphthalene-2,2′-diol (binol) has impacted asymmetric catalysis profoundly.[15] Used widely as a chiral ligand and as a precursor to chiral ligands and catalysts, binol is best prepared by the oxidative dimerization of 2-naphthol (Scheme 4).[16]

[15] (a) Brunel, J. M. *Chem. Rev.* **2005**, *105*, 857. (b) Wang, H. *Chirality* **2010**, *22*, 827.
[16] For selected examples of oxidative dimerization of naphthols, see: (a) Guo, Q.-X.; Wu, Z.-J; Luo, Z.-B.; Liu, Q.-Z.; Ye, J.-L.; Luo, S.-W.; Cun, L.-F.; Cun, L.-F.; Gong, L.-Z. *J. Am. Chem. Soc.* **2007**, *129*, 13927. (b) Egami, H.; Matsumoto, K.; Oguma, T.; Kunisu, T.; Katsuki, T. *J. Am. Chem. Soc.* **2010**, *132*, 13633.

Scheme 4: A Representative Example of the Preparation of Binol by Oxidative Dimerization

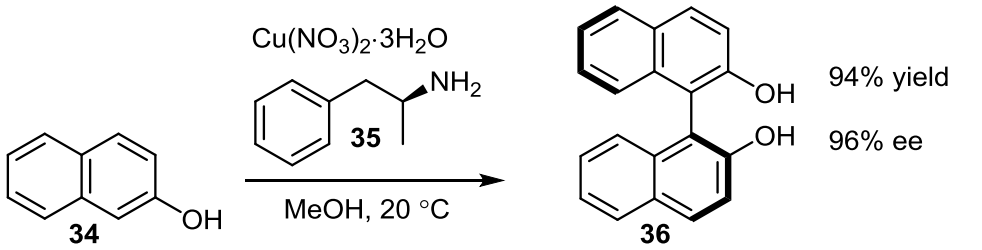

Binol derivatives, particularly those with substituents at the 3,3′-positions, allow fine-tuning of steric and electronic properties as well as sculpting of the scaffold's chiral environment, thereby greatly enhancing the utility of this scaffold.[17,18,19] Such 3,3′-disubstituted binols are nearly always made through a multistep sequence starting from a preformed binol (Scheme 5), since the direct oxidative dimerization of 3-substituted naphthols is impractical given the limited availability of such naphthol precursors.[20]

[17] Reviews: (a) Y.; Yekta, S.; Yudin, A. K. *Chem. Rev.* **2003**, *103*, 3155. (b) Berthod, M.; Mignani, G.; Woodward, G.; Lemaire, M. *Chem. Rev.* **2005**, *105*, 1801. (c) Shibasaki, M.; Matsunaga, S. *Chem. Soc. Rev.* **2006**, *35*, 269. (d) Pereira, M. M.; Calvete, M. J. F.; Carrilho, R. M. B.; Abreu, A. R. *Chem. Soc. Rev.* **2013**, *42*, 6990.

[18] For selected examples of binol derivatives in catalysis, see: (a) Bao, J.; Wulff, W. D.; Dominy, J. B.; Fumo, M. J.; Grant, E. B.; Rob, A. C.; Whitcomb, M. C.; Yeung, S.-M.; Ostrander, R. L.; Rheingold, A. L. *J. Am. Chem. Soc.* **1996**, *118*, 3392. (b) Knöpfel, T. F.; Aschwanden, P.; Ichikawa, T.; Watanabe, T.; Carreira, E. M. *Angew. Chem. Int. Ed.* **2004**, *43*, 5971. (c) Unni, A. K.; Takenaka, N.; Yamamoto, H.; Rawal, V. H. *J. Am. Chem. Soc.* **2005**, *127*, 1336. (d) Li, G.-Q.; Gao, H.; Keene, C.; Devonas, M.; Ess, D. H.; Kürti, L. *J. Am. Chem. Soc.* **2013**, *135*, 7414.

[19] A particularly important class of binol derivatives are chiral phosphoric acids: (a) Cannon, S. J. *Angew. Chem. Int. Ed.* **2006**, *45*, 3909. (b) Terada, M. *Synthesis* **2010**, *12*, 1929. For pioneering applications, see: (c) Akiyama, T.; Itoh, J.; Yokota, K.; Fuchibe, K. *Angew. Chem. Int. Ed.* **2004**, *43*, 1566. (d) Uraguchi, D.; Terada, M. *J. Am. Chem. Soc.* **2004**, *126*, 5356.

[20] (a) Simonsen, K. B.; Gothelf, K. V.; Jørgensen, K. A. *J. Org. Chem.* **1998**, *63*, 7536. (b) Maruoka, K.; Itoh, T.; Araki, Y.; Shirasaka, T.; Yamamoto, H. *Bull. Chem. Soc. Jpn.* **1998**, *61*, 2975. (c) Huang, W.-S.; Pu, L. *Tetrahedron Lett.* **2000**, *41*, 145. (d) Romanov-Michailidis, F.; Guénée, L.; Alexakis, A. *Angew. Chem. Int. Ed.* **2013**, *52*, 9266.

Scheme 5: Multi-Step Sequence Employed Towards the Preparation of 3,3'-Disubstituted Binols

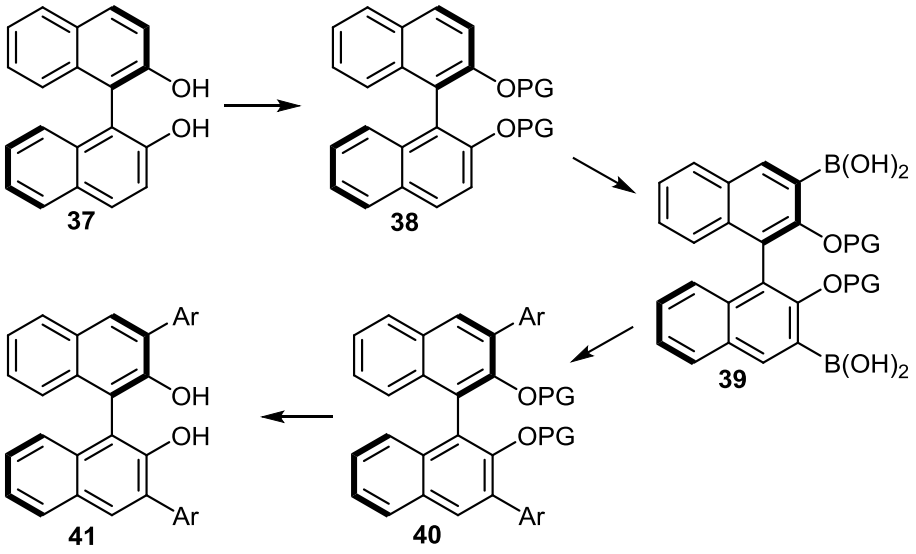

I.4.2 Previous Work Towards Accessing Substituted Naphthalenes, Anthracene

In 2012, our group (Dr. Yunus E. Türkmen) reported a general route of 3-substituted naphthol silyl ethers via a silver salt-catalyzed formal Inverse Electron-Demand Diels-Alder (IEDDA) reaction between phthalazines and siloxy alkynes (Scheme 6).[21] It should be noted that this reaction was a rare example of a metal-catalyzed formal IEDDA reaction. Shortly thereafter, a procedure describing the one-pot synthesis of phthalazines from aldehydes was reported by Wegner and co-workers.[22] This section describes the extension of the formal [4+2] cycloaddition reaction towards catalysis by other metals (Copper(I)/Nickel(0)) and towards other substrates derived from Wegner's one-pot methodology.[23]

[21] Türkmen, Y. E.; Montavon, T. J.; Kozmin, S. A.; Rawal, V. H. *J. Am. Chem. Soc.* **2012**, *134*, 9062.
[22] Kessler, S. N.; Wegner, H. A. *Org. Lett.* **2012**, *14*, 3268.
[23] Sumaria, C. S.; Türkmen, Y. E.; Rawal, V. H. *Org. Lett.* **2014**, *16*, 3236.

Scheme 6: Silver(I) Catalyzed Formal [4+2] Cycloaddition Reaction of 1,2-Diazines and Siloxy Alkynes

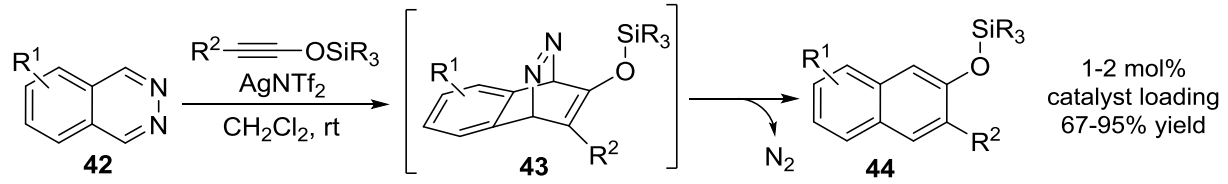

I.4.3 Accessing Heterocycles and Their Potential Application Towards Binols

Scheme 7: A Potential 3-step Synthesis of Substituted Binols Facilitated by the Formal [4+2] Cycloaddition Reaction of Siloxy Alkynes and 1,2-Diazines

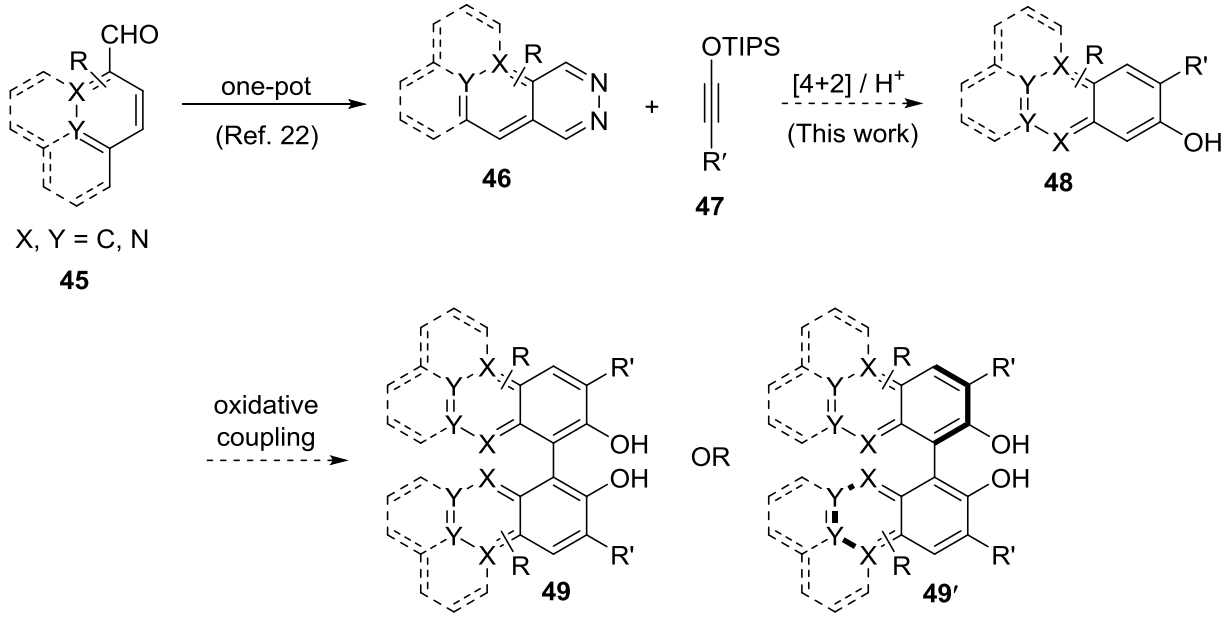

Since phthalazines are prepared by a one-pot procedure from aromatic aldehydes, a methodology to access 2-hydroxy naphthol derivatives would facilitate the synthesis of a variety of 2-hydroxy naphthalene derivatives,[24] potential precursors to modified binol ligands (Scheme 7).[16]

[24] For reviews on the synthesis of substituted naphthalenes, see: (a) Katritzky, A. R.; Li, J.; Xie, L. *Tetrahedron* **1999**, *55*, 8263. (b) Rousseau, A. L.; de Koning, C. B.; van Otterlo, W. A. L. *Tetrahedron* **2003**, *59*, 7. For recent examples for the synthesis of 2-naphthols, see: (c) Juteau, H.; Gareau, Y.; Lachance, H. *Tetrahedron Lett.* **2005**, *46*, 4547. (d) Zhang, X.; Sarkar, S.; Larock, R. C. *J. Org. Chem.* **2006**, *71*, 236. (e) Dai, Y.; Feng, X.; Liu, H.; Jiang, H.; Bao, M. *J. Org.*

We also envisioned that extending the chemistry towards other azadienes would greatly expand the scope of this reaction. Substituted heterocycles such as quinolines, isoquinolines, indoles, phenanthrenes, benzofurans and benzothiofurans could potentially be accessed in just two steps from commercially available starting materials (Figure 2). It should be noted that over 80% of top small molecule drugs (by US retail sales, 2010) contain at least one heterocycle,[25] and that 59% of all FDA approved drugs contain at least one *N*-heterocycle.[26] As a result, an investigation into catalysis by other metals, and towards other heterocycles was undertaken. Our calculations of HOMO/LUMO values showed that the scope of this chemistry may be greatly expanded (Figure 3).[27]

Figure 2: Heterocycles That Can Potentially Be Accessed via a [4+2] Cycloaddition Reaction of Azadienes and Siloxy Alkynes

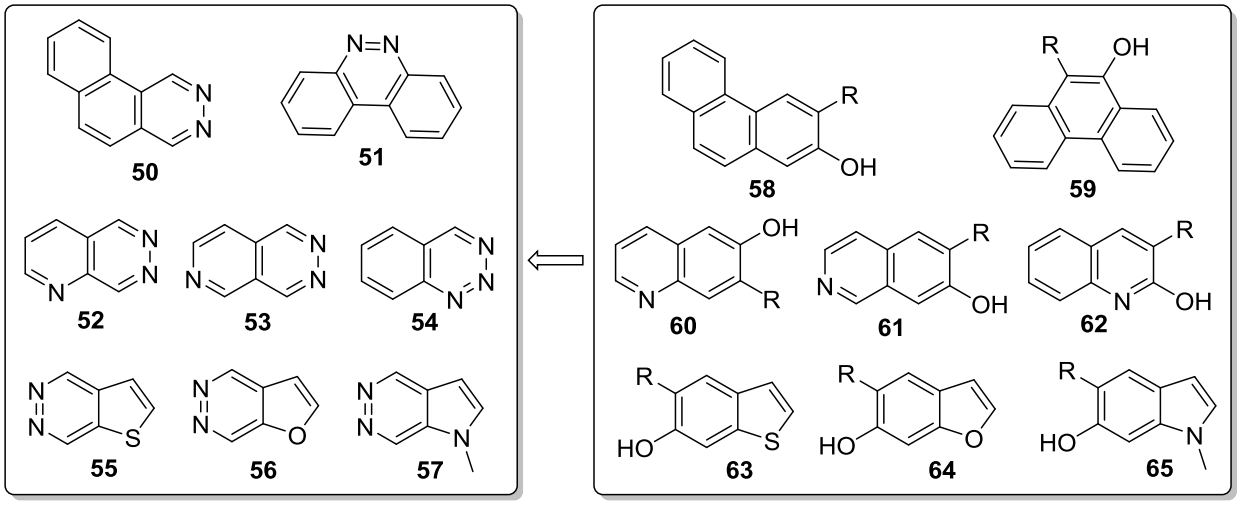

Chem. **2011**, *76*, 10068. (f) Xia, Y.; Qu, P.; Liu, Z.; Ge, R.; Xiao, Q.; Zhang, Y.; Wang, J. *Angew. Chem. Int. Ed.* **2013**, *52*, 2543. (g) He, Y.; Zhang, X.; Shen, N.; Fan, X. *J. Org. Chem.* **2013**, *78*, 10178. (h) Chang, M.-Y.; Chan, C.-K.; Lin, S.-Y. *Tetrahedron* **2013**, *69*, 1532.

[25] Gomtsyan, A. *Chem. Heterocycl. Compd.* **2012**, *48*, 7.

[26] Vitaku, E.; Smith, D. T.; Njardarson, J. T. *J. Med. Chem.* **2014**, *57*, 10257.

[27] Calculations were carried out using Spartan '08, Wavefunction, Inc., Irvine, CA.

Figure 3: Calculated HOMO/LUMO Values (in eV) with HF 3-21G Level of Theory (Solvent: DCM)

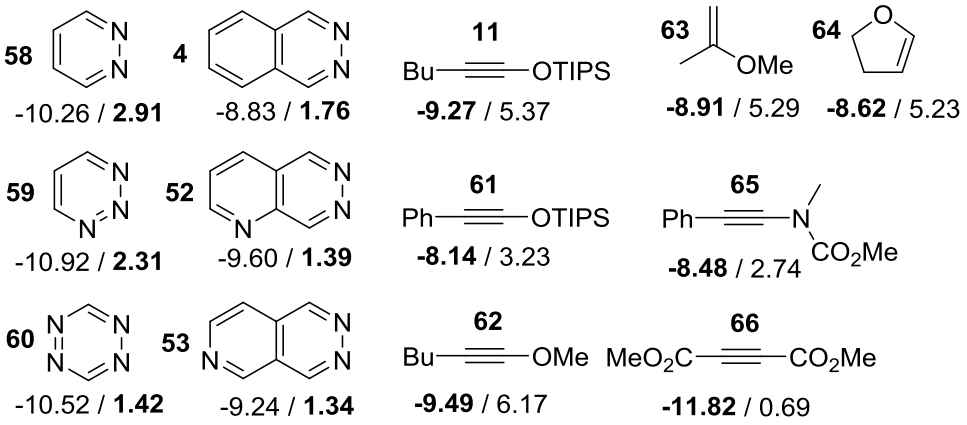

I.4.4 Optimization of Reaction Conditions

The contrasting reactivity displayed by pyridinium salts and silver salts combined with a desire to identify non-precious metals for catalysis motivated us to examine a broader range of metal complexes for the IEDDA reaction of phthalazine and 1-siloxy hexyne (Table 3). Commonly employed Lewis acids, such as $ZnBr_2$, $TiCl_4$, $Yb(OTf)_3$, $Sc(OTf)_3$, $Bi(OTf)_3$, $Co(BF_4)_2$, $La(OTf)_3$, $In(OTf)_3$ and $BF_3{\cdot}OEt_2$, all failed to catalyze the reaction.[28] Interestingly, while $NiCl_2$ was also ineffective, the corresponding Ni(0) complexes, $Ni(PPh_3)_4$ and $Ni(cod)_2$, afforded the desired cycloadduct **67** in 21% and 43% yields, respectively (entries 1-2). This result suggests that the metal is not activating the diazine simply through Lewis acid/base interaction, since Ni(0) complexes are expected to be weakly Lewis acidic, certainly compared to $NiCl_2$. We were pleased to find that $Ni(CO)_2(PPh_3)_2$, at 10 mol% catalyst loading, nicely catalyzed the cycloaddition at room temperature, affording the product in 80% yield (entry 3). Further addition of PPh_3 or $P(OMe)_3$ to the Ni(0) complex gave the product in diminished yields (entries 4-5). Isoelectronic with Ag(I) and Ni(0), Cu(I) salts were expected to also catalyze the cycloaddition

[28] Please see the Experimental Section for a complete list of metal complexes evaluated.

reactions. Indeed, CuCl when used in conjunction with 2,2′-bipyridine did catalyze the reaction, albeit poorly (not shown).

Table 3: Reaction Development and Optimization[a]

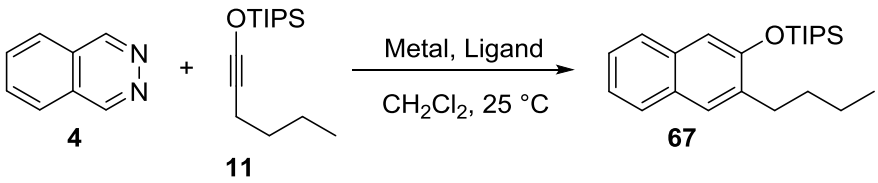

entry	catalyst (mol%)	ligand (mol%)	time (h)	yield (%)[b]
1	$Ni(PPh_3)_4$ (10)	-	24	21
2	$Ni(cod)_2$ (10)	-	24	43
3	$Ni(CO)_2(PPh_3)_2$ (10)	-	24	**81 (80)**[c]
4	$Ni(CO)_2(PPh_3)_2$ (10)	PPh_3 (10)	24	67
5	$Ni(CO)_2(PPh_3)_2$ (10)	$P(OMe)_3$ (10)	24	35
6[d]	CuOTf (5)	bpy (5)	24	34
7[d]	$Cu(MeCN)_4OTf$ (5)	bpy (5)	24	38
8[d]	$Cu(MeCN)_4PF_6$ (5)	bpy (5)	24	49
9	$Cu(MeCN)_4PF_6$ (10)	bpy (10)	4	79
10	$Cu(MeCN)_4BF_4$ (10)	bpy (10)	4	67
11	$Cu(MeCN)_4PF_6$ (10)	bpy (7.5)	4	**83 (80)**[c]
12	$Cu(MeCN)_4PF_6$ (10)	1,10-phenanthroline (10)	24	32
13	$Cu(MeCN)_4PF_6$ (10)	pyr (20)	16	72
14	$Cu(MeCN)_4PF_6$ (10)	4,4'-di-*tert*-butyl-2,2'-dipyridine (10)	24	60
15	$Cu(MeCN)_4PF_6$ (10)	2,2′:6′,2″-terpyridine (10)	24	28

[a]All reactions were carried out using 0.5 mmol of **1** and 1.0 mmol of **2** in 1 mL CH_2Cl_2. [b]Yields were determined by ^1H NMR using 1,3,5-trimethoxybenzene as an internal standard. [c]Isolated yield. [d]Reaction was carried out using 1.5 equivalents of **2** per equivalent of **1** in CH_2Cl_2 (0.5 mmol of **1** in 1.0 mL CH_2Cl_2).

The efficacy of Cu(I) salts improved with decreasing nucleophilicity of the counterion, as evidenced by increasing yields on going from CuI to CuCl to Cu(OTf). Even better results were obtained with highly dissociated counter ions, such as PF_6^- and BF_4^- (entries 7-10). The best result was obtained using 10 mol% of tetrakis(acetonitrile)copper(I) hexafluorophosphate with

2,2'-bipyridine as the ligand, which provided naphthalene **67** in 80% isolated yield after 4 hours reaction time (entry 11). Several other ligands were examined, but they did not better the yields (entries 12-15). Reactions proceeded in lower yields in acetonitrile and 1,4-dioxane, and no product was formed in chloroform or in protic solvents, such as methanol and water. The interchangeable use of silver, copper, or nickel complexes for catalysis of formal cycloadditions is noteworthy.[29,30]

I.4.5 Substrate Scope

Having defined effective conditions for Cu(I) and Ni(0) catalyzed cycloaddition of the parent system, we next evaluated the substrate scope for the new catalyst systems (Table 4, 5). The two catalysts were expected to behave differently, since $Ni(CO)_2(PPh_3)_2$ is hindered, having a sterically-crowded neutral Ni(0) center, whereas Cu(I), as a soft Lewis acid, was expected to coordinate more strongly.[31]

Indeed, as noted above, while both provided silyl ether **67** in the same yield, the reaction was noticeably faster with the Cu(I) catalyst. Additionally, the two complexes begot differing regioselectivities with unsymmetrical phthalazines. Whereas Cu(I) gave 1:1 mixture of the two regioisomeric products of 6-methoxy phthalazine, the Ni(0) catalyst gave **69** in a 1.5:1 preference over its regioisomer (not shown).

[29] Bullock, R. M., Ed. *Catalysis Without Precious Metals*; Wiley-VCH: Weinheim, 2010.
[30] For an example of silver and copper complexes giving two different products from the same precursor, see: Fang, Y.; Wang, C.; Su, S.; Yu, H.; Huang, Y. *Org. Biomol. Chem.* **2014**, *12*, 1061.
[31] Ho, T.-L. *Chem. Rev.* **1975**, *75*, 1.

Table 4: Investigation of Cu(I) Catalyzed Formal [4+2] Cycloaddition Reactions of 1,2-Diazines and Siloxy Alkynes

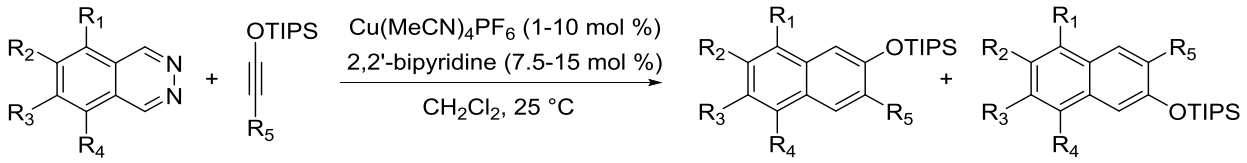

entry[a]	substrate	time (hours)	product	yield[b] (%)	ratio of regioisomers[c]
1	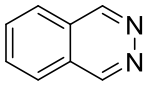 **4**	4	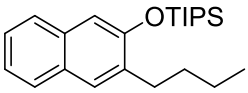 **67**	80	-
2	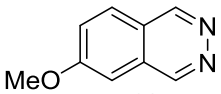 **68**	8	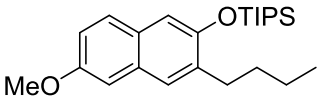 **69a (+69b)**	80	50:50
3	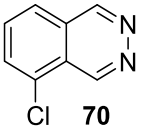 **70**	5	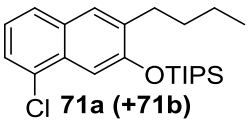 **71a (+71b)**	79	55:45
4	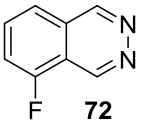 **72**	3.5	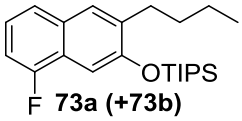 **73a (+73b)**	76	50:50
5	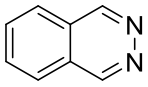 **4**	2.5	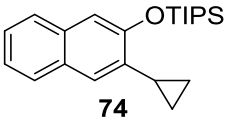 **74**	73	-
6	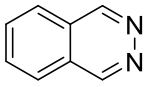 **4**	4	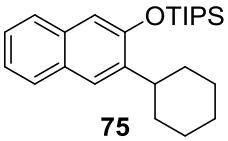 **75**	76	-

Table 4, continued

7[d]	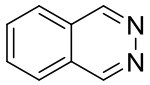 **4**	7	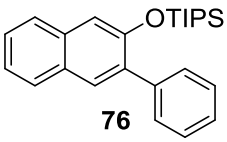 **76**	88	-
8	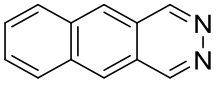 **23**	3.5	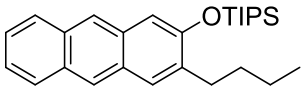 **77**	74	-
9[d]	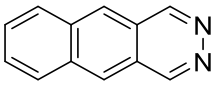 **23**	4	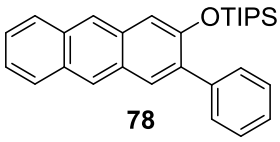 **78**	76	-
10	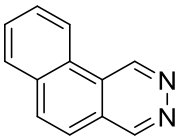 **79**	14	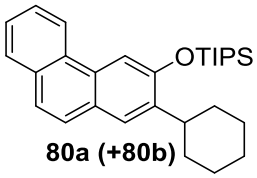 **80a (+80b)**	70	64:36
11	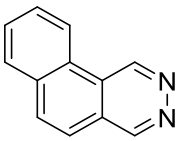 **79**	14	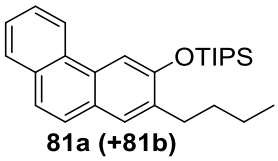 **81a (+81b)**	71	73:27
12	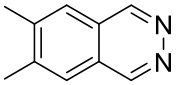 **82**	12	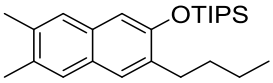 **83**	74	-
13	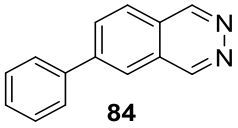 **84**	7	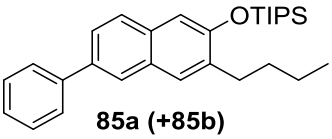 **85a (+85b)**	72	60:40

[a]Unless otherwise stated, the reaction was carried out using 0.5 mmol of 1,2-diazine with 10 mol% catalyst loading & 2.0 equivalents of siloxy alkyne [b]Combined isolated yield of the two regioisomers. [c]Major isomer corresponds to the product shown in the table. [d]Reaction carried out using 1 mol% of $Cu(MeCN)_4PF_6$.

A similar preference was observed with 5-chlorophthalazine and 5-fluorophthalazine, which produced naphthalenes **71** and **73**, respectively, as the major products. In these instances, the slower reaction was also the more regioselective one. Other alkyl and aryl siloxy alkynes were examined, and all gave the naphthalene products in good yields. Benzo-fused derivatives of phthalazine enabled the synthesis of anthracene and phenanthrene derivatives. Thus, benzo[*g*]phthalazine gave anthracene products **77** and **78**, whereas benzo[*f*]phthalazine gave phenanthrenes **80** and **81**.

As the relatively slow Ni(0) catalyzed reactions were generally found to be more selective, we wondered if a slower reaction is likely to be more regioselective in general. Thus, we used a lower catalyst loading of $Ni(CO)_2(PPh_3)_2$ under otherwise similar conditions and indeed found the ratio of regioisomers to be different (Table 6). While this is likely to result from altered kinetics for one product versus another, a certain threshold of catalyst loadings and concentration was necessary for the reaction to be synthetically useful.

Table 5: Investigation of Ni(0) Catalyzed Formal [4+2] Cycloaddition Reactions of 1,2-Diazines and Siloxy Alkynes

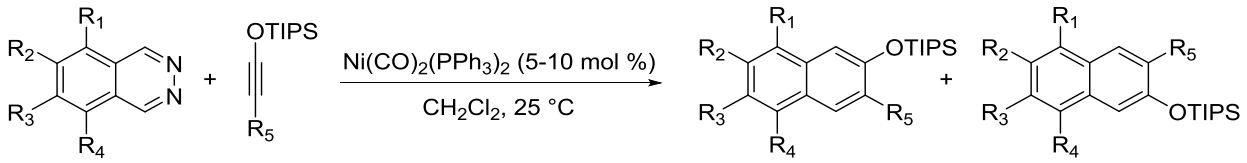

entry[a]	substrate	time (hours)	product	yield[b] (%)	ratio of regioisomers[c]
1	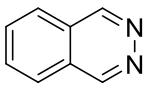 **4**	24	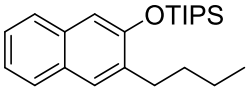 **67**	80	-

Table 5, continued

2	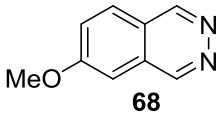 **68**	24	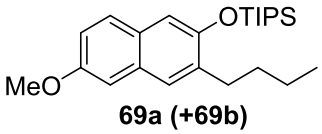 **69a (+69b)**	75	62:38
3	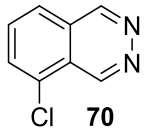 **70**	24	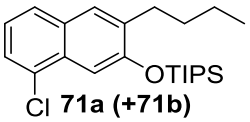 **71a (+71b)**	74	74:26
4	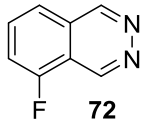 **72**	48	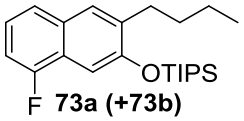 **73a (+73b)**	70	67:33
5	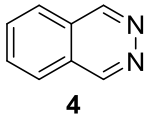 **4**	48	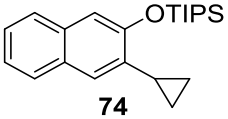 **74**	88	-
6	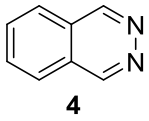 **4**	24	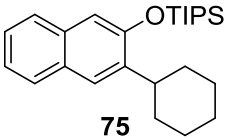 **75**	82	-
7[d]	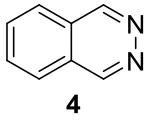 **4**	7	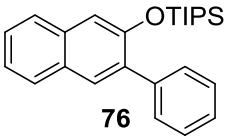 **76**	94	-
8	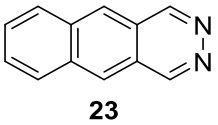 **23**	24	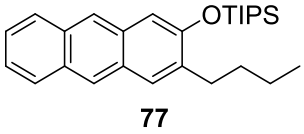 **77**	64	-
9[d]	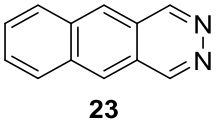 **23**	6	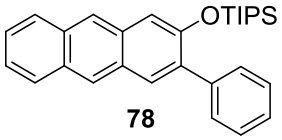 **78**	83	-
10[e]	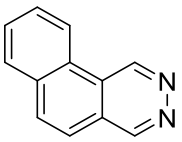 **79**	120	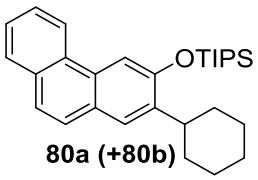 **80a (+80b)**	57	44:56

Table 5, continued

11[e]	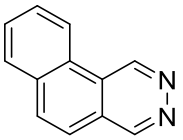 **79**	120	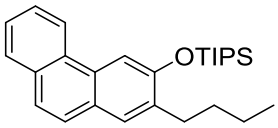 **81a (+81b)**	78	40:60
12	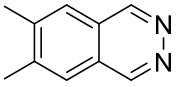 **82**	24	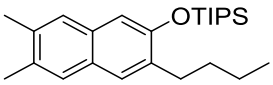 **83**	76	-
13	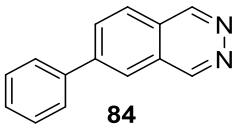 **84**	96	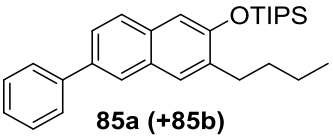 **85a (+85b)**	21	50:50

[a]Unless otherwise stated, the reaction was carried out using 0.5 mmol of 1,2-diazine with 10 mol% catalyst loading & 2.0 equivalents of siloxy alkyne [b]Combined isolated yield of the two regioisomers. [c]Major isomer corresponds to the product shown in the table. [d]Reaction carried out using 5 mol% of $Ni(CO)_2(PPh_3)_2$. [e]Note the reversal in regioselectivity upon changing from Cu(I) to Ni(0).

Table 6: Dependence of Regioselectivity upon Catalyst Loadings

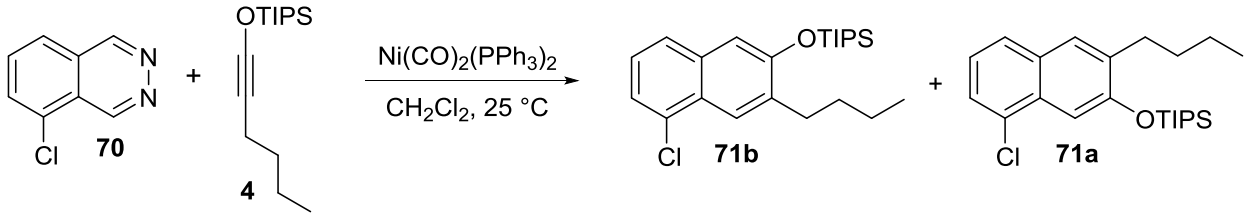

entry	catalyst loading (mol%)	reaction time (hours)	yield (%)	ratio of regioisomers **71b**:**71a**
1[a]	10	24	74	26:74
2[b]	1	120	30	12:88

[a]See Table 5 for further details. [b]Reaction carried out on a 0.15 mmol scale and the yield was obtained using NMR spectroscopy and by using 2,4,6-trimethoxybenzene as an internal standard.

We had early recognized that extending the IEDDA reactions to pyridopyridazines would open up a new route to quinolines and isoquinolines, but had found the silver catalyst to be ineffective

with most such substrates. We are delighted to note that this limitation can be overcome with the Cu-catalyst. The reaction of pyrido[2,3-*d*]pyridazine and 1-siloxy-hexyne **11**, under standard Cu-catalysis conditions, gave small amounts of the quinoline product (Table 7). When the same reaction was carried out in refluxing DCE, siloxy quinoline **86** was isolated in 41% yield, as a mixture of regioisomers.[32] The related trifluoromethane-substituted pyrido[2,3-*d*]pyridazine **88** reacted smoothly at room temperature, thus affording the corresponding product mixture **89** in 64% yield.[33] As observed with phthalazine, the reaction with the phenyl-substituted siloxy alkyne was more facile, giving the regioisomers of siloxy quinoline **87** in 74% yield. Similar success was enjoyed in the reaction between pyrido[3,4-*d*]pyridazine **53** and phenyl siloxy alkyne, which gave the regioisomeric isoquinoline products **90** in 67% yield.

Table 7: Investigation of Cu(I) Catalyzed Formal [4+2] Cycloaddition Reactions of Pyridopyridazines and Siloxy Alkynes[a]

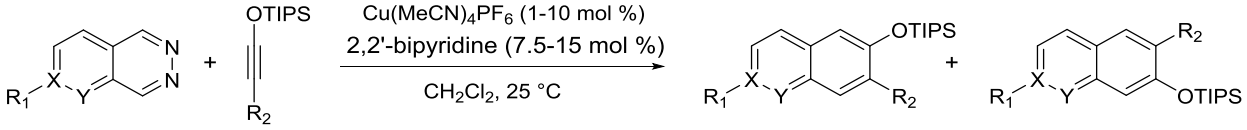

entry	substrate	time (hours)	product	yield[b] (%)	ratio of regioisomers[c]
1[d]	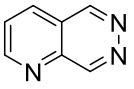 **52**	24	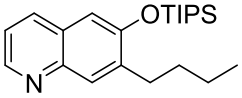 **86a (+86b)**	41	55:45-

[32] The Ag(I) and Ni(0) catalysts did not promote this reaction.
[33] Interestingly, the reaction of the trifluoromethyl-substituted pyrido[2,3-*d*]pyridazine, wherein the adjacent nitrogen atom is expected to be less basic, can also be catalyzed by 5 mol% $AgNTf_2$ to give the cycloadduct in 71% yield. See the supporting information for a detailed procedure.

Table 7, continued

2	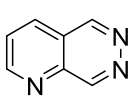 **52**	6	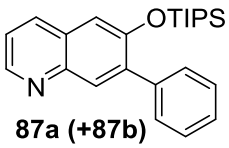 **87a (+87b)**	74	73:27
3[e]	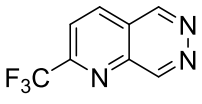 **88**	6	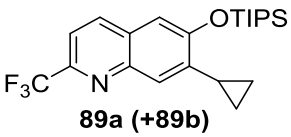 **89a (+89b)**	64	55:45
4	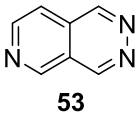 **53**	5	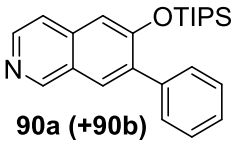 **90a (+90b)**	67	54:46

[a]Unless otherwise stated, the reaction was carried out using 0.5 mmol of 1,2-diazine with 10 mol% catalyst loading & 2.0 equivalents of siloxy alkyne [b]Combined isolated yield of the two regioisomers. [c]Major isomer corresponds to the product shown in the table. [d]Reaction was carried out in refluxing DCE. [e]Due to the electron-withdrawing nature of the trifluoromethyl group, the adjacent nitrogen atom is less basic, and the reaction with this substrate can also be catalyzed by 5 mol% $AgNTf_2$ (See experimental section for more details).

We hoped to evaluate the effect of these substituents on the formation of one regioisomer over the other, thus expanding the substrate scope and simultaneously providing an insight into the mechanism of our reaction. Unfortunately, we did not see a strong preference for one regioisomer over the other, rather almost equal amounts of both regioisomers were formed in some cases.

I.4.6 Evaluation of Other Azadienes

The following azadienes reported in literature were evaluated with Cu(I) and Ni(0) based methodology under a variety of conditions (Figure 4). However, no conversion to the corresponding addition product was observed.

Figure 4: Other Substrates Evaluated With the Copper(I)/Nickel(0) Methodology

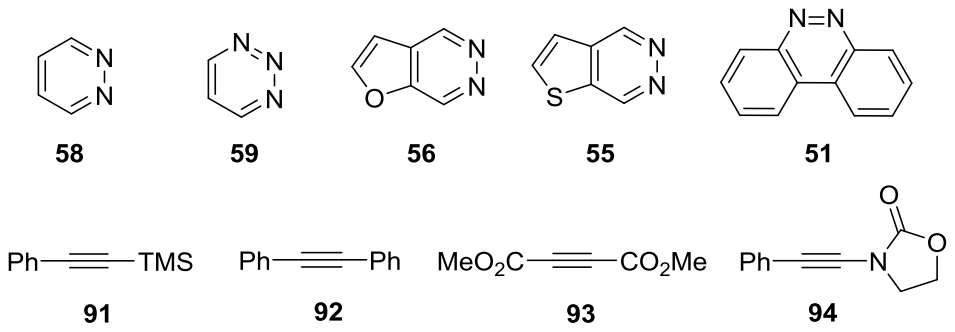

I.5 The Copper(I)-Catalyzed Formal [2+2] Cycloaddition Reaction

I.5.1 Previous Report of a [2+2] Cycloaddition Reaction with Siloxy Alkynes

The fruitful switch from a silver catalyst to a nickel or copper catalyst spurred a brief look at other reactions that might be amenable to such a change. Among the reactions of siloxy alkynes, we examined its formal [2+2]-cycloaddition with cyclohexenone, a transformation reported by Kozmin et al. to be catalyzed by $AgNTf_2$.[34] While we employ 1,2-diazines for the previous two reactions, the use of an electron-poor double bond instead of an electron-poor diene limited the scope of a formal cycloaddition reaction to that of a [2+2] while maintaining a desired HOMO/LUMO gap between the two reactants.

I.5.2 Optimization of Reaction Conditions

Scheme 8: Optimizing the formal [2+2] cycloaddition reaction of cyclohexenone and siloxy alkyne

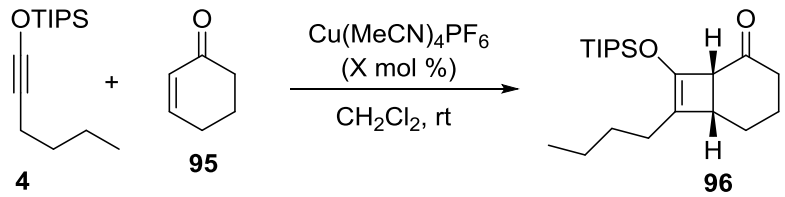

[34] Sweis, R. F.; Schramm, M. P.; Kozmin, S. A. *J. Am. Chem. Soc.* **2004**, *126*, 7442.

For the above reaction, using a 1 mol% of catalyst loading led to only 32% yield over 24 hours (Scheme 8). The yields improved upon further increasing the catalyst loading, however, saturation could be seen at 5 mol% catalyst loading. No significant increase in yield was observed upon increasing the catalyst loading from 5 mol% to 10 mol%. See Figure 5 for a graphical representation of the saturation of the reaction yield with increasing catalyst loadings.

Figure 5: Graph of Percentage Yield vs. Catalyst Loading (mol%) for the $Cu(MeCN)_4PF_6$ catalyzed [2+2] cycloaddition reaction of cyclohexenone and siloxy alkyne

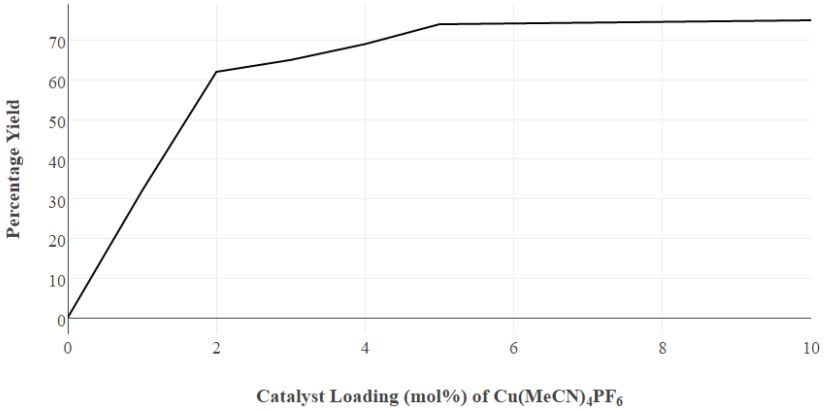

When 10 mol% of 2,2'-bipyridine was used as an additive along with a 5 mol% of $Cu(MeCN)_4PF_6$, no conversion could be seen even after 24 hours. Similarly, use of the isoelectronic Ni(0) complex, $Ni(CO)_2(PPh_3)_2$ failed to afford any conversion. When the reaction was repeated on a 0.5 mmol scale, the product **96** was isolated in 74% yield (Scheme 9).

Scheme 9: The Cu(I)-catalyzed formal [2+2] cycloaddition reaction[a,b]

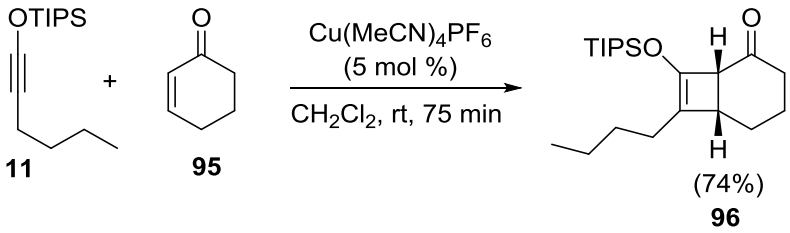

[a]Isolated yield; [b]The above reaction was not catalyzed by $Ni(CO)_2(PPh_3)_2$

I.5.3 Proposed Reaction Mechanism

Kozmin and co-workers found that the [2+2] cycloaddition reaction of phenyl vinyl ketone and *n*-butyl siloxy alkyne was catalyzed by Lewis acids such as $Sc(OTf)_3$, $TiCl_4$, TIPSOTf and BF_3OEt_2. As with the previous reactions, the role of Cu(I) is likely that of a 'soft' Lewis acid. Thus, two possible reaction mechanisms were deemed likely, based either upon the activation of the enone or upon the activation of the siloxy alkyne (Figure 6). We discuss the proposed mechanisms for the [2+2+2] and the [2+2] cycloaddition reactions for the reader to get a better understanding of the mechanism for the Ni(0) catalyzed [4+2] cycloaddition reaction.

Figure 6: Proposed reaction mechanism for Cu(I)-catalyzed the [2+2] Cycloaddition Reaction

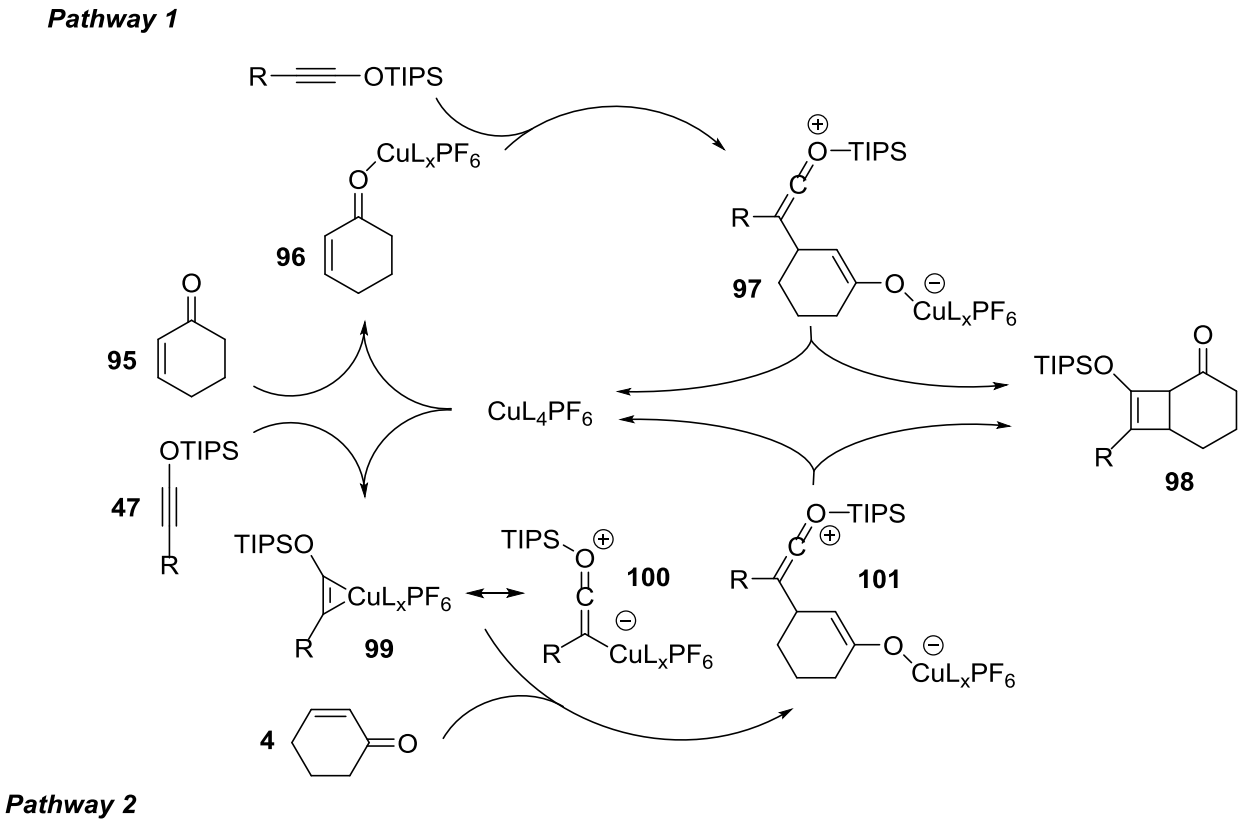

I.6 Concluding Remarks

In conclusion, we have demonstrated complementary reactivity with metal and Brønsted catalysis. We have also shown the utility of complexes of non-precious metals such as Cu(I) and Ni(0) towards the catalysis of the formal [4+2] cycloaddition reaction of 1,2-diazines and siloxy alkynes to give siloxy derivatives of naphthalene, anthracene, and phenanthrene. The copper catalyst was also effective in promoting the corresponding cycloaddition to generate quinoline and isoquinoline derivatives, as well as for the [2+2]-cycloaddition of siloxy alkyne and cyclohexenone. This study provides another demonstration of the feasibility of switching from a precious metal to more economical, isoelectronic metals for catalyzing reactions. It also demonstrates the unique advantage that one isoelectronic metal could possess over other metals.

CHAPTER II

THE DEVELOPMENT AND APPLICATION OF CHIRAL, BIFUNCTIONAL DELTIC UREAS AS DUAL HYDROGEN-BOND DONOR CATALYSTS

II.1 Significance of Hydrogen-Bond Donor Catalysis

The significance of chirality in the pharmaceutical industry has been widely recognized. As most enzymes are chiral, different enantiomers often exhibit different biological activities.[1] Thus, it is not surprising that racemic compounds constitute an ever smaller share of worldwide drug approvals,[2,3] and that half of all drugs currently marketed are chiral. Given the global spending on pharmaceutical drugs of over $ 1 trillion, the goal of developing new methods towards the synthesis of functionalized, chiral molecules is commendable.[4] While methods such as enzymatic processes and chemical resolution play a significant role, asymmetric catalysis is emerging as a prominent tool to achieve such an end-goal.[5]

Until the early 2000s, asymmetrical catalysis was considered synonymous with metal-catalyzed processes.[6] Due to the dramatic expansion of the area of organocatalysis over the last two decades, it has been realized that organocatalysis represents a fundamental concept by itself.[7] In contrast to metal catalysis, organocatalysts are stable to air and water, relatively non-toxic, easily

[1] (a) Casy, A. F. Medicinal Chemistry, 3rd ed.; Wiley-Interscience: New York, **1970**; 81. (b) Chen, A. M.; Wang, Y. *Org. Process. Res. Dev.* **2008**, *12*, 282
[2] Craner, H.; Groner, E.; Levy, L.; Agranat, I. *Drug Discov. Today* **2004**, *9*, 105.
[3] Wainschtein, S. R.; Zusman, E. Z.; Agranat, I. *Nat. Rev. Drug Discov.* **2012**, *11*, 972.
[4] "Drug Spending to Reach $1.3 Trillion by 2018, Report Forecasts.", New Rochelle (New York): *Mary Ann Liebert, Inc.*; **2014** Nov 21. Available from: http://www.genengnews.com/gen-news-highlights/drug-spending-to-reach-1-3-trillion-by-2018-report-forecasts/81250626/
[5] Trost, B. M. *Science* **1991**, *254*, 1471.
[6] Nugent, W. A. *Angew. Chem. Int. Ed.* **2012**, *51*, 8936.
[7] Hegedus, L. S. *J. Am. Chem. Soc.* **2009**, *131*, 17995.

handled experimentally and readily separated from crude reaction mixture without arduous work-up.[7] Often, both enantiomers are readily available to synthesize organocatalysts in a few steps.

Figure 7: Modes of Activation by Non-Covalent Hydrogen-Bonding Interactions

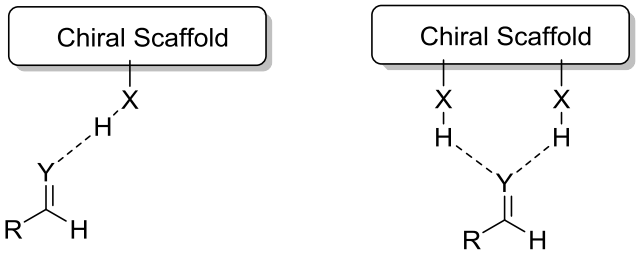

In particular, we focus on organocatalysts that rely on non-covalent hydrogen-bonding interactions. For catalysis using small molecules, hydrogen-bonding interactions are typically classified into two major types: a) mono hydrogen-bond donor catalysis and b) dual hydrogen-bond donor catalysis (Figure 7).[8] Please see reports by Jacobsen, Rawal, Takemoto and others (Figure 8) for pioneering examples of hydrogen-bond donor catalysis.[9,10]

[8] Please see the following review (and references therein) for a discussion of the various design elements: Auvil, T. J.; Schafer, A. G.; Mattson, A. E. *Eur. J. Org. Chem.* **2014**, 2633.

[9] (a) Sigman, M. S.; Jacobsen, E. N. *J. Am. Chem. Soc.* **1998**, *120*, 4901. (b) Wenzel, A. G.; Jacobsen, E. N. *J. Am. Chem. Soc.* **2002**, *124*, 12964. (c) Huang, Y.; Unni, A. K.; Thadani, A. N. Rawal, V. H. *Nature* **2003**, 146. (c) Okino, T.; Hoashi, Y.; Takemoto, Y. *J. Am. Chem. Soc.* **2003**, 12672. (d) Nugent, B. M.; Yoder, R. A.; Johnston, J. N. *J. Am. Chem. Soc.* **2004**, *126*, 3418. (e) Malerich J. P.; Hagihara, K.; Rawal, V. H. *J. Am. Chem. Soc.* **2008**, *130*, 14416.

[10] General reviews: (a) Doyle, A. G.; Jacobsen, E. N. *Chem. Rev.* **2007**, *107*, 713. (b) *Hydrogen Bonding in Organic Synthesis*; Pihko, P. M., Ed.; Wiley-VCH: Weinheim, **2009**. (c) Türkmen, Y. E.; Zhu, Y.; Rawal, V. H. Brønsted Acids. In *Comprehensive Enantioselective Organocatalysis*; Dalko, P. I., Ed.; Wiley-xVCH: Weinheim, **2013**; Vol. 2, Chpt. 10

Figure 8: Timeline of the Development of Major Dual Hydrogen-Bond Donor Scaffolds

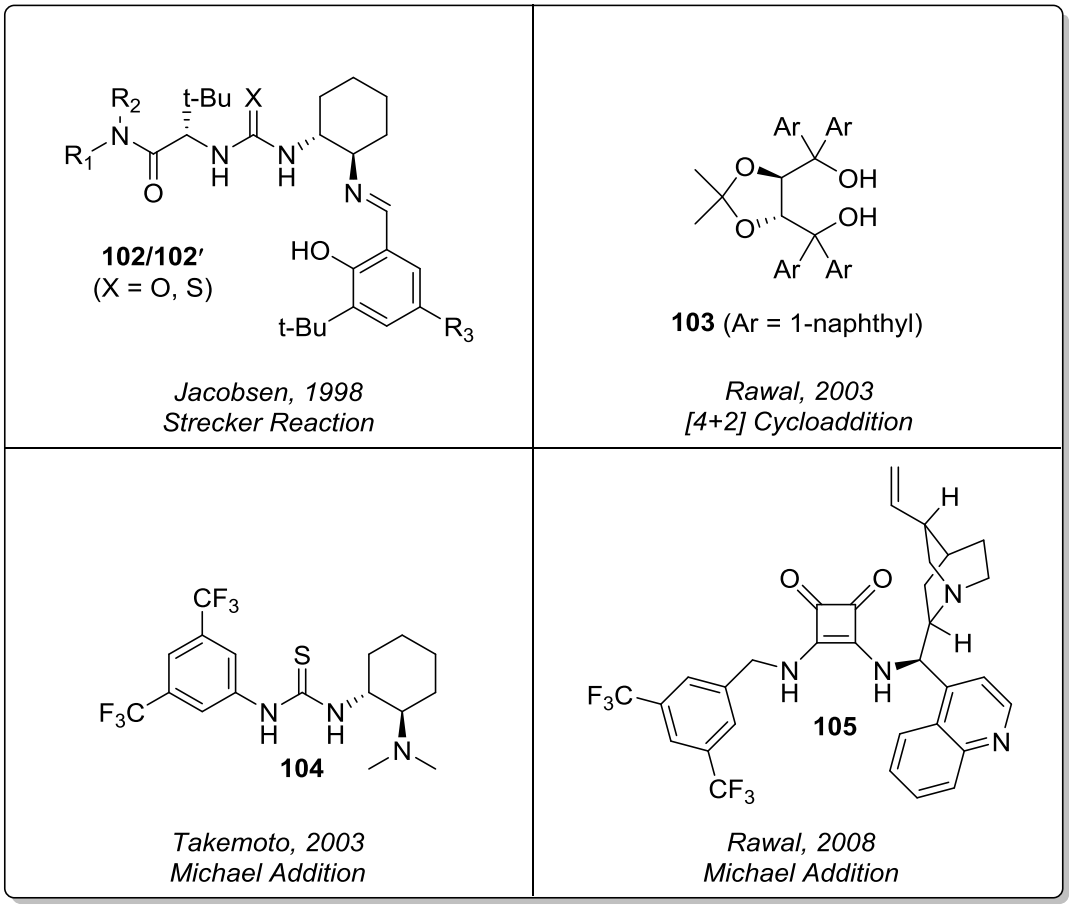

II.2 Design Principles and the Deltic Urea Scaffold

In a quest to design superior hydrogen-bond donor (HBD) catalysts towards asymmetric transformations, numerous permutations and combinations of achiral, chiral scaffolds have been explored (Figure 9). However, the use of core functional groups such as thioureas and squaramides has largely persisted in literature.[11,12] A potential driving force for the heavy use of

[11] For a review of thiourea catalysis, see: (a) Takemoto, Y. *Chem. Pharm. Bull.* **2010**, *58*, 593. (b) Siau, W. -Y.; Wang, J. *Catal. Sci. Tech.* **2011**, *1*, 1298.
[12] For review of squaramide catalysis, see: (a) Aciro, C.; Jones, L. H. Storer, R. I. *Chem. Soc. Rev.* **2011**, *40*, 2330. (b) Alemán, J.; Parra, A.; Jiang, H.; Jørgensen, K. A. *Chem. Eur. J.* **2011**,

these functional groups may have been the established chemistry underlying the synthesis of such molecules. In this chapter, we describe our progress towards the synthesis of a 'Deltic Urea' (amide of deltic acid) functional group, and elaborate upon it's applications as organocatalysts. Note that 'Detic Ureas' may also be referred to as 'Deltamides'.

Figure 9: Using a Different Core for Catalysts[8]

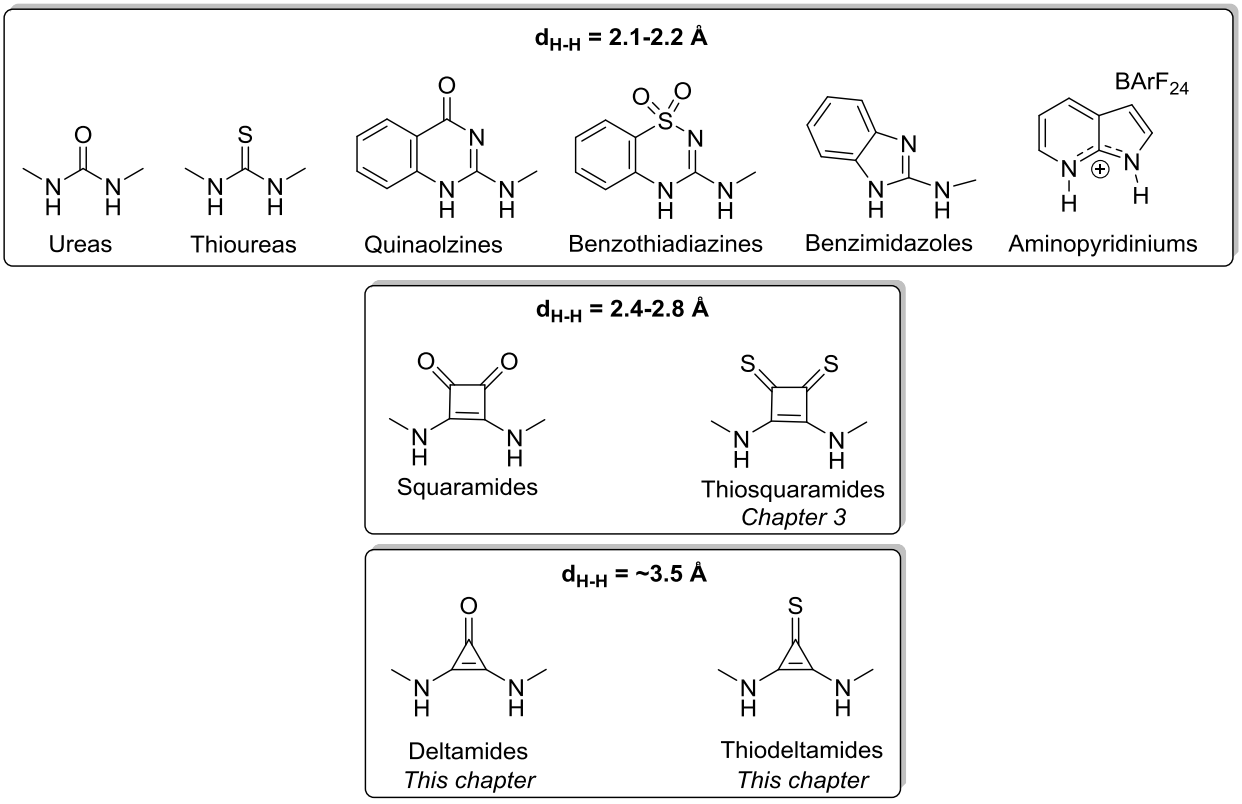

The success of squaramides is in no small part due to the aromatic nature of cyclobutenedione core. Such an aromatic core not only leads to stronger N-H bonds, but also positions the two hydrogen atoms in a unique geometry. Also, squaramides are among the few reported functional groups that exhibit an increased H-H distance. A statistical analysis of N-H···O=C bonds in protein crystal structures revealed that there is a distinct preference for N-H···O=C bonds to

17, 6890. (c) Chauhan, P.; Mahajan, S.; Kaya, U.; Hack, D.; Enders, D. *Adv. Synth. Catal.* **2015**, *357*, 253.

form in, or near to, the direction of sp^2 lone pairs.[13] The same report (by Taylor and co-workers) put the ideal H-H distance between 3.0 Å and 3.7 Å, and the ideal N-N distance at 4.0 Å and 5.7 Å (Figure 10).

Figure 10: A graphical representation of dual hydrogen-bonding interactions with a carbonyl group

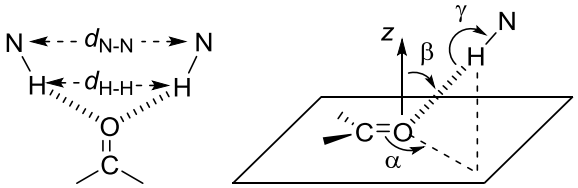

While nature uses complex architecture to position active functional groups, chemists are limited to small molecules to achieve end-goals. Thus, the use of an aromatic cyclopropenone[14] core to position N-H groups represented an intriguing possibility, especially given the increased H-H distances (Table 8). In thioureas and squaramides, polar N-H bonds are employed to activate electrophiles, and often an amine group is tethered to activate a nucleophile in tandem. Hence, our ultimate goal was to synthesize deltic ureas with a tethered amine group. Also, deltic ureas may not only be used to better activate existing electrophiles but also be used to activate a different class of electrophiles. In this chapter, we present the chemistry needed to synthesize various classes of deltic ureas, and offer preliminary evidence that deltic ureas are indeed capable of forming strong hydrogen-bonds to a carbonyl group. We also demonstrate the capability of deltic ureas to catalyze a reaction enantioselectively, albeit with low enantioselectivity.[15]

---

[13] (a) Taylor, R.; Kennard, O.; Versichel, W. *J. Am. Chem. Soc.* **1983**, *105*, 5761. (b) Taylor, R.; Kennard, O. *Acc. Chem. Res.* **1984**, *17*, 320.

[14] For a discussion regarding the aromaticity of cyclopropenone, see: *Chem. Eng. News* **1983**, *61*, 33.

[15] Cyclopropenimines have been employed towards asymmetric catalysis: (a) Nacsa, E. D.; Lambert, T. H. *J. Am. Chem. Soc.* **2015**, *137*, 10246. (b) Bandar, J. S.; Lambert, T. H. *J. Am. Chem. Soc.* **2013**, *135*¸11799.

Table 8: 6-31G* Hartree-Fock Calculations for Equilibrium Geometry in Vacuum[16]

Compound	Calculated H-H Distance
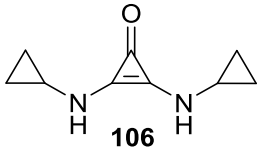 **106**	3.489 Å
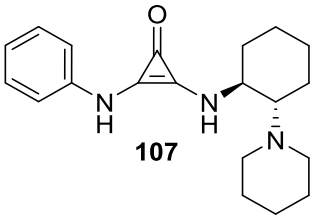 **107**	3.484 Å
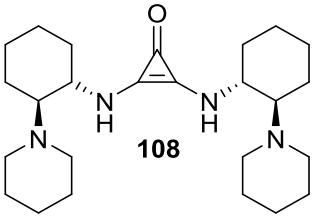 **108**	3.508 Å

II.3 Towards the Synthesis of Simple Deltic Ureas

While deltic ureas represented an ideal scaffold for use as dual hydrogen-bond donor catalyst, the challenges of synthesizing such molecules can be summed up in Table 9. Nonetheless, note an increase in stability as one changes the substituents on the cyclopropenone ring system from 'Cl' to 'OH' to 'OEt' to 'NR_2'.[17]

Table 9: Relative Stability of Deltic Urea Analogues

Compound	Reported Comments on Stability
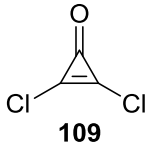 **109**	Dichlorocyclopropenone[18] "The neat liquid decomposes rapidly, and sometimes explosively at room temperature"

[16] Carried out using Spartan '08, Wavefunction, Inc., CA.
[17] For an reviews on the chemistry of cyclopropenones, see: (a) Potts, K. T.; Baum, J. S. *Chem. Rev.* **1974**, *74*, 189. (b) Komatsu, K.; Kitagawa, T. *Chem. Rev.* **2003**, *103*, 1371.
[18] West, R.; Chickos, J.; Osawa, E. *J. Am. Chem. Soc.* **1968**, *90*, 3885.

Table 9, continued

	Deltic Acid[19]
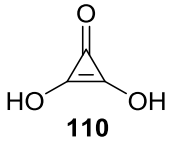 **110**	"When dissolved in ethanol-water at room temperature, partial decomposition occurs within hours" "Explosive decomposition has also occurred, more frequently on rapid heating at temperatures as low as 140 °C"
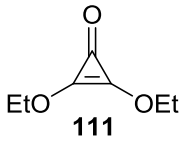 **111**	Diethoxycyclopropenone[20] "…briefly survives aqueous NaOH…"
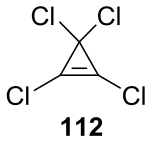 **112**	Tetrachlorocyclopropene[21] "Can be hydrolyzed at room temperature"
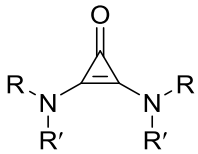 **113**	Bis(dialkylamino)cyclopropenones[22] Air stable solids

In order to synthesize these strained deltic ureas, different approaches were envisioned. While squaramides are prepared by reacting primary amines with methoxy squarates,[23] little is known about the reactivity of dialkoxycyclopropenones. The direct reaction of a *n*-butyl amine and

[19] (a) Eggerding, D.; West, R. *J. Am. Chem. Soc.* **1975**, 207. (b) Eggerding, D.; West, R. *J. Am. Chem. Soc.* **1976**, *98*, 3641. (c) Pericas, M. A.; Serratosa, F. *Tetrahedron Lett.* **1977**, *50*, 4437.
[20] Dehmlow, E. V. *Tetrahedron Lett.* **1972**, *13*, 1271.
[21] Tobey, S. W.; West, R. *Tetrahedron Lett.* **1963**, *18*, 1179.
[22] Yoshida, Z.; Konishi, H.; Tawara, Y.; Nishikawa, K.; Ogoshi, H. *Tetrahedron Lett.* **1973**, *14*, 2619.
[23] Storer, R. I. **2013**. Squaramide. e-EROS Encyclopedia of Reagents for Organic Synthesis.

diethoxycyclopropenone **111** failed to give the corresponding deltic urea.[24] Although dihydroxycyclopropenones are prepared by photolysis of bis(trimethylsilyl)squarate, direct photolysis of a squaramide also failed to deliver results (Scheme 10).

Using dichlorocyclopropenone **109** as the entry point presents its own risks, given the explosive nature of this reagent. Tetrachlorocyclopropene (TCCP) **112**, on the other hand, can easily be prepared in multigram quantities, and has been used to synthesize diaminocyclopropenones **113**. A direct reaction between primary amines and TCCP **112** failed to give either the corresponding deltic urea or the cyclopropeniminium species. This necessaited the use of a protecting group to form diaminocyclopropenone **113** via secondary amines, followed by subsequent deprotection. Note that the result related to the use of the 2,4-dimethoxybenzyl (DMB) protecting group was provided to us by the research group of Prof. Tristan H. Lambert.

Scheme 10: Different Entry-points Towards Deltic Ureas

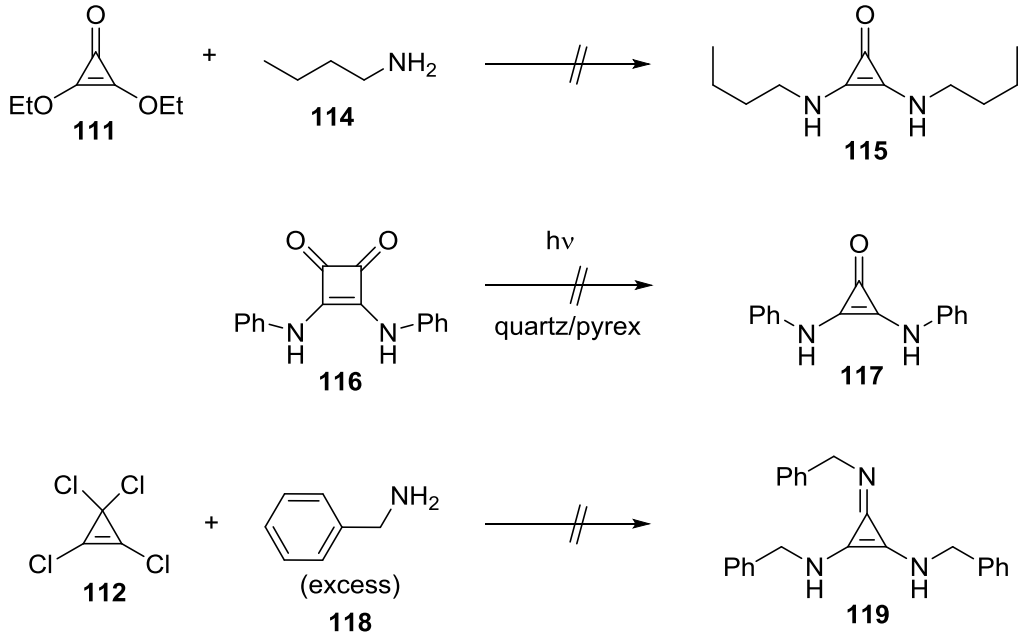

[24] Note that this is an unpublished result from our group (Dr. Ye Zhu).

In order to better understand the reactivity of the result provided to us by Prof. Lambert's group, we set out to optimize the given reaction. Best results were obtained with low concentrations of secondary amine and at temperatures above room temperature (Tables 10, 11 and 12).

Table 10: Optimization of Reaction Conditions with Respect to Concentration of Secondary Amine and Temperature

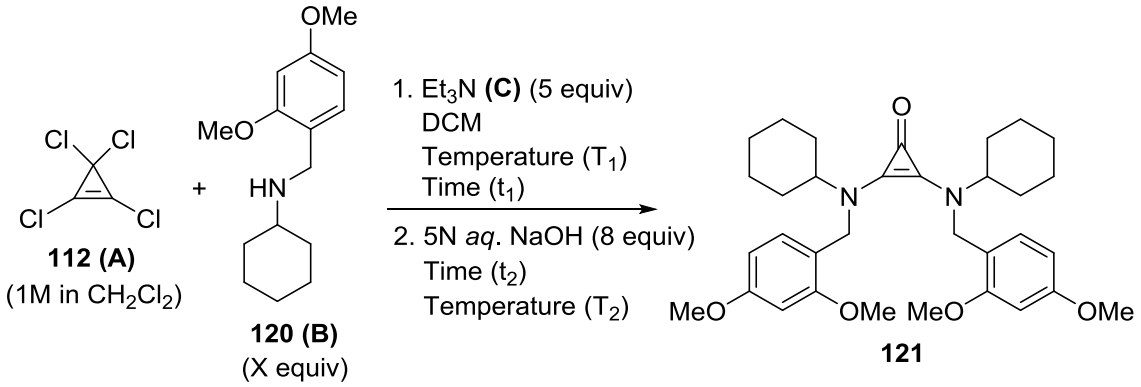

X	Concentration Of 2° Amine	T_1	t_1	T_2	t_2	Order of Addition	NMR Yield[a]
1.6	**0.2M**	0 °C	30min	0 °C – rt	90min	A-B-C	45
4.0	**0.5M**	0 °C	30min	0 °C – rt	90min	A-B-C	26
1.0	**0.2M**	0 °C	30min	0 °C – rt	90min	A-B-C	47
1.6	**2M**	0 °C	30min	0 °C – rt	90min	A-B-C	27
1.6	0.2M	0 °C	**2h**	0 °C – rt	90min	A-B-C	42
1.6	0.2M	**0 °C + rt**	**2h + 48h**	**rt**	90min	A-B-C	23
1.6	0.2M	0 °C	30min	0 °C – rt	**24h**	A-B-C	56
2.5	0.25M	0 °C	30min	0 °C – rt	**30min**	A-B-C	29
2.0	0.25M	0 °C	30min	0 °C – rt	90min	A-B-C	53
2.0	0.25M	**rt**	30min	**rt**	90min	A-B-C	61
2.0	0.25M	**reflux**	30min	**41 °C**	90min	A-B-C	66

[a]All reactions were carried out with 0.2 mmol of TCCP, and the yield was measured via ^{1}H NMR spectroscopy with 1,3,5-trimethoxybenzene as an internal standard. Order of addition 'A-B-C' implies that B was added to A, followed by the addition of C.

Table 11: Optimization of Reaction Conditions with Respect to Solvent and Base

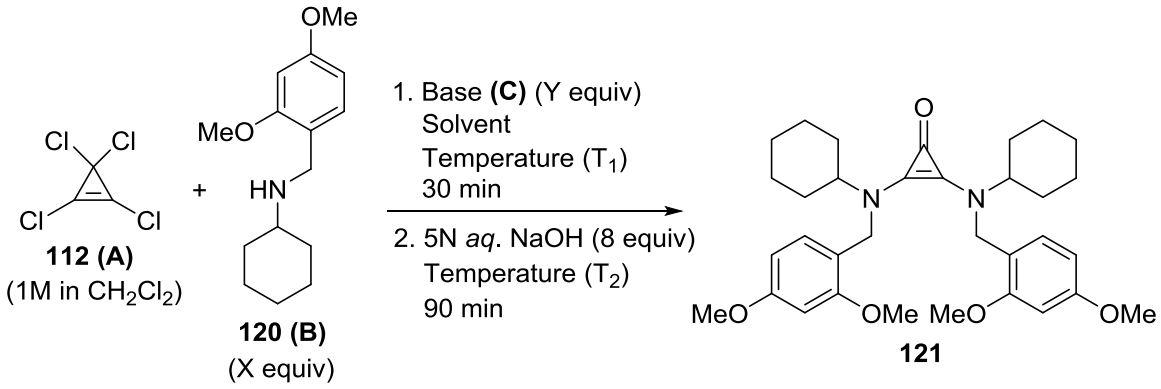

X	Conc. Of 2° Amine	Base C	Y	Solvent	T_1	T_2	Order of Addition	NMR Yield[a]
2.0	0.2M	**DIPEA**	5	DCM	rt	rt	A-B-C	22
2.0	0.2M	**Pyr**	5	DCM	rt	rt	A-B-C	0
2.0	0.2M	**DABCO**	5	DCM	rt	rt	C-B-A	4
2.0	0.2M	**DMAP**	5	DCM	rt	rt	C-B-A	0
2.0	0.2M	**KO*t*-Bu**	5	DCM	rt	rt	C-B-A	18
2.0	0.2M	**NaOH**	5	DCM	rt	rt	C-B-A	18
2.0	0.2M	**Na_2CO_3**	5	DCM	rt	rt	C-B-A	15
2.0	0.2M	**$NaHCO_3$**	5	DCM	rt	rt	C-B-A	0
2.0	0.2M	**No base**	-	DCM	rt	rt	**A-B**	32
2.0	0.25M	TEA	**1**	DCM	0 °C	0 °C – rt	A-B-C	57
2.0	0.25M	TEA	**25**	DCM	0 °C	0 °C – rt	A-B-C	26
2.0	0.2M	TEA	1	**DCE**	**reflux**	84 °C	A-B-C	67
2.0	0.2M	TEA	1	**Acetone**	rt	rt	A-B-C	62
2.0	0.2M	TEA	1	**MeCN**	rt	rt	A-B-C	39
2.0	0.2M	TEA	1	**THF**	rt	rt	A-B-C	44
2.2	0.2M	TEA	**2**	**Acetone**	**reflux**	reflux	A-B-C	20
2.2	0.2M	TEA	**2**	DCM	**reflux**	reflux	A-B-C	20

[a]All reactions were carried out with 0.2 mmol of TCCP, and the yield was measured via ^{1}H NMR spectroscopy with 1,3,5-trimethoxybenzene as an internal standard. Order of addition 'A-B-C' implies that B was added to A, followed by the addition of C.

Commonly used bases such as pyridine and DMAP proved to be too nucleophilic to afford any conversion to the product **121**.[25] This rules out the use of cinchona alkaloids towards the synthesis of chiral deltic ureas. The use of inorganic bases did not result in any improvement

[25] Both TCCP and diphenylcyclopropenone have been reported to react with pyridine to form indolizine derivatives: (a) Johlman, C. L; Ijames, C. F.; Wilkins, C. L.; Morton, T. H. *J. Org. Chem.* **1983**, *48*, 2629. (b) Lown, J. W.; Matsumoto, K. *Can. J. Chem.* **1971**, *49*, 1165.

over carrying out the reaction in the absence of a base, while DIPEA was not as effective as Et_3N. Also, acetone was as beneficial as CH_2Cl_2 towards this transformation (Table 11).

During the course of this study, we realized that the base Et_3N is not merely a spectator, but Et_3N itself quickly reacts with TCCP.[26] Thus, it was not surprising that a decrease in yield results upon the use of excess base, and the use of 1.6-2.0 equiv or base was found to be ideal (Table 12). The initial concentration of TCCP was found to have a modest effect on the yield, and the use of additives such as NaCl and NaI did not lead to any improvements.

Table 12: Optimizing Conditions Using the Lessons Learned with Previous Optimizations

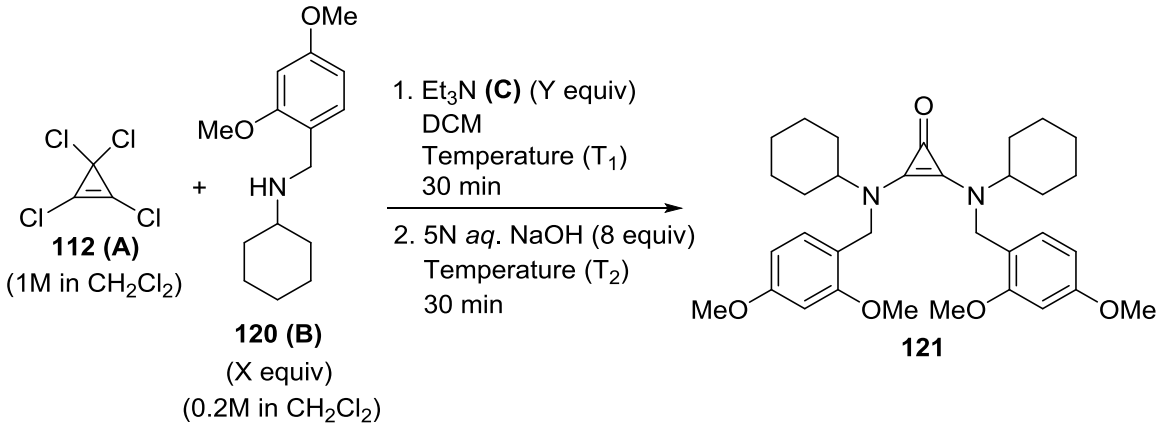

X	Conc. Of 2° Amine	Y	T1	T2	Order of Add.	NMR Yield[a]
1.6	0.2M	5	**0 °C**	0 °C - rt	A-B-C	69
2.2	0.2M	**2**	**rt**	rt	A-B-C	10
1.6	0.2M	5	**rt**	rt	A-B-C	90
1.6	0.2M	**2**	**reflux**	rt	A-B-C	**96**
1.6	0.2M	**2**	**rt**	rt	A-B-C	**98**

[a]All reactions were carried out under N_2 atmosphere in a test-tube using 0.2 equivalents of TCCP. NMR yields were measured using 1,3,5-trimethoxybenzene as an internal standard.

[26] See section II.7 for NMR experiments with triethylamine and TCCP.

Scheme 11: Gram-Scale Synthesis of a Dicyclohexyl Deltic Urea

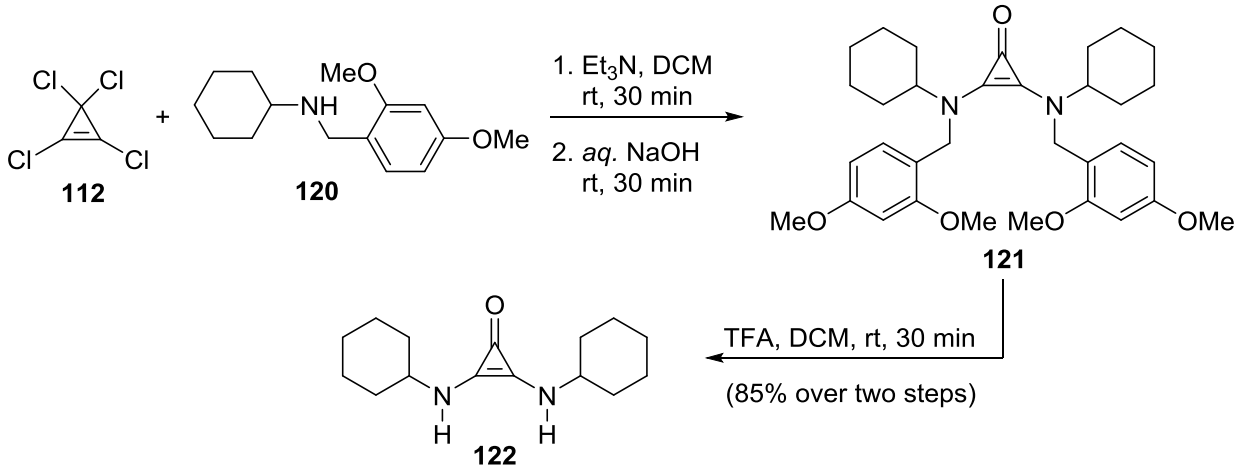

Shortly thereafter, we found that it was possible to carry out the reaction on gram-scale (Scheme 11). The high isolated yield for the first step (91%) rules out the formation of a cyclopropeniminium intermediate. Though this is a formal substitution reaction followed by hydrolysis, the remarkable efficiency of this reaction can be seen with the formation of the sterically crowded cyclopropenone **124** in fair yield (Table 13 and Scheme 12). Also, the deprotection of the 2,4-dimethoxybenzyl protecting group could be carried out using TFA.[27]

Table 13: Optimization of Reaction Conditions with a Sterically Crowded Secondary Amine

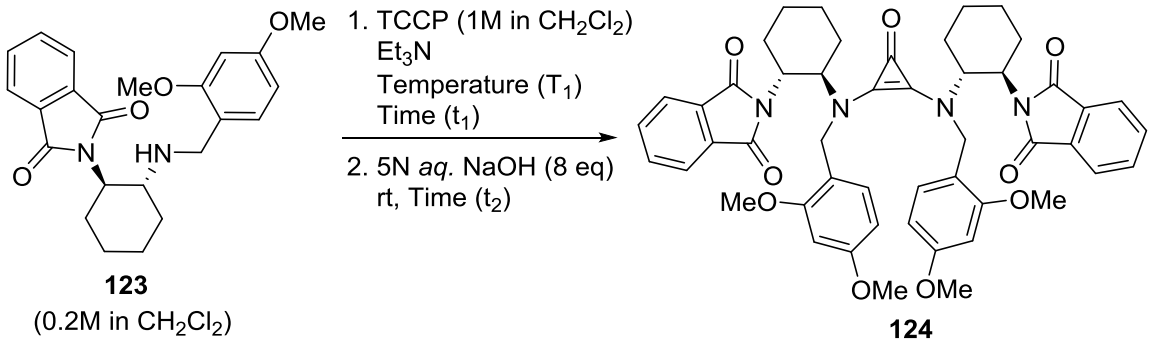

Equivalents of 2° Amine	Equivalents of Et_3N	T_1	t_1	t_2	Yield[a]
1.6	5	0 °C	30 min	30 min	9
1.6	2	rt	30 min	30 min	23

[27] Nussbaumer, P.; Baumann, K.; Dechat, T.; Harasek, M. *Tetrahedron* **1991**, *47*, 4591.

Table 13, continued

1.6	2	rt	4h	30 min	40
3.0	2	rt	30 min	30 min	21
1.6	2	rt	16h	30 min	42
1.6	2	rt	16h	4h	52[b]
1.6	2	reflux	16h	30 min	41
1.6	2	rt	48h	4h	50

[a]All reactions were carried out with 0.2 mmol of TCCP, and the yield was measured via ^{1}H NMR spectroscopy with 1,3,5-trimethoxybenzene as an internal standard. [b]These conditions were employed towards a large-scale reaction which led to the product in 45% isolated yield.

Scheme 12: Synthesis of a Chiral Deltic Urea

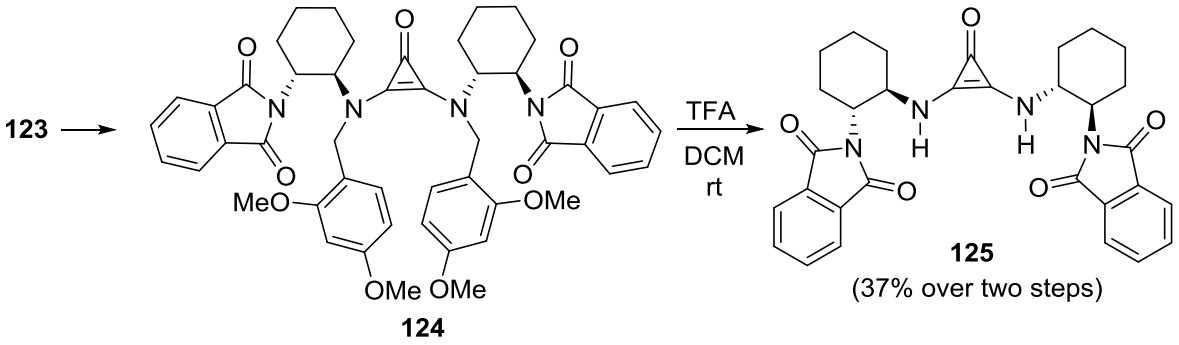

It was soon realized that the above reaction failed to provide diaryl deltic ureas. Prof. Lambert's group communicated to us that the use of stronger hydrolysis condition is required, however, the intermediate was not known and was presumed to be compound **128**. We found that the reaction of an aniline derivative with TCCP, in the presence of a base, instead leads to the formation of the corresponding cyclopropeniminium chloride species **127**.[28] As communicated by Prof. Lambert, hydrolysis of this compound under relatively vigorous conditions, followed by deprotection, afforded diphenyl deltic urea **130** (Scheme 13). While the exact mechanism is not known, presumably, the kinetics favor the expedient conversion of the disubstituted product to the trisubstituted product **127**.[29]

[28] Hertel, M.; Weiss, R. *J.C.S. Chem. Comm.* **1980**, 223.
[29] In a previous study, different results were obtained with different secondary amines: Yoshida, Z. -I.; Tawara, Y. *J. Am. Chem. Soc.* **1971**, *93*, 2573.

Scheme 13: Synthesis of Diaryl Deltic Ureas

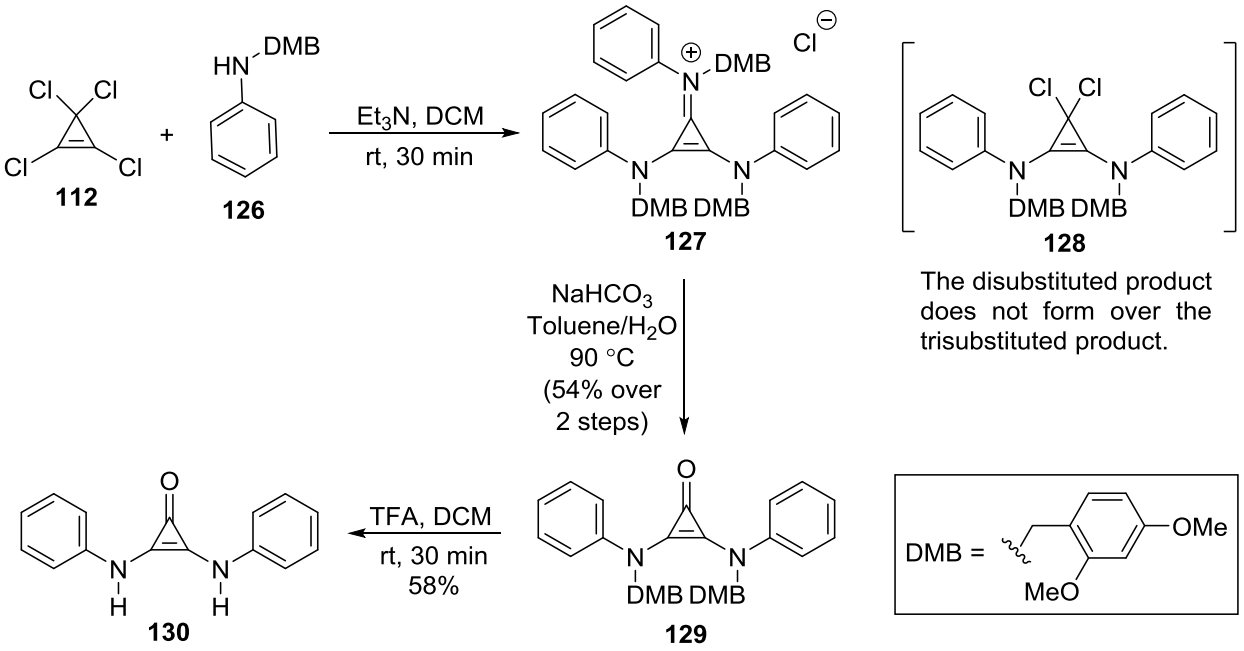

We also found that the use of an electron-withdrawing group (EWG) on the phenyl ring leads to lower yields (not shown). While EWGs decrease the nucleophilicity of the secondary amine, it possibly destabilizes the cyclopropenone core, as it has thrice the effect on the tri-substituted cyclopropeniminium compound. Also, TFA-catalyzed DMB deprotection is relatively difficult and proceeds in lower yields, as evident by the formation of the deltic guanidinium species **132** (Scheme 14).

Scheme 14: Deprotection to Form a Deltic Guanidinium Derivative with EWGs

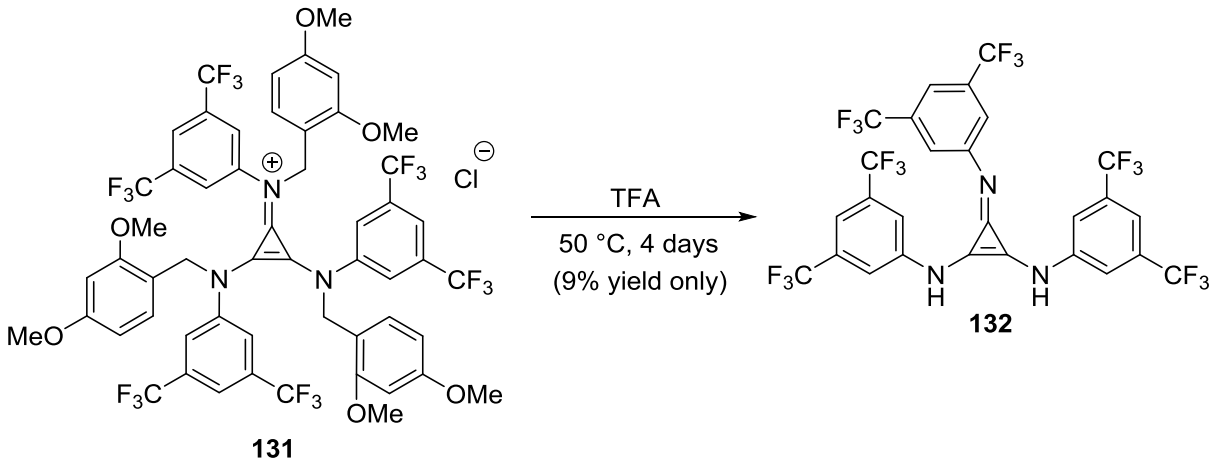

II.4 X-ray Crystal Structures of Dicyclohexyl and Diphenyl Deltic Ureas

While diphenyl deltic urea **130** is insoluble in all solvents except DMSO, dicyclohexyl deltic urea **122** has a much better solubility profile in common solvents such as chloroform, dichloromethane and ethyl acetate. This difference in solubilities motivated us to get a crystal structure for both compounds, and as could be expected, π- π stacking was responsible for the low solubility of **130** (Figures 11 and 12). We were also pleased to find that cyclohexyl deltic ureas **122** form strong H-bonds (2.26 Å) to the carbonyl group of another deltic urea in the crystal. While the calculated H-H distance for a dialkyl deltic urea in vacuum is 3.49 Å, the observed H-H distance was 3.22 Å. On the other hand, the H-H distance for the π-stacked compound **130** was found to be 3.6 Å. As **122** forms hydrogen-bonds to a carbonyl, one may conclude that deltic ureas may be employed as H-bond donors to a host of 'larger' electrophilic functional groups such as the nitro, thiocarbonyl, sulfoxide, dicarbonyls etc.

Figure 11: X-Ray Crystal Structure of Deltic Urea **122**

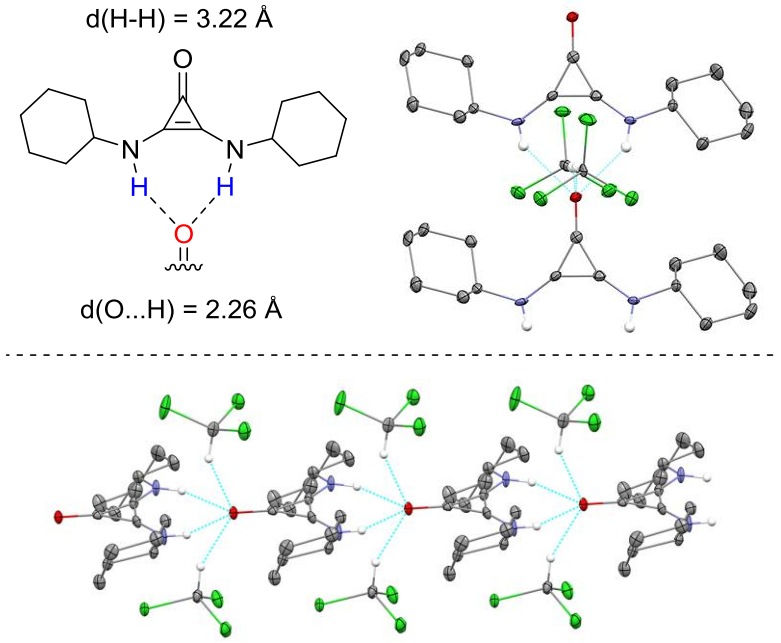

Figure 12: X-Ray Crystal Structure of Deltic Urea **130**

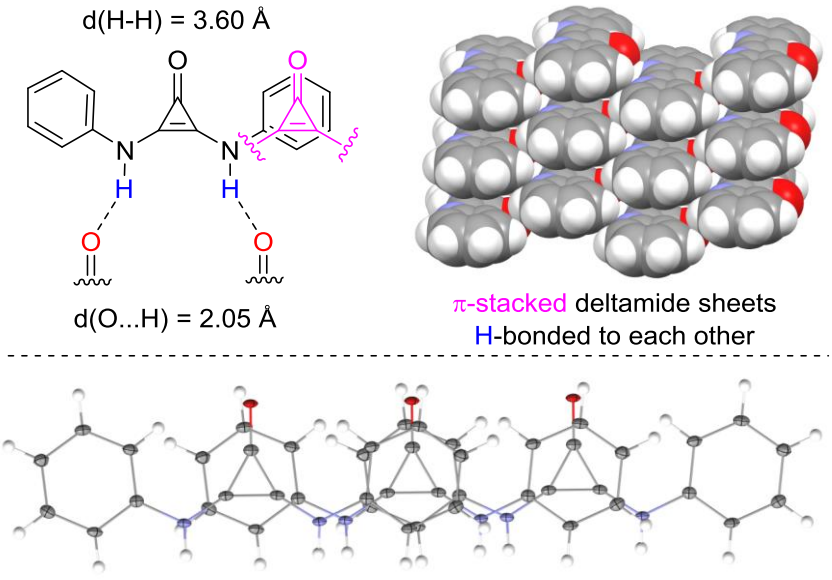

II.5 Cross-Substituted Deltic Ureas

Next, we turned our attention to cross substituted deltic ureas. We were pleased to find that the kinetic differences between alkyl and aryl amines could be exploited to synthesize deltic ureas such as **135**, albeit with lower yields (Table 14 and Scheme 15). To the best of our knowledge, this represents the only example of substitution reaction with TCCP to lead to cross-substituted cyclopropenone system.

Table 14: Optimization of Reaction Conditions Towards the Cross-Substitution Reaction

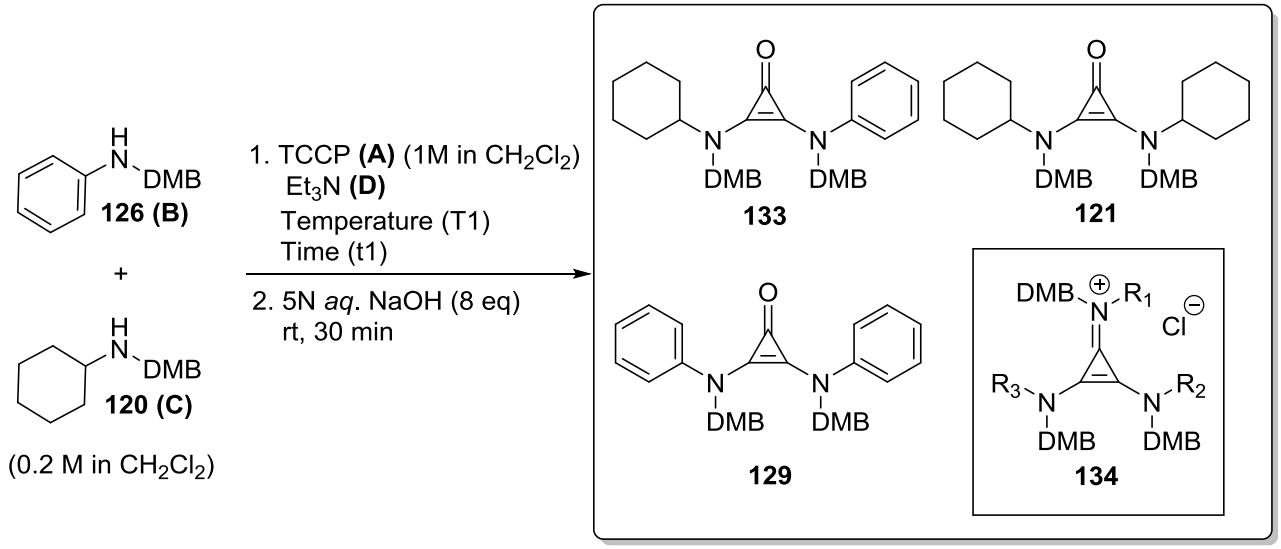

Equiv. of **126**	Conc. of **126**	Eq. of **120**	Eq.of **TEA**	T_1 (°C)	t_1 (min)	Order of Addition	**P1** : **P2 : P3**	Yield[a] (**133**)
0.8	0.2M	0.8	5	0	30	A-C-B-D	1.21 : 1.0 : 0.29	27%
0.5	0.2M	**0.5**	5	0	30	A-C-B-D	1.22 : 1.0 : 0.23	27%
0.8	0.2M	0.8	**2**	0	30	A-C-B-D	1.48 : 1.0 : 0.22	32%
0.8	0.2M	0.8	2	rt	30	A-C-B-D	1.44 : 1.0 : 0.12	31%
0.8	0.2M	0.8	2	0	**120**	A-C-B-D	1.47 : 1.0 : 0.16	32%
1.6	0.2M	0.8	2	0	30	A-C-B-D	**121**, **129** nd	14%
3.2	0.2M	0.8	2	0	30	A-C-B-D	--	~0%
1.6	**0.4M**	0.8	2	0	30	A-(C+B)-D	**121**, **129** nd	25%
3.2	**0.8M**	0.8	2	0	30	A-(C+B)-D	--	~0%

nd = not detected in significant quantities. [a]All reactions were carried out with 0.2 mmol of TCCP, and the yield was measured via NMR spectroscopy with 1,3,5-trimethoxybenzene as an internal standard. [b]See Scheme 15 below for isolated yields obtained on a reaction carried out on a large scale.

Scheme 15: First Examples of a Cross Substitution Reaction on a Cyclopropenone System

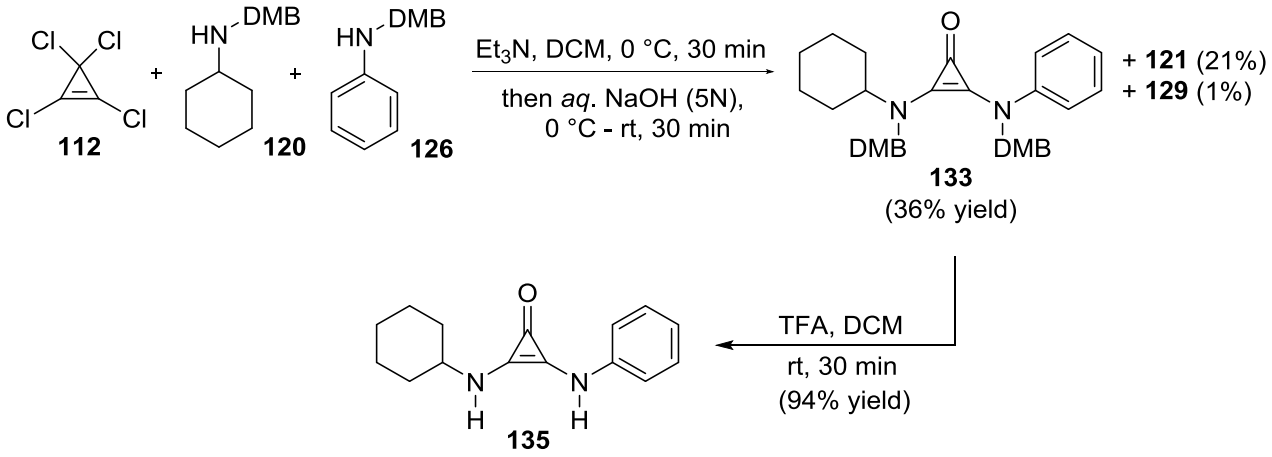

Reaction was carried out on gram-scale to afford 1.45 g of the product **133**. Surprisingly, the reaction yield was higher when carried out on a larger scale. Please see Experimental Section for further details.

Furthermore, sterically crowded amines can also be incorporated to form molecules such as **137** and **138** (Table 15 and Scheme 16). Notably, use of an excess Et_3N at 0 °C was required for optimum results. The precise mechanism of this cross-substitution reaction is not known, but we believe that Et_3N does not merely act as a base, but possibly reacts with TCCP or it's derivatives. Attempts to carry out the reaction at temperatures below -20 °C with extended reaction times failed to provide the cross-substitution product.

Table 15: Optimization of the Cross-Substitution Reaction Towards Compound **137**

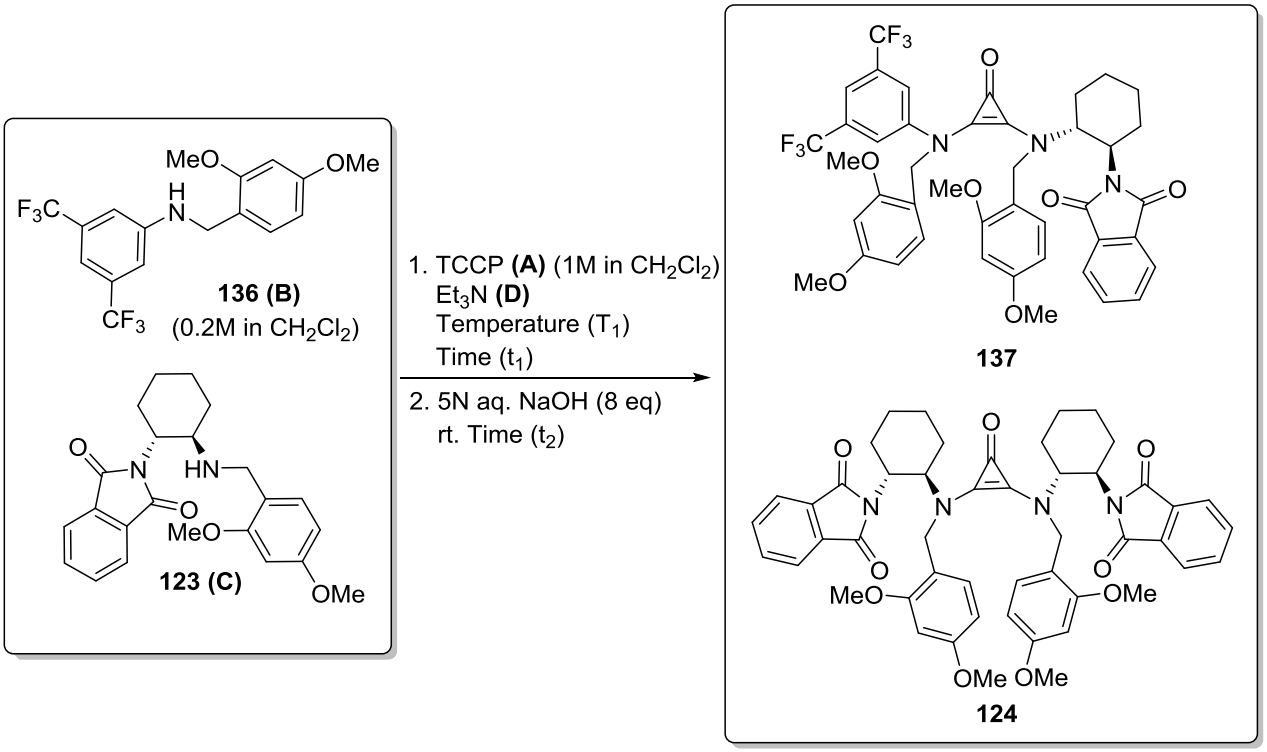

Eq. of **B** & **C**	Conc. of **C**	Eq. of **D**	T_1	t_1	t_2	Order of Addition	**137**:**124**[a]	Yield (**137**)[b]
0.8	0.2M	2	rt	30 min	30 min	A-B-C-D	1:1.5	8
0.8	0.2M	2	rt	30 min	30 min	A-C-B-D	1:1.5	11
0.8	0.2M	2	rt	30 min	30 min	A-(B+C)-D	1:1.5	8
0.8	0.2M	0	rt	30 min	30 min	A-C-B	0:1	0
0.8	0.2M	5	0 °C	30 min	30 min	A-C-B-D	4:1	21
0.8	0.13M	2	rt	30 min	30 min	A-C-B-15min-D	1:1.1	9
0.8	0.13M	5	rt	30 min	30 min	A-C-B-D	1:1.4	5
0.8	0.13M	25	0 °C	30 min	30 min	A-C-B-D	>10:1	13
0.8	0.13M	25	rt	30 min	30 min	A-C-B-D	1:1.3	6
0.8	0.2M	2	0 °C	30 min	30 min	A-C-B-D	1.9:1	12
0.5	0.2M	5	0 °C	30 min	30 min	A-C-B-D	5.5:1	22[c]
1.1	0.2M	5	0 °C	30 min	30 min	A-C-B-D	1:1.2	3
0.8	0.2M	5	0 °C	30 min	30 min	A-C-(B+D)	1.6:1	14
0.8	0.2M	5	0 °C	3 h	30 min	A-C-B-D	1:1.1	9

[a]Approximate ratio of the two compounds determined by ^{1}H NMR Spectroscopy. [b]All reactions were carried out with 0.2 mmol of TCCP, and the yield was measured via NMR spectroscopy with 1,3,5-trimethoxybenzene as an internal standard. [c]See Scheme 16 below for isolated yields obtained on a reaction carried out on a large scale.

Scheme 16: Synthesis of a Cross-Substituted Chiral Deltic Ureas

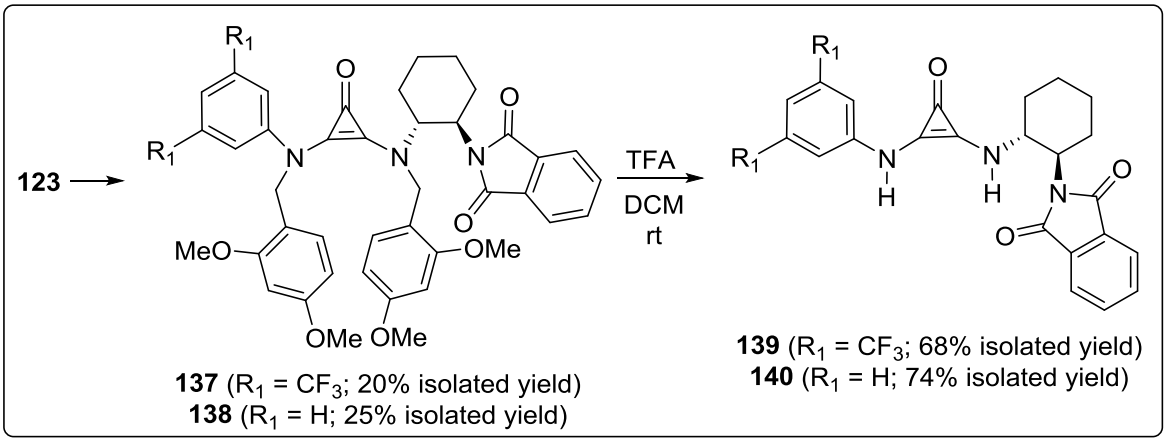

For R_1 = CF_3, TFA-mediated DMB-deprotection fails to deliver product **139** in the presence of small quantities (~0.01-0.1 equiv) of Et_3N (TEA).

II.6 An Ideal Scaffold Towards the First Bifunctional Deltic Urea

The molecule **139** closely resembles the framework of some of the widely successful chiral bifunctional thioureas and squaramides,[30] except the presence of a tertiary amine instead of a phthalimide group (Scheme 17). We hypothesized that the presence of EWG groups leads compound **139** to be relatively unstable, and leads to the slow decomposition in solution (chloroform/methanol) over 2-3 days. Thus, we wished to synthesize **152** as a tertiary amine would essentially give us a bifunctional catalyst, but also as it would serve as proof-of-concept with respect to the EWG nature of the bis(trifluoromethyl)aniline substituent.

[30] (a) Yang, K. S.; Nibbs, A. E.; Turkmen, Y. E.; Rawal, V. H. *J. Am. Chem. Soc.* **2013**, *135*, 16050. (b) Zhang, X.-J.; Liu, S.-P.; Lao, J.; Du, G.; Yan, M.; Chan, A. S. C. *Tetrahedron:Asymmetry* **2009**, *20*, 1451. (c) Mukherjee, S.; Muller, T. N.; Cleemann, F.; Roland, K.; Brandenburg, M.; Neudorfl, J.; Berkessel, A. *Org. Biomol. Chem.* **2006**, *4*, 4319.

Scheme 17: A Widely Successful Chiral Scaffold

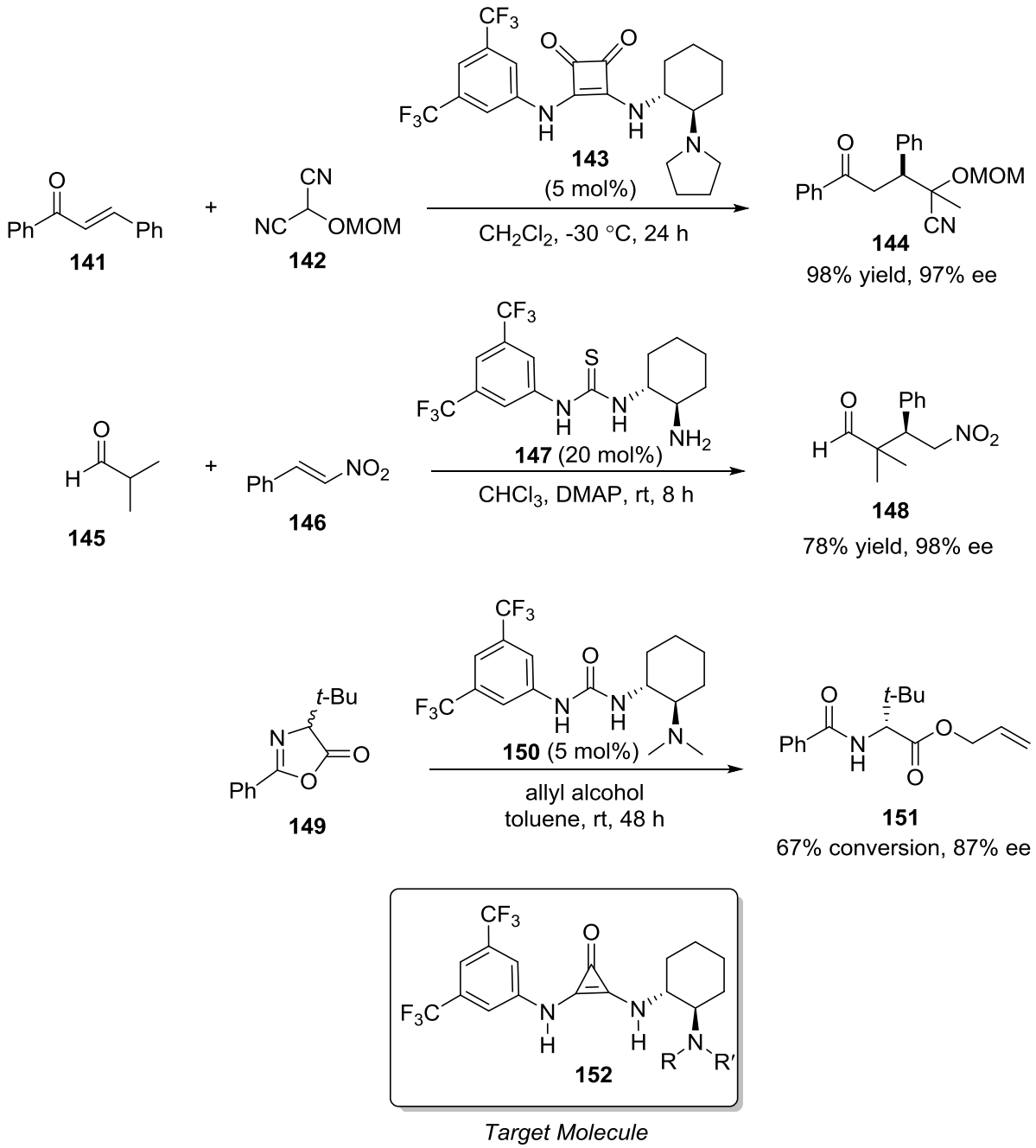

Towards this scaffold, we repeated our standard reaction reaction with amine **153**, but could not isolate the product (Scheme 18). NMR experiments revealed that triethylamine reacts with TCCP

112,[31] and thus the presence of a tertiary amine along with a secondary amine in **153** likely leads to the formation of various undesirable by-products, hindering isolation (See Supporting Information for details regarding NMR experiments).

Scheme 18: Towards the Bifunctional Catalyst 152

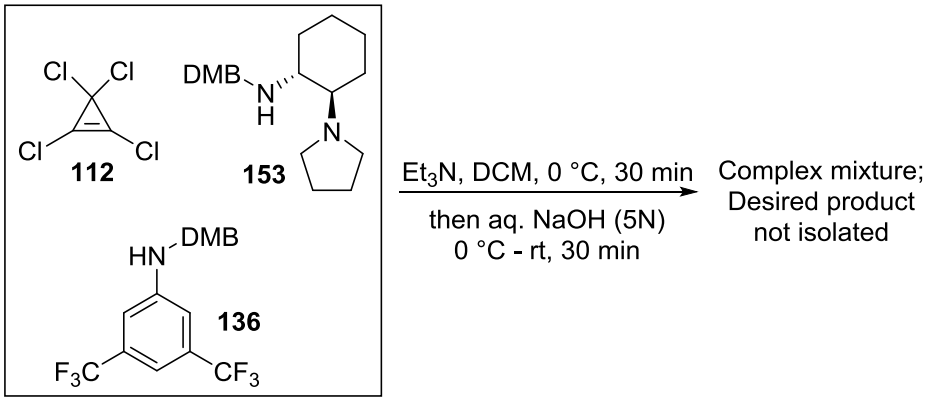

II.7 NMR Experiments with TCCP

II.7.1 TCCP + TEA

Conditions: 0.3 mmol NEt_3 + 0.3 mL CD_2Cl_2 + (0.3 mmol TCCP)

Observation: Within the first 10 minutes, the only quartet of Et_3N in CD_2Cl_2 ($\delta = 2.46$) splits into 5 different downfield quartets and one multiplet upon the addition of tetrachlorocyclopropene (TCCP, 1 equiv). The triplet of Et_3N ($\delta = 0.97$) similarly also splits into multiple downfield triplets and a multiplet. After 3 hours, many new signals appear in the spectrum.

Conclusion: This indicates that Et_3N does not just absorb the acid formed during the course of the reaction but itself reacts with TCCP. Only three peaks would be expected if only the mono-, di- and tri- addition products formed, the other peaks might correspond to absorption of H^+ and ring-opening reactions. This may explain the complications arising from the presence of a secondary amine and a tertiary amine on the same molecule:

[31] See Section II.7 for NMR Experiments with Et_3N and TCCP.

II.7.2 TCCP + 2° amine + TEA

Conditions: 0.3 mmol *i*Pr_2NH + 0.3 mL CD_2Cl_2 + (0.3 mmol TCCP) + (1.5 mmol NEt_3)

Observation: Within the first 10 minutes, the only septet of diisopropylamine in CD_2Cl_2 (δ = 2.86) splits into 3 different downfield multiplets upon the addition of TCCP. The only doublet (δ = 0.98) splits into 2 downfield doublets upon the addition of TCCP (1 equiv). Also, one broad singlet (δ = 9.45) appears. Surprisingly, these peaks do not change when the NMR is taken after 3 hours. Thus, the reaction that occurs is complete in the first few minutes at room temperature. Upon the addition of 1 equivalent of Et_3N, multiple peaks appear and the original multiplets shift a bit upfield. The singlet shifts from δ = 9.45 to δ = 9.64, while a new singlet at δ = 11.7 appears.

Conclusion: Secondary amines are quick to react with TCCP, but addition of Et_3N can possibly displace the original product and multiple products are likely to be in equilibrium.

II.7.3 TCCP + Electron-deficient Amine

Conditions: 0.3 mmol 'compound **136** + 0.3 mL CD_2Cl_2 + (0.3 mmol TCCP)

Observation: Within the first 15 minutes, the singlet corresponding to the NH proton in amine **136** merely broadens upon the addition of TCCP (1 equiv). No significant change in the spectra is seen when the NMR is taken again after 1 hour. However, when I wait for 64 hours, the benzyl peak (δ = 4.32) has split into multiple downfield singlets. Also, similar to the case for diisopropylamine, broad singlets appear at δ = 9.98 and δ = 13.2.

Conclusions: Amine **136** does react slowly as expected, but eventually may form a similar product as formed upon the addition of diisopropylamine. Broadening of the N-H peak suggests partial bond formation between N/H and TCCP. Also, as Et_3N reacts with TCCP much faster, its addition does not speed up the formation of the corresponding deltamide pre-cursor. But also

hints at why amine **136** can in-turn be captured by a mono-aliphatic-amine-DMB-substituted-TCCP.

II.8 Towards the First Bifunctional Deltic Urea

Scheme 19: Towards the Bifunctional Catalyst **152** II

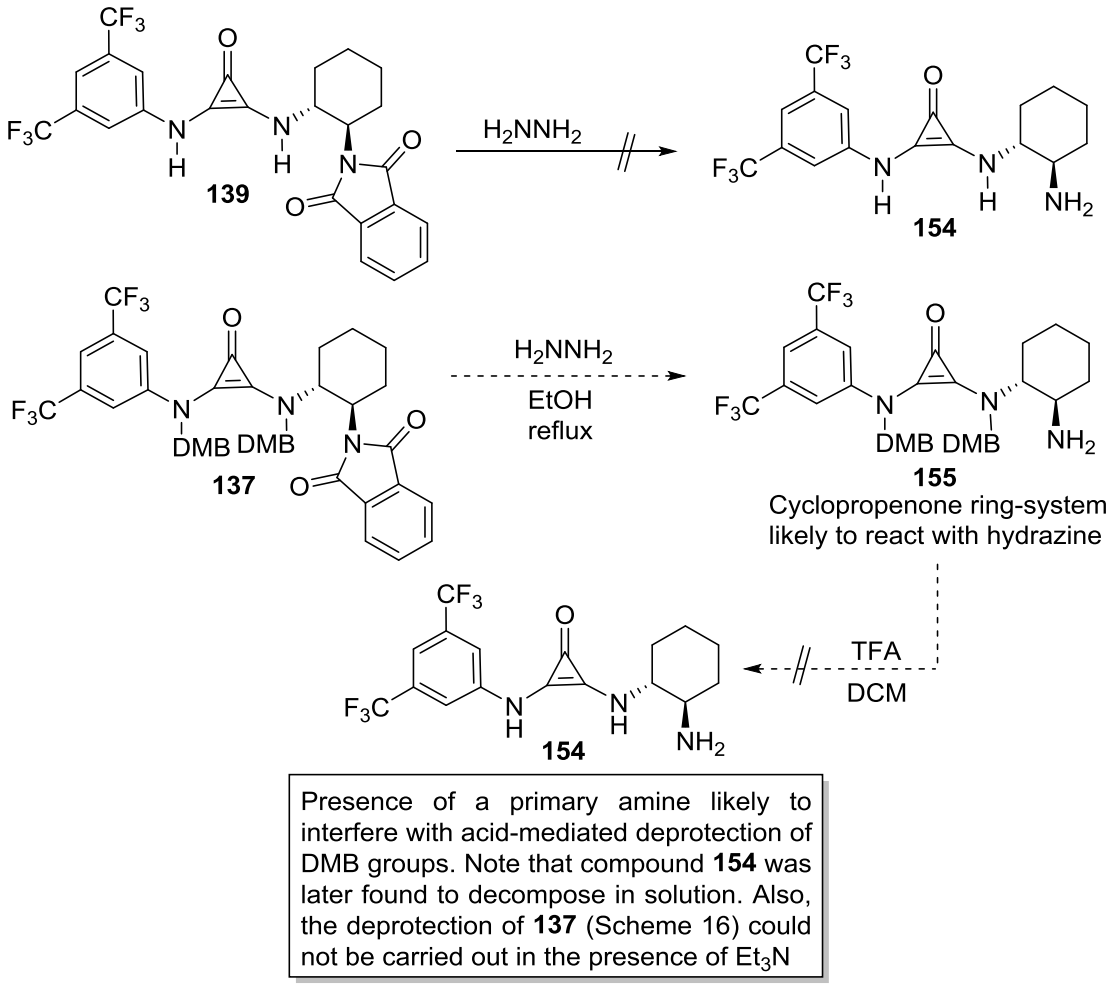

The phthalimide deprotection of **139** with hydrazine failed to give the corresponding amine under a variety of conditions. This was not surprising, given that tosylhydrazine reacts with cyclopropenones under similar conditions to form the corresponding tosylhydrazone.[32]

[32] Jones, W. M.; Stowe, M. E.; Wells Jr., E. E.; Lester, E. W. *J. Am. Chem. Soc.* **1968**, *90*, 1849.

Also, hydroxylamine reacts with *n*-pentyl cyclopropenone to form the corresponding *n*-pentylmethyl glyoxime via a ring-opening reaction.[33]

Scheme 20: Synthesis of Target **159** and a Ring-Opening Side-Reaction

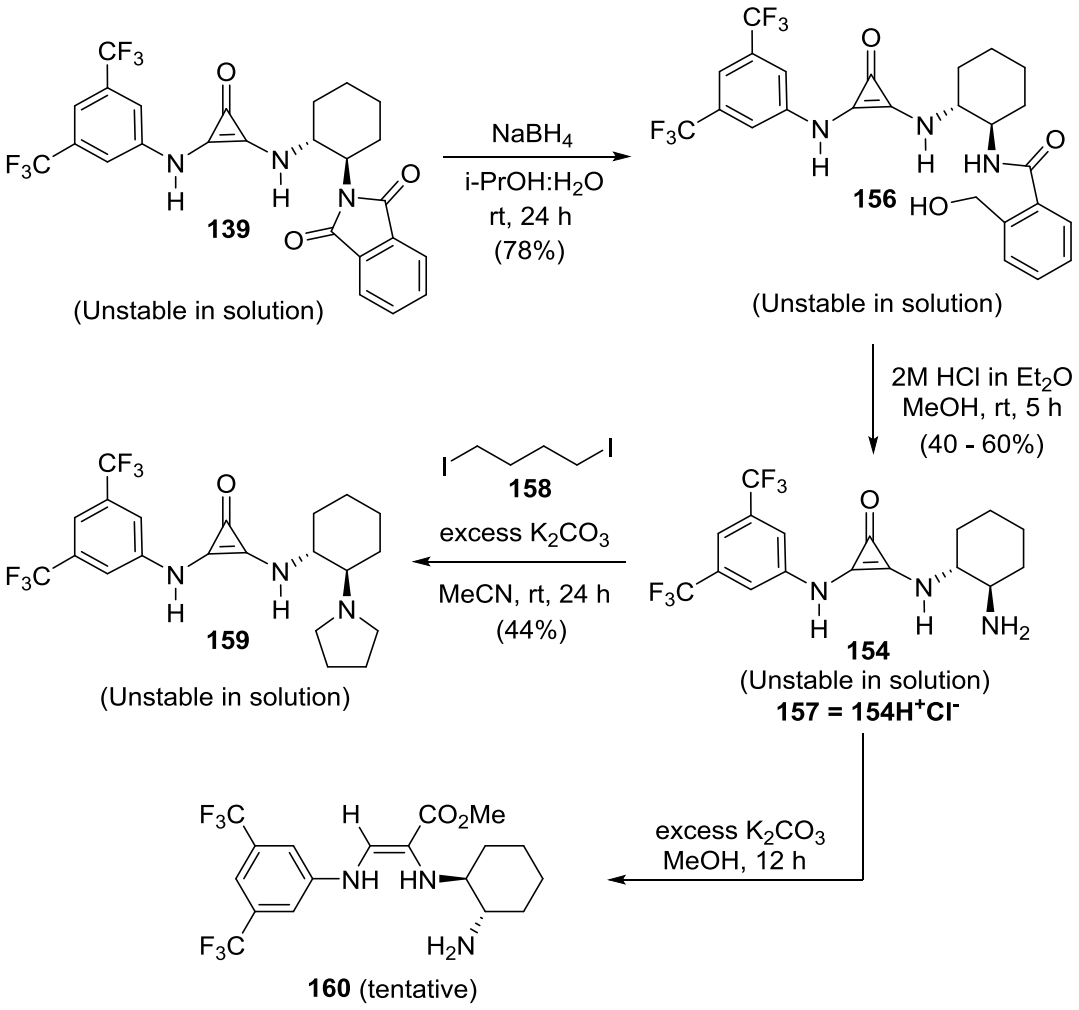

Fortunately, the deprotection could be carried out under milder conditions, with the use of sodium borohydride reduction,[34] followed by treatment with HCl (Scheme 20). Using acetic acid

[33] McCorkindale, N. J.; Raphael, R. A.; Scott, W. T.; Zwanenburg, B. *Chem. Commun.* **1966**, 133.

[34] This reaction surprisingly proceeds under good yields, given that ethyl phenyl cyclopropenone reacts with $NaBH_4$ to result in the corresponding ring-opening products: Dehmlow, E. V. *Justus Liebigs Ann. Chem.* **1969**, *729*, 64.

instead of HCl led to deprotection, but afforded the corresponding acetate salt instead.[35] Then, the tertiary amine could be synthesized with 1,4-diiodobutane in the presence of potassium carbonate.

It should be noted, however, that compounds **139, 154, 156, 159** decompose (over 1-4 days) in certain solvents such as methanol/chloroform, but are stable as a solid. This is evident with the ring-opening of **154** in the presence of a base in methanol (Scheme 20).[36,37] Nonetheless, as this represents our "how far you can push it" approach with the bis(trifluoromethyl)aniline substituent, the use of ring systems with less EWG groups than the bis(trifluoromethyl)aniline would likely lead to catalysts and intermediates that are stable in solution for extended times.

[35] Osby, J. O.; Martin, M. G.; Ganem, B. *Tetrahedron Lett.* **1984**, *25*, 2093.
[36] Similar ring-opening reaction of a *N*,*N*'-disubstituted deltamide has been reported: Yoshida, Z.; Konishi, H.; Tawara, Y.; Nishikawa, K.; Ogoshi, H. *Tetrahedron Lett.* **1973**, *28*, 2619.
[37] This was concluded based on preliminary ^{1}H NMR and MS $(M+H)^{+}$ data, and the corresponding product could be obtained consistently over two trials. Note that the alkene isomer shown in Table 20 is tentative.

Scheme 21: The Synthesis of Compound **159**: Taking a Step Back

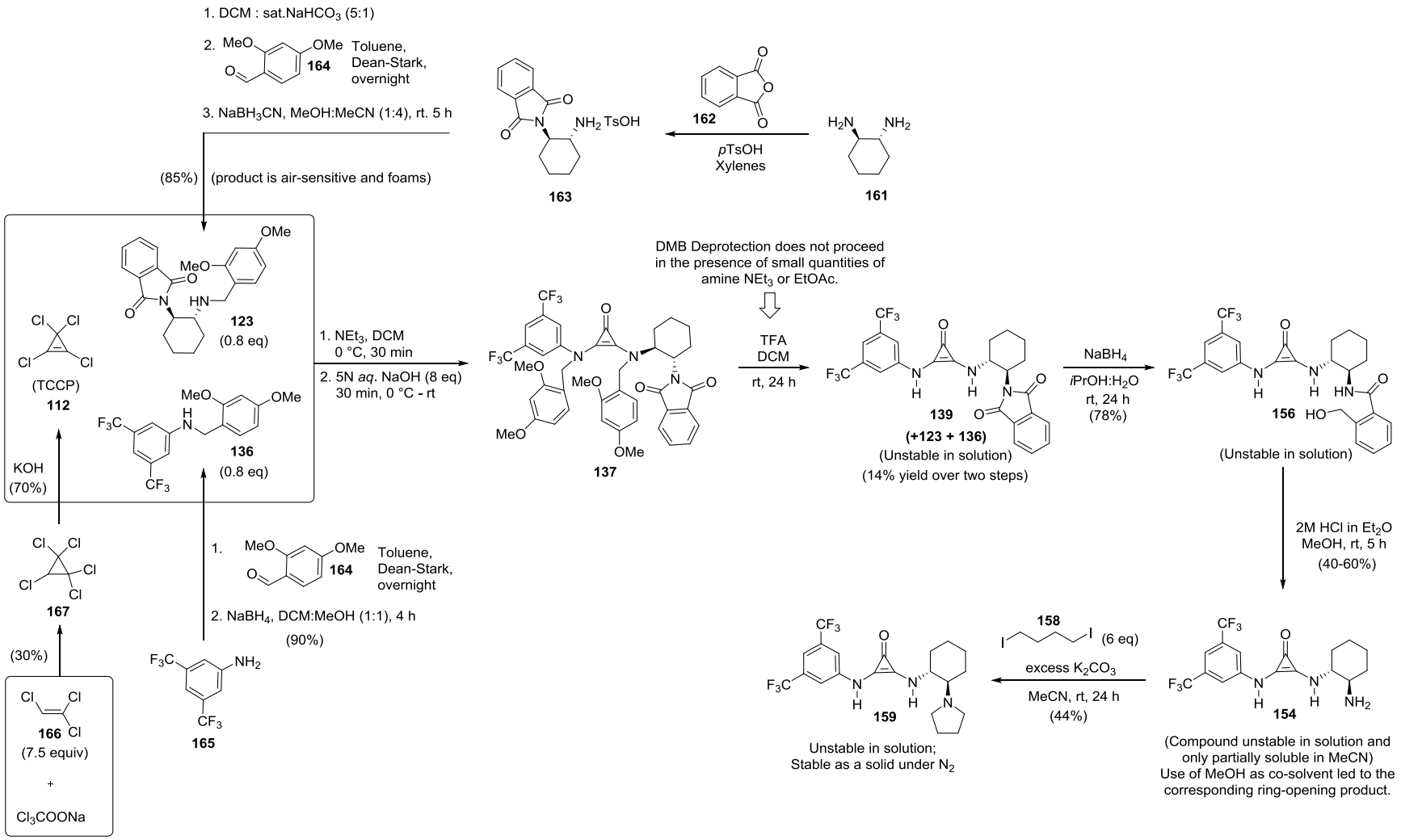

II.9 A Shorter Route Towards Potentially Accessing Compound 159

While direct installation of a tertiary amine onto a deltic urea proved to be messy (Scheme 18), deltic urea with a secondary amine could be formed (Scheme 22). It was found to decompose in solution. This was surprising as DMB protected derivatives were thought to be very stable, and the instability only arose after DMB-deprotection. It could not be purified completely and when the compound with one impurity present was subjected to TFA/DCM, deprotection does not occur, and the product decomposes. Nonetheless, one can hope that an alternate mild deprotection strategy might afford a bifunctional deltic urea in a shorter sequence.

Scheme 22: A Potential Shorter Route Towards Accessing Bifunctional Deltic Ureas

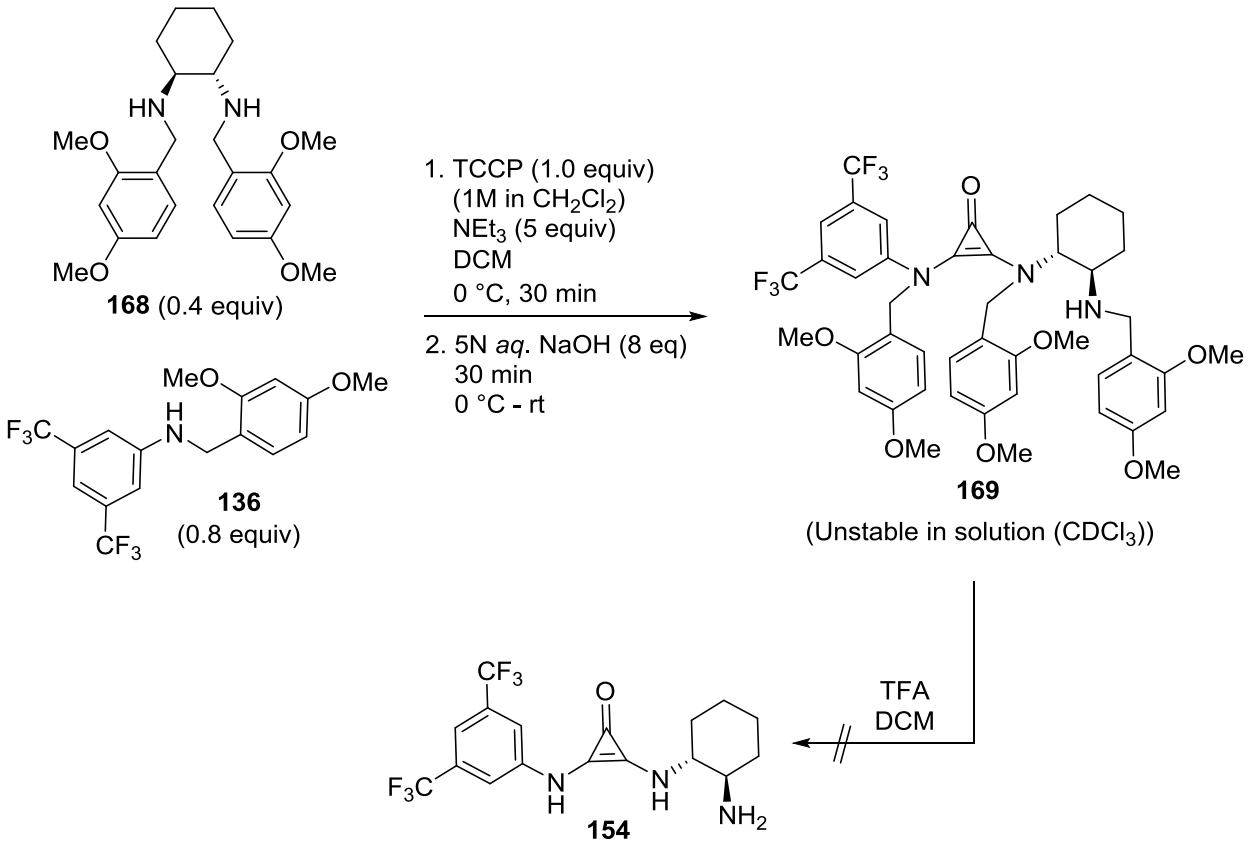

II.10 A C_2 Symmetric Bifunctional Deltic Urea

Scheme 23: Direct reduction with Borane-dimethylsulfide complex

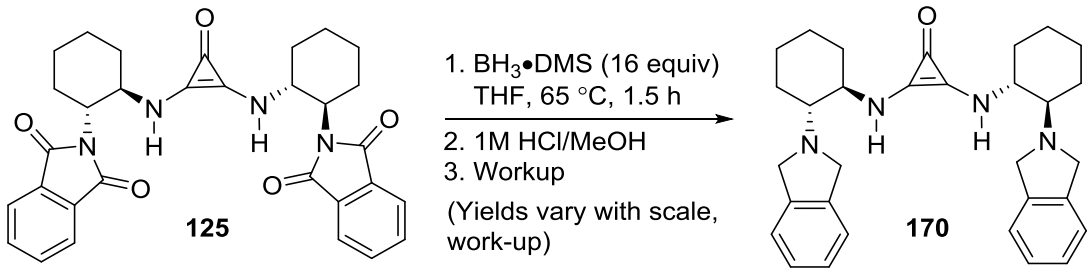

Our next step was to synthesize a bifunctional deltic urea that is stable in solution. Thankfully, the phthalimide groups on the C_2-symmetric molecule can be reduced with borane-dimethyl sulfide complex. While these relatively harsh conditions could not be applied to **139**, the dialkyl deltic ureas **125** did not quickly decompose under such conditions. We optimized the reduction conditions for this substrate as higher reaction times or stronger reducing agents[38] lead to decomposition. Borane reduction, however leads to the formation of an unknown borane adduct, which then leads to **170** after treatment with 1M HCl in methanol followed by acid-base extraction. When starting with less than 40 mg of the starting material **125**, the reaction could be applied successfully, however, the product was found to be unstable in solution, and decomposed over a period of 2-3 days. Based on our previous hypothesis, we had assumed that this compound would be stable because it lacks electron-withdrawing groups. We re-examined the stability of dicyclohexyl deltic urea and diphenyl deltic urea, and found them to be perfectly stable in solution ($CDCl_3$) up to 3 days. This led us revisit our hypothesis, and we now believe that both

[38] For reports on the reduction of a phthalimide to isoindolines, see: (a) Das, S.; Addis, D.; Knopke, L. R.; Bentrup, U.; Junge, K.; Bruckner, A.; Beller, M. *Angew. Chem. Int. Ed.* **2011**, *50*, 9180. (b) Huang, K.; Marciales-Oritz, M.; Correa, W.; Pomales, E.; Lopez, X. Y. *J. Org. Chem.* **2009**, *74*, 4195. (c) Gali, H.; Prabhu, K. R.; Karra, S. R.; Katti, K. V. *J. Org. Chem.* **2000**, *65*, 676.

EWG groups and an intramolecular tertiary amine can lead to a decrease in the stability of deltic ureas.

II.11 A ^{1}H NMR Comparison Between Similar Catalysts

Table 16: Acidity of Deltic Acid, Squaric Acid and Croconic Acid[a]

Compound	pK_1	pK_2
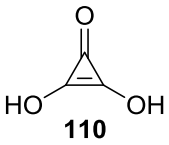 **110**	2.57	6.03
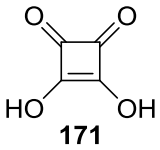 **171**	0.54	3.48
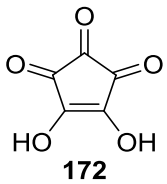 **172**	0.80	2.24

[a]This table was reproduced from reference 40.

In the past, various studies have linked organocatalyst acidity to it's catalytic activity.[39] Given the similarities between deltic acid **110** and deltic urea **159** (Section II.12), we wondered if the deltic ureas would be particularly acidic. While we expected the aromatic nature of the cyclopropenone ring system to positively influence acidity, literature suggested otherwise (Table 16).[40] In order to better understand the acidity of our bifunctional deltic urea, we carried out a direct comparison

[39] Increased acidity of a catalyst has been found to correlate with increased activity and capability. See, inter alia, (a) Wittkopp, A.; Schreiner, P.R. *Chem. Eur. J.* **2003**, *9*, 407. (b) Jensen, K. H.; Sigman, M. S. *Angew. Chem. Int. Ed.* **2007**, *46*, 4748. (c) Jensen, K. H.; Sigman, M. S. *J. Org. Chem.* **2010**, *75*, 7194. (d) Parmar, D.; Sugiono, E.; Raja, S.; Rueping, M. *Chem. Rev.* **2014**, *114*, 9047.

[40] Eggerding, D.; West, R. *J. Am. Chem. Soc.* **1976**, *98*, 3641.

between the ^{1}H NMRs of similar compounds (Table 17). Note that an ideal comparison can only be made if the ^{1}H NMR spectra were recorded in the same solvent, however, other entries have been included for reference. If a linear correlation between ^{1}H NMR peaks and acidity were valid, one can conclude that deltic ureas are less acidic than thioureas and squaramides, but comparable in acidity to ureas. Please see Chapter 4 for measurements of deltic urea pK_a using Bordwell's method of overlapping indicators.

Table 17: A ^{1}H NMR Comparison of Analogous Compounds with Different Functional Groups[41]

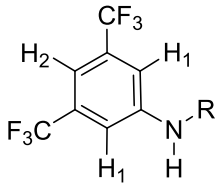

Entry	Compound	Solvent	Peak 1 (2H)	Peak 2 (1H)
1	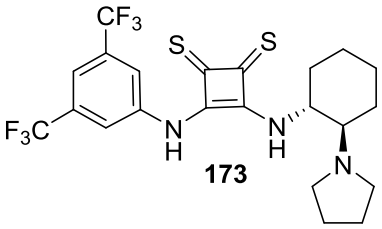 **173**	CD_3OD	8.33	7.75
2	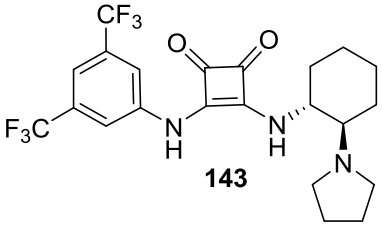 **143**	DMSO-d6	8.06	7.66

[41] For the source of ^{1}H NMR data, see: (a) Yang, K. S.; Nibbs, A. E.; Turkmen, Y. E.; Rawal, V. H. *J. Am. Chem. Soc.* **2013**, *135*, 16050. (b) Zhang, X.-J.; Liu, S.-P.; Lao, J.; Du, G.; Yan, M.; Chan, A. S. C. *Tetrahedron:Asymmetry* **2009**, *20*, 1451. (c) Mukherjee, S.; Muller, T. N.; Cleemann, F.; Roland, K.; Brandenburg, M.; Neudorfl, J.; Berkessel, A. *Org. Biomol. Chem.* **2006**, *4*, 4319. (d) For thiosquaramide, please see the Experimental Section for Chapter 3.

Table 7, continued

3	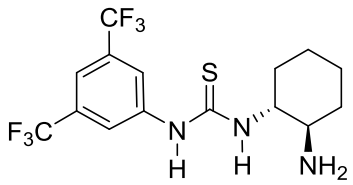 **147**	CD_3OD	8.11	7.52
4	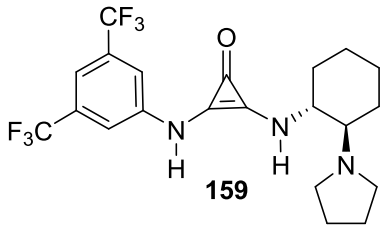 **159**	CD_3OD	7.79	7.51
5	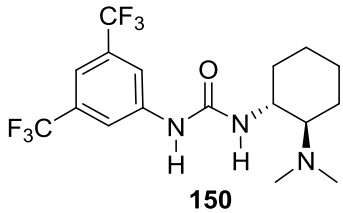 **150**	$CDCl_3$	7.80	7.36

II.12 Comments on the Relative Instability of the Cross-Substituted Bifunctional Deltic Urea

As we carried out the final few steps towards compound **159**, we found multiple similarities between bifunctional deltic ureas **159** and deltic acid **110**. Just as with deltic acid, bifunctional deltic urea intermediates are also insoluble in nonhydroxylic solvents (chloroform:methanol being the exception). Hence, all earlier attempts to carry out the final step with methanol as the co-solvent led to slow decomposition, and concomitant loss in yield. As with the acidity of deltic acid, the table above indicates that the peaks of

bis(trifluoromethyl)aniline portion are upfield, just as deltic acid has been described as an 'unexpectedly' weak acid. Also, as with deltic acid, a ring-opening reaction takes place in methanol to afford vinylogous ester **160**. Similarly, at each step, from **139** to **159** (Scheme 20), some loss in yield may be attributed to ring-opening reactions. As with deltic acid, these compounds are stable as a solid at room temperature.

II.13 A Direct Synthesis of Thiodeltic Ureas

In the past, an increase in acidity has corroborated with better catalyst performance, as shown by the proliferation of thiourea and squaramide based catalysts. To this end, thiodeltic ureas are an attractive class of potential H-bond donor scaffolds. However, the increased polarization of the C-S bond potentially makes the cyclopropenone core more vulnerable to ring-opening reactions. Collaborative reports from Prof. Lambert's group communicated to us that simple dialkyl thiodeltic ureas could be prepared by the use of Na_2S instead of NaOH during workup. We found that dialkyl thiodeltic ureas can also be prepared by thionylation of dialkyl deltic ureas using Lawesson's reagent (Scheme 24).

Scheme 24: Synthesis of Thiodeltic Ureas

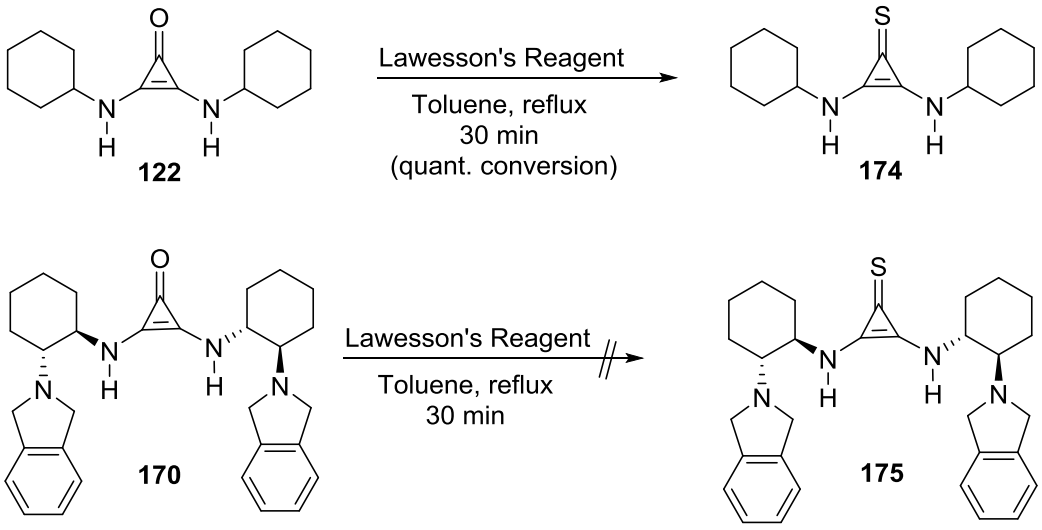

II.14 Synthesis of Simple Deltic Compounds

Parallel efforts by us and Prof. Lambert's group[42] simultaneously led to the synthesis of unsubstituted deltic urea (Scheme 25).

Scheme 25: Synthesis of Deltic Urea

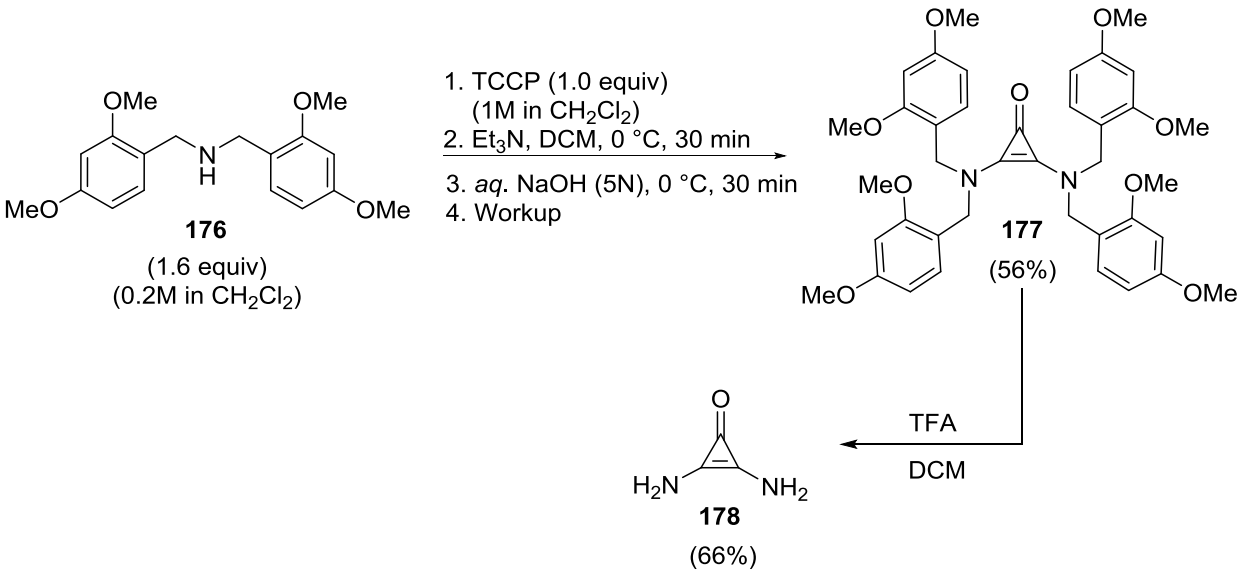

II.15 Evaluation of Bifunctional Deltic Ureas as Asymmetric Organocatalysts

As the preparation of deltic urea **159** involved a number of steps to form the relatively unstable product, a limited number of reactions were carried out using this catalyst. While a select number of reactions are being reported in Schemes 26 and 27, we were happy to find that deltic urea **170** can catalyze the addition reaction of *N*,*N'*-diphenylbarbituric acid **181** and β-nitrostyrene **146** in quantitative yield and 45% ee.[43]

[42] Mishiro, K.; Hu, F.; Paley, D. W.; Min, W.; Lambert, T. H. *Eur. J. Chem.* **2016**, 1655.

[43] Note that the conjugate addition products have long retention times and broad peaks when examined by chiral HPLC, presumably a result of its high acidity and the presence of significant enol content. The ee was measured by chlorinating the product at the 5-position with NCS/DCM. Please see chapter 3 for a representative procedure.

Scheme 26: Initial Results for Addition to β-nitrostyrene[a]

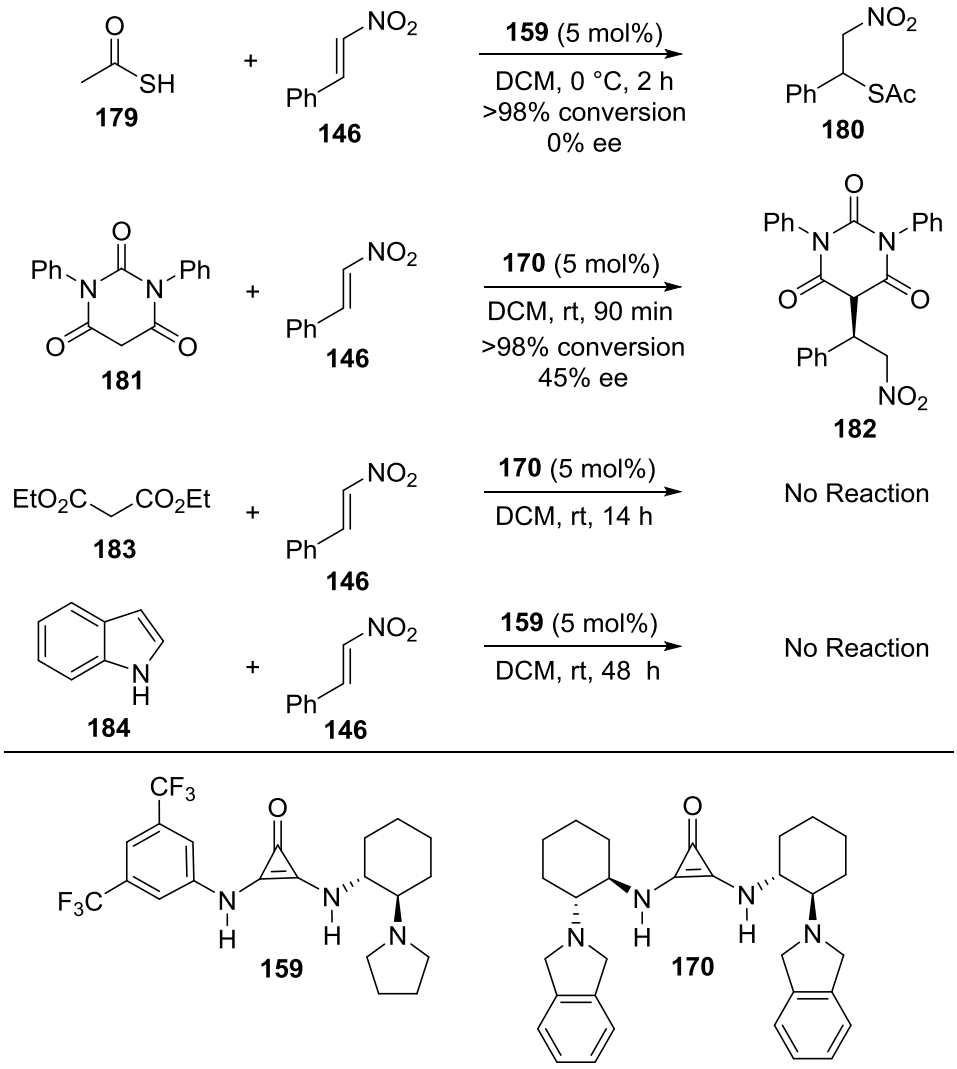

[a]While reactions 1,3 and 4 were carried out according to reported literature protocols, please see the experimental section of chapter 3 for more information regarding reaction 2, i.e. the Michael addition of barbituric acid to β-nitrostyrene

Further efforts towards the synthesis of similar bifunctional catalysts, and towards identifying judicious applications of bifunctional deltic ureas as asymmetric organocatalysts are warranted.

Scheme 27: Initial Results for Addition to Cyclohexenone

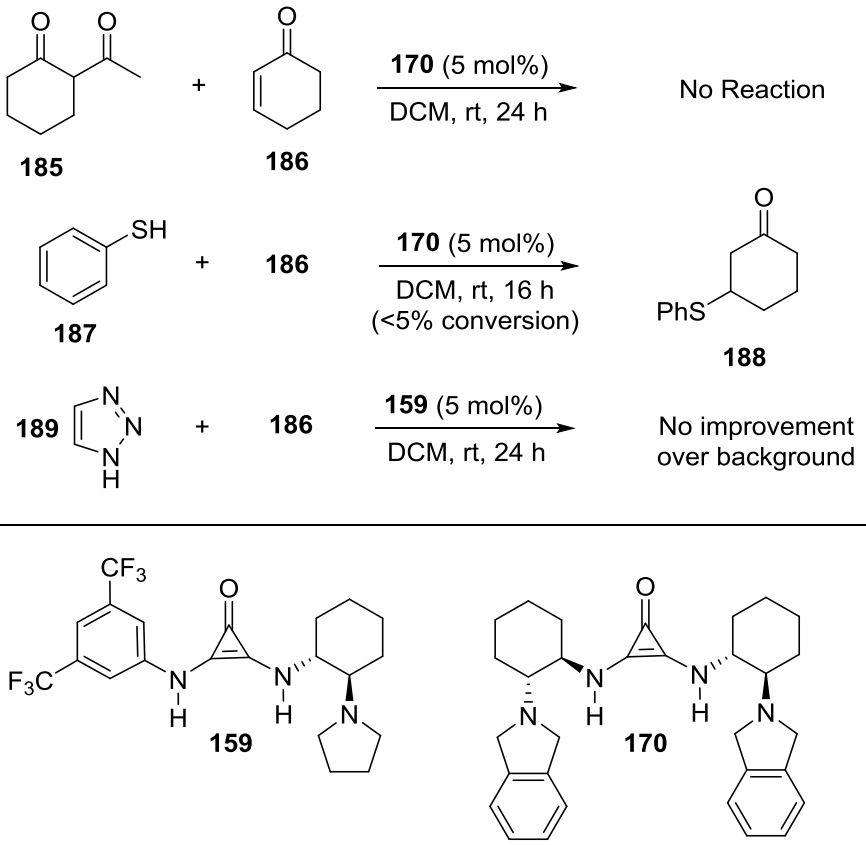

II.16 Concluding Remarks

In this chapter, we report chemistry towards bifunctional deltic ureas, analogues of the widely successful thioureas and squaramides. The synthesis of these highly strained molecules have little precedent, and the corresponding diaryl cyclopropenones are known to easily undergo ring-opening reactions. In one of our own concluding steps, we were also able to identify a by-product that resulted from the ring-opening reaction of a deltic urea. A direct conversion of a deltic urea to a thiodeltic urea is also being reported. Furthermore, we describe an example of an asymmetric reaction catalyzed by a bifunctional deltic urea, albeit with low enantioselectivity. During the course of our research, we were able to form multiple hypotheses regarding the stability of bifunctional deltic ureas. According to our current understanding, deltic ureas are

more prone to ring-opening reactions when an electron-withdrawing group is present within the molecule. Also, bifunctionality, by itself tends to reduce the stability of deltic ureas in solution. Neverthelesss, these deltamides are stable in solution over conventional reaction times, and we hope to develop interesting and unique applications of these motifs.

CHAPTER III

APPLYING CHIRAL, BIFUNCTIONAL THIOSQUARAMIDES: ENANTIOSELECTIVE MICHAEL ADDITION REACTIONS

III.1 Introduction

Over the past two decades, chemists have witnessed an explosive growth in enantioselective reactions catalyzed through activation by chiral hydrogen bond donors.[1,2] In a quest to design superior hydrogen-bond donor (HBD) catalysts towards asymmetric transformations, numerous permutations and combinations of achiral, chiral scaffolds have been explored. Nevertheless, the use of core functional groups such as thioureas, and squaramides has largely persisted. (Figure 13).[3,4] On various occasions, it has been demonstrated that activity and ability to induce enantioselectivity depend upon the acidity of the HBD catalyst.[5]

---

[1] For selected pioneering examples of enantioselective hydrogen-bond donor catalysis, see: (a) Sigman, M. S.; Jacobsen, E. N. *J. Am. Chem. Soc.* **1998**, *120*, 4901. (b) Wenzel, A. G.; Jacobsen, E. N. *J. Am. Chem. Soc.* **2002**, *124*, 12964. (c) Huang, Y.; Unni, A. K.; Thadani, A. N.; Rawal, V. H. *Nature* **2003**, *424*, 146. (d) Nugent, B. M.; Yoder, R. A.; Johnston, J. N. *J. Am. Chem. Soc.* **2004**, *126*, 3418.

[2] For a review of hydrogen-bond donor catalysis, see: (a) Doyle, A. G.; Jacobsen, E. N. *Chem. Rev.* **2007**, *107*, 5713. (b) *Hydrogen Bonding in Organic Synthesis*; Pihko, P. M., Ed.; Wiley-VCH: Weinheim, **2009**. (c) Türkmen, Y. E.; Zhu, Y.; Rawal, V. H. Brønsted Acids. *Comprehensive Enantioselective Organocatalysis*; Dalko, P. I., Ed.; Wiley-VCH: Weinheim, **2013**; Vol. 2, Chapt. 10.

[3] For a review of bifunctional thiourea catalysis, see: (a) Takemoto, Y. *Chem. Pharm. Bull.* **2010**, *58*, 593. (b) Siau, W. -Y.; Wang, J. *Catal. Sci. Tech.* **2011**, *1*, 1298.

[4] For a review of squaramide catalysis, see: (a) Aciro, C.; Jones, L. H. Storer, R. I. *Chem. Soc. Rev.* **2011**, *40*, 2330. (b) Alemán, J.; Parra, A.; Jiang, H.; Jørgensen, K. A. *Chem. Eur. J.* **2011**, *17*, 6890. (c) Chauhan, P.; Mahajan, S.; Kaya, U.; Hack, D.; Enders, D. *Adv. Synth. Catal.* **2015**, *357*, 253.

[5] Increased acidity of a catalyst has been found to correlate with increased activity and capability. See, inter alia, (a) Wittkopp, A.; Schreiner, P.R. *Chem. Eur. J.* **2003**, *9*, 407. (b) Jensen, K. H.;

Figure 13: Increasing Acidity While Maintaining A Higher H-H Distance

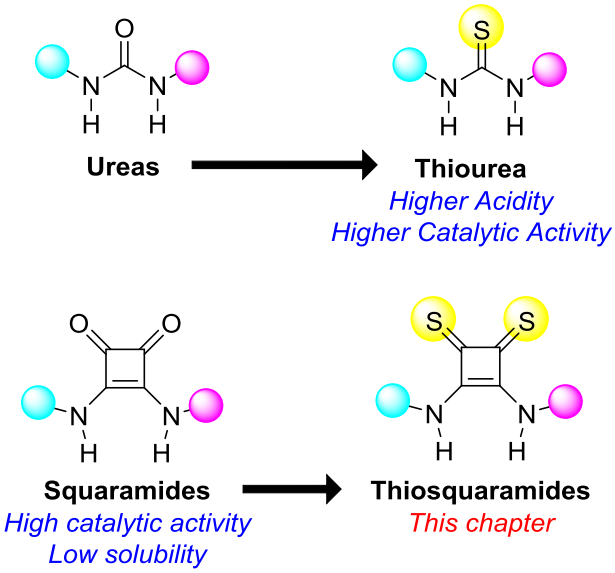

This design principle has not only led to the development of new classes of chiral catalysts, but is also evident throughout their historical development. In thioureas, increased polarization of C-S bonds (over C-O bonds in ureas) has translated to relatively acidic N-H groups, and thus thioureas were able to transcend ureas as HBD catalysts.[6] Similarly, the aromaticity of the cyclobutenedione functional group in squaramides results in more acidic N-H groups, and partly explains the success of squaramides.[7] However, we believe that an increased H-H distance in squaramides is yet another design element that has spearheaded squaramides' efficacy.

Sigman, M. S. *Angew. Chem. Int. Ed.* **2007**, *46*, 4748. (c) Jensen, K. H.; Sigman, M. S. *J. Org. Chem.* **2010**, *75*, 7194. (d) Parmar, D.; Sugiono, E.; Raja, S.; Rueping, M. *Chem. Rev.* **2014**, *114*, 9047.

[6] For early examples of thiourea based bifunctional catalysis, see: (a) Okino, T.; Hoashi, Y.; Takemoto, Y. *J. Am. Chem. Soc.* **2003**, *125*, 12672. (b) Yoon, T.; Jacobsen, E. N. *Angew. Chem. Int. Ed.* **2005**, *44*, 466.

[7] For the first applications of squaramides as asymmetric organocatalysts, see: (a) Malerich, J. P.; Hagihara, K.; Rawal, V. H. *J. Am. Chem. Soc.* **2008**, *130*, 14416. (b) Lee, J. W.; Ryu, T. H.; Oh, J. S.; Bae, H. Y.; Jang, H. B.; Song, C. E. *Chem. Commun.* **2009**, 7224. (c) Zhu, Y.; Malerich, J. P.; Rawal, V. H. *Angew. Chem. Int. Ed.* **2010**, *49*, 153.

Chart 1: Reconstructed Images for 'Ladder' Arrangement in Squaramides

Dibenzyl squaramide	3-((3,5-bis(trifluoromethyl)benzyl)amino)-4-(cinchonan-9-ylamino)-3-cyclobutene-1,2-dione

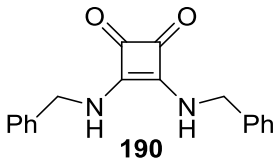

190

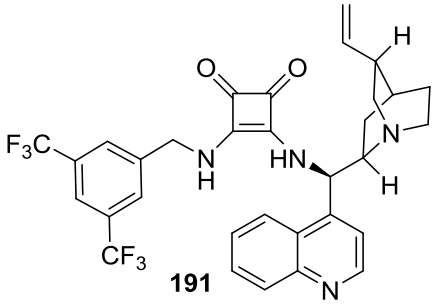

191

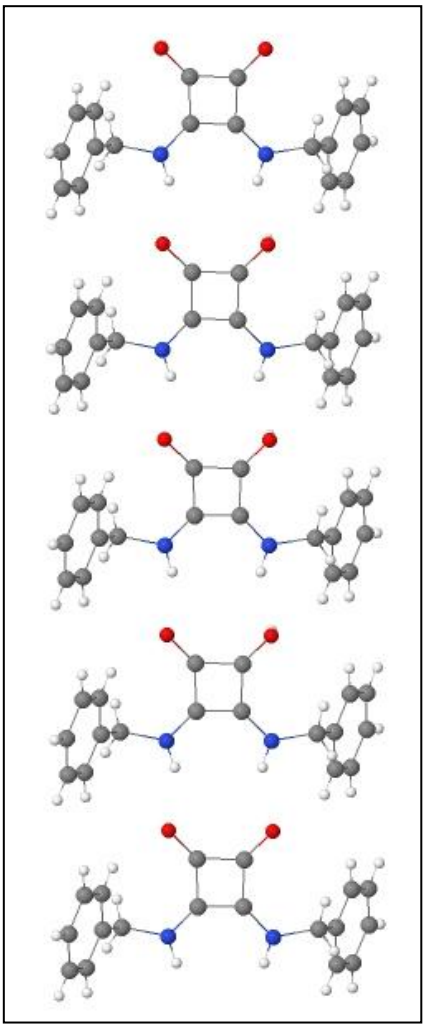

Source: Portell, A.; Barbas, R.; Braga, D.; Polito, M.; Puigjaner, C.; Prohens, R. *CrystEngComm* **2009**, *11*, 52.

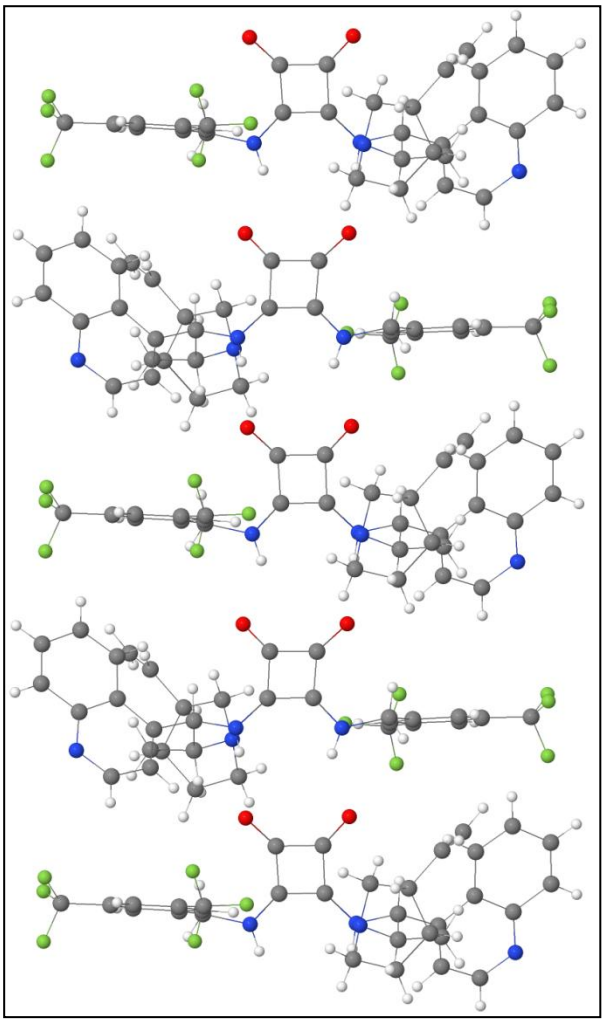

Source: Malerich, J. P.; Hagihara, K.; Rawal, V. H. *J. Am. Chem. Soc.* **2008**, *130*, 14416.

This design element affects the direction of hydrogen bonds, and in case of an oxygen nucleophile, leads to the formation of hydrogen bonds along the direction of oxygen's lone pair electrons.[8] Also, as seen in Chart 1, squaramides tend to hydrogen-bond in a 'ladder' arrangement, thus resulting in poor solubility in most solvents.[9]

In light of the two design principles, enhanced acidity of a thiosquaramide core opens the prospective for superior catalytic activity. To the best of our knowledge, a synergistic combination of increased C-S polarization and cyclobutenedione aromaticity has not been evaluated towards asymmetric HBD catalysis.

Table 18: Equilibrium Geometry in Vacuum Calculated Using Hartree-Fock 3-21G Level of Theory[10]

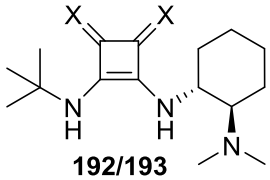

192/193

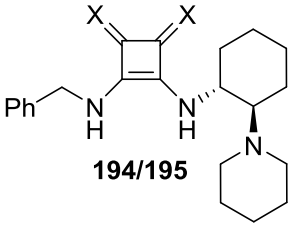

194/195

	Compound	Compound
X = O	(**192**) 2.616 Å	(**194**) 2.695 Å
X = S	(**193**) 2.504 Å	(**195**) 2.464 Å

Having calculated equilibrium geometries in vacuum (Table 18), we had expected the large sulfur groups to push the thiosquaramide substituents, thus resulting in rigid skeleton and relatively smaller H-H distances. Indeed, when a crystal structure was later elucidated in our

[8] (a) Taylor, R.; Kennard, O.; Versichel, W. *J. Am. Chem. Soc.* **1983**, *105*, 5761. (b) Taylor, R.; Kennard, O. *Acc. Chem. Res.* **1984**, *17*, 320.

[9] (a) Portell, A.; Barbas, R.; Braga, D.; Polito, M.; Puigjaner, C.; Prohens, R. *CrystEngComm* **2009**, *11*, 52. (b) Prohens, R.; Portell, A.; Alcobé, X. *Cryst. Growth Des.* **2012**, *12*, 4548. (c) Portell, A.; Font-Bardia, M.; Bauzá, A.; Frontera, A.; Prohens, R. *Cryst. Growth Des.* **2014**, *14*, 2578. (d) Portell, A.; Bardia-Font, M.; Bauzá, A.; Frontera, A.; Prohens, R. *CrystEngComm* **2016**, *18*, 6437.

[10] Calculated using Spartan '08, Wavefunction, Inc., CA.

group, the H-H distance of compound **193** was found to be 2.43 Å and 2.64 Å (for two isomers respectively).[11]

III.2 Towards the Synthesis of Bifunctional Thiosquaramides

While the use of squaramide as a chiral scaffold has inspired numerous groups to develop new enantioselective reactions, the core structure of squaramide has yet to be modified for use in asymmetric catalysis. An obvious means of modifying the nature of the squaramide core is to convert a squaramide into a thiosquaramide. While conversion of squaric acid derivatives into their respective thio forms was first investigated over thirty years ago there has been surprisingly little research done over the subsequent years.[12]

Scheme 28: Synthesis of simple thiosquaramides by Gale and co-workers

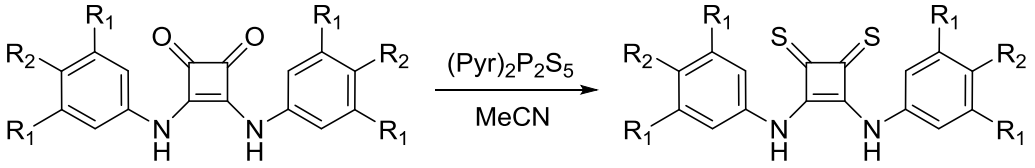

196a-199a

196b: R_1 = H; R_2 = H
197b: R_1 = H; R_2 = CF_3
198b: R_1 = CF_3; R_2 = H
199b: R_1 = *t*Bu; R_2 = H

A notable example of recent development in this field has been the preparation of achiral bis-aryl thiosquaramides for use in anion transportation by Jolliffe and coworkers (Scheme 28).[13] A possible advantage of thiosquaramide catalysts lies in the increased acidity of the core amines.

[11] Details of the X-ray crystal structure are beyond the scope of this dissertation, and would be reported as a publication in due course.
[12] For reports of thionation of squaric acid derivatives, see: (a) Eggerding, D.; West, R. *J. Org. Chem.* **1976**, *41*, 3904. (b) Frauenhoff, G. R.; Takusagawa, F.; Busch, D. H. *Inorg. Chem.* **1992**, *31*, 4002. (c) Müller, M.; Heileman, M. J.; Moore, H. W.; Schaumann, E.; Adiwidjaja, G. *Synthesis* **1997**, 50.
[13] Busschaert, N.; Elmes, R. B. P.; Czech, D. D.; Wu, X.; Kirby, I. L.; Peck, E. M.; Hendzel, K. D.; Shaw, S. K.; Chan, B.; Smith, B. D.; Jolliffe, K. A.; Gale, P. A. *Chem. Sci.* **2014**, *5*, 3617.

As the N-H bond polarizes (becomes more acidic) it becomes a better hydrogen bond donor. As large sulfur groups are unlikely to lead to strongly hydrogen-bonded ladder arrangements, one can expect improved solubility of thiosquaramides as compared to squaramides, which are generally poorly soluble in non-protic solvents.

Scheme 29: Synthesis of Thiosquaramides by Direct Thionylation of Bifunctional Squaramides

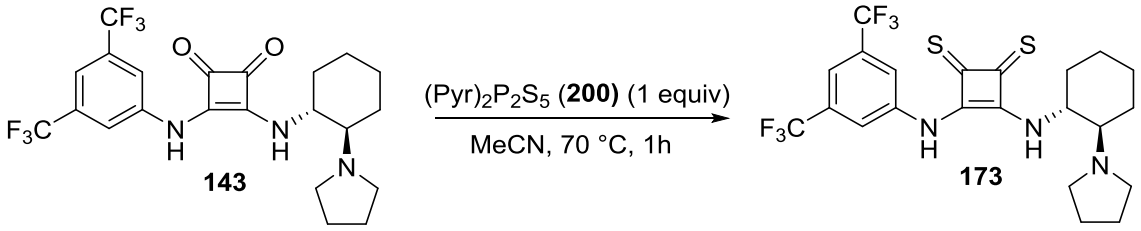

Thiosquaramide **143** could be synthesized from A and pyridine-P_2S_5 complex **200**. It should be noted that this step was initially developed by Dr. Thomas D. Montgomery. It was found that compound B decomposed during silica gel chromatography, but a reasonably pure sample could be obtained via an base-acid extraction protocol (see Experimental Section for detailed procedure). However, the compound gradually decomposed in methanol and dichloromethane. Based on crude ^{1}H NMR spectra, we hypothesized that one of the decomposition products was bis(trifluoromethyl)aniline. Surprisingly, the ^{1}H NMR of the compound **173** in $CDCl_3$ displayed 3 broad peaks in the $\delta = 8.5$ to $\delta = 11$ region. We realized that during the final step of the acid-base extraction, the aqueous layer was acidified to a pH of 1-2, and hence, the possibility that the tertiary amine in compound **173** was protonated could not be ruled out. All attempts to acidify/basify an aqueous solution to a pH of 4-6, and subsequent extraction in CH_2Cl_2 failed to give the product. On the contrary, we found that reactions typical of bifunctional catalysis could be performed using our compound, and hence it is debatable if the tertiary amine is protonated or not. It should also be noted that the compound was found to be stable in solution in acetone, acetonitrile and chloroform.

Figure 14: Compounds Subjected to the Direct Thionylation Procedure

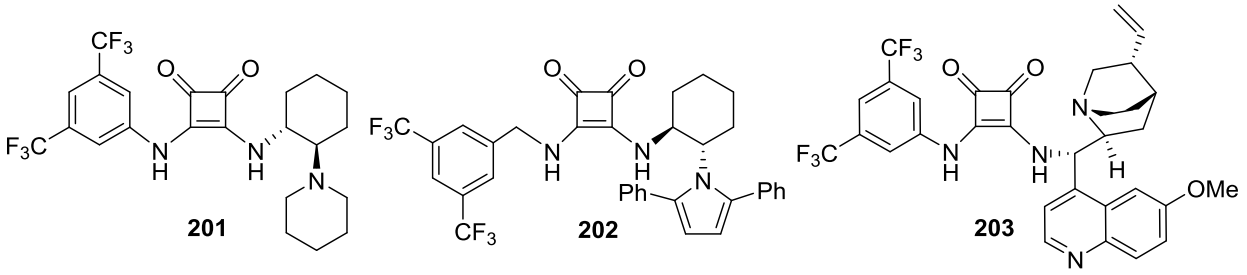

Furthermore, the above direct thionylation protocol could be applied to compound **201**, but not towards compounds **202** and **203** (see Experimental Section for related ^{1}H NMR data). In each case, the thiosquaramide product could be formed by modifying the thionylation agent, concentration, reaction time and temperature. However, the instability of these thiosquaramides towards silica gel chromatography leaves one with few other options towards it's purification, and base-acid extraction did not prove to be consistently successful due to the presence of by-products. Thus, an alternative approach was explored to access such thiosquaramides. As the presence of a tertiary amine reduced the stability of thiosquaramides towards silica gel chromatography, the bifunctionality was introduced at the end of the synthetic sequence.

The preferred route to bifunctional thiosquaramides proceeded through the butyl squarate ester **204**, rather than the more common vinylogous methyl ester. Treatment of vinylogous butyl ester-amide **205** with one equivalent of Lawesson's reagent gave the easily isolated dithionation product **206**, which is moderately stable at room temperature. Carrying out these steps on the corresponding methyl ester gave little or no product, depending on the substrate. Coupling of **206** with a chiral diamine provided bifunctional catalyst **207**, which was purified by trituration to give yellow to amber, bench-stable solids (depending upon R_1). As expected, unlike their widely used oxo-counterparts, which are at best sparingly soluble in common organic solvents,

thiosquaramides are significantly more soluble in a range of solvents.[14] Note that this alternative approach was developed after collaborative discussions with Michael Rombola and Dr. Thomas D. Montgomery, and the strategy pioneered by Michael Rombola (Please see Experimental Section for an example of the synthesis).

Scheme 30 An Alternate Approach Towards the Synthesis of Thiosquaramides

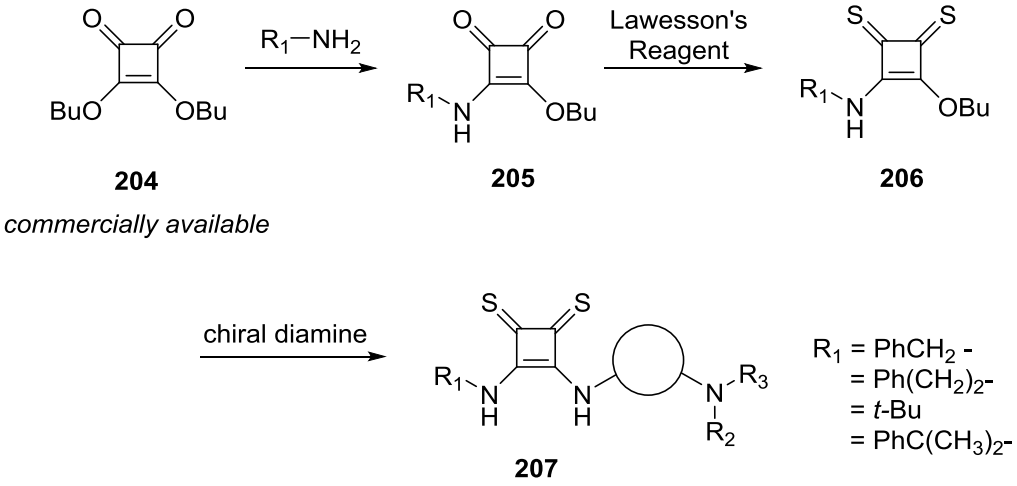

III.3 Evaluation of Thiosquaramides as Asymmetric Organocatalysts

Thiosquaramides developed above were evaluated towards a variety of reactions, of which selected examples are shown in Scheme 31. The reaction of chalcones with the MAC reagent could be catalyzed in 90% ee, however, this was not pursued further as the reaction has previously been developed for high enantioselectivities.[15] The addition of thioacetic acid **179** to compound **211** could not be catalyzed with thiosquaramide **173**. The addition of thioacetic acid to chalcones could be catalyzed in good conversions, albeit with low enantioselectivity (Scheme 31).

[14] Thiosquaramides were found to possess superior solubility in toluene by an order of >30.
[15] Yang, K. S.; Nibbs, A. E.; Türkmen, Y. E.; Rawal, V. H. *J. Am. Chem. Soc.* **2013**, *135*, 16050.

Scheme 31: Selected Initial Results with Addition Reactions

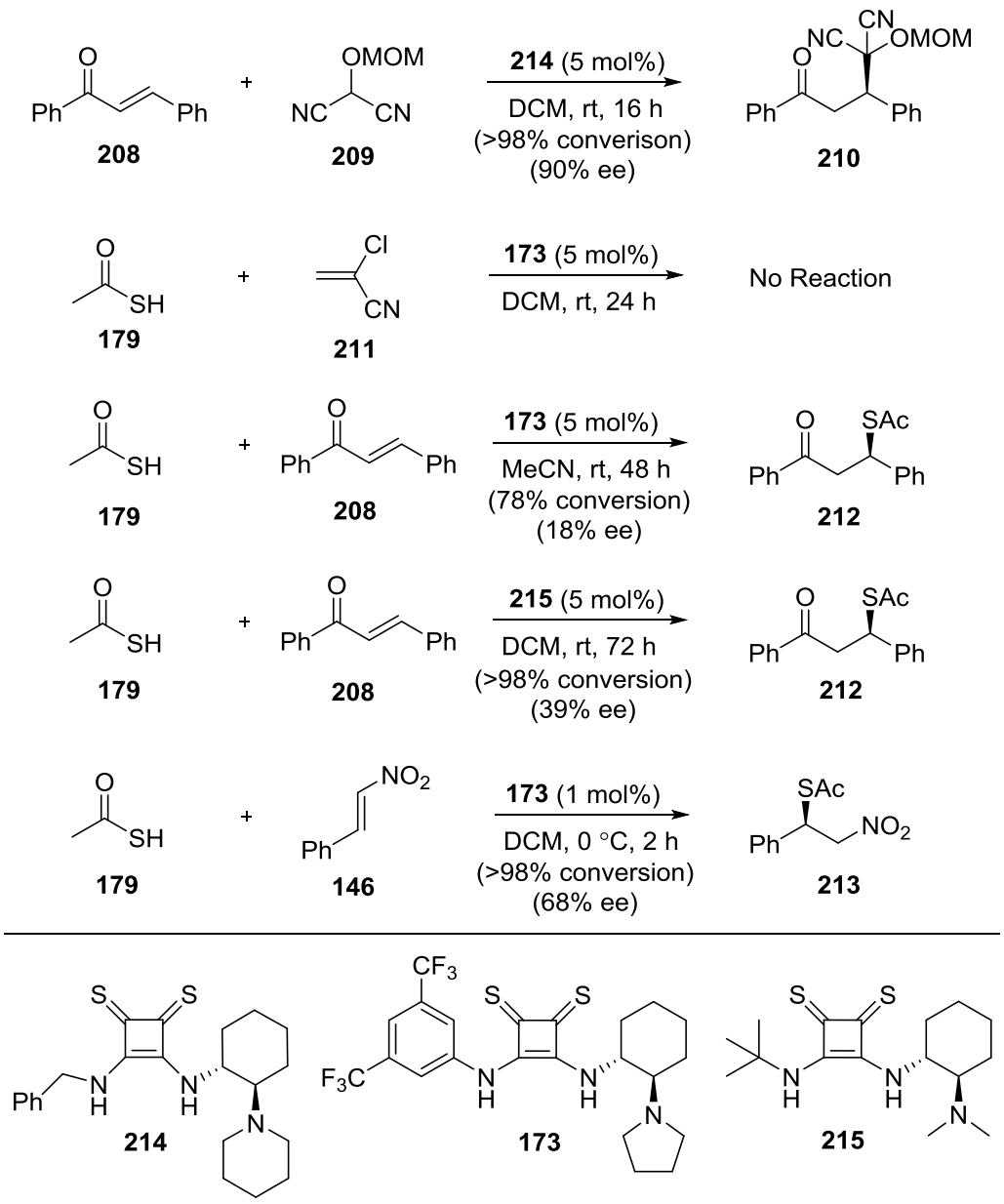

Next, we embarked on optimizing the Michael addition reaction of thioacetic acid to β-nitrostyrene (Table 19).[16] While various reaction conditions failed to provide the product in high ee, thiosquaramides also failed to reliably catalyze this asymmetric reaction. Only a small drop in ee (4%) was observed when the ee of a solid sample under nitrogen was measured after 16 hours.

[16] For a previous report of this reaction with *N*-sulfinyl urea, see: Kimmel, K. L.; Robak, M. T.; Ellman, J. A. *J. Am. Chem. Soc.* **2009**, *131*, 8754.

Stirring this product with toluene at 0 °C for 1 hour, followed by filtration through a plug of silica, and subsequent concentration did not lead to any reduction in ee. Similarly, stirring the product in the presence of 1% catalyst **215** and subsequent work-up led to only 2% loss in ee. The reaction was carried out under a variety of conditions, however, the source of this variation in ee could not be pin-pointed. In the absence of a catalyst, the background reaction is fairly slow (entry 1), and hence, a possible pathway could result from the decomposition of the thiosquaramide catalyst in the presence of thioacetic acid, followed by an amine catalyzed formation of the achiral product. We ruled out reversibility of this reaction, and also found that the best results were instead obtained with oxosquaramides. As a result, we then focused our attention towards another reaction, i.e. the Michael addition of barbituric acids to β-nitrostyrene.

III.4 Catalyzing the Enantioselective Michael Addition of Barbituric Acids to Nitroolefins

The selection of barbituric acid derivatives to test the capability of new thiosquaramides was motivated by their known biomedical applications.[17,18] Historically used as sedatives, anti-convulsants, and analgesics, barbiturates have recently been shown to possess anti-tumor, immune system modulatory, and anti-depressive activity. The varied biological properties of barbituric acids and the limited reports on their use in enantioselective reactions, and none using

[17] (a) Gulliya, K. S. Anti-Cancer Uses for Barbituric Acid Analogs. US Patent 5674870 A, October 7, 1997. (b) Gulliya, K. S. Uses for Barbituric Acid Analogs. US 5869494 A, February 9, 1999. (c) Kaur, M.; Verma, P.; Singh, P. *Bioorg. Med. Chem. Lett*. **2009**, *19*, 3054. (d) Dhorajiya, B. D.; Ibrahim, A. S.; Badria, F. A.; Dholakiya, B. Z. *Med. Chem. Res.* **2014**, *23*, 839. (e) Penthala, N. R.; Ketkar, A.; Sekhar, K. R.; Freeman, M. L.; Eoff, R. L.; Balusu, R.; Crooks, P. A. *Bioorg. Med. Chem.* **2015**, *23*, 7226.

[18] To the best of our knowledge, the only use of barbituric acids as nucleophiles in asymmetric catalysis has been in palladium-catalyzed allylation reactions: (a) Brunner, H.; Deml, I.; Dirnberger, W.; Nuber, B.; Reiβer, W. *Eur. J. Inorg. Chem.* **1998**, 43. (b) Brunner, H.; Deml, I.; Dirnberger, W.; Ittner, K.-P.; Reiβer, W.; Zimmerman, M. *Eur. J. Inorg. Chem.* **1999**, 51. (c) Trost, B. M.; Schroeder, G. M. *J. Org. Chem.* **2000**, *65*, 1569.

organic catalysts, prompted us to select them as nucleophiles for demonstrating the effectiveness of chiral thiosquaramide catalysts.

Table 19: Selected Results for the Optimization of the Addition Reaction of Thioacetic Acid and β-nitrostyrene

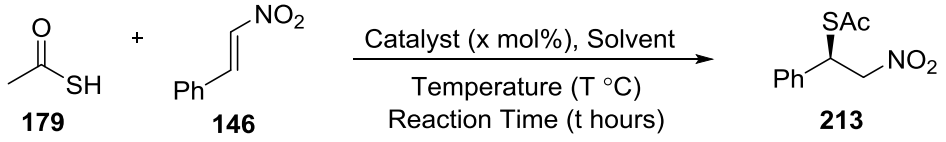

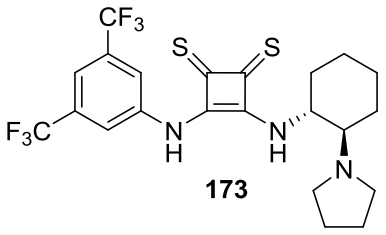

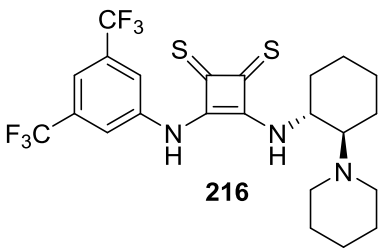

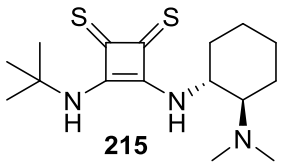

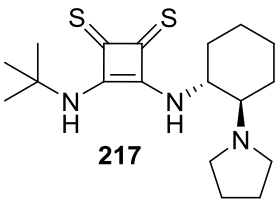

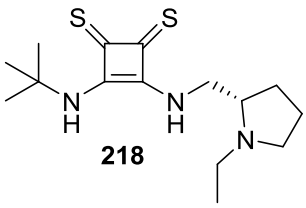

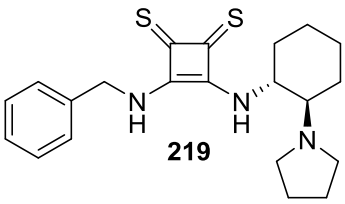

Catalyst	Solvent (Volume)	**146**:**179**	T	t	Conversion[a]	ee[b]
None	Et_2O	1.1:1	0	24	3%	-
173	DCM (1.4 mL)	1.1:1	0	2	>98%	68%
173	Toluene (1.4 mL)	2:1	0	1	>98%	19%
173	α,α,α-Trifluorotoluene (1.4 mL)	2:1	0	1	>98%	30%
173	THF (1.4 mL)	2:1	25	14	>98%	59%
173	Et_2O (1.4 mL)	2:1	25	14	>98%	49%
216	Et_2O (1.4 mL)	2:1	0	2	>98%	63%
216	DCM (1.4 mL)	2:1	0	2	>98%	71%
216	α,α,α-Trifluorotoluene (1.4 mL)	2:1	0	2	>98%	56%
215	THF (1.4 mL)	1.1:1	0	2	>98%	31%
215	DCM (0.7 mL)	1.1:1	0	2	>98%	36%
215	Et_2O (1.4 mL)	1.1:1	0	2	>98%	44%
215	$CHCl_3$ (0.7 mL)	1.1:1	0	2	>98%	35%
215	Et_2O (0.7 mL)	2:1	-20	3	>98%	44%
215	Toluene (0.7 mL)	2:1	-20	3	>98%	24%
215	Et_2O:DCM (1:1; 2.8 mL total)	2:1	0	2	>98%	13%
217	DCM (2.8 mL)	2:1	0	2	>98%	18%
217	Et_2O (2.8 mL)	2:1	0	2	>98%	27%
218	Et_2O (2.8 mL)	2:1	0	2	>98%	7%

Table 19, continued

219	DCM (2.8 mL)	2:1	0	1	>98%	28%
219	Et_2O (2.8 mL)	2:1	0	1	>98%	19%

All reactions were carried out using 0.5 mmol (1.0 equiv) of β-nitrostyrene. [a]Conversion was measured by ^1H NMR spectroscopy. [b]ee was measured using the following HPLC conditions (OD-H, 88:12 Hexanes:iPrOH, 1.0mL/min): t_{major} = 13.8 min, t_{minor} = 24.7 min.

As evident from Table 20, our catalyst of choice gave good enantioselectivities in all solvents except methanol.[19] In order to accurately measure ee, the compound was further derivatized. It was found that stirring the compound with NBS in the presence of benzyl peroxide gave the corresponding brominated product, however, the difficulty of quickly separating benzoyl peroxide via a pipette column chromatography led us to look for another method. It was found that NCS leads to the corresponding chlorinated product **220** (X = Cl) within 30 minutes at room temperature. It should be noted that the Michael reaction did not occur in the absence of a catalyst. Further reduction of catalyst loading to 0.1 mol% increased the reaction time only slightly, from 0.5 h to 2 h, with no effect on ee. Even at a catalyst loading of 0.05 mol%, the reaction proceeded smoothly, going to full conversion within 10 h, with essentially no diminution in ee. The reaction worked even when the catalyst level was reduced to 0.02 mol%, but gave the product in 72% ee. The conjugate addition can also be carried out on gram-scale, affording 1.65 grams of the product in 96% yield and 96.5% ee. Note that many of the above reactions were carried out without special precautions, under an air atmosphere and using reagent grade solvents right out of a bottle.

[19] This was expected as methanol can potentially act as a competing hydrogen-bond donor.

Table 20: Optimization of the Michael Addition Reaction of *N,N'*-Disubstituted Barbituric Acid and β-nitrostyrene

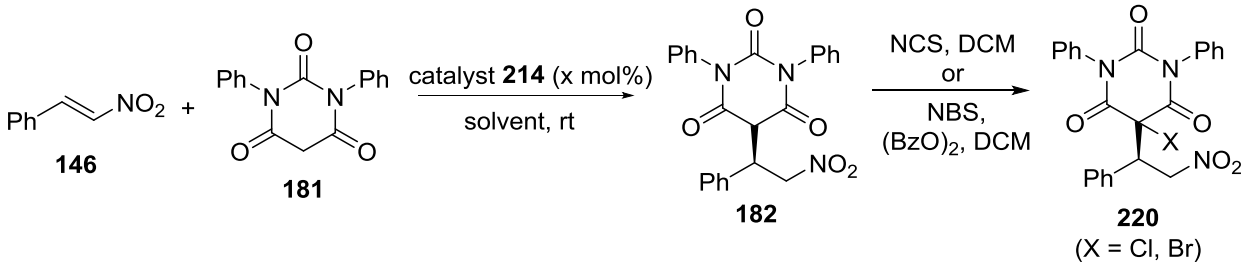

146 **181** **182** **220** (X = Cl, Br)

Catalyst Loading (mol%)[a]	T	Solvent (Volume)	Reaction Time	Conversion[b]	ee
0.5[e]	rt	DCM (0.25 mL)	1 h	>98%	90[c]
0.5[e]	rt	Toluene (0.5 mL)	30 min	>98%	97[c]
0.5[e]	rt	Et_2O (0.25 mL)	3 h	34%	-
0.5[e]	rt	MeCN (0.25 mL)	1 h	88%	79[c]
0.5	rt	DCE (0.5 mL)	30 min	>98%	93[c]
0.5	rt	DCM (0.5 mL)	30 min	>98%	94[c]
0.5	rt	Acetone (0.5 mL)	90 min	>98%	87[c]
0.5	rt	MeOH (0.5 mL)	6 h	>98%	38[c]
0.5	rt	EtOAc (0.5 mL)	30 min	>98%	92[c]
0.5	rt	$CHCl_3$ (0.5 mL)	30 min	>98%	91[c]
0.5	rt	m-Xylene (0.5 mL)	90 min	>98%	96[c]
0.5	rt	TCE (0.5 mL)	30 min	>98%	96[c]
0.5	rt	α,α,α-trifluorotoluene (0.5 mL)	60 min	>98%	95[c]
0.5	rt	Benzene (0.5 mL)	30 min	>98%	96[c]
0.5	rt	o-Xylene	24 h	54%	-
0.5	rt	DME	60 min	>98%	89[c]
0.5	rt	1:1 DCM:Cyclohexane (0.5 mL total)	30 min	>98%	94[c]
0.5	rt	3:1 DCM:Cyclohexane (0.5 mL total)	30 min	>98%	92[c]
0.5	rt	1:3 DCM:Cyclohexane (0.5 mL total)	30 min	>98%	95[c]
0.5	rt	1:1 DCM:Toluene (0.5 mL total)	30 min	>98%	94[d]
0.5	rt	1:1 DCM:Cyclohexane (0.5 mL total)	30 min	>98%	95[d]
0.5	rt	1:1 DCM:*n*-hexane (0.5 mL total)	30 min	>98%	95[d]
0.5	rt	1:1 DCM:pentane (0.5 mL total)	30 min	>98%	93[d]
0.5	rt	1:1 DCM:*n*-heptane (0.5 mL total)	30 min	>98%	93[d]

0.5	rt	1:1 DCM:*iso*-octane (0.5 mL total)	30 min	>98%	95[d]

Table 20, continued

0.5[e,f]	rt	Toluene (0.5 mL)	30 min	>98%	97[d]
0.5[e,f]	rt	1:1 DCM:Toluene (0.2 mL total)	30 min	>98%	96[d]
0.5[e,f]	rt	1:1 DCM:Toluene (0.5 mL total)	30 min	>98%	96[d]
0.5[e,f]	rt	1:1 DCM:Toluene (2 mL total)	30 min	>98%	96[d]
0.5[e,f]	rt	1:1 DCM:Toluene (5 mL total)	30 min	>98%	95[d]
0.02[e,f]	rt	Toluene	10 h	83%	72[d]
0.05[e,f]	Rt	Toluene (0.5 mL)	10 h	>98%	96[d]
0.1[e,f]	rt	Toluene (0.5 mL)	2 h	>98%	97[d]
5[e,f]	rt	Toluene (0.5 mL)	30 min	>98%	97[d]
0.5[e,f,g]	rt	Toluene (0.5 mL)	30 min	>98%	95[d]
0.5[e,f]	rt	Toluene (0.2 mL)	30 min	>98%	97[d]
0.5[e,f]	rt	Toluene (0.5 mL)	30 min	>98%	97[d]
0.5[e,f]	rt	Toluene (2 mL)	30 min	>98%	97[d]
0.5[e,f]	rt	Toluene (5 mL)	30 min	>98%	97[d]
0.5[e,f]	-20 °C	Toluene (5 mL)	30 min	>98%	97[d]

[a]Unless otherwise noted, all reactions were carried out on a 0.2 mmol scale of barbituric acid and 0.22 mmol of β-nitrostyrene under open-air conditions using regular solvent out of bottle. [b]Conversion was determined by ^{1}H NMR spectroscopy. [c]ee was determined by brominating the product. Bromination was carried out by stirring the product with 0.5 equiv of ethylenebis(*N*-methylimidazolium)ditribromide in acetonitrile at room temperature for 20 minutes.[20] Alternatively, *N*-bromosuccinimide with benzoyl peroxide in dichloromethane afforded the product within 30 minutes at room temperature. [d]ee was determined by chlorinating the product by stirring it with 1.0 equiv of *N*-chlorosuccinimide (NCS) in dichloromethane for 20 minutes at room temperature. [e]Reaction carried out under N_2 atmosphere. [f]Carried out using anhydrous solvent. [g]3.0 equivalents of β-nitrostyrene was used.

Among the catalysts possessing the *N*,*N'*-dimethylated cyclohexanediamine unit, reduction in steric bulk on the distal thiosquaramide nitrogen corresponded with lower ee for the Michael addition product (Table 21). Of the piperidine containing thiosquaramides examined, the benzyl-substituted catalyst performed better than the one possessing a phenethyl unit. Catalyst **224**, the oxo-analogue of **215**, was also effective, but gave lower ee (entries 5 and 6). The seemingly small difference in ee observed with catalysts **214** and **227** (97% vs 95%) corresponds to

[20] Hosseinzadeh, R.; Tajbakhsh, M.; Mohadjerani, M.; Lasemi, Z. *Monatsh Chem* **2009**, *140*, 57.

selectivity ratios of 70:1 and 40:1, respectively. Catalyst **222**, the thiourea analogue also provided the product in quantitative yield, but in much lower ee (97% vs 85%). Surprisingly, Takemoto's catalyst **221** also led to much lower enantiomeric excess.

Table 21: Optimization of the Michael Addition Reaction of *N*,*N*'-Disubstituted Barbituric Acid and β-nitrostyrene

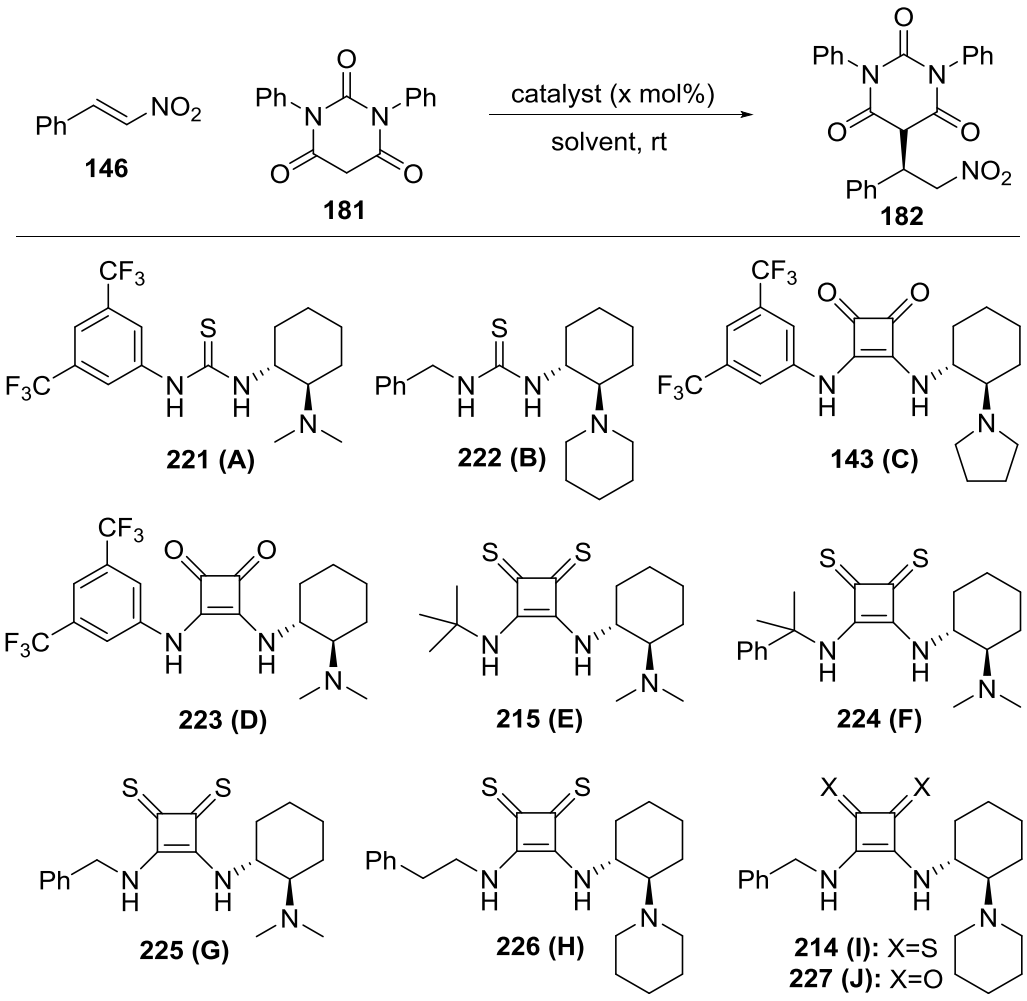

Catalyst[a]	Catalyst Loading (mol%)	Solvent	Time	Conversion[b]	ee[c]
A	0.5	PhMe	0.5 h	>98%	76%
B	0.5	PhMe	0.5 h	>98%	85%
C	0.5	PhMe	0.5 h	>98%	80%
D	0.5	PhMe	0.5 h	>98%	72%
E	0.5	PhMe	0.5 h	>98%	54%

Table 21, continued

F	0.5	PhMe	0.5 h	>98%	45%
G	0.5	PhMe	0.5 h	>98%	88%
H	0.5	PhMe	0.5 h	>98%	91%
I	0.5	PhMe	0.5 h	>98%	97%
J	0.5	PhMe	0.5 h	>98%	95%

[a]All reactions were carried out using 0.2 mmol of barbituric acid with 1.1 equivalents of β-nitrostyrene, and with regular solvent under open air conditions. [b]Conversion was determined by ^{1}H NMR spectroscopy. [c]ee was determined by chlorinating the product by stirring it with 1.0 equiv of *N*-chlorosuccinimide (NCS) in dichloromethane for 20 minutes at room temperature.

Table 22: Employing Low Catalyst Loadings for the Michael Addition Reaction of Barbituric Acid and β-nitrostyrene

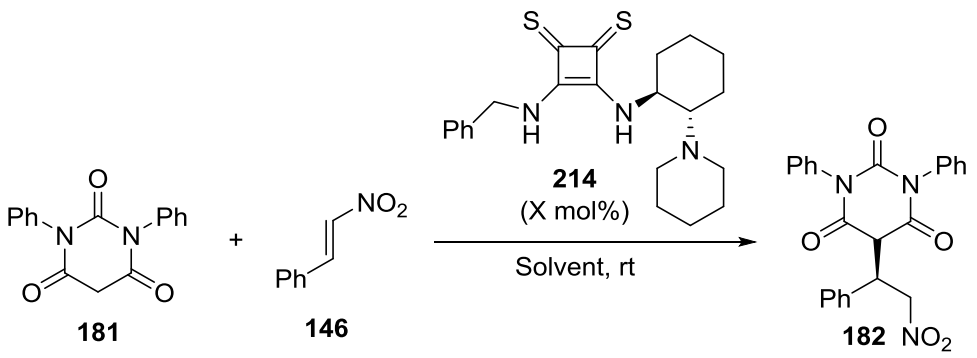

Catalyst Loading[a]	Scale (mmol)	Solvent (Volume)	Apparatus	Reaction Time	Conversion[b]	ee[c]
0.01 mol%	0.2	Toluene (0.5 mL)	Test-tube	48 h	42%	-
0.01 mol%	0.2	DCM (0.25 mL)	Cylindrical Vial	48 h	91%	33%
0.01 mol%	0.2	DCM (0.25 mL)	Cylindrical Vial	48 h	76%	-
0.01 mol%	0.4	DCM (0.2 mL)	V-bottomed vial	10 h	37%[d]	-

[a]Experiments were carried out by preparing a stock solution of the catalyst in corresponding solvents, and the stock solution was added immediately after preparation. Also, 0.01 mol% corresponds to 0.0001 equivalents of catalyst. [b]Conversion was determined by ^{1}H NMR spectroscopy. [c]We noticed a drop in ee upon lowering catalyst loadings. See Table 21 for experiments with 0.02-0.05 mol% catalyst loadings. [d]Due to the V-shape of the vial, dichloromethane dries out quickly, and hence, the low conversion.

At higher catalyst loadings, most transformations could be carried out with quantitative conversions. However, at catalyst loadings less than 0.01 mol% (0.0001 equiv), the reaction did not proceed to complete conversion even after 2 days. In this case, the chlorination of the product

competed with the chlorination of the starting material, nonetheless, the mixture could be subjected to chlorination with less than 1.0 equiv of NCS. The fact that the chlorination of product **182** is faster than the chlorination of the starting material **181** makes it possible to use greater than 1.0 equiv of NCS, as NCS is otherwise difficult to separate from the product due to close R_f values (Figure 15).

Figure 15: Kinetics of chlorination of the addition product in the presence of the starting material

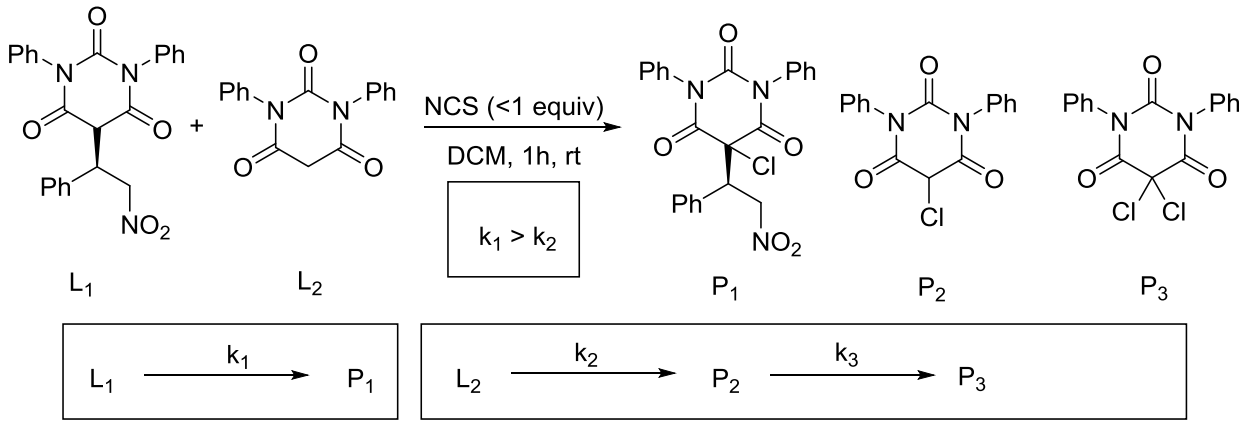

The substrate scope of this reaction was examined next. Different combinations of nitroolefins and *N*,*N*′-disubstituted-barbituric acids were reacted in the presence of 0.5 mol% of catalyst **214** (Scheme 32). The reactions gave high yields and high enantioselectivities for most of the reactants examined. Brominated nitrostyrenes gave excellent results, although the rate of the reaction was considerably slower when the bromine is ortho to the alkene substituent, presumably due to the steric hindrance. A similar effect on rate was observed with other hindered substrates, and with alkenyl and alkyl substituted nitroalkenes.

Scheme 32: Substrate Scope for the Thiosquaramide Catalyzed Michael Addition of Barbituric Acid to β-Nitrostyrene

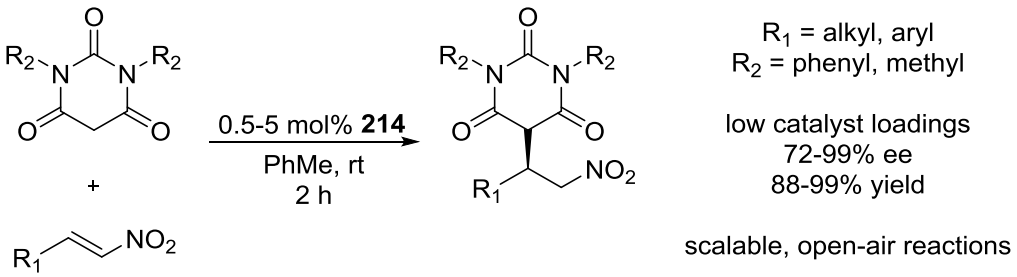

A discussion of individual substrates is beyond the scope of this dissertation.Results will be shortly communicated via a publication.

Please note that the substrate scope was examined in collaboration with Michael Rombola; with major contributions from Michael Rombola and minor contributions from the author of this dissertation, and hence a detailed discussion is beyond the scope of this chapter.

III.5 Reversibility of the Barbituric Acid Addition Reaction

While the product **182** of the asymmetric reaction could be easily chlorinated and brominated at the 5-position, we wondered of other ways in which this product can be functionalized. Reaction of **182** with allyl chloride in the presence of NEt_3 or K_2CO_3 failed to give the corresponding 5-allyl derivative. A second Michael reaction of **182** with acrolein in the presence of K_2CO_3 also failed to provide the corresponding product.

Scheme 33: Reaction reversibility in the Presence of a Mild Base

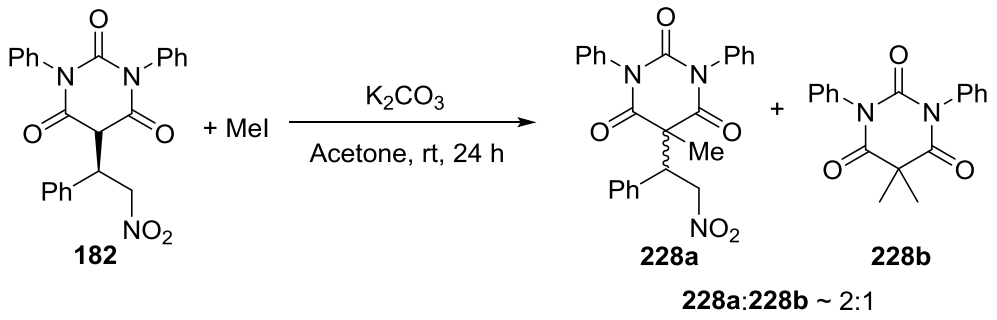

Nonetheless, we found that the quaternary center could be formed by reacting **182** with MeI to afford the product **228a**, with almost complete conversion of the starting material to the products **228a** and **228b** (Scheme 33). However, this made us realize that the retro-Michael reaction can take place in the presence of a base, and this could lead to a loss of ee over the course of the reaction (Scheme 34). Hence, this method was not pursued further.

Scheme 34: Loss in ee upon Methylation of **182**

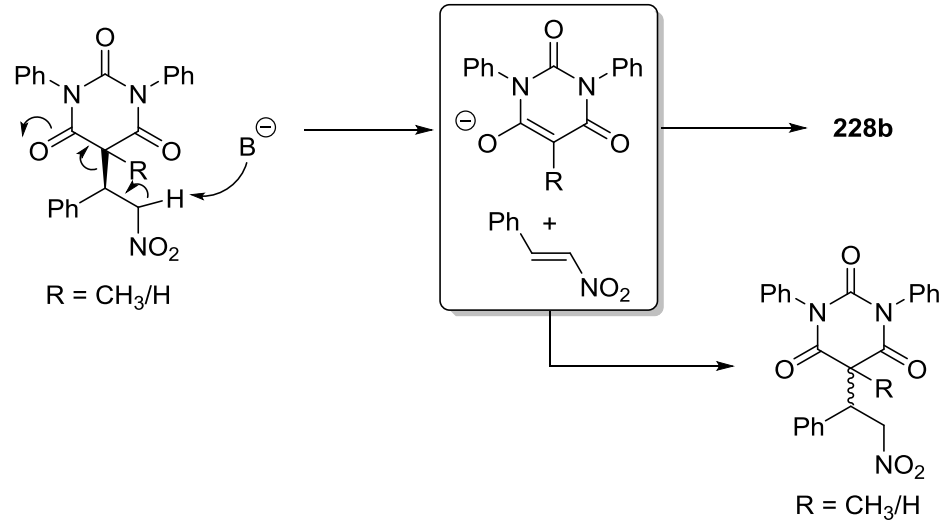

Scheme 35: Forming a Quaternary Center a via 5-allyl barbituric acid

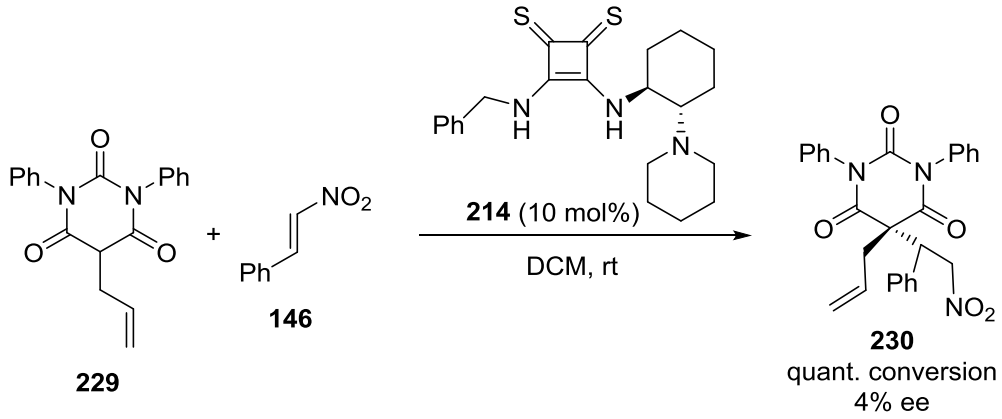

We next turned our attention towards an alternate way of constructing the quaternary center with adjacent chirality. When 2-allyl malonic acid was condensed with 1,3-diphenylurea, the

corresponding 5-allyl-*N*,*N*'-diphenylbarbituric acid **229** could be prepared.[21] While the thiosquaramide-catalyzed Michael addition reaction did lead to the corresponding quaternary center, the reaction was not asymmetric. As the 5-allylbarbituric acid is relatively sterically hindered, one explanation could be that the kinetics of the reaction are equally favorable towards both Michael and retro-Michael reaction, thus diminishing ee.

III.6 Concluding Remarks

In conclusion, we have developed a general method for the synthesis of chiral thiosquaramides, a class of bifunctional catalysts not previously described in the literature. Thiosquaramides are more acidic and significantly more soluble in non-polar solvents than their "oxo"-squaramide counterparts. Thiosquaramides are excellent catalysts for the unreported, enantioselective conjugate addition reaction of the barbituric acid pharmacaphore to nitroalkenes, delivering the chiral barbiturate derivatives in high yields and high enantioselectivities, even with catalyst loadings as low as 0.05 mol%. However, thiosquaramides are also effective at other asymmetric transformations, and possess the potential to replace squaramides as excellent organocatalysts.

[21] Vazakas, A. J.; Bennetts Jr., W. W. *J. Med. Chem.* **1964**, *7*, 342.

CHAPTER IV

MEASUREMENT OF EQUILLIBRIUM ACIDITIES OF DELTIC UREAS AND THIOSQUARAMIDES IN DMSO

IV.1 Introduction

Fundamental physical organic parameters such as acidity are useful for the understanding of catalytic activity and catalyst design. As hydrogen-bonding interactions likely determine catalyst activity with deltic ureas and thiosquaramides, an understanding of pK_a values can help understand activation of specific nucleophiles/electrophiles by these organocatalysts.[12]

Over the past century, various acidity scales have been developed, but the most extensive scale for organic compounds is that developed by Bordwell and co-workers (in DMSO).[3,4] As opposed to pK_a measurement in H_2O, polar non-H-bond-donor solvent such as DMSO are an excellent solvent for pK_a measurement of organic compounds. Not only are organic compounds more

[1] Increased acidity of a catalyst has been found to correlate with increased activity and capability. See, inter alia, (a) Wittkopp, A.; Schreiner, P.R. *Chem. Eur. J.* **2003**, *9*, 407. (b) Jensen, K. H.; Sigman, M. S. *Angew. Chem. Int. Ed.* **2007**, *46*, 4748. (c) Jensen, K. H.; Sigman, M. S. *J. Org. Chem.* **2010**, *75*, 7194. (d) Parmar, D.; Sugiono, E.; Raja, S.; Rueping, M. *Chem. Rev.* **2014**, *114*, 9047.

[2] For reviews discussing design strategies for dual hydrogen bond donor catalysts, see: (a) Taylor, M. S.; Jacobsen, E. N. *Angew. Chem. Int. Ed.* **2006**, *45*, 1520. (b) Takemoto, Y. *J. Synth. Org. Chem. Jpn.* **2006**, *64*, 1139.(c) Connon, S. J. *Synlett* **2009**, *3*, 0354. (d) Sohtome, Y.; Nagasawa, K. *Synlett* **2010**, *1*, 1.(e) Auvil, T. J.; Schafer, A. G.; Mattson, A. E. *Eur. J. Org. Chem.* **2014**, *13*, 2633.

[3] For an elaborate procedure, see: Matthews, W. S.; Bares, J. E.; Bartmess, J. E.; Bordwell, F. G.; Cornforth, F. J.; Drucker, G. E.; Margolin, Z.; McCallum, R. J.; McCollum, G. J.; Vanier, N. R. *J. Am. Chem. Soc.* **1975**, *97*, 7006.

[4] Prof. Bordwell's group has determined the pK_a values of over 1200 compounds. For more information, see Bordwell, F. G. *Acc. Chem. Res.***1988**, *21*, 456.

soluble in DMSO, the polar aprotic solvent also suppress ion pairing, thus providing pK_a values termed "absolute".[5]

Figure 16: Previously Reported pK_a Values of Analogous Compounds in DMSO

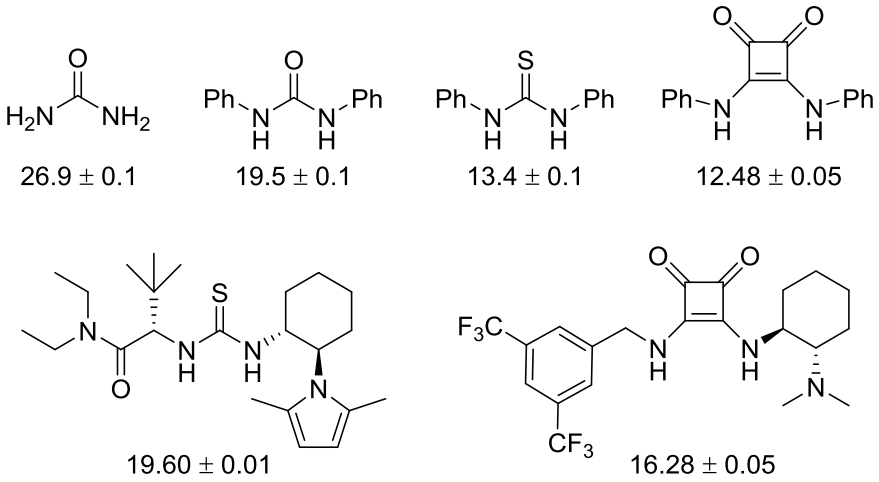

Cheng and co-workers determined the pK_a values of bifunctional thiourea and squaramide catalysts in DMSO.[6] Similarly, Schreiner and co-workers determined pK_a values of additional thiourea and urea organocatalysts.[7] Furthermore, pK_a values of TADDOLs and chiral Brønsted acids have also been reported.[8] While pK_a values of achiral thiosquaramides in acetonitrile-water (9:1 v/v) have been reported, however, to the best our knowledge, the pK_a values of thiosquaramides in DMSO are not known.[9] Inspired by reports of organocatalyst pK_a

[5] Bordwell, F. G.; Branca, J. C.; Hughes, D. L.; Olmstead, W. N. *J. Org. Chem.* **1980**, *45*, 3305.
[6] (a) Li, X.; Deng, H., Zhang, B.; Li, J.; Zhang, L.; Luo, S.; Cheng, J.-P. *Chem. Eur. J.* **2010**, *16*, 450. (b) Ni, X.; Li, X.; Wang, Z.; Cheng, J.-P. *Org. Lett.* **2014**, *16*, 1786.
[7] Jakab, G.; Tancon, C.; Zhang, Z.; Lippert, K. M.; Schreiner, P. R. *Org. Lett.* **2012**, *14*, 1724.
[8] (a) Christ, P.; Lindsay, A. G.; Vormittag, S. S.; Neudörfl, J.-M.; Berkessel, A.; O'Donoghue, A. C. *Chem. Eur. J.* **2011**, *17*, 8524. (b) Seebach, D.; Beck, A. K.; Bichsel, H. U.; Pichota, A.; Sparr, C.; Wünsch, R.; Schweizer, W. B. *HeIv. Chim. Acta* **2012**, *95*, 1303. (c) Kaupmees, K.; Tolstoluzhsky, N.; Raja, S.; Rueping, M.; Leito, I. *Angew. Chem., Int. Ed.* **2013**, *52*, 11569.
[9] Busschaert, N.; Elmes, R. B. P.; Czech, D. D.; Wu, X.; Kirby, I. L.; Peck, E. M.; Hendzel, K. D.; Shaw, S. K.; Chan, B.; Smith, B. D.; Jolliffe, K. A.; Gale, P. A.*Chem. Sci.* **2014**, *5*, 3617.

measurement by Cheng, Schreiner and Berkessel, we decided to determine the pK_a values of deltic ureas and thiosquaramides.[10]

Figure 17: Determination of pK_a Using the Overlapping Indicator Method

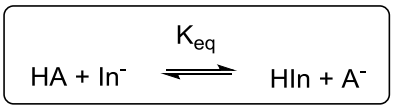

$$\Delta[In^-] = \Delta[HA]$$

$$pK_{HA} = pKH_{In} - \log_{10}K_{eq}$$

$$pK_{HA} = pKH_{In} - \log_{10}([HIn][A^-]/[In^-][HA])$$

The pK_a was measured by the spectrophotometric method of overlapping indicators. The method is based upon the equilibrium of the compound (HA), the indicator (HIn) and their anions (Figure 17). Determining the precise concentrations of the four species would afford the K_{eq}, thus affording the pK_a of the desired compound. A precondition for choosing an indicator is such that the indicator pKa should not be more than 1.5 units away from the compound's pK_a. However, as the compound's pK_a is not known, multiple indicators may be needed to evaluate the pK_a of a given compound, such that each indicator would only give an estimate until a measurement is made such that the pKa of the indicator is less than 1.5 units away from the determined pK_a of the compound.

A solution of K-dimsyl in DMSO is used as the starting point. As the indicator (HIn) solution in DMSO is added in measured increments to the K-dimsyl solution in DMSO, immediate formation of the indicator anion (In^-) solution results, and an increase in intensity is observed on the spectrophotometer. Once the K-dimsyl has exhausted, no further conversion of the indicator to the indicator anion is observed via the spectrophotometer. This saturation is intensity allows

[10] For pKa's of achiral ureas and thioureas, see: (a) Bordwell, F. G.; Algrim, D. J.; Harrelson, J. A. *J. Am. Chem. Soc.* **1988**, *110*, 5903. (b) Bordwell, F. G.; Ji, G. Z. *J. Am. Chem. Soc.* **1991**, *113*, 8398.

one to plot the Beer-Lambert plot and subsequently calculate the precise concentrations of HIn and In^-. The experiment is carried out at low concentrations, and owing to the high dielectric constant of DMSO, ion association can be neglected. Then, the compound (HA) whose acidity is to be measured is added in small increments, and the corresponding change in intensity is observed. Then, the equilibrium pK_a of the compound can then be calculated using the equations in Figure 17.[11]

IV.2 Initial Results

The pK_a values for compounds **122, 130, 215 and 231** in DMSO were determined using procedure described above (Table 23). The pK_a of a sample compound **231** was measured first, and found to be within range of reported value. When the pK_a of diphenyl deltic urea was measured using fluorene as the indicator, it was found to be out of range. A different indicator was hence used, and the pK_a of **122** was found to be 23.3. The pK_a of **130** was about 18.2. The pK_a of thiosquaramide **215** was then determined using **232** as the indicator and was found to be 13.96 ± 0.32. While a R^2 of 0.9999 was obtained with this measurement, a small drift was nonetheless observed in the pKa value. Nonetheless, further work would be needed to improvise upon these values.

[11] Please see the Experimental Section for a detailed discussion regarding pK_a measurement and calculation.

Table 23: Preliminary Data Towards the pK_a Values of Deltic Ureas and Thiosquaramides

Compound	Indicator	pK_a (Indicator)	pK_a (Compound)
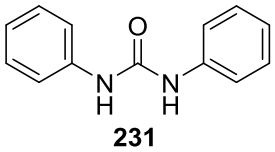 **231**	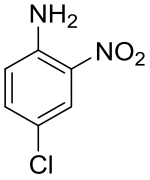 **232**	18.9	Reported value = 19.5 Experimental value = 19.48 ± 0.06
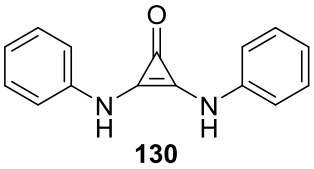 **130**	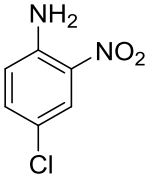 **232**	18.9	18.16 ± 0.29
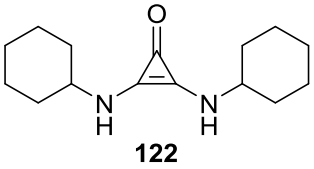 **122**	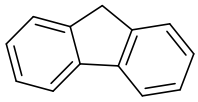 **233**	22.6	23.33 ± 0.23
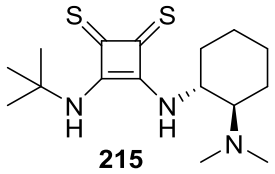 **215**	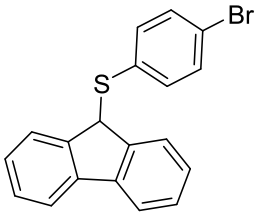 **234**	14.8	13.96 ± 0.32

IV.3 Concluding Remarks

In conclusion, we have employed Bordwell's method of overlapping indicators to get preliminary data on the pK_a values of two deltic ureas and one thiosquaramide. We hope that this data aids towards the rational design of these catalysts. In the experimental section, we describe the various pitfalls encountered towards successful measurements, and outline our measurements leading to an ideal Beer plots. While our measurements certainly help us rule out specific pK_a ranges for individual compounds, we hope to improve upon existing values reported herein.

CHAPTER V

EXPERIMENTAL SECTION

V.I General Information

General: Reactions were run in flame-dried glassware under an atmosphere of argon, with septa dried over P_2O_5. Methylene chloride was purified by passage over activated alumina, through an Innovative Technologies Solvent Drying system. Thin-layer chromatography (TLC) was performed using Whatman silica gel 60 Å F254 plates (250 μm) with F-254 fluorescent indicator and visualized by UV fluorescence quenching, ceric ammonium molybdate or potassium permanganate staining. SiliCycle SiliaFlash P60 silica gel (particle size 40–63 μm) was used for flash chromatography. NMR spectra were measured on Bruker DRX and DMX spectrometers at 500 MHz for ^1H spectra and 125 MHz for ^{13}C spectra and calibrated from either TMS ($\delta = 0$ for ^1H) or residual $CHCl_3$ ($\delta = 7.26$ for ^1H and $\delta = 77.0$ for ^{13}C). Mass spectral analysis was measured on Agilent technologies 6224 TOF LC/MS. Infrared spectra were recorded on a Nicolet 6700 FT-IR spectrometer and are reported in frequency of absorption (cm^{-1}) using NaBr salt plates using a thin film. Data are reported as follows: chemical shift, (multiplicity (s = singlet, d = doublet, t = triplet, q = quartet, ddd = doublet of doublet of doublets, dddd = doublet of doublet of doublet of doublets br = broad, m = multiplet), coupling constants in Hertz (Hz), and integration). ^{13}C NMR spectra were recorded on a Bruker DMX-500 instrument using residual solvent peaks as internal standards ($CDCl_3$ δ 77.23, CD_2Cl_2: δ 5.32 DMSO-d6: δ 39.51). Preparative HPLC (compounds **25 - 32**) consisted of the following components of a Waters system: Waters 2545 binary gradient module, Waters 515 HPLC pump, Waters 3100 quadrupole mass spectrometer, Waters system fluidics organizer, Waters 2767 sample manager, Waters 2489

dual channel UV-Vis detector, Waters 2424 evaporative light scattering detector, and Masslynx software v4.1. Preparative HPLC conditions: Waters X-bridge Prep C18 5 μm OBD 19×150 mm column, flow rate 19.0 mL/min, injection volume 1.0 mL; mobile phase A: water with 0.1% formic acid; mobile phase B: methanol with 0.1% formic acid; typical gradient: 0-1.25 min 40-63% B, 1.25-7.25 min 63-77% B, 7.25-8.25 min 77-92% B, 8.25-11.85 min 92-100% B, 11.85-12 min 100-40% B.

Materials: Distilled reagents were sealed under an inert atmosphere and stored in a freezer. All other reagents were stored in a desiccator.

V.2 Experimental Procedures and Characterization Data - Chapter I

V.2.1 Preparation of 1,2-Diazines

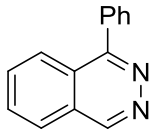

21

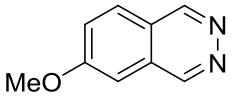

68

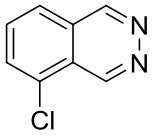

70

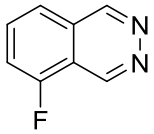

72

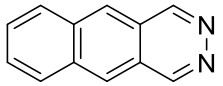

23

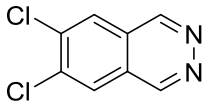

22

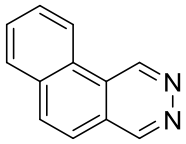

79

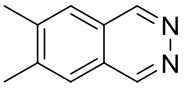

82

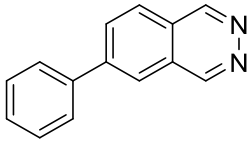

84

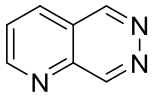

52

The previously known 1,2-diazines **22**[1], **23**[1], **82**[1], **52**[2], **68**[2], **70**[2], **72**[2], **79**[2], **84**[2] were prepared according to reported procedures.

[1] Türkmen, Y. E.; Montavon, T. J.; Kozmin, S. A.; Rawal, V. H. *J. Am. Chem. Soc.* **2012**, *134*, 9062.
[2] Kessler, S. N., Wegner, H. A. *Org. Lett.* **2012**, *14*, 3268.

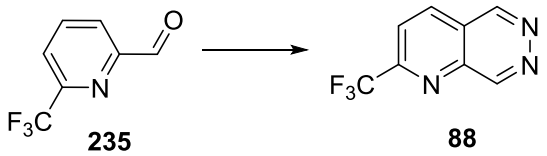

Compound **88** was prepared by modifying a procedure reported by Wegner and co-workers.[2] *n*-BuLi (2.00 ml, 3.20 mmol, 1.6 M in hexane, 1.07 equiv) was added dropwise under nitrogen to a stirred solution of *bis*(2-methoxyethyl)amine (0.49 mL, 3.30 mmol, 1.10 equiv) in a mixture of anhydrous hexanes (10 ml) and THF (2.5 ml) at –25 °C. After the addition, the mixture was stirred at –25 °C for 30 min to form the lithium amide. A solution of 6-(trifluoromethyl)pyridine-2-carboxaldehyde **235** (525.3 mg, 3.00 mmol, 1.00 equiv) in THF (2 mL) was added dropwise over a period of 30 min at –25 °C. The reaction mixture was stirred at -20 °C for 45 min and additional *n*-BuLi (2.80 ml, 4.50 mmol, 1.6 M in hexane, 1.50 equiv) was added at -20 °C. The reaction mixture was then stirred for another 2 h at the same temperature. After cooling to –78 °C, THF (3 ml) and DMF (0.70 ml, 9.0 mmol, 3.00 equiv) were added, and the resulting mixture was stirred for 10 min. It was then allowed to warm to 0 °C and stirred for 1.5 h. The reaction was quenched with a solution of NH_4Cl (0.48 g, 9.0 mmol, 3.00 equiv) and $N_2H_4 \bullet H_2O$ (0.70 ml, 11.5 mmol, 80% in H_2O, 3.80 equiv) in H_2O (3 ml). The reaction was allowed to warm to room temperature and stirred overnight. It was then diluted with ethyl acetate (10 ml) and the two phases were partitioned. The aqueous phase was extracted with ethyl acetate (3 × 15 ml), and the combined organic layers were dried over $MgSO_4$, filtered and thoroughly concentrated *in vacuo* to remove DMF. Purification by two successive flash column chromatographies over SiO_2 (first with 1:2 acetone:hexanes and second with ethyl acetate as eluent) afforded product **88** (401 mg, 67% yield) as a pale yellow solid.

88: ^{1}H NMR (500 MHz, $CDCl_3$) δ 9.95 (s, 1H), 9.74 (s, 1H), 8.59 (d, *J* = 8.5 Hz, 1H), 8.21 (d, *J* = 8.5 Hz, 1H).

^{13}C NMR (125 MHz, $CDCl_3$) δ 154.2, 153.9, 152.8, 150.4, 140.8, 137.0, 123.46, 123.44, 122.4, 121.6, 119.4.

^{19}F NMR (470 MHz, $CDCl_3$) δ -68.1.

HRMS (ESI) calcd for $C_8H_5F_3N_3^+$ $(M+H)^+$: 200.0430, Found: 200.0428.

R_f 0.30-0.40 (ethyl acetate).

Melting Point 147-148 °C.

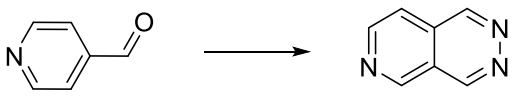

236 **53**

Compound **53** was prepared by modifying a procedure reported by Wegner and co-workers[1]. *n*-BuLi (4.00 ml, 6.40 mmol, 1.6 M in hexane, 1.07 equiv) was added dropwise under nitrogen to a stirred solution of *bis*(2-methoxyethyl)amine (0.98 mL, 6.60 mmol, 1.10 equiv) in a mixture of anhydrous hexanes (10 ml) and THF (6 ml) at –25 °C. After the addition, the mixture was stirred at –25 °C for 30 min to form the lithium amide. A solution of 4-pyridinecarboxaldehyde **236** (643 mg, 6.00 mmol, 1.00 equiv) in THF (5 mL) was added dropwise over a period of 1 hour at –25 °C. The reaction mixture was stirred for 45 min and additional *n*-BuLi (5.60 ml, 9.00 mmol, 1.6 M in hexane, 1.50 equiv) was added at –25 °C. The reaction mixture was then stirred for another 2 h at the same temperature. After cooling to –78 °C, THF (5 ml) and DMF (1.40 ml, 18.0 mmol, 3.00 equiv) were added, and the resulting mixture was stirred for 10 min. It was then allowed to warm to 0 °C and stirred for 1.5 h. The reaction was quenched with a solution of NH_4Cl (0.96 g, 18.0 mmol, 3.00 equiv) and N_2H_4•H_2O (0.70 ml, 11.5 mmol, 80% in H_2O, 1.90 equiv) in H_2O (5 ml). The reaction was allowed to warm to room temperature and stirred overnight. It was then diluted with ethyl acetate (15 ml) and the two phases were partitioned. The

aqueous phase was extracted with ethyl acetate (3 × 20 ml), and the combined organic layers were dried over $MgSO_4$, filtered and concentrated *in vacuo*. Purification by flash column chromatography over SiO_2 (3:1-20:1 EtOAc:hexanes) afforded product **53** (208 mg, 26% yield) as a pale yellow solid.

53: ^{1}H NMR (500 MHz, $CDCl_3$) δ 9.70 (s, 1H), 9.68 (s, 1H), 9.51 (s, 1H), 9.10 (d, *J* = 5.8 Hz, 1H), 7.82 (d, *J* = 5.8 Hz, 1H)

^{13}C NMR (125 MHz, $CDCl_3$) δ 151.3, 150.43, 150.42, 149.6, 128.7, 120.5, 117.9

HRMS (ESI) calcd for $C_7H_6N_3^+$ $(M+H)^+$: 132.0556, Found: 132.0556

R_f 0.25-0.35 (10% methanol in ethyl acetate)

Melting Point 168 °C

V.2.2 Preparation of Siloxy Alkynes

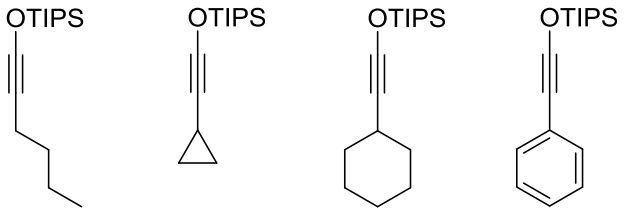

11 **237** **238** **239**

Siloxy alkynes **11**[3], **237**[4], **238**[4] and **239**[5] were prepared according to reported procedures.

V.2.3 Three-component [2+2+2] cycloaddition reactions to form mixed products

[3] Shubinets, V., Schramm, M. P., Kozmin, S. A. *Org. Synth*. **2010**, *87*, 253.
[4] Montavon, T. J., Li, J., Cabrera-Pardo, J. R., Mrksich, M., Kozmin, S. A. *Nat. Chem*. **2012**, *4*, 45.
[5] Sun, J., Keller, V. A., Meyer, S. T., Kozmin, S. A. *Adv. Synth. Catal.* **2010**, *352*, 839.

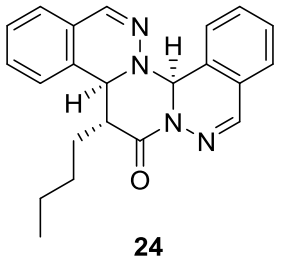

24

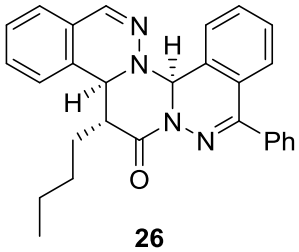

26

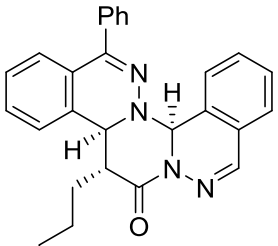

27

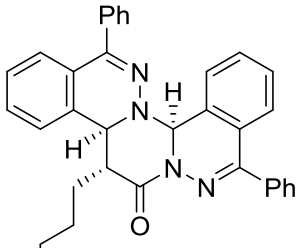

25

(6b*RS*,13b*SR*,14*RS*)-14-Butyl-13b,14-dihydropyrimido[2,1-a:4,3-a']diphthalazin-15(6bH)-one (**24**), **(6b*RS*,13b*SR*,14*RS*)-14-Butyl-2-phenyl-13b,14-dihydropyrimido[2,1-a:4,3-a']diphthalazin-15(6bH)-one** (**26**), **(6b*RS*,13b*SR*,14*RS*)-14-Butyl-9-phenyl-13b,14-dihydropyrimido[2,1-a:4,3-a']diphthalazin-15(6bH)-one** (**27**) **and (6b*RS*,13b*SR*,14*RS*)-14-Butyl-2,9-diphenyl-13b,14-dihydropyrimido[2,1-a:4,3-a']diphthalazin-15(6bH)-one** (**25**).

The three-component reaction was carried out following the general cycloaddition procedure with siloxy alkyne **11** (62.1 μL, 50.9 mg, 0.2 mmol), phthalazine **4** (39.0 mg, 0.3 mmol) and 1-phenylphthalazine **21** (61.9 mg, 0.3 mmol). The residue was purified by flash chromatography (DCM – 30% EtOAc/DCM) to give mainly two product mixtures. These two product mixtures were then further purified by preparative thin layer chromatography to afford 11.7 mg of **24** (0.0326 mmol, 16% yield), 11.3 mg of **26** (0.0260 mmol, 13% yield), 12.9 mg of **27** (0.0297 mmol, 15% yield) and 11.8 mg of **25** (0.0231 mmol, 12% yield) as white solids. While the ^{1}H

NMR assignments for **24** and **25** matched those reported in collaboration with Prof. Sergey A. Kozmin,[6] the tentative assignments for **26** and **27** are as follows:

26: ^{1}H NMR (500 MHz, $CDCl_3$, 295 K) δ 7.73 (s, 1H), 7.57-7.48 (m, 3H), 7.46-7.38 (m, 5H), 7.37-7.32 (m, 3H), 7.32-7.28 (m, 2H), 6.64 (s, 1H), 4.64 (d, *J* = 12 Hz, 1H), 3.17 (dt, J = 16.5, 4.0 Hz, 1H), 2.07-1.98 (m, 1H), 1.63-1.50 (m, 1H), 1.47-1.28 (m, 3H), 0.92 (t, *J* = 7.0 Hz, 3H); ^{13}C NMR (125 MHz, $CDCl_3$, 295 K) δ 169.2, 152.2, 143.9, 135.4,135.0, 131.4, 131.0, 130.4, 129.0, 128.7, 128.6, 128.3, 126.9, 126.6, 126.4, 124.7, 124.1, 74.1, 57.8, 41.9, 28.1, 26.2, 23.0, 14.0; HRMS (ESI) calculated for $C_{28}H_{27}N_4O$ $[M+H]^+$ 435.2185, found 435.2177.

27: ^{1}H NMR (500 MHz, $CDCl_3$, 295 K) δ 7.81 (s, 1H), 7.70-7.64 (m, 2H), 7.55-7.42 (7H), 7.37-7.31 (m, 3H), 7.24-7.20 (m, 1H), 6.64 (s, 1H), 4.63 (d, *J* = 11.5 Hz, 1H), 3.15 (dt, J = 11.5, 4.0 Hz, 1H), 2.01-1.92 (m, 1H), 1.58-1.42 (m, 2H), 1.42-1.23 (m, 3H), 0.91 (t, *J* = 7.0 Hz, 3H); ^{13}C NMR (125 MHz, $CDCl_3$, 295 K) δ 169.4, 152.7, 143.6, 135.3, 133.4, 131.3, 131.2, 131.0, 129.5, 129.2, 128.9, 128.4, 128.3, 127.6, 126.8, 126.0, 125.9, 125.0, 123.9, 73.7, 57.4, 42.1, 28.0, 26.2, 23.0, 13.9; HRMS (ESI) calculated for $C_{28}H_{27}N_4O$ $[M+H]^+$ 435.2185, found 435.2176.

[6] Montavon, T. J.; Türkmen, Y. E.; Shamsi, N. A.; Miller, C.; Sumaria, C. S.; Rawal, V. H.; Kozmin, S. A. *Angew. Chem. Int. Ed.* **2013**, *52*, 13576.

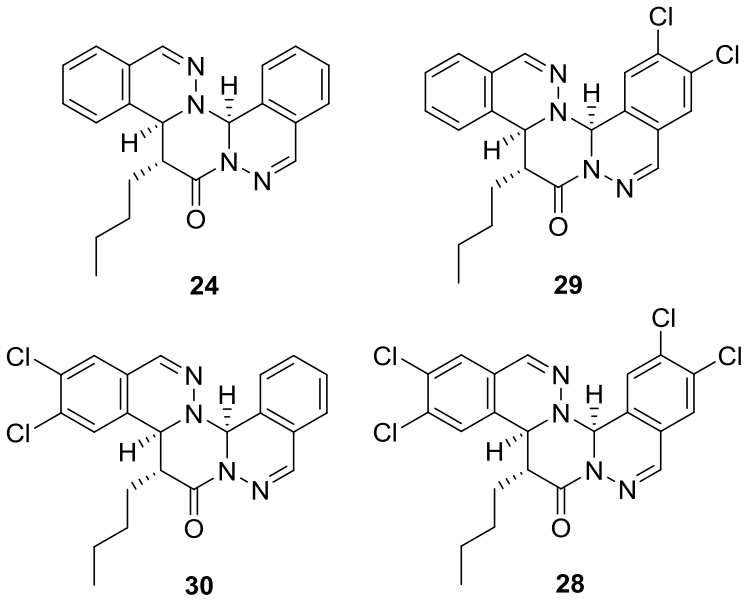

(6b*RS*,13b*SR*,14*RS*)-14-Butyl-13b,14-dihydropyrimido[2,1-a:4,3-a']diphthalazin-15(6bH)-one (**24**), **(6b*RS*,13b*SR*,14*RS*)-14-butyl-4,5 -dichloro-13b,14-dihydropyrimido[2,1-a:4,3-a']diphthalazin-15(6bH)-one** (**29**), **(6b*RS*,13b*SR*,14*RS*)-14-butyl-11,12-dichloro-13b,14-dihydropyrimido[2,1-a:4,3-a']diphthalazin-15(6bH)-one** (**30**) **and (6b*RS*,13b*SR*,14*RS*)-14-butyl-4,5,11,12-tetrachloro-13b,14-dihydropyrimido[2,1-a:4,3-a']diphthalazin-15(6bH)-one** (**28**).

The three-component reaction was carried out following the general cycloaddition procedure with siloxy alkyne **11** (62.1 μL, 50.9 mg, 0.2 mmol), phthalazine **4** (39.0 mg, 0.3 mmol) and 6,7-dichlorophthalazine **22** (59.7 mg, 0.3 mmol). The residue was purified by preparative HPLC to afford 1.5 mg of **24** (0.0042 mmol, 2% yield), 17.5 mg of **29** (0.041 mmol, 21% yield), 10.4 mg of **30** (0.024 mmol, 12% yield) and 8.0 mg of **28** (0.016 mmol, 8% yield) as white solids. While the ^{1}H NMR assignments for **24** and **28** matched those reported in collaboration with Prog. Sergey A. Kozmin,[6] the tentative assignments for **29** and **30** are as follows:

29: ^{1}H NMR (500 MHz, $CDCl_3$, 295 K) δ 7.71 (s, 1H), 7.69 (s, 1H), 7.50-7.45 (m, 1H), 7.43-7.36 (m, 3H), 7.34-7.30 (m, 1H), 7.28 (s, 1H), 6.60 (s, 1H), 4.57 (d, *J* = 11.5 Hz, 1H), 3.06 (dt, *J* = 11.0, 4.5 Hz), 2.05-1.96 (m, 1H), 1.55-1.44 (m, 2H), 1.44-1.30 (m, 3H), 0.93 (t, *J* = 7.0 Hz, 3H); ^{13}C NMR (125 MHz, $CDCl_3$, 295 K) δ 168.7, 143.1, 141.3, 134.9, 133.2, 132.5, 131.9, 129.4, 129.2, 127.9, 127.5, 126.8, 126.5, 124.2, 123.2, 73.3, 56.7, 42.8, 27.9, 26.5, 22.9, 13.9; HRMS (ESI) calculated for $C_{22}H_{21}Cl_2N_4O$ $[M+H]^+$ 427.1092, found 427.1089.

30: ^{1}H NMR (500 MHz, $CDCl_3$, 295 K) δ 7.78 (s, 1H), 7.63 (s, 1H), **7**.52 (s, 1H), 7.50 (td, *J* = 7.5, 1.0 Hz, 1H), 7.46 (td, *J* = 7.5, 1.0 Hz), 7.40 (s, 1H), 7.35 (dd, *J* = 7.3, 1.2 Hz, 1H), 7.19 (d, *J* = 7.0 Hz, 1H), 6.52 (s, 1H), 4.57 (d, *J* = 11.5 Hz, 1H), 3.08 (dt, *J* = 11.5, 4.5 Hz, 1H), 2.02-1.94 (m, 1H), 1.55-1.44 (m, 1H), 1.41-1.27 (m, 3H), 0.91 (t, *J* = 7.0 Hz, 3H); ^{13}C NMR (125 MHz, $CDCl_3$, 295 K) δ 169.2, 144.2, 140.5, 136.0, 133.7, 133.0, 131.6, 129.4, 129.1, 129.0, 128.0, 126.2, 126.0, 124.1, 123.5, 72.7, 57.3, 42.9, 27.9, 26.4, 22.9, 13.9; HRMS (ESI) calculated for $C_{22}H_{21}Cl_2N_4O$ $[M+H]^+$ 427.1092, found 427.1089.

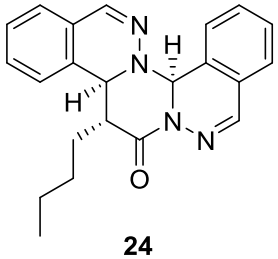

24

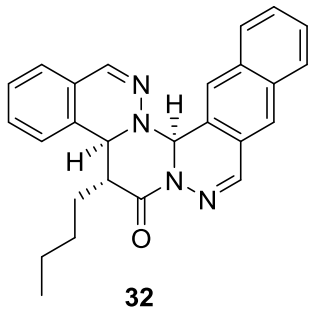

32

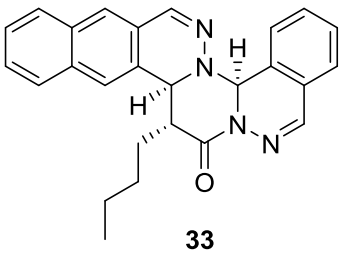

33

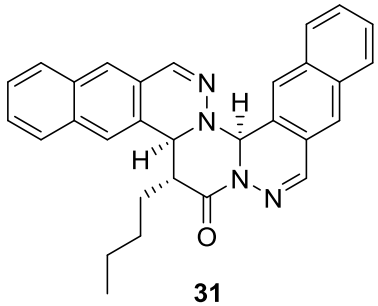

31

(6b*RS*,13b*SR*,14*RS*)-14-Butyl-13b,14-dihydropyrimido[2,1-a:4,3-a']diphthalazin-15(6bH)-one (**24**), **Lactams 31, 32 and 33**.

The three-component reaction was carried out following the general cycloaddition procedure with siloxy alkyne **11** (62.1 μL, 50.9 mg, 0.2 mmol), phthalazine **4** (39.0 mg, 0.3 mmol) and benzo[g]phthalazine **23** (54.1 mg, 0.3 mmol). The residue was purified by preparative HPLC to afford 37.4 mg of **32** (0.0916 mmol, 46% yield) and 20.6 mg of **31** (0.0449 mmol, 23% yield) as white solids. While the ^{1}H NMR assignment for **31** matched that reported in collaboration with Prof. Sergey A. Kozmin,[6] the tentative assignment for **32** is as follows:

32: ^{1}H NMR (500 MHz, $CDCl_3$, 295 K) δ 7.93-7.87 (m, 3H), 7.79 (s, 1H), 7.71 (s, 1H), 7.61-7.53 (m, 3H), 7.49-7.44 (m, 2H), 7.42-7.37 (m, 1H), 7.33-7.29 (m, 1H), 6.66 (s, 1H), 4.76 (d, *J* = 11.0 Hz, 1H), 3.14 (dt, J = 11.0, 4.5 Hz, 1H), 2.08-1.99 (m, 1H), 1.65-1.50 (m, 2H), 1.47-1.20 (m, 3H), 0.93 (t, *J* = 7.0 Hz, 3H); ^{13}C NMR (125 MHz, $CDCl_3$, 295 K) δ 169.1, 143.6, 142.9, 134.4, 133.3, 131.8, 130.7, 129.9, 129.0, 128.8, 127.9, 127.7, 127.0, 126.7, 126.6, 126.0, 124.8, 124.4, 121.5 73.5, 58.2, 43.1, 27.9, 26.8, 23.0, 13.9; HRMS (ESI) calculated for $C_{26}H_{25}N_4O$ $[M+H]^+$ 409.2028, found 409.2022.

V.2.4 The Formal [4+2] Cycloaddition Reaction of 1,2-Diazines and Siloxy Alkynes

General procedure 1 for the cycloaddition reaction of 1,2-diazines and siloxy alkynes catalyzed by $Cu(MeCN)_4PF_6$

Tetrakis(acetonitrile)copper(I) hexafluorophosphate, $Cu(MeCN)_4PF_6$ (typically 0.1 equiv) and 1,2-diazine (1.0 equiv) were added to a a flame-dried test-tube or a round-bottomed flask equipped with a stir bar. The test-tube/round-bottom flask is then subjected to vacuum, flushed with argon, sealed with a septum, and connected to an argon balloon to maintain positive argon

pressure throughout the remainder of the experiment. A stock solution of 2,2′-bipyridine (0.075-0.15 equiv) in CH_2Cl_2 was then used to add 2,2′-bipyridine via a syringe, followed by the addition of remaining CH_2Cl_2. This mixture was allowed to stir for 15 minutes before the addition of recently distilled siloxy alkyne (1.5-2.0 equiv) using a syringe, and the reaction monitored by thin-layer chromatography (TLC). After consumption of 1,2-diazine, the reaction was quenched by passing the reaction mixture through a plug of silica (washing with CH_2Cl_2), and was concentrated under reduced pressure. The excess unreacted siloxy alkyne was removed by Kugelrohr distillation, and the purified product was obtained by flash column chromatography.

General procedure 2 for the cycloaddition reaction of 1,2-diazines and siloxy alkynes catalyzed by $Ni(CO)_2(PPh_3)_2$

Bis(triphenylphosphine)nickel dicarbonyl, $Ni(CO)_2(PPh_3)_2$ (typically 0.1 equiv) and 1,2-diazine were added to a flame-dried test-tube equipped with a stir bar. This test-tube was then subjected to vacuum, flushed with argon, sealed with a septum, and connected to an argon balloon to maintain positive argon pressure throughout the remainder of the experiment. CH_2Cl_2 was added by a syringe and the mixture was allowed to stir for 15 minutes before the addition of freshly distilled siloxy alkyne (1.5-2.0 equiv) using another syringe. After complete consumption of 1,2-diazine (as monitored by TLC), the reaction was quenched by passing the reaction mixture through a plug of silica (washing with hexanes), and was concentrated under reduced pressure. The excess unreacted siloxy alkyne was removed by Kugelrohr distillation, and the purified product was obtained by flash column chromatography.

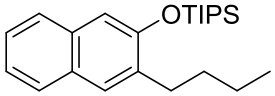

67

(3-butyl-naphth-2-yloxy)triisopropylsilane 67

General procedure 1 was employed for the cycloaddition of phthalazine **4** (65.1 mg, 0.5 mmol, 1.0 equiv) and 1-(triisopropylsiloxy)-1-hexyne **11** (254 mg, 1.0 mmol, 2.0 equiv) using a catalyst combination of tetrakis(acetonitrile)copper(I) hexafluorophosphate (18.6 mg, 0.05 mmol, 0.1 equiv) and 2,2′-bipyridine (5.86 mg, 0.0375 mmol, 0.075 equiv) in 1.0 mL of CH_2Cl_2. The reaction was quenched after a period of 4 h. Flash column chromatography (after Kuglerohr distillation) with hexanes as the eluent afforded compound **67** (143 mg, 80%) as a colorless oil.

General procedure 2 was employed for the cycloaddition of phthalazine **4** (65.1 mg, 0.5 mmol, 1.0 equiv) and 1-(triisopropylsiloxy)-1-hexyne **11** (254 mg, 1.0 mmol, 2.0 equiv) using bis(triphenylphosphine)nickel(0) dicarbonyl (32.0 mg, 0.05 mmol, 0.1 equiv) as catalyst in 1.0 mL of CH_2Cl_2. The reaction was quenched after a period of 24 h. Flash column chromatography (after Kuglerohr distillation) with hexanes as the eluent afforded compound **67** (143 mg, 80%) as a colorless oil.

^{1}H NMR (500 MHz, $CDCl_3$) δ 7.69 (d, *J* = 8.0 Hz, 1H), 7.62 (d, *J* = 8.0 Hz, 1H), 7.56 (s, 1H), 7.34 (dt, *J* = 8.1, 1.2, Hz, 1H), 7.28 (dt, *J* = 7.5, 1.2 Hz, 1H), 7.09 (s, 1H), 2.77 (t, *J* = 7.8 Hz, 2H), 1.68-1.63 (m, 2H), 1.44-1.37 (m, 5H), 1.15 (d, *J* = 7.5 Hz, 18H), 0.95 (t, *J* = 7.3 Hz ,3H)

^{13}C NMR (125 MHz, $CDCl_3$) δ 153.0, 135.0, 133.2, 129.0, 128.2, 127.0, 126.0, 125.1, 123.4, 112.4, 32.2, 31.2, 22.8, 18.1, 14.1, 13.1

HRMS (ESI) calcd for $C_{23}H_{37}OSi^+$ $(M+H)^+$: 357.2608, Found: 357.2605

IR (film): 2945, 2867, 1499, 1466, 1258, 1180, 929, 882, 862, 744, 685 cm^{-1}

R_f 0.57 (hexanes)

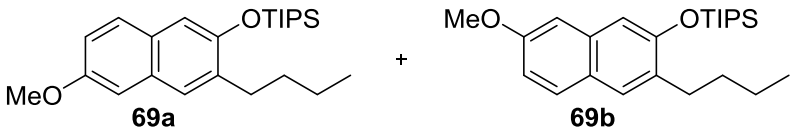

69a **69b**

(3-butyl-6-methoxy-naphth-2-yloxy)triisopropylsilane 69a and (3-butyl-7-methoxy-naphth-2-yloxy)triisopropylsilane 69b:

General procedure 1 was employed for the cycloaddition of 6-methoxy phthalazine **68** (80.1 mg, 0.5 mmol, 1.0 equiv) and 1-(triisopropylsiloxy)-1-hexyne **11** (254 mg, 1.0 mmol, 2.0 equiv) using a catalyst combination of tetrakis(acetonitrile)copper(I) hexafluorophosphate (18.6 mg, 0.05 mmol, 0.1 equiv) and 2,2′-bipyridine (11.7 mg, 0.075 mmol, 0.15 equiv) in 3.0 mL of CH_2Cl_2. The reaction was quenched after a period of 8 h. Flash column chromatography (after Kuglerohr distillation) with 2% EtOAc in hexanes as the eluent afforded 155 mg (80%) of a product mixture consisting of regioisomers **69a** and **69b** (**69a**:**69b** = 50:50) as a pale yellow oil.

General procedure 2 was employed for the coupling of 6-methoxy phthalazine **68** (80.1 mg, 0.5 mmol, 1.0 equiv) and 1-(triisopropylsiloxy)-1-hexyne **11** (254 mg, 1.0 mmol, 2.0 equiv) using bis(triphenylphosphine)nickel(0) dicarbonyl (32.0 mg, 0.05 mmol, 0.1 equiv) as catalyst in 3.0 mL of CH_2Cl_2. The reaction was quenched after a period of 24 h. Flash chromatography (after Kuglerohr distillation) with 2% EtOAc in hexanes as the eluent afforded 144 mg (75%) of a product mixture consisting of regioisomers **69a** and **69b** (**69a**:**69b** = 62:38) as a pale yellow oil.

69a: ^{1}**H NMR** (500 MHz, $CDCl_3$) δ 7.52 (d, *J* = 9 Hz, 1H), 7.47 (s, 1H), 7.06-6.99 (m, 2H), 6.97-6.92 (m, 1H), 3.88 (s, 3H), 2.76 (t, *J* = 8.0 Hz, 2H), 1.70-1.60 (m, 2H), 1.46-1.34 (m, 5H), 1.14 (d, *J* = 7.5 Hz, 18H), 0.95 (t, *J* = 7.5 Hz, 3H)

69b: ^{1}**H NMR** (500 MHz, $CDCl_3$) δ 7.58 (d, *J* = 8.5 Hz, 1H), 7.48 (s, 1H), 7.06-6.99 (m, 2H), 6.97-6.92 (m, 1H), 3.90 (s, 3H), 2.73 (t, *J* = 8.0 Hz, 2H), 1.70-1.60 (m, 2H), 1.46-1.34 (m, 5H), 1.16 (t, *J* = 7.5 Hz, 18H), 0.94 (t, *J* = 7.0 Hz, 3H)

^{13}C NMR (125 MHz, $CDCl_3$) δ 157.4, 156.1, 153.6, 151.3, 135.3, 134.3, 132.3, 129.8, 128.5, 128.4, 128.0, 127.5, 127.1, 124.5, 117.7, 115.9, 112.5, 111.8, 105.4, 104.4, 55.2 (2C), 32.32, 32.25, 31.18, 30.96, 22.8 (2C), 18.14, 18.13 14.1 (2C), 13.14, 13.10

HRMS (ESI) calcd for $C_{24}H_{39}O_2Si^+$ $(M+H)^+$: 387.2714, Found: 387.2715

IR (film): 2946, 2867, 1504, 1464, 1390, 1251, 883 cm^{-1}

R_f 0.20 (2% EtOAc in hexanes)

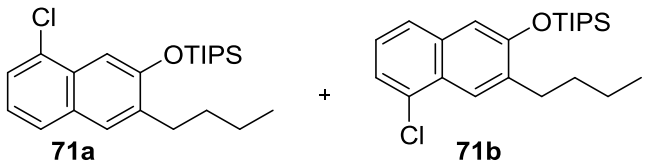

(3-butyl-8-chloro-naphth-2-yloxy)triisopropylsilane 71a and (3-butyl-5-chloro-naphth-2-yloxy)triisopropylsilane 71b:

General procedure 1 was employed for the cycloaddition of 5-chloro phthalazine **70** (82.3 mg, 0.5 mmol, 1.0 equiv) and 1-(triisopropylsiloxy)-1-hexyne **11** (254 mg, 1.0 mmol, 2.0 equiv) using a catalyst combination of tetrakis(acetonitrile)copper(I) hexafluorophosphate (18.6 mg, 0.05 mmol, 0.1 equiv) and 2,2′-bipyridine (7.8 mg, 0.05 mmol, 0.10 equiv) in 1.5 mL of CH_2Cl_2. The reaction was quenched after a period of 5 h. Flash column chromatography (after Kuglerohr distillation) with hexanes as the eluent afforded 155 mg (79%) of a product mixture consisting of regioisomers **71a** and **71b** (**71a**:**71b** = 55:45) as a colorless oil.

General procedure 2 was employed for the coupling of 5-chloro phthalazine **70** (82.3 mg, 0.5 mmol, 1.0 equiv) and 1-(triisopropylsiloxy)-1-hexyne **11** (254 mg, 1.0 mmol, 2.0 equiv) using bis(triphenylphosphine)nickel(0) dicarbonyl (32.0 mg, 0.05 mmol, 0.1 equiv) as catalyst in 1.5 mL of CH_2Cl_2. The reaction was quenched after a period of 24 h. Flash column chromatography

(after Kuglerohr distillation) with hexanes as the eluent afforded 145 mg (74%) of a product mixture consisting of regioisomers **71a** and **71b** (**71a**:**71b** = 74:26) as a colorless oil.

71a: ^{1}H NMR (500 MHz, $CDCl_3$) δ 7.61 (d, *J* = 8.5 Hz, 1H), 7.57 (s, 1H), 7.55 (s, 1H), 7.44 (dd, *J* = 7.5, 1.1 Hz, 1H), 7.19 (t, *J* = 7.5 Hz, 1H), 2.78 (t, *J* = 8.0 Hz, 2H), 1.71-1.62 (m, 2H), 1.48-1.36 (m, 5H), 1.17 (d, *J* = 7.5 Hz, 18H), 0.95 (t, *J* = 7.5 Hz, 3H)

71b: ^{1}H NMR (500 MHz, $CDCl_3$) δ 7.98 (s, 1H), 7.55-7.52 (m, 1H), 7.364 (dd, *J* = 7.5, 1.1 Hz, 1H), 7.24 (t, *J* = 8.0 Hz, 1H), 7.10 (s, 1H), 2.82 (t, *J* = 8.0 Hz, 2H), 1.71-1.62 (m, 2H), 1.48-1.36 (m, 5H), 1.15 (d, *J* = 8.5 Hz, 18H), 0.96 (t, *J* = 7.3 Hz, 3H)

^{13}C NMR (125 MHz, $CDCl_3$) δ 154.1, 153.7, 136.4, 135.9, 134.5, 131.2, 130.7, 130.0, 129.9, 128.6, 126.1, 125.29, 125.26, 125.1, 124.9, 123.7, 123.2, 123.1, 112.7, 109.3, 32.3, 32.1, 31.4, 31.0, 22.84, 22.77, 18.13, 18.10, 14.06, 14.05, 13.1, 13.0

HRMS (ESI) calcd for $C_{23}H_{36}ClOSi^{+}$ $(M+H)^{+}$: 391.2218, Found: 391.2225

IR (film): 2946, 2867, 1493, 1460, 1263, 1127, 882, 833, 681 cm^{-1}

R_f 0.74 (hexanes)

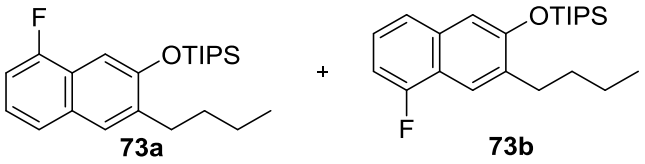

73a **73b**

(3-butyl-8-fluoro-naphth-2-yloxy)triisopropylsilane 73a and (3-butyl-5-fluoro-naphth-2-yloxy)triisopropylsilane 73b:

General procedure 1 was employed for the cycloaddition of 5-fluoro phthalazine **72** (74.1 mg, 0.5 mmol, 1.0 equiv) and 1-(triisopropylsiloxy)-1-hexyne **11** (254 mg, 1.0 mmol, 2.0 equiv) using a catalyst combination of tetrakis(acetonitrile)copper(I) hexafluorophosphate (18.6 mg, 0.05 mmol, 0.1 equiv) and 2,2′-bipyridine (7.8 mg, 0.05 mmol, 0.10 equiv) in 3.5 mL of CH_2Cl_2.

The reaction was quenched after a period of 3.5 h. Flash column chromatography (after Kuglerohr distillation) with hexanes as the eluent afforded 141.5 mg (76%) of a product mixture consisting of regioisomers **73a** and **73b** (**73a**:**73b** = 50:50) as a colorless oil.

General procedure 2 was employed for the coupling of 5-fluoro phthalazine **72** (74.1 mg, 0.5 mmol, 1.0 equiv) and 1-(triisopropylsiloxy)-1-hexyne **11** (254 mg, 1.0 mmol, 2.0 equiv) using bis(triphenylphosphine)nickel(0) dicarbonyl (32.0 mg, 0.05 mmol, 0.1 equiv) as catalyst in 3.5 mL of CH_2Cl_2. The reaction was quenched after a period of 48 h. Flash column chromatography (after Kuglerohr distillation) with hexanes as the eluent afforded 131 mg (70%) of a product mixture consisting of regioisomers **73a** and **73b** (**73a**:**73b** = 67:33) as a colorless oil.

73a: ^{1}**H NMR** (500 MHz, $CDCl_3$) δ 7.58 (s, 1H), 7.47 (d, *J* = 8.3 Hz, 1H), 7.33 (s, 1H), 7.21-7.15 (m, 1H), 7.01 (ddd, *J* = 10.9, 7.7, 0.9 Hz, 1H), 2.82-2.75 (m , 2H), 1.71-1.62 (m, 2H), 1.48-1.36 (m, 5H), 1.16 (d, *J* = 7.5 Hz, 18H) , 0.95 (t, *J* = 7.4 Hz, 3H)

73b: ^{1}**H NMR** (500 MHz, $CDCl_3$) δ 7.83 (s, 1H), 7.39 (d, *J* = 8.3 Hz, 1H), 7.27-7.22 (m, 1H), 7.10 (d, *J* = 1.8 Hz, 1H), 6.94 (ddd, *J* = 11.1, 7.7, 0.9, 1H), 2.82-2.75 (m, 2H), 1.71-1.62 (m, 2H), 1.48-1.36 (m, 5H), 1.15 (d, *J* = 7.5 Hz, 18H), 0.95 (t, *J* = 7.4 Hz, 3H)

^{13}**C NMR** (125 MHz, $CDCl_3$) δ 159.7, 158.8, 157.7, 156.8, 153.9, 153.4, 136.1, 135.6, 135.5, 135.1, 130.7, 130.6, 128.1, 128.0, 125.1, 125.0, 123.4, 123.2, 122.9, 122.8, 122.7, 122.6, 121.8, 120.9, 120.8, 119.1, 119.0, 112.2, 108.7, 108.5, 107.1, 106.9, 105.1, 32.2, 32.1, 31.3, 31.2, 22.8, 18.1, 14.1, 13.1, 13.0

73a: ^{19}**F NMR** (470 MHz, $CDCl_3$) δ -125.0

73b: ^{19}**F NMR** (470 MHz, $CDCl_3$) δ -124.1

HRMS (ESI) calcd for: $C_{23}H_{36}FOSi^{+}$ $(M+H)^{+}$: 375.2514, Found: 375.2495

IR (film): 2946, 2868, 1607, 1497, 1457, 1262, 1211, 1150, 908, 883, 866, 685 cm^{-1}

R_f 0.56 (hexanes)

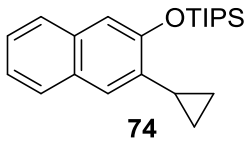

74

(3-cyclopropyl-naphth-2-yloxy)triisopropylsilane 74

General procedure 1 was employed for the cycloaddition of phthalazine **4** (65.1 mg, 0.5 mmol, 1.0 equiv) and 2-cyclopropyl-1-(triisopropylsiloxy)ethyne **237** (238 mg, 1.0 mmol, 2.0 equiv) using a catalyst combination of tetrakis(acetonitrile)copper(I) hexafluorophosphate (18.6 mg, 0.05 mmol, 0.1 equiv) and 2,2′-bipyridine (5.86 mg, 0.0375 mmol, 0.075 equiv) in 1.3 mL of CH_2Cl_2. The reaction was quenched after a period of 2.5 h. Flash column chromatography (after Kuglerohr distillation) with hexanes as the eluent afforded 124 mg (73%) of compound **74** as a colorless oil.

General procedure 2 was employed for the coupling of phthalazine **4** (65.1 mg, 0.5 mmol, 1.0 equiv) and 2-cyclopropyl-1-(triisopropylsiloxy)ethyne **237** (238 mg, 1.0 mmol, 2.0 equiv) using bis(triphenylphosphine)nickel(0) dicarbonyl (32.0 mg, 0.05 mmol, 0.1 equiv) as catalyst in 1.3 mL of CH_2Cl_2. The reaction was quenched after a period of 48 h. Flash column chromatography (after Kuglerohr distillation) with hexanes as the eluent afforded 150 mg (88%) of compound **74** as a colorless oil.

^{1}H NMR (500 MHz, $CDCl_3$) δ 7.65 (d, *J* = 8.0 Hz, 1H), 7.61 (d, *J* = 8.0 Hz, 1H), 7.37-7.23 (m, 3H), 7.11 (s, 1H), 2.33-2.25 (m, 1H), 1.41 (septet, *J* = 7.5 Hz, 3H), 1.16 (d, *J* = 7.5 Hz, 18H), 1.02-0.94 (m, 2H), 0.79-0.71 (m, 2H)

^{13}C NMR (125 MHz, $CDCl_3$) δ 153.8, 135.9, 132.9, 129.1, 127.0, 126.0, 125.1, 123.6, 123.4, 112.4, 18.1, 13.1, 10.9, 8.0

HRMS (ESI) calcd for $C_{22}H_{33}OSi^{+}$ $(M+H)^{+}$: 341.2295, Found: 341.2295

IR (film): 2944, 2866, 1498, 1472, 1179, 930, 883, 744, 684 cm^{-1}

R_f 0.44 (hexanes)

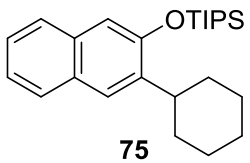

75

(3-cyclohexyl-naphth-2-yloxy)triisopropylsilane 75

General procedure 1 was employed for the cycloaddition of phthalazine **4** (65.1 mg, 0.5 mmol, 1.0 equiv) and 2-cyclohexyl-1-(triisopropylsiloxy)ethyne **238** (281 mg, 1.0 mmol, 2.0 equiv) using a catalyst combination of tetrakis(acetonitrile)copper(I) hexafluorophosphate (18.6 mg, 0.05 mmol, 0.1 equiv) and 2,2′-bipyridine (5.86 mg, 0.0375 mmol, 0.075 equiv) in 1.3 mL of CH_2Cl_2. The reaction was quenched after a period of 4 h. Flash column chromatography (after Kuglerohr distillation) with hexanes as the eluent afforded 145 mg (76%) of compound **75** as a colorless oil, which solidifies upon standing in the refrigerator to form a white solid.

General procedure 2 was employed for the coupling of phthalazine **4** (65.1 mg, 0.5 mmol, 1.0 equiv) and 2-cyclohexyl-1-(triisopropylsiloxy)ethyne **238** (281 mg, 1.0 mmol, 2.0 equiv) using bis(triphenylphosphine)nickel(0) dicarbonyl (32.0 mg, 0.05 mmol, 0.1 equiv) as catalyst in 1.3 mL of CH_2Cl_2. The reaction was quenched after a period of 24 h. Flash column chromatography (after Kuglerohr distillation) with hexanes as the eluent afforded 158 mg (82%) of compound **75** as a colorless oil, which solidifies upon standing in the refrigerator to form a white solid.

^{1}H NMR (500 MHz, $CDCl_3$) δ 7.71 (d, *J* = 8.0 Hz, 1H), 7.61 (d, *J* = 8.0 Hz, 2H), 7.59 (s, 1H), 7.34 (dt, *J* = 7.5, 1.2 Hz, 1H), 7.27 (dt, *J* = 7.5, 1.2 Hz, 1H), 7.09 (s, 1H), 3.10 (br t, 1H), 1.98 (br

d, 2H), 1.87 (m, 2H), 1.79 (br d, *J* = 13.0 Hz, 1H), 1.49-1.37 (m, 7H), 1.34-1.25 (m, 1H), 1.16 (d, *J* = 7.5 Hz, 18H)

^{13}C NMR (125 MHz, $CDCl_3$) δ 152.4, 139.7, 132.8, 129.2, 127.2, 125.9, 125.2, 125.1, 123.3, 112.3, 37.5, 33.5, 27.2, 26.5, 18.2, 13.1

HRMS (ESI) calcd for $C_{25}H_{39}OSi^+$ $(M+H)^+$: 383.2765, Found: 383.2771

IR (film): cm^{-1}: 2925, 2866, 2361, 1653, 1497, 1465, 1448, 1252, 1179

R_f 0.62 (hexanes)

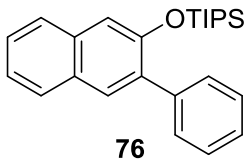

76

(3-phenyl-naphth-2-yloxy)triisopropylsilane 76

General procedure 1 was employed for the cycloaddition of phthalazine **4** (65.1 mg, 0.5 mmol, 1.0 equiv) and 2-phenyl-1-(triisopropylsiloxy)ethyne **239** (206 mg, 0.75 mmol, 1.5 equiv) using a catalyst combination of tetrakis(acetonitrile)copper(I) hexafluorophosphate (1.86 mg, 0.005 mmol, 0.01 equiv) and 2,2′-bipyridine (0.78 mg, 0.005 mmol, 0.01 equiv) in 1.0 mL of CH_2Cl_2. Note that instead of using a stock solution to add 2,2′-bipyridine, stock solutions were prepared to add both $Cu(MeCN)_4PF_6$ and 2,2′-bipyridine. The reaction was quenched after a period of 7 h. Flash column chromatography (after Kuglerohr distillation) with hexanes as the eluent afforded 166 mg (88%) of compound **76** as a colorless oil.

General procedure 2 was employed for the coupling of phthalazine **4** (65.1 mg, 0.5 mmol, 1.0 equiv) and 2-phenyl-1-(triisopropylsiloxy)ethyne **239** (206 mg, 0.75 mmol, 1.5 equiv) using bis(triphenylphosphine)nickel(0) dicarbonyl (16.0 mg, 0.025 mmol, 0.05 equiv) as catalyst in 1.0 mL of CH_2Cl_2. The reaction was quenched after a period of 7 h. Flash column chromatography

(after Kuglerohr distillation) with hexanes as the eluent afforded 178 mg (94%) of compound **76** as a colorless oil.

^{1}H NMR (500 MHz, $CDCl_3$) δ 7.77 (d, *J* = 8.0 Hz, 1H), 7.75 (s, 1H), 7.68 (d, *J* = 8.0 Hz, 1H), 7.57 (d, *J* = 7.5 Hz, 2H), 7.43-7.39 (m, 3H), 7.33 (dt, *J* = 7.7, 1.1 Hz, 2H), 7.24 (s, 1H), 1.20 (sept, *J* = 7.5 Hz, 3H), 0.99 (d, *J* = 7.5 Hz, 18H)

^{13}C NMR (125 MHz, $CDCl_3$) δ 151.7, 139.1, 134.9, 133.9, 129.91, 129.86, 129.1, 127.7, 127.6, 126.9, 126.1, 126.0, 123.8, 113.8, 17.9, 12.9

HRMS (ESI) calcd for $C_{25}H_{33}OSi^{+}$ $(M+H)^{+}$: 377.2295, Found: 377.2296

IR (film): cm^{-1}: 2944, 2866, 1462, 1437, 1201, 1179, 857, 685

R_f 0.24 (hexanes)

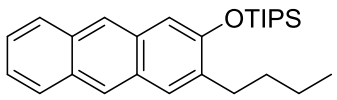

77

(3-butylanthrac-2-yloxy)triisopropylsilane 77

General procedure 1 was employed for the cycloaddition of benzo[*g*]phthalazine **23** (90.1 mg, 0.5 mmol, 1.0 equiv) and 1-(triisopropylsiloxy)-1-hexyne **11** (254 mg, 1.0 mmol, 2.0 equiv) using a catalyst combination of tetrakis(acetonitrile)copper(I) hexafluorophosphate (18.6 mg, 0.05 mmol, 0.1 equiv) and 2,2′-bipyridine (7.8 mg, 0.05 mmol, 0. 10 equiv) in 2.0 mL of CH_2Cl_2. The reaction was quenched after a period of 3.5 h. Flash column chromatography (after Kuglerohr distillation) with hexanes as the eluent afforded 151 mg (74%) of compound **77** as a colorless oil.

General procedure 2 was employed for the coupling of benzo[*g*]phthalazine **23** (90.1 mg, 0.5 mmol, 1.0 equiv) and 1-(triisopropylsiloxy)-1-hexyne **11** (254 mg, 1.0 mmol, 2.0 equiv) using

bis(triphenylphosphine)nickel(0) dicarbonyl (32.0 mg, 0.05 mmol, 0.1 equiv) as catalyst in 2.0 mL of CH_2Cl_2. The reaction was quenched after a period of 24 h. Flash column chromatography (after Kuglerohr distillation) with hexanes as the eluent afforded 130 mg (64%) of compound **77** as a colorless oil.

^{1}H NMR (500 MHz, $CDCl_3$) δ 8.24 (s, 1H), 8.17 (s, 1H), 7.90 (t, *J* = 8.5 Hz, 2H), 7.71 (s, 1H), 7.41-7.31 (m, 2H), 7.22 (s, 1H), 2.81 (t, *J* = 7.8 Hz, 2H), 1.74-1.68 (m, 2H), 1.49-1.40 (m, 5H), 1.17 (d, *J* = 7.5 Hz, 18H), 0.97 (t, *J* = 7.3 Hz, 3H)

^{13}C NMR (125 MHz, $CDCl_3$) δ 153.0, 136.2, 132.0, 131.5, 130.4, 128.5, 128.1, 127.8, 127.5, 125.0, 124.9, 124.1, 123.3, 110.7, 32.1, 31.4, 22.8, 18.2, 14.1, 13.1

HRMS (ESI) calcd for $C_{27}H_{39}OSi^+$ $(M+H)^+$: 407.2765, Found: 407.2764

IR (film): 2945, 2866, 1634, 1459, 1279, 1214, 1148, 882, 739, 685 cm^{-1}

R_f 0.42 (hexanes)

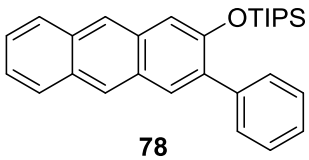

78

(3-phenylanthrac-2-yloxy)triisopropylsilane 78

General procedure 1 was employed for the cycloaddition of benzo[*g*]phthalazine **23** (90.1 mg, 0.5 mmol, 1.0 equiv) and 2-phenyl-1-(triisopropylsiloxy)ethyne **239** (206 mg, 0.75 mmol, 1.5 equiv) using a catalyst combination of tetrakis(acetonitrile)copper(I) hexafluorophosphate (1.86 mg, 0.005 mmol, 0.01 equiv) and 2,2′-bipyridine (0.78 mg, 0.005 mmol, 0.01 equiv) in 2.0 mL of CH_2Cl_2. Note that instead of using a stock solution to add 2,2′-bipyridine, stock solutions were prepared to add both $Cu(MeCN)_4PF_6$ and 2,2′-bipyridine. The reaction was quenched after a

period of 4 h. Flash column chromatography (after Kuglerohr distillation) with hexanes as the eluent afforded 162 mg (76%) of compound **78** as pale yellow oil.

General procedure 2 was employed for the coupling of benzo[*g*]phthalazine **23** (90.1 mg, 0.5 mmol, 1.0 equiv) and 2-phenyl-1-(triisopropylsiloxy)ethyne **239** (206 mg, 0.75 mmol, 1.5 equiv) using bis(triphenylphosphine)nickel(0) dicarbonyl (16.0 mg, 0.025 mmol, 0.05 equiv) as catalyst in 2.0 mL of CH_2Cl_2. The reaction was quenched after a period of 6 h. Flash column chromatography (after Kuglerohr distillation) with hexanes as the eluent afforded 178 mg (83%) of compound **78** as pale yellow oil.

^{1}H NMR (500 MHz, $CDCl_3$) δ 8.33 (s, 1H), 8.23 (s, 1H), 7.96-7.89 (m, 3H), 7.61 (dt, *J* = 7.5, 1.5 Hz, 2H), 7.45-7.31 (m, 6H), 1.24 (sept, *J* = 7.5 Hz, 3H), 1,00 (d, *J* = 7.5 Hz, 18 H)

^{13}C NMR (125 MHz, $CDCl_3$) δ 151.6, 139.0, 136.1, 132.3, 132.0, 130.61, 130.60, 129.9, 128.4, 128.2, 127.7, 127.6, 127.0, 126.1, 125.4, 124.4, 123.5, 112.2, 17.9, 12.9

HRMS (ESI) calcd for $C_{29}H_{35}OSi^+$ $(M+H)^+$: 427.2452, Found: 427.2434

IR (film): cm^{-1}: 2944, 2866, 1457, 1436, 1211, 1175, 899, 884, 698

R_f 0.26 (hexanes)

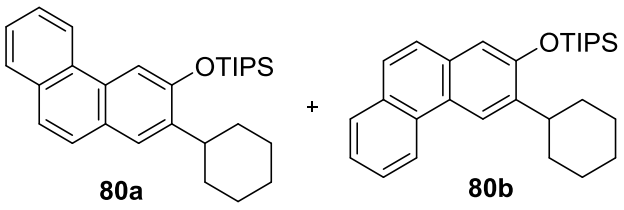

80a **80b**

(2-cyclohexylphenanthr-3-yloxy)triisopropylsilane 80a and (3-cyclohexylphenanthr-2-yloxy)triisopropylsilane 80b:

General procedure 1 was employed for the cycloaddition of benzo[*f*]phthalazine **79** (90.1 mg, 0.5 mmol, 1.0 equiv) and 2-cyclohexyl-1-(triisopropylsiloxy)ethyne **238** (281 mg, 1.0 mmol, 2.0

equiv) using a catalyst combination of tetrakis(acetonitrile)copper(I) hexafluorophosphate (18.6 mg, 0.05 mmol, 0.1 equiv) and 2,2′-bipyridine (7.8 mg, 0.05 mmol, 0.10 equiv) in 10.0 mL of CH_2Cl_2. The reaction was quenched after a period of 14 h. Flash column chromatography (after Kuglerohr distillation) with hexanes as the eluent afforded 152 mg (70%) of a product mixture consisting of regioisomers **80a** and **80b** (**80a**:**80b** = 64:36) as a colorless oil.

General procedure 2 was employed for the coupling of benzo[*f*]phthalazine **79** (90.1 mg, 0.5 mmol, 1.0 equiv) and 2-cyclohexyl-1-(triisopropylsiloxy)ethyne **238** (281 mg, 1.0 mmol, 2.0 equiv) using bis(triphenylphosphine)nickel(0) dicarbonyl (32.0 mg, 0.05 mmol, 0.1 equiv) as catalyst in 10.0 mL of CH_2Cl_2. The reaction was quenched after a period of 120 h. Flash column chromatography (after Kuglerohr distillation) with hexanes as the eluent afforded 124 mg (57%) of a product mixture consisting of regioisomers **80a** and **80b** (**80a**:**80b** = 44:56) as a colorless oil.

80a: ^{1}**H NMR** (500 MHz, $CDCl_3$) δ 8.63 (d, *J* = 8.3 Hz, 1H), 8.47 (s, 1H), 7.86-7.80 (m, 1H), 7.67-7.47 (m, 4H), 7.18 (d, *J* = 1.4 Hz, 1H), 3.25-3.12 (m, 1H), 2.07-1.98 (m, 2H), 1.95-1.86 (m, 2H), 1.85-1.77 (m, 1H), 1.62-1.28 (m, 8H), 1.17 (d, 18H, *J* = 7.5 Hz)

80b: ^{1}**H NMR** (500 MHz, $CDCl_3$) δ 8.43 (d, *J* = 8.1, 1H), 7.99 (s, 1H), 7.86-7.80 (m, 1H), 7.67-7.47 (m, 5H), 3.25-3.12 (m, 1H), 2.07-1.98 (m, 2H), 1.95-1.86 (m, 2H), 1.85-1.77 (m, 1H), 1.62-1.28 (m, 8H), 1.20 (d, *J* = 7.5 Hz, 18H)

^{13}**C NMR** (125 MHz, $CDCl_3$) δ 153.0, 152.8, 139.0, 138.9, 132.0, 131.3, 131.1, 130.4, 129.6, 129.3, 128.52, 128.51, 126.9, 126.7, 126.34, 126.29, 126.26, 126.02, 125.98, 125.96, 125.3, 124.6, 124.2, 122.2, 122.1, 120.5, 114.5, 109.5, 37.7, 37.4, 33.7, 33.4, 27.3, 27.2, 26.51, 26.48, 18.23, 18.18, 13.2 (2C)

HRMS (ESI) calcd for $C_{29}H_{41}OSi^{+}$ $(M+H)^{+}$: 433.2921, Found: 433.2921

IR (film): 2866, 2851, 2361, 2339, 1498, 1461, 1265, 1222, 999, 879, 743, 684, 668 cm^{-1}

R_f 0.34 (hexanes)

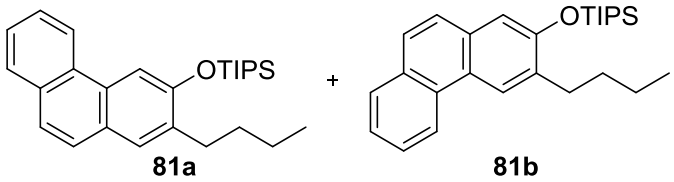

81a **81b**

(2-butylphenanthr-3-yloxy)triisopropylsilane 81a and (3-butylphenanthr-2-yloxy)triisopropylsilane 81b:

General procedure 1 was employed for the cycloaddition of benzo[*f*]phthalazine **79** (90.1 mg, 0.5 mmol, 1.0 equiv) and 1-(triisopropylsiloxy)-1-hexyne **11** (254 mg, 1.0 mmol, 2.0 equiv) using a catalyst combination of tetrakis(acetonitrile)copper(I) hexafluorophosphate (18.6 mg, 0.05 mmol, 0.1 equiv) and 2,2′-bipyridine (7.8 mg, 0.05 mmol, 0.10 equiv) in 10.0 mL of CH_2Cl_2. The reaction was quenched after a period of 14 h. Flash column chromatography (after Kuglerohr distillation) with hexanes as the eluent afforded 145 mg (71%) of a product mixture consisting of regioisomers **81a** and **81b** (**81a**:**81b** = 73:27) as a colorless oil.

General procedure 2 was employed for the coupling of benzo[*f*]phthalazine **79** (90.1 mg, 0.5 mmol, 1.0 equiv) and 1-(triisopropylsiloxy)-1-hexyne **11** (254 mg, 1.0 mmol, 2.0 equiv) using bis(triphenylphosphine)nickel(0) dicarbonyl (32.0 mg, 0.05 mmol, 0.1 equiv) as catalyst in 10.0 mL of CH_2Cl_2. The reaction was quenched after a period of 120 h. Flash column chromatography (after Kuglerohr distillation) with hexanes as the eluent afforded 159 mg (78%) of a product mixture consisting of regioisomers **81a** and **81b** (**81a**:**81b** = 40:60) as a colorless oil.

81a: **^{1}H NMR** (500 MHz, $CDCl_3$) δ 8.58 (d, *J* = 8.0 Hz, 1H), 8.41 (s, 1H), 7.80-7.77 (m, 1H), 7.62-7.43 (m, 4H), 7.19 (s, 1H), 2.88 (t, *J* = 7.9 Hz, 2H), 1.77-1.66 (m, 2H), 1.51-1.35 (m, 5H), 1.154 (d, *J* = 7.5 Hz, 18H), 0.97 (t, *J* = 7.5 Hz, 3H)

81b: **^{1}H NMR** (500 MHz, $CDCl_3$) δ 8.44 (d, J = 8.0 Hz, 1H), 8.00 (s,1H), 7.82-7.78 (m, 1H), 7.62-7.43 (m, 5H), 2.814 (t, *J* = 7.9 Hz, 2H), 1.77-1.66 (m, 2H), 1.51-1.35 (m, 5H), 1.186 (d, *J* = 7.5 Hz, 18H), 0.96 (t, *J* = 7.5 Hz, 3H)

^{13}C NMR (125 MHz, $CDCl_3$) δ 153.6, 153.4, 134.22, 134.20, 132.0, 131.7, 131.1, 130.3, 129.69, 129.68, 129.3, 128.55, 128.49, 126.8, 126.5, 126.32, 126.29, 126.05, 126.0, 125.3, 124.58, 124.57, 124.3, 123.9, 122.2, 122.1, 114.6, 109.5, 32.6, 32.3, 31.6, 30.9, 22.9, 22.8, 18.19, 18.15, 14.13, 14.11, 13.18, 13.14

HRMS (ESI) calcd for $C_{27}H_{39}OSi^{+}$ $(M+H)^{+}$: 407.2765, Found: 407.2753

IR (film): 2945, 2866, 1499, 1460, 1274, 1224, 1152, 999, 882, 866, 742, 646 cm^{-1}

R_f 0.41 (hexanes)

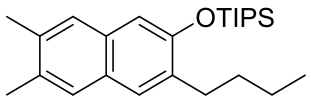

83

(3-butyl-6,7-dimethylnaphth-2-yloxy)triisopropylsilane 83

General procedure 1 was employed for the cycloaddition of 6,7-dimethylphthalazine **82** (79.1 mg, 0.5 mmol, 1.0 equiv) and 1-(triisopropylsiloxy)-1-hexyne **11** (254 mg, 1.0 mmol, 2.0 equiv) using a catalyst combination of tetrakis(acetonitrile)copper(I) hexafluorophosphate (18.6 mg, 0.05 mmol, 0.1 equiv) and 2,2′-bipyridine (7.8 mg, 0.05 mmol, 0. 10 equiv) in 6.0 mL of CH_2Cl_2. The reaction was quenched after a period of 12 h. Flash column chromatography (after Kuglerohr distillation) with hexanes as the eluent afforded 143 mg (74%) of compound **83** as a colorless oil.

General procedure 2 was employed for the coupling of 6,7dimethylphthalazine **82** (79.1 mg, 0.5 mmol, 1.0 equiv) and 1-(triisopropylsiloxy)-1-hexyne **11** (254 mg, 1.0 mmol, 2.0 equiv) using

bis(triphenylphosphine)nickel(0) dicarbonyl (32.0 mg, 0.05 mmol, 0.1 equiv) as catalyst in 6.0 mL of CH_2Cl_2. The reaction was quenched after a period of 48 h. Flash column chromatography (after Kuglerohr distillation) with hexanes as the eluent afforded 146 mg (76%) of compound **83** as a colorless oil.

^{1}H NMR (500 MHz, $CDCl_3$) δ 7.44 (s, 2H), 7.39 (s, 1H), 7.00 (s, 1H), 2.74 (t, *J* = 7.8 Hz, 2H), 2.37 (s, 3H), 2.36 (s, 3H), 1.67-1.61 (m, 2H), 1.44-1.34 (m, 5H), 1.14 (d, *J* = 7.5 Hz, 18H), 0.94 (t, *J* = 7.5 Hz, 3H)

^{13}C NMR (125 MHz, $CDCl_3$) δ 152.4, 134.6, 133.9, 132.7, 132.0, 127.9, 127.2, 126.5, 125.7, 111.6, 32.3, 31.1, 22.7, 20.1, 20.0, 18.1, 14.1, 13.1

HRMS (ESI) calcd for $C_{25}H_{41}OSi^+$ $(M+H)^+$: 385.2921, Found: 385.2918

IR (film): 2944, 2867, 1498, 1466, 1372, 1253, 1208, 1146, 905, 882 cm^{-1}

R_f 0.56 (hexanes)

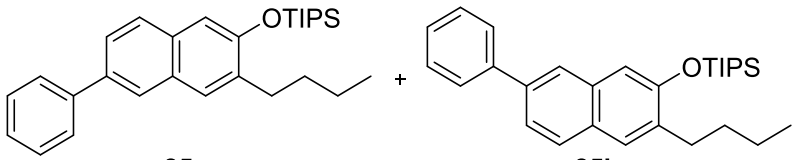

85a **85b**

(3-butyl-6-phenyl-naphth-2-yloxy)triisopropylsilane 85a and (3-butyl-7-phenyl-naphth-2-yloxy)triisopropylsilane 85b:

General procedure 1 was employed for the cycloaddition of 6-phenyl phthalazine **84** (103.1 mg, 0.5 mmol, 1.0 equiv) and 1-(triisopropylsiloxy)-1-hexyne **11** (254 mg, 1.0 mmol, 2.0 equiv) using a catalyst combination of tetrakis(acetonitrile)copper(I) hexafluorophosphate (18.6 mg, 0.05 mmol, 0.1 equiv) and 2,2′-bipyridine (7.8 mg, 0.05 mmol, 0.10 equiv) in 8.0 mL of CH_2Cl_2. The reaction was quenched after a period of 7 h. Flash column chromatography (after Kuglerohr

distillation) with hexanes as the eluent afforded 156 mg (72%) of a product mixture consisting of regioisomers **85a** and **85b** (**85a**:**85b** = 60:40) as a colorless oil.

General procedure 2 was employed for the coupling of 6-phenyl phthalazine **84** (103.1 mg, 0.5 mmol, 1.0 equiv) and 1-(triisopropylsiloxy)-1-hexyne **11** (254 mg, 1.0 mmol, 2.0 equiv) using bis(triphenylphosphine)nickel(0) dicarbonyl (32.0 mg, 0.05 mmol, 0.1 equiv) as catalyst in 8.0 mL of CH_2Cl_2. The reaction was quenched after a period of 96 h. Flash column chromatography (after Kuglerohr distillation) with hexanes as the eluent afforded 46 mg (21%) of a product mixture consisting of regioisomers **85a** and **85b** (**85a**:**85b** = 50:50) as a colorless oil.

85a: ^{1}**H NMR** (500 MHz, $CDCl_3$) δ 7.91 (s, 1H), 7.79-7.53 (m, 5H), 7.49-7.42 (m, 2H), 7.38-7.31 (m, 1H), 7.12 (s, 1H), 2.84-2.76 (m, 2H), 1.73-1.63 (m, 2H), 1.50-1.38 (m, 5H), 1.16 (d, *J* = 7.5 Hz, 18H), 0.96 (t, *J* = 7.4 Hz, 3H)

85b: ^{1}**H NMR** (500 MHz, $CDCl_3$) δ 7.83 (s, 1H), 7.79-7.53 (m, 5H), 7.49-7.42 (m, 2H), 7.38-7.31 (m, 1H), 7.16 (m, 1H), 2.84-2.76 (m, 2H), 1.73-1.63 (m, 2H), 1.50-1.38 (m, 5H), 1.16 (d, *J* = 7.5 Hz, 18H), 0.96 (t, *J* = 7.4 Hz, 3H)

^{13}**C NMR** (125 MHz, $CDCl_3$) δ 153.4, 153.2, 141.56, 141.52, 137.9, 136.3, 135.5, 135.2, 133.5, 132.4, 129.3, 128.74, 128.71, 128.6, 128.3, 128.0, 127.5, 127.4, 127.2, 127.1, 126.9, 126.6, 125.0, 124.9, 124.1, 123.2, 112.7, 112.2, 32.23, 32.22 31.2 (2C), 22.8 (2C), 18.2 (2C), 14.1 (2C), 13.1 (2C)

HRMS (ESI) calcd for $C_{29}H_{41}OSi^{+}$ $(M+H)^{+}$: 433.2921, Found: 433.2910

IR (film): 2946, 2867, 1466, 1253, 1217, 884, 696 cm^{-1}

$\mathbf{R_f}$ 0.34 (hexanes)

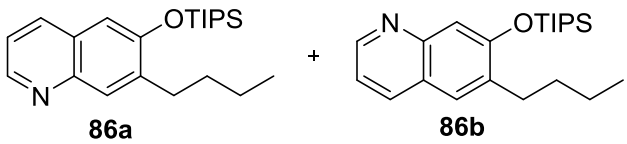

86a **86b**

(7-butyl-6-quinolyloxy)-triisopropylsilane 86a and (6-butyl-7-quinolyloxy)-triisopropylsilane 86b

Tetrakis(acetonitrile)copper(I) hexafluorophosphate, $Cu(MeCN)_4PF_6$ (18.6 mg, 0.05 mmol, 0.1 equiv) and pyrido[2,3-*d*]pyridazine **52** (65.6 mg, 0.5 mmol, 1.0 equiv) were added to a a flame-dried test-tube equipped with a stir bar. This test-tube was subjected to vacuum, flushed with argon, sealed with a septum, and connected to an argon balloon to maintain positive argon pressure throughout the remainder of the experiment. A stock solution (0.4 mL) of 2,2′-bipyridine in anhydrous 1,2-dichloroethane was then used to add 2,2′-bipyridine (11.7 mg, 0.075 mmol, 0.15 equiv) via a syringe, followed by the addition of another 0.6 mL of anhydrous 1,2-dichloroethane. The test-tube was transferred to an oil bath at about 85 °C for 1,2-dichloroethane to undergo reflux over the sides of the test-tube. The reaction mixture was then allowed to stir for 15 minutes before the addition of freshly distilled 1-(triisopropylsiloxy)-1-hexyne **11** (254 mg, 1.0 mmol, 2.0 equiv) with a syringe. After 48 h, heating was discontinued to cool the reaction mixture to room temperature. The catalyst was separated by passing it through a plug of silica (washing with CH_2Cl_2), thus quenching the reaction. The mixture was consequently concentrated and the excess unreacted siloxy alkyne removed by Kugelrohr distillation. By using a 10% ethyl acetate in hexanes solvent mixture as an eluent, flash column chromatography (after Kuglerohr distillation) afforded 74 mg (41%) of a product mixture consisting of **86a** and **86b** (**86a**:**86b** = 55:45).

86a: **^{1}H NMR** (500 MHz, $CDCl_3$) δ 8.72 (dd, *J* = 4.3, 1.7 Hz, 1H), 7.94 (d, *J* = 8.0 Hz, 1H), 7.85 (s, 1H), 7.28-7.24 (m, 1H), 7.032 (s, 1H), 2.82 (t, *J* = 7.8 Hz, 2H), 1.73-1.63 (m, 2H), 1.52-1.35 (m, 5H), 1.16 (d, *J* = 7.5 Hz, 18H), 0.95 (t, *J* = 7.4 Hz, 3H)

86b: **^{1}H NMR** (500 MHz, $CDCl_3$) δ 8.75 (dd, *J* = 4.3, 1.7 Hz, 1H), 8.00 (d, *J* = 8.1 Hz, 1H), 7.52 (s, 1H), 7.39 (s, 1H), 7.21 (dd, *J* = 4.3, 3.9, 1H), 2.80 (t, *J* = 7.8 Hz, 2H), 1.73-1.63 (m, 2H), 1.52-1.35 (m, 5H), 1.16 (d, *J* = 7.5 Hz, 18H), 0.96 (t, *J* = 7.4 Hz, 3H)

^{13}C NMR (125 MHz, $CDCl_3$) δ 156.2, 153.3, 149.2, 147.6, 144.2, 139.2, 136.1, 135.2, 134.2, 129.3, 127.8, 127.4, 123.7, 120.3, 118.8, 117.7, 113.4, 111.5, 32.0, 31.8, 31.1, 31.0, 22.7, 22.6, 18.04, 18.03 13.97, 13.95 13.03, 12.99

HRMS (ESI) calcd for $C_{22}H_{36}NOSi^{+}$ $(M+H)^{+}$: 358.2561, Found: 358.2570

IR (film): 2945, 2866, 1498, 1462, 1271, 1223, 908, 882, 865, 742, 683, 645 cm^{-1}

R_f 0.40-0.45 (1:3 ethyl acetate:hexanes)

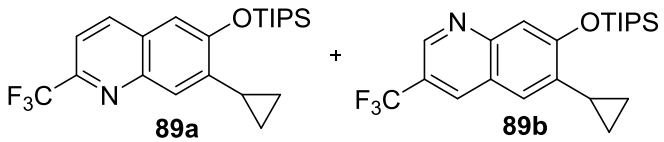

7-cyclopropyl-2-(trifluoromethyl)-6-(triisopropylsiloxy)quinoline 89a and 6-cyclopropyl-2-(trifluoromethyl)-7-(triisopropylsiloxy)quinoline 89b

General procedure 1 was employed for the cycloaddition of 2-(trifluoromethyl)-pyrido[2,3-*d*]pyridazine **88** (99.6 mg, 0.5 mmol, 1.0 equiv) and 2-cyclopropyl-1-(triisopropylsiloxy)ethyne **237** (238 mg, 1.0 mmol, 2.0 equiv) using a catalyst combination of tetrakis(acetonitrile)copper(I) hexafluorophosphate (18.6 mg, 0.05 mmol, 0.1 equiv) and 2,2′-bipyridine (7.8 mg, 0.05 mmol, 0.10 equiv) in 1.0 mL of CH_2Cl_2. The reaction was quenched after a period of 6 h. Flash column chromatography (after Kuglerohr distillation) with 2% EtOAc in hexanes solvent mixture as the

eluent afforded 132 mg (64%) of a product mixture consisting of regioisomers **89a** and **89b** (**89a**:**89b** = 55:45) as pale yellow oil.

Catalysis by $AgNTf_2$: Silver bis(trifluoromethanesulfonyl)imide, $AgNTf_2$ (9.3 mg, 0.025 mmol, 0.05 equiv) and 2-(trifluoromethyl)-pyrido[2,3-*d*]pyridazine **88** (99.6 mg, 0.5 mmol, 1.0 equiv) were added to a flame-dried test-tube equipped with a stir bar. The test-tube is then subjected to vacuum, flushed with N_2, sealed with a septum, and positive N_2 pressure throughout the remainder of the experiment. 2,2′-bipyridine (3.90 mg, 0.025 mmol, 0.05 equiv) in CH_2Cl_2 (0.2 mL) was added via a syringe, followed by the addition of 0.8 mL of CH_2Cl_2. This mixture was allowed to stir for 15 minutes before the addition of 2-cyclopropyl-1-(triisopropylsiloxy)ethyne **237** (238 mg, 1.0 mmol, 2.0 equiv) using a syringe, and the reaction monitored by thin-layer chromatography (TLC). After 2 hours, the reaction was quenched by passing the reaction mixture through a plug of silica (washing with CH_2Cl_2), and was concentrated under reduced pressure. Flash column chromatography (after Kuglerohr distillation to remove unreacted siloxy alkyne) with 2% ethyl acetate in hexanes as the eluent afforded 145 mg (71%) of a product mixture consisting of regioisomers **89a** and **89b** (**89a**:**89b** = 67:33) as pale yellow oil.

89a: ^{1}**H NMR** (500 MHz, $CDCl_3$) δ 8.14-8.08 (m, 1H), 7.64 (s, 1H), 7.58 (d, *J* = 8.5Hz, 1H), 7.11 (s, 1H), 2.40-2.30 (m, 1H), 1.42 (septet, *J* = 7.5 Hz, 3H), 1.16 (d, *J* = 7.5 Hz, 18H), 1.14-1.04 (m, 2H), 0.88-0.83 (m, 2H)

89b: ^{1}**H NMR** (500 MHz, $CDCl_3$) δ 8.14-8.08 (m, 1H), 7.53 (d, *J* = 8.5 Hz, 1H), 7.45 (s, 1H), 7.30 (s, 1H), 2.40-2.30 (m, 1H), 1.48 (septet, *J* = 7.5 Hz, 3H), 1.16 (d, *J* = 7.5 Hz, 18H), 1.14-1.04 (m, 2H), 0.81-0.76 (m, 2H)

^{13}C NMR (125 MHz, $CDCl_3$) δ 158.0, 155.7, 147.5, 147.1, 146.9, 145.6, 143.4, 142.5, 139.8, 136.5, 135.6, 128.31, 128.30, 125.2, 124.5, 122.9, 122.7, 122.6, 120.77, 120.76, 115.89, 115.87, 114.44, 114.42, 113.95, 113.94, 111.2, 18.01, 17.97, 13.06, 13.02, 11.0, 10.8, 9.2, 8.4

89a: ^{19}F NMR (470 MHz, $CDCl_3$) δ -67.3

89b: ^{19}F NMR (470 MHz, $CDCl_3$) δ -67.3

HRMS (ESI) calcd for $C_{22}H_{31}F_3NOSi^+$ $(M+H)^+$: 410.2122, Found: 410.2118

IR (film): 2947, 2869, 1473, 1334, 1229, 1183, 1090, 883 cm^{-1}

R_f 0.5-0.6 (5% ethyl acetate in hexanes)

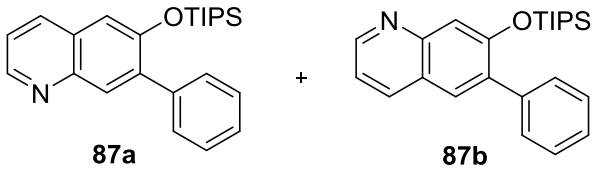

87a **87b**

(7-phenyl-6-quinolyloxy)-triisopropylsilane 87a and (6-phenyl-7-quinolyloxy)-triisopropylsilane 87b

General procedure 1 was employed for the cycloaddition of pyrido[2,3-*d*]pyridazine **52** (65.6 mg, 0.5 mmol, 1.0 equiv) and 2-phenyl-1-(triisopropylsiloxy)ethyne **239** (275 mg, 1.0 mmol, 2.0 equiv) using a catalyst combination of tetrakis(acetonitrile)copper(I) hexafluorophosphate (18.6 mg, 0.05 mmol, 0.1 equiv) and 2,2′-bipyridine (7.8 mg, 0.05 mmol, 0.10 equiv) in 1.0 mL of CH_2Cl_2. The reaction was quenched after a period of 6 h. Flash column chromatography (after Kuglerohr distillation) with 5-20% EtOAc in hexanes solvent mixture as the eluent afforded 140 mg (74%) of a product mixture consisting of regioisomers **87a** and **87b** (**87a**:**87b** = 73:27) as pale brown oil.

87a: **^{1}H NMR** (500 MHz, $CDCl_3$) δ 8.77 (dd, *J* = 4.0, 1.5 Hz, 1H), 8.06 (s, 1H), 8.00 (d, *J* = 8.5 Hz, 1H), 7.63-7.33 (m, 5H), 7.30 (q, *J* = 4.2 Hz, 1H), 7.19 (s, 1H), 1.20 (septet, *J* = 7.5 Hz, 3H), 0.99 (d, *J* = 7.5 Hz, 18H)

87b: **^{1}H NMR** (500 MHz, $CDCl_3$) δ 8.82 (dd, *J* = 4.0, 1.5 Hz, 1H), 8.09-8.04 (m, 1H), 7.70 (s, 1H), 7.63-7.33 (m, 6H), 7.24 (q, *J* = 4.2 Hz, 1H), 1.28 (septet, *J* = 7.5 Hz, 3H) 1.00 (d, *J* = 7.0 Hz, 18H)

^{13}C NMR (125 MHz, $CDCl_3$) δ 154.9, 152.0, 150.3, 149.0, 148.4, 144.3, 138.4, 138.3, 135.8, 135.5, 134.1, 131.1, 129.8, 129.76, 129.74, 129.1, 128.5, 127.78, 127.76, 127.3, 127.2, 123.6, 121.0, 119.2, 115.1, 113.1, 17.78, 17.75, 12.81, 12.80

HRMS (ESI) calcd for $C_{24}H_{32}NOSi^{+}$ $(M+H)^{+}$: 378.2248, Found: 378.2248

IR (film): 2945, 2867, 1479, 1458, 1436, 1329, 1229, 932, 882, 868, 767, 698 cm^{-1}

R_f 0.51-0.60 (1:3 ethyl acetate:hexanes)

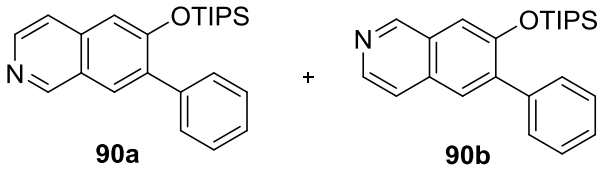

90a + **90b**

(7-phenyl-6-isoquinolyloxy)-triisopropylsilane 90a and (6-phenyl-7-isoquinolyloxy)-triisopropylsilane 90b

General procedure 1 was employed for the cycloaddition of pyrido[3,4-*d*]pyridazine **53** (65.6 mg, 0.5 mmol, 1.0 equiv) and 2-phenyl-1-(triisopropylsiloxy)ethyne **239** (275 mg, 1.0 mmol, 2.0 equiv) using a catalyst combination of tetrakis(acetonitrile)copper(I) hexafluorophosphate (18.6 mg, 0.05 mmol, 0.1 equiv) and 2,2′-bipyridine (7.8 mg, 0.05 mmol, 0.10 equiv) in 1.0 mL of CH_2Cl_2. The reaction was quenched after a period of 6 h. Flash chromatography (after Kuglerohr distillation) with 5-20% ethyl acetate in hexanes solvent mixture as the eluent afforded 127 mg

(67%) of a product mixture consisting of regioisomers **90a** and **90b** (**90a**:**90b** = 54:46) as pale yellow oil.

90a: ^{1}**H NMR** (500 MHz, $CDCl_3$) δ 9.13 (s, 1H), 8.43 (d, *J* = 6.0 Hz, 1H), 7.87 (s, 1H), 7.57-7.53 (m, 2H), 7.50 (d, *J* = 6.0 Hz), 7.45-7.41 (m, 2H), 7.39-7.35 (m, 1H), 7.17 (s, 1H), 1.32-1.20 (m, 3H), 0.99 (d, *J* = 7.5 Hz, 18H)

90b: ^{1}**H NMR** (500 MHz, $CDCl_3$) δ 9.11 (s, 1H), 8.41 (d, *J* = 5.0 Hz, 1H), 7.74 (s, 1H), 7.58 (d, *J* = 5.5 Hz, 1H), 7.57-7.53 (m, 2H), 7.45-7.41 (m, 2H), 7.40-7.35 (m, 1H), 7.32 (s, 1H), 7.31-7.19 (m, 3H), 0.99 (d, *J* = 7.5 Hz, 18H)

^{13}**C NMR** (125 MHz, $CDCl_3$) δ 155.5, 152.7, 151.8, 150.6, 143.0, 141.4, 139.7, 138.11, 138.09, 136.7, 136.5, 131.2, 129.7, 129.6, 128.4, 127.83, 127.82, 127.5, 127.3, 112.9, 112.0, 17.74, 17.72, 12.8 (2C)

HRMS (ESI) calcd for $C_{24}H_{32}NOSi^{+}$ $(M+H)^{+}$: 378.2248, Found: 378.2245

IR (film): 2943, 2866, 1625, 1487, 1459, 1413, 1263, 1216, 1206, 883, 854, 697, 687, 644 cm^{-1}

R_f 0.20-0.30 (1:3 ethyl acetate:hexanes)

Table 24: Evaluating Different Metal Complexes Towards the [4+2] Cycloadditoin Reaction[a]

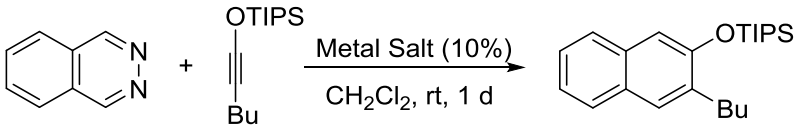

Metal Salt	Yield (%)[b]
$Sc(OTf)_3$	3
$MnBr_2$	0
$Mn(OAc)_3{\cdot}2H_2O$	62
$FeCl_2$	0
$FeCl_3$	0
$Co(BF_4)_2.6H_2O$	0
$NiCl_2$	0

Table 24, continued

$ZnBr_2$	0
$CdCl_2.2H_2O$	0
$CrCl_2$	4
$CrCl_3$	0
LiBr	0
$CeCl_3$	0
$Yb(OTf)_3$	0
$La(OTf)_3$	0
$ZrCl_4.(THF)_2$	0
$In(OTf)_3$	0
$Bi(OTf)_3$	0

[a]All reactions were carried out using 0.5 mmol of phthalazine and 0.75 mmol of siloxy alkyne.
[b]Yield was measured using 1,3,5-trimethoxybenzene as an internal standard.

Table 25: Evaluation of Cu(II) salts and changing the nucleophilicity of the anion[a]

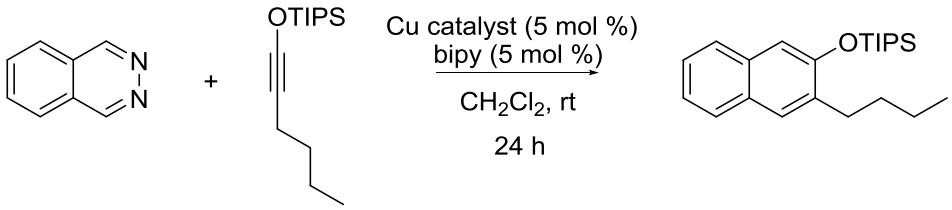

Catalyst (mol%)	Yield
CuOTf (5)	34%
Cu(1,10-phenanthroline)(PPh_3)Br (5)	NR
CuI (5)	NR
$CuBr.(CH_3)_2S$ (5)	NR
CuCl (5)	5%
$Cu(OTf)_2$ (5)	16%
Cu(hexafluoroacetylacetonate)$_2$ (5)	4%
$Cu(MeCN)_4OTf$ (5)	38%
$Cu(MeCN)_4PF_6$ (5)	49%

[a]All reactions were carried out using 0.5 mmol of phthalazine and 0.75 mmol of siloxy alkyne.
[b]Yield was measured using 1,3,5-trimethoxybenzene as an internal standard.

V.2.5 Copper-Catalyzed Formal [2+2] Cycloaddition Reaction of Siloxy Alkynes and Cyclohexenone

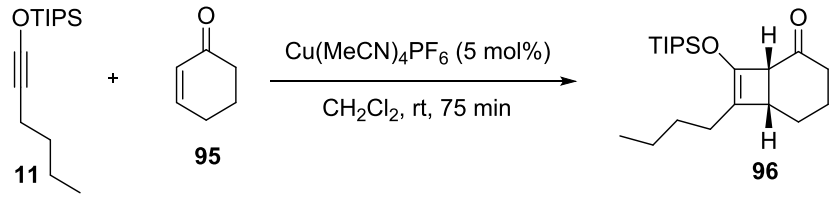

An oven-dried test-tube fitted with a septum was charged with 1-(triisopropylsiloxy)-1-hexyne **11** (153.0 mg, 0.6 mmol, 1.2 equiv) and 3.0 mL of anhydrous CH_2Cl_2 in an inert atmosphere. Neat cyclohexenone **95** (48 µL, 0.5 mmol, 1.0 equiv) was added followed by the addition of $Cu(MeCN)_4PF_6$ (9.3 mg, 0.025 mmol, 0.05 equiv) dissolved in 1.0 mL of CH_2Cl_2 (using a stock solution). The resulting clear light yellow solution is stirred at room temperature under nitrogen for 75 minutes. The mixture was then passed through a plug of silica and washed with CH_2Cl_2 in order to remove the catalyst. The mixture was purified by flash column chromatography (after Kuglerohr distillation), using 2-5% ethyl acetate in hexanes solvent mixture as eluent to afford the 130 mg (74%) of the product **96** as colorless oil. Spectral data is consistent with that reported earlier.[7]

96: ^{1}H NMR (500 MHz, $CDCl_3$) δ 3.38 (s, 1H), 2.81 (s, 1H), 2.56-2.50 (m, 1H), 2.14-2.09 (m, 2H), 1.92-1.86 (m, 3H), 1.68-1.61 (m, 1H), 1.59-1.54 (m, 1H), 1.43-1.31 (m, 4H), 1.15-1.10 (m, 3H), 1.08 (d, *J* = 7.0 Hz, 18H), 0.91 (t, *J* = 7.0 Hz, 3H)

^{13}C NMR (125 MHz, $CDCl_3$) 211.5, 138.3, 122.1, 58.0, 40.1, 34.8, 29.6, 25.1, 24.8, 23.3, 18.1, 17.9, 14.2, 13.0

HRMS (ESI) calcd for $C_{21}H_{39}O_2Si^+$ $(M+H)^+$: 351.2714, Found: 351.2708

IR (film): 2943, 2868, 1699, 1465, 1283, 1255, 1001, 884, 687, 668 cm^{-1}

[7] Sweis, R. F.; Schramm, M. P.; Kozmin, S. A. *J. Am. Chem. Soc.* **2004**, *126*, 7442.

R_f ~ 0.4 (15:85 ethyl acetate:hexanes)

V.3 Data for Chapter II

V.3.1 Experimental Procedures and Characterization Data

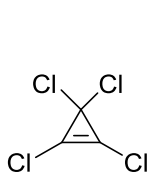

112

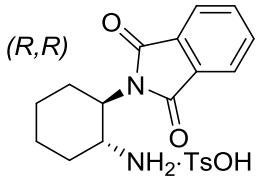

163

Compounds **112**[8] and **163**[9] were prepared by procedures previously reported.

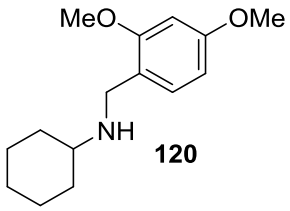

120

Commercially available cyclohexylamine (3.57 g, 36 mmol, 1 eq) and 2,4-dimethoxybenzaldehyde **164** (6 g, 36 mmol, 1.0 eq) were dissolved in toluene and the mixture was refluxed overnight for 12 h. The round-bottom flask was attached to a Dean-Stark apparatus to collect water generated during the course of the formation of the imine (not shown). After 12 h, the system was bought to room temperature, and the toluene was removed using a rotary evaporator. The imine, without any purification, was then dissolved in a 1:1 mixture of dichloromethane and methanol under inert atmosphere, and the solution was cooled to 0 °C using an ice-bath. Sodium borohydride (1.81 g, 47.9 mmol, 1.33 eq) was added in portions to this solution at 0 °C, and the round-bottom flask was subsequently allowed to slowly warm to room temperature by removing the ice-bath. The reaction mixture was allowed to stir for 3 h, after

[8] Sepiol, J.; Solulen, R. L. *J. Org. Chem.* **1975**, *40*, 3791.
[9] Kaik, M.; Gawronski, J. *Tetrahedron: Asymmetry* **2003**, *14*, 1559.

which it was diluted with ethyl acetate and washed with water and then brine. The aqueous layer was washed with ethyl acetate, and the combined organic layers were dried with brine and Na_2SO_4, and concentrated. No further purification was carried out as ^{1}H NMR indicated a pure product, and 8.79 g (98 %) of compound **120** was thus obtained as a pale yellow oil. The amine is stored as a solution in dichloromethane for future uses.

120: ^{1}H NMR (500 MHz, $CDCl_3$) δ 7.12 (d, *J* = 8.5 Hz, 1H), 6.45-6.38 (m, 2H), 3.80 (s, 3H), 3.79 (s, 3H), 3.73 (s, 2H), 2.41 (dt, *J* = 13.0, 3.5 Hz, 1H), 1.88 (d, 11.0 Hz, 2H), 1.75-1.68 (m, 2H), 1.62-1.58 (m, 1H), 1.30-1.05 (m, 5H).

^{13}C NMR (125 MHz, CDl_3) δ 159.8, 158.5, 130.1, 121.4, 103.6, 98.4, 55.6, 55.2, 55.1, 45.7, 33.4, 26.2, 24.9.

HRMS (ESI) calcd for $(M+H)^+$, $C_{15}H_{24}NO_2^+$: 250.1802, Found: 250.1808.

IR: 2924, 2850, 2361, 2338, 1733, 1717, 1700, 1684, 1652, 1647, 1635, 1616, 1588, 1576, 1540, 1521, 1506, 1472, 1457, 1287, 1208, 1155, 1038 cm^{-1}

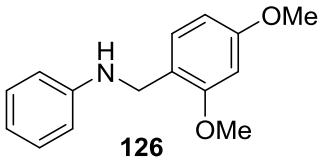

126

Compound **126** was prepared according to a previously reported procedure.[10]

126: ^{1}H NMR (500 MHz, $CDCl_3$) δ 7.24 (d, *J* = 8.0 Hz, 1H), 7.20 (t, *J* = 7.5 Hz, 2H), 6.73 (t, *J* = 7.5 Hz, 1H), 6.69 (d, *J* = 7.5 Hz, 2H), 6.51 (d, *J* = 2.5 Hz, 1H), 6.47 (dd, *J* = 8.0, 2.5 Hz, 1H), 4.29 (s, 2H), 4.08 (br s, 1H), 3.87 (s, 3H), 3.83 (s, 3H).

^{13}C NMR (125 MHz, CDl_3) δ 160.2, 158.4, 148.5, 129.7, 129.1, 119.8, 117.2, 113.1, 103.9, 98.6, 55.3 (2C), 43.1.

[10] Gauthier, D.; Dodd, R. H.; Dauban, P. *Tetrahedron* **2009**, *65*, 8542.

HRMS (ESI) calcd for ($2M^+$) $C_{15}H_{18}NO_2^+$: 244.1332, Found: 244.134

IR: 3853, 3744, 2631, 1653, 1559, 1540, 1506 cm^{-1}

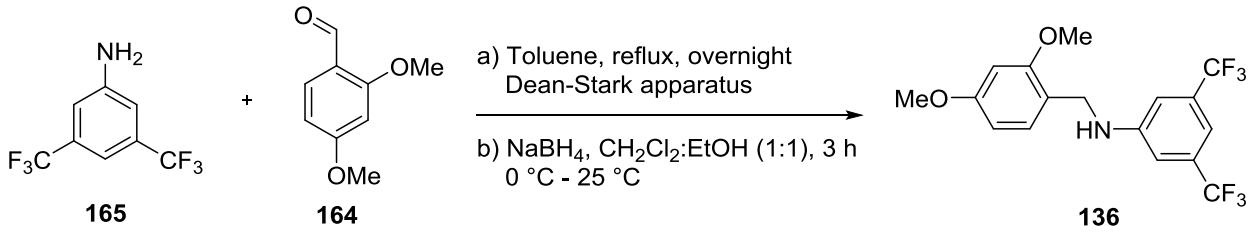

Commercially available bis(trifluoromethyl)aniline **165** (9.17 g, 40 mmol, 1 eq) and 2,4-dimethoxybenzaldehyde **164** (6.78 g, 40.8 mmol, 1.02 eq) were dissolved in toluene and the mixture was refluxed overnight for 12 h. The round-bottom flask was attached to a Dean-Stark apparatus to collect water generated during the course of the formation of the imine (not shown). After 12 h, the system was bought to room temperature, and the toluene was removed using a rotary evaporator. The imine, without any purification, was then dissolved in a 1:1 mixture of dichloromethane and ethanol under inert atmosphere, and the solution was cooled to 0 °C using an ice-bath. Sodium borohydride (2.01 g, 53.2 mmol, 1.33 eq) was added in portions to this solution at 0 °C, and the round-bottom flask was subsequently allowed to slowly warm to room temperature by removing the ice-bath. The reaction mixture was allowed to stir for 3 h, after which it was diluted with ethyl acetate and extracted with saturated sodium bicarbonate. The aqueous layer was washed with ethyl acetate, and the combined organic layers were dried with brine and $MgSO_4$, and concentrated. The mixture was purified by flash chromatography, using a 20:1 mixture of hexanes and ethyl acetate as the eluent to obtain 14.01 g (92%) of compound **136**.

136: ^{1}H NMR (500 MHz, $CDCl_3$) δ 7.14 (d, *J* = 8.0 Hz, 1H), 7.11 (s, 1H), 6.97 (s, 2H), 6.48 (s, 1H), 6.44 (d, 8.0 Hz, 1H), 4.49 (br s, 1H), 4.26 (d, *J* = 5.5 Hz, 2H), 3.81 (s, 3H), 3.78 (s, 3H).

^{13}C NMR (125 MHz, CDl_3) δ 160.7, 158.5, 148.9, 132.6, 132.4, 132.1, 131.9, 130.0, 126.9, 124.8, 122.6, 120.4, 118.2, 112.1, 112.0, 109.9, 109.8, 104.2, 98.7, 55.3, 42.8.

HRMS (ESI) calcd for (M^+) $C_{17}H_{15}F_6NO_2^+$: 379.1001, Found: 379.0939.

IR: 3392, 1615, 1508, 1280, 1170, 1156, 1134, 1117, 1074 cm^{-1}

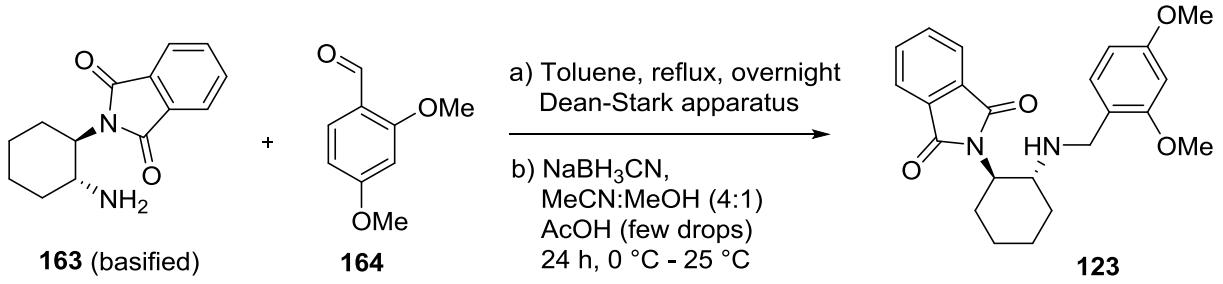

163 (basified) **164** **123**

Compound **163** (5.02 g, 20.55 mmol, 1.0 equiv) is basified according to literature procedure.[9] Then, the primary amine and 2,4-dimethoxybenzaldehyde **164** (3.42 g, 20.55 mmol, 1.0 equiv) were dissolved in toluene (100 mL) and the mixture was refluxed overnight for 16 h. The round-bottom flask was attached to a Dean-Stark apparatus to collect water generated during the course of the formation of the imine (not shown). After 16 h, the system was bought to room temperature, and the toluene was removed using a rotary evaporator. The imine, without any purification, was dissolved in a 4:1 mixture of acetonitrile:methanol (100mL:25mL) and a few drops of acetic acid were added to this solution. Under inert atmosphere, the solution was cooled to 0 °C using an ice-bath. Fresh sodium cyanoborohydride (2.58 g, 41.1 mmol, 2.0 equiv) was added in portions to this solution at 0 °C, and the round-bottom flask was subsequently allowed to slowly warm to room temperature by removing the ice-bath. The conversion was monitored by ^{1}H NMR, and the reaction mixture was allowed to stir until no further improvement in conversion was observed. The solvent was evaporated, and the solid diluted with ethyl acetate and extracted with saturated $NaHCO_3$. The aqueous layer was washed with ethyl acetate, and the combined organic layers were dried with brine and $MgSO_4$, and concentrated. The mixture was

purified by flash chromatography, using CH_2Cl_2 to load the mixture on to the column. Then, the eluent is varied in polarity from 1:4 EtOAc:DCM to 10% MeOH in EtOAc to obtain 7.01 g (86%) of compound **123** as a pale yellow solid. Note that this compound is air-sensitive, and has a tendency to foam upon concentration. This problem was averted by using a large round-bottom flask and high rotation speeds on the rotary evaporator. The round bottom is typically subjected to high vacuum and the product flushed with N_2. For storage over extended periods, an efficient method is to keep the product dissolved in either EtOAc or CH_2Cl_2 under an atmosphere of N_2, and then concentrate the material prior to use.

123: ^{1}H NMR (500 MHz, $CDCl_3$) δ 7.79 (dd, *J* = 5.0, 3.0 Hz, 2H), 7.69 (dd, J = 5.0, 3.0, 2H), 6.95 (d, *J* = 8.0 Hz, 1H), 6.28 (dd, *J* = 8.0, 2.0 Hz, 1H), 6.18 (d, *J* = 2.0 Hz, 1H), 3.97 (dt, 11.5, 3.2 Hz, 1H), 3.73 (s, 1H), 3.70 (d, *J* = 13.0 Hz, 1H), 3.52 (d, *J* = 13.0 Hz, 1H), 3.40 (s, 3H), 3.25 (dt, *J* = 11.0, 4.0 Hz, 1H), 2.27-2.15 (m, 2H), 1.83-1.71 (m, 3H), 1.61 (br s, 1H), 1.40-1.30 (m, 2H), 1.22-1.11 (m, 1H)

^{13}C NMR (125 MHz, $CDCl_3$) δ 168.4, 159.7, 158.3, 133.5, 131.9, 130.1, 122.9, 121.2, 103.4, 98.3, 55.8, 55.7, 55.1, 54.7, 46.1, 32.9, 29.3, 25.6, 24.8

HRMS (ESI) calcd for $C_{23}H_{27}N_2O_4^+$: 395.1965, Found: 395.1971.

IR: 3853, 3744, 3675, 3649, 2918, 2361, 2337, 1701, 1653, 1559, 1506 cm^{-1}

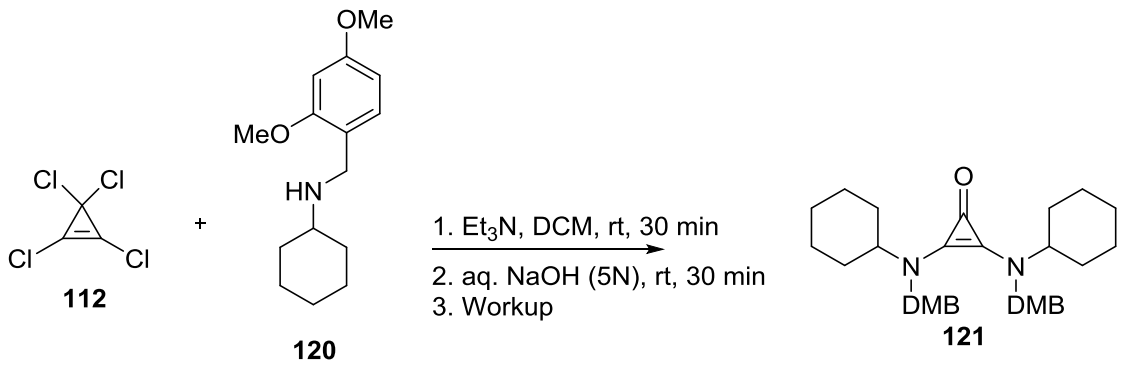

Small Scale Reaction:[11] To a stirred solution of tetrachlorocyclopropene **112** (178 mg, 1.0 mmol) in DCM (1 mL), a solution of **120** (399 mg, 1.6 mmol, 1.6 eq) in DCM (8 mL) was added at rt. Then triethylamine (280 µL, 2 mmol) was added dropwise to the reaction mixture at rt. After stirring for 30 min at rt, *aqueous* 5N NaOH (1.6 mL, 8 mmol) was added and the heterogeneous reaction mixture allowed to stir for 30 min. The organic layer was separated using a phase separator (IST, 120-1905-C, 6 mL capacity), washed with H_2O and concentrated *in vacuo*. (Alternatively, the organic layer can be separated, dried over $MgSO_4$ and then concentrated *in vacuo*). The residue was purified by SiO_2 column (AcOEt : hexane = 1:1 – 1:0) to give a white colorless solid of **121** (392 mg, 89%).

Gram Scale Reaction: To a stirred solution of tetrachlorocyclopropene **112** (1.33 g, 7.5 mmol, 1.0 equiv) in DCM (7.5 mL), a solution of **120** (2.99 g, 12 mmol, 1.6 eq) in DCM (60 mL) was added at rt. Then triethylamine (2.1 mL, 15 mmol, 2.0 equiv) was added dropwise to the reaction mixture. After stirring for 30 min at rt, *aqueous* 5N NaOH (12 mL) was added and the heterogeneous reaction mixture allowed to stir for 30 min. The organic layer was separated using a separatory funnel, washed with H_2O, brine, dried over $MgSO_4$ and concentrated *in vacuo*. The residue was purified by SiO_2 column (AcOEt : CH_2Cl_2 = 0:1 – 1:1) to give a white colorless solid of **121** (2.818 g, 86%).

121: ^{1}H NMR (500 MHz, $CDCl_3$) δ 6.97 (d, *J* = 6.0 Hz, 2H), 6.38-6.28 (m, 4H), 4.21 (s, 4H), 3.76 (s, 6H), 3.68 (s, 6H), 2.81 (s, 2H), 1.85-1.72 (m, 8H), 1.72-1.60 (m, 4H), 1.58-1.50 (m, 2H), 1.22-1.14 (m, 6H).

^{13}C NMR (125 MHz, $CDCl_3$) δ 159.8, 157.5, 132.1, 127.9, 118.9, 118.1, 103.4, 97.8, 60.1, 54.8, 54.6, 49.1, 31.7, 25.5, 24.9.

[11] Note that this reaction was reported to us by Prof. Tristan H. Lambert in a private communication. The initial yield of 37% was further optimized by our group.

HRMS (ESI) calcd for $C_{33}H_{45}N_2O_5^+$: 549.3323, Found: 549.3327.

IR: 2930, 2853, 2361, 2337, 1900, 1559, 1540, 1506, 1418, 1301, 1257, 1208, 1156, 1035, 834 cm^{-1}

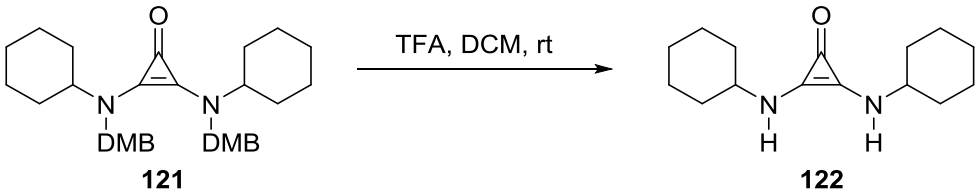

121 **122**

Gram Scale Reaction:[12] TFA was added to a stirred solution of **121** (2.25 g, 4.1 mmol) in DCM (10 mL) at rt. A white precipitate (DMB derived byproduct) was gradually generated. After 30 min, the mixture was diluted with Et_2O (80 mL) and MeOH (8 mL), and filtered through short SiO_2 column to remove the precipitate. The filtrate was concentrated *in vacuo* to give a mixture of **1** and TFA as an oil. The residue was dissolved in DCM, washed with sat. $NaHCO_3$ aq and brine, dried over $MgSO_4$, filtered and concentrated *in vacuo* to give a pale yellow solid. The solid was washed with Et_2O to give **122** an off-white solid (1.001 g, 97%).

122: ^{1}H NMR (500 MHz, $CDCl_3$) δ 4.47 (br s, 2H), 3.20-3.12 (m, 2H), 2-1.94 (m, 4H), 1.76 (dt, *J* = 13.2, 3.8 Hz, 4H), 1.62 (dt, *J* = 9.0, 3.8 Hz, 2H), 1.37-1.14 (m, 10H).

^{13}C NMR (125 MHz, $CDCl_3$) δ 131.5, 117.4, 54.6, 34.0, 25.4, 24.6.

HRMS (ESI) calcd for $C_{15}H_{25}N_2O^+$ $(M+H)^+$: 249.1961, Found: 249.1975.

IR 3187, 2928, 2853, 2362, 1910, 1567, 1488, 1446, 1418, 1365, 1343, 1305, 1110 cm^{-1}

[12] Note that this reaction was also communicated to us by Prof. Tristan H. Lambert. Herein, we report a gram-scale version.

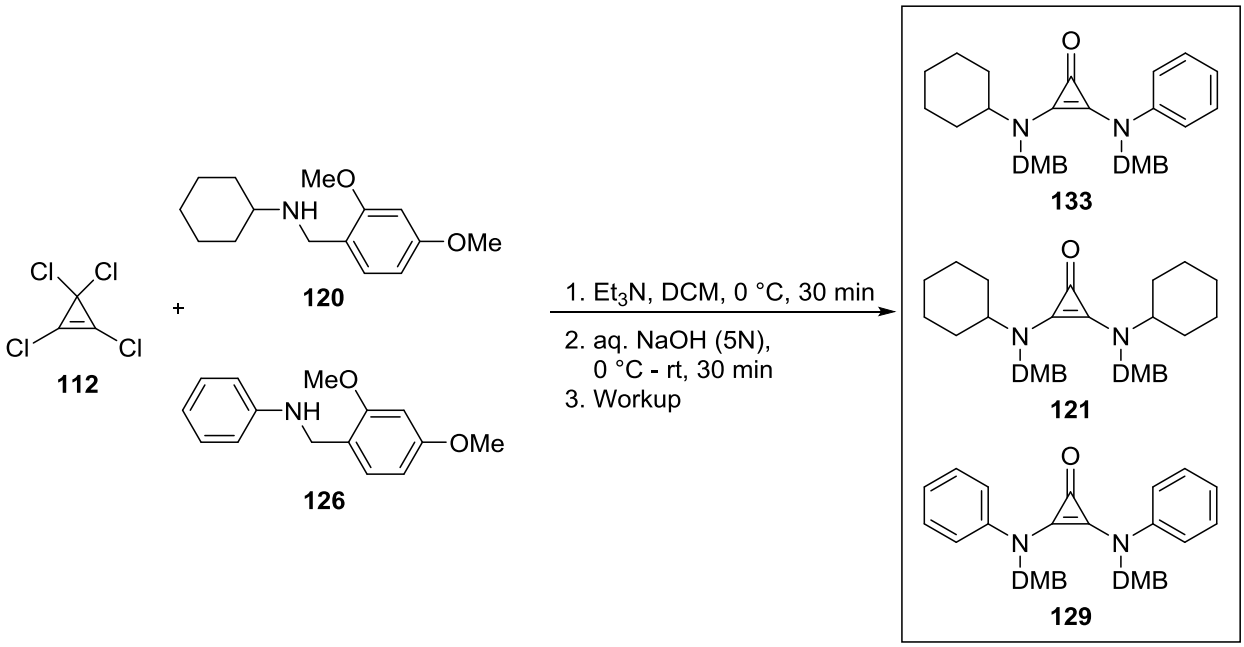

A solution of **120** (1.845 g, 7.4 mmol, 0.8 eq) in DCM (8 mL) was added over two minutes to a stirred solution of tetrachlorocyclopropene **112** (1.645 g, 9.25 mmol, 1 equiv) in DCM (9.25 mL) at 0 °C. This was then followed by the addition of **126** (1.8 g, 7.4 mmol, 0.8 equiv) at 0 °C over two minutes, and then triethylamine (2.58 mL, 18.5 mmol, 2 equiv) (added at once) to the reaction mixture at 0 °C. After stirring for 30 min, aq. 5N NaOH (mL, 4 mmol, 8 equiv) was added and the heterogeneous reaction mixture stirred for 30 min at rt (after removal of the ice-bath). The organic layer was separated using a separatory funnel, washed with H_2O, brine, dried over $MgSO_4$, and concentrated *in vacuo*. The residue was purified by SiO_2 column (DCM – 1:1 DCM:EtOAc) to give a compounds **121** (868 mg, 21%), **133** (1.448 g, 36%) and **129** (41 mg, 1%) as off-white solids. **121** has been characterized above.

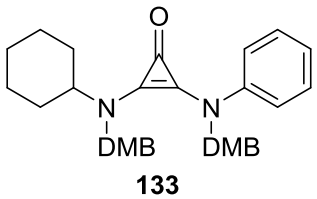

133

133: **^{1}H NMR** (500 MHz, $CDCl_3$) δ 7.32-7.24 (m, 4H), 6.92 (t, J = 7.0 Hz, 1H), 6.86 (dd, *J* = 16.5, 8.5 Hz, 2H), 6.33 (dd, *J* = 15.5, 2.0 Hz, 2H), 6.29 (dd, *J* = 8.0, 2.0 Hz, 2H), 4.73 (s, 2H), 4.19 (s, 2H), 3.76 (s, 3H), 3.74 (s, 3H), 3.69 (s, 3H), 3.66 (s, 3H), 2.89-2.82 (tt, *J* = 11.7, 3.6 Hz, 1H), 1.80 (t, *J* = 12.2 Hz, 4H), 1.72-1.61 (m, 2H), 1.60-1.53 (m, 1H), 1.28-1.09 (m, 3H).

^{13}C NMR (125 MHz, $CDCl_3$) δ 160.1, 160.0, 157.7, 157.3, 143.4, 133.4, 129.2, 128.0, 126.9, 123.1, 121.4, 117.6, 116.1, 115.8, 113.8, 103.7, 103.5, 98.1, 60.9, 55.1, 54.9, 54.8, 49.6, 49.1, 31.9, 25.7, 25.0.

HRMS (ESI) calcd for $C_{33}H_{39}N_2O_5^+$ $(M+H)^+$: 543.2853, Found: 543.2862.

IR 2934, 2854, 1906, 1610, 1506, 1417, 1365, 1335, 1302, 1209, 1157, 1121, 1038, 921, 834, 752, 731 cm^{-1}

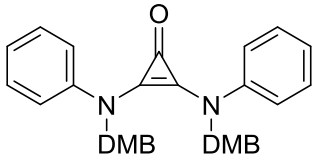

129

129: **^{1}H NMR** (500 MHz, $CDCl_3$) δ 7.31-7.23 (m, 8H), 6.98 (t, J = 6.7, 1.6 Hz, 2H), .6.82 (d, J = 8.4 Hz, 2H), 6.34 (d, *J* = 2.0 Hz, 2H), 6.25 (dd, *J* = 8.4, 2.4 Hz, 2H), 4.67 (s, 4H), 3.74 (s, 6H), 3.69 (s, 6H).

^{13}C NMR (125 MHz, $CDCl_3$) δ 160.2, 157.5, 143.1, 134.3, 129.4, 127.1, 122.6, 118.6, 117.0, 115.9, 103.7, 98.4, 55.2, 55.0, 50.0.

HRMS (ESI) calcd for $C_{33}H_{33}N_2O_5^+$ $(M+H)^+$: 537.2384, Found: 537.2401.

IR 3853, 2361, 2337, 1653, 1616, 1588, 1559, 1506, 1457, 1387, 1208 cm^{-1}

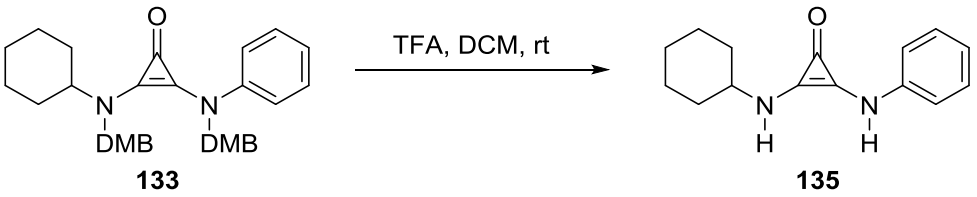

133 **135**

TFA (0.43 mL, 5.6 mmol, 7.5 equiv) was added to a stirred solution of **133** (405 mg, 0.75 mmol, 1 equiv) in DCM (1.6 mL) at rt. A white precipitate (DMB derived byproduct) was gradually generated. After 1 hour, the mixture was diluted with a 3:1 mixture of chloroform and methanol, and filtered through a short SiO_2 column to remove the precipitate. The filtrate was concentrated *in vacuo* to give a maroon oil. This oil was purified by flash column chromatography (1:4 Hexanes:EtOAc to 1:9 MeOH:EtOAc) to give **135** as a white solid (170 mg, 94 %). Note that the compound is sparingly soluble in chloroform or methanol, but is soluble in mixtures of chloroform and methanol.

135: ^{1}H NMR (500 MHz, 1:1 $CDCl_3$:CD_3OD) δ 7.33-7.20 (m, 2H), 7.18-7.12 (m, 2H), 6.94 (t, *J* = 7.5 Hz, 1H), 3.34-3.27 (m, 1H), 2.04-1.96 (m, 2H), 1.84-1.76 (m, 2H), 1.68-1.60 (m, 1H), 1.45-1.18 (m, 5H).

This 1H NMR spectrum was calibrated with respect to the TMS signal at δ = 0 ppm. Peaks corresponding to $CHCl_3$, CH_3OD, HDO and H_2O can be observed, albeit at different δ values because a 1:1 mixture of $CDCl_3$ and CD_3OD was used as the NMR solvent.

^{13}C NMR (125 MHz, 1:1 $CDCl_3$:CD_3OD) δ 140.3, 130.0, 128.9, 121.0, 119.1, 114.2, 110.7, 53.9, 33.2, 24.7, 24.0.

This ^{13}C NMR spectrum was calibrated with respect to $CDCl_3$ triplet at δ = 77.0 ppm.

HRMS (ESI) calcd for $C_{15}H_{19}N_2O^+$: 243.1492, Found: 243.1499.

IR 3853, 2927, 2850, 1653, 1616, 1559, 1540, 1507, 1457, 1298, 1207 cm^{-1}

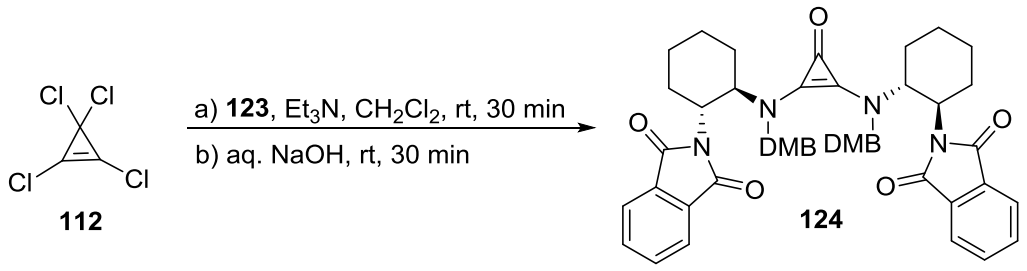

To a stirred 1M solution of tetrachlorocyclopropene **112** (2.24 g, 12.6 mmol) in DCM (13 mL), a 0.2M solution of **123** (20.2 mmol, 1.6 equiv) in DCM (101 mL) was slowly added at room temperature. Then triethylamine (3.5 mL, 25.2 mmol, 2 equiv) was added, and the reaction mixture stirred for 16 hours. At the end of 16 hours, 5N *aq.* NaOH (20.1 mL, 100.8 mmol, 8 equiv) was added, and the heterogeneous reaction mixture allowed to stir for 4 hours at rt. The organic layer was separated, washed with H_2O, dried with brine and $MgSO_4$ and concentrated *in vacuo*. The residue was purified by SiO_2 column (MeOH : EtOAc = 1:20 – 1:10) to give **124** as a pale white solid (3.836 g, 45%).

124: ^{1}H NMR (500 MHz, $CDCl_3$) δ 7.72 (br s, 2H), 7.64 (s, 4H), 7.55 (br s, 2H), 6.80 (d, *J* = 8.0 Hz, 2H), 6.06 (d, *J* = 6.5 Hz, 2H), 5.75 (s, 2H), 4.57 (td, *J* = 11.0, 3.8 Hz, 2H), 4.37 (d, *J* = 15.0 Hz, 2H), 3.94 (s, *J* = 15.0 Hz, 2H), 3.63 (s, 6H), 3.39 (s, 6H), 2.31-2.22 (m, 2H), 2.02 (br s, 4H), 1.89-1.55 (m, 10H), 1.36 (br s, 2H).

^{13}C NMR (125 MHz, $CDCl_3$) δ 167.5, 160.1, 157.9, 134.6, 133.1, 131.9, 130.1, 122.6, 119.1, 117.9, 103.4, 97.9, 59.5, 54.9, 54.5, 52.9, 31.1, 29.0, 25.0, 24.7.

HRMS (ESI) calcd for $C_{49}H_{51}N_4O_9^+$: 839.3651, Found: 839.3653.

IR (cm^{-1}): 2934, 2361, 2338, 1710, 1587, 1559, 1507, 1457, 1419, 1389, 1376, 1291, 1209, 1157, 719.

R_f (10% MeOH in EtOAc): ~0.5

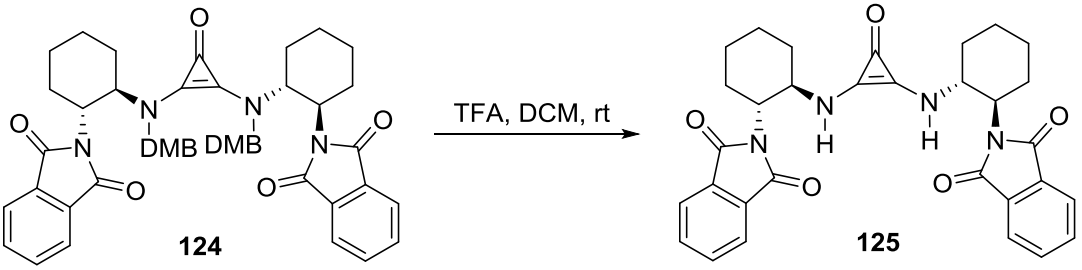

Trifluoroacetic acid (TFA) (1.08 mL, 14.0 mmol, 20 equiv) was added to compound **124** (584 mg, 0.70 mmol, 1 equiv) in anhydrous CH_2Cl_2 (7 mL) and stirred for 24 hours (The color of reaction mixture gradually changes to pink during the course of this reaction). Then, the reaction mixture is concentrated *in vacuo*, dissolved in MeOH:$CHCl_3$ (1:1) and filtered through a plug of silica. The filtrate is then concentrated and purified by SiO_2 column ($CHCl_3$ – 2% MeOH in $CHCl_3$) to afford **125** (312 mg, 83%). Note that the compound is only sparingly soluble in methanol and chloroform, but is very soluble in a mixture of methanol and chloroform. Also, note the higher reaction times in comparison to **122**, likely due to steric factors.

125: ^{1}H NMR (500 MHz, 1:1 $CDCl_3$: CD_3OD) δ 7.77 (s, 8H), 4.00-3.93 (m, 2H), 3.89-3.82 (m, 2H), 2.28-2.13 (m, 2H), 2.01-1.96 (m, 2H), 1.88-1.72 (m, 6H), 1.48-1.30 (m, 6H).

^{13}C NMR (125 MHz, 1:1 $CDCl_3$: CD_3OD) δ 167.9, 133.5, 131.1, 129.2, 122.4, 116.6, 54.7, 54.3, 32.8, 28.5, 24.3, 24.0.

IR (cm^{-1}): 2935, 2361, 2339, 1701, 1653, 1586, 1559, 1506, 1466, 1457, 1436, 1394, 1379, 1080, 751, 718, 668.

HRMS (ESI) calcd for $C_{23}H_{27}N_2O_4^+$: 539.2289, Found: 539.2275.

R_f (10% MeOH in $CHCl_3$): ~ 0.3

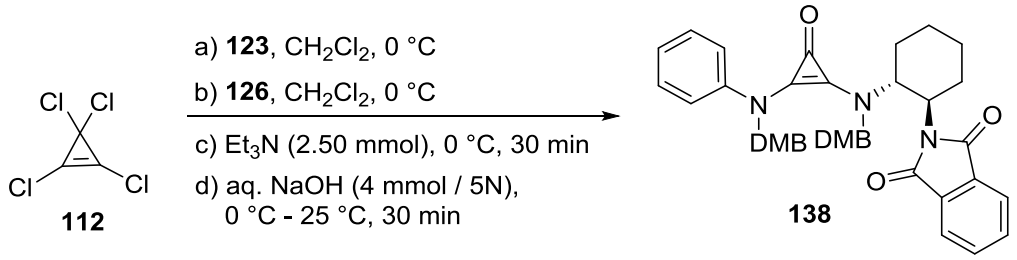

To a stirred 1M solution of tetrachlorocyclopropene **112** (88.9 mg, 0.5 mmol, 1 equiv) in DCM, a 1M solution of **123** (157.8 mg, 0.4 mmol, 0.8 equiv) in DCM was slowly added at 0 °C, followed by the slow addition of a 1M solution of **126** (97.3 mg, 0.4 mmol, 0.8 equiv) at 0 °C. Then triethylamine (0.35 mL, 2.5 mmol, 5 equiv) was added slowly to the reaction mixture. After stirring for 30 min at 0 °C, 5N *aq.* NaOH (0.8 mL, 4 mmol, 8 equiv) was added and the heterogeneous reaction mixture allowed to stir for 30 min at rt. The organic layer was separated, washed with H_2O, dried over $MgSO_4$ and concentrated *in vacuo*. The residue was purified by SiO_2 column with 3:1 EtOAc:Hexanes as eluent to give a white solid (69.5 mg, 25%).

138: ^{1}**H NMR** (500 MHz, $CDCl_3$) δ 7.81-7.55 (m, 4H), 7.33 (d, *J* = 8.0 Hz, 2H), 7.28-7.24 (m, 2H), 6.94 (t, *J* = 7.0 Hz, 1H), 6.90 (d, *J* = 8.5 Hz, 1H), 6.71 (d, *J* = 7.5 Hz), 6.30 (s, 1H), 6.24 (d, *J* = 8.0 Hz, 1H), 6.07 (d, *J* = 7.5 Hz, 1H), 5.96 (s, 1H), 4.94 (d, *J* = 18.0 Hz, 1H), 4.83 (d, *J* = 17.5 Hz, 1H), 4.54 (t, *J* = 9.3 Hz, 1H), 3.94 (s, 2H), 3.75-3.65 (m, 1H), 3.70 (s, 3H), 3.69 (s, 3H), 3.60 (s, 3H), 3.47 (s, 3H), 2.27-2.19 (m, 1H), 1.85-1.72 (m, 5H), 1.59-1.48 (m, 1H), 1.35-1.20 (m, 1H).

^{13}**C NMR** (125 MHz, $CDCl_3$) δ 160.4, 160.0, 158.1, 157.4, 143.5, 134.8, 133.3, 130.2, 129.2, 127.2, 122.9, 122.5, 121.5, 117.0, 116.4, 116.1, 114.6, 104.0, 103.4, 98.2(2C), 59.6, 55.2, 55.0 (2C), 54.7, 53.0, 48.8, 31.6, 29.6, 29.1, 24.9, 24.7.

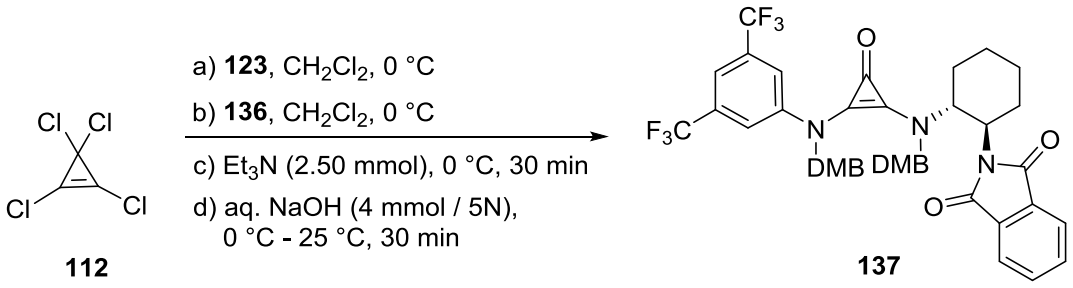

112 **137**

To a stirred 1M solution of tetrachlorocyclopropene **112** (2.76 g, 15.5 mmol, 1 equiv) in DCM (15.5 mL), a 0.2M solution of **123** (4.90 g, 12.4 mmol, 0.8 equiv) in DCM (62 mL) was slowly added at 0 °C, followed by the slow addition of a 0.2M solution of **136** (4.71 g, 12.4 mmol, 0.8 equiv) at 0 °C. Then triethylamine (10.8 mL, 77.5 mmol, 5 equiv) was added slowly to the reaction mixture. After stirring for 30 min at 0 °C, 5N *aq.* NaOH (24.8 mL, 124 mmol, 8 equiv) was added and the heterogeneous reaction mixture allowed to stir for 30 min at rt. The organic layer was separated, washed with H_2O, dried over $MgSO_4$ and concentrated *in vacuo*. The residue was purified by SiO_2 column (30% EtOAc in Hexanes to 45% EtOAc in Hexanes, using $CHCl_3$ to deposit the compound onto the column) to give a white solid (2.05 g, 20%).

137: ^{1}H NMR (500 MHz, $CDCl_3$) δ 7.88 (s, 1H), 7.78 (s, 1H), 7.68 (s, 2H), 7.60 (s, 1H), 7.41 (s, 1H), 6.91 (d, *J* = 8.5 Hz, 1H), 6.80 (d, *J* = 7.5 Hz, 1H), 6.35 (d, *J* = 2.0 Hz, 1H), 6.27 (dd, *J* = 8.5, 4.0 Hz, 1H), 6.17 (dd, *J* = 8.3, 4.0 Hz, 1H),

^{13}C NMR (125 MHz, $CDCl_3$) δ 144.6, 134.8, 133.4, 133.0, 132.8, 132.5, 132.2, 130.6, 127.6, 126.6, 124.4, 123.8, 122.9, 122.2, 120.1, 116.3, 115.6, 114.8, 114.5, 114.4 (3C), 112.5, 104.6, 103.6, 98.4, 98.3, 77.3, 77.0, 76.7, 59.7, 55.2, 55.1 (2C), 54.7, 53.1, 48.1, 31.8, 29.0, 24.9, 24.7.

HRMS (ESI) calcd for $C_{43}H_{40}F_6N_3O_7^+$: 824.2765, Found: 824.2768.

IR 2937, 2361, 2337, 1710, 1684, 1616, 1507, 1392, 1278, 1210, 1133, 1037, 720 cm^{-1}

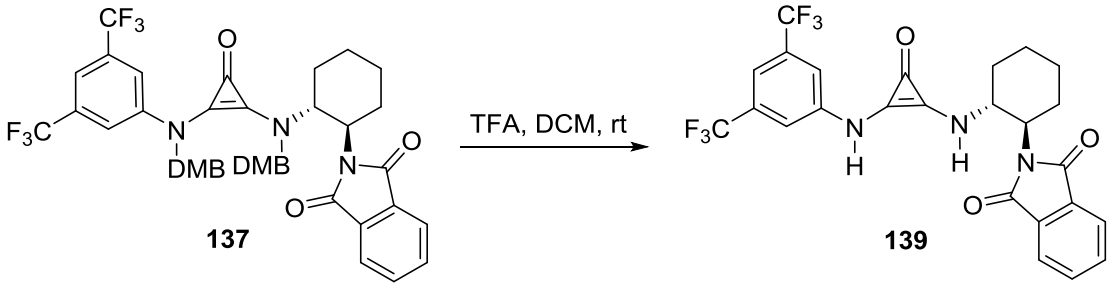

Compound **137** was purified so as to afford it in greater than 97% purity. Then, traces of solvent were removed (by heating to about 60 °C on high vacuum for about 1 hour) to result in a pale yellow powder. Note that this reaction is sensitive to the purity of the starting material: Trifluoroacetic acid (TFA) (1.08 mL, 14 mmol, 10 equiv) was added to compound **137** (1.15 g, 1.40 mmol, 1 equiv) in anhydrous CH_2Cl_2 (14 mL) and stirred for 24 hours (The color of reaction mixture gradually changes to pink during the course of this reaction). The reaction mixture is concentrated *in vacuo*, dissolved in MeOH:$CHCl_3$ (1:3) and filtered through a plug of silica. As the compound slowly decomposes in solution, this filtrate is then quickly concentrated and purified by SiO_2 column (75:25:0.5 ethyl acetate:hexanes:NH_4OH) to afford **139** (501.2 mg, 68%) as a white solid. Note that the product, while insoluble in most nonhydroxylic solvents, slowly decomposes in a mixture of $CHCl_3$ and MeOH, and thus alternatively, the next step can be carried out without purifying **139**..

139: ^{1}H NMR (500 MHz, $CDCl_3$) δ 8.05 (br s, 1H), 7.70 (s, 2H), 7.63 (s, 2H), 7.50 (s, 2H), 7.39 (1H), 5.88 (br s, 1H), 4.14 (d, *J* = 9.0 Hz, 1H), 4.06-4.00 (m, 1H), 2.30-2.10 (m, 2H), 1.95-1.70 (m, 3H), 1.58-1.30 (m, 3H).

HRMS (ESI) calcd for $C_{25}H_{20}F_6N_3O_3^+$: 524.1403, Found: 524.1402.

IR 3330, 2937, 1707, 1618, 1471, 1384, 1277, 1173, 1129, 720 cm^{-1}

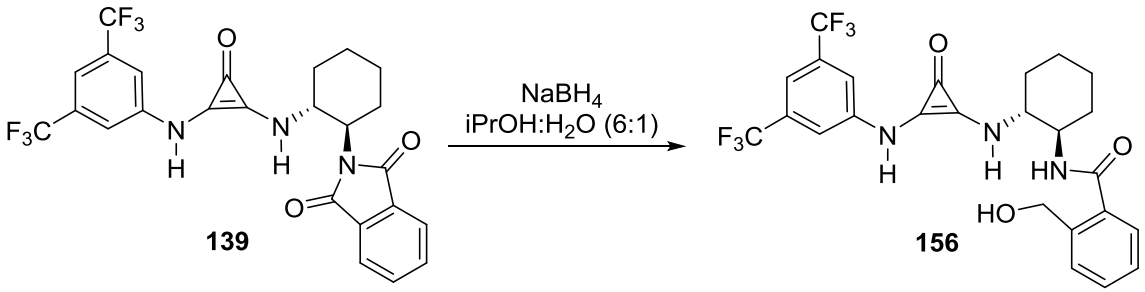

Sodium borohydride (36.1 mg, 0.955 mmol, 5 equiv) is added to a solution of **139** (100.0 mg, 0.191 mmol, 1 equiv) in 6:1 iPrOH:H_2O (2 mL total), and the resulting reaction mixture is stirred at room temperature for 24 h. Additional $NaBH_4$ (up to 10 equiv) is used if **139** wasn't purified via chromatography in the earlier step. The reaction is then concentrated, and the solid is re-dissolved in a 3:1 mixture of chloroform and methanol. This is dried over $MgSO_4$, and then filtered through celite, with further washings using the same mixture of chloroform and methanol. The filtrate is quickly concentrated, and purified by flash column chromatography using ethyl acetate as the eluent to afford **156** (79.8 mg, 78%) as a white solid. Note that the product, while insoluble in most nonhydroxylic solvents, slowly decomposes in $CHCl_3$ and MeOH, and thus alternatively, the next step can be carried out without purifying **156**.

156: ^{1}H NMR (500 MHz, CD_3OD) δ 7.59 (s, 2H), 7.45 (d, *J* = 7.5 Hz, 1H), 7.41 (s, 1H), 7.36 (d, *J* = 7.0 Hz, 1H), 7.31 (t, *J* = 7.0 Hz, 1H), 7.20 (t, *J* = 7.0 Hz, 1H), 4.65 (d, *J* = 12.5 Hz, 1H), 4.60 (d, *J* = 13.0 Hz, 1H), 3.95 (dt, *J* = 10.5, 7.7 Hz, 1H), 3.35-3.25 (m, 1H), 2.13-2.02 (m, 2H), 1.85-1.75 (m, 4H), 1.57-1.38 (m, 4H).

^{13}C NMR (125 MHz, CD_3OD) δ 172.1, 144.7, 140.4, 136.8, 134.5, 134.3, 134.0, 133.7, 132.8, 131.6, 130.4, 129.0, 128.8, 128.1, 125.9, 123.8, 123.5, 121.6, 116.0, 115.1, 110.2, 63.9, 61.0, 55.0, 33.9, 33.2, 32.8, 25.7.

HRMS (ESI) calcd for $C_{25}H_{24}F_6N_3O_3^+$: 528.1716, Found: 528.1717.

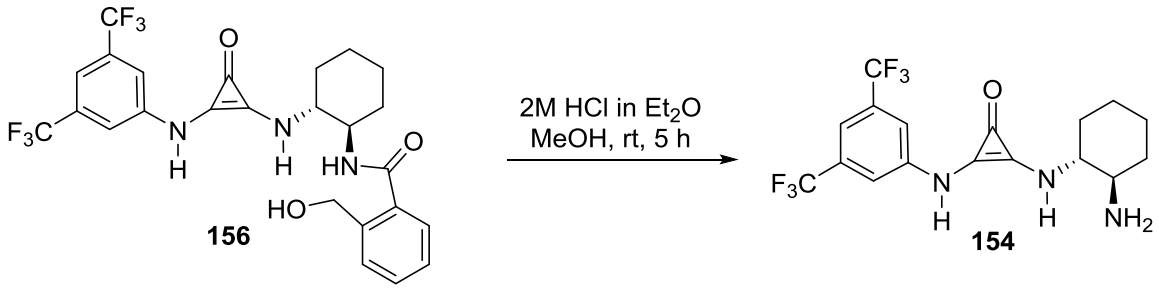

A solution of HCl (2M in diethyl ether) (30 equiv) is added to a solution of compound **156** (10.0 mg, 0.0019 mmol, 1.0 equiv) in 1.5 mL of MeOH. The reaction is monitored by TLC for the consumption of **156**. After 5 hours, the reaction mixture was concentrated, redissolved in $CHCl_3$, washed with x/10 sat. $NaHCO_3$ and concentrated again and subjected to high vacuum. It was then purified by quick flash column chromatography using $CHCl_3$:MeOH (20:1-3:1) as the eluent. The fractions are quickly concentrated to afford **154** as an off-white solid. Varying yields (40-60%) have been obtained, however, the reaction has been carried out reliably (1 – 40 mg scale). This solid is stable over several days at room temperature under inert atmosphere. Note that we could not ascertain if compound **154** exists with the primary amine in the protonated or the unprotonated form. The protonated chloride salt has been referred to as compound **157**.

154(/157): ^{1}H NMR (500 MHz, CD_3OD) δ 7.77 (s, 2H), 7.52 (s, 1H), 3.42-3.32 (m, 1H), 3.09 (t, *J* = 10.5 Hz, 1H), 2.17 (d, *J* = 13.0 Hz, 1H), 2.10 (d, *J* = 11.0 Hz, 1H), 1.88 (d, *J* = 8.0 Hz, 2H), 1.59-1.44 (m, 4H), 1.34-1.25 (m, 2H).

ESI/MS $(M+H)^+$: 394.1.

HRMS (ESI) calcd for $C_{17}H_{18}F_6N_3O^+$: 394.1349, Found: 394.1360.

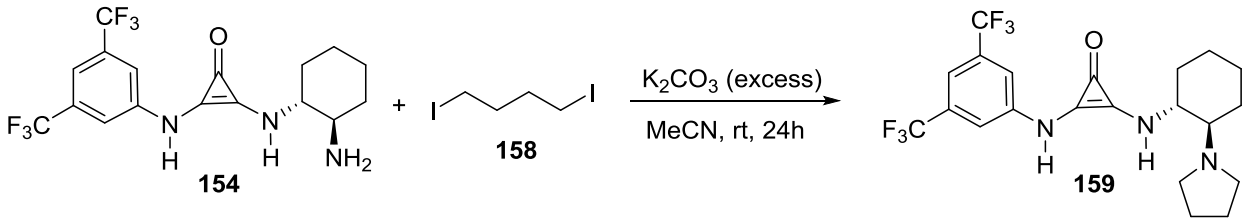

Excess anhydrous potassium carbonate is added to a mixture of **154** (1.0 equiv) and acetonitrile (Note that **159** is only sparingly soluble in acetonitrile, while under the same conditions in methanol, **159** primarily undergoes a ring-opening reaction). This is followed by the addition of diiodobutane **158** (2.0 equiv) via a syringe, and the reaction mixture is stirred at room temperature for 24 h, while being monitored by TLC. The compound **159** (Rf ~ 0.55 in 1:3 MeOH:$CHCl_3$) is slightly less polar than **154** (Rf ~ 0.5 in 1:3 MeOH:$CHCl_3$). This hints towards the absence of **157** over **154**.

For a trial-run carried out with 8 mg of **154**, 4.0 mg (44%) of the product **159** was obtained. Nonetheless, note that the yields may be improved upon.

159: ^{1}H NMR (500 MHz, CD_3OD) δ 7.79 (s, 2H), 7.51 (s, 1H), 3.53 (m 1H), 3.19 (m, 5H), 2.17 (m, 2H), 2.01 (m, 3H), 1.85 (m, 2H), 1.57 (m, 3H), 1.47 (m, 2H).

ESI/MS $(M+H)^+$: 448.2.

HRMS (ESI) calcd for $C_{17}H_{18}F_6N_3O^+$: 448.1818, Found: 448.1820.

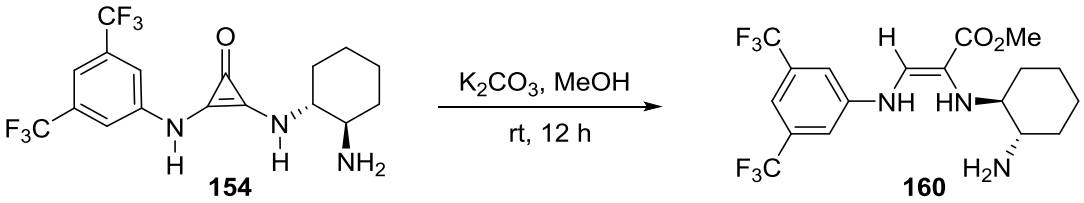

As compound **154** was insoluble in most non-hydroxylic solvents, it was attempted to use methanol as a co-solvent with acetonitrile in the above reaction. However, that led to the isolation of compound **160** (tentative structure). This reaction was repeated with 1.0 mg of **154** in 0.2 mL of MeOH and excess K_2CO_3. After stirring the reaction mixture for 12 hours, compound **160** was isolated via preparative TLC. The yield will be determined, reported in due course by carrying out the reaction on a larger scale.

The structure was assigned tentatively by considering the following data: 1) The peak at 7.70 implies that the ester is *cis* to the alkene proton. Had the ester been in a *trans* or *gem* position, one may expect a lower δ value. This would also be expected given the starting material geometry. 2) An *N*-aryl imine can be ruled out, given the absence of peaks above δ = 8.5. c) While ^{1}H NMR cannot rule out the other isomer with the ester *cis* to the alkene proton, we arrived a tentative structure given that a ring-opening reaction would be irreversible. For the proposed intermediate, see structure below.

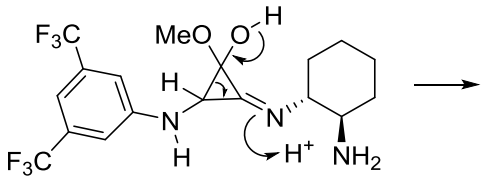

160: ^{1}H NMR (500 MHz, CD_3OD) δ 7.70 (s, 1H), 7.11 (s, 1H), 7.04 (s, 2H), 3.69 (s, 3H), 3.0-2.9 (m, 1H), 2.74-2.62 (m, 1H), 2.1-1.2 (m, 8H).

ESI/MS $(M+H)^{+}$: 426.2.

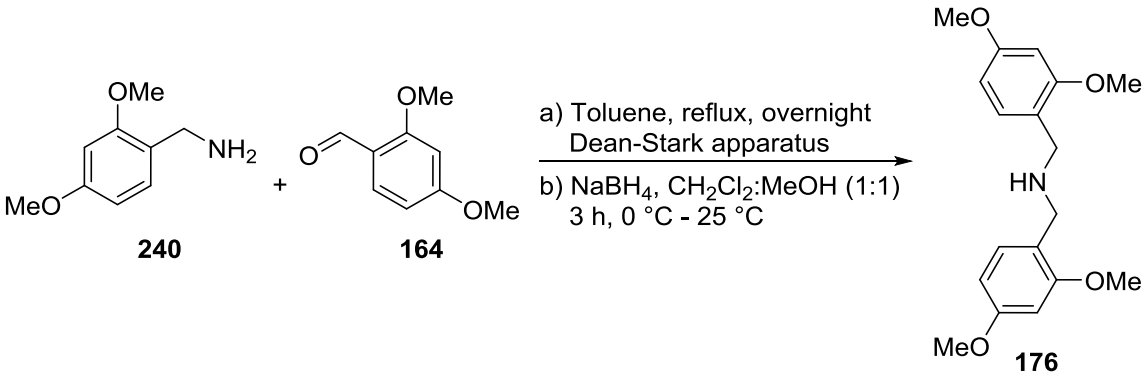

Commercially available 2,4-dimethoxybenzylamine **240** (5.07 g, 30.33 mmol, 1.0 equiv) and 2,4-dimethoxybenzaldehyde **164** (5.04g, 30.33 mmol, 1.0 equiv) were dissolved in toluene (75 mL) and the mixture was refluxed overnight for 12 h. The round-bottom flask was attached to a Dean-Stark apparatus to collect water generated during the course of the formation of the imine

(not shown). After 12 h, the system was bought to room temperature, and the toluene was removed using a rotary evaporator. The imine, without any purification, was then dissolved in a 1:1 mixture of dichloromethane and methanol under inert atmosphere, and the solution was cooled to 0 °C using an ice-bath. Sodium borohydride (1.53 g, 40.33 mmol, 1.33 equiv) was added in portions to this solution at 0 °C, and the round-bottom flask was subsequently allowed to slowly warm to room temperature by removing the ice-bath. The reaction mixture was allowed to stir for 3 h, after which it was diluted with ethyl acetate and extracted with saturated sodium bicarbonate. The aqueous layer was washed with ethyl acetate, and the combined organic layers were dried with brine and $MgSO_4$, and concentrated. The mixture was purified by flash chromatography, using a 20:1 mixture of hexanes and ethyl acetate as the eluent to obtain 9.43 g (98%) of compound **176**.

176: ^{1}H NMR (500 MHz, $CDCl_3$) δ.7.16 (d, *J* = 8.0 Hz, 2H), 6.43 (m, 4H), 3.80 (s , 6H), 3.79 (s, 6H), 3.71 (s, 4H), 2.1 (br s, 1H).

^{13}C NMR (125 MHz, CDl_3) δ. 159.3, 158.6, 130.3, 121.2, 103.7, 98.5, 55.3, 55.2, 48.1.

ESI/MS $(M+H)^+$: 318.2.

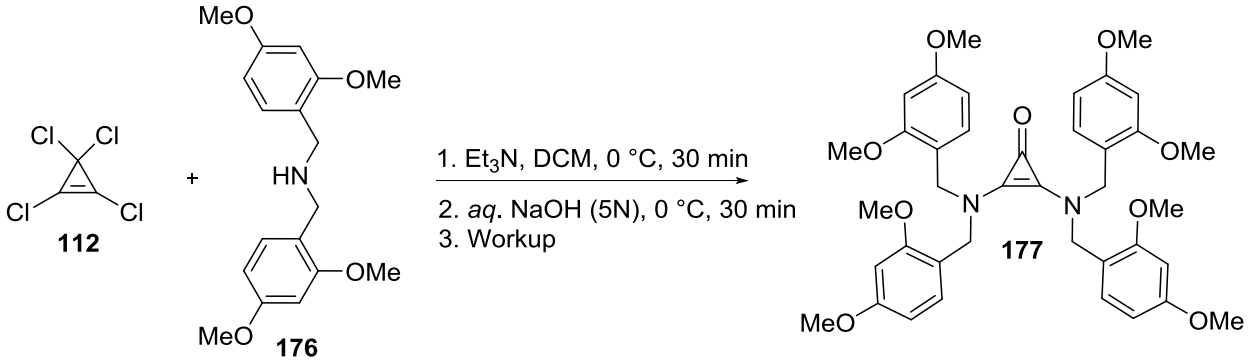

To a stirred solution of tetrachlorocyclopropene **112** (347 mg, 1.95 mmol, 1.0 equiv) in DCM (2 mL), a solution of **176** (990 mg, 3.12 mmol, 1.6 eq) in DCM (15 mL) was slowly added at 0 °C.

Then triethylamine (540 µL, 3.90 mmol, 2.0 equiv) was added dropwise to the reaction mixture at 0 °C within 1 minute of the addition of **176**. After stirring for 30 min at 0 °C, 5N aq. NaOH (3.1 mL, 15.6 mmol, 8 equiv) was added and the heterogeneous reaction mixture allowed to stir for 30 min and simultaneously allowed to slowly come to room temperature. The organic layer was separated, washed with H_2O, The organic layer separated again, the aqueous layer washed with DCM. The combined organic layers were dried over brine and over $MgSO_4$, and concentrated *in vacuo*. The residue was purified by SiO_2 column (loaded on to the column using CH_2Cl_2, and eluted with AcOEt to 5% MeOH in EtOAc to give a white colorless solid **177** (594 mg, 56%).

177: ^{1}H NMR (500 MHz, $CDCl_3$) δ 7.10 (d, *J* = 8.5 Hz, 2H), 6.39 (d, *J* = 8.5 Hz, 2H), 6.36 (d, *J* = 2.0 Hz), 4.25 (s, 4H), 3.76 (s, 6H), 3.65 (s, 6H).

^{13}C NMR (125 MHz, $CDCl_3$) δ 160.0, 158.2, 129.6, 120.1, 117.6, 103.5, 97.9, 54.8, 54.6, 48.8.

HRMS (ESI) calcd for $C_{39}H_{45}N_2O_9^+$: 685.3120, Found: 686.3168.

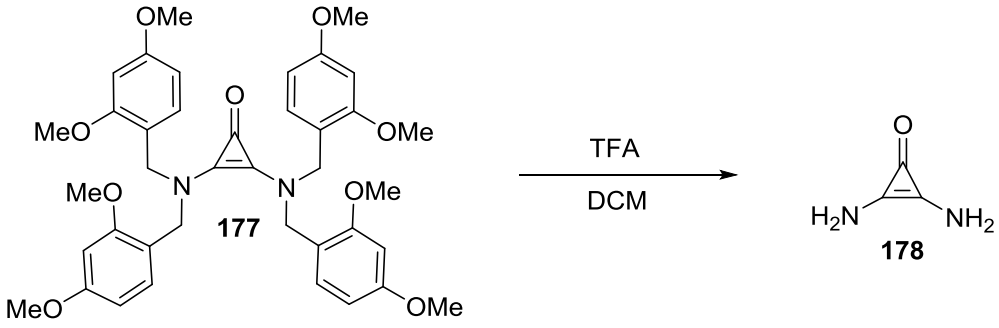

Trifluoroacetic acid (547 mg, 4.8 mmol, 10 equiv) was added to a solution of **177** (330 mg, 0.48 mmol, 1 equiv) in DCM (7.5 mL), and the reaction mixture was stirred for 24 hours. It should be noted that the color slowly turns pink as the reaction progresses. At the end of 24 hours, the reaction mixture is diluted with a 25% MeOH solution in $CHCl_3$, and filtered through a plug of silica, in order to remove the DMB-TFA by-product. The flask is washed (3 times) with 25%

MeOH in $CHCl_3$ solvent and passed through the same plug of silica. The clear solution is then concentrated, and the product **178** purified by flash column chromatography, using 15-25% MeOH in $CHCl_3$ as the eluent. 26.8 mg (66%) of **178** was isolated as a pale yellow solid.

178: ^{1}H NMR (500 MHz, d_6-DMSO) δ 6.02 (s, 4H).

^{13}C NMR (125 MHz, d_6-DMSO) δ 131.6, 118.8.

HRMS (ESI) calcd for $C_3H_5N_2O^+$: 85.0396, Found: 85.0176.

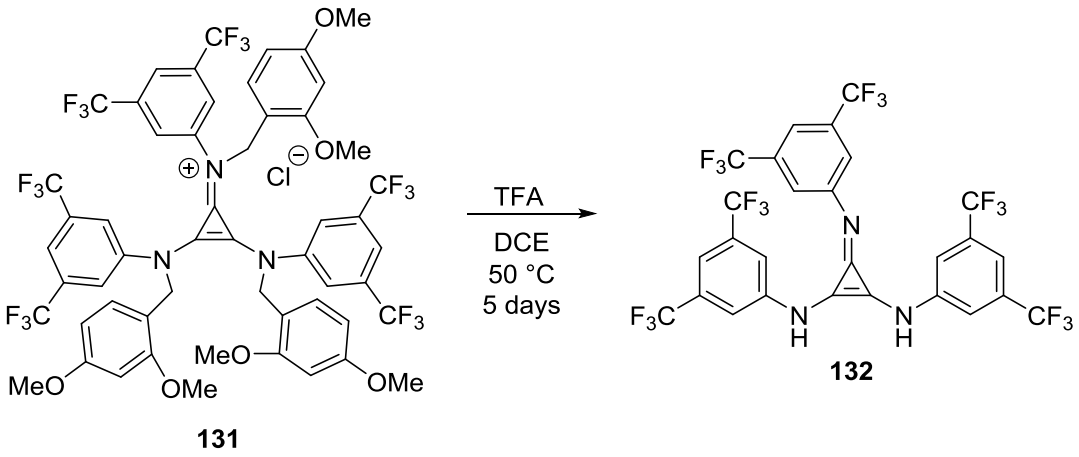

Trifluoroacetic acid (1.9 mL, 25 mmol, 50 equiv) is added to a solution of **131** (603 mg, 0.5 mmol, 1 equiv) in DCE (1.9 mL) and the mixture is stirred at 50 °C for 5 days. The resulting solution is cooled to room temperature, diluted with 25% MeOH in $CHCl_3$ and filtered through a plug of silica. The product is then isolated using flash column chromatography ($CHCl_3$ to 5% MeOH in $CHCl_3$) to afford 33.1 mg (9%) of the product **132**.

132: ^{1}H NMR (500 MHz, CD_3OD) δ.7.62 (s, 6H), 7.44 (s, 3H).

^{13}C NMR (125 MHz, CD_3OD) δ 150.1, 132.8, 132.5, 132.2, 131.8, 126.5, 124.3, 122.1, 120.0, 118.2, 114.8.

HRMS (ESI) calcd for $C_{27}H_{12}F_{18}N_3^+$: 720.0738, Found:. 720.0735.

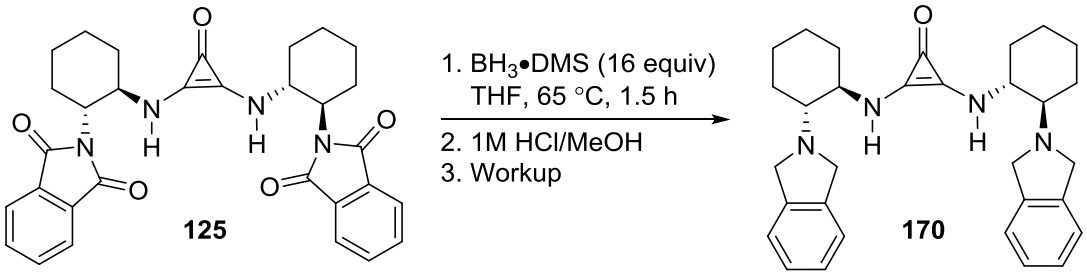

To a stirred solution of **125** (40 mg, 0.074 mmol, 1 equiv) in anhydrous THF (2.4 mL) under nitrogen was added a commercially available 2.0M solution of $BH_3 \cdot Me_2S$ in THF (1.19 mmol, 16 equiv). The mixture was stirred at 65 °C, and was quenched by the slow addition of MeOH until bubbling stops. The solvent and $B(OMe)_3$ were removed by applying high vacuum for 2 hours, and the solid subsequently obtained was heated with 1M HCl solution in MeOH (3 mL) at 65 °C for 1 hour. The solvent was evaporated under reduced pressure, and the semi-solid mixture was dissolved in a minimal quantity of H_2O, and this aqueous layer was washed with DCM (4x by volume) thrice. The aqueous layer is basified with sat. $NaHCO_3$ (pH > 8), and this basified layer is extracted with $CHCl_3$ thrice. Any insoluble material in the organic layer is removed using gravity filtration, and the filtrate is concentrated, and then quickly purified by preparative TLC (18% MeOH in $CHCl_3$). The product **170** is colorless, but appears below yellow impurity-bands. With the above procedure, the compound **170** was obtained as an off white solid, however, yields were found to vary with scale and work-up, typically ranging from 25-60%. Note that this compound is unstable in solution (chloroform), and decomposes completely over 4 days.

170: ^{1}H NMR (500 MHz, $CDCl_3$) δ 7.18 (s, 8H), 5.61 (br s, 2H), 3.99 (s, 8H), 3.12 (dt, *J* = 10.2, 4.4 Hz, 2H), 2.62-2.5 (m, 4H), 1.88-1.75 (m, 6H), 1.4-1.27 (8H).

ESI/MS $(M+H)^+$: 483.3.

R_f (18% MeOH in $CHCl_3$) ~ 0.65

V.3.2 X-ray crystal structure of 122

General information: a colorless block (0.18 x 0.22 x 0.39 mm) was mounted on a Dual-Thickness MicroMount^{tm} (MiTeGen) with 75 μm sample aperture. The diffraction data were measured at 100 K on a Bruker D8 VENTURE with PHOTON 100 CMOS detector system equipped with a Mo-target X-ray tube (λ = 0.71073 Å). Data reduction and integration were performed with the Bruker APEX2 software package. Data were corrected for absorption effects using the empirical methods as implemented in SADABS. The structure was solved and refined by full-matrix least-squares procedures using the Bruker SHELXTL software package. Crystallographic data and details of the data collection and structure refinement are listed in Table 1.

Specific details for structure refinement: Structure was refined as a 2-component perfect inversion twin. All atoms were refined with anisotropic thermal parameters. Hydrogen atoms were included in idealized positions for structure factor calculations except those involved in hydrogen bonding (See Table 2 below). These hydrogen atoms were located on the difference Fourier map and their coordinates allowed to be refined while their thermal parameters were constrained to be 1.2 times of the U_{eq} value of the N or C atoms they are attached to.

Table 26: Crystal Data and Structure Refinement for **122**

Empirical formula	$C_{17}H_{26}Cl_6N_2O$
Formula weight	487.10
Temperature	100(2) K
Wavelength	0.71073 Å
Crystal system	Monoclinic
Space group	*C*2
Unit cell dimensions	a = 51.623(5) Å α= 90°.
	b = 5.6432(5) Å β= 95.216(2)°.
	c = 11.4929(11) Å γ = 90°.
Volume	3334.3(5) $Å^3$
Z	6
Density (calculated)	1.456 Mg/m^3
Absorption coefficient	0.783 mm^{-1}
F(000)	1512
Crystal size	0.390 x 0.220 x 0.180 mm^3
Theta range for data collection	2.273 to 27.083°.
Index ranges	-65<=h<=64, -7<=k<=7, -14<=l<=14
Reflections collected	15810
Independent reflections	7037 [R(int) = 0.0344]
Completeness to theta = 25.242°	99.3 %
Absorption correction	Semi-empirical from equivalents
Max. and min. transmission	0.563 and 0.353
Refinement method	Full-matrix least-squares on F^2
Data / restraints / parameters	7037 / 1 / 371
Goodness-of-fit on F^2	1.051
Final R indices [I>2sigma(I)]	R1 = 0.0476, wR2 = 0.1007
R indices (all data)	R1 = 0.0540, wR2 = 0.1036
Largest diff. peak and hole	0.634 and -0.492 $e \cdot Å^{-3}$

$R_{int} = \Sigma \mid F_o^2 - \langle F_o^2 \rangle \mid / \Sigma \mid F_o^2 \mid$

$R1 = \Sigma \mid \mid F_o \mid - \mid F_c \mid \mid / \Sigma \mid F_o \mid$

$wR2 = [\Sigma [w (F_o^2 - F_c^2)^2] / \Sigma [w (F_o^2)^2]]^{1/2}$

$Goodness\text{-}of\text{-}fit = [\Sigma [w (F_o^2 - F_c^2)^2] / (n-p)]^{1/2}$

Figure 18: ORTEP Diagram Drawn with the 40% Probability Ellipsoids and Showing Atom Labeling

Selected bond lengths: C8-O1 1.264(6); C7-C9 1.371(6); C7-C8 1.389(7); C8-C9 1.400(7); N1-C7 1.337(7); N1-C4 1.464(6)

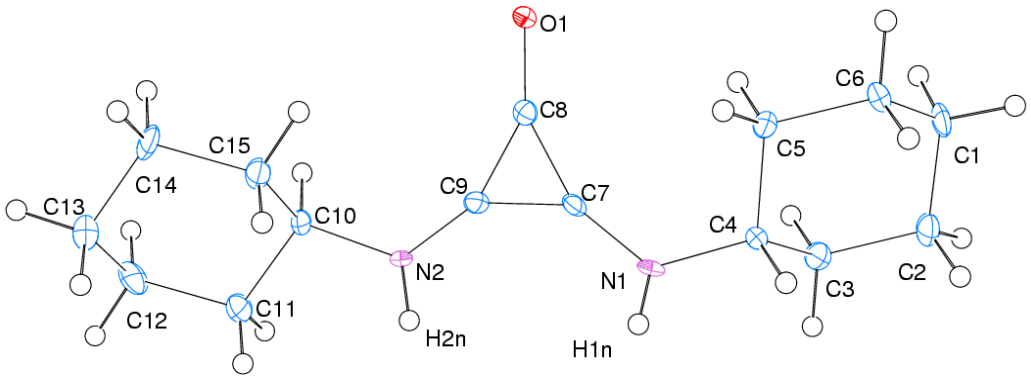

Figure 19: ORTEP Diagram Drawn with the 40% Probability Ellipsoids and Showing Chair Conformation of both Cyclohexyl Substituents

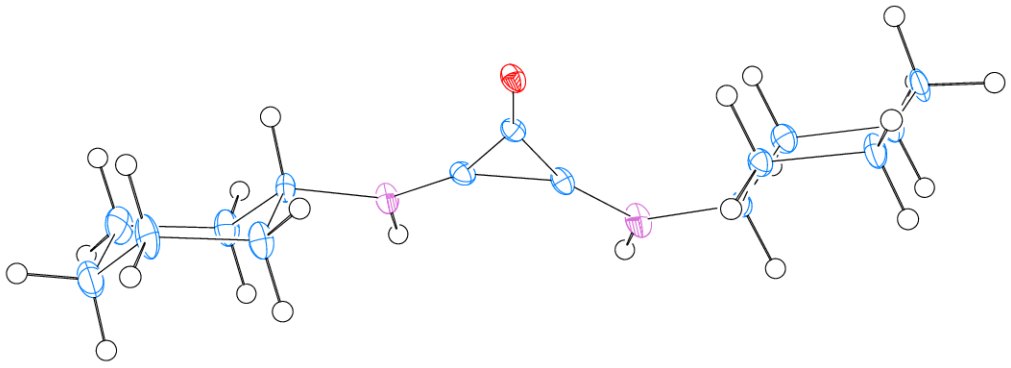

Figure 20: Different views of intermolecular hydrogen bonds (see Table 27 for bond lengths and angles)

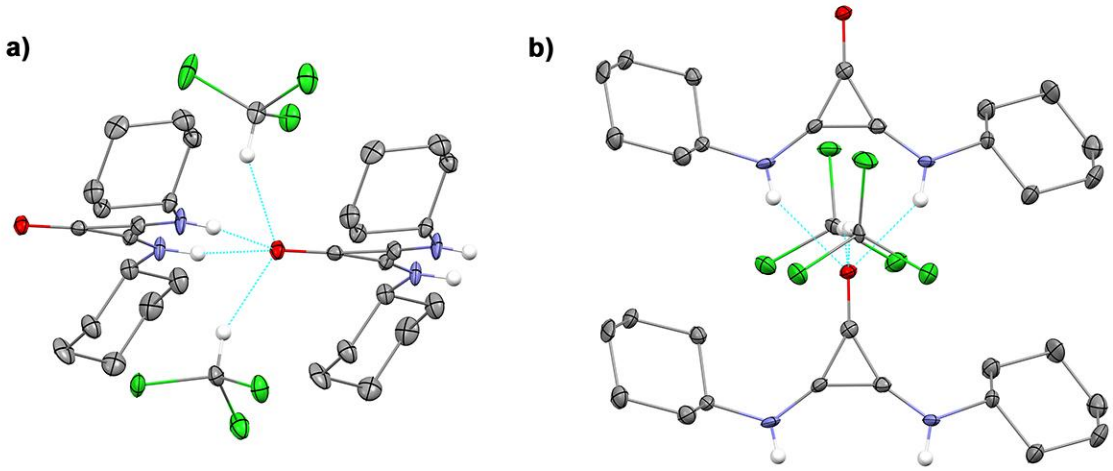

Table 27: Hydrogen Bonds and Angles for **122** [Å and °]

D-H···A	d(D-H)	d(H···A)	d(D···A)	<(DHA)
N(1)-H(1N)···O(1)#2	0.77(7)	2.29(6)	2.967(5)	147(6)
N(2)-H(2N)···O(1)#2	0.84(6)	2.22(6)	2.943(6)	144(5)
N(3)-H(3N)···O(2)#2	0.78(7)	2.28(6)	2.967(6)	147(6)
C(24)-H(24)···O(1)	0.94(5)	2.22(5)	3.064(6)	149(5)
C(25)-H(25)···O(2)#2	0.92(6)	2.20(6)	3.093(6)	161(5)
C(26)-H(26)···O(1)	0.98(6)	2.19(6)	3.126(6)	161(5)

Symmetry transformations used to generate equivalent atoms:

#1 -x+1,y,-z+1 #2 x,y+1,z

Figure 21: 1D Chain via Intermolecular Hydrogen Bonds

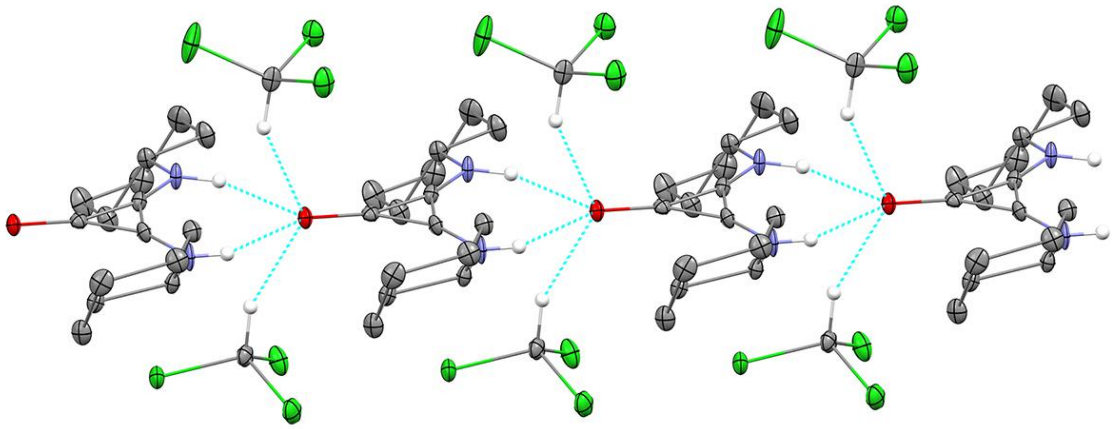

Figure 22: Space Filling Drawing of Intermolecular Hydrogen Bonding with (left) and without (right) $CHCl_3$ Molecule

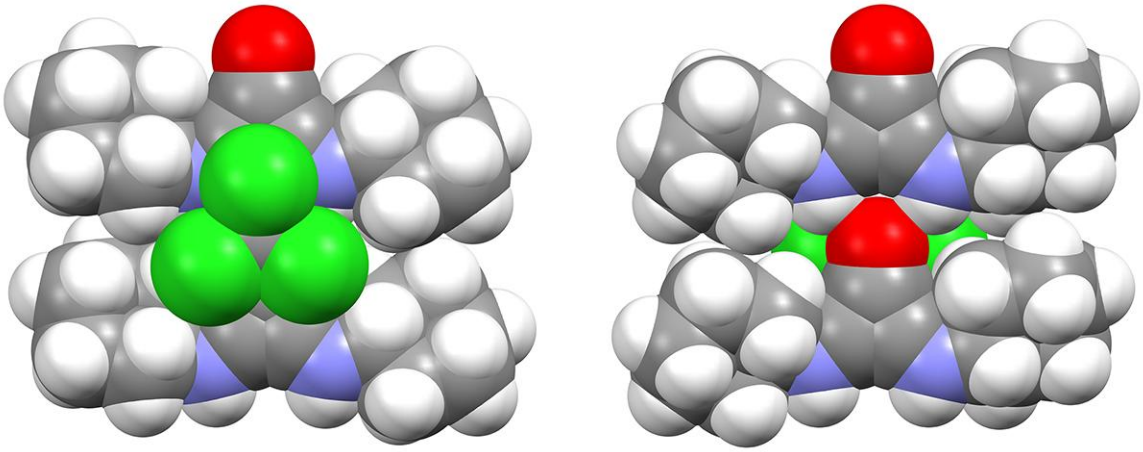

Table 28: Atomic Coordinates (x 10^4) and Equivalent Isotropic Displacement Parameters ($Å^2$x 10^3) of **122**

U(eq) is defined as one third of the trace of the orthogonalized U^{ij} tensor

	x	y	z	U(eq)
N(1)	3538(1)	8246(8)	6485(4)	21(1)
N(2)	3098(1)	8267(8)	3968(4)	17(1)

Table 28, continued

N(3)	5240(1)	2586(8)	6191(4)	19(1)
O(1)	3332(1)	2464(6)	5168(3)	15(1)
O(2)	5000	-3184(9)	5000	14(1)
Cl(1)	2665(1)	2874(2)	5705(1)	26(1)
Cl(2)	2972(1)	2837(2)	7956(1)	30(1)
Cl(3)	2758(1)	-1501(3)	6964(1)	41(1)
Cl(4)	3717(1)	1796(2)	2352(1)	28(1)
Cl(5)	3835(1)	-2578(2)	3597(1)	22(1)
Cl(6)	4028(1)	1866(2)	4581(1)	26(1)
Cl(7)	4335(1)	6818(2)	5971(1)	27(1)
Cl(8)	4698(1)	6758(3)	8043(1)	30(1)
Cl(9)	4523(1)	2358(2)	6955(1)	26(1)
C(1)	3802(1)	4728(10)	9711(4)	23(1)
C(2)	3727(1)	7339(10)	9737(4)	22(1)
C(3)	3558(1)	8051(9)	8632(4)	19(1)
C(4)	3693(1)	7478(9)	7548(4)	14(1)
C(5)	3755(1)	4835(9)	7505(4)	17(1)
C(6)	3928(1)	4152(10)	8602(4)	21(1)
C(7)	3401(1)	6841(9)	5721(4)	15(1)
C(8)	3324(1)	4701(9)	5202(4)	14(1)
C(9)	3231(1)	6862(9)	4733(4)	15(1)
C(10)	2968(1)	7448(9)	2859(4)	15(1)
C(11)	2851(1)	9587(10)	2212(5)	24(1)
C(12)	2724(1)	8902(11)	1007(5)	28(1)
C(13)	2913(1)	7634(11)	285(4)	28(1)
C(14)	3025(1)	5476(10)	935(5)	28(1)
C(15)	3154(1)	6154(9)	2126(4)	22(1)
C(16)	5499(1)	-988(11)	9403(5)	27(1)
C(17)	5435(1)	1625(11)	9439(4)	26(1)
C(18)	5267(1)	2386(9)	8340(4)	22(1)
C(19)	5397(1)	1771(9)	7250(4)	16(1)
C(20)	5453(1)	-867(9)	7197(4)	19(1)
C(21)	5624(1)	-1623(10)	8286(4)	24(1)
C(22)	5092(1)	1208(9)	5465(4)	17(1)
C(23)	5000	-928(12)	5000	14(1)
C(24)	2885(1)	1257(9)	6650(4)	17(1)
C(25)	4601(1)	5339(9)	6717(5)	18(1)
C(26)	3770(1)	454(9)	3739(5)	19(1)

Table 29: Bond Lengths [Å] and Angles [°] for **122**

N(1)-C(7)	1.337(7)	C(11)-H(11A)	0.9900
N(1)-C(4)	1.464(6)	C(11)-H(11B)	0.9900
N(1)-H(1N)	0.77(7)	C(12)-C(13)	1.516(8)
N(2)-C(9)	1.327(6)	C(12)-H(12A)	0.9900
N(2)-C(10)	1.462(6)	C(12)-H(12B)	0.9900
N(2)-H(2N)	0.84(6)	C(13)-C(14)	1.515(8)
N(3)-C(22)	1.331(7)	C(13)-H(13A)	0.9900
N(3)-C(19)	1.473(6)	C(13)-H(13B)	0.9900
N(3)-H(3N)	0.78(7)	C(14)-C(15)	1.517(7)
O(1)-C(8)	1.264(6)	C(14)-H(14A)	0.9900
O(2)-C(23)	1.273(8)	C(14)-H(14B)	0.9900
Cl(1)-C(24)	1.755(5)	C(15)-H(15A)	0.9900
Cl(2)-C(24)	1.768(5)	C(15)-H(15B)	0.9900
Cl(3)-C(24)	1.741(5)	C(16)-C(17)	1.513(8)
Cl(4)-C(26)	1.763(5)	C(16)-C(21)	1.531(8)
Cl(5)-C(26)	1.755(5)	C(16)-H(16A)	0.9900
Cl(6)-C(26)	1.764(5)	C(16)-H(16B)	0.9900
Cl(7)-C(25)	1.763(5)	C(17)-C(18)	1.528(7)
Cl(8)-C(25)	1.754(5)	C(17)-H(17A)	0.9900
Cl(9)-C(25)	1.757(5)	C(17)-H(17B)	0.9900
C(1)-C(6)	1.520(7)	C(18)-C(19)	1.515(6)
C(1)-C(2)	1.524(8)	C(18)-H(18A)	0.9900
C(1)-H(1A)	0.9900	C(18)-H(18B)	0.9900
C(1)-H(1B)	0.9900	C(19)-C(20)	1.519(7)
C(2)-C(3)	1.528(7)	C(19)-H(19)	1.0000
C(2)-H(2A)	0.9900	C(20)-C(21)	1.526(7)
C(2)-H(2B)	0.9900	C(20)-H(20A)	0.9900
C(3)-C(4)	1.518(6)	C(20)-H(20B)	0.9900
C(3)-H(3A)	0.9900	C(21)-H(21A)	0.9900
C(3)-H(3B)	0.9900	C(21)-H(21B)	0.9900
C(4)-C(5)	1.527(7)	C(22)-C(22)#1	1.362(10)
C(4)-H(4)	1.0000	C(22)-C(23)	1.385(8)
C(5)-C(6)	1.527(7)	C(23)-C(22)#1	1.385(8)
C(5)-H(5A)	0.9900	C(24)-H(24)	0.94(5)
C(5)-H(5B)	0.9900	C(25)-H(25)	0.92(6)
C(6)-H(6A)	0.9900	C(26)-H(26)	0.98(6)
C(6)-H(6B)	0.9900	C(7)-N(1)-C(4)	126.1(4)
C(7)-C(9)	1.371(6)	C(7)-N(1)-H(1N)	115(5)
C(7)-C(8)	1.389(7)	C(4)-N(1)-H(1N)	119(5)
C(8)-C(9)	1.400(7)	C(9)-N(2)-C(10)	123.9(4)
C(10)-C(11)	1.514(7)	C(9)-N(2)-H(2N)	117(4)
C(10)-C(15)	1.523(7)	C(10)-N(2)-H(2N)	117(4)
C(10)-H(10)	1.0000	C(22)-N(3)-C(19)	125.3(5)
C(11)-C(12)	1.527(8)	C(22)-N(3)-H(3N)	114(5)

Table 29, continued

C(19)-N(3)-H(3N)	120(5)	C(7)-C(9)-C(8)	60.2(4)
C(6)-C(1)-C(2)	110.6(4)	N(2)-C(10)-C(11)	107.9(4)
C(6)-C(1)-H(1A)	109.5	N(2)-C(10)-C(15)	111.7(4)
C(2)-C(1)-H(1A)	109.5	C(11)-C(10)-C(15)	110.8(4)
C(6)-C(1)-H(1B)	109.5	N(2)-C(10)-H(10)	108.8
C(2)-C(1)-H(1B)	109.5	C(11)-C(10)-H(10)	108.8
H(1A)-C(1)-H(1B)	108.1	C(15)-C(10)-H(10)	108.8
C(1)-C(2)-C(3)	111.4(4)	C(10)-C(11)-C(12)	111.3(4)
C(1)-C(2)-H(2A)	109.4	C(10)-C(11)-H(11A)	109.4
C(3)-C(2)-H(2A)	109.4	C(12)-C(11)-H(11A)	109.4
C(1)-C(2)-H(2B)	109.4	C(10)-C(11)-H(11B)	109.4
C(3)-C(2)-H(2B)	109.4	C(12)-C(11)-H(11B)	109.4
H(2A)-C(2)-H(2B)	108.0	H(11A)-C(11)-H(11B)	108.0
C(4)-C(3)-C(2)	110.8(4)	C(13)-C(12)-C(11)	111.9(5)
C(4)-C(3)-H(3A)	109.5	C(13)-C(12)-H(12A)	109.2
C(2)-C(3)-H(3A)	109.5	C(11)-C(12)-H(12A)	109.2
C(4)-C(3)-H(3B)	109.5	C(13)-C(12)-H(12B)	109.2
C(2)-C(3)-H(3B)	109.5	C(11)-C(12)-H(12B)	109.2
H(3A)-C(3)-H(3B)	108.1	H(12A)-C(12)-H(12B)	107.9
N(1)-C(4)-C(3)	111.4(4)	C(14)-C(13)-C(12)	110.2(4)
N(1)-C(4)-C(5)	111.2(4)	C(14)-C(13)-H(13A)	109.6
C(3)-C(4)-C(5)	110.4(4)	C(12)-C(13)-H(13A)	109.6
N(1)-C(4)-H(4)	107.9	C(14)-C(13)-H(13B)	109.6
C(3)-C(4)-H(4)	107.9	C(12)-C(13)-H(13B)	109.6
C(5)-C(4)-H(4)	107.9	H(13A)-C(13)-H(13B)	108.1
C(6)-C(5)-C(4)	109.1(4)	C(13)-C(14)-C(15)	111.1(5)
C(6)-C(5)-H(5A)	109.9	C(13)-C(14)-H(14A)	109.4
C(4)-C(5)-H(5A)	109.9	C(15)-C(14)-H(14A)	109.4
C(6)-C(5)-H(5B)	109.9	C(13)-C(14)-H(14B)	109.4
C(4)-C(5)-H(5B)	109.9	C(15)-C(14)-H(14B)	109.4
H(5A)-C(5)-H(5B)	108.3	H(14A)-C(14)-H(14B)	108.0
C(1)-C(6)-C(5)	112.0(4)	C(14)-C(15)-C(10)	111.8(4)
C(1)-C(6)-H(6A)	109.2	C(14)-C(15)-H(15A)	109.3
C(5)-C(6)-H(6A)	109.2	C(10)-C(15)-H(15A)	109.3
C(1)-C(6)-H(6B)	109.2	C(14)-C(15)-H(15B)	109.3
C(5)-C(6)-H(6B)	109.2	C(10)-C(15)-H(15B)	109.3
H(6A)-C(6)-H(6B)	107.9	H(15A)-C(15)-H(15B)	107.9
N(1)-C(7)-C(9)	143.1(5)	C(17)-C(16)-C(21)	111.2(5)
N(1)-C(7)-C(8)	155.8(5)	C(17)-C(16)-H(16A)	109.4
C(9)-C(7)-C(8)	61.0(4)	C(21)-C(16)-H(16A)	109.4
O(1)-C(8)-C(7)	150.7(5)	C(17)-C(16)-H(16B)	109.4
O(1)-C(8)-C(9)	150.4(5)	C(21)-C(16)-H(16B)	109.4
C(7)-C(8)-C(9)	58.9(3)	H(16A)-C(16)-H(16B)	108.0
N(2)-C(9)-C(7)	143.8(5)	C(16)-C(17)-C(18)	111.2(5)
N(2)-C(9)-C(8)	156.0(5)	C(16)-C(17)-H(17A)	109.4

Table 29, continued

C(16)-C(17)-H(17B)	109.4	N(3)-C(22)-C(22)#1	144.3(3)
C(18)-C(17)-H(17B)	109.4	H(21A)-C(21)-H(21B)	108.0
H(17A)-C(17)-H(17B)	108.0	N(3)-C(22)-C(23)	155.2(5)
C(19)-C(18)-C(17)	111.0(4)	C(22)#1-C(22)-C(23)	60.5(3)
C(19)-C(18)-H(18A)	109.4	O(2)-C(23)-C(22)#1	150.5(3)
C(17)-C(18)-H(18A)	109.4	O(2)-C(23)-C(22)	150.5(3)
C(19)-C(18)-H(18B)	109.4	C(22)#1-C(23)-C(22)	58.9(5)
C(17)-C(18)-H(18B)	109.4	Cl(3)-C(24)-Cl(1)	110.9(3)
H(18A)-C(18)-H(18B)	108.0	Cl(3)-C(24)-Cl(2)	110.3(3)
N(3)-C(19)-C(18)	111.1(4)	Cl(1)-C(24)-Cl(2)	111.3(3)
N(3)-C(19)-C(20)	111.4(4)	Cl(3)-C(24)-H(24)	108(3)
C(18)-C(19)-C(20)	111.0(4)	Cl(1)-C(24)-H(24)	107(3)
N(3)-C(19)-H(19)	107.7	Cl(2)-C(24)-H(24)	109(3)
C(18)-C(19)-H(19)	107.7	Cl(8)-C(25)-Cl(9)	110.7(3)
C(20)-C(19)-H(19)	107.7	Cl(8)-C(25)-Cl(7)	110.7(3)
C(19)-C(20)-C(21)	109.8(4)	Cl(9)-C(25)-Cl(7)	110.4(3)
C(19)-C(20)-H(20A)	109.7	Cl(8)-C(25)-H(25)	108(4)
C(21)-C(20)-H(20A)	109.7	Cl(9)-C(25)-H(25)	110(3)
C(19)-C(20)-H(20B)	109.7	Cl(7)-C(25)-H(25)	106(4)
C(21)-C(20)-H(20B)	109.7	Cl(5)-C(26)-Cl(4)	110.5(3)
H(20A)-C(20)-H(20B)	108.2	Cl(5)-C(26)-Cl(6)	110.4(3)
C(20)-C(21)-C(16)	111.5(4)	Cl(4)-C(26)-Cl(6)	110.5(3)
C(20)-C(21)-H(21A)	109.3	Cl(5)-C(26)-H(26)	112(3)
C(16)-C(21)-H(21A)	109.3	Cl(4)-C(26)-H(26)	106(3)
C(20)-C(21)-H(21B)	109.3	Cl(6)-C(26)-H(26)	107(3)
C(16)-C(21)-H(21B)	109.3		

Symmetry transformations used to generate equivalent atoms: #1 -x+1,y,-z+1

Table 30: Anisotropic Displacement Parameters for **122** ($Å^2 x\ 10^3$).

	U^{11}	U^{22}	U^{33}	U^{23}	U^{13}	U^{12}
N(1)	35(3)	5(2)	20(2)	2(2)	-5(2)	2(2)
N(2)	30(2)	6(2)	15(2)	-1(2)	-5(2)	-1(2)
N(3)	29(2)	11(2)	17(2)	-2(2)	-6(2)	-2(2)
O(1)	22(2)	10(2)	13(2)	1(1)	0(1)	1(1)
O(2)	20(2)	11(2)	10(2)	0	-1(2)	0
Cl(1)	30(1)	22(1)	24(1)	3(1)	-8(1)	2(1)
Cl(2)	39(1)	22(1)	25(1)	-5(1)	-10(1)	-1(1)
Cl(3)	72(1)	17(1)	30(1)	7(1)	-13(1)	-18(1)
Cl(4)	42(1)	20(1)	20(1)	1(1)	-1(1)	8(1)
Cl(5)	25(1)	10(1)	32(1)	-1(1)	2(1)	0(1)

Table 30, continued

Cl(6)	28(1)	19(1)	29(1)	-8(1)	-5(1)	-1(1)
Cl(7)	28(1)	20(1)	32(1)	3(1)	-7(1)	0(1)
Cl(8)	44(1)	21(1)	23(1)	-7(1)	-5(1)	1(1)
Cl(9)	33(1)	13(1)	32(1)	0(1)	2(1)	-1(1)
C(1)	30(3)	27(3)	11(3)	7(2)	-7(2)	-3(2)
C(2)	28(3)	26(3)	12(2)	-1(2)	-2(2)	2(2)
C(3)	24(3)	18(3)	16(2)	-1(2)	1(2)	1(2)
C(4)	19(2)	11(2)	12(2)	2(2)	-3(2)	-1(2)
C(5)	22(3)	16(2)	13(2)	-1(2)	-1(2)	-3(2)
C(6)	27(3)	18(3)	15(3)	4(2)	-6(2)	3(2)
C(7)	19(2)	11(2)	13(2)	3(2)	0(2)	4(2)
C(8)	14(2)	15(2)	12(2)	1(2)	4(2)	1(2)
C(9)	19(2)	11(2)	15(2)	1(2)	2(2)	-2(2)
C(10)	18(2)	15(2)	12(2)	0(2)	-4(2)	2(2)
C(11)	31(3)	19(3)	20(3)	1(2)	-6(2)	6(2)
C(12)	30(3)	26(3)	25(3)	9(3)	-10(2)	6(3)
C(13)	38(3)	29(3)	16(3)	0(2)	-2(2)	-2(3)
C(14)	43(3)	28(3)	12(3)	-10(2)	-3(2)	6(3)
C(15)	29(3)	21(3)	15(3)	-3(2)	-2(2)	5(2)
C(16)	27(3)	35(3)	17(3)	9(2)	-4(2)	-4(2)
C(17)	34(3)	32(3)	13(2)	1(2)	-1(2)	-4(3)
C(18)	26(3)	19(3)	19(2)	-6(2)	1(2)	1(2)
C(19)	17(2)	17(2)	12(2)	0(2)	-6(2)	-3(2)
C(20)	26(3)	20(3)	11(2)	2(2)	1(2)	0(2)
C(21)	24(3)	22(3)	23(3)	10(2)	-5(2)	-2(2)
C(22)	21(3)	15(2)	15(2)	0(2)	5(2)	0(2)
C(23)	19(4)	10(3)	13(3)	0	2(3)	0
C(24)	25(3)	18(3)	7(2)	-1(2)	-6(2)	-3(2)
C(25)	25(3)	12(2)	18(3)	-2(2)	1(2)	-2(2)
C(26)	23(3)	15(2)	18(3)	-6(2)	2(2)	-2(2)

The anisotropic displacement factor exponent takes the form: $-2\pi^2[h^2 a^{*2}U^{11} + ... + 2 h k a^* b^* U^{12}]$

Table 31: Hydrogen Coordinates (x 10^4) and Isotropic Displacement Parameters for **122** ($Å^2$x 10^3)

	x	y	z	U(eq)
H(1N)	3524(12)	9570(120)	6360(50)	25
H(2N)	3124(11)	9730(110)	4040(50)	21
H(3N)	5222(11)	3940(120)	6070(50)	23
H(1A)	3924	4354	10401	28
H(1B)	3644	3738	9750	28
H(2A)	3887	8319	9810	27
H(2B)	3631	7646	10429	27
H(3A)	3390	7195	8601	23
H(3B)	3521	9771	8654	23
H(4)	3862	8366	7600	17
H(5A)	3592	3905	7461	21
H(5B)	3846	4480	6802	21
H(6A)	3966	2433	8582	25
H(6B)	4096	5011	8610	25
H(10)	2824	6341	3025	19
H(11A)	2988	10777	2125	29
H(11B)	2718	10315	2673	29
H(12A)	2573	7859	1099	33
H(12B)	2659	10349	588	33
H(13A)	2822	7139	-472	33
H(13B)	3055	8724	122	33
H(14A)	3154	4707	472	33
H(14B)	2884	4323	1032	33
H(15A)	3306	7184	2024	26
H(15B)	3219	4704	2543	26
H(16A)	5338	-1926	9442	32
H(16B)	5620	-1401	10092	32
H(17A)	5598	2557	9509	32
H(17B)	5341	1959	10135	32
H(18A)	5096	1583	8315	26
H(18B)	5236	4117	8365	26
H(19)	5567	2625	7293	19
H(20A)	5543	-1223	6491	23
H(20B)	5288	-1764	7146	23
H(21A)	5795	-832	8293	28
H(21B)	5653	-3356	8262	28

Table 31, continued

H(24)	3036(11)	1020(100)	6260(50)	21
H(25)	4736(11)	5430(100)	6240(50)	22
H(26)	3613(11)	740(100)	4130(50)	22

V.3.3 X-ray crystal structure of 130

General information: The diffraction data were measured at 100 K on a Bruker D8 VENTURE diffractometer equipped with a microfocus Cu-target X-ray tube (λ = 1.54178 Å) and PHOTON 100 CMOS detector system. Data reduction and integration were performed with the Bruker APEX3 software package (Bruker AXS, version 2015.5-2, 2015). Data were scaled and corrected for absorption effects using the multi-scan procedure as implemented in SADABS (Bruker AXS, version 2014/5, 2015, part of Bruker APEX3 software package). The structure was solved by SHELXT (Version 2014/5: Sheldrick, G. M. *Acta Crystallogr*. **2015**, *A**71***, 3-8) and refined by a full-matrix least-squares procedure using OLEX2 (O. V. Dolomanov, L. J. Bourhis, R. J. Gildea, J. A. K. Howard and H. Puschmann. J. Appl. Crystallogr. **2009**, *42*, 339-341) (XL refinement program version 2014/7, Sheldrick, G. M. *Acta Crystallogr*. **2008**, *A64*, 112-122; Sheldrick, G. M. *Acta Crystallogr*. **2015**, *C71*, 3-8). Crystallographic data and details of the data collection and structure refinement are listed in Table 1.

Specific details for structure refinement: All atoms were refined with anisotropic thermal parameters. Hydrogen atoms were included in idealized positions for structure factor calculations except the H atom of NH group which was refined freely. All structures are drawn with thermal ellipsoids at 50% probability.

Table 32: Crystal Data and Structure Refinement for **130**

Identification code	0131_cu_a
Empirical formula	$C_{15}H_{12}N_2O$
Formula weight	236.27
Temperature/K	100(2)
Crystal system	orthorhombic
Space group	$C222_1$
a/Å	5.4151(5)
b/Å	11.1365(11)
c/Å	18.5853(17)
α/°	90
β/°	90
γ/°	90
Volume/Å^3	1120.79(18)
Z	4
ρ_{calc}g/cm^3	1.400
μ/mm^{-1}	0.716
F(000)	496.0
Crystal size/mm^3	0.32 × 0.1 × 0.01
Radiation	CuKα (λ = 1.54178)
2Θ range for data collection/°	9.518 to 134.212
Index ranges	$-6 \leq h \leq 5$, $-13 \leq k \leq 13$, $-22 \leq l \leq 22$
Reflections collected	9881
Independent reflections	1001 [R_{int} = 0.0742, R_{sigma} = 0.0312]
Data/restraints/parameters	1001/0/87
Goodness-of-fit on F^2	1.183
Final R indexes [I>=2σ (I)]	R_1 = 0.0433, wR_2 = 0.1151
Final R indexes [all data]	R_1 = 0.0446, wR_2 = 0.1159
Largest diff. peak/hole / e Å^{-3}	0.20/-0.20

$R_{int} = \Sigma \mid F_o^2 - \langle F_o^2 \rangle \mid / \Sigma \mid F_o^2 \mid$

$R1 = \Sigma \mid \mid F_o \mid - \mid F_c \mid \mid / \Sigma \mid F_o \mid$

$wR2 = [\Sigma [w (F_o^2 - F_c^2)^2] / \Sigma [w (F_o^2)^2]]^{1/2}$

Goodness-of-fit = $[\Sigma [w (F_o^2 - F_c^2)^2] / (n-p)]^{1/2}$

n: number of independent reflections; p: number of refined parameters

Figure 23: Front View of **130** and Atom Labeling

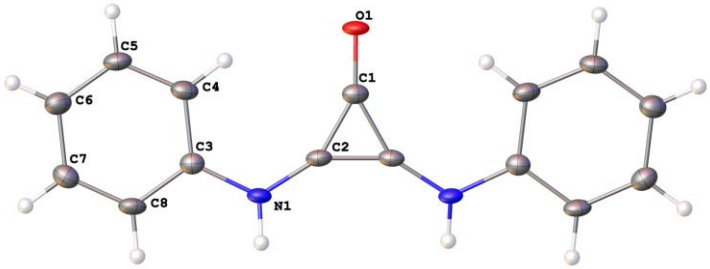

Figure 24: Front View and Side View of Three π-Stacked Molecules of **130**

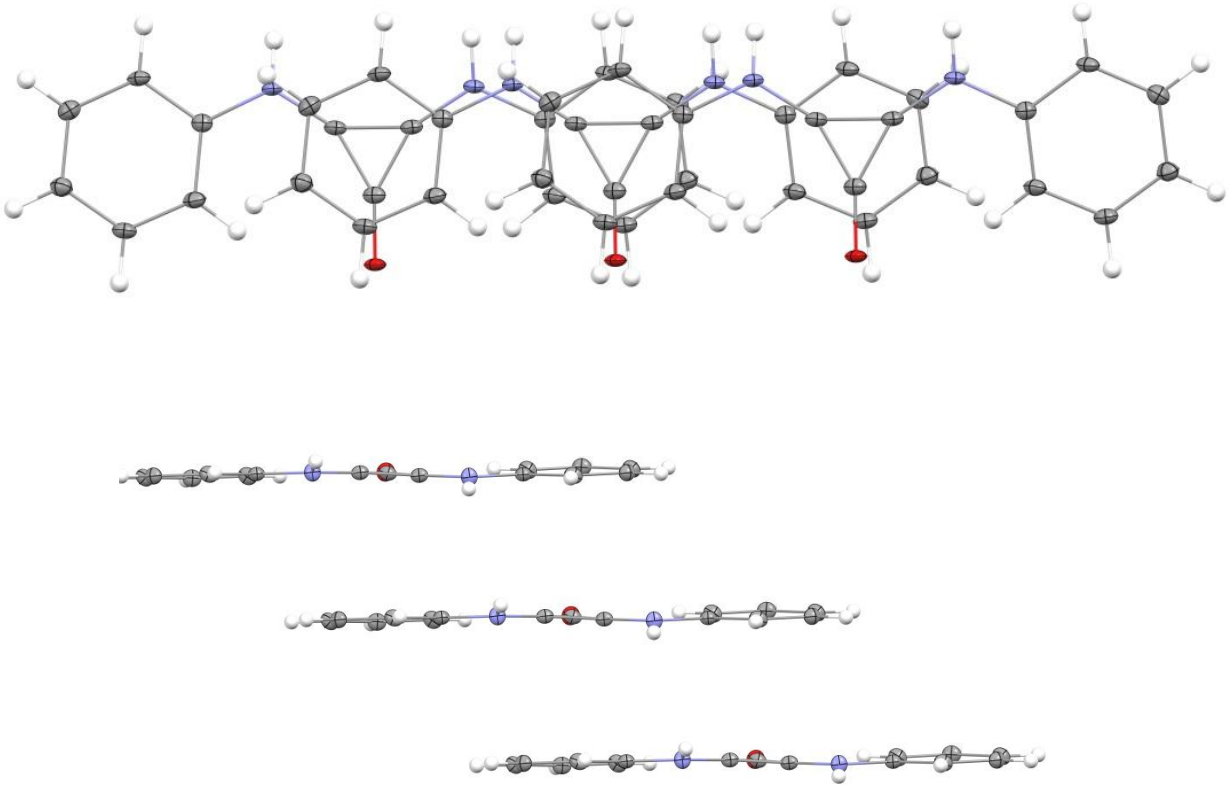

Figure 25: A Side View of Hydrogen-Bonding in **130**

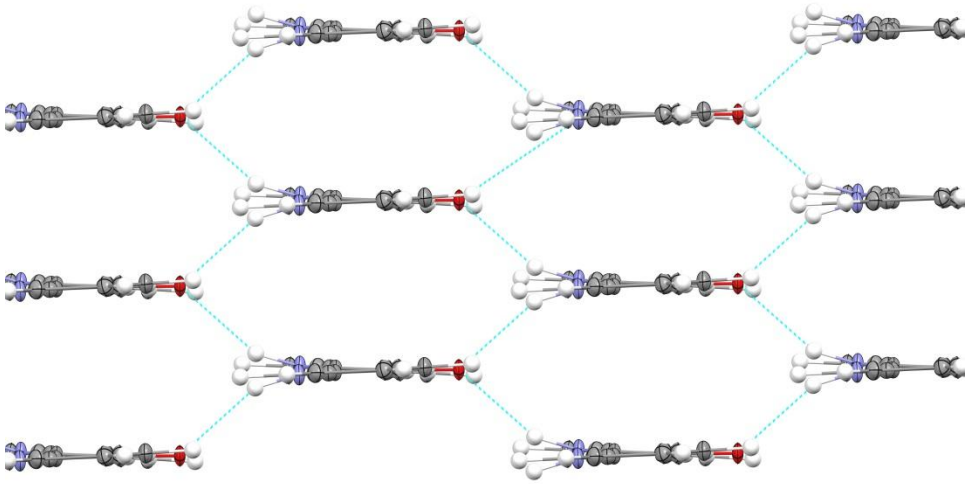

Table 33: Fractional Atomic Coordinates ($\times 10^4$) and Equivalent Isotropic Displacement Parameters ($Å^2 \times 10^3$) for **130**.

Atom	*x*	*y*	*z*	U(eq)
O1	0	5054(3)	2500	22.4(8)
N1	2718(5)	7916(2)	3074.6(14)	20.3(7)
C1	0	6178(4)	2500	20.3(10)
C2	1042(6)	7272(3)	2712.4(17)	18.3(7)
C3	4527(6)	7376(3)	3514.2(16)	19.3(7)
C4	4666(7)	6132(3)	3596.6(17)	23.7(8)
C5	6461(6)	5648(3)	4039.0(18)	23.4(8)
C6	8140(7)	6367(3)	4396.3(18)	25.0(8)
C7	7983(7)	7606(3)	4318.1(18)	24.1(8)
C8	6194(7)	8109(3)	3881.1(18)	21.9(8)

Table 34: Anisotropic Displacement Parameters ($Å^2×10^3$) for **130**

The Anisotropic displacement factor exponent takes the form: $-2\pi^2[h^2a^{*2}U_{11}+2hka^*b^*U_{12}+\ldots]$.

Atom	U_{11}	U_{22}	U_{33}	U_{23}	U_{13}	U_{12}
O1	27.9(18)	7.6(13)	31.7(18)	0	-0.7(15)	0
N1	25.9(16)	8.8(12)	26.2(14)	0.2(10)	-2.7(12)	-1.3(11)
C1	27(3)	15(2)	19(2)	0	3.7(19)	0
C2	22.4(16)	10.8(14)	21.8(15)	1.3(12)	4.5(12)	0.6(13)
C3	20.5(17)	17.6(15)	19.6(14)	0.2(12)	3.6(13)	0.3(12)
C4	33(2)	14.1(15)	24.5(16)	-2.1(14)	0.3(15)	-1.8(15)
C5	30(2)	13.0(14)	27.6(17)	1.9(13)	2.8(15)	1.3(14)
C6	32(2)	19.8(17)	23.2(16)	1.9(13)	-0.5(15)	0.9(15)
C7	25.5(18)	21.3(16)	25.3(16)	-3.2(13)	1.4(15)	-3.6(15)
C8	31(2)	11.2(14)	23.6(16)	0.8(13)	2.3(14)	-2.4(13)

Table 35: Bond Lengths for **130**

Atom	Atom	Length/Å	Atom	Atom	Length/Å
O1	C1	1.252(6)	C3	C4	1.395(4)
N1	C2	1.339(4)	C3	C8	1.395(5)
N1	C3	1.410(4)	C4	C5	1.383(5)
C1	$C2^1$	1.399(5)	C5	C6	1.382(5)
C1	C2	1.399(5)	C6	C7	1.390(5)
C2	$C2^1$	1.377(7)	C7	C8	1.383(5)

^{1}-X,+Y,1/2-Z

Table 36: Bond Angles for **130**

Atom	Atom	Atom	Angle/°	Atom	Atom	Atom	Angle/°
C2	N1	C3	122.3(3)	C8	C3	N1	118.9(3)
O1	C1	$C2^1$	150.53(17)	C8	C3	C4	119.5(3)
O1	C1	C2	150.53(17)	C5	C4	C3	119.4(3)
C2	C1	$C2^1$	58.9(3)	C6	C5	C4	121.5(3)
N1	C2	C1	151.9(3)	C5	C6	C7	119.0(3)
N1	C2	$C2^1$	147.55(18)	C8	C7	C6	120.4(3)
$C2^1$	C2	C1	60.53(17)	C7	C8	C3	120.2(3)
C4	C3	N1	121.6(3)				

^{1}-X,+Y,1/2-Z

Table 37: Torsion Angles for **130**

A	B	C	D	Angle/°	A	B	C	D	Angle/°
O1	C1	C2	N1	-2.8(8)	C3	N1	C2	C2[1]	173.6(6)
O1	C1	C2	C2[1]	180.000(2)	C3	C4	C5	C6	-0.7(5)
N1	C3	C4	C5	-179.4(3)	C4	C3	C8	C7	0.5(5)
N1	C3	C8	C7	179.8(3)	C4	C5	C6	C7	1.2(5)
C2	N1	C3	C4	-0.1(5)	C5	C6	C7	C8	-0.9(5)
C2	N1	C3	C8	-179.3(3)	C6	C7	C8	C3	0.0(5)
C2[1]	C1	C2	N1	177.2(8)	C8	C3	C4	C5	-0.2(5)
C3	N1	C2	C1	-1.9(8)					

[1]-X,+Y,1/2-Z

Table 38: Hydrogen Atom Coordinates (Å×10[4]) and Isotropic Displacement Parameters (Å[2]×10[3]) for **130**

Atom	*x*	*y*	*z*	U(eq)
H1	2950(80)	8700(40)	2950(20)	28(11)
H4	3537.96	5623.17	3351.1	28
H5	6541.64	4801.55	4098.58	28
H6	9382.9	6020.3	4691.11	30
H7	9111.99	8110.52	4566.45	29
H8	6099.93	8956.87	3830.51	26

V.4 Experimental Procedures and Characterization Data - Chapter III

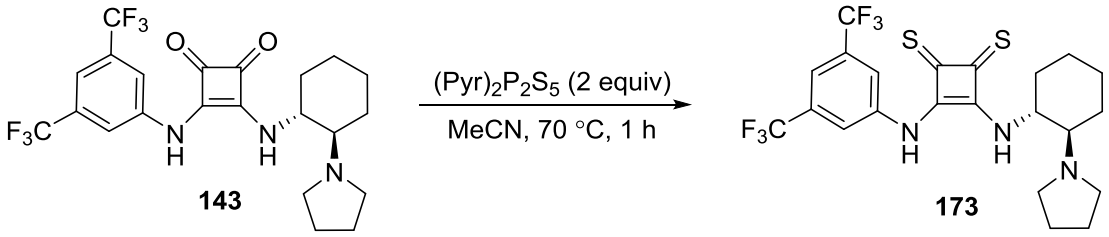

Squaramide **143** (100 mg, 0.210 mmol, 1.0 equiv) and P_4S_{10}-Pyridine complex (159.8 mg, 0.420 mmol, 2.0 equiv) were added to an oven-dried test-tube which was then flushed with nitrogen

(3x). Then, 4.0 mL of anhydrous MeCN was added at the reaction mixture stirred at 65 °C for 1 hour.

After 1 hour, the reaction mixture was cooled to room temperature, and the solvent removed *in vacuo*. The solids were than dissolved in methanol. The undissolved solids were filtered through a cotton plug, and the filtrate was concentrated, then dissolved in a minimum amount of methanol, followed by 3x volume of hexanes. This organic layer was washed thrice with *aq.* 1M NaOH, and any suspended black solids are filtered off from the aqueous layer with a cotton plug. The combined aqueous layers were washed once with hexanes, and then acidified with 1M HCl to pH < 3. After acidification, the aqueous layer is extracted thrice with DCM, and the combined DCM layers are dried with brine, Na_2SO_4, and concentrated. This afforded 67 mg of moderately pure **173** as a yellow-brown solid. See NMRs of this sample in CD_3OD and $CDCl_3$ in Appendix. It was found to show 3 broad peaks in the $\delta = 7.5 - 11$ region, and hence it was concluded that the compound potentially exists as the HCl salt after the acidic workup. Also, note that this procedure was initially developed by Dr. Thomas D. Montgomery.

173: ^{1}H NMR (500 MHz, d_6-DMSO) 8.31 (s, 2H), 7.76 (s, 1H), 5.55-5.47 (m, 1H), 3.79-3.66 (m, 2H), 3.58-3.48 (m, 2H), 3.47-3.4 (m, 1H), 2.31-2.21 (m, 2H), 2.3-1.45 (m, 10H).

ESI/MS $(M+H)^+$: 508.1.

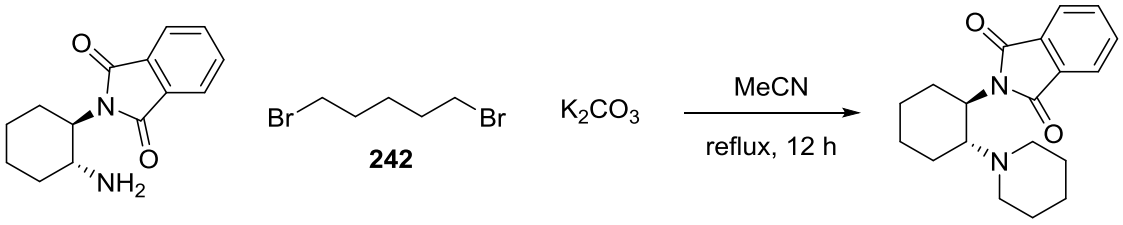

241 **242** **243**

2-((1*R*,2*R*)-2-(piperidin-1-yl)cyclohexyl)isoindoline-1,3-dione **243**

To a solution of **241** (1.51 g, 6.18 mmol, 1.0 eqv) and 1,5-dibromopentane **242** (1.56 g, 6.80 mmol, 1.1 eqv) in MeCN (30 mL) was added K_2CO_3 (1.88 g, 13.59 mmol, 2.2 eqv) at room temperature. The reaction mixture was then brought to reflux. After 12 h at reflux, the reaction was allowed to cool and diluted with water. The reaction mixture was then extracted three times with CH_2Cl_2, dried with $MgSO_4$, and concentrated. The residue was chromatographed on silica gel ($CHCl_3$) to afford impure **243**, which was further purified by heating on the Kugelrohr to remove remaining starting material. The resulting residue was allowed to solidify, and was then ground up and washed with Et_2O to afford pure **243** (1.51 g, 78%) as a light yellow solid.

^{1}H NMR (500 MHz, $CDCl_3$) δ 7.81 (dd, *J* = 5.4, 3.1 Hz, 2H), 7.69 (dd, *J* = 5.4, 3.0 Hz, 2H), 4.13 (td, *J* = 11.9, 4.0 Hz, 1H), 3.16 (td, *J* = 11.5, 3.4 Hz, 1H), 2.56 (m, 2H), 2.24 (m, 3H), 1.86 (m, 4H), 1.28 (m, 9H).

^{13}C NMR (125 MHz, $CDCl_3$) δ 169.1, 133.7, 132.5, 123.0, 63.9, 52.5, 50.0, 30.3, 27.1, 26.0, 25.6, 25.1, 24.8.

HRMS (ESI) calcd for $C_{19}H_{25}N_2O_2^+(M+H)^+$: 313.1911, Found: 313.1916.

IR (film): 2930, 2854, 2799, 1766, 1707, 1391, 1371, 718 cm^{-1}

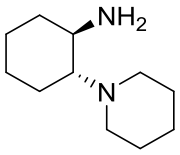

244

(1*R*,2*R*)-2-(piperidin-1-yl)cyclohexan-1-amine **244**

To a solution of **243** (446 mg, 1.43 mmol, 1.0 eqv) in EtOH (4 mL) was added H_2NNH_2 (33 wt. % in H_2O, 0.54 mL, 5.72 mmol, 4.0 eqv). The reaction was placed in a preheated oil bath and refluxed for 1 h, after which time it was allowed to cool to room temperature. Et_2O (20 mL) was added, and the slurry was stirred at 0 °C for 15 min. The mixture was then filtered, and the

filtrate concentrated to afford the desired product **244** (161 mg, 62%) as a pale yellow solid. Analytical data matched previously reported values.

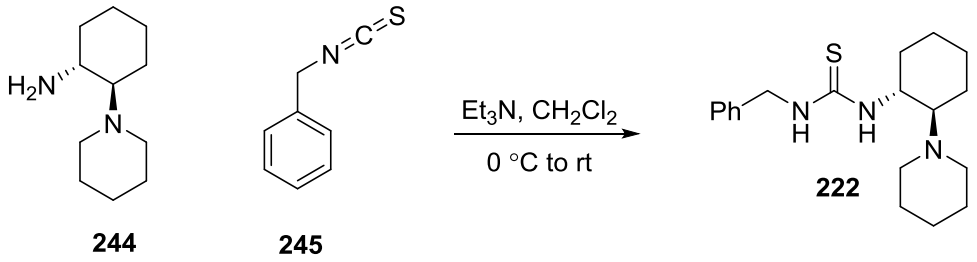

244 **245** **222**

A solution of **244** (266 mg, 1.46 mmol, 1.1 equiv) in dichloromethane (4 mL) was cooled to 0 °C followed by the addition of triethylamine (0.37 mL, 2.66 mmol, 2.0 equiv). Benzyl isothiocyanate **245** (199 mg, 1.33 mmol, 1.0 equiv) was added and the reaction mixture was stirred at room temperature for 12 hours (monitored by TLC). The reaction mixture was washed with water, brine, and the organic layers were dried with $MgSO_4$ and concentrated. The crude product was purified by silica gel chromatography using methanol:chloroform:NH_4OH (5:94:1) as the eluent to give catalyst **222** (312 mg, 71%) as a white solid.

^{1}H NMR (500 MHz, $CDCl_3$) δ 7.35-7.31 (m, 4H), 7.30-7.26 (m, 1H), 6.45 (br s, 1H), 4.8-4.5 (m, 2H), 3.59 (br s, 1H), 2.7-2.5 (m, 3H), 2.38-2.24 (m, 3H), 1.87 (d, *J* = 12.0 Hz, 1H), 1.82-1.76 (m, 1H), 1.71-1.64 (m, 1H), 1.46-1.02 (m, 11H).

^{13}C NMR (125 MHz, $CDCl_3$) δ 128.7, 127.6, 127.5, 68.7, 55.7, 49.5 (br), 48.3, 33.1, 26.2, 25.3, 24.4, 23.4.

HRMS (ESI) calcd for $C_{19}H_{30}N_3S^+(M+H)^+$: 332.2155, Found:332.216.

IR (film): 3853, 3258, 2930, 2853, 2361, 2337, 1540 cm^{-1}

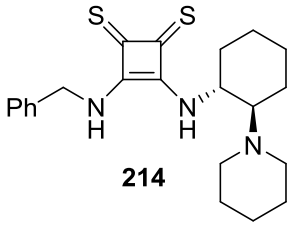

214

To a solution of **206** (R_1 = benzl) (306 mg, 1.05 mmol, 1.05 eqv) in dry Et_2O (26 mL) at 0 °C was added **244** (182 mg, 1.00 mmol, 1.00 eqv) in 4 mL dry Et_2O. The mixture was stirred at 0 °C for 5 min, then allowed to warm to room temperature and stirred an additional 1 h. The reaction mixture was then concentrated and the orange solid thus obtained was washed with pentane to afford the desired product **244** (332 mg, 83%) as an orange solid. The product is rotameric in DMSO at room temperature. Note that this procedure was developed by Michael Rombola, and has been included to give the reader an example of a synthesis of bifunctional deltic urea.

^{1}H NMR (500 MHz, DMSO-d_6, T = 60 °C) δ8.74 (br s, 1H), 8.25 (br s, 1H), 7.38 (m, 5H), 5.34 (m, 2H), 4.87 (brs, 1H), 2.68 (m, 2H), 2.30 (m, 3H), 2.10 (m, 1H), 1.87 (brs, 1H), 1.75 (brs, 1H), 1.66 (brs, 1H), 1.27 (m, 10H).

^{13}C NMR (125 MHz, DMSO-d_6) δ 204.4, 201.5, 170.3, 170.2, 137.6, 137.4, 128.7, 128.5, 128.4, 127.9, 127.8, 127.7, 127.3, 67.4, 66.9, 55.5, 53.4, 49.7, 49.1, 46.0, 45.9, 45.5, 34.5, 26.2, 24.8, 24.5, 24.3, 24.1, 23.8, 23.3.

HRMS (ESI) calcd for $C_{22}H_{30}N_3S_2^+(M+H)^+$: 400.1876, Found: 400.1869.

IR (film): 3173, 2931, 1707, 1575, 1451, 1233 cm^{-1}

General Procedure for the Synthesis of 5-Substituted Barbituric Acids

0.4 mg (0.001 mmol, 0.005 equiv, 0.5 mol%)of **214** in 0.5 mL PhMe was added to a mixture of nitroolefin (0.20mmol, 1.0eqv) and *N,N'*-disubstitutedbarbituric acid (0.22 mmol, 1.1 eqv). The reaction was stirred at room temperature, and the conversion monitored by TLC. Upon complete conversion, the reaction mixture was loaded directly onto column and eluted with a gradient of 0:1 to 1:1 EtOAc:CH_2Cl_2.

Note: Enantiomeric excesses are measured after C-5 chlorination of the addition product (see below).

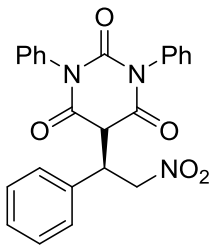

182

(*R*)-5-(2-nitro-1-phenylethyl)-1,3-diphenylpyrimidine-2,4,6(1*H*,3*H*,5*H*)-trione **182**

Flash column chromatography afforded **182** (83.5 mg, 97%) as an off-white solid.

^{1}H NMR (500 MHz, $CDCl_3$) δ7.46 (m, 9H), 7.28 (m, 2H), 7.05 (br s, 2H), 6.91 (br s, 2H), 5.32 (dd, *J* = 14.3, 8.0 Hz, 1H), 5.04 (dd, *J* = 14.3, 7.7 Hz, 1H), 4.67 (td, 7.8, 3.5 Hz, 1H), 4.20 (d, *J* = 3.5 Hz, 1H).

^{13}C NMR (125 MHz, $CDCl_3$) δ 166.9, 166.7, 150.1, 134.3, 133.8, 133.7, 129.9, 129.8, 129.6, 129.6, 129.6, 129.5, 128.5, 128.3, 76.0, 52.0, 45.9.

HRMS (ESI) calcd for $C_{24}H_{20}N_3O_5^+$ $(M+H)^+$: 430.1397, Found: 430.1398.

IR (film): 1697, 1554, 1492, 1372, 1220 cm^{-1}

HPLC (after chlorination: AS-H, 88:12 Hexanes:iPrOH, 1.0mL/min, 210 nm): t_{major} = 19.5 min, t_{minor} = 14.0 min, 97% ee.

Procedure for the Determination of Enantiomeric Excess

Due to poor solubility, high retention times, and a tendency to streak, barbituric acids were chlorinated prior to ee measurement. A representative example is shown below for **182:**

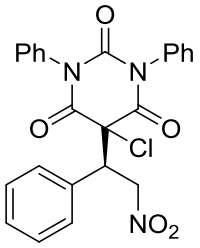

220 (X = Cl)

(*R*)-5-chloro-5-(2-nitro-1-phenylethyl)-1,3-diphenylpyrimidine-2,4,6(1*H*,3*H*,5*H*)-trione **220** (X = Cl)

To a solution of **182** (43 mg, 0.1 mmol, 1.0 eqv) in CH_2Cl_2 (1.0 mL) was added N-chlorosuccinimide (13 mg, 0.1 mmol, 1.0 eqv). The mixture was stirred at room temperature for 20 min, and then filtered through a plug of silica gel (eluting with CH_2Cl_2) to afford the desired product **220** (41.9 mg, 90%) as a white solid.

^{1}H NMR (500 MHz, $CDCl_3$) δ 7.49 (m, 6H), 7.42 (m, 3H), 7.33 (m, 2H), 7.13 (d, *J* = 6.4 Hz, 2H), 6.84 (br s, 2H), 5.49 (dd, *J* = 14.5, 3.4 Hz, 1H), 5.39 (dd, *J* = 14.4, 10.9 Hz, 1H), 4.86 (dd, *J* = 10.9, 3.4 Hz, 1H).

^{13}C NMR (125 MHz, $CDCl_3$) δ 165.4, 164.6, 148.5, 133.4, 133.4, 131.9, 130.4, 130.0, 130.0, 129.9, 129.9, 129.8, 129.7, 128.1, 128.1, 75.8, 62.9, 50.8.

HRMS (ESI) calcd for $C_{24}H_{19}ClN_3O_5^+$ $(M+H)^+$: 464.1008, Found: 464.1007.

IR (film): 1708, 1557, 1491, 1370, 1224 cm^{-1}

V.5 Experimental Procedures - Chapter IV

General Information

General: Spectrophotometric measurements were carried out using Shimadzu UV-2401 PC spectrometer, and the data was analyzed using UVPC software. Optical glass cuvettes with a 3-way stopcock were customized and were purchased from Starna Cells, Inc. Atascadero, CA.

During the course of measurement, the cuvettes were subjected to positive N_2 pressure, and the setup was covered using a black cloth. Potassium hydride (25-35% dispersion in mineral oil) was bought from Acros Organics, and the dispersion was thoroughly stirred before being transferred with a syringe (18G needle; 1.25 mm O.D.). Dimethyl sulfoxide (BP231-1) was purchased from Fisher Chemicals, and freshly distilled prior to use. Sodium amide and triphenylmethane were purchased from Sigma-Aldrich.

Experimental Details:

Ideal results were obtained by following Bordwell's procedure[13] as closely as possible. The following additional precautions may be followed:

a. DMSO undergoes appreciable disproportionation to dimethyl sulfide and dimethyl sulfone when heated above temperatures 90 C.[14] For best results, DMSO should be distilled using a strong vacuum such that DMSO distills at temperatures less than 60 °C. Results vary widely with the quality of DMSO, and thus, DMSO was used within 48 hours of distillation.
b. Layout all glassware before flame-drying them. In practice, one can wash all apparatus and let them dry in an oven overnight. The next morning, they can all be laid out for operational simplicity before flame-drying (Figure 26).
c. All operations are best carried out using flame-dried apparatus, and it is important to maintain a constant positive pressure of nitrogen/argon. Using a cuvette with a rubber septa was inferior to cuvettes with 3-way stopcock (Figure 27).

[13] Matthews, W. S.; Bares, J. E.; Bartmess, J. E.; Bordwell, F. G.; Cornforth, F. J.; Drucker, G. E.; Margolin, Z.; McCallum, R. J.; McCollum, G. J.; Vanier, N. R. *J. Am. Chem. Soc.* **1975**, *97*, 7006.
[14] Corey, E. J.;Chaykovsky, M. *Org. Synth., Coll. Vol.* **1973**, *5*, 755.

d. Schlenk flasks can be used effectively, however, avoid using rubber septa as DMSO reacts with the rubber to form a black solid. If used, replace them periodically.

e. Best results were obtained when the K-dimsyl anion solution was freshly prepared. Use of (<0.2 mg) triphenylmethane is highly recommended as the light pink color is a good indicator of K-dimsyl solution quality. If the solution turns from light pink to colorless/yellow, then the K-dimsyl solution may need to be freshly prepared (Figure 28). It is best stored in a Schlenk under positive N_2 while being covered with aluminum foil.

f. When K-dimsyl anion solution (<0.1 mL) is added to DMSO (2.0-2.5 mL) in the cuvette, a minimal color change should be observed. If the color changes to pale yellow, then the quality of DMSO or K-dimsyl may need to be re-examined.

g. The dryness of DMSO can be measured using a Karl-Fischer apparatus. DMSO routinely had H_2O levels below 25 ppm. Using activated 4 Å molecular sieves over multiple days gave optimum results.

h. Do not use excess $NaNH_2$ during distillation as that may lead to bumping. Furthermore, bumping of the viscous DMSO-$NaNH_2$ solution can be avoided by stirring at high speeds during distillation.

i. A setup is required to maintain positive N_2 pressure throughout the course of the experiment (see figure 29).

j. Dismiss outliers in data. Use of a weighing machine to gravimetrically determine the mass after every incremental addition is important to get a high R^2 with the Beer-Lambert plot.

Figure 26: Laying Out Glassware for the Titration

Figure 27: Flame-drying a Cuvette with a 3-Way Stopcock

Figure 28: Preparation of K-dimsyl Solution Followed by Addition of <0.2 mg Triphenylmethane

Figure 29: Applying Positive N_2 Pressure During the Course of the Experiment

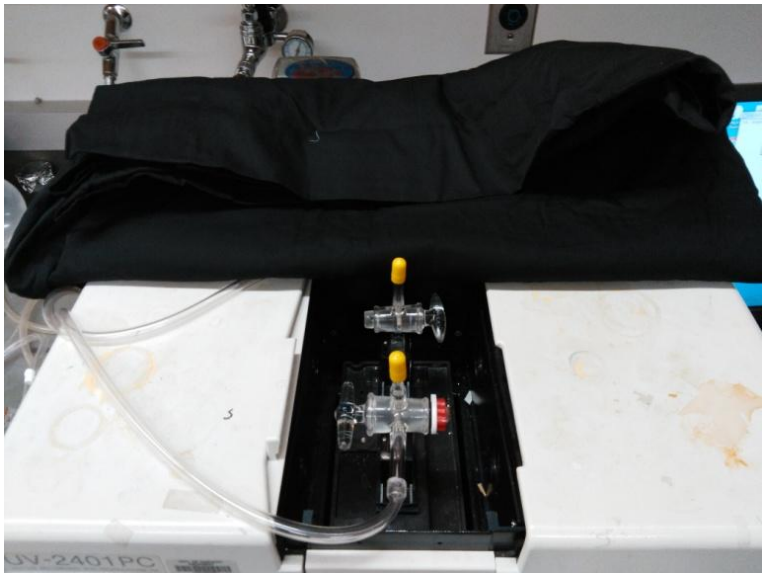

Spectrophotometric Measurements

After the data was recorded, the calculations are carried out using Microsoft Excel 2007. As an example, see Figure 30 for data corresponding to incremental addition of HIn, and Figure 31 for data corresponding to subsequent incremental addition of HA (absorbs <475 nm). Then, see Figure 32 for sample calculation. Note the use of 'regression' function in Microsoft Excel to get the slope and co-efficient for the best-fit straight line.

Figure 30: Sample Dataset for Incremental Addition of HIn

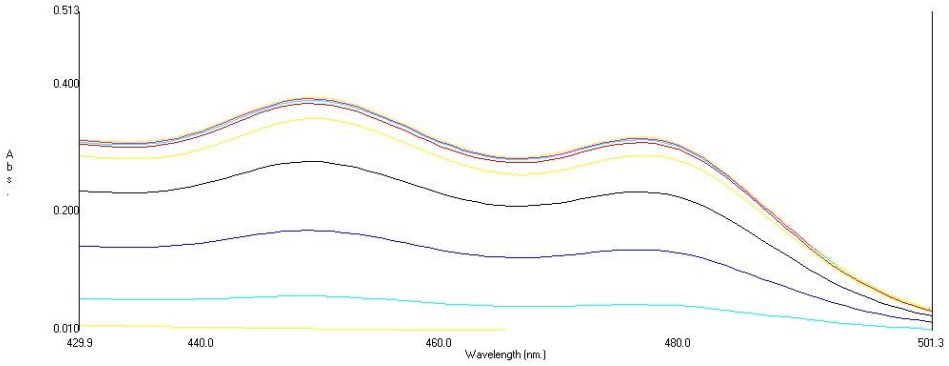

Figure 31: Sample Dataset for Subsequent Incremental Addition of HA

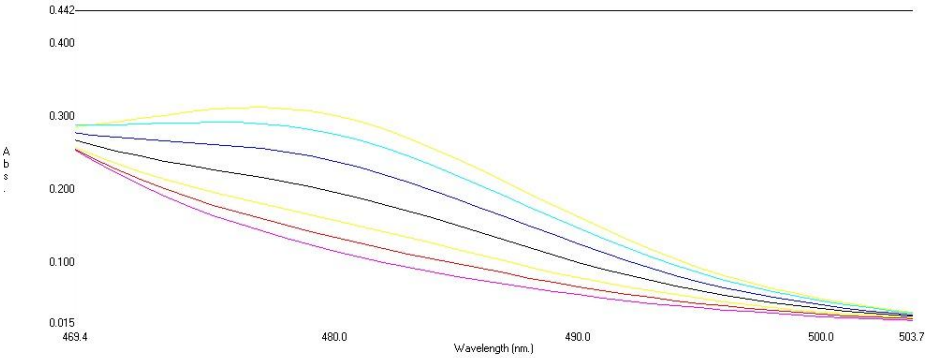

	A	B	C	D	E	F	G	H	I	J	K	L	M	N	O	P	Q	R
1	Wavelength Range =		400 - 650 nm															
2	Wavelength for Abs =		485 nm															
3																		
4	Concentration of Indicator =			0.00283														
5																		
6	Expt	Mass	δmass-I2	Σmass-I2	δvolume-I2	Σvolume-I2	Total System Volum	[HIn] + [In]	Absorbance [In]		[HIn]							
7	Initial	86.2542					2		0									
8	DAS3	86.3482	0.094		0.08545455	0	2.085454545	0	0.0056									
9	B01	86.3674	0.0192	0.0192	0.01745455	0.017454545	2.102909091	2.34947E-05	0.0386	2.34E-05	5.15E-08							
10	B02	86.4104	0.043	0.0622	0.03909091	0.056545455	2.142	7.47238E-05	0.1052	7.48E-05	########							
11	B03	86.4585	0.0481	0.1103	0.04372727	0.100272727	2.185727273	0.000129858	0.1767	1.30E-04	########							
12	B04	86.4943	0.0358	0.1461	0.03254545	0.132818182	2.218272727	0.000169482	0.2143	1.59E-04	1.06E-05							
13	B05	86.5389	0.0446	0.1907	0.04054545	0.173363636	2.258818182	0.000217249	0.2374	1.77E-04	4.06E-05							
14	B06	86.5998	0.0609	0.2516	0.05536364	0.228727273	2.314181818	0.00027977	0.2414	1.80E-04	1.00E-04							
15	B07	86.6512	0.0514	0.303	0.04672727	0.275454545	2.360909091	0.000330257	0.2442	1.82E-04	1.48E-04							
16	B08	86.7532	0.102	0.405	0.09272727	0.368181818	2.453636364	0.00042475	0.241	1.79E-04	2.45E-04							
17																		
18										Regression applied to top 4 points								
19										Coefficient	0.00077064							
20	Concentration of HA =		0.00215							Intercept =	-6.3035E-06							
21																		
22	Expt	Mass	δmass-H.	Σmass-H.	δvolume-HA	Σvolume-HA	Total System Volum	[HA]+[A]										
23	B08	86.7532	0	0	0	0	2.453636364	0										
24	C01	86.7883	0.0351	0.0351	0.03190909	0.031909091	2.485454545	2.76058E-05										
25	C02	86.8375	0.0492	0.0843	0.04472727	0.076636364	2.562181818	6.43179E-05										
26	C03	86.8881	0.0506	0.1349	0.046	0.122636364	2.684818182	9.82226E-05										
27	C04	86.9344	0.0463	0.1812	0.04209091	0.164727273	2.849545455	0.000124307										
28	C05	86.9834	0.049	0.2302	0.04454545	0.209272727	3.058818182	0.000147118										
29	C06	87.0432	0.0598	0.29	0.05436364	0.263636364	3.322454545	0.000170629										

Figure 32: Sample Calculations (partial) with Microsoft Excel

APPENDIX

^{1}H NMR, ^{13}C NMR SPECTRA

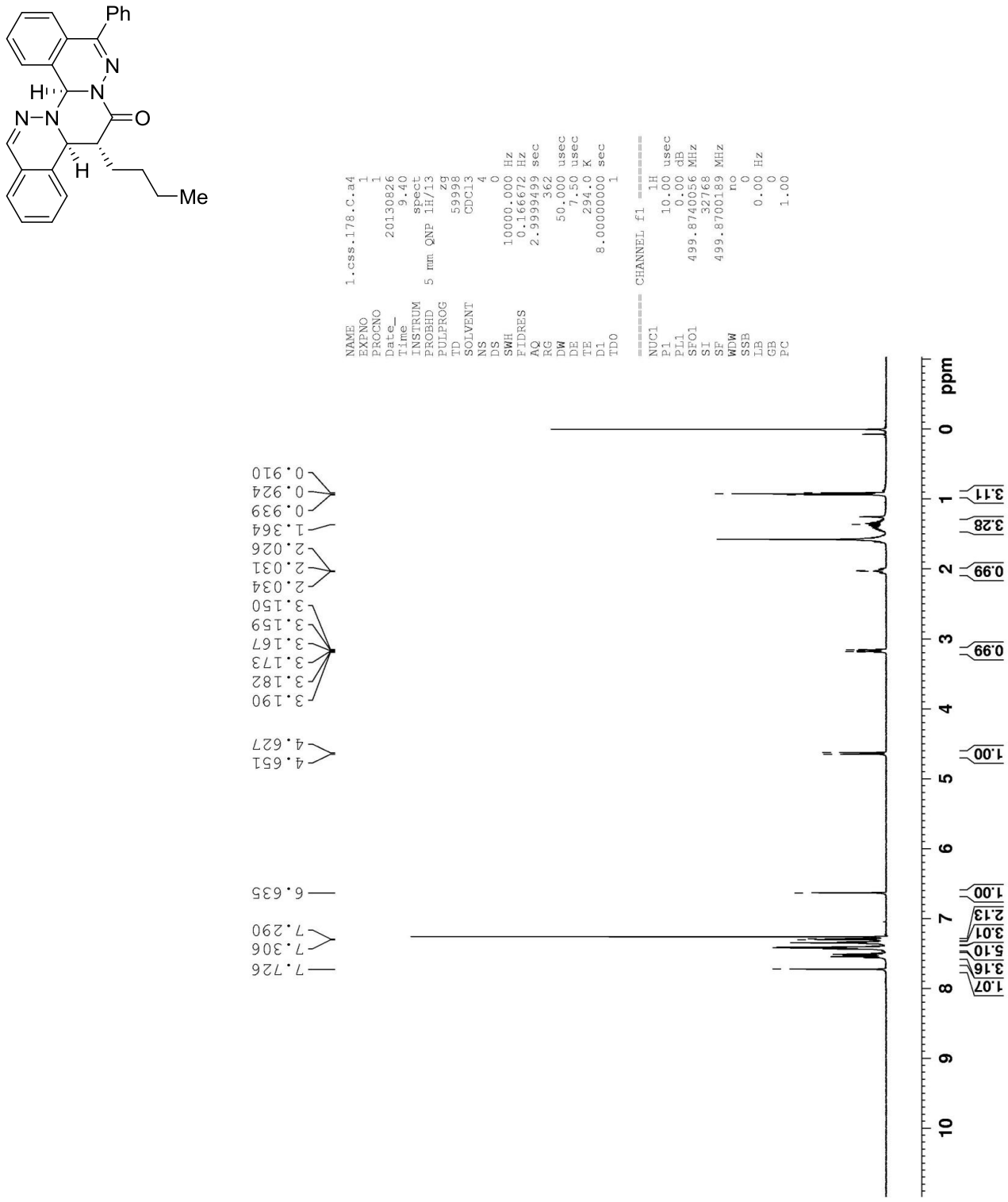

Figure 33: ^{1}H NMR Spectrum of 26 (500 MHz, $CDCl_3$, 298K)

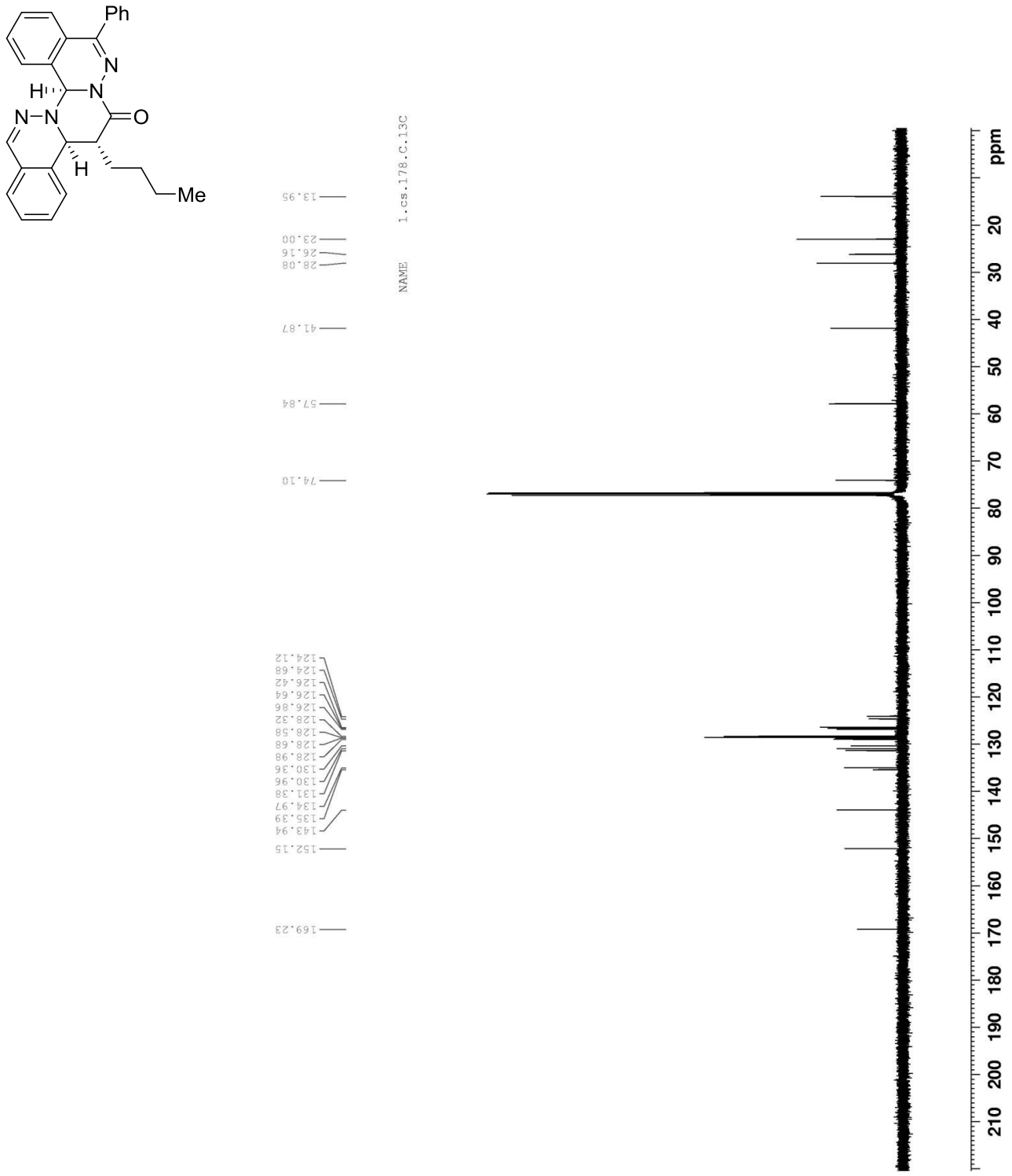

Figure 34: ^{13}C NMR Spectrum of 26 (125 MHz, $CDCl_3$, 298K)

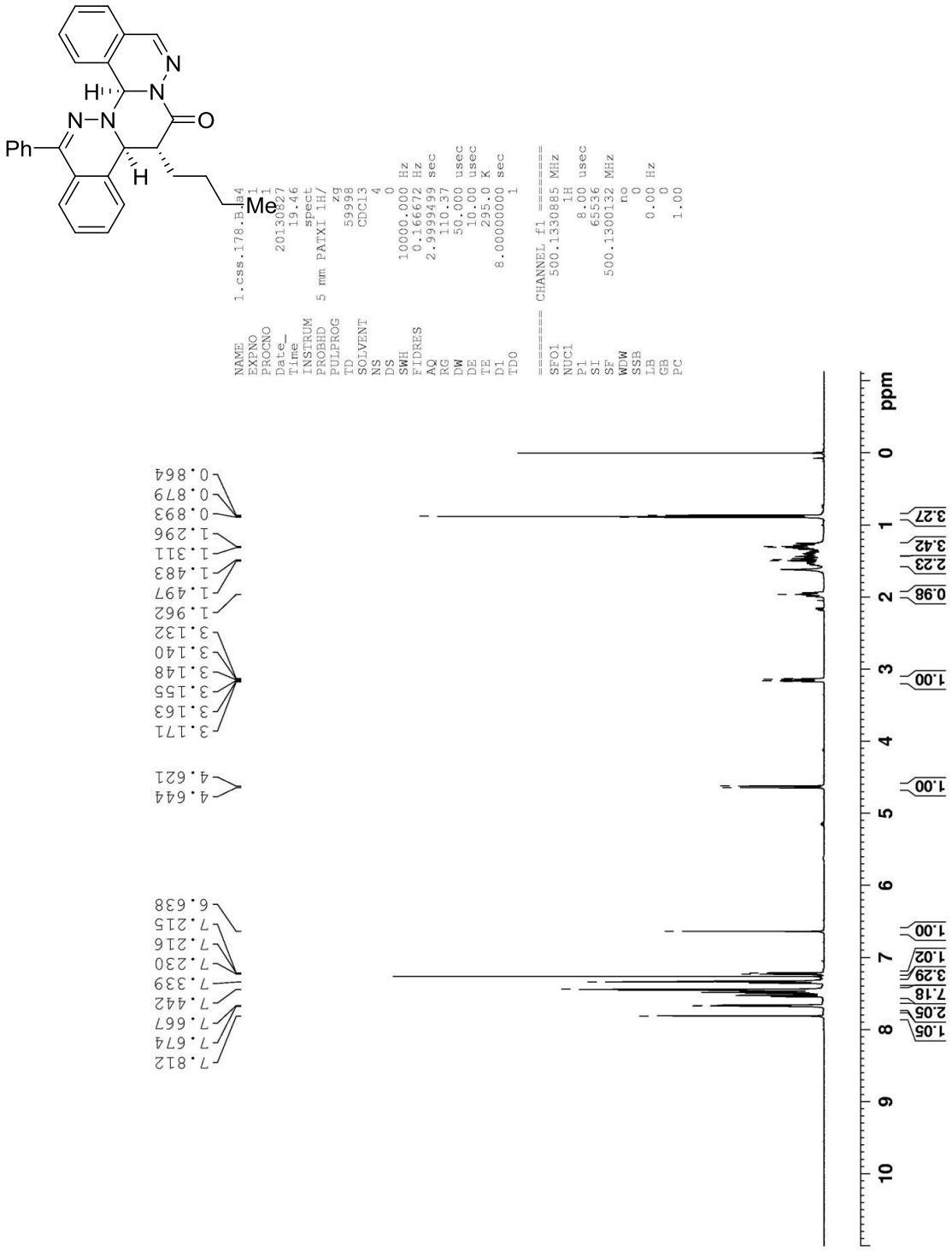

Figure 35: ^{1}H NMR Spectrum of 27 (500 MHz, $CDCl_3$, 298K)

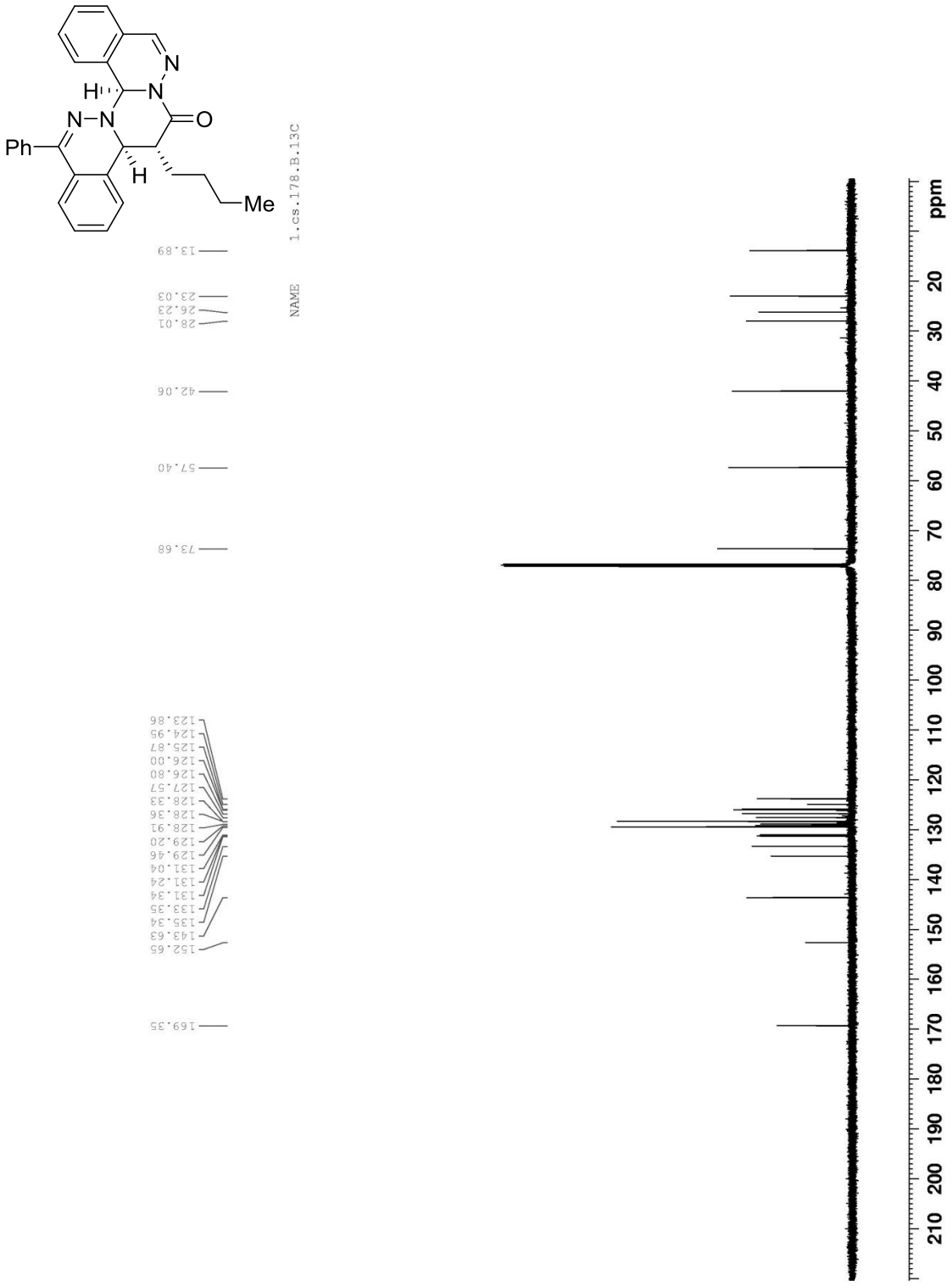

Figure 36: ^{13}C NMR Spectrum of 27 (125 MHz, $CDCl_3$, 298K)

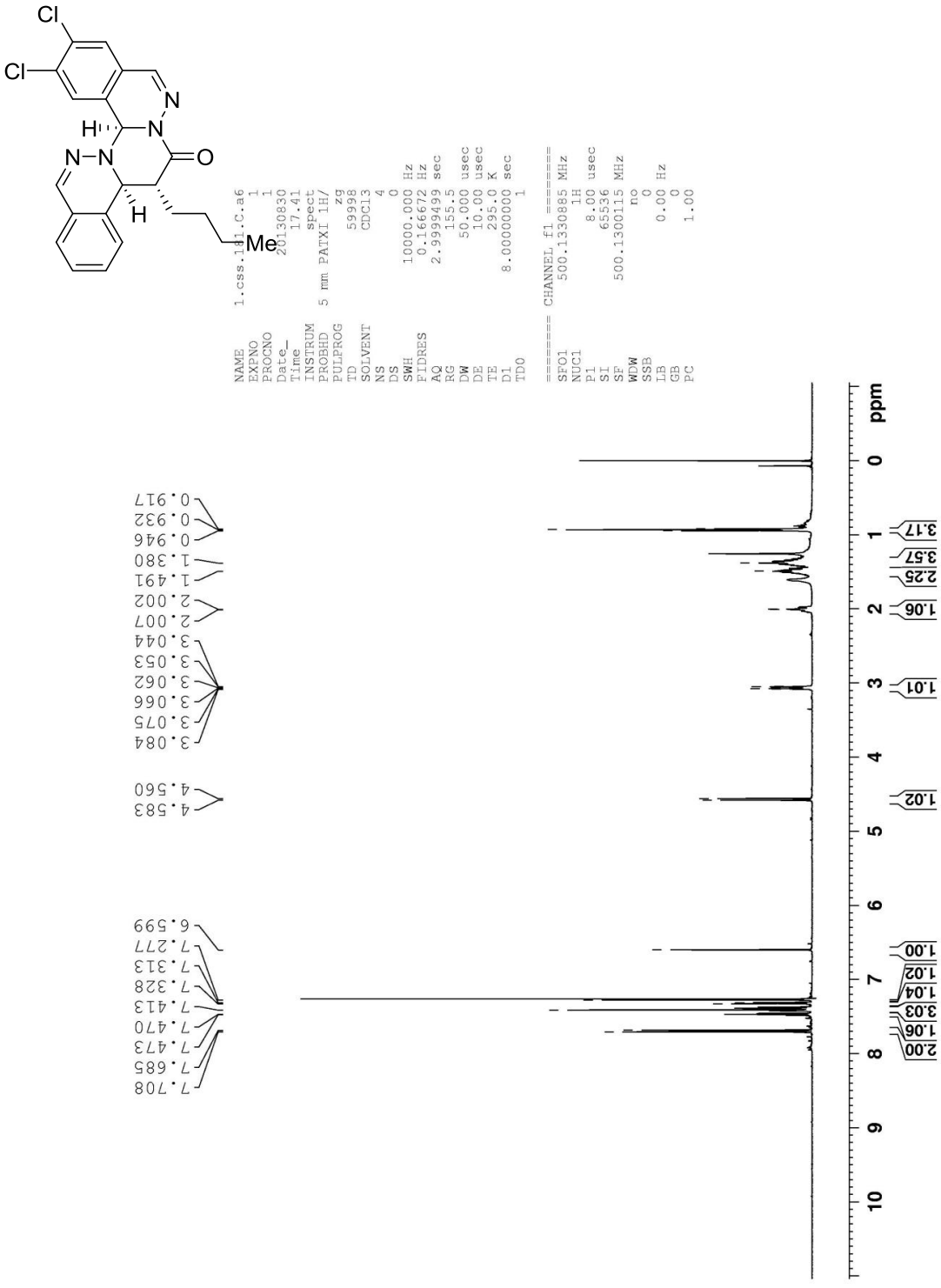

Figure 37: ^{1}H NMR Spectrum of 29 (500 MHz, $CDCl_3$, 298K)

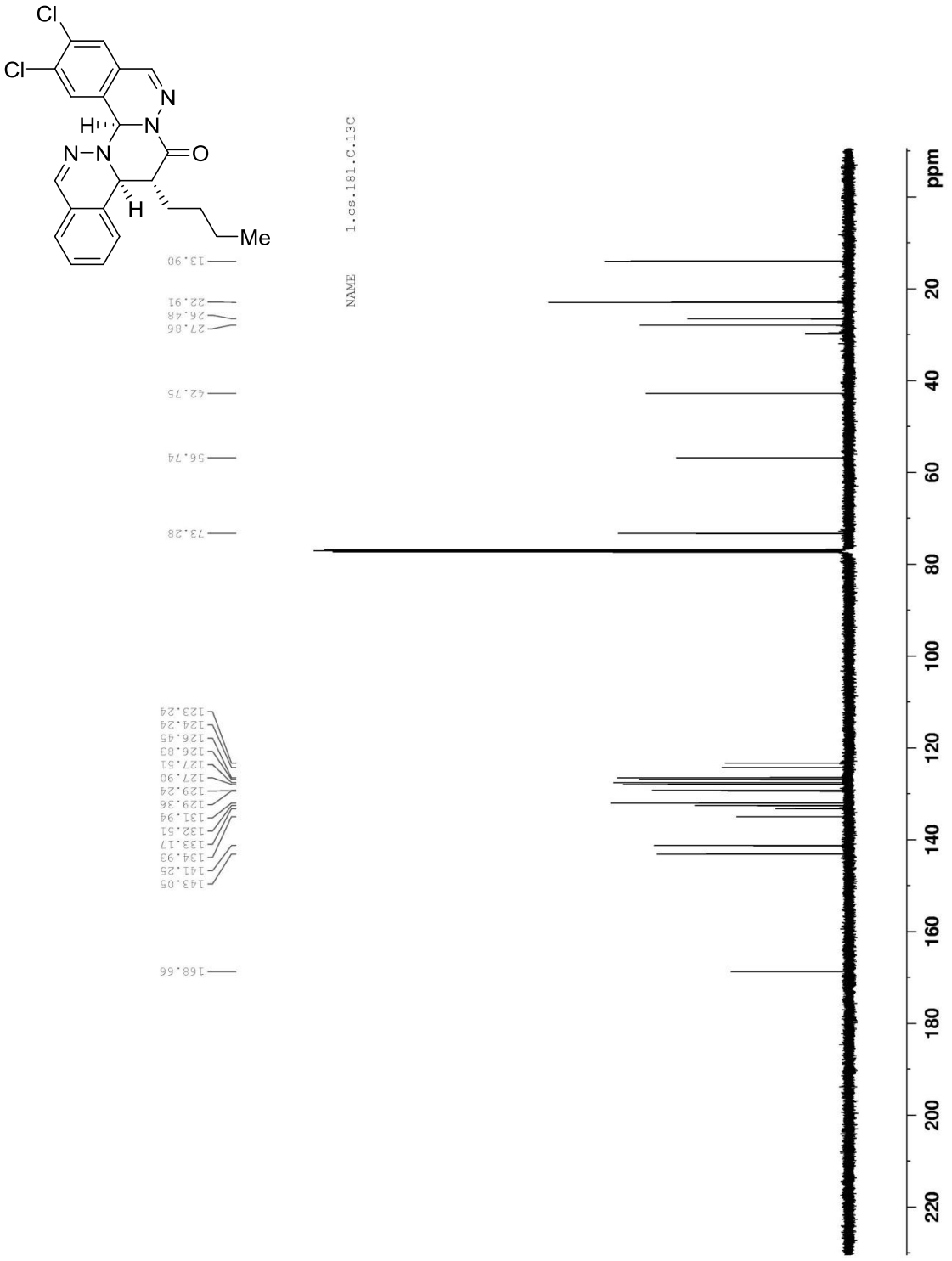

Figure 38: ^{13}C NMR Spectrum of 29 (125 MHz, $CDCl_3$, 298K)

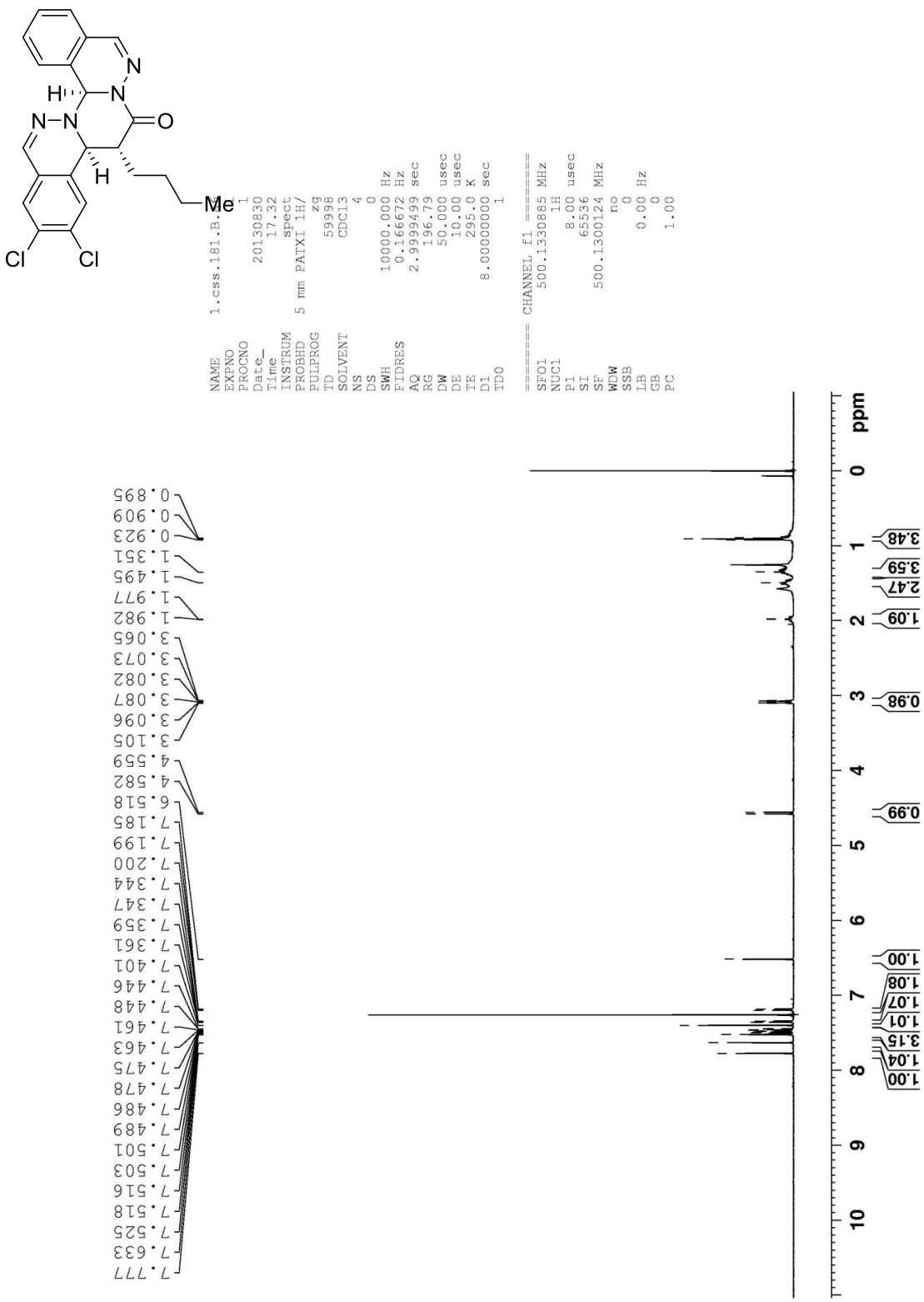

Figure 39: ^{1}H NMR Spectrum of 30 (500 MHz, $CDCl_3$, 298K)

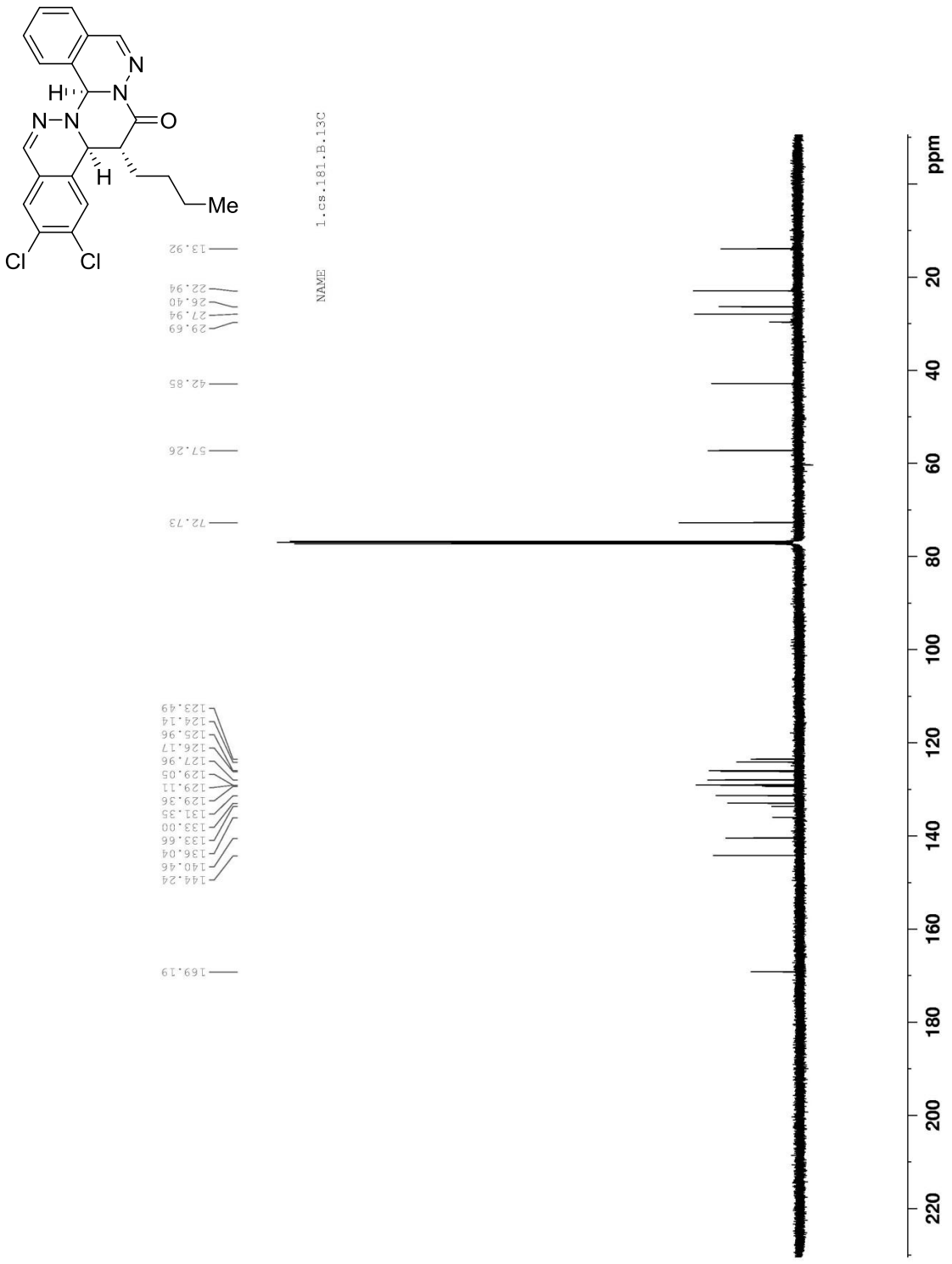

Figure 40: ^{13}C NMR Spectrum of 30 (125 MHz, $CDCl_3$, 298K)

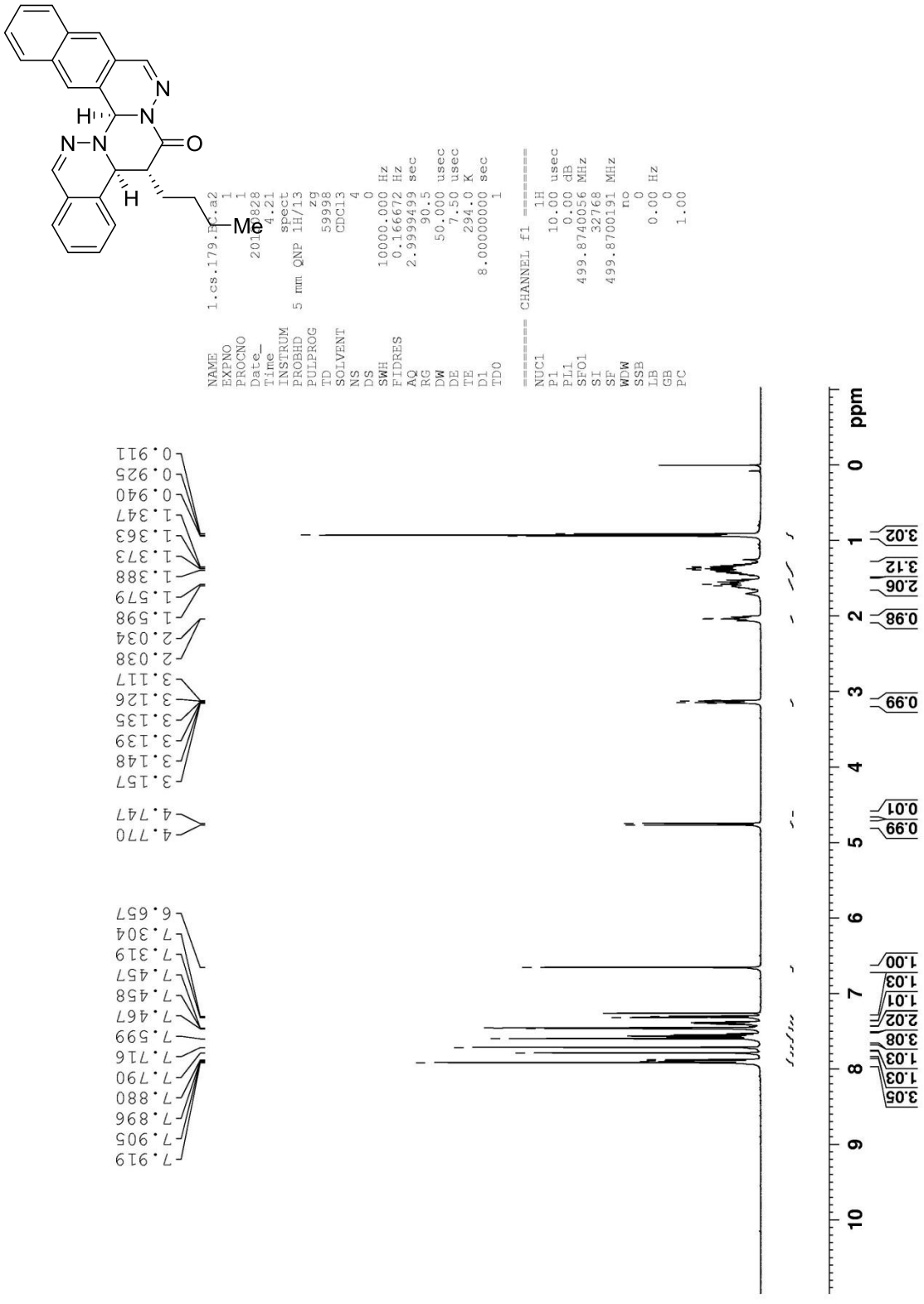

Figure 41: ^{1}H NMR Spectrum of 32 (500 MHz, $CDCl_3$, 298K)

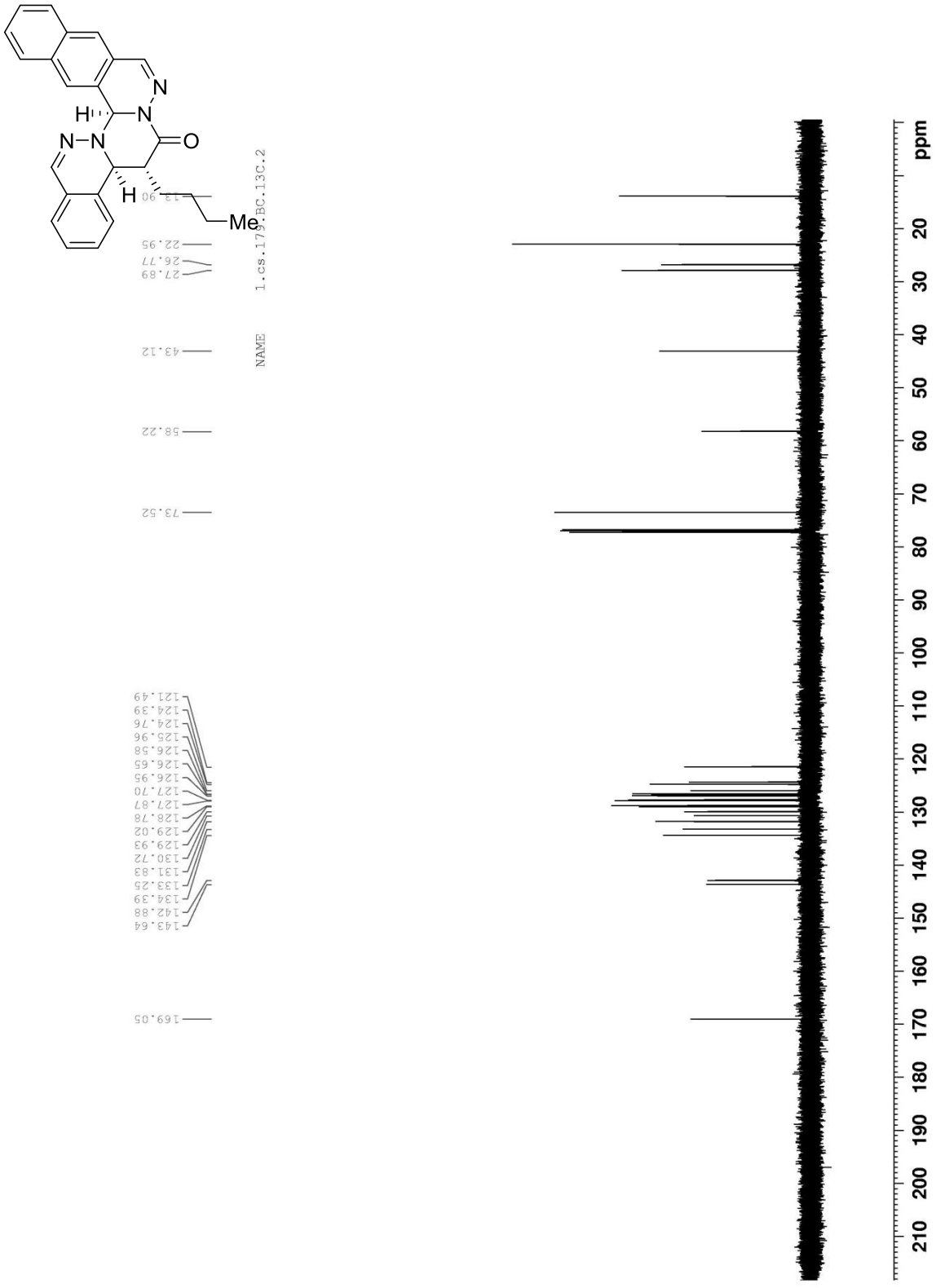

Figure 42: ^{13}C NMR Spectrum of 32 (125 MHz, $CDCl_3$, 298K)

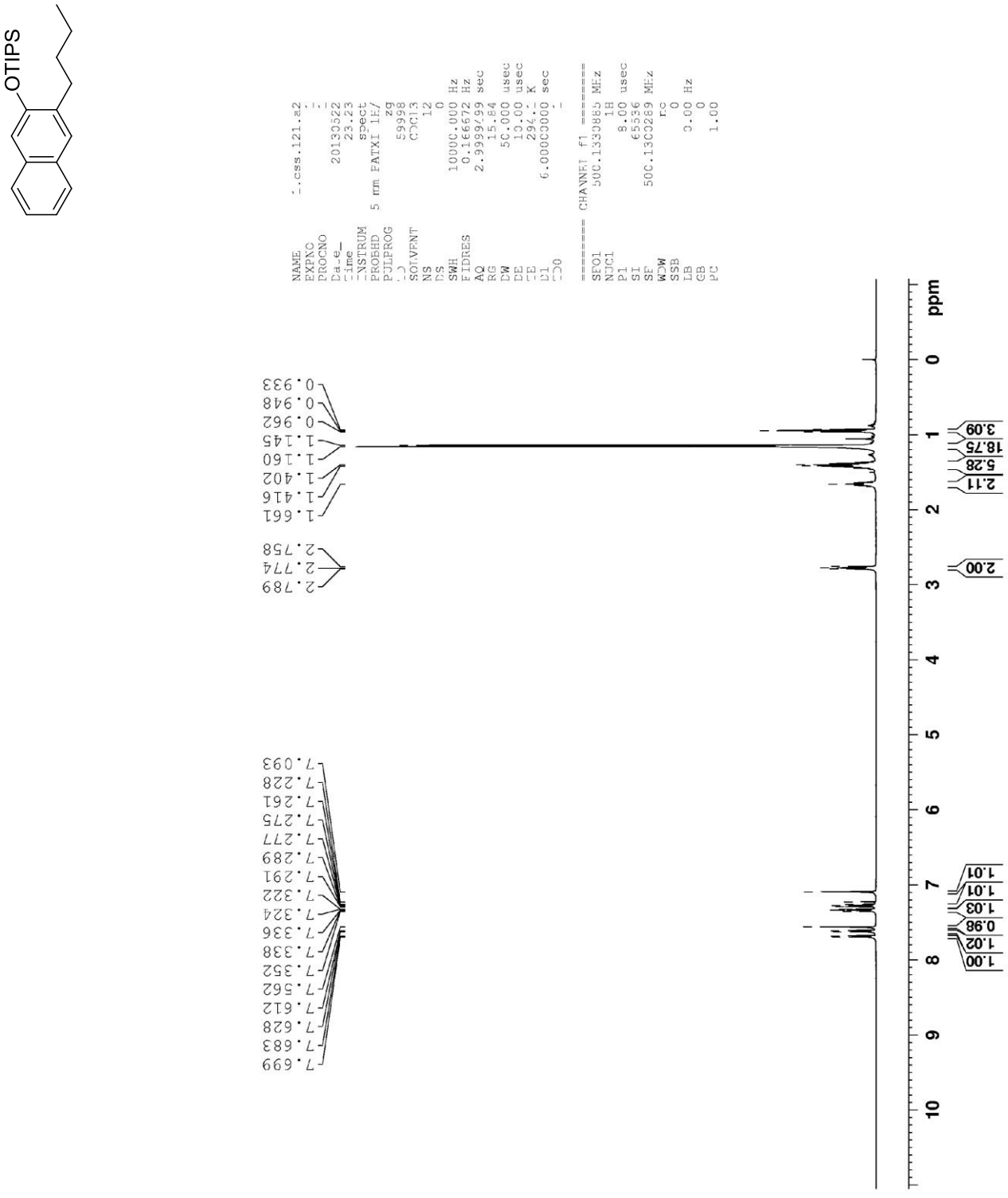

Figure 43: ^{1}H NMR Spectrum of 67 (500 MHz, $CDCl_3$, 298K)

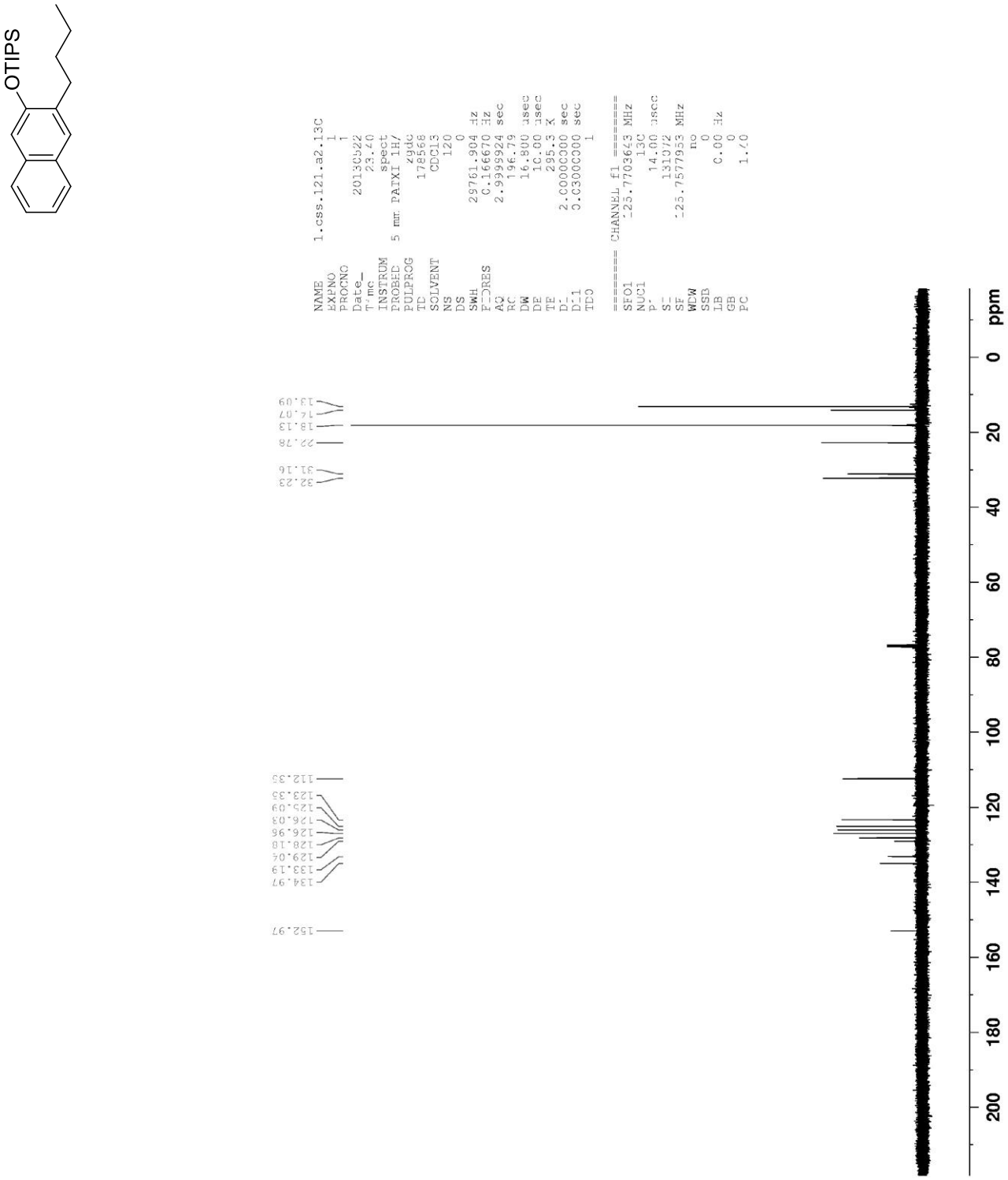

Figure 44: ^{13}C NMR Spectrum of 67 (125 MHz, $CDCl_3$, 298K)

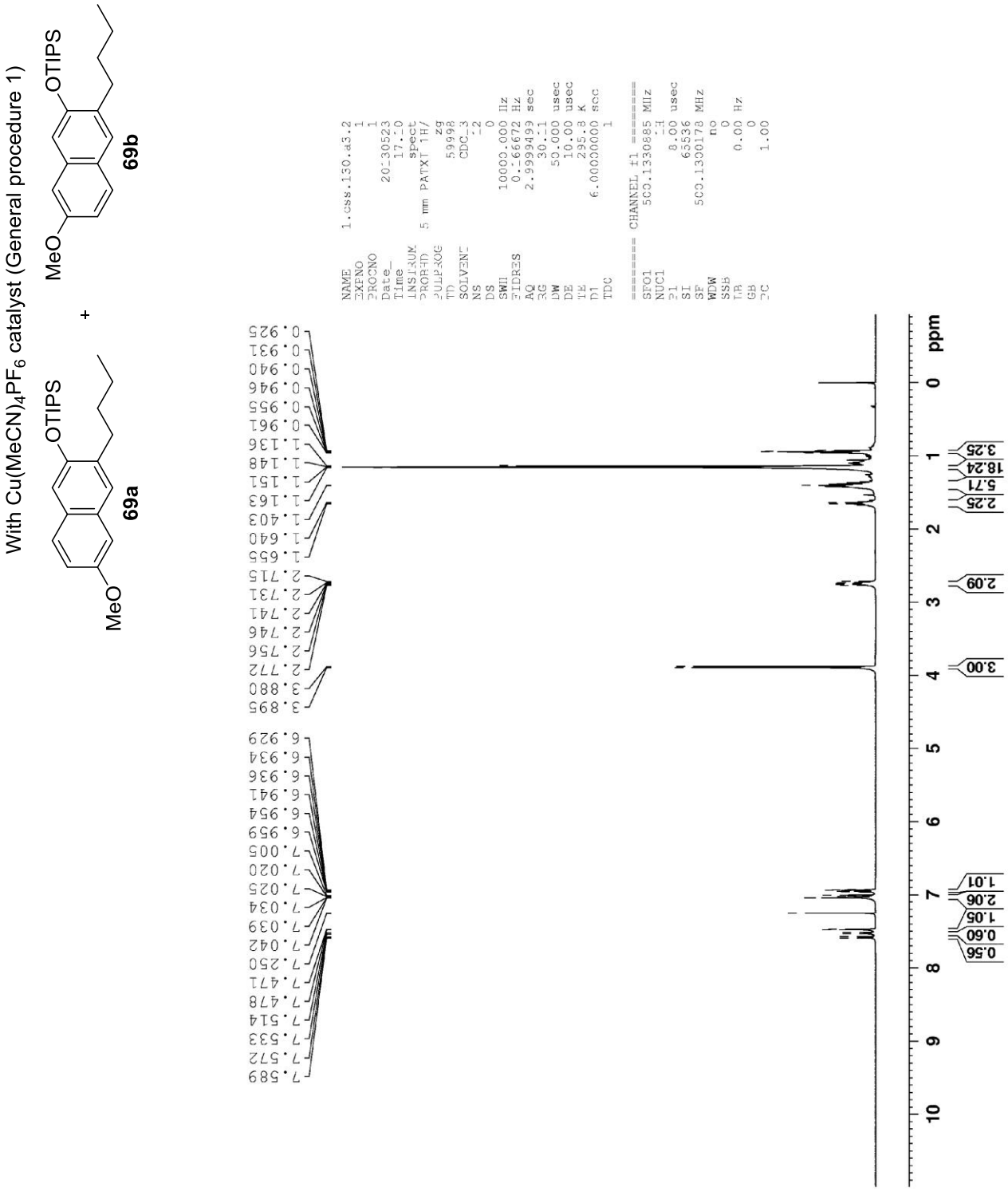

Figure 45: ^{1}H NMR Spectrum of 69a+69b (500 MHz, $CDCl_3$, 298K)

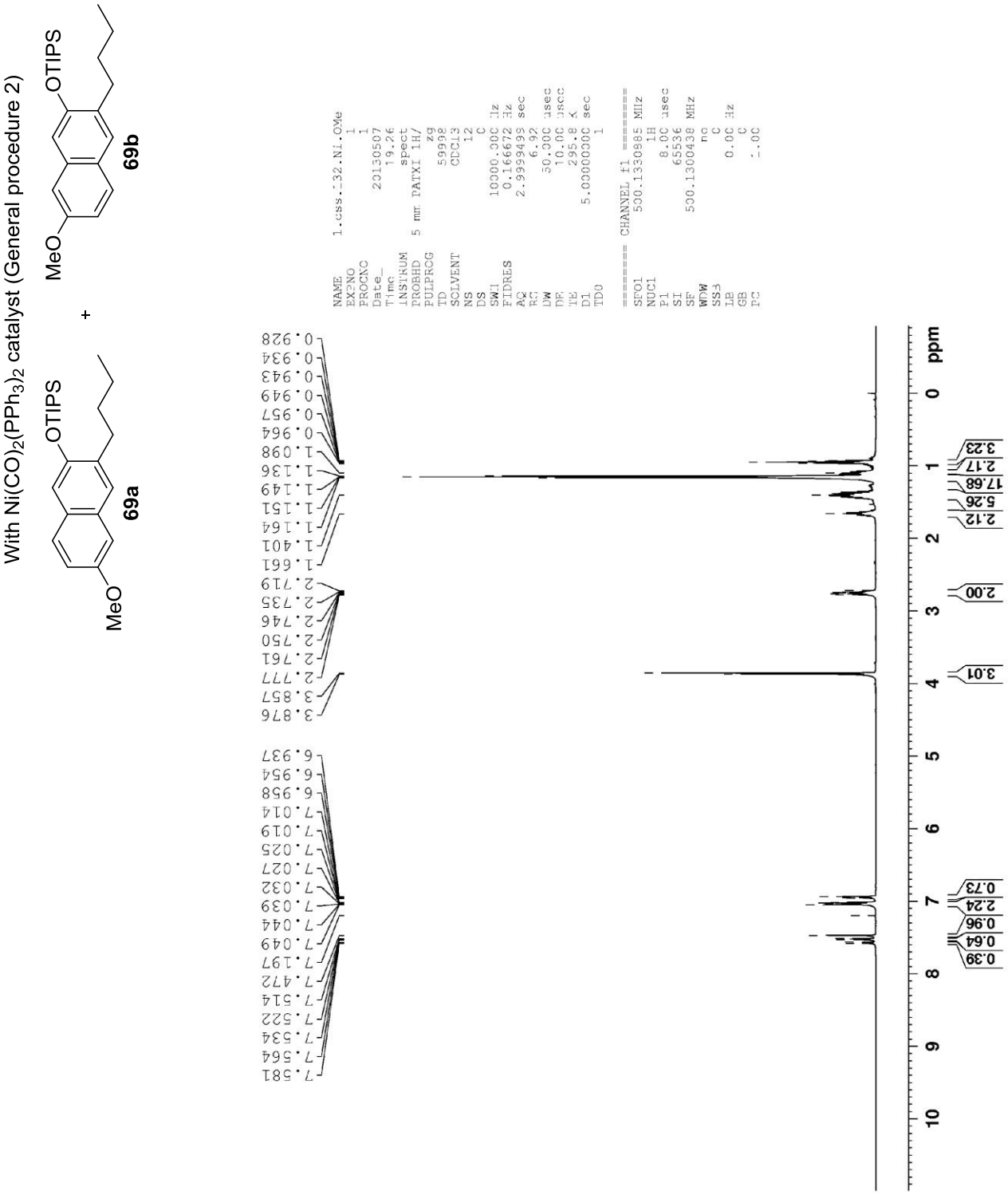

Figure 46: ^{1}H NMR Spectrum of 69a+69b (500 MHz, $CDCl_3$, 298K)

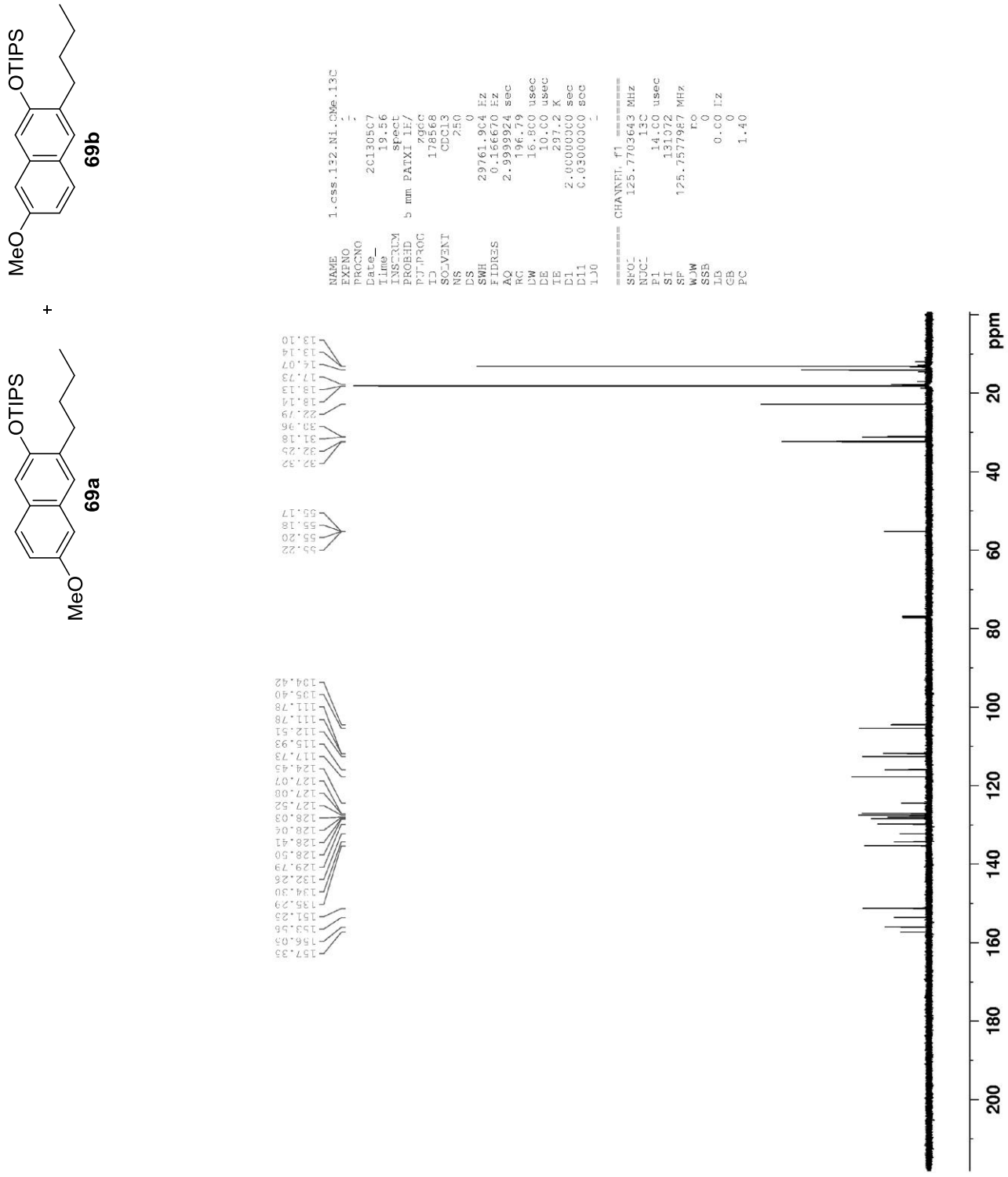

Figure 47: ^{13}C NMR Spectrum of 69a+69b (125 MHz, $CDCl_3$, 298K)

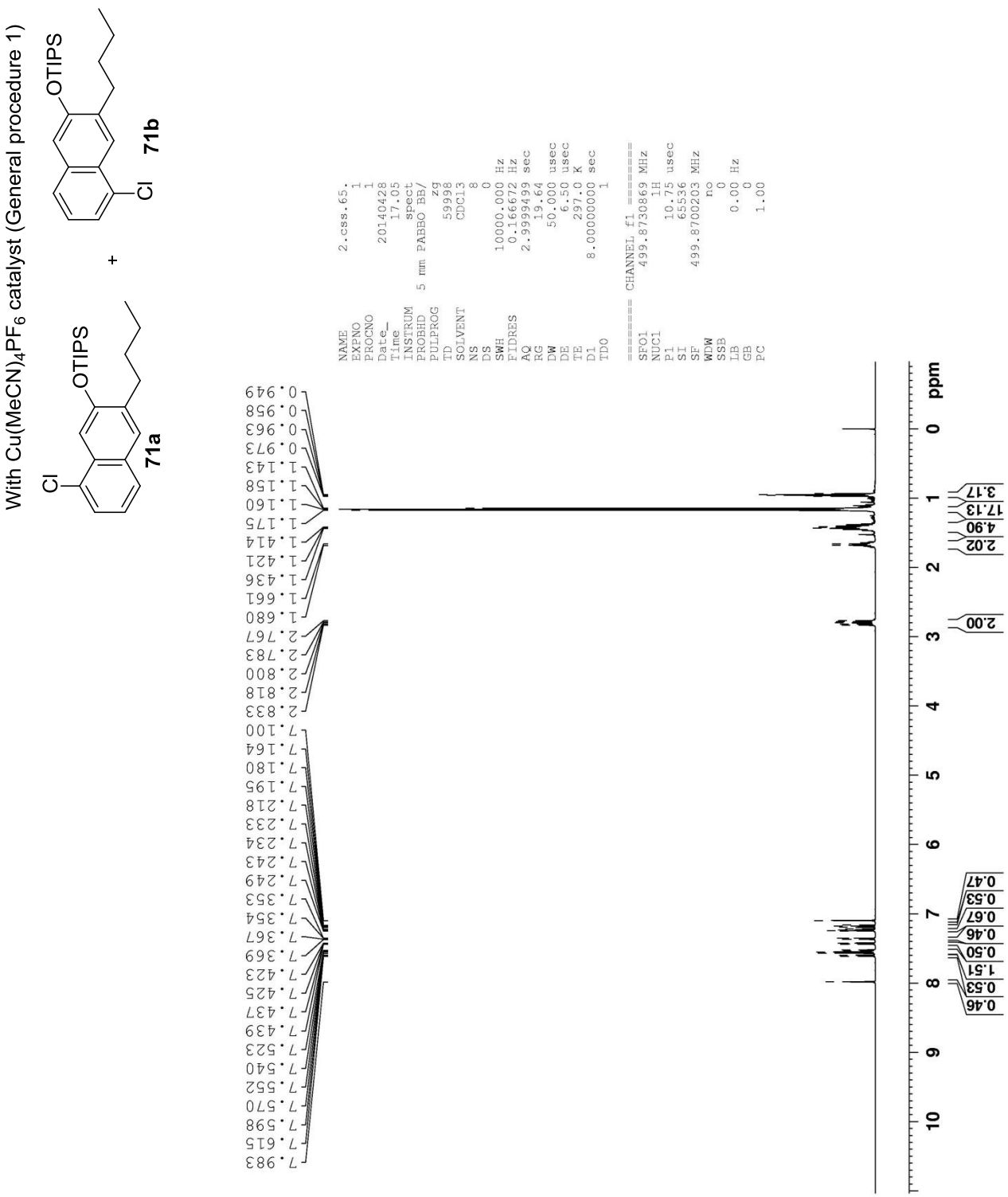

Figure 48: ^{1}H NMR Spectrum of 71a+71b (500 MHz, $CDCl_3$, 298K)

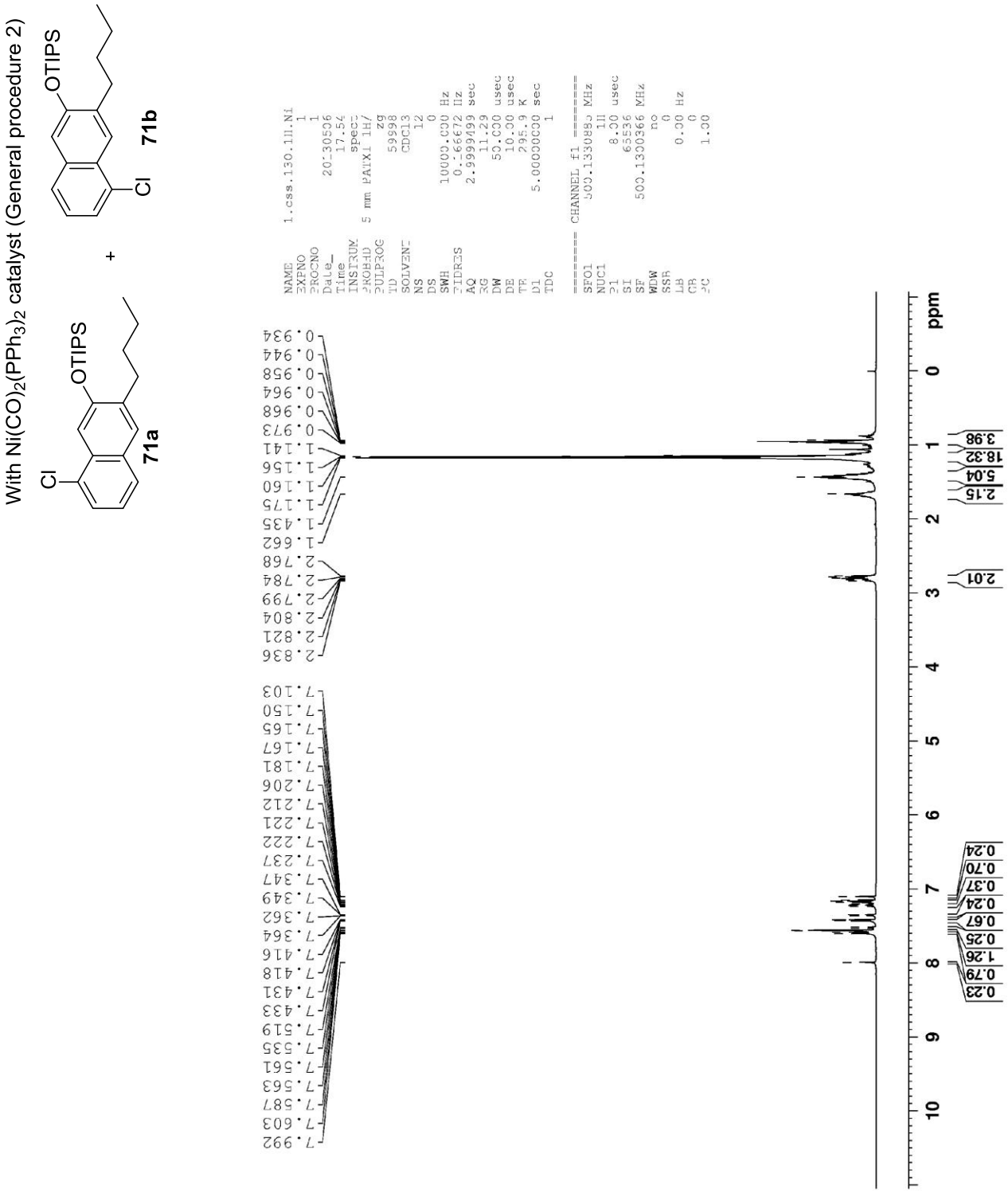

Figure 49: ^{1}H NMR Spectrum of 71a+71b (500 MHz, $CDCl_3$, 298K)

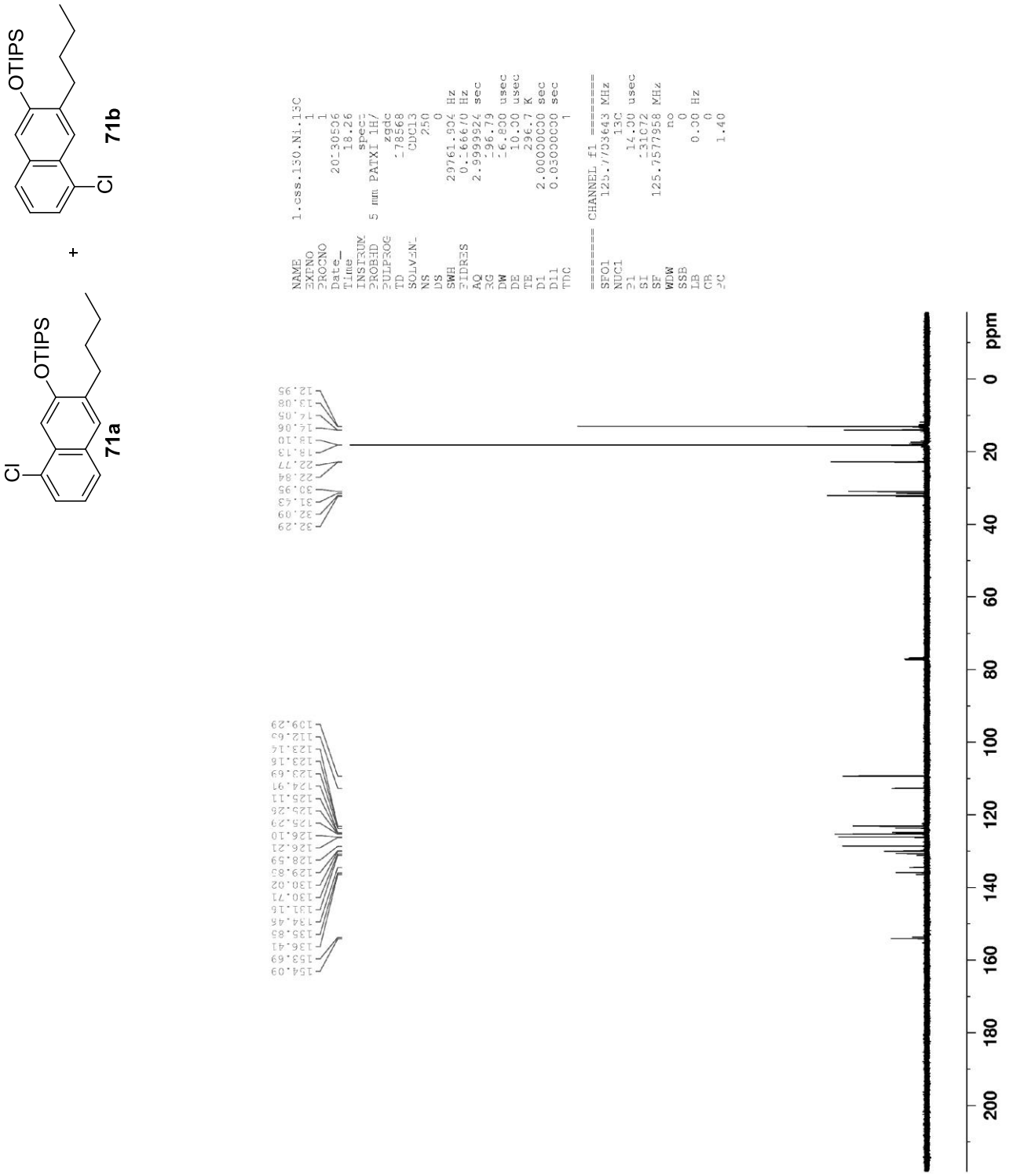

Figure 50: ^{13}C NMR Spectrum of 71a+71b (125 MHz, $CDCl_3$, 298K)

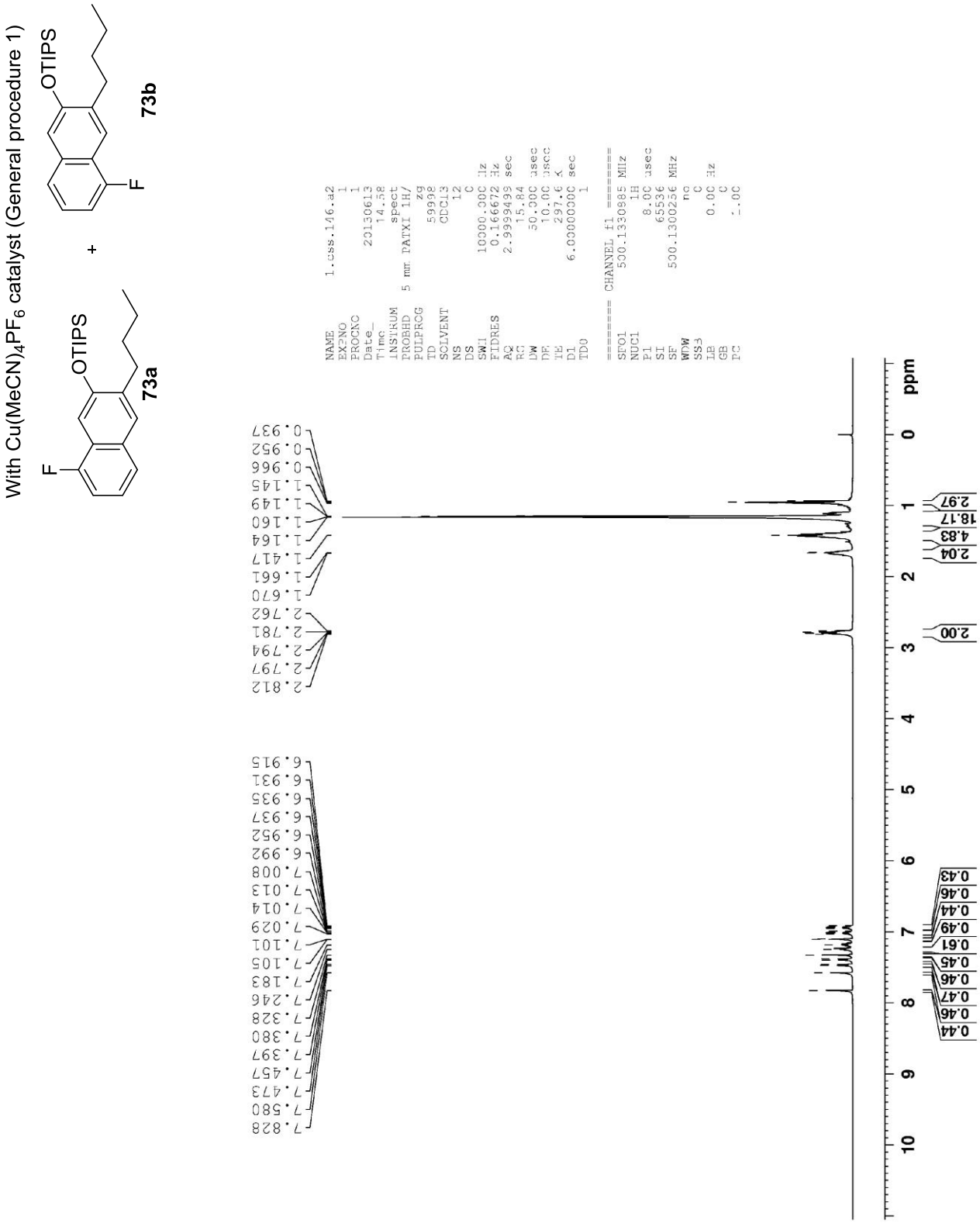

Figure 51: ^{1}H NMR Spectrum of 73a+73b (500 MHz, $CDCl_3$, 298K)

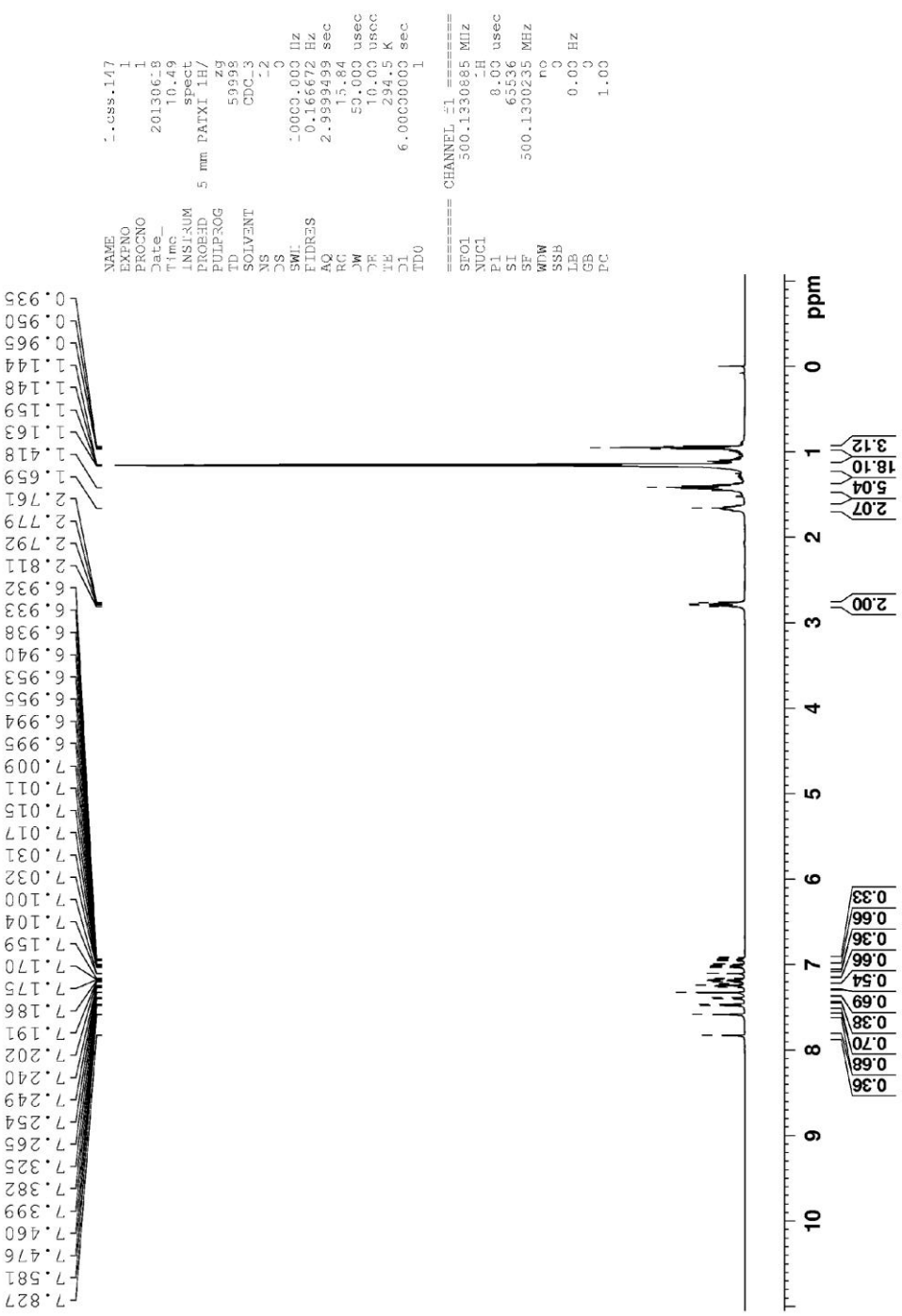

Figure 52: ^{1}H NMR Spectrum of 73a+73b (500 MHz, $CDCl_3$, 298K)

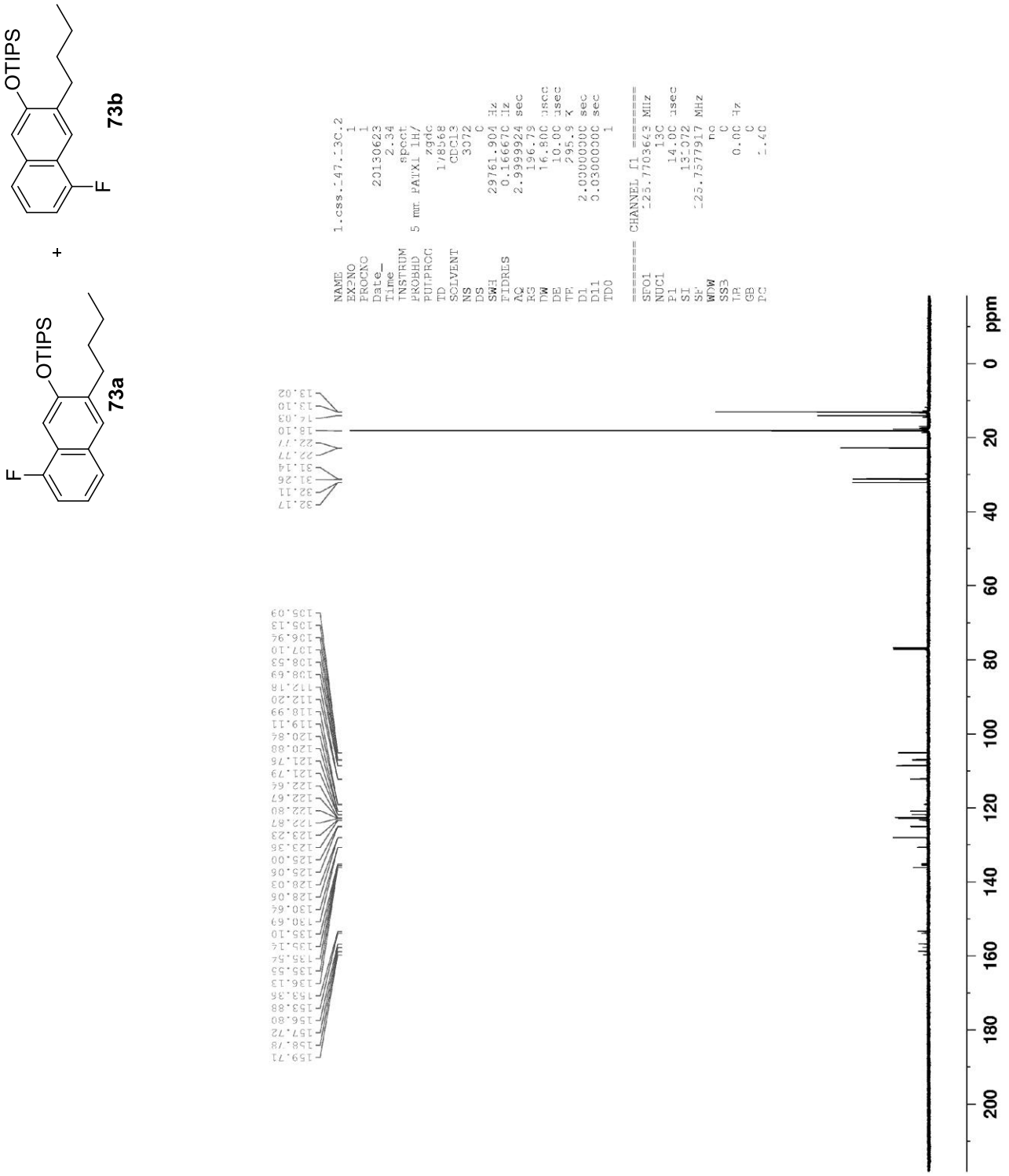

Figure 53: ^{13}C NMR Spectrum of 73a+73b (125 MHz, $CDCl_3$, 298K)

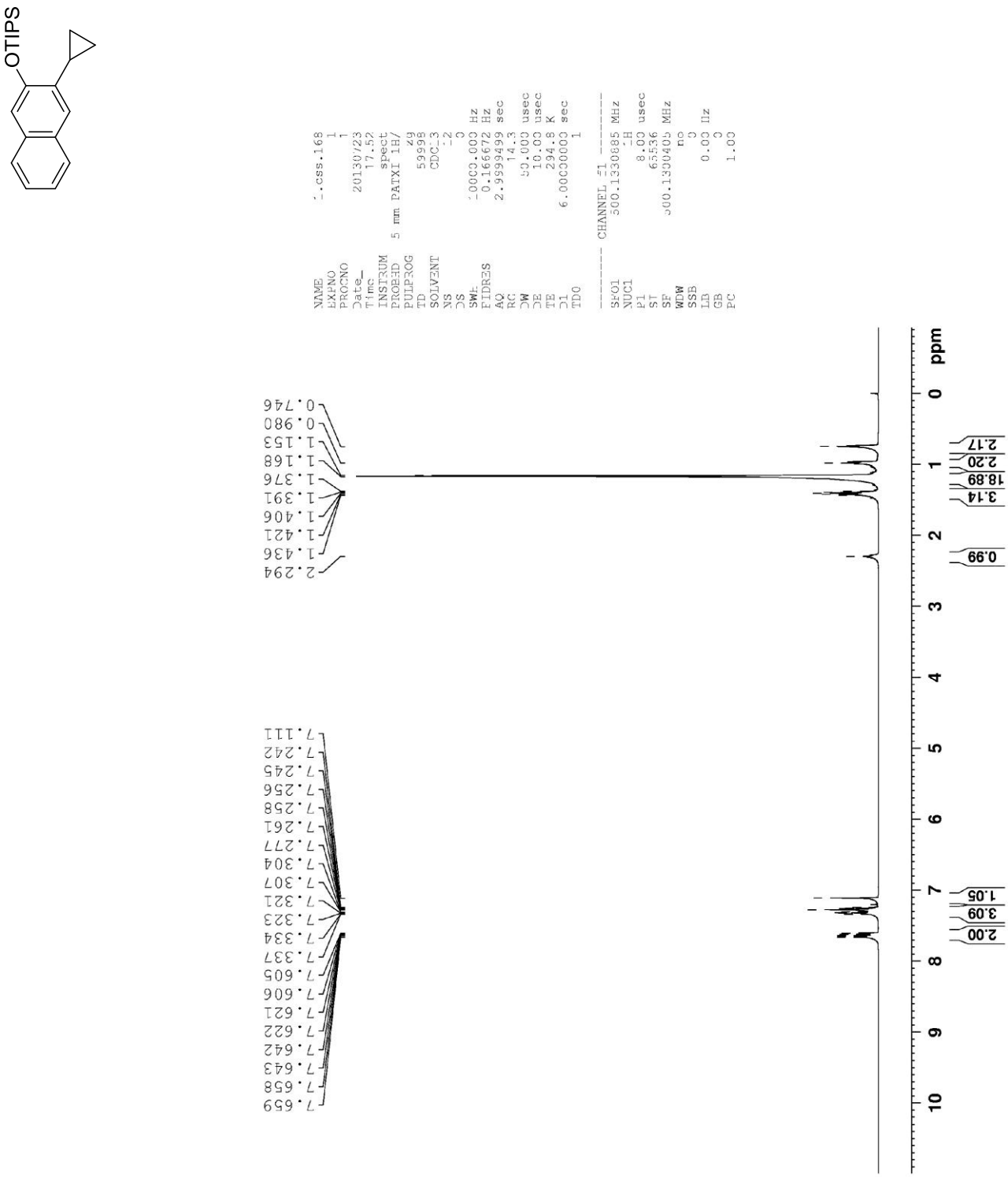

Figure 54: ^{1}H NMR Spectrum of 74 (500 MHz, $CDCl_3$, 298K)

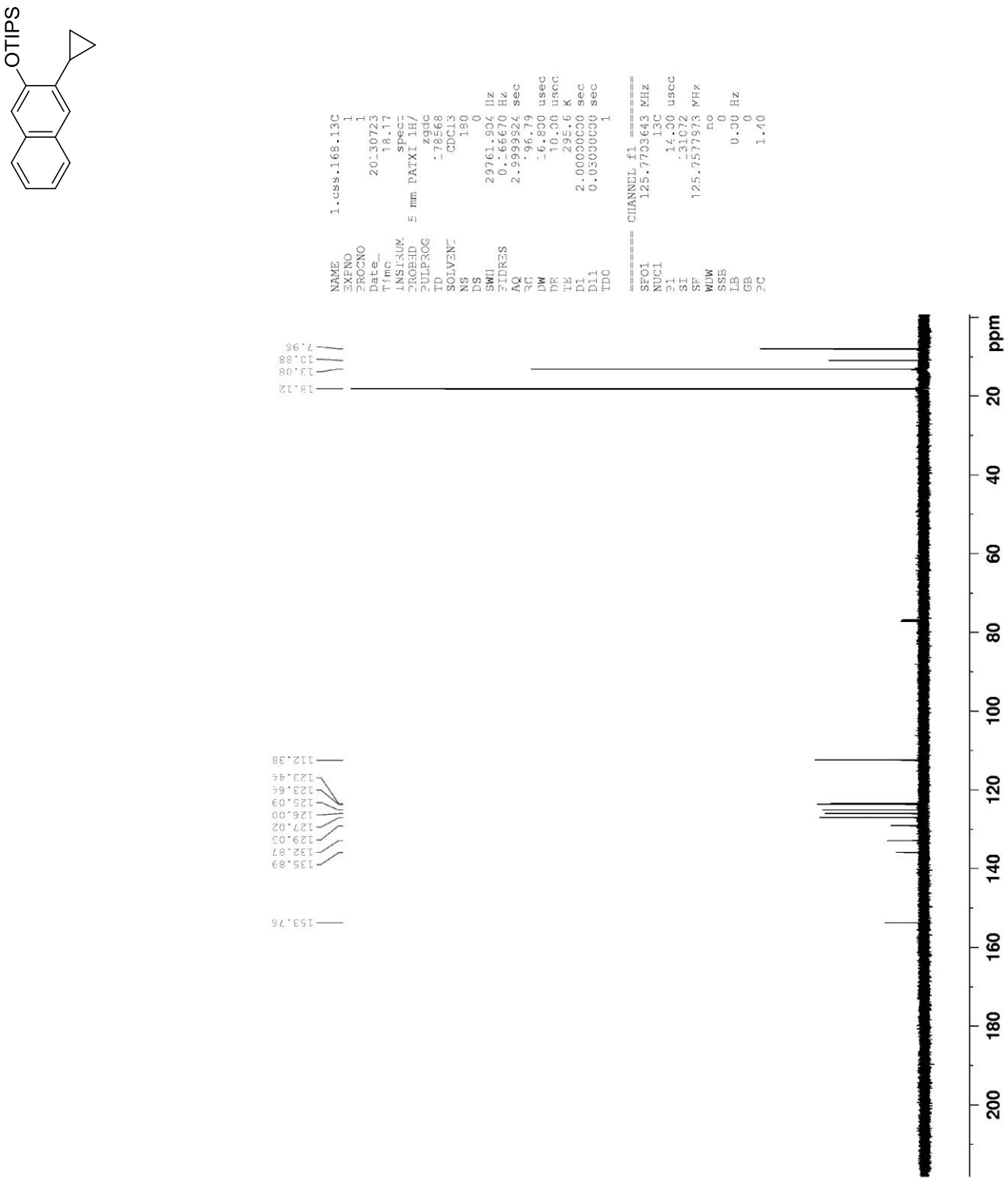

Figure 55: ^{13}C NMR Spectrum of 74 (125 MHz, $CDCl_3$, 298K)

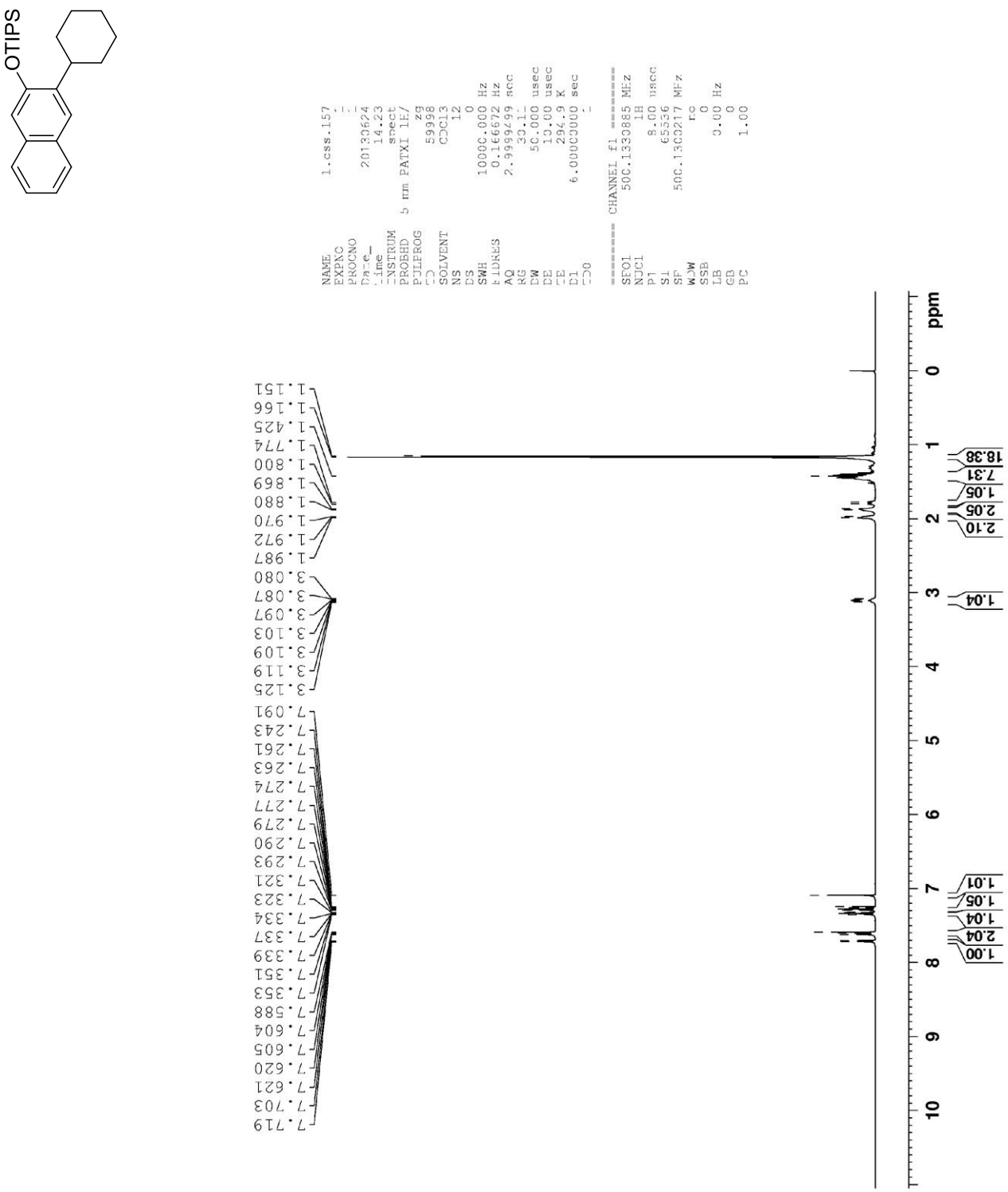

Figure 56: ^{1}H NMR Spectrum of 75 (500 MHz, $CDCl_3$, 298K)

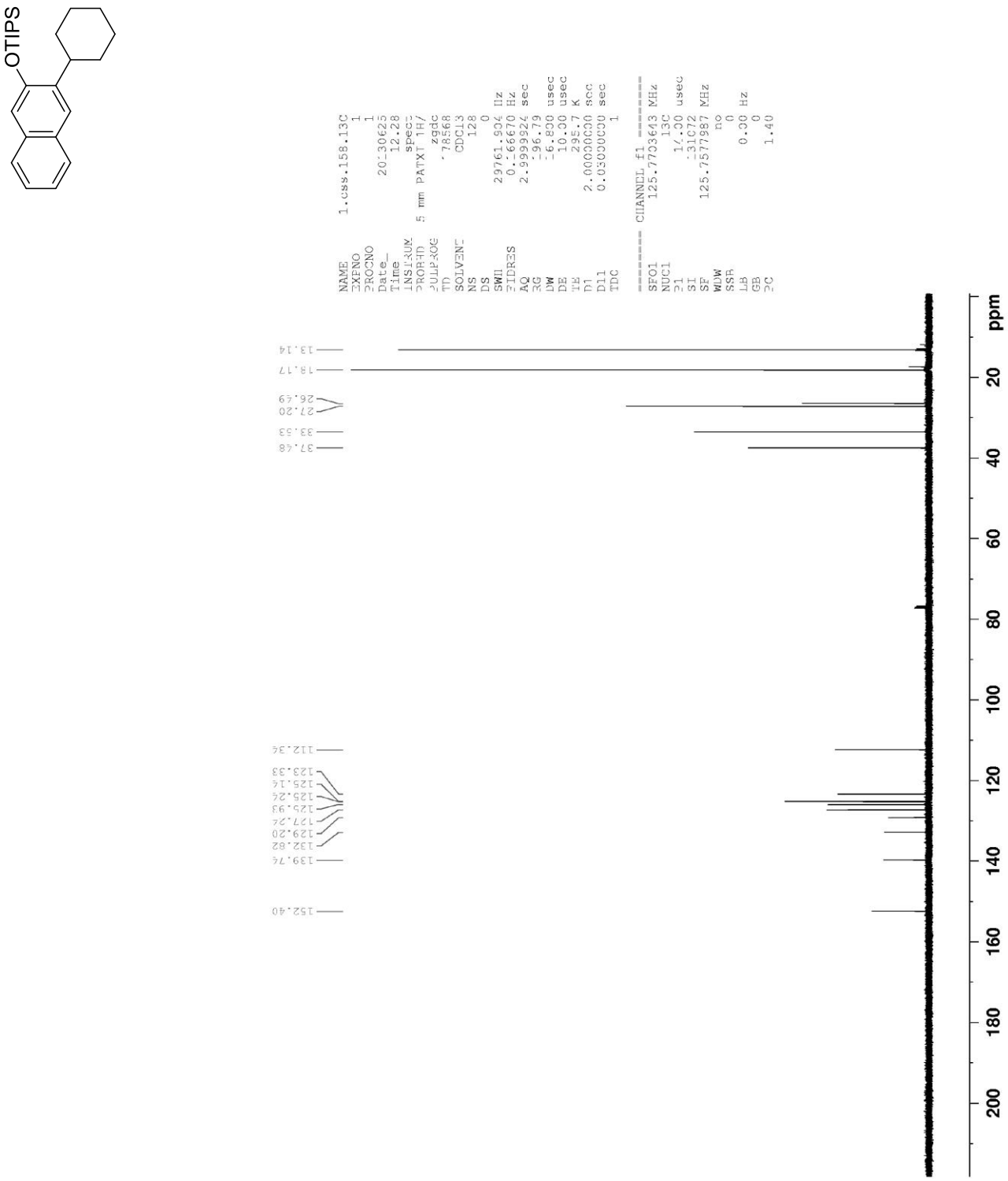

Figure 57: ^{13}C NMR Spectrum of 75 (125 MHz, $CDCl_3$, 298K)

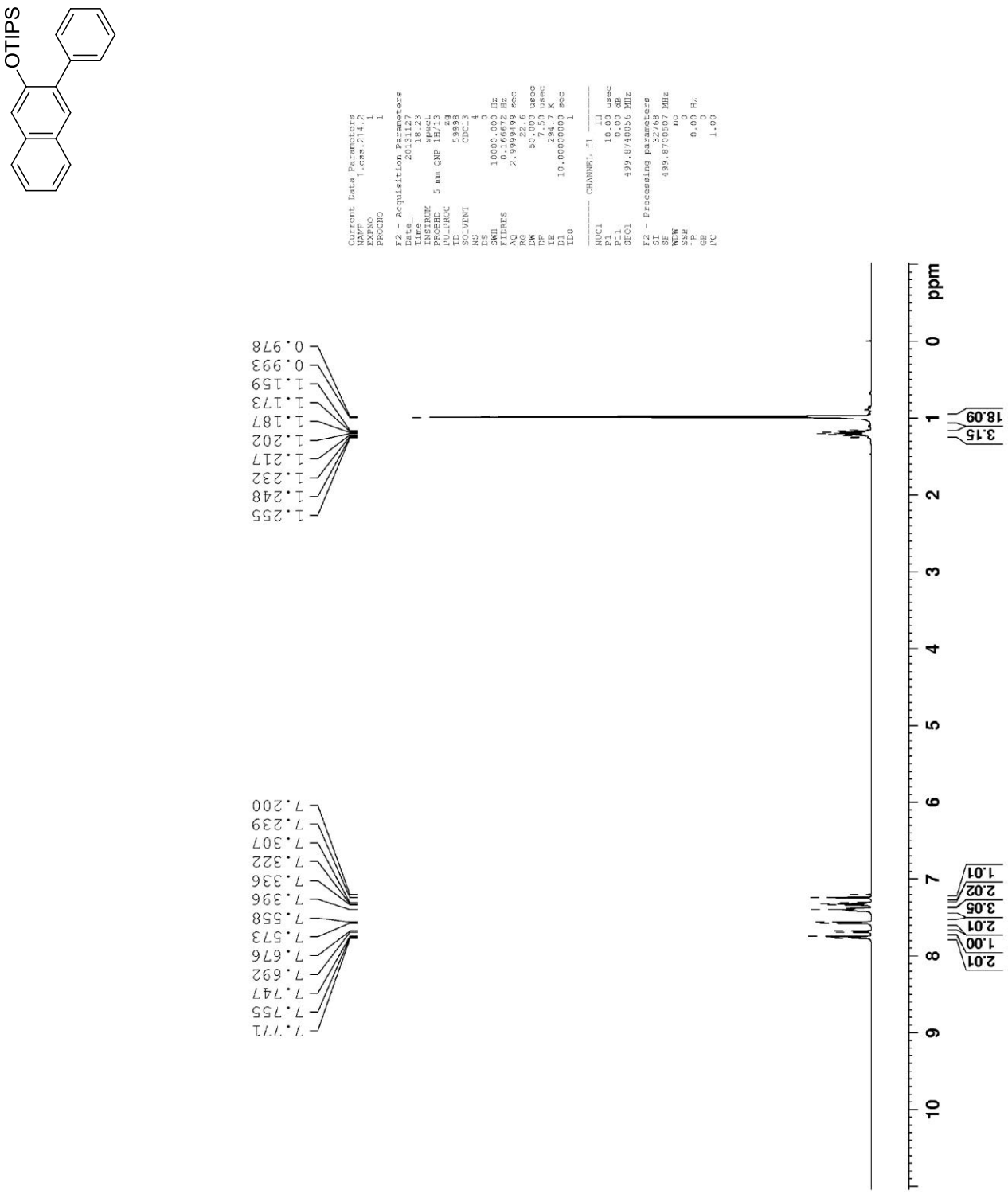

Figure 58: ^{1}H NMR Spectrum of 76 (500 MHz, $CDCl_3$, 298K)

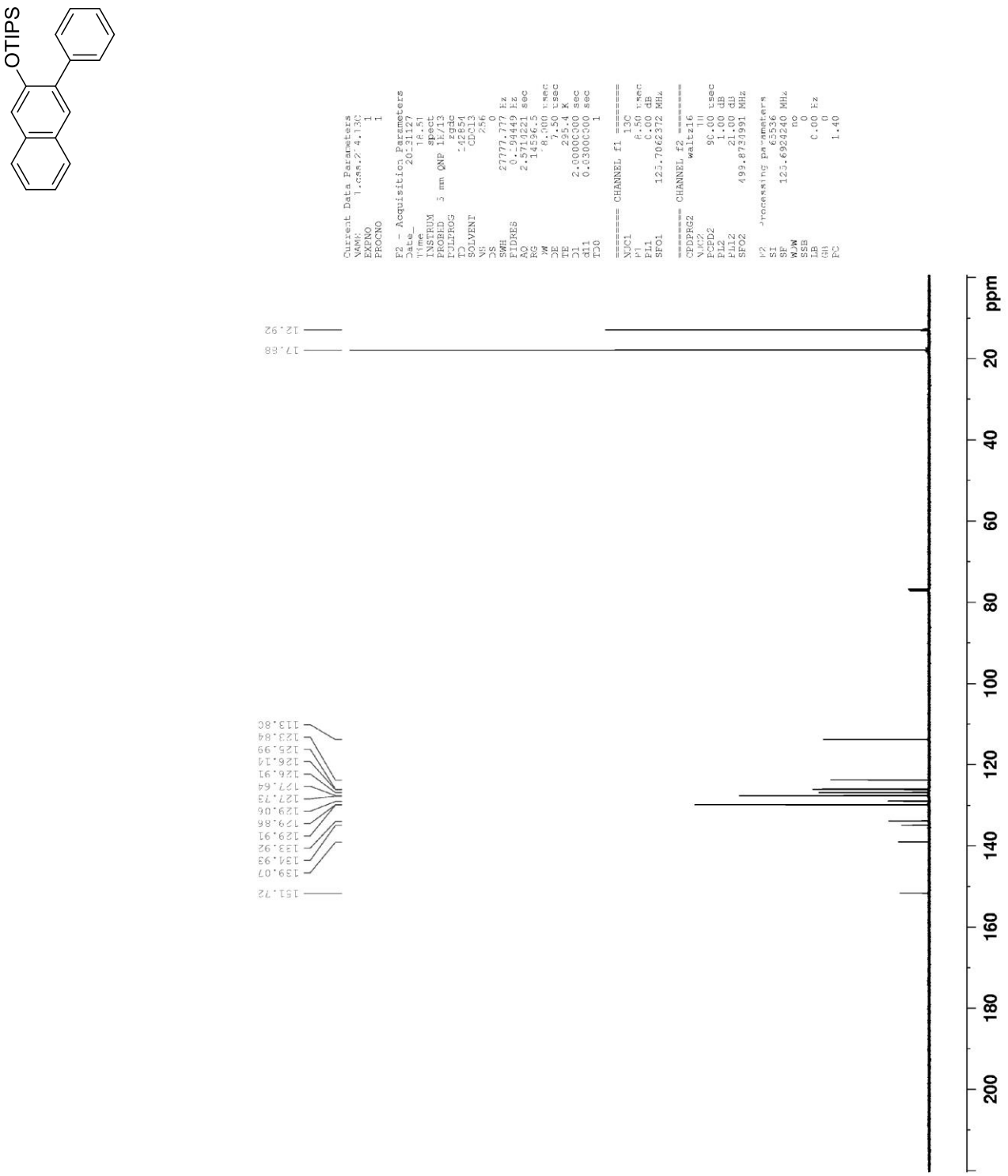

Figure 59: ^{13}C NMR Spectrum of 76 (125 MHz, $CDCl_3$, 298K)

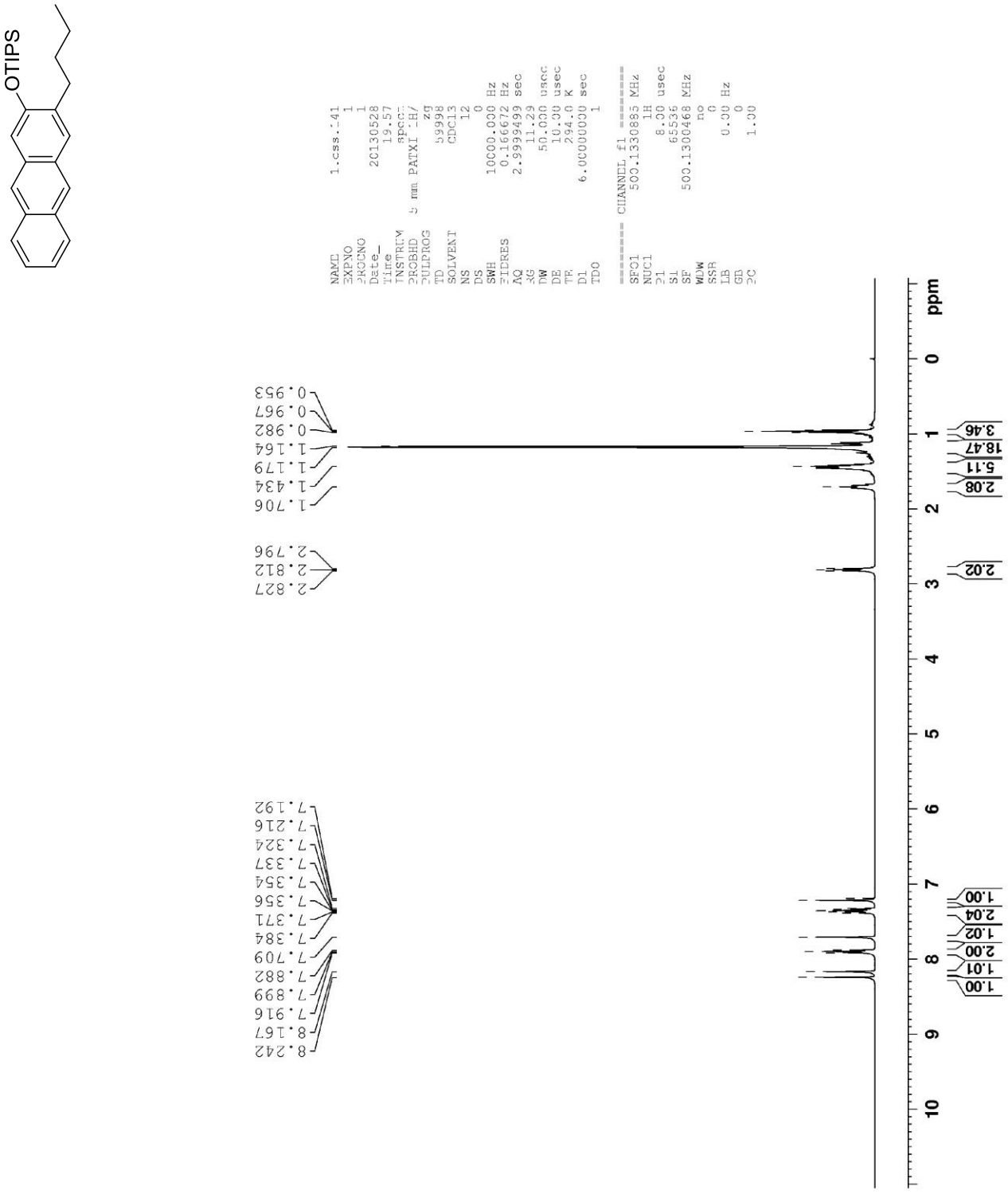

Figure 60: ^{1}H NMR Spectrum of 77 (500 MHz, $CDCl_3$, 298K)

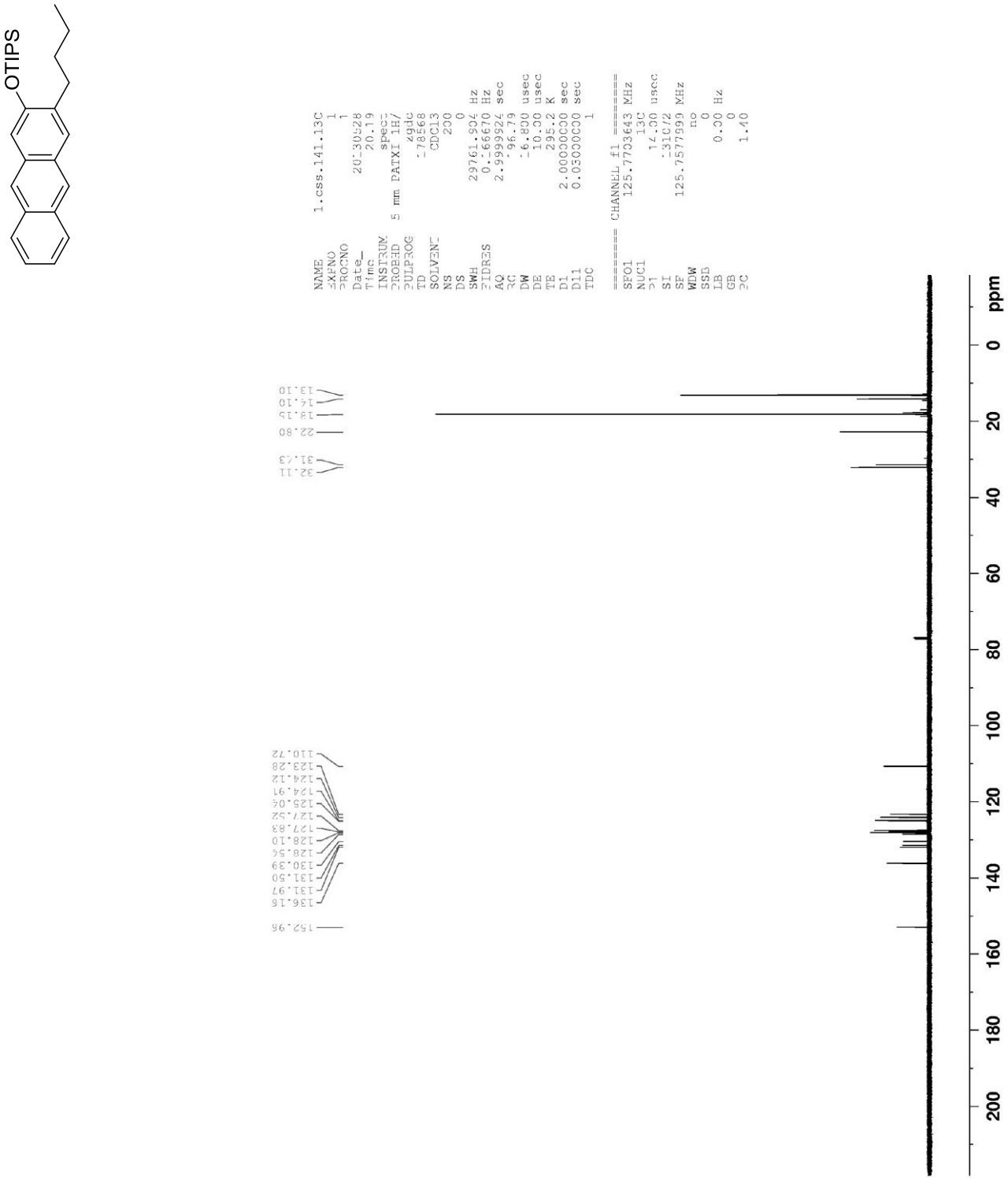

Figure 61: ^{13}C NMR Spectrum of 77 (125 MHz, $CDCl_3$, 298K)

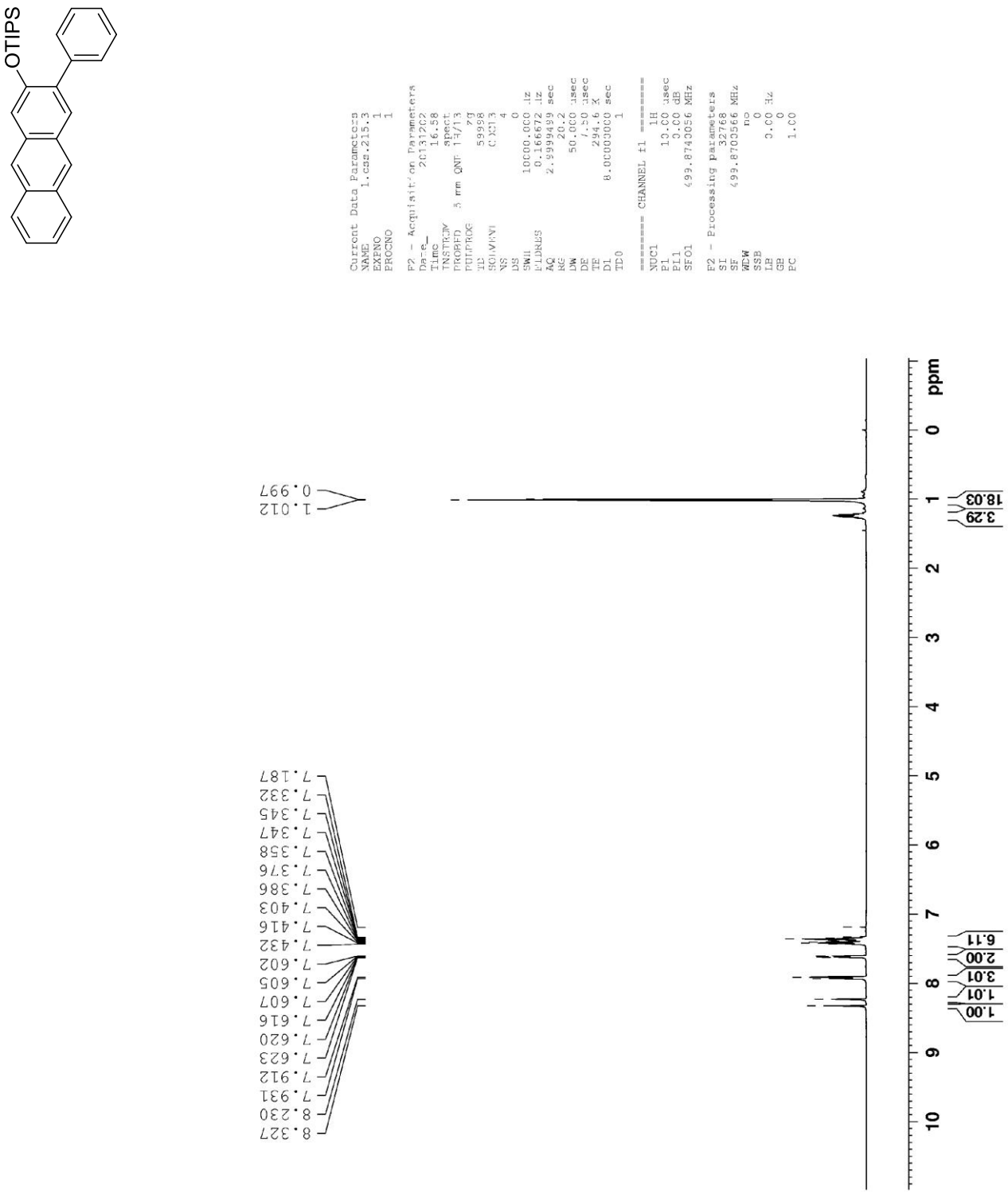

Figure 62: ^{1}H NMR Spectrum of 78 (500 MHz, $CDCl_3$, 298K)

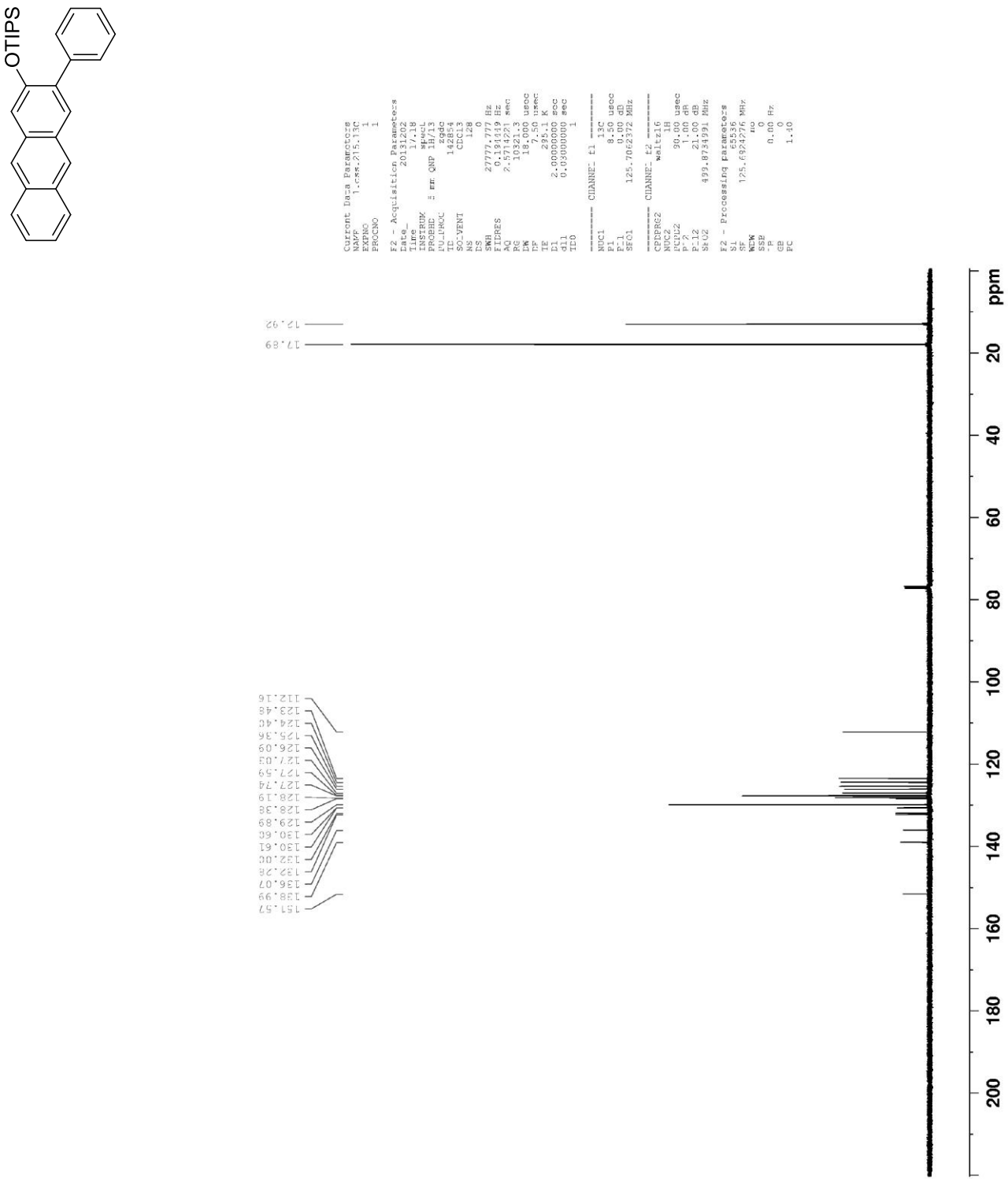

Figure 63: ^{13}C NMR Spectrum of 78 (125 MHz, $CDCl_3$, 298K)

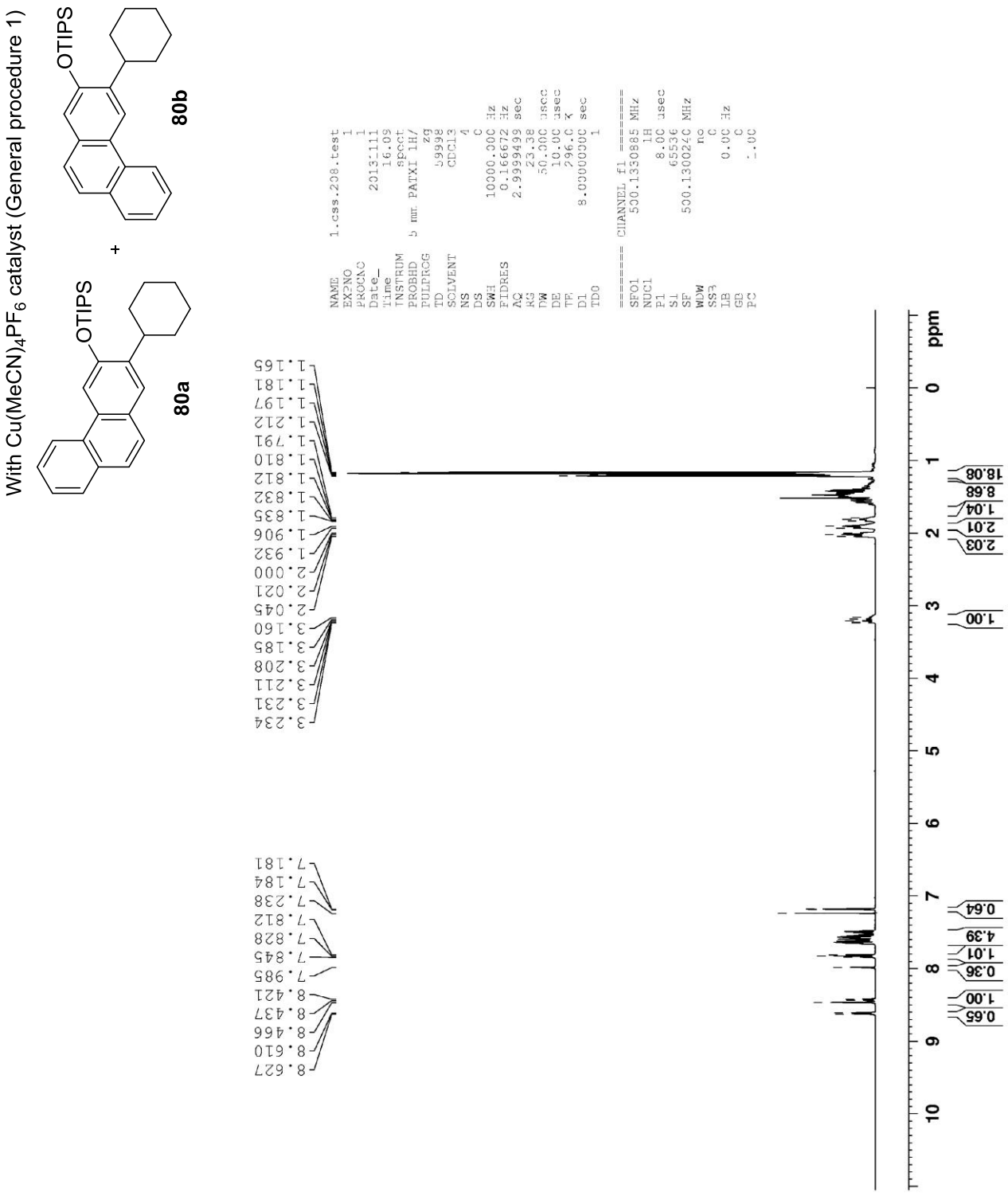

Figure 64: ^{1}H NMR Spectrum of 80a+80b (500 MHz, $CDCl_3$, 298K)

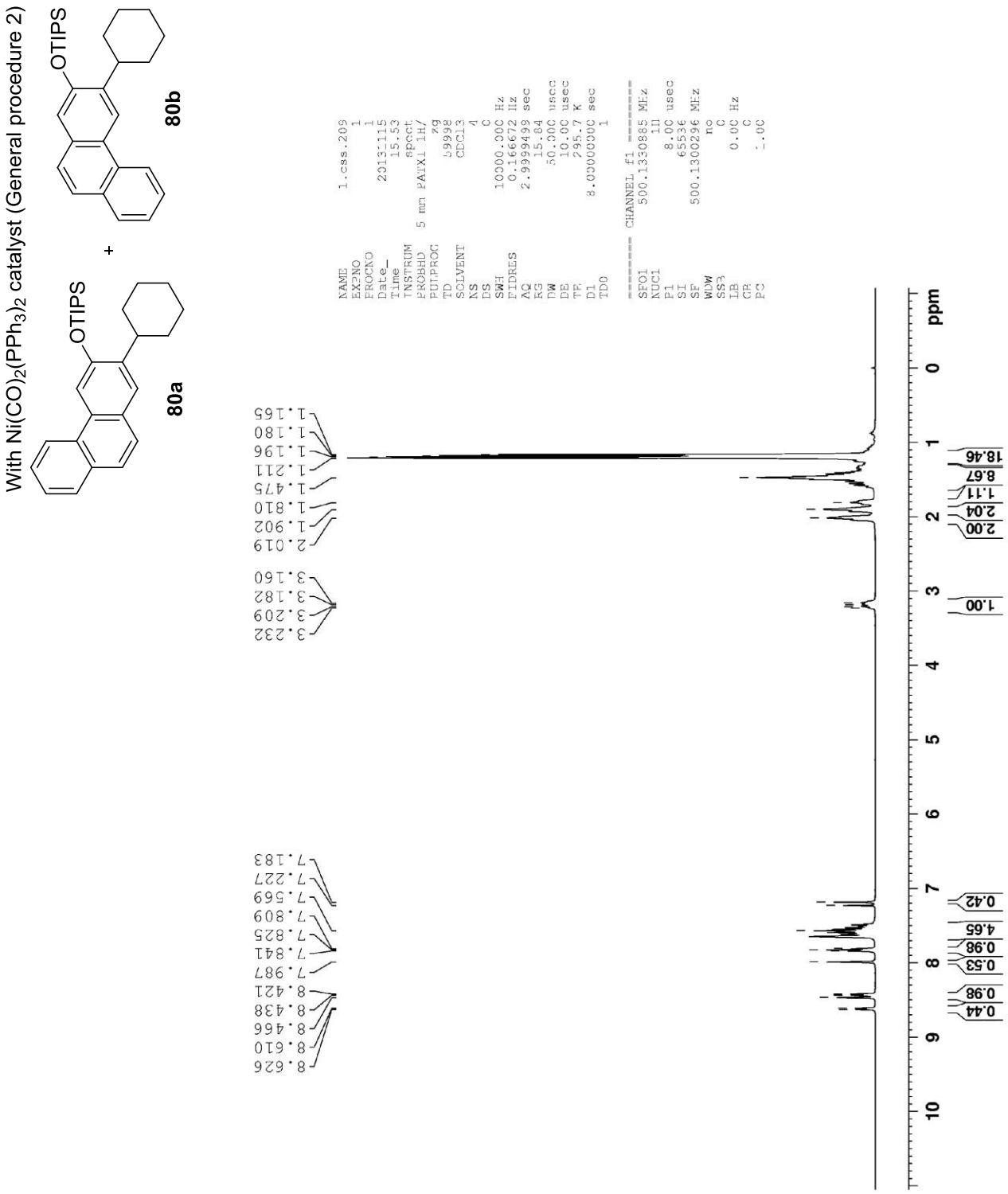

Figure 65: ^{1}H NMR Spectrum of 80a+80b (500 MHz, $CDCl_3$, 298K)

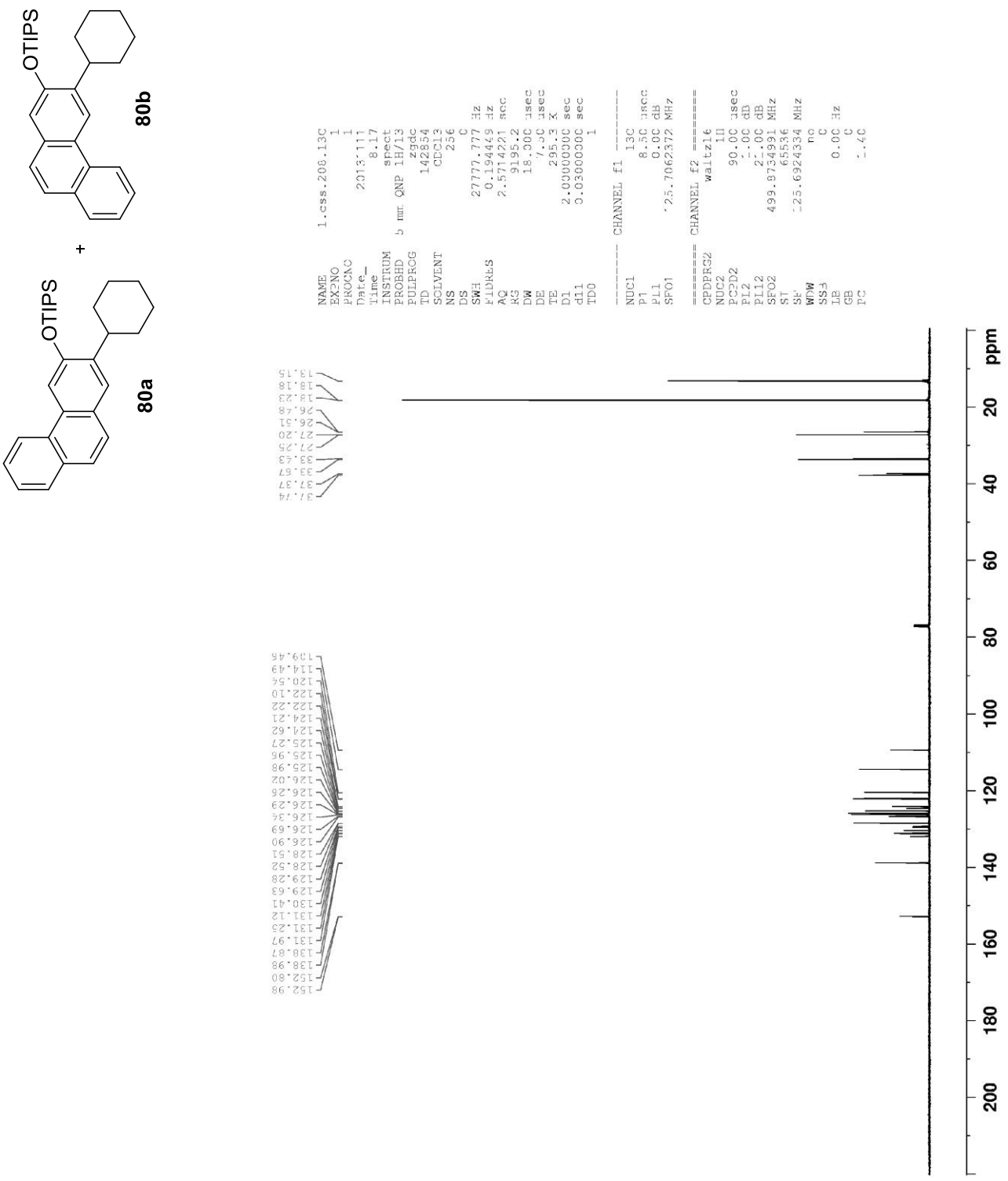

Figure 66: ^{13}C NMR Spectrum of 80a+80b (125 MHz, $CDCl_3$, 298K)

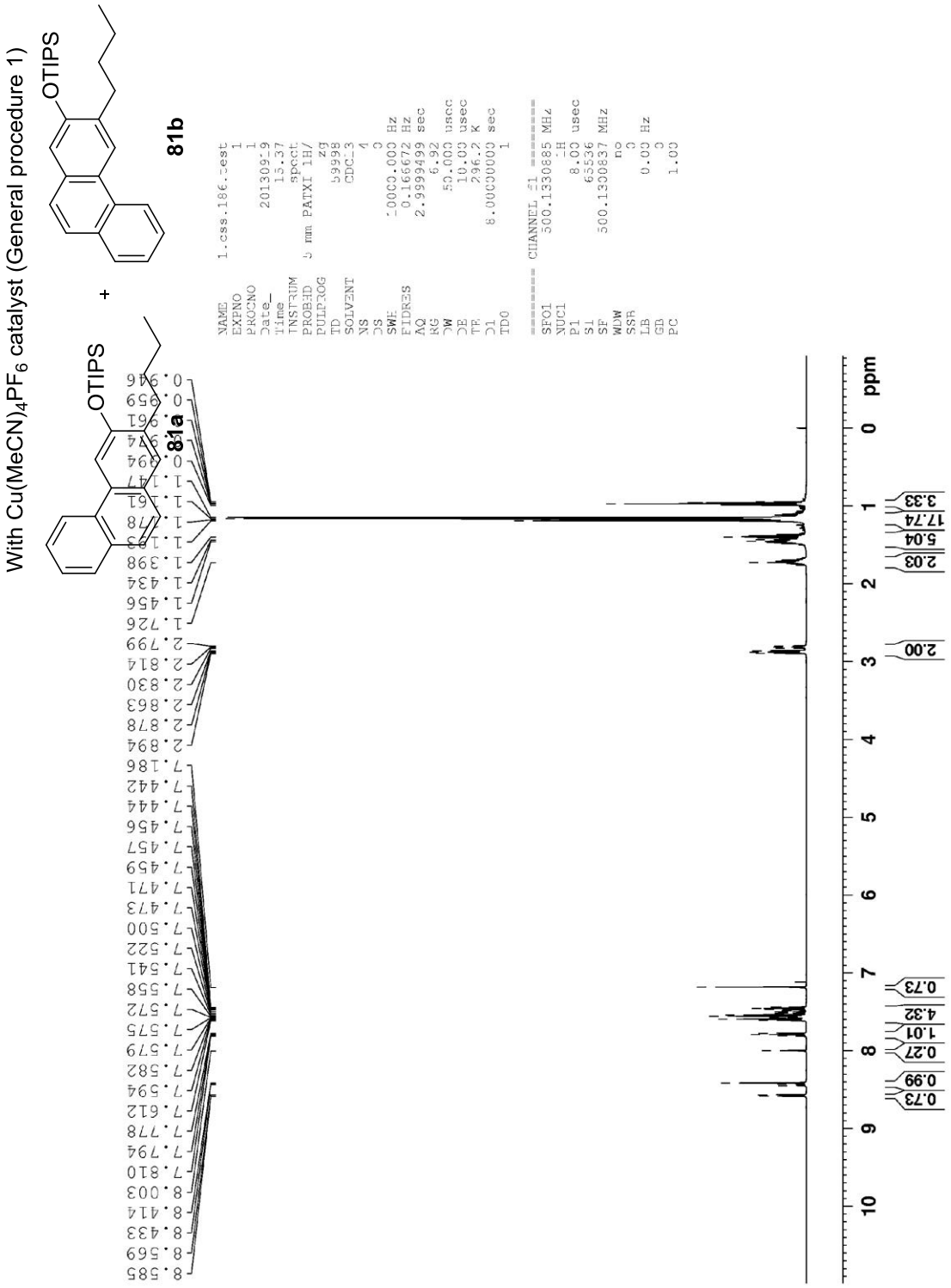

Figure 67: ^{1}H NMR Spectrum of 81a+81b (500 MHz, $CDCl_3$, 298K)

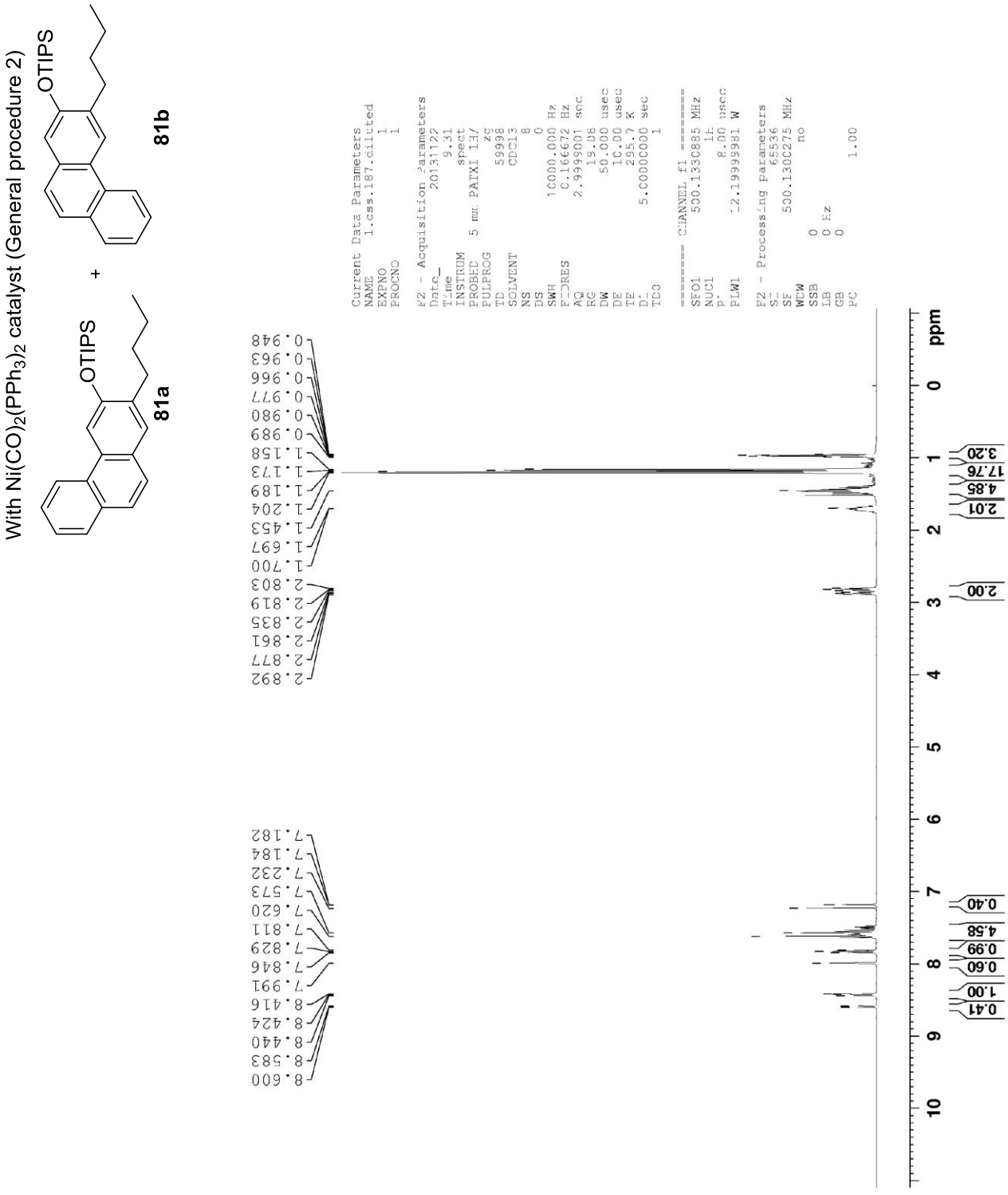

Figure 68: ^{1}H NMR Spectrum of 81a+81b (500 MHz, $CDCl_3$, 298K)

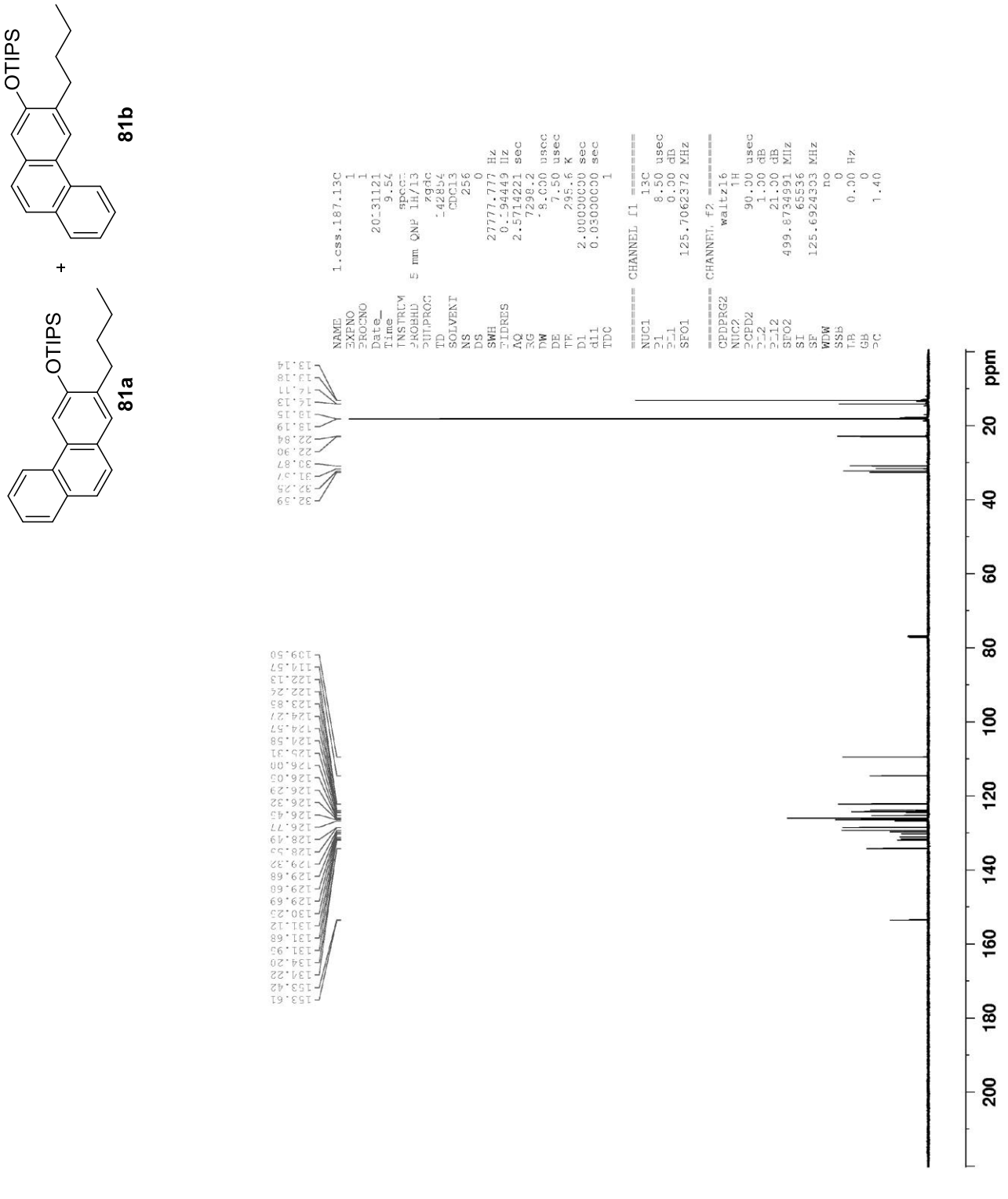

Figure 69: ^{13}C NMR Spectrum of 81a+81b (125 MHz, $CDCl_3$, 298K)

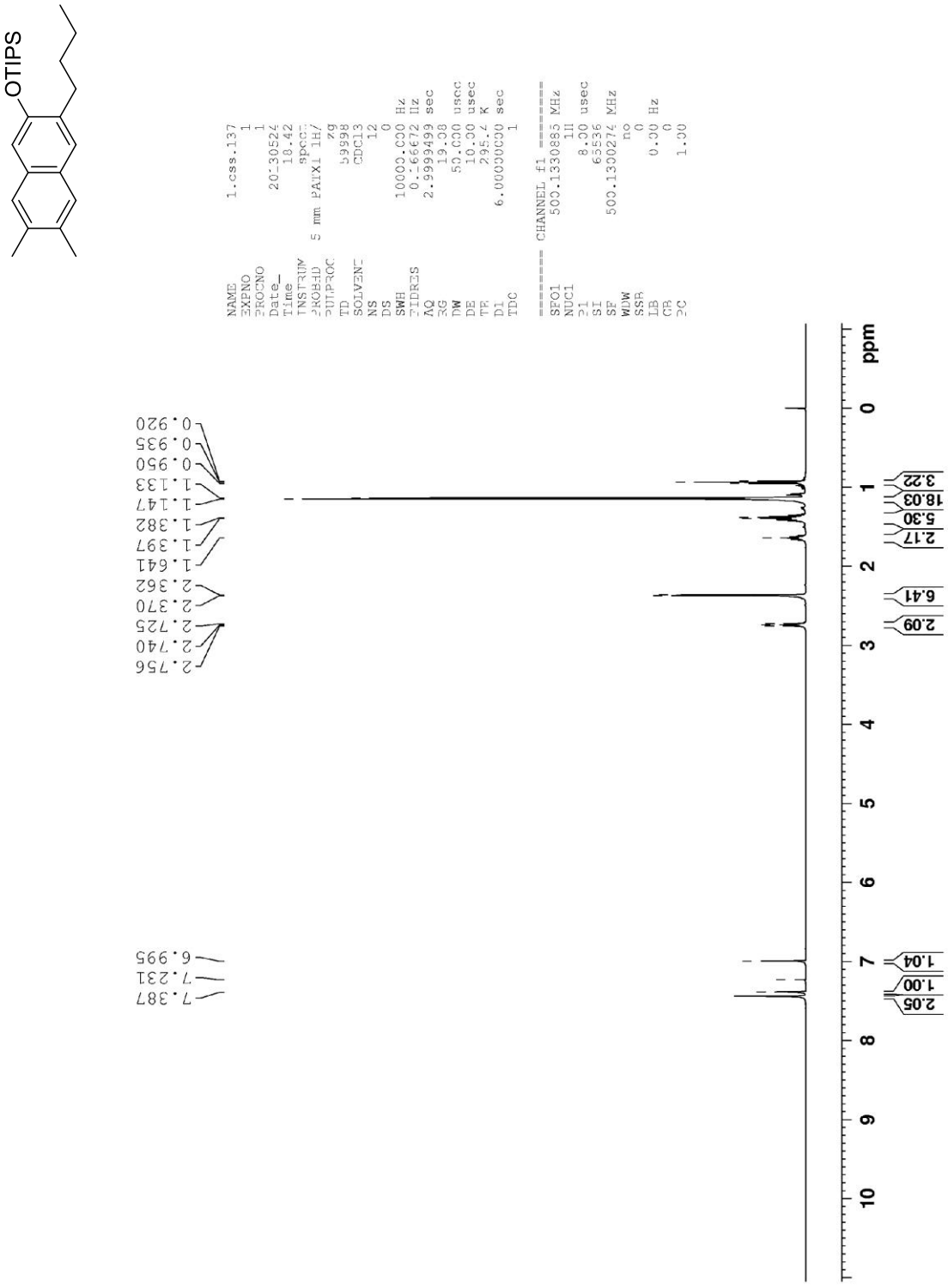

Figure 70: ^{1}H NMR Spectrum of 83 (500 MHz, $CDCl_3$, 298K)

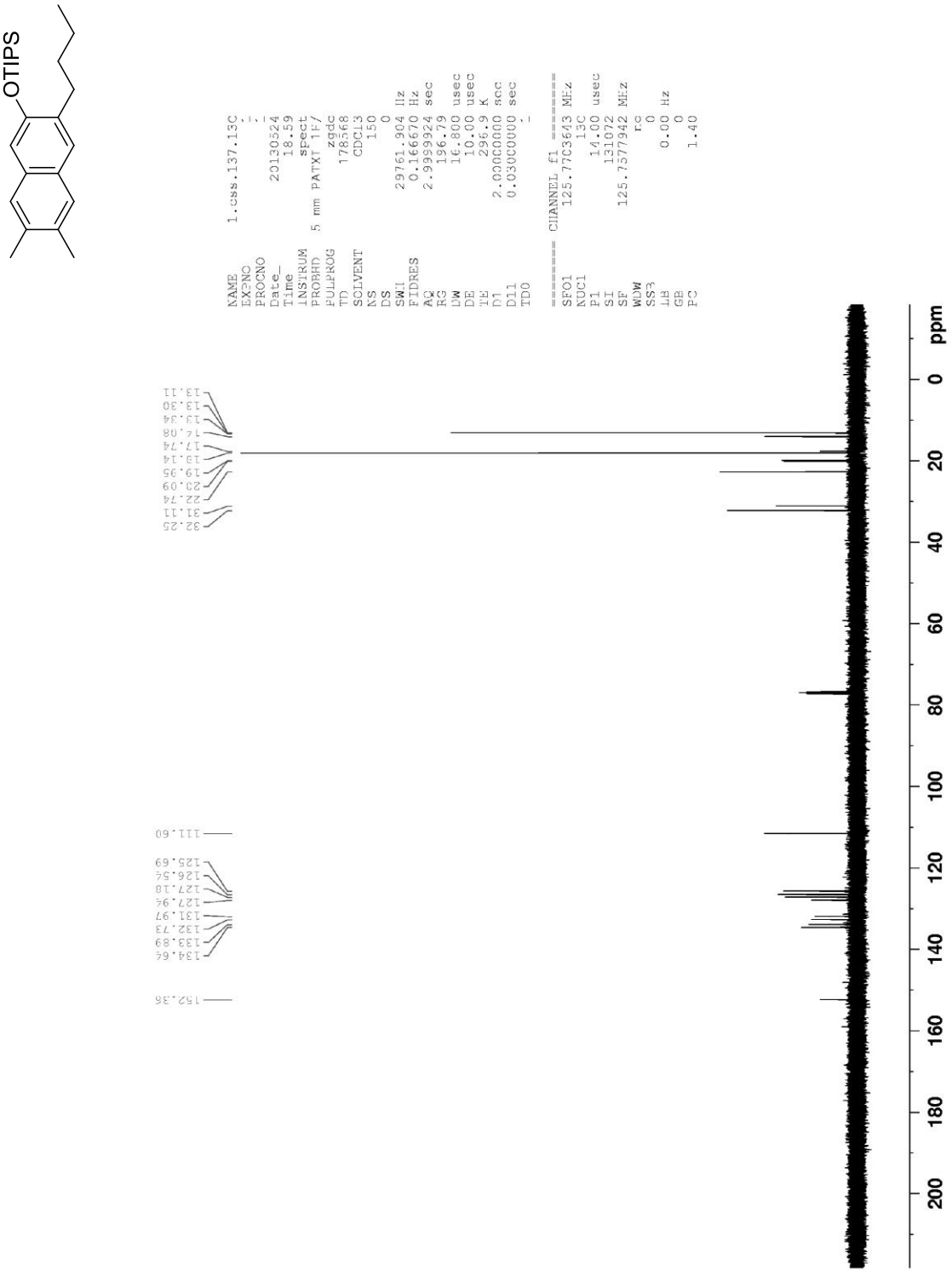

Figure 71: ^{13}C NMR Spectrum of 83 (125 MHz, $CDCl_3$, 298K)

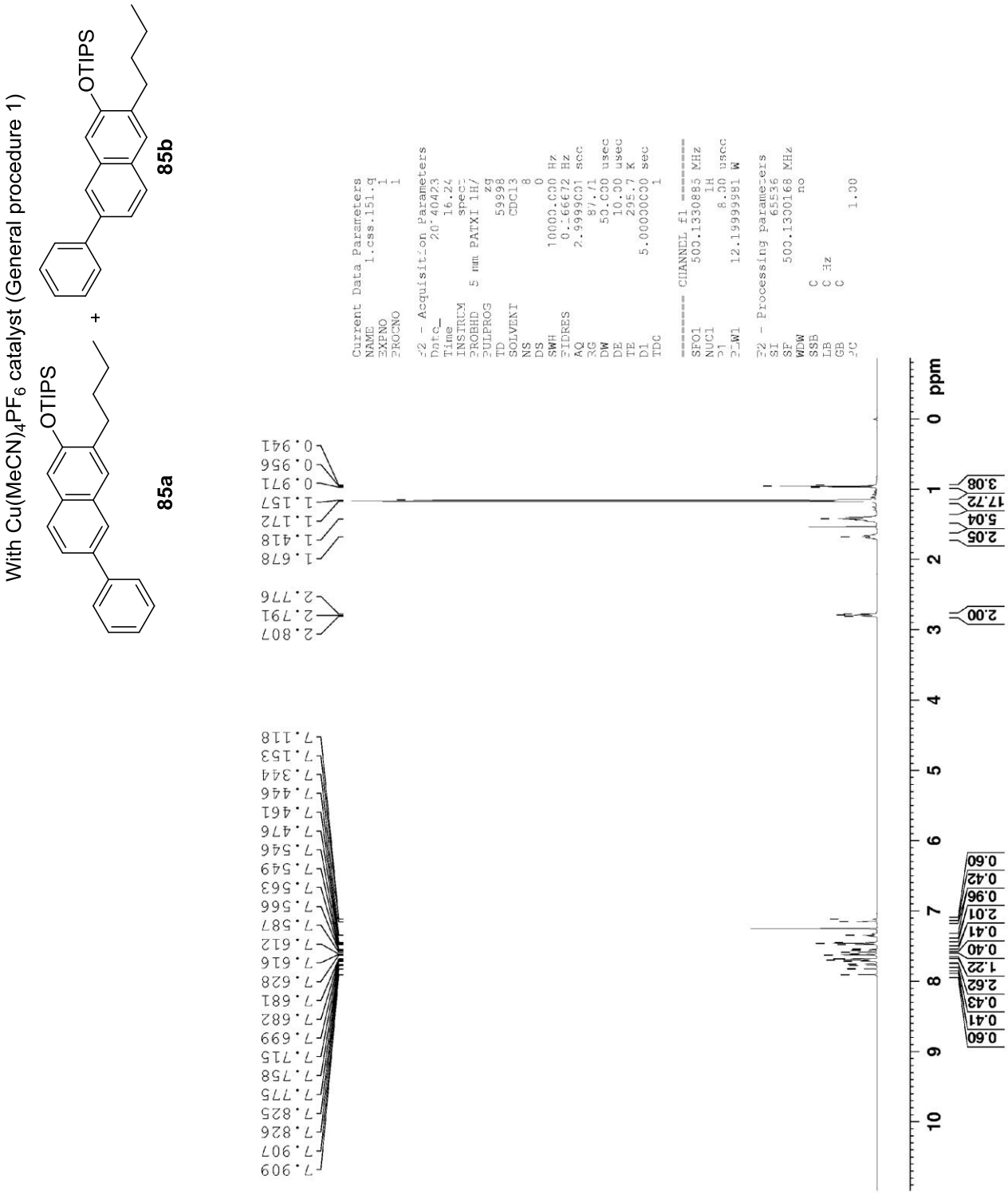

Figure 72: ^{1}H NMR Spectrum of 85a+85b (500 MHz, $CDCl_3$, 298K)

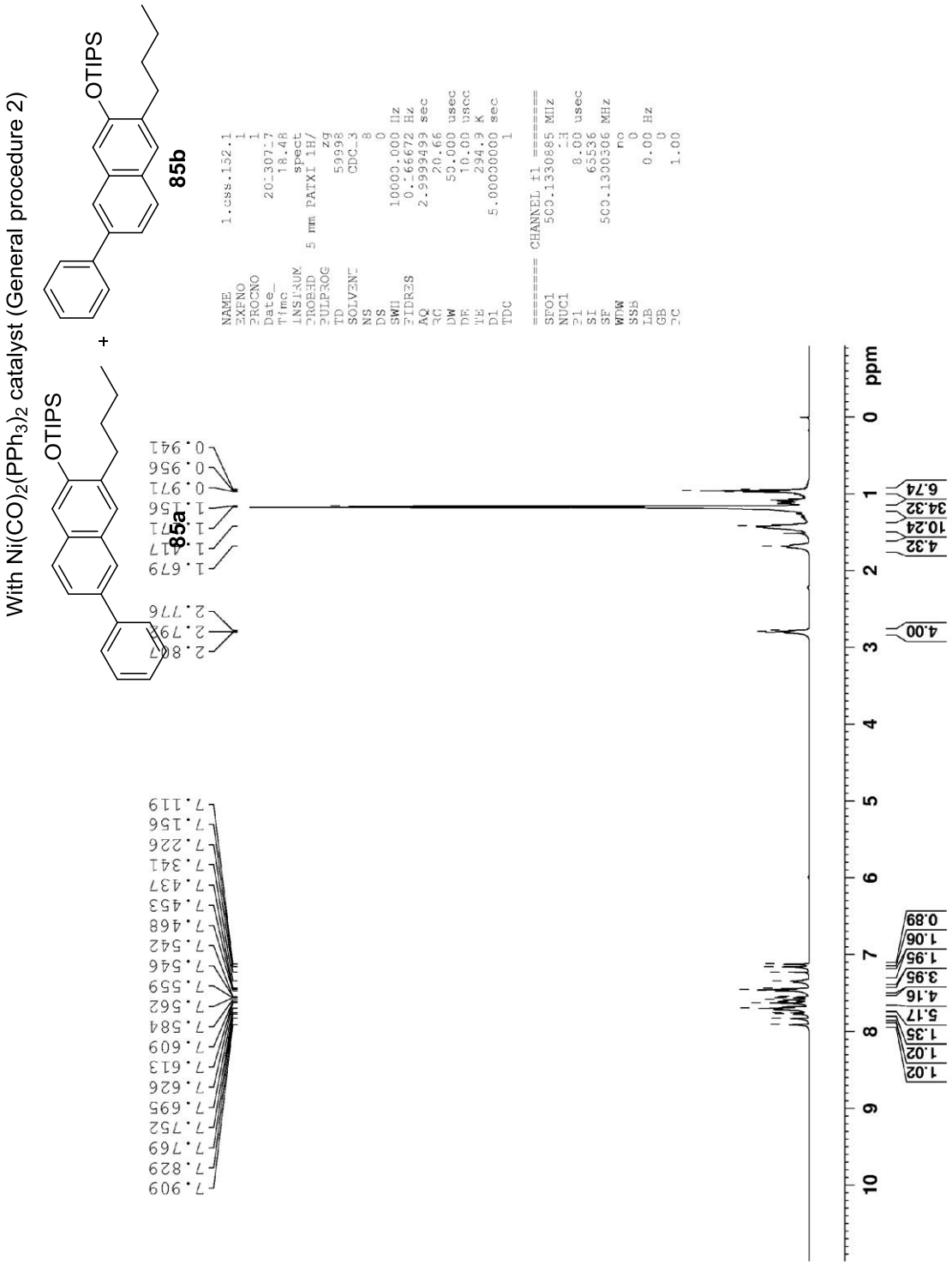

Figure 73: ^{1}H NMR Spectrum of 85a+85b (500 MHz, $CDCl_3$, 298K)

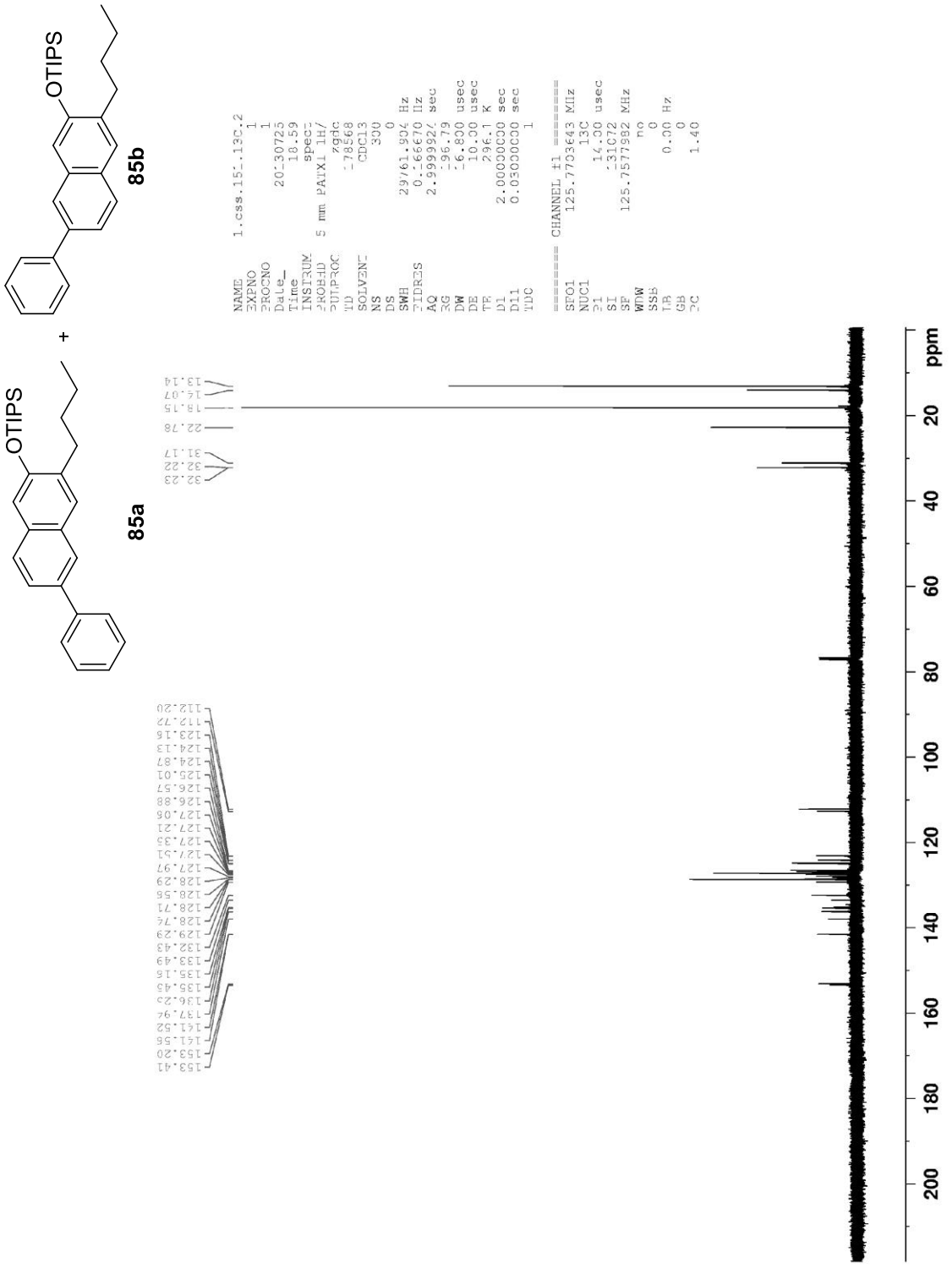

Figure 74: ^{13}C NMR Spectrum of 85a+85b (125 MHz, $CDCl_3$, 298K)

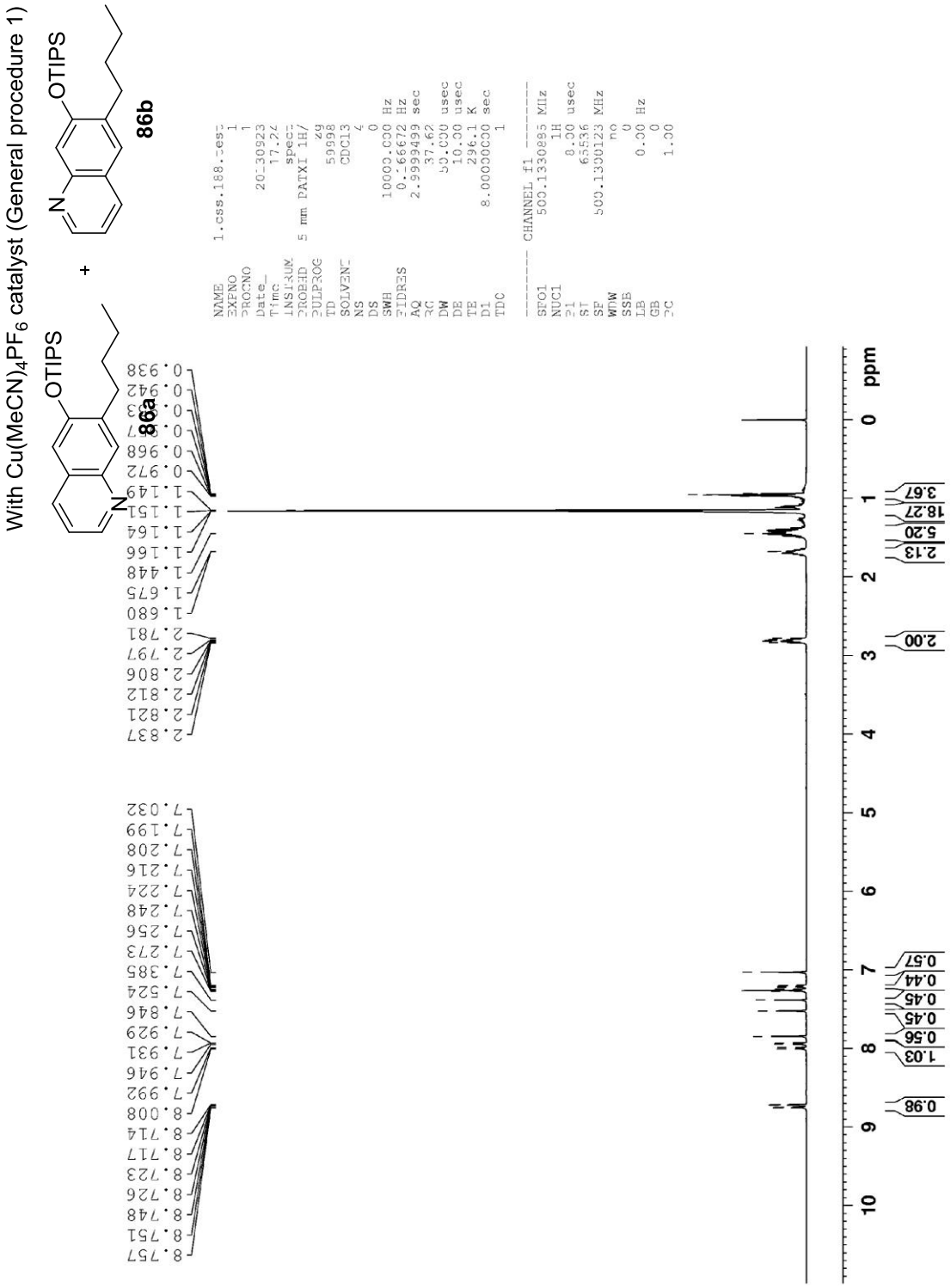

Figure 75: ^{1}H NMR Spectrum of 86a+86b (500 MHz, $CDCl_3$, 298K)

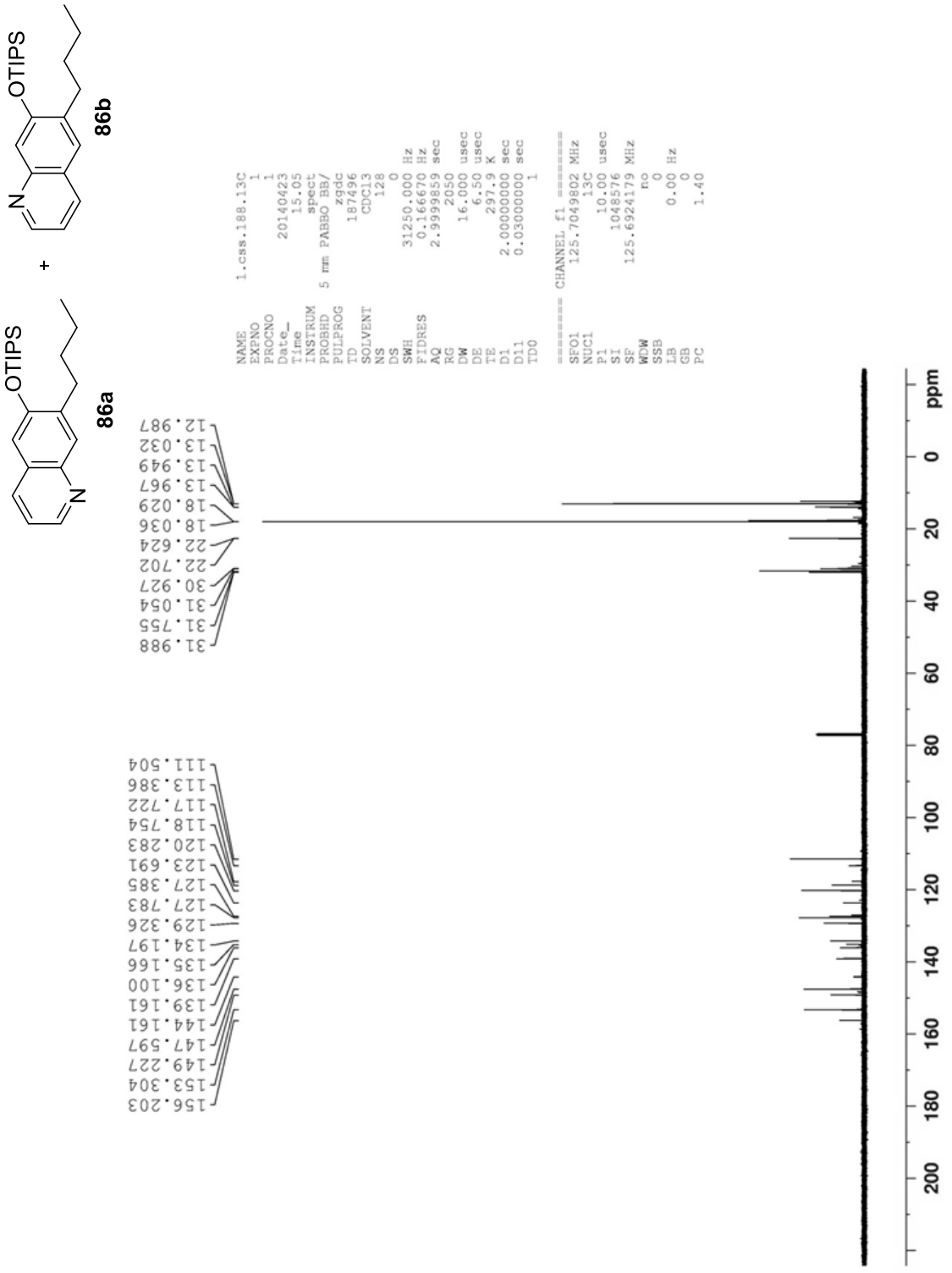

Figure 76: ^{13}C NMR Spectrum of 86a+86b (125 MHz, $CDCl_3$, 298K)

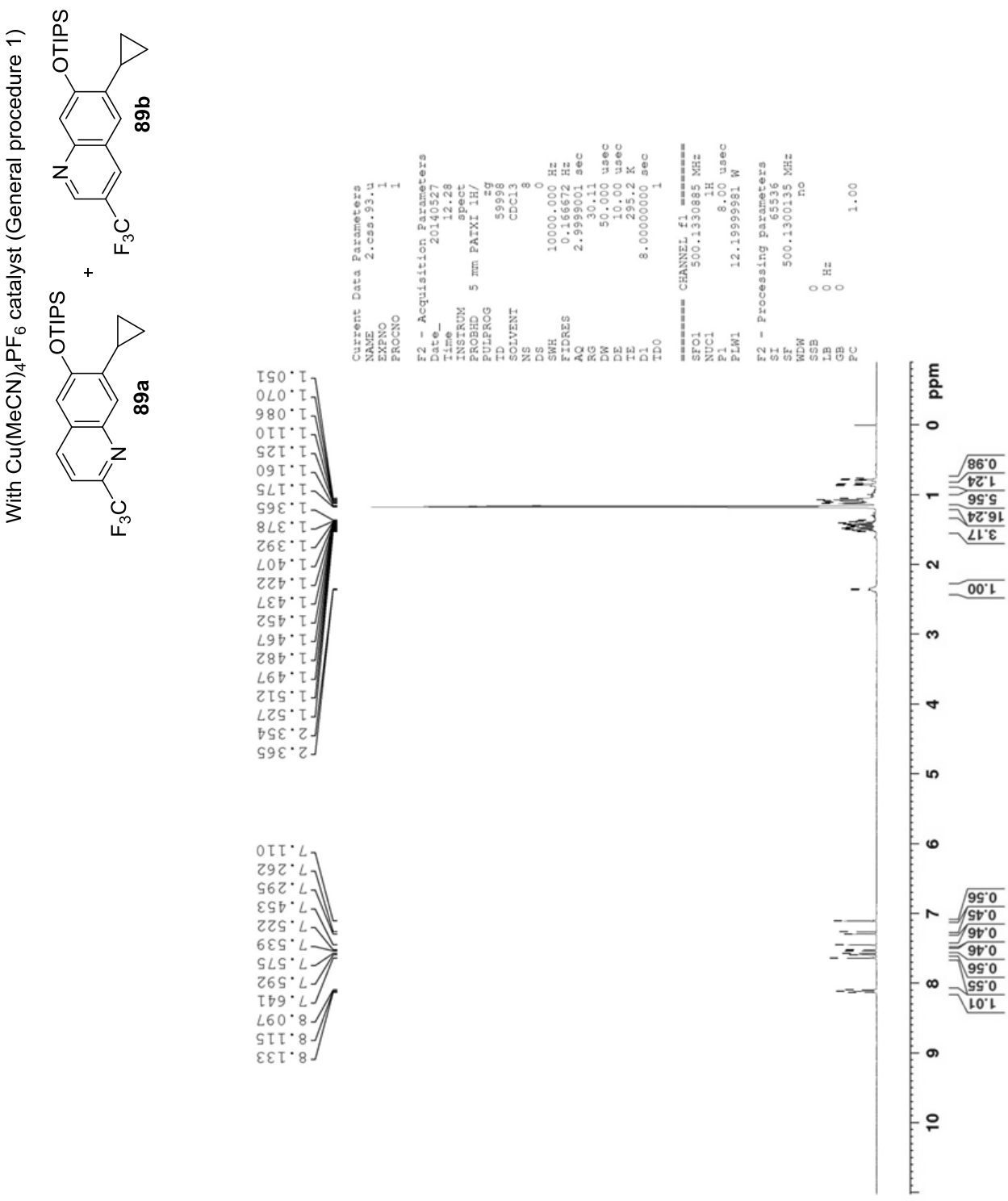

Figure 77: ^{1}H NMR Spectrum of 89a+89b (500 MHz, $CDCl_3$, 298K)

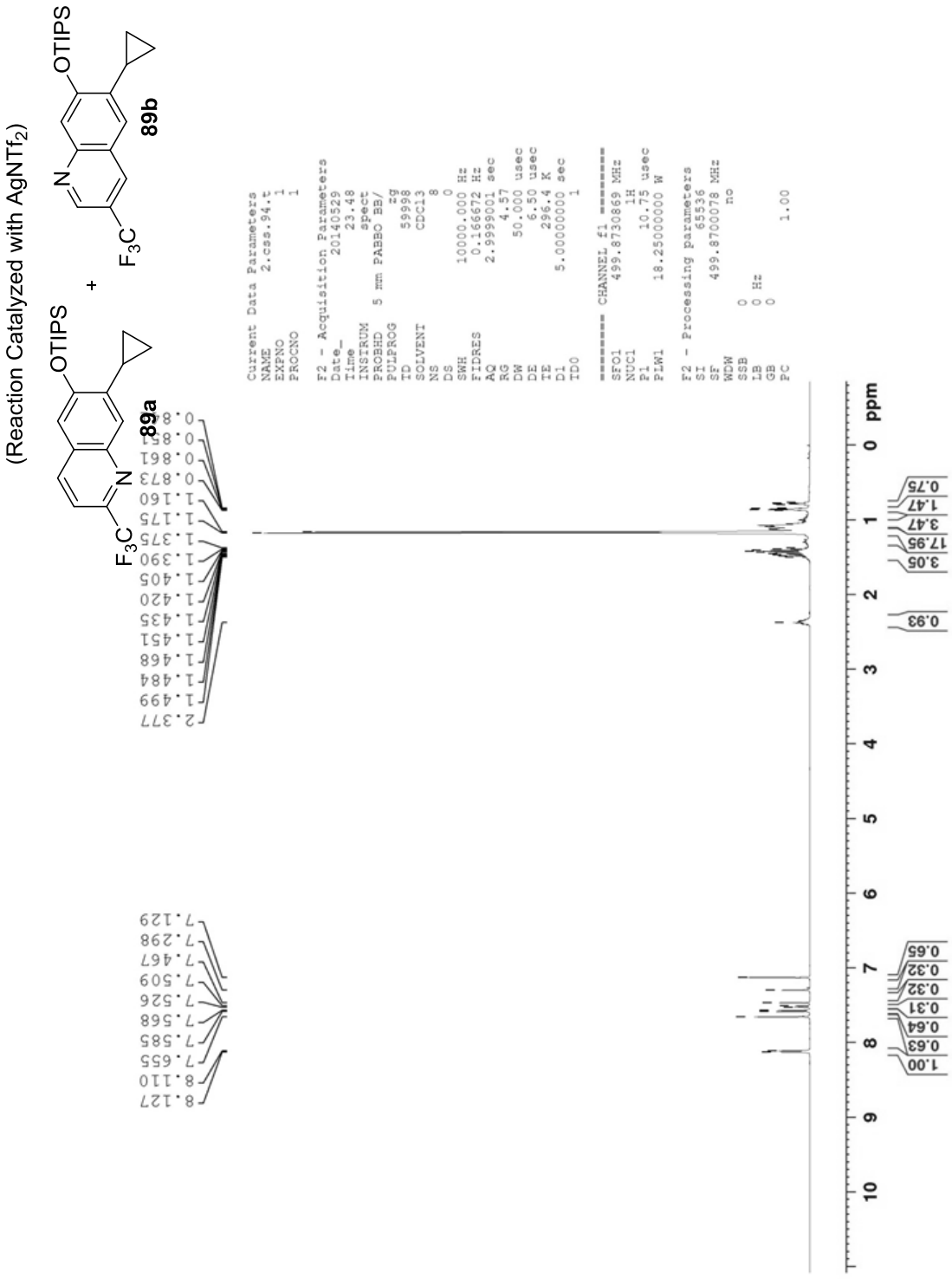

Figure 78: ^{1}H NMR Spectrum of 89a+89b (500 MHz, $CDCl_3$, 298K)

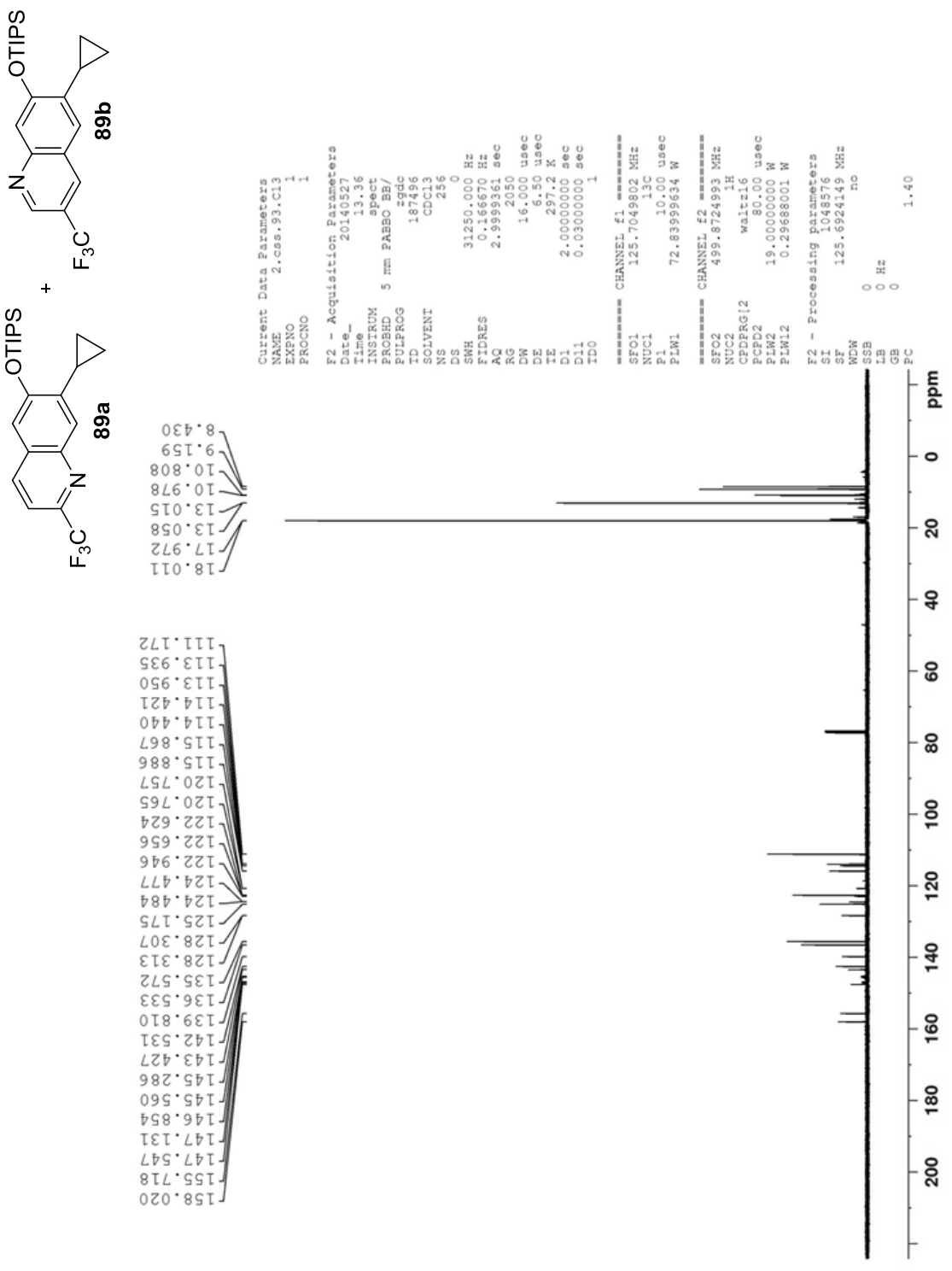

Figure 79: ^{13}C NMR Spectrum of 89a+89b (125 MHz, $CDCl_3$, 298K)

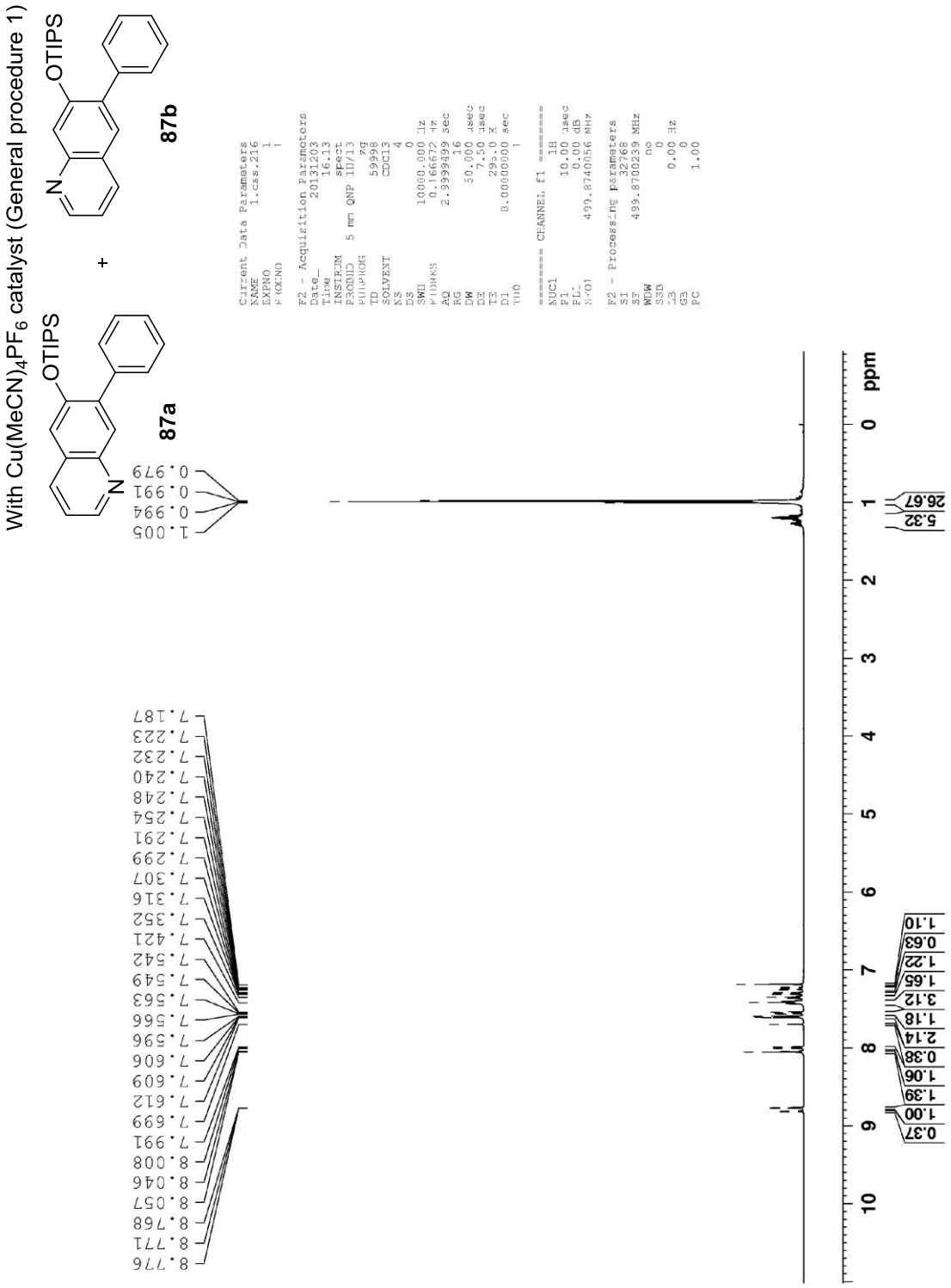

Figure 80: ^{1}H NMR Spectrum of 87a+87b (500 MHz, $CDCl_3$, 298K)

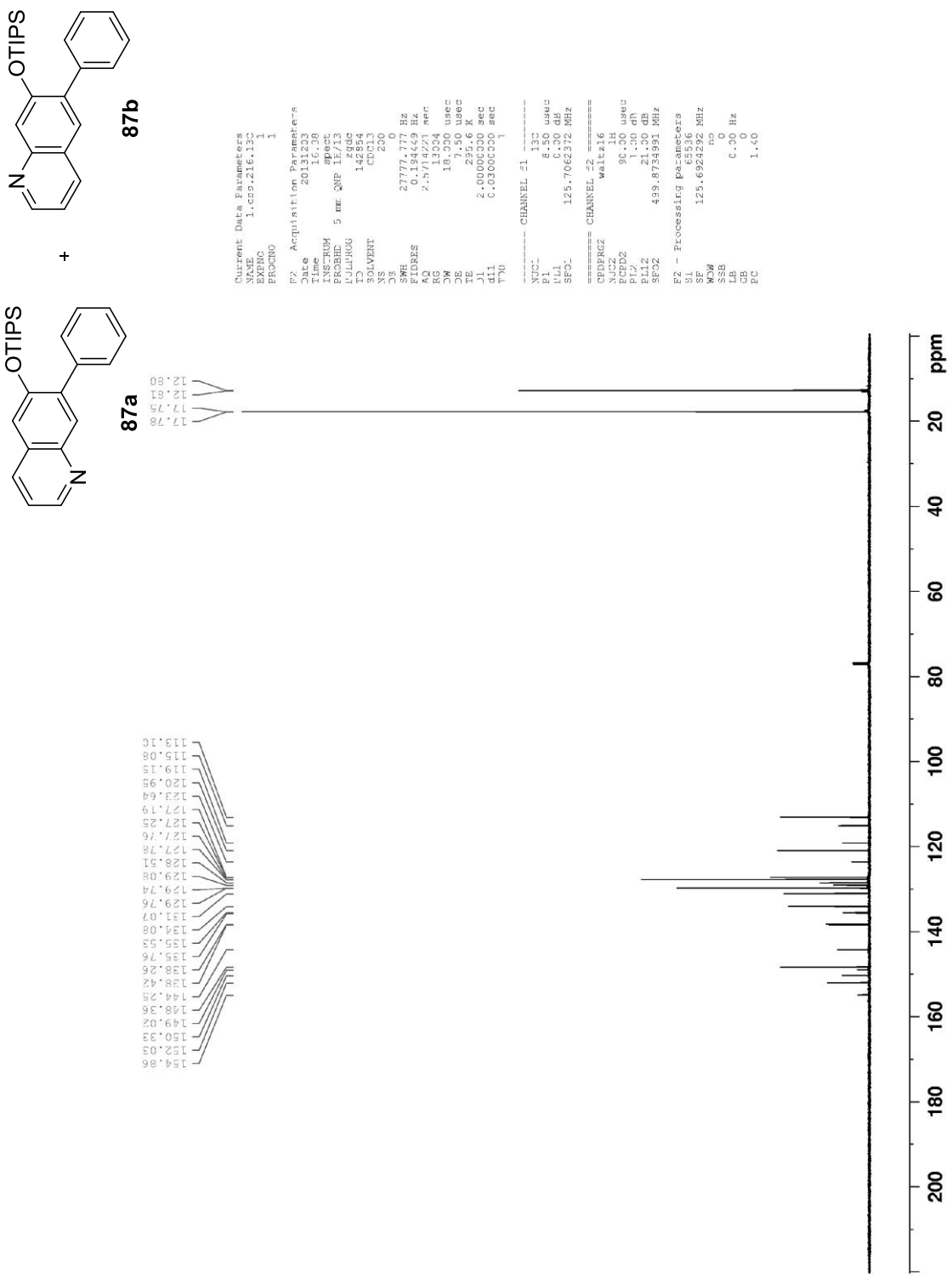

Figure 81: ^{13}C NMR Spectrum of 87a+87b (125 MHz, $CDCl_3$, 298K)

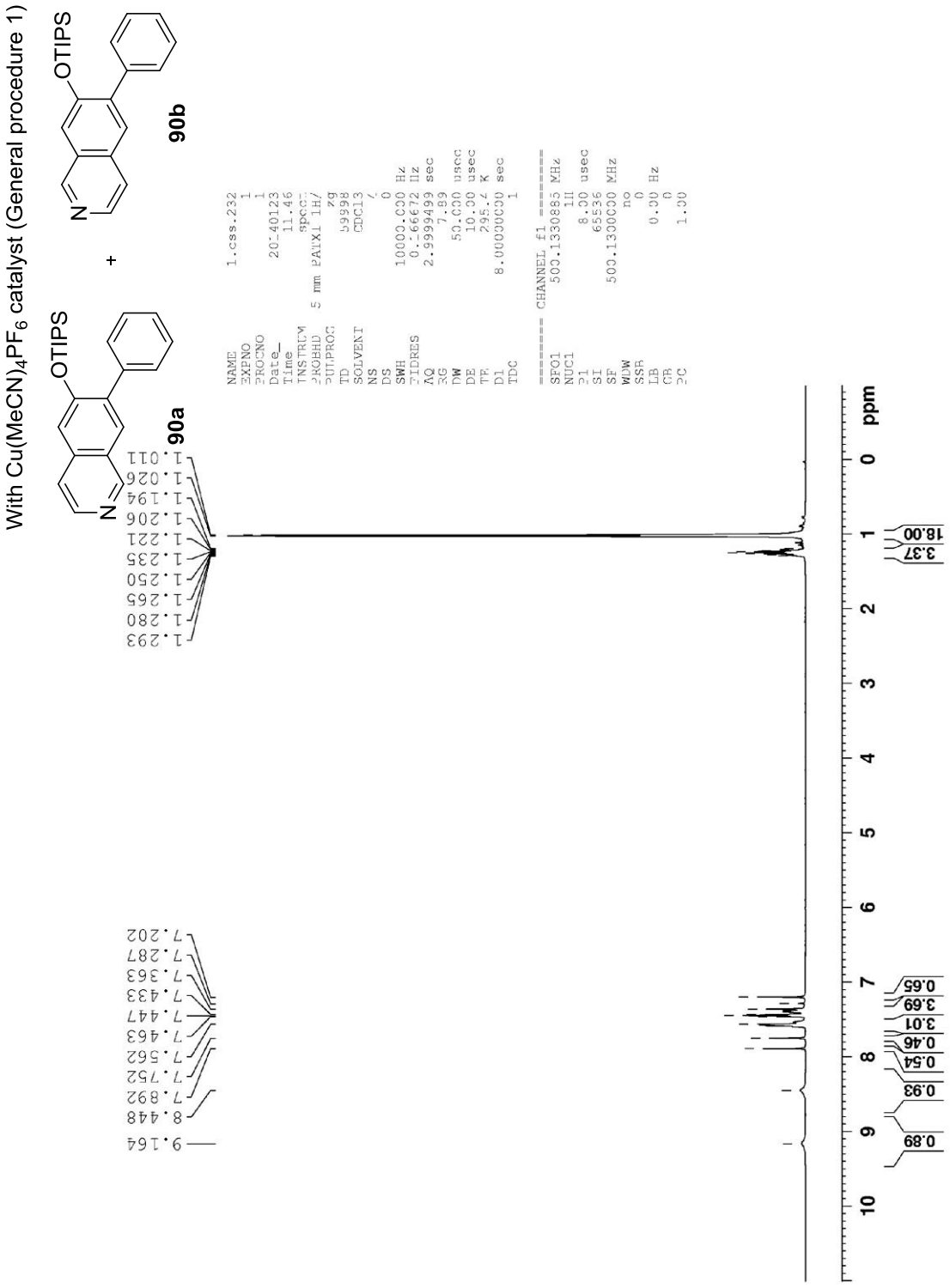

Figure 82: ^{1}H NMR Spectrum of 90a+90b (500 MHz, $CDCl_3$, 298K)

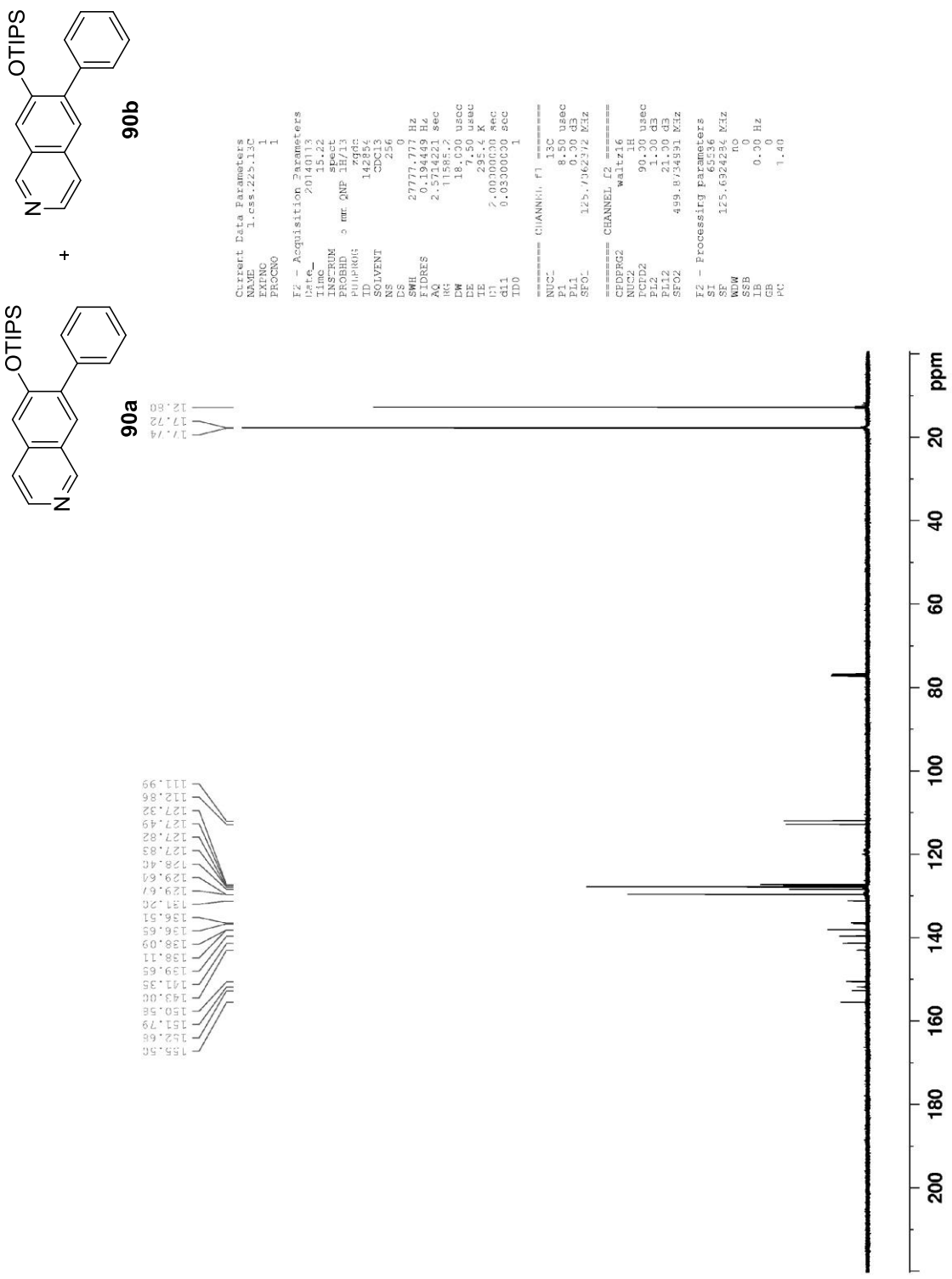

Figure 83: ^{13}C NMR Spectrum of 90a+90b (125 MHz, $CDCl_3$, 298K)

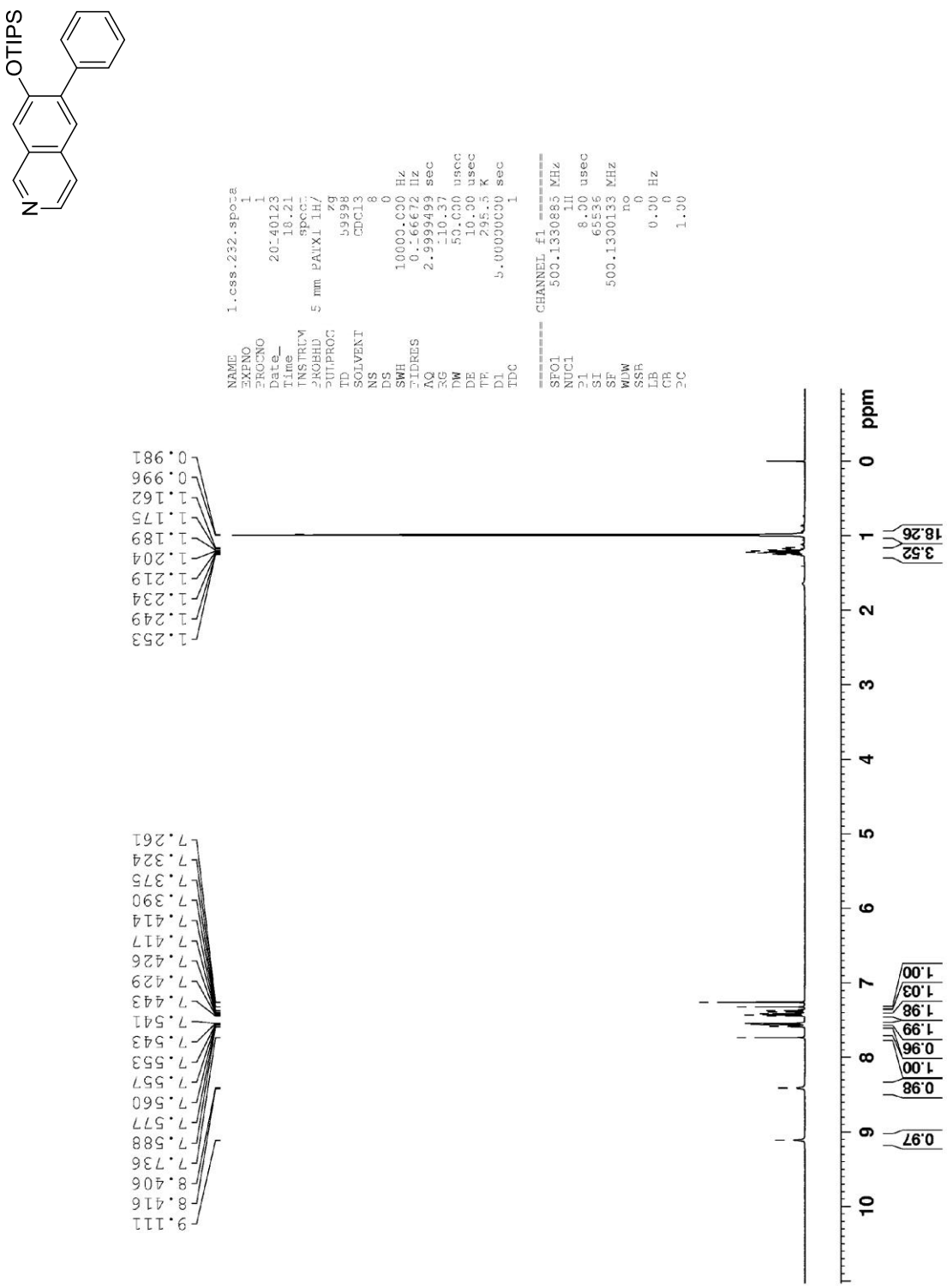

Figure 84: ^{1}H NMR Spectrum of 90b (500 MHz, $CDCl_3$, 298K)

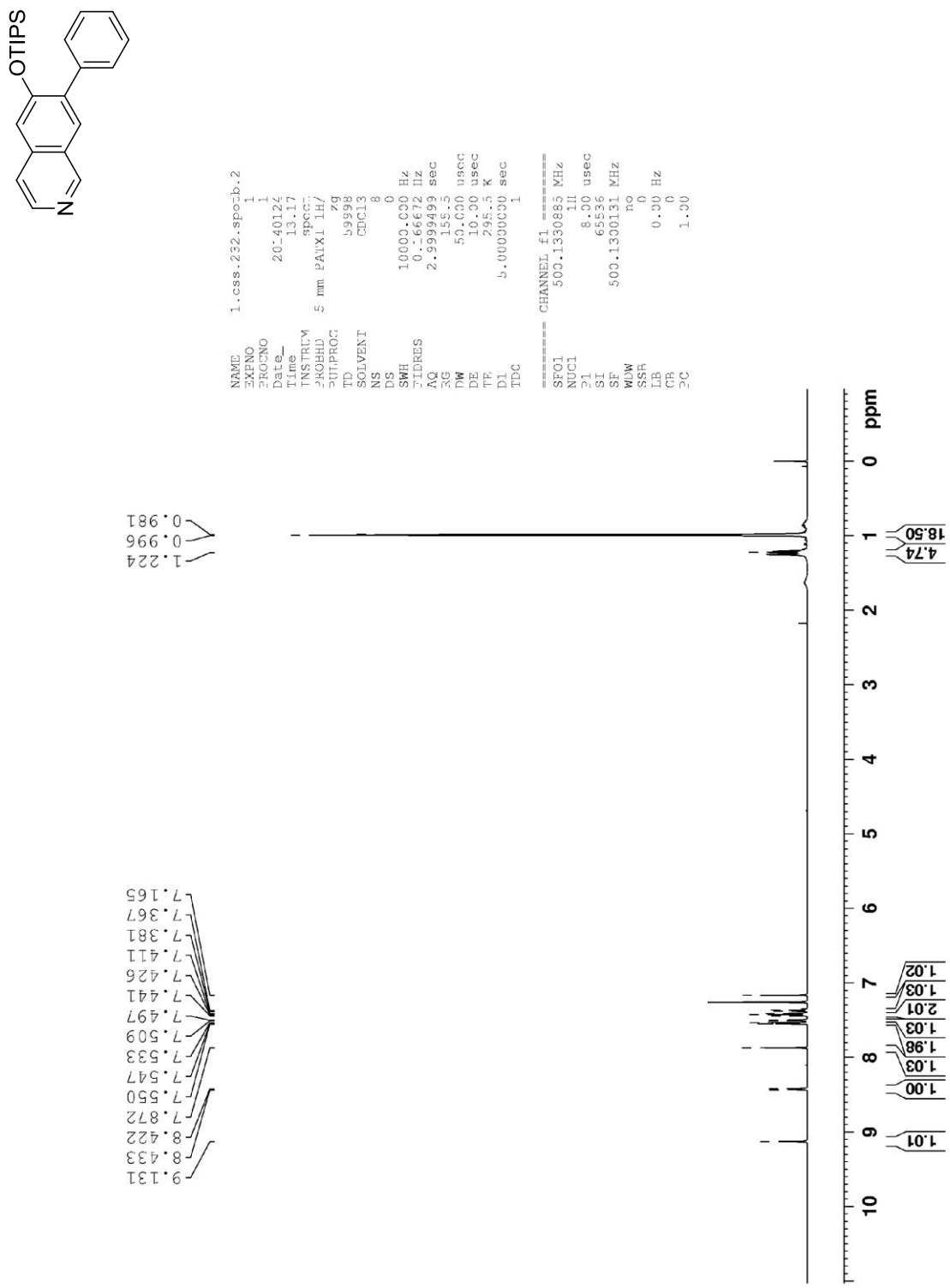

Figure 85: ^{1}H NMR Spectrum of 90a (500 MHz, $CDCl_3$, 298K)

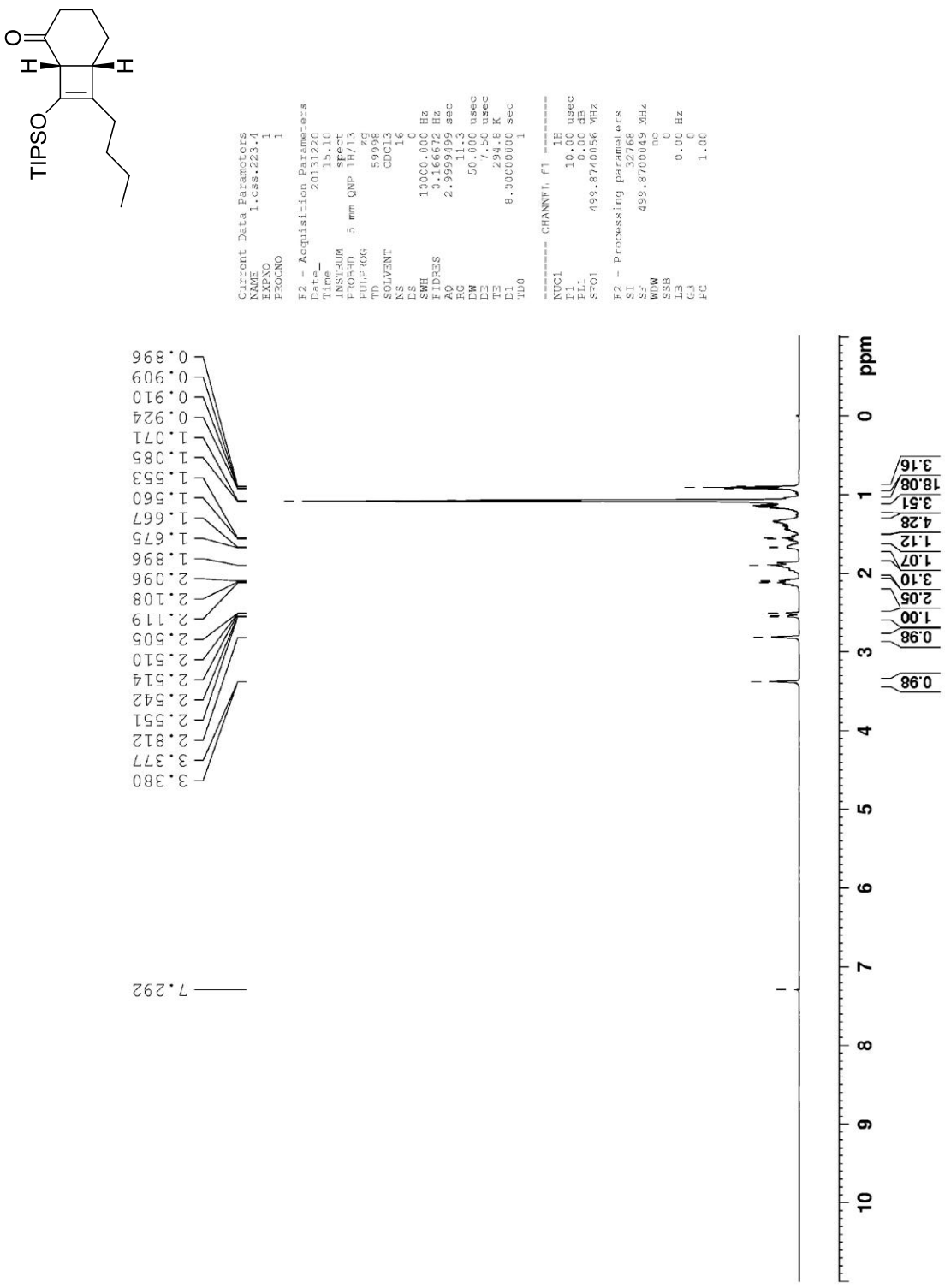

Figure 86: ^{1}H NMR Spectrum of 96 (500 MHz, $CDCl_3$, 298K)

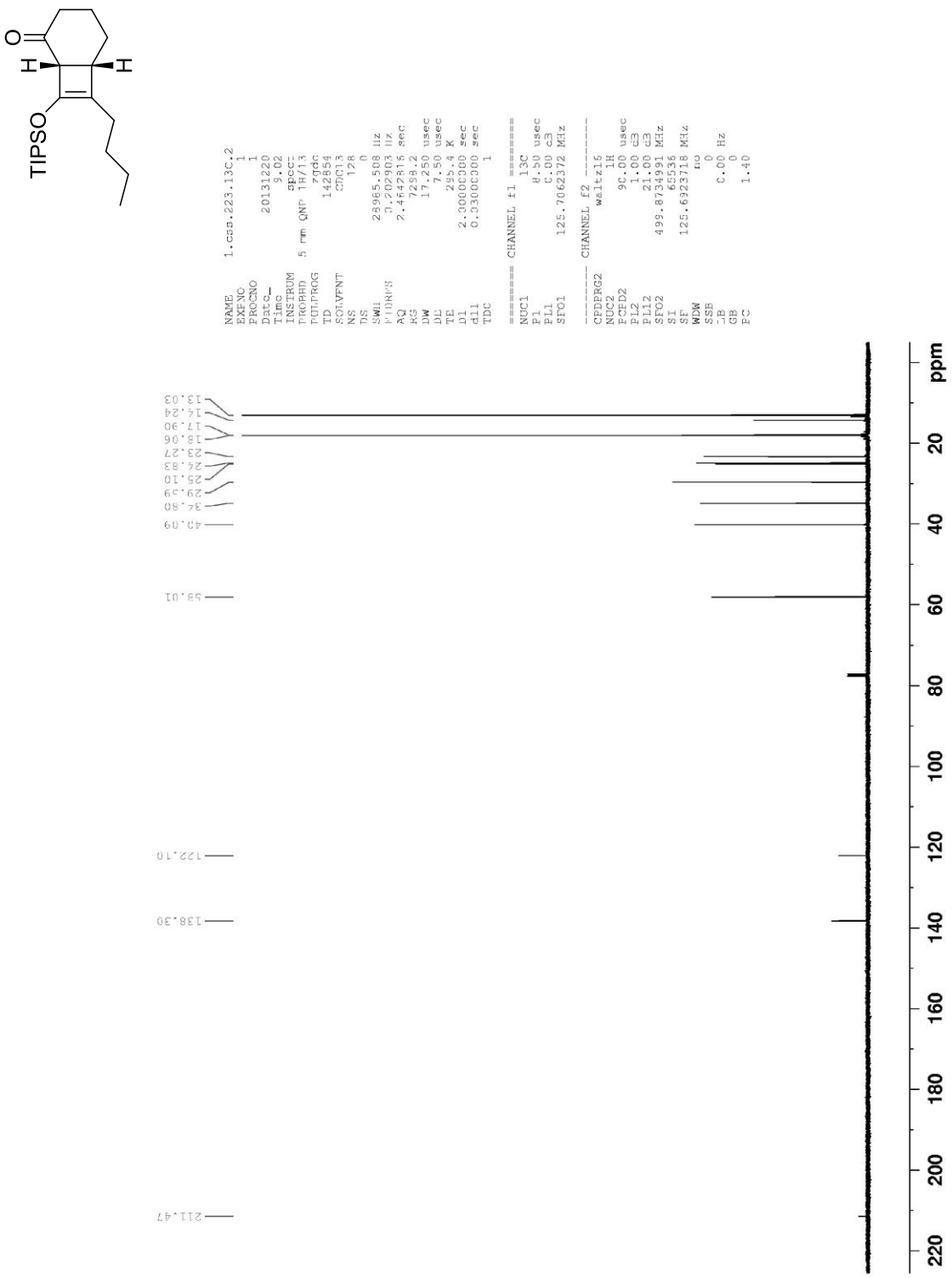

Figure 87: ^{13}C NMR Spectrum of 96 (125 MHz, $CDCl_3$, 298K)

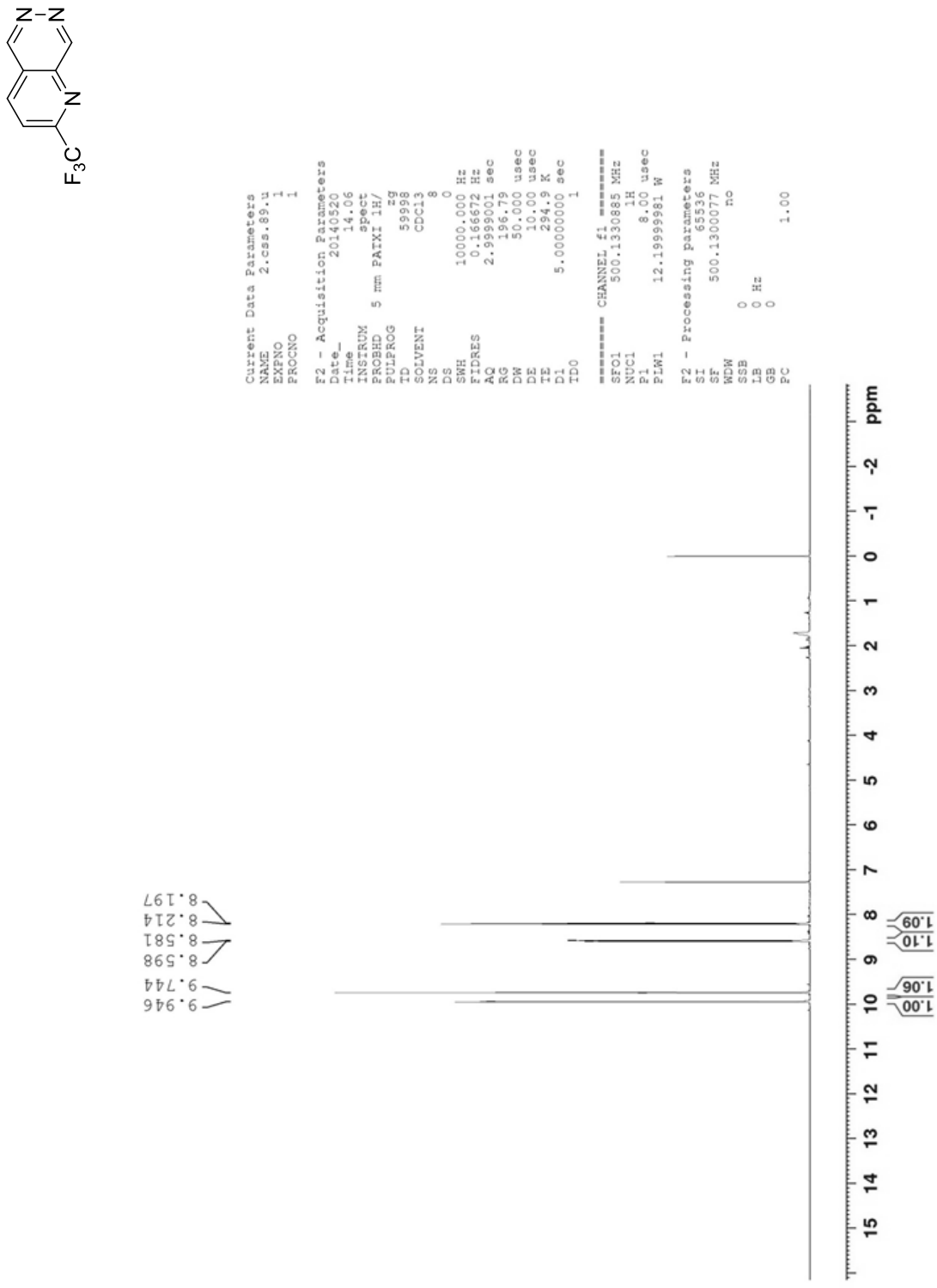

Figure 88: ^{1}H NMR Spectrum of 88 (500 MHz, $CDCl_3$, 298K)

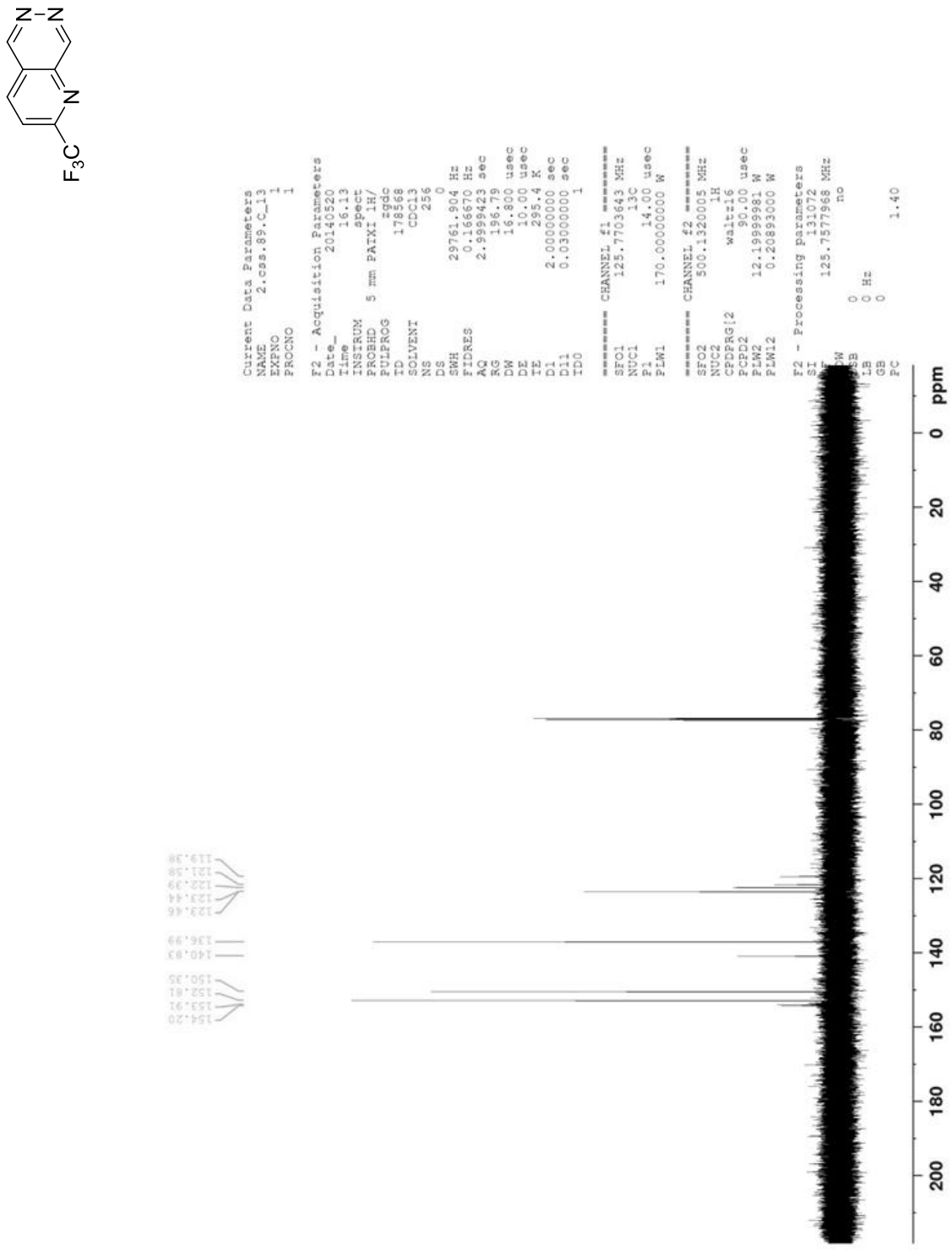

Figure 89: ^{13}C NMR Spectrum of 88 (125 MHz, $CDCl_3$, 298K)

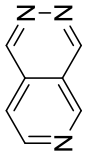

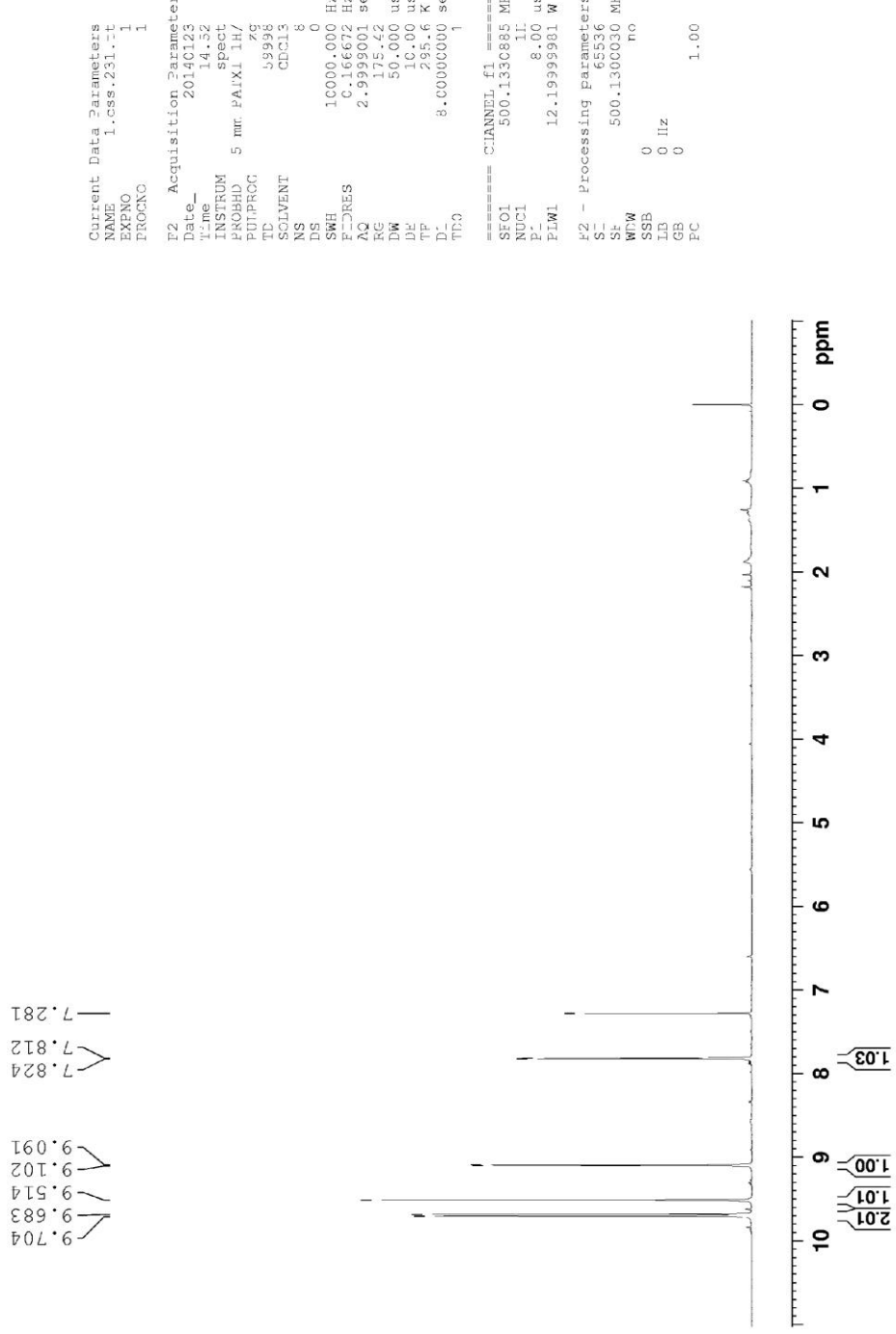

Figure 90: ^{1}H NMR Spectrum of 53 (500 MHz, $CDCl_3$, 298K)

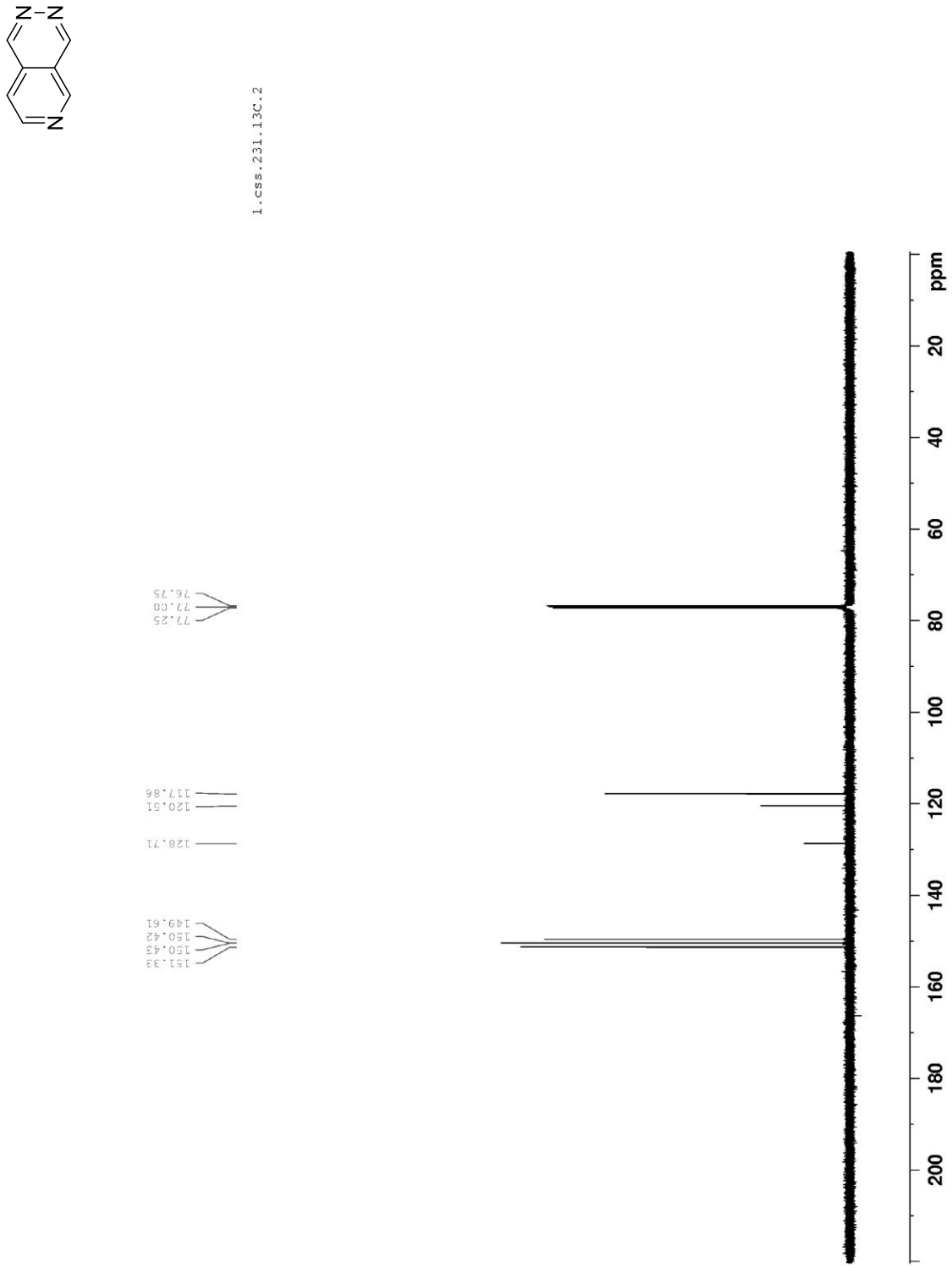

Figure 91: ^{13}C NMR Spectrum of 53 (125 MHz, $CDCl_3$, 298K)

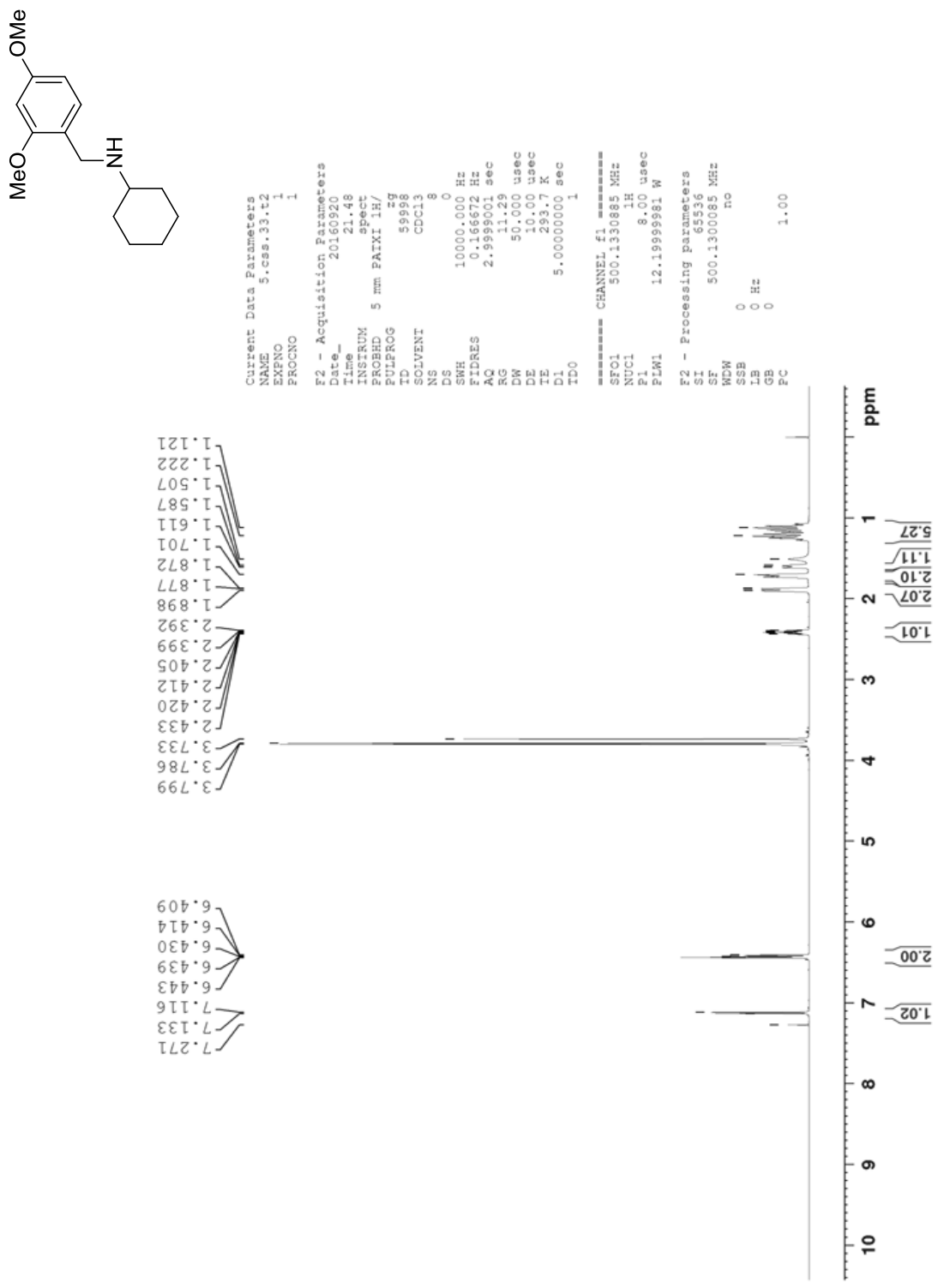

Figure 92: ^{1}H NMR Spectrum of 120 (500 MHz, $CDCl_3$, 298K)

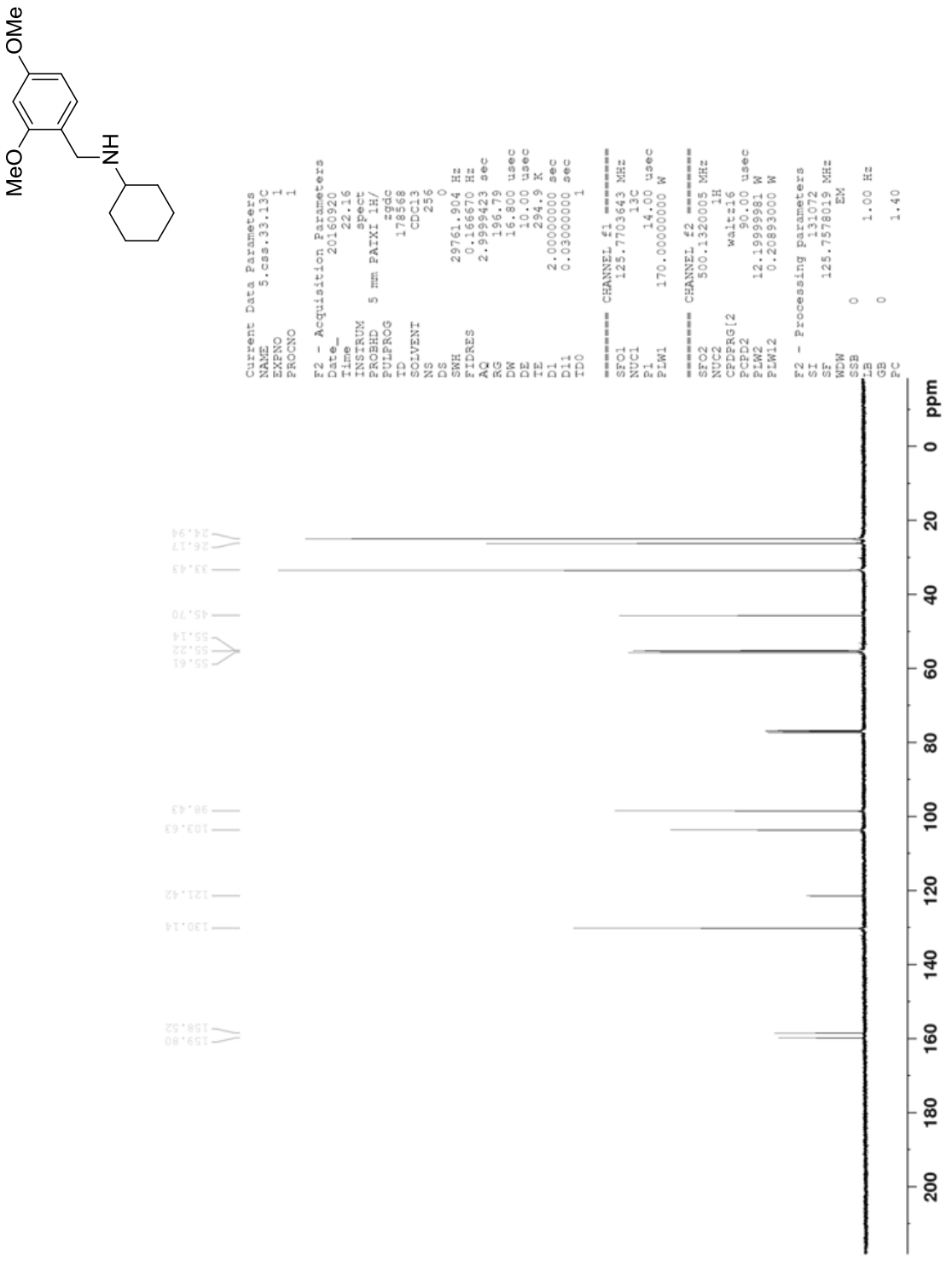

Figure 93: ^{13}C NMR Spectrum of 120 (125 MHz, $CDCl_3$, 298K)

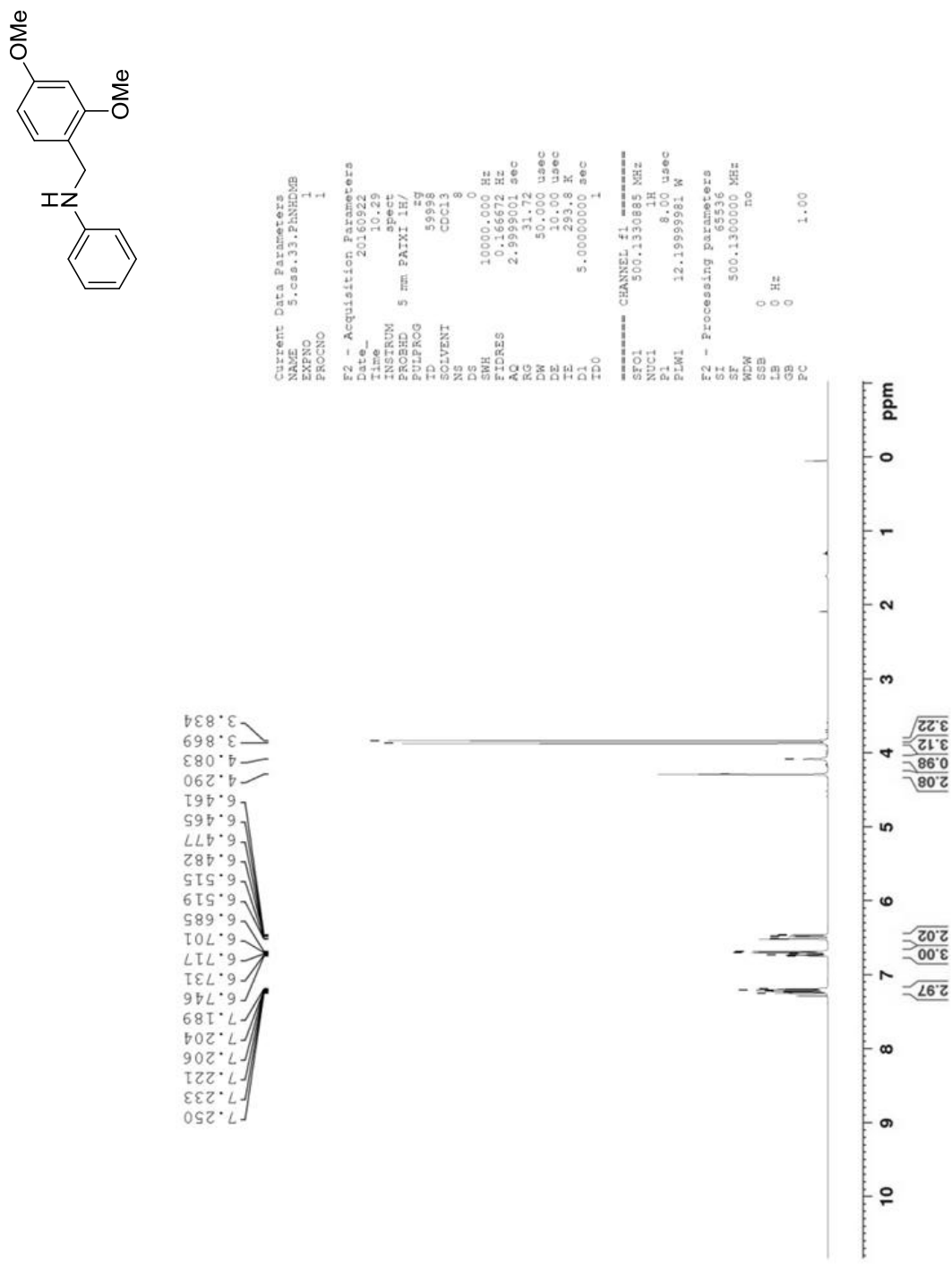

Figure 94: ^{1}H NMR Spectrum of 126 (500 MHz, $CDCl_3$, 298K)

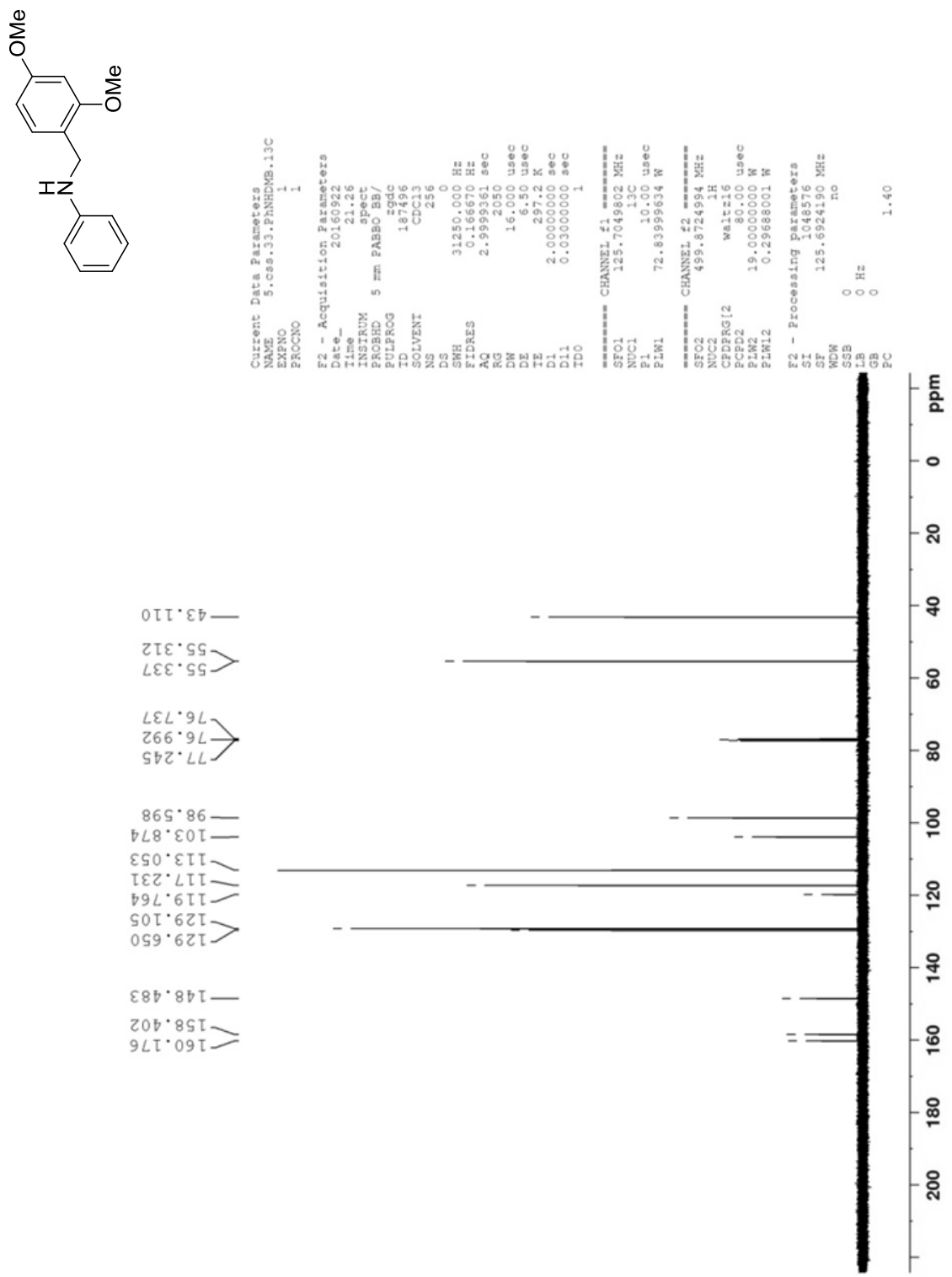

Figure 95: ^{13}C NMR Spectrum of 126 (125 MHz, $CDCl_3$, 298K)

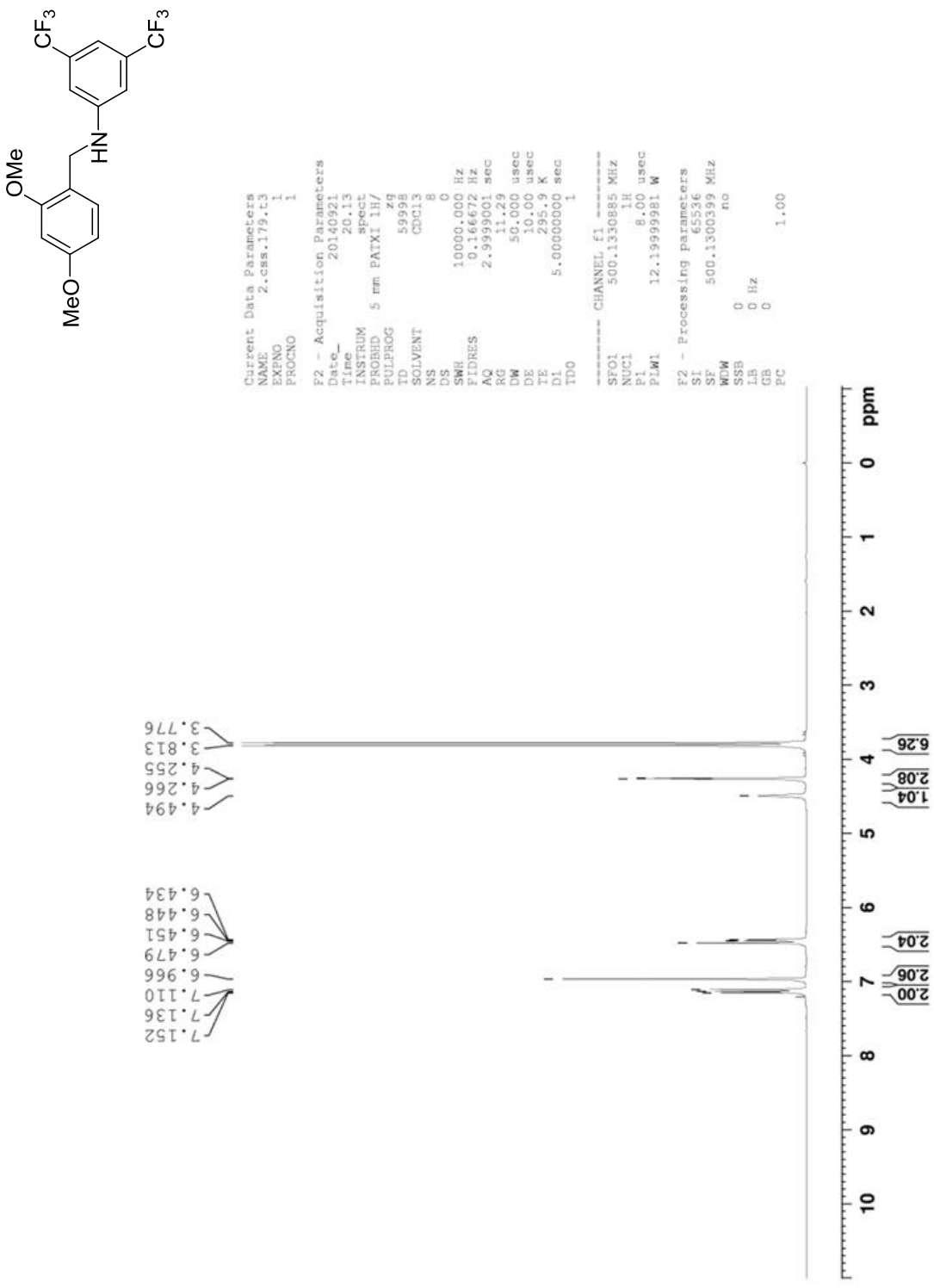

Figure 96: ^{1}H NMR Spectrum of 136 (500 MHz, $CDCl_3$, 298K)

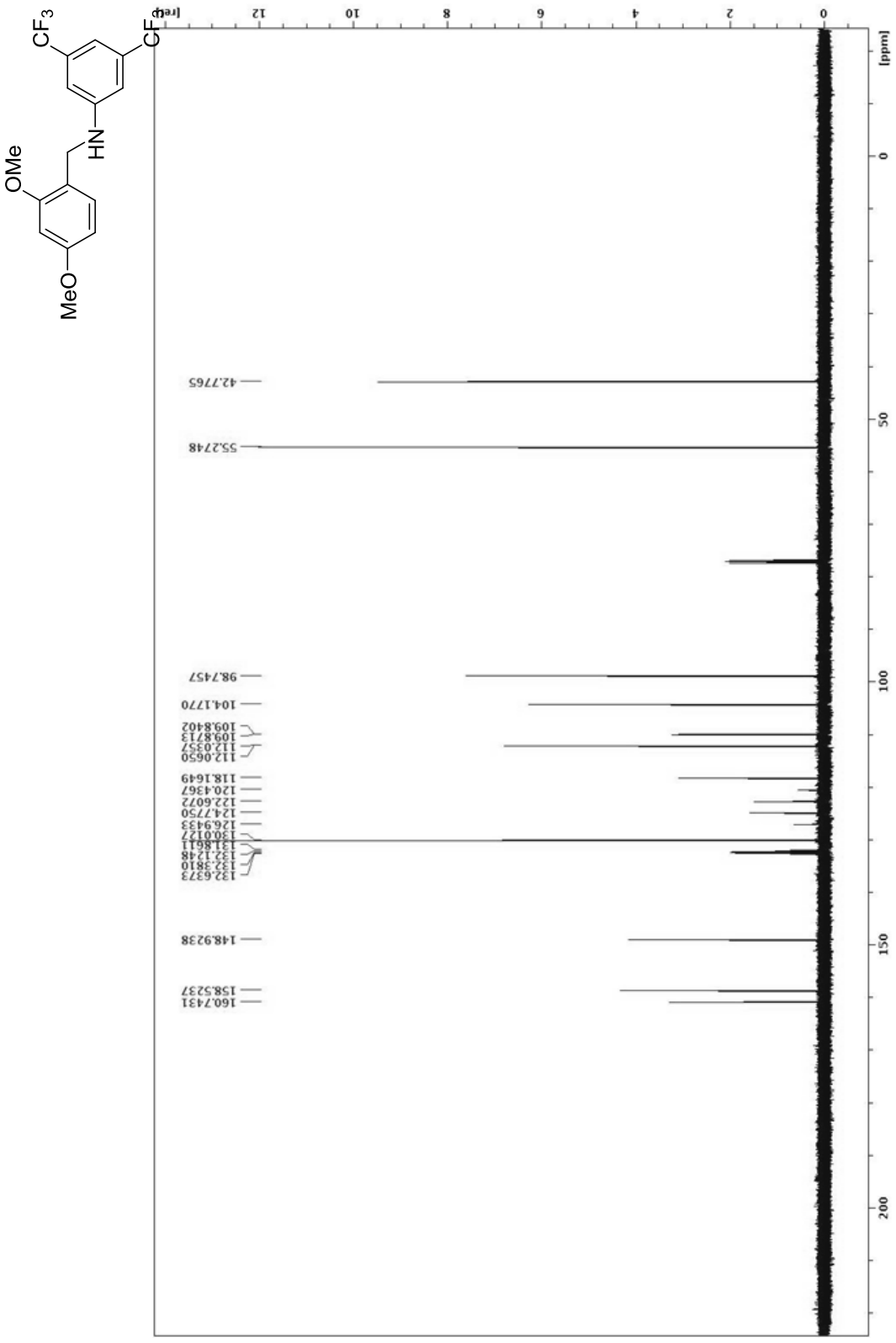

Figure 97: ^{13}C NMR Spectrum of 136 (125 MHz, $CDCl_3$, 298K)

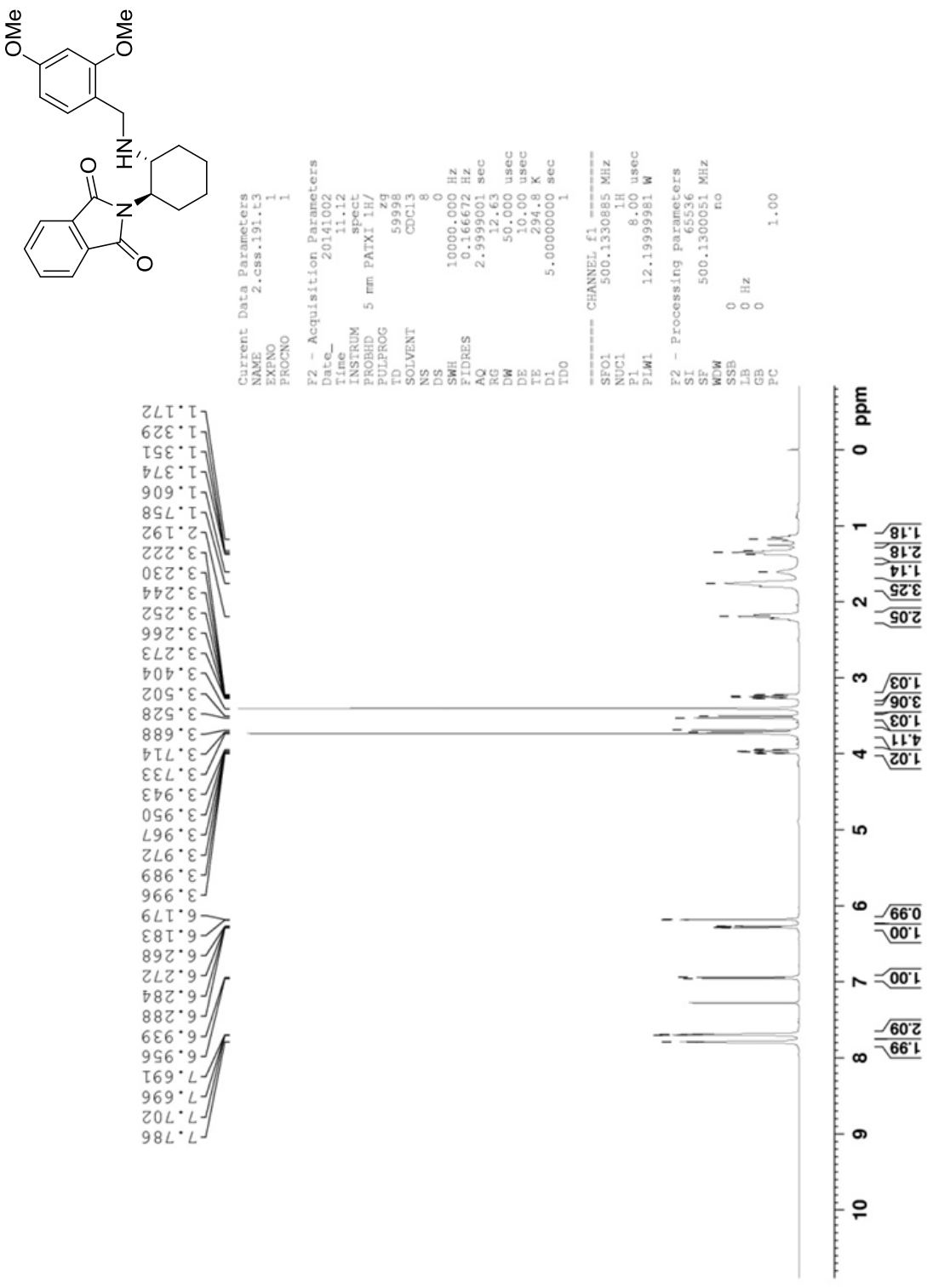

Figure 98: ^{1}H NMR Spectrum of 123 (500 MHz, $CDCl_3$, 298K)

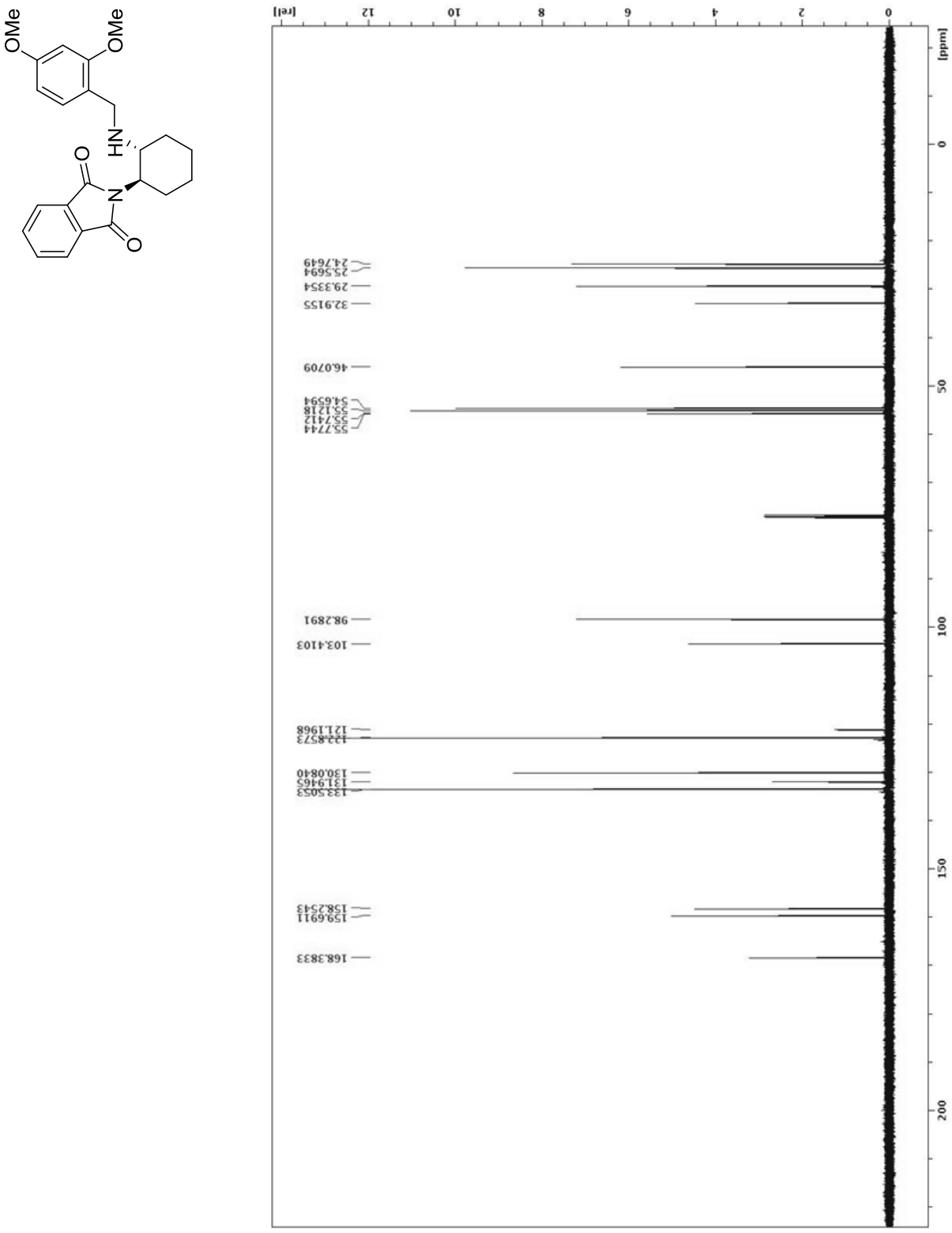

Figure 99: ^{13}C NMR Spectrum of 123 (125 MHz, $CDCl_3$, 298K)

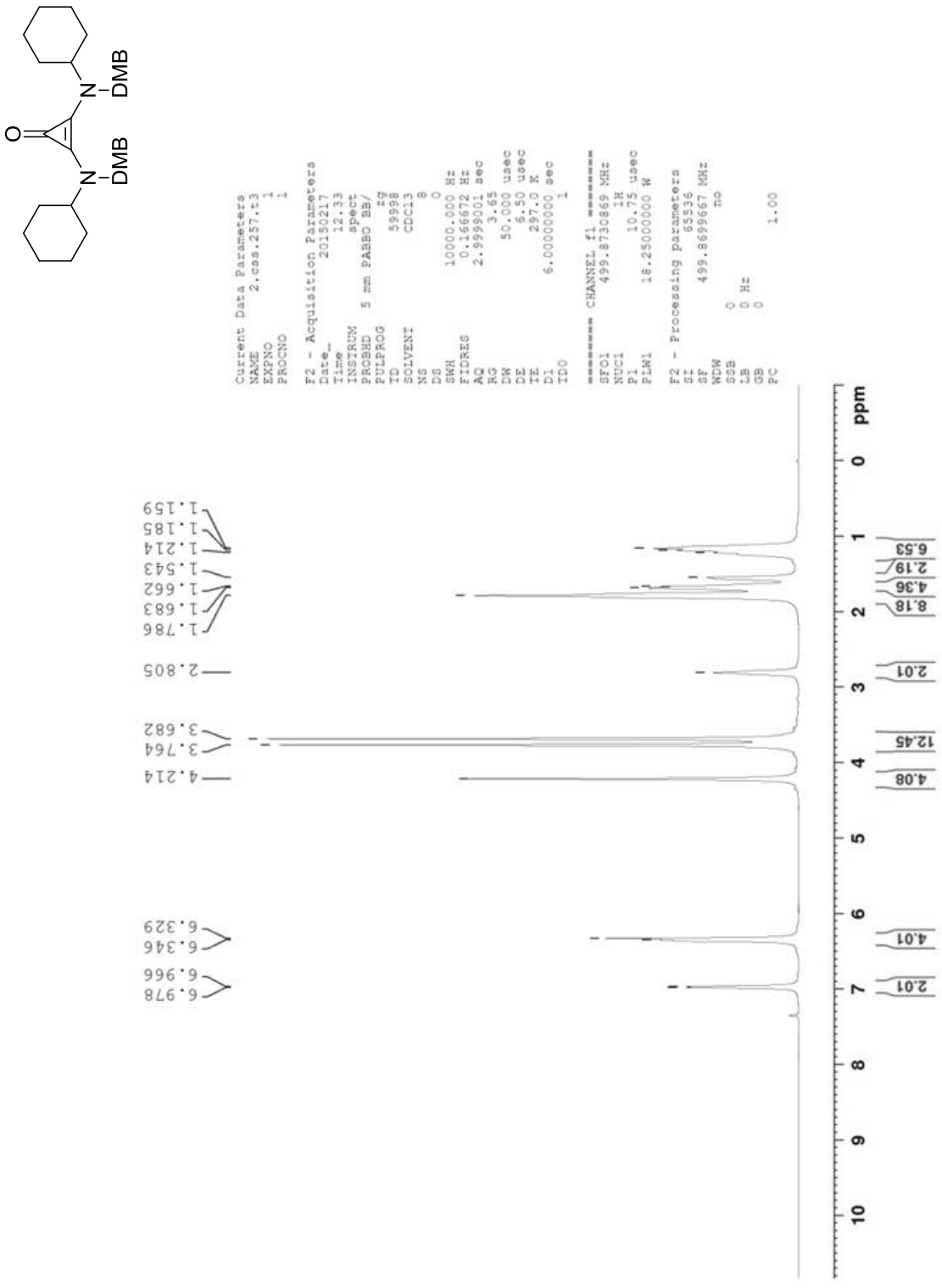

Figure 100: ^{1}H NMR Spectrum of 121 (500 MHz, $CDCl_3$, 298K)

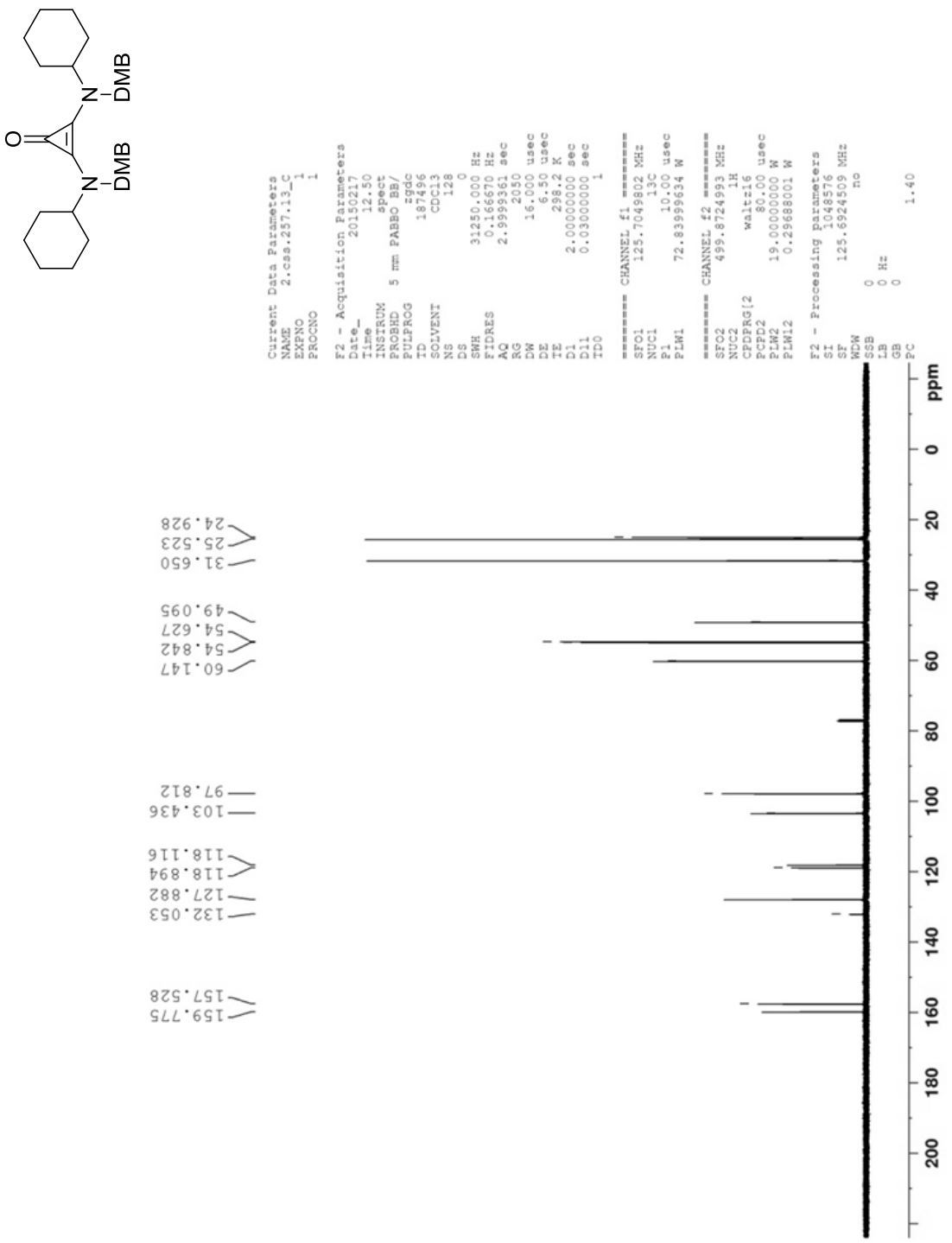

Figure 101: ^{13}C NMR Spectrum of 121 (125 MHz, $CDCl_3$, 298K)

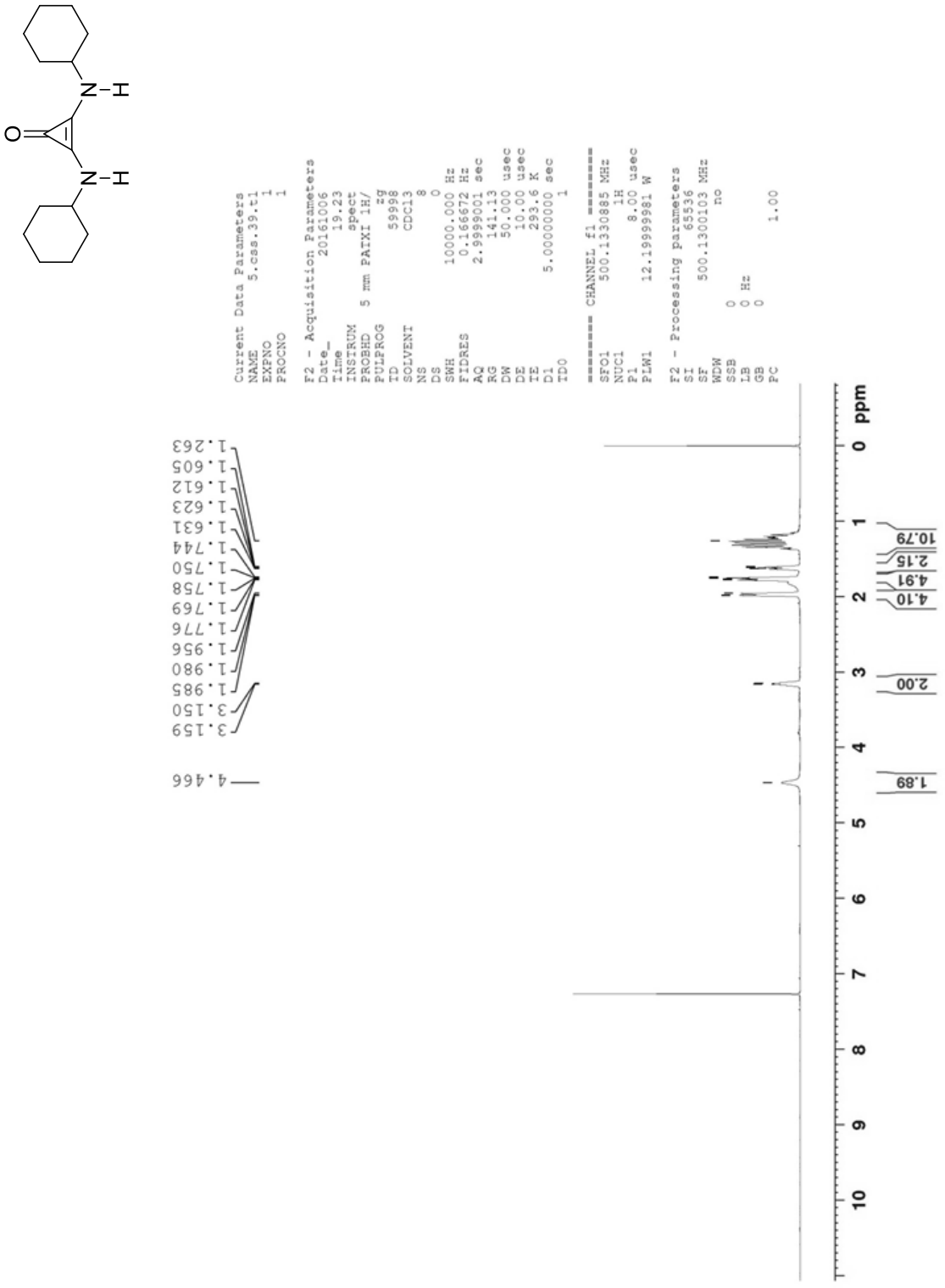

Figure 102: ^{1}H NMR Spectrum of 122 (500 MHz, $CDCl_3$, 298K)

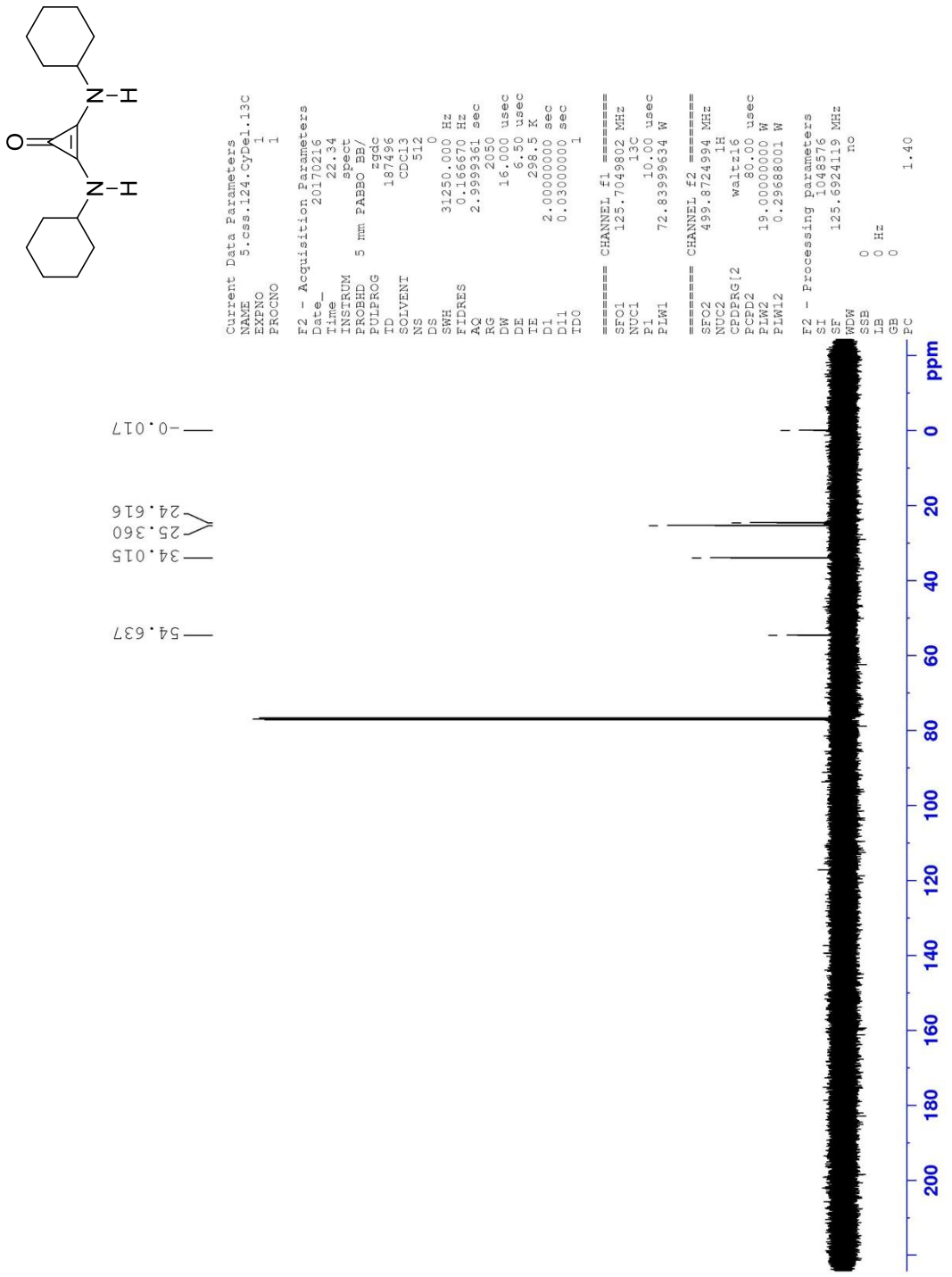

Figure 103: ^{13}C NMR Spectrum of 122 (125 MHz, $CDCl_3$, 298K)

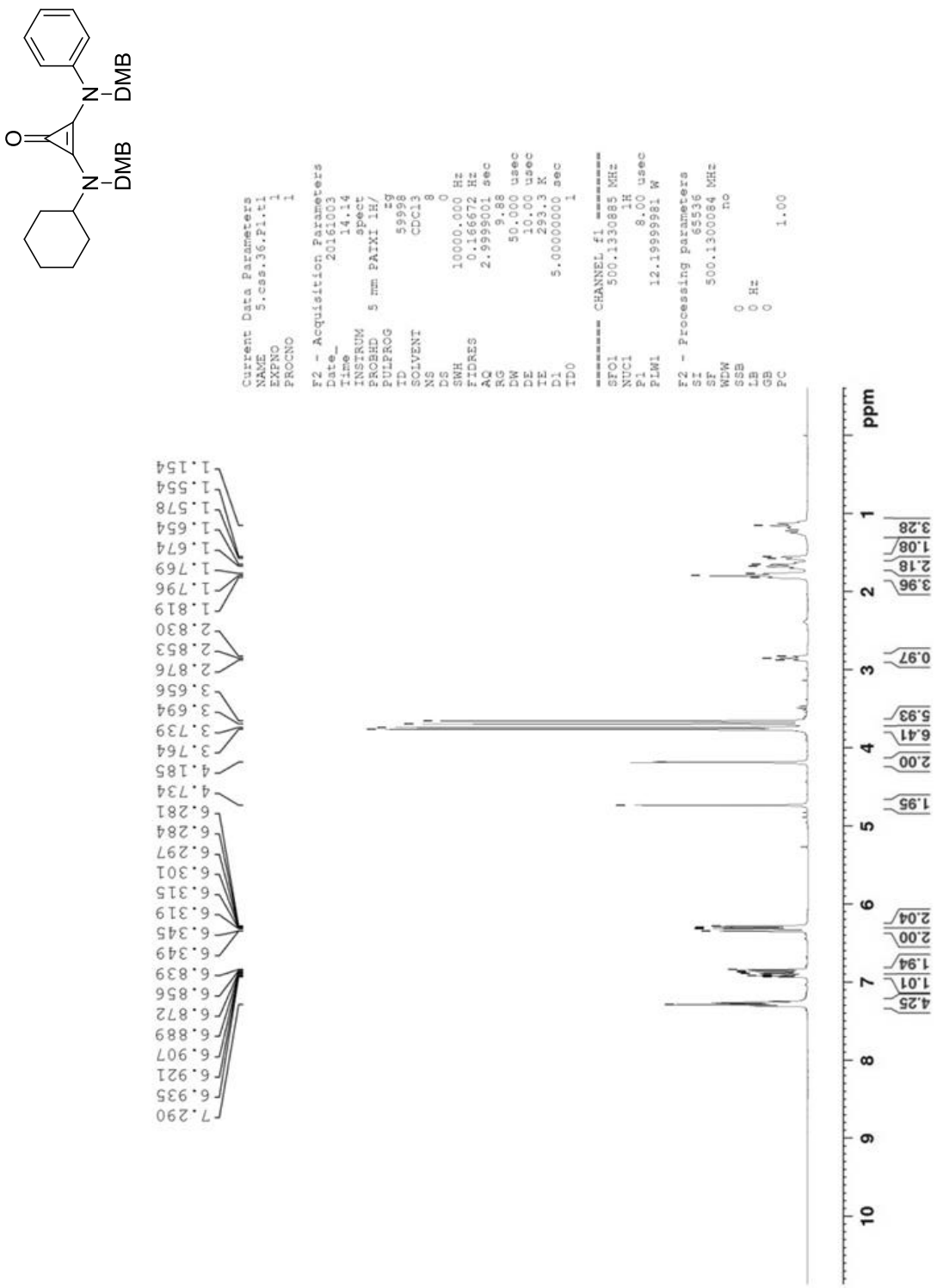

Figure 104: ^{1}H NMR Spectrum of 133 (500 MHz, $CDCl_3$, 298K)

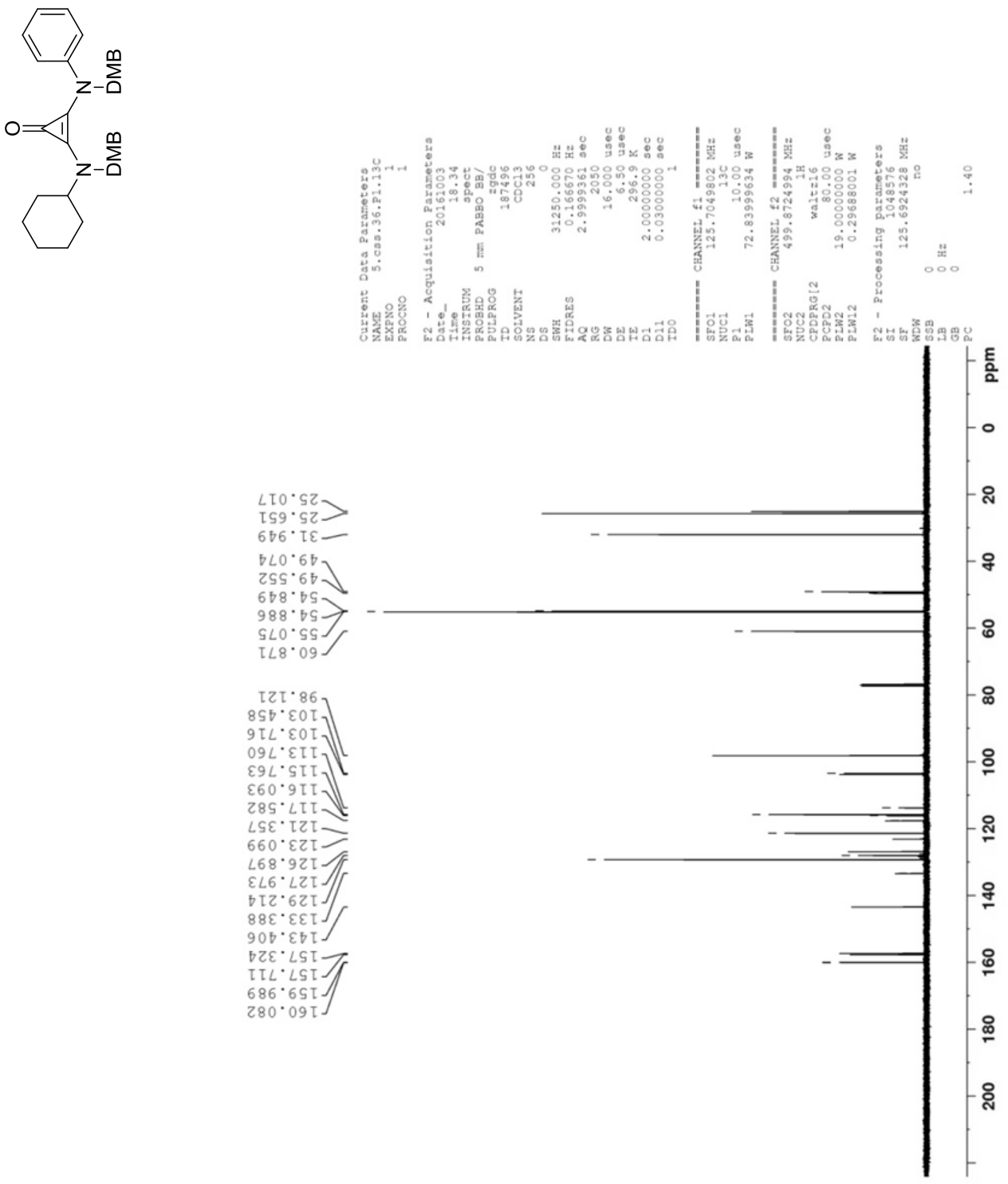

Figure 105: ^{13}C NMR Spectrum of 133 (125 MHz, $CDCl_3$, 298K)

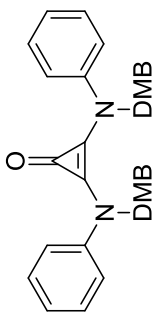

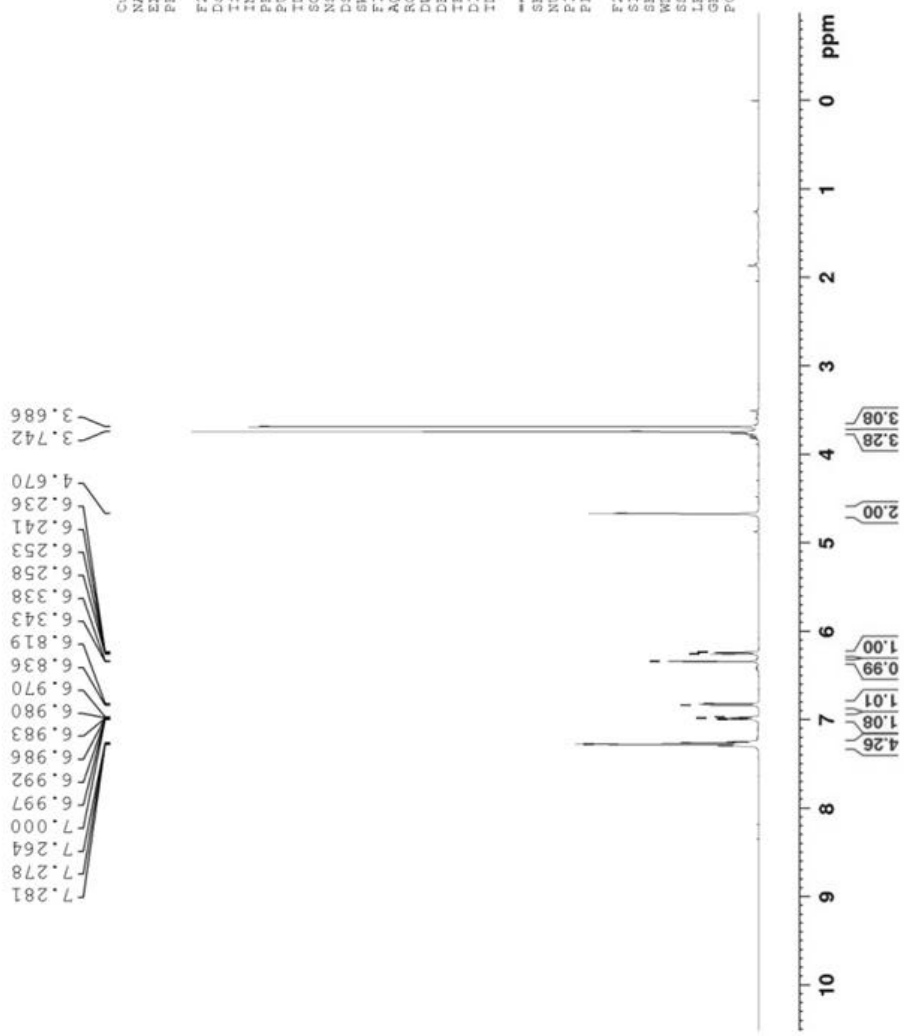

Figure 106: ^{1}H NMR Spectrum of 129 (500 MHz, $CDCl_3$, 298K)

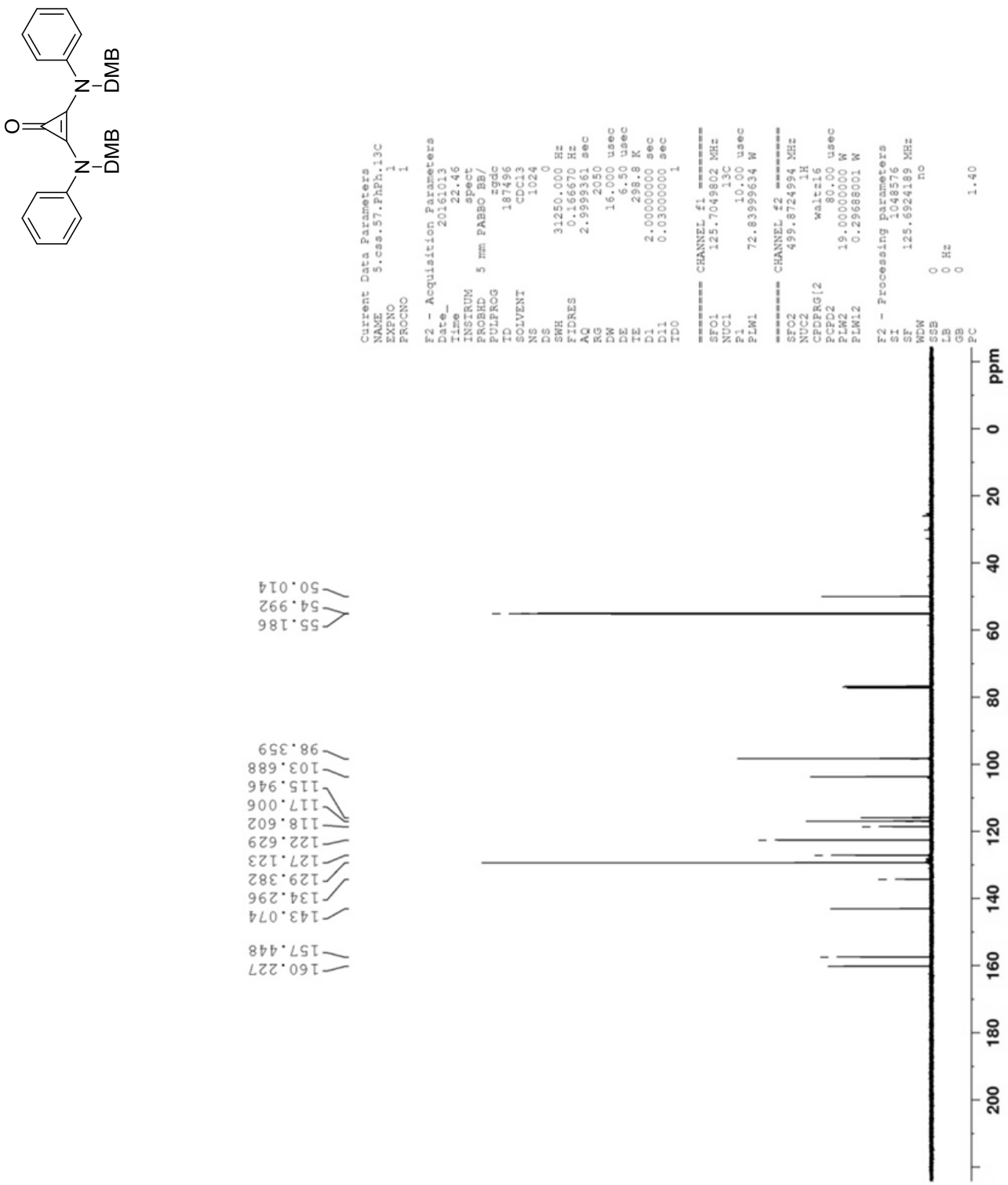

Figure 107: ^{13}C NMR Spectrum of 129 (125 MHz, $CDCl_3$, 298K)

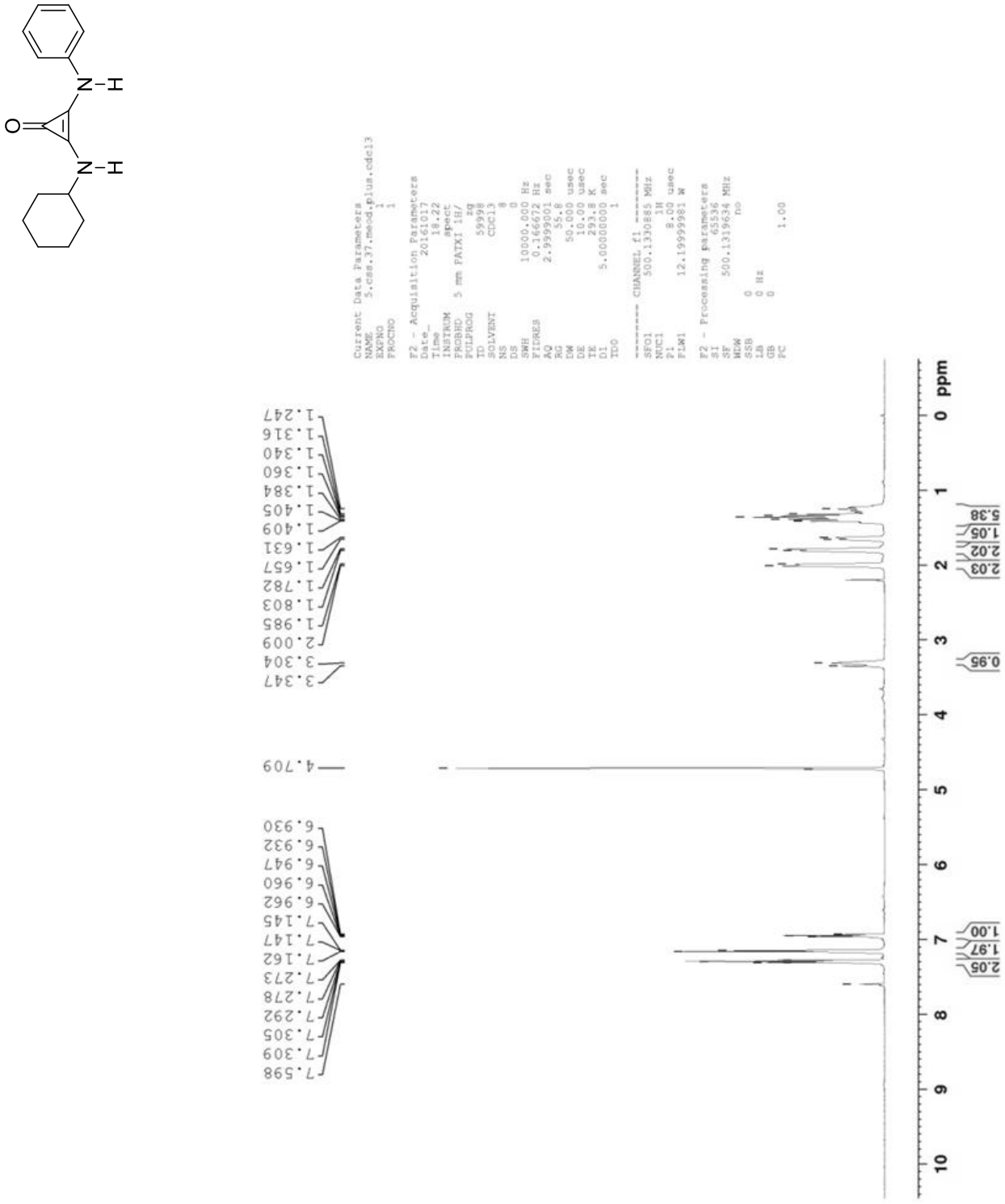

Figure 108: ^{1}H NMR Spectrum of 135 (500 MHz, $CDCl_3$, 298K)

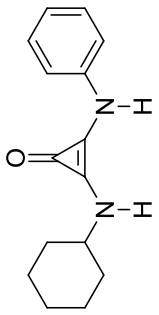

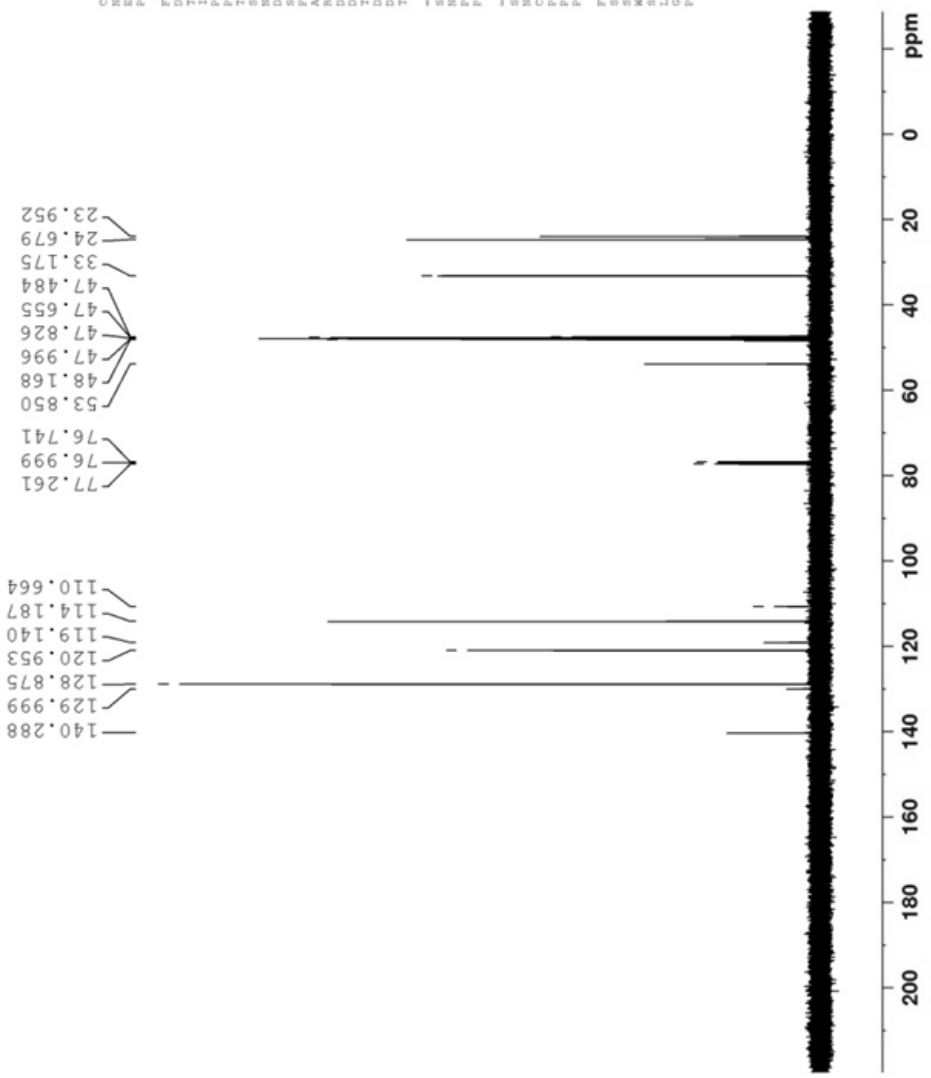

Figure 109: ^{13}C NMR Spectrum of 135 (125 MHz, $CDCl_3$, 298K)

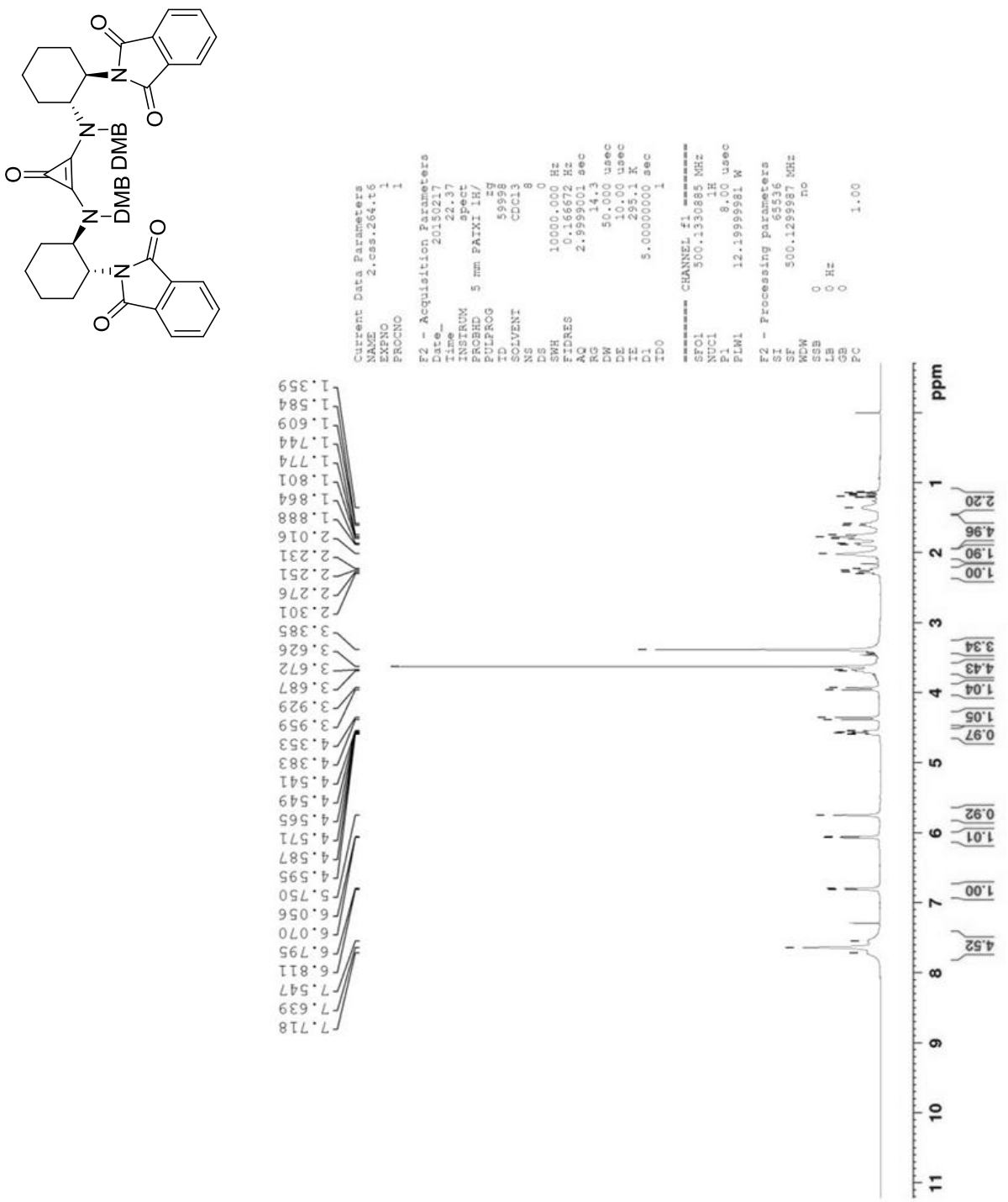

Figure 110: ^{1}H NMR Spectrum of 124 (500 MHz, $CDCl_3$, 298K)

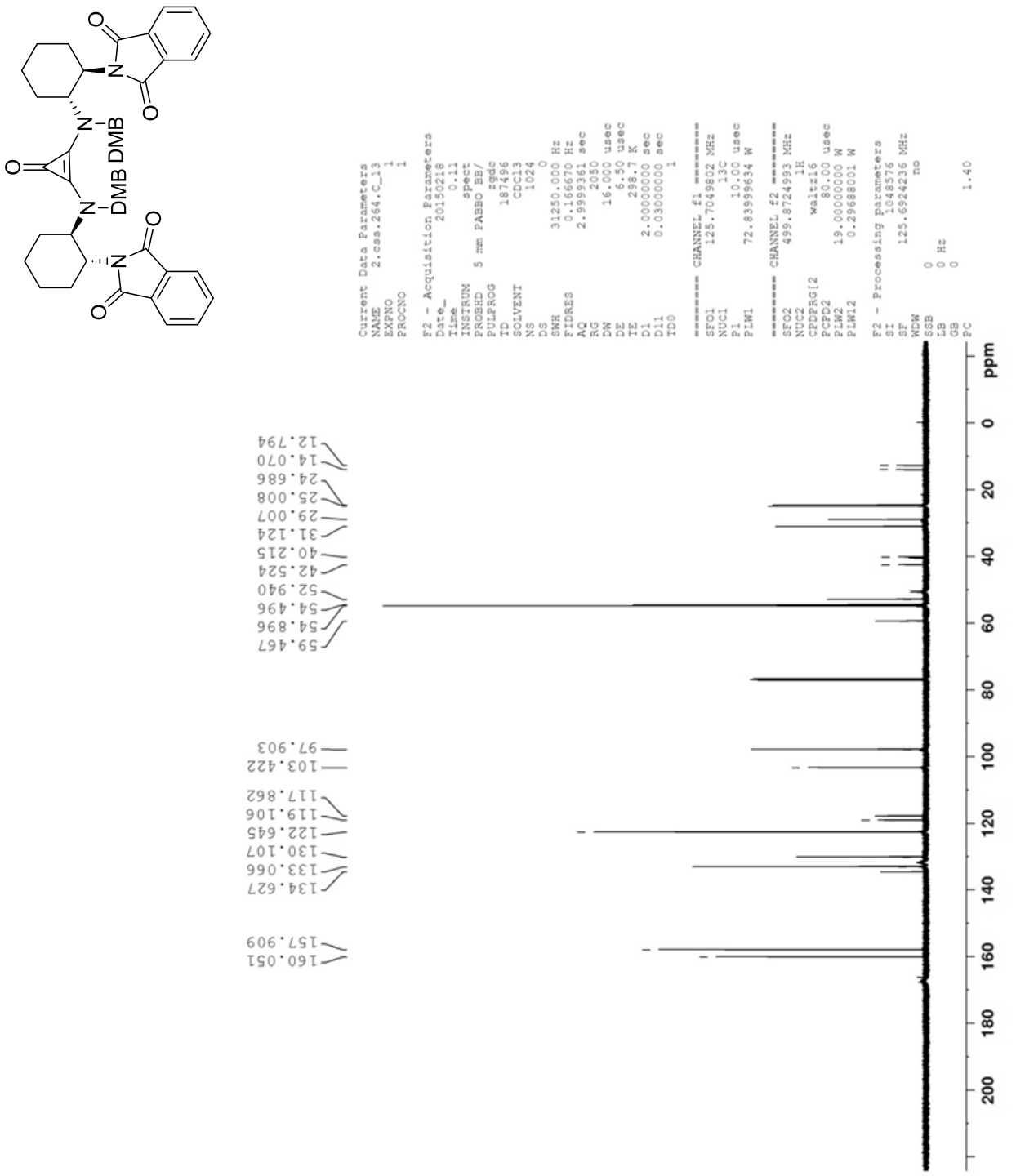

Figure 111: ^{13}C NMR Spectrum of 124 (125 MHz, $CDCl_3$, 298K)

Figure 112: ^{1}H NMR Spectrum of 125 (500 MHz, 1:1 $CDCl_3$:CD_3OD, 298K)

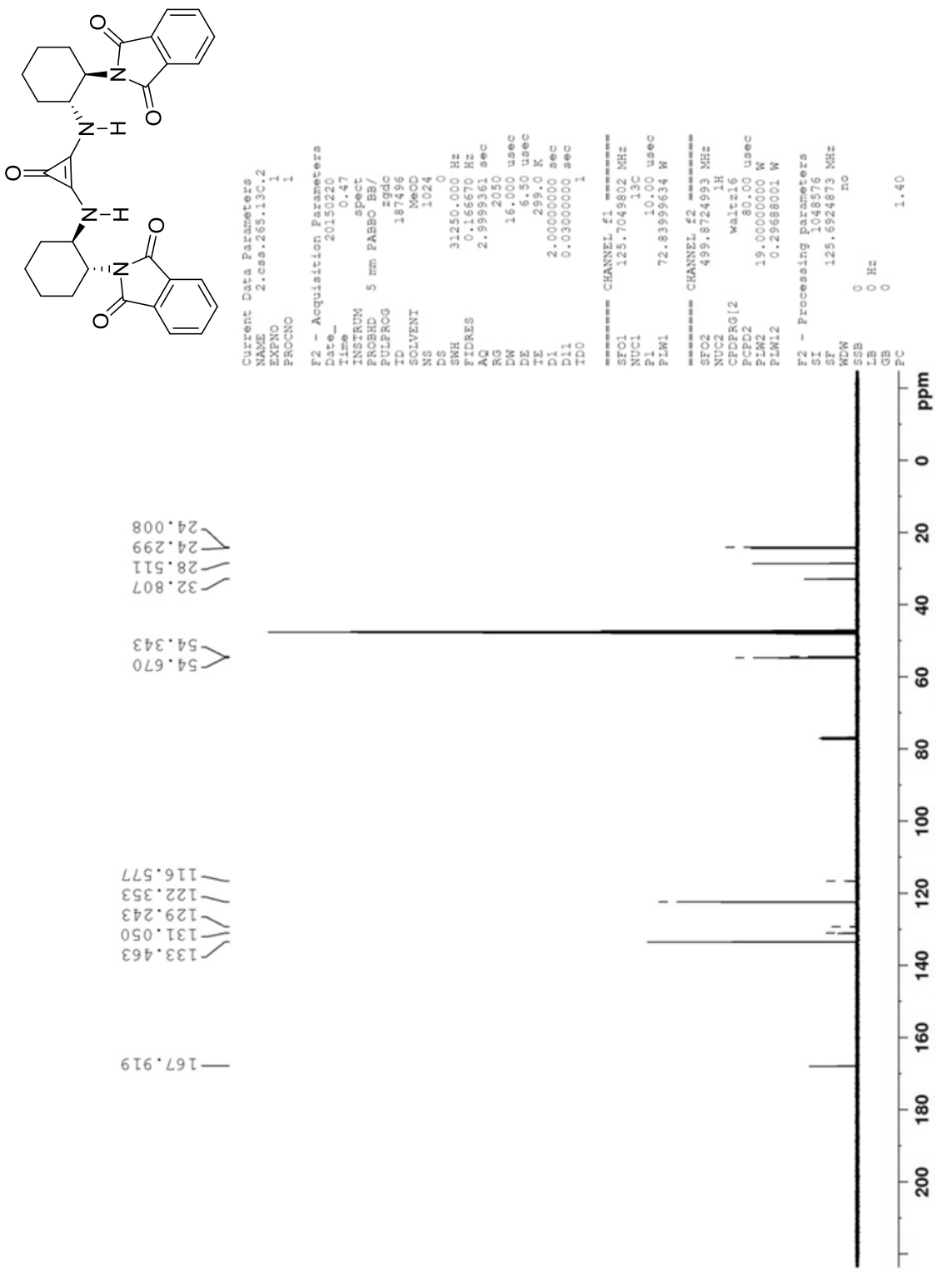

Figure 113: ^{13}C NMR Spectrum of 125 (125 MHz, 1:1 $CDCl_3$:CD_3OD, 298K)

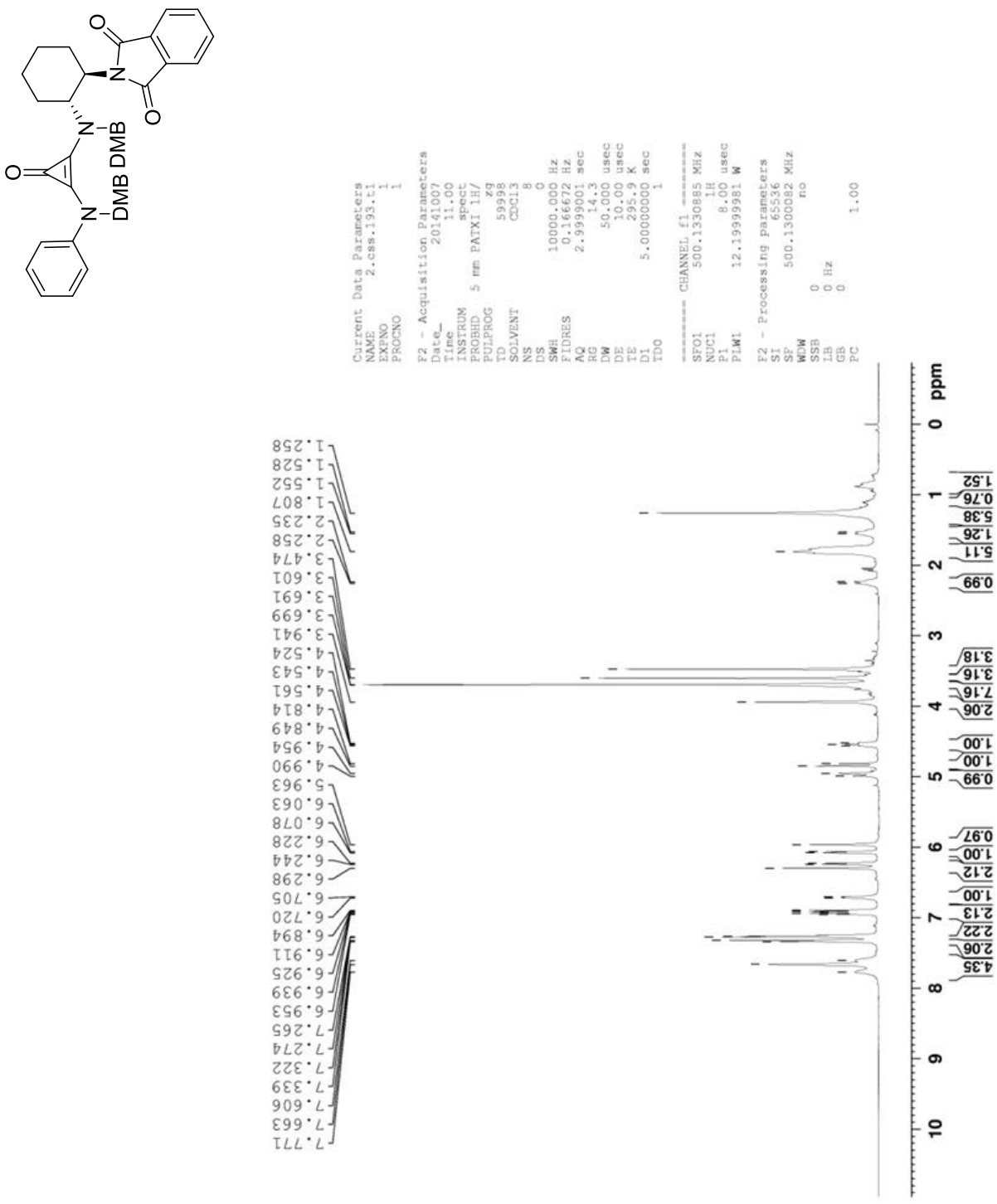

Figure 114: ^{1}H NMR Spectrum of 138 (500 MHz, $CDCl_3$, 298K)

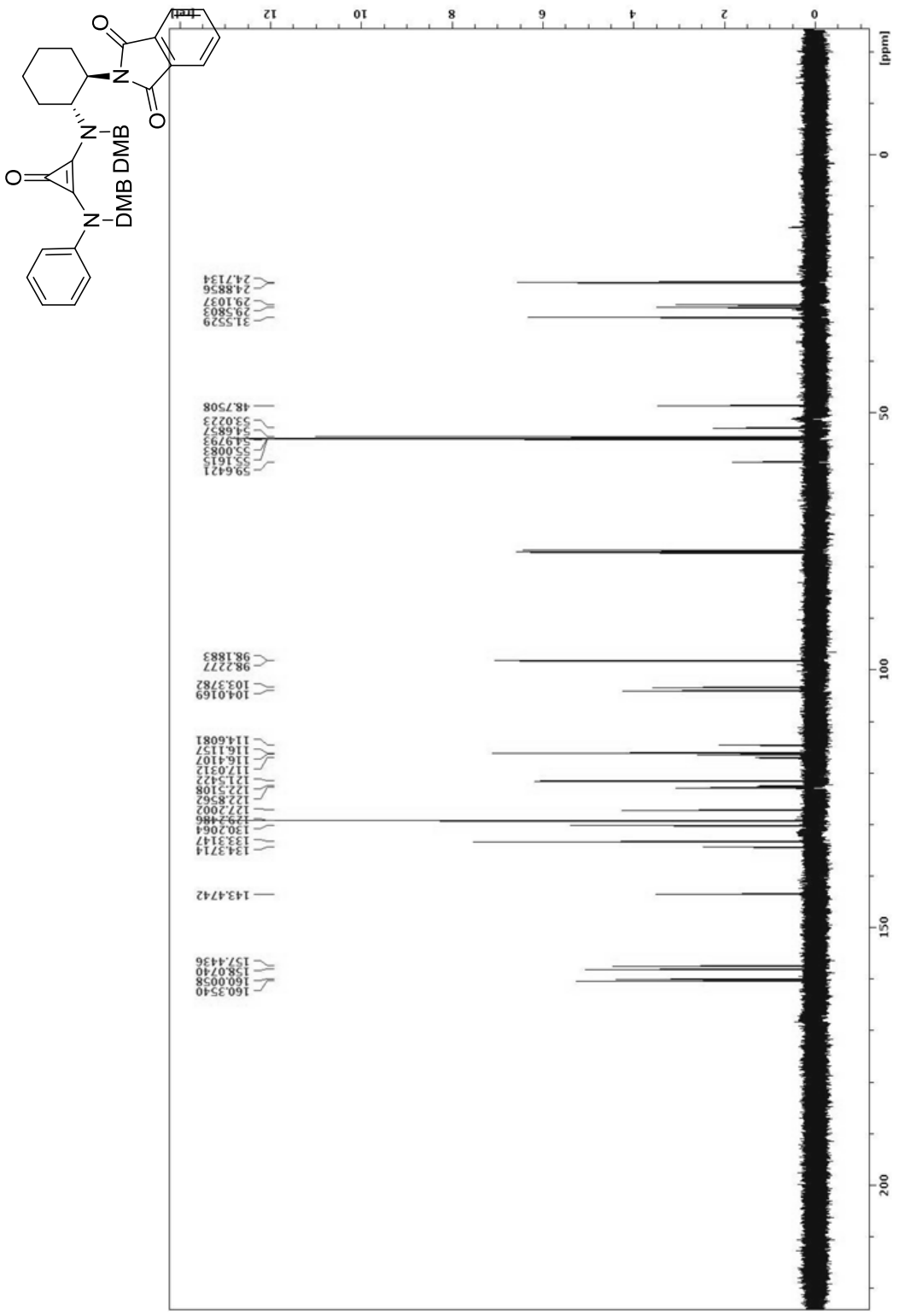

Figure 115: ^{13}C NMR Spectrum of 138 (125 MHz, $CDCl_3$, 298K)

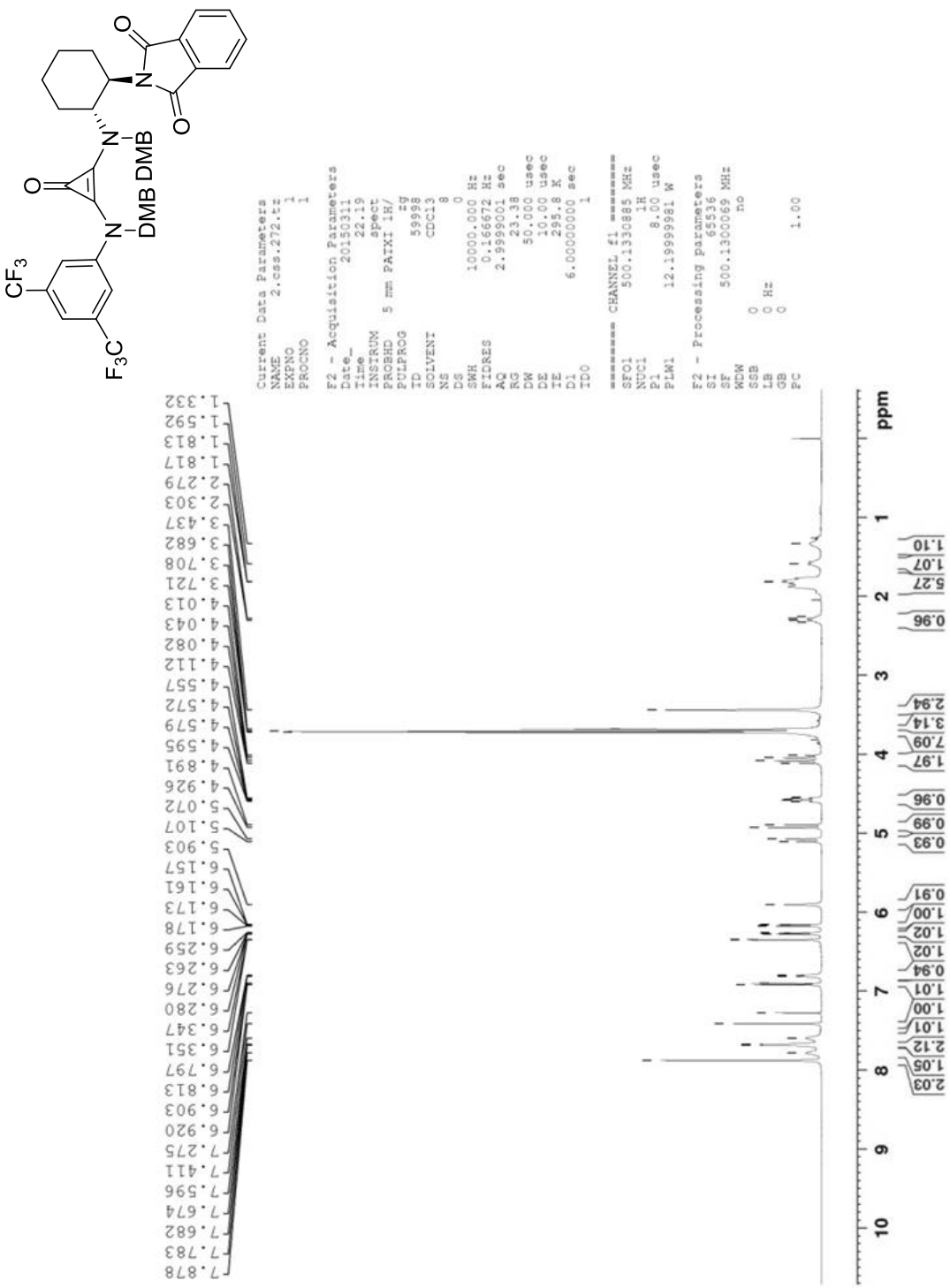

Figure 116: ^{1}H NMR Spectrum of 137 (500 MHz, $CDCl_3$, 298K)

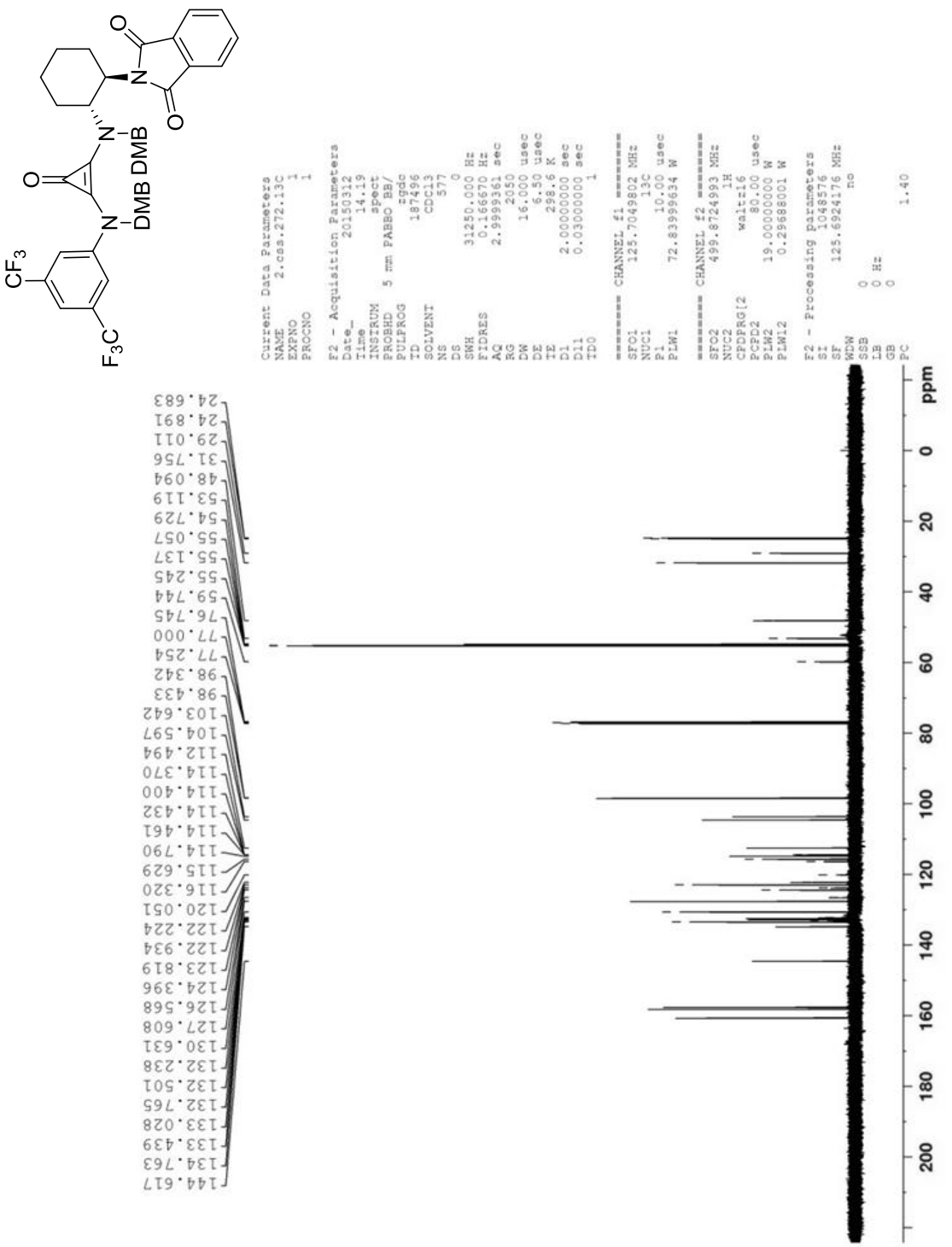

Figure 117: ^{13}C NMR Spectrum of 137 (125 MHz, $CDCl_3$, 298K)

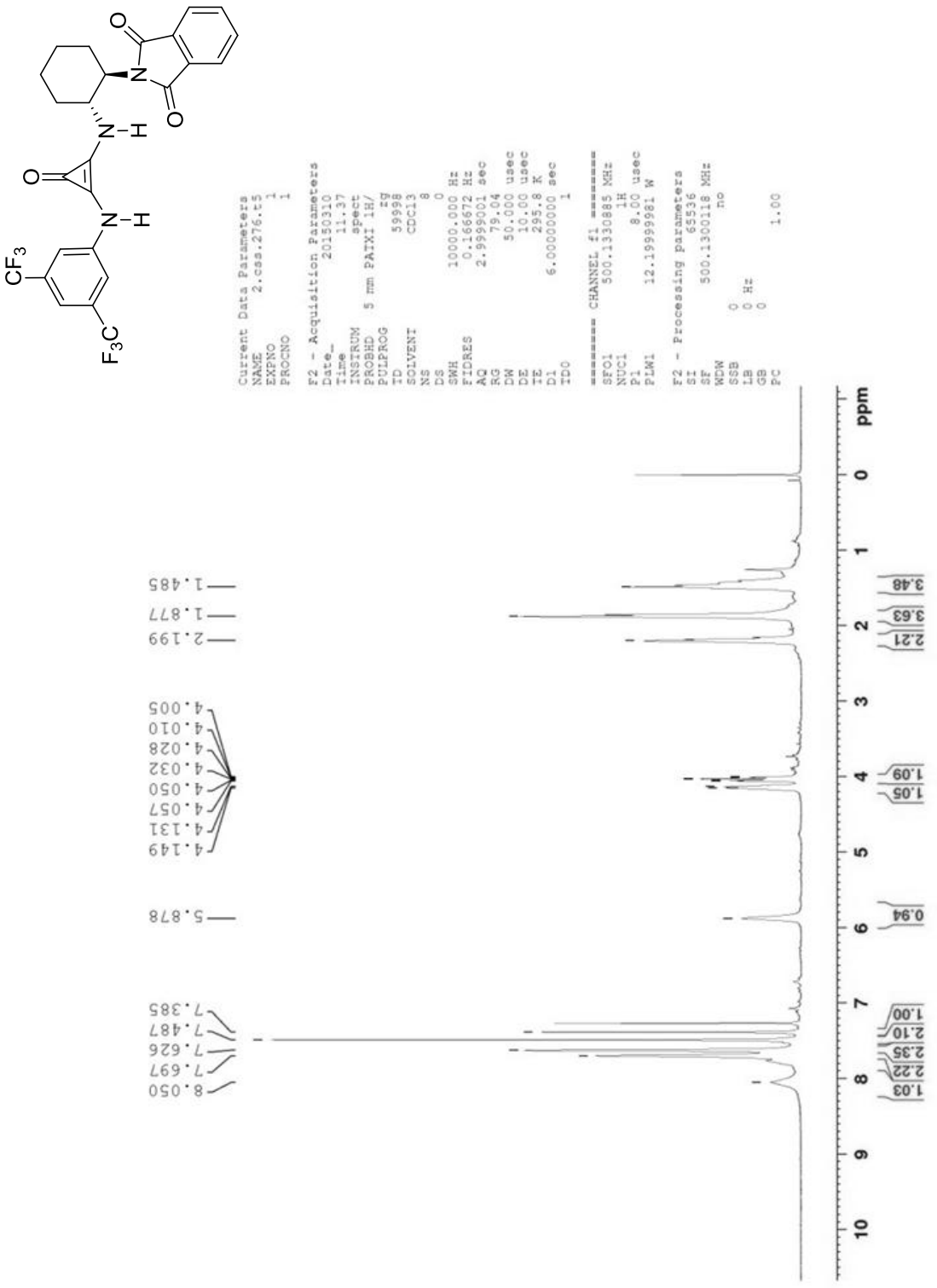

Figure 118: ^{1}H NMR Spectrum of 139 (500 MHz, $CDCl_3$, 298K)

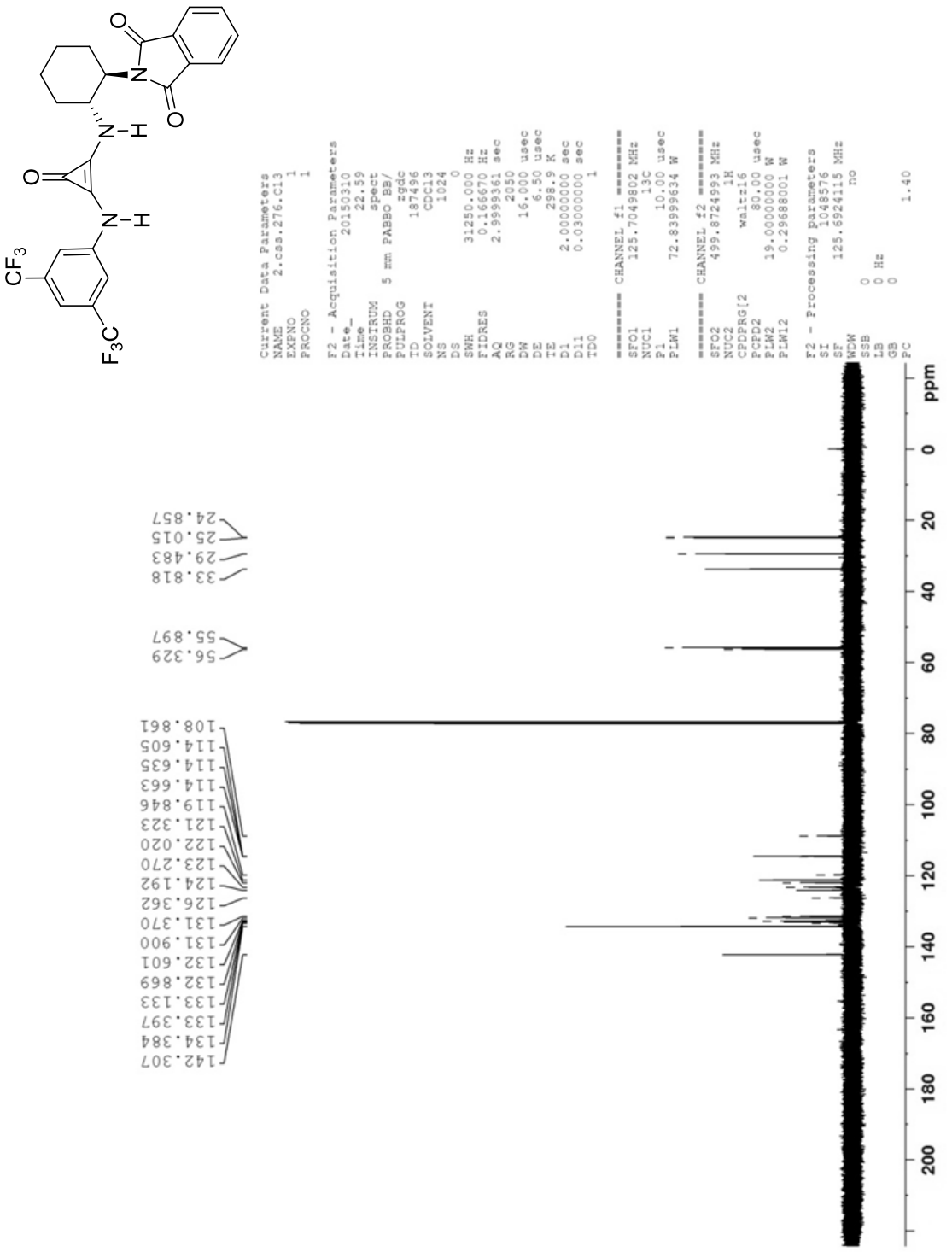

Figure 119: ^{13}C NMR Spectrum of 139 (125 MHz, $CDCl_3$, 298K)

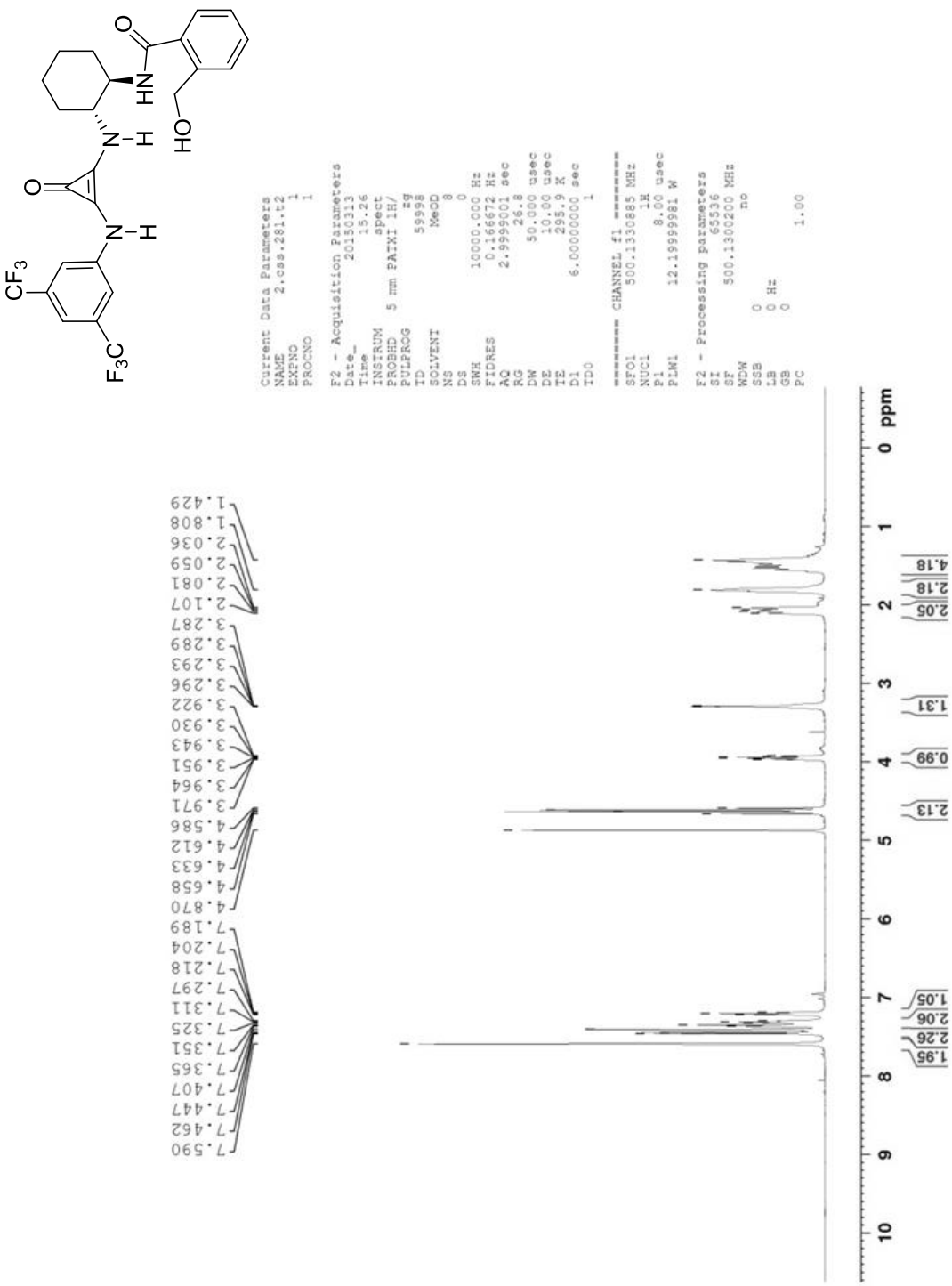

Figure 120: ^{1}H NMR Spectrum of 156 (500 MHz, CD_3OD, 298K)

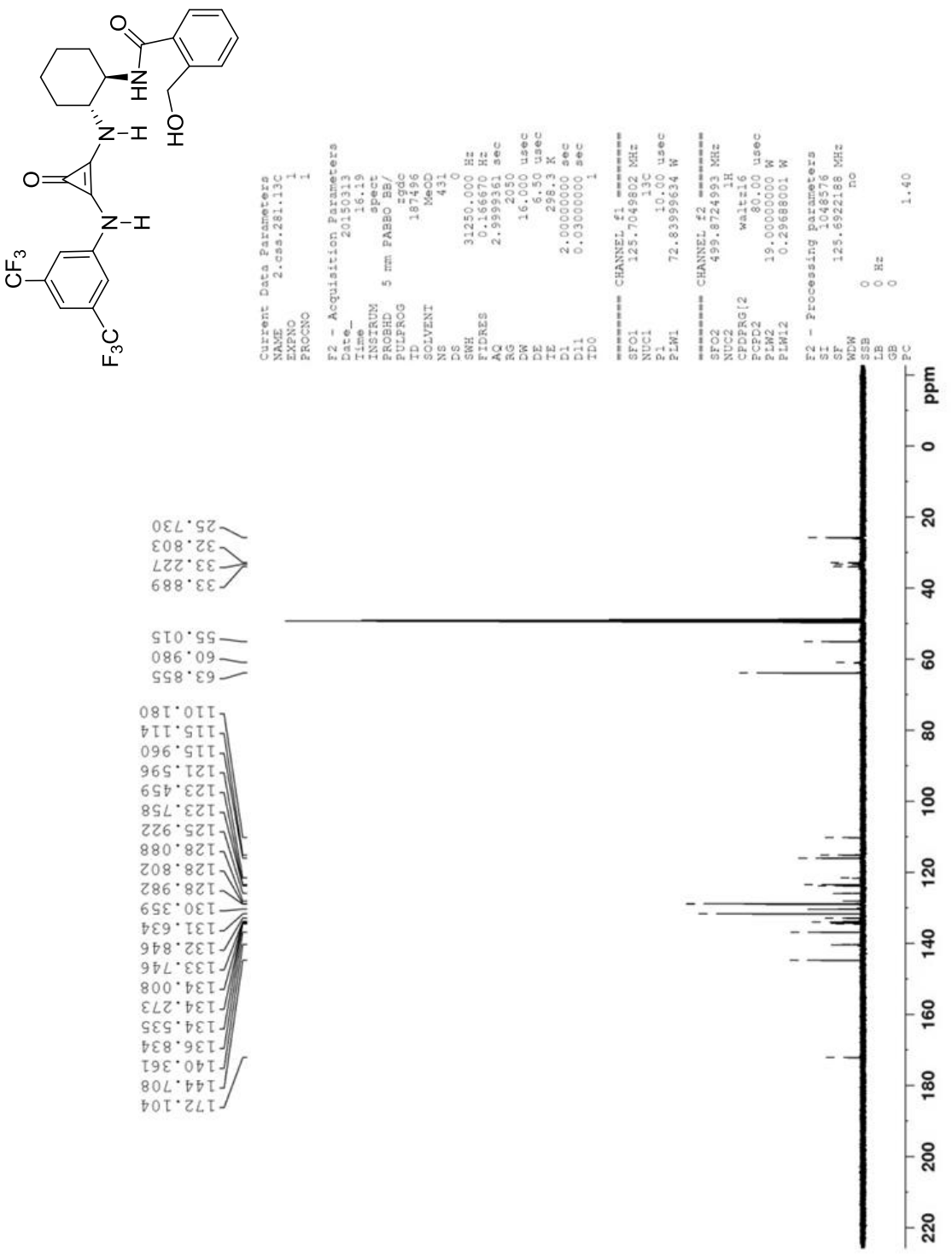

Figure 121: ^{13}C NMR Spectrum of 156 (125 MHz, CD_3OD, 298K)

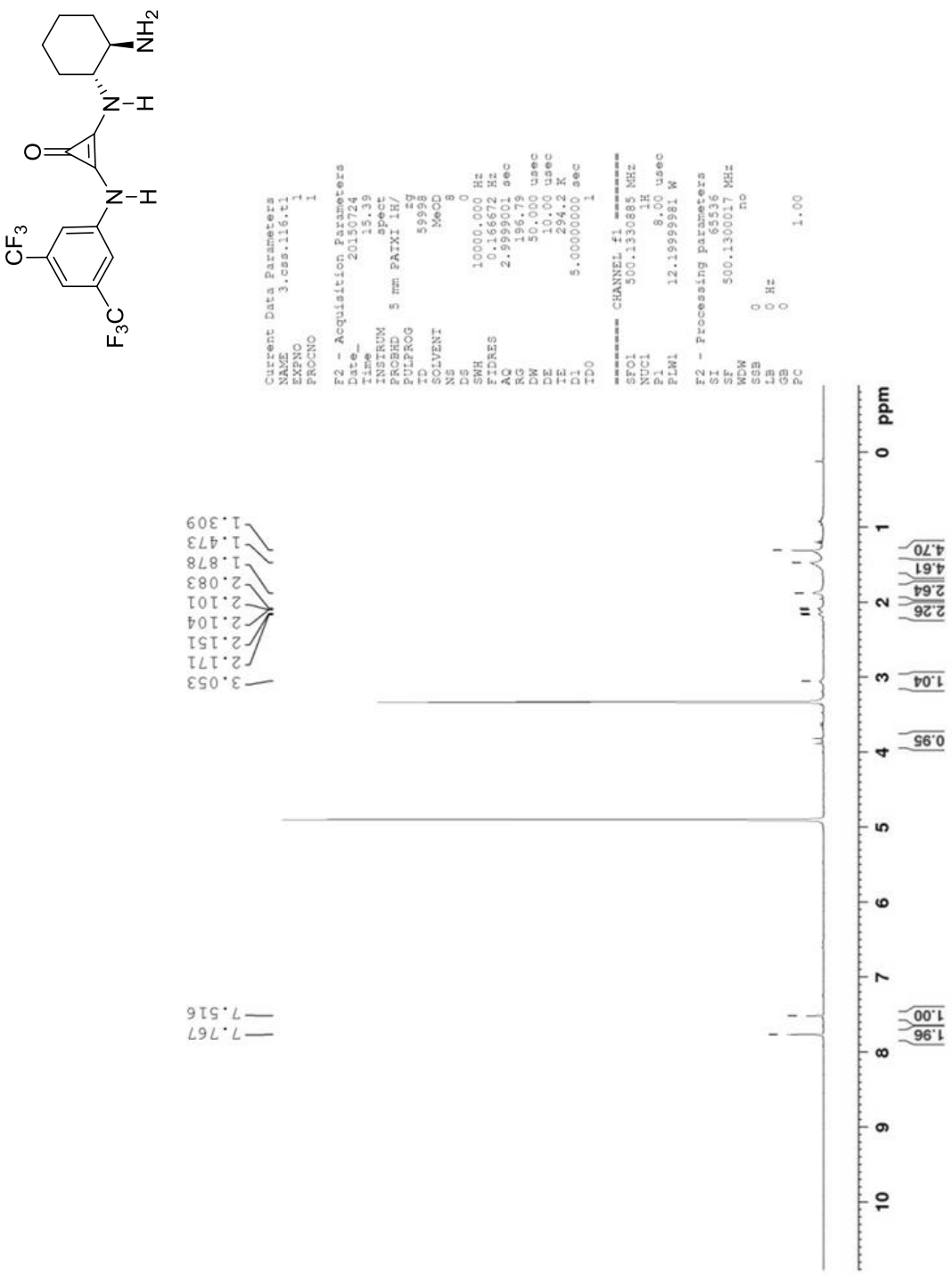

Figure 122: ^{1}H NMR Spectrum of 154 (500 MHz, CD_3OD, 298K)

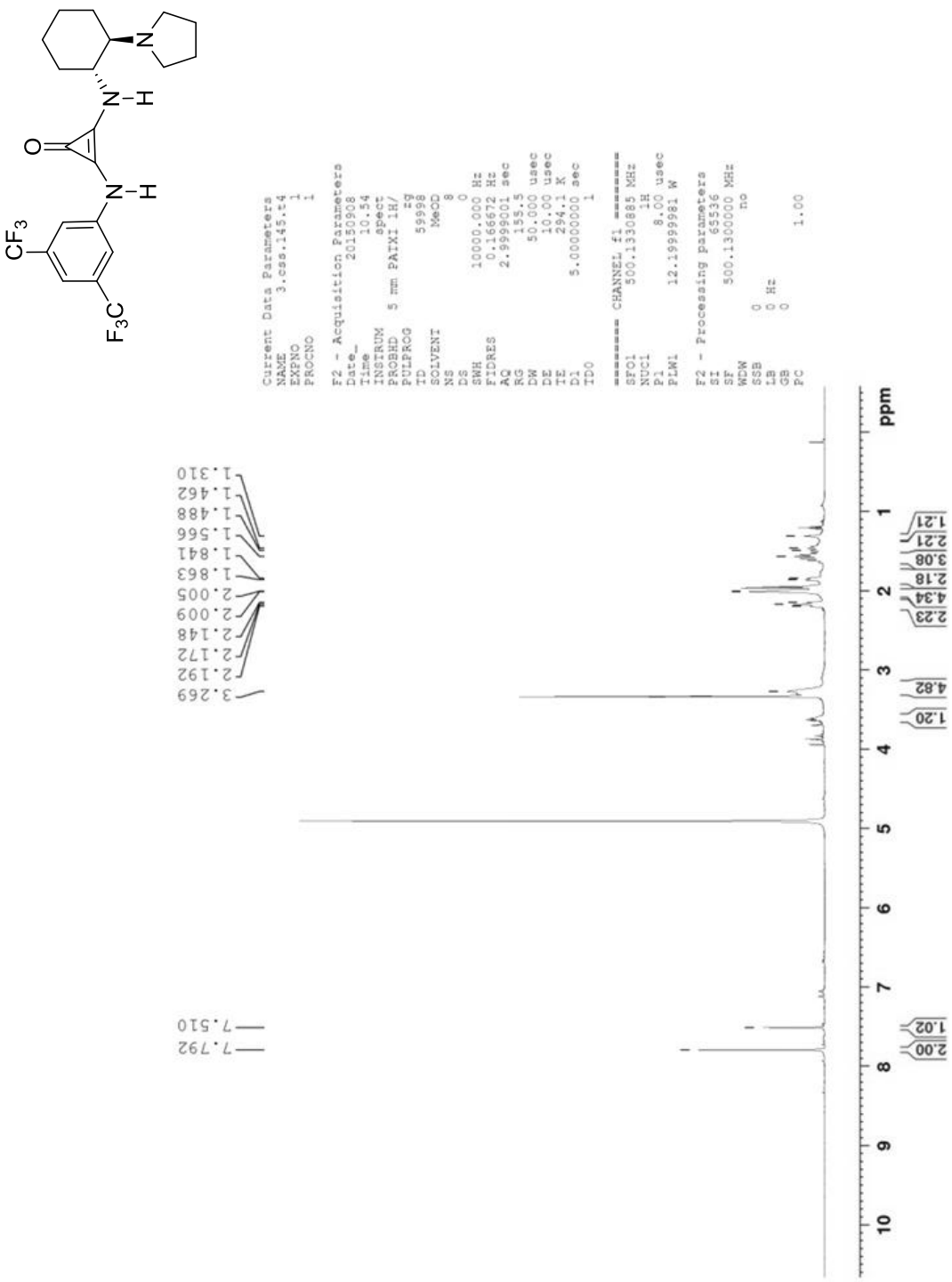

Figure 123: ^{1}H NMR Spectrum of 159 (500 MHz, CD_3OD, 298K)

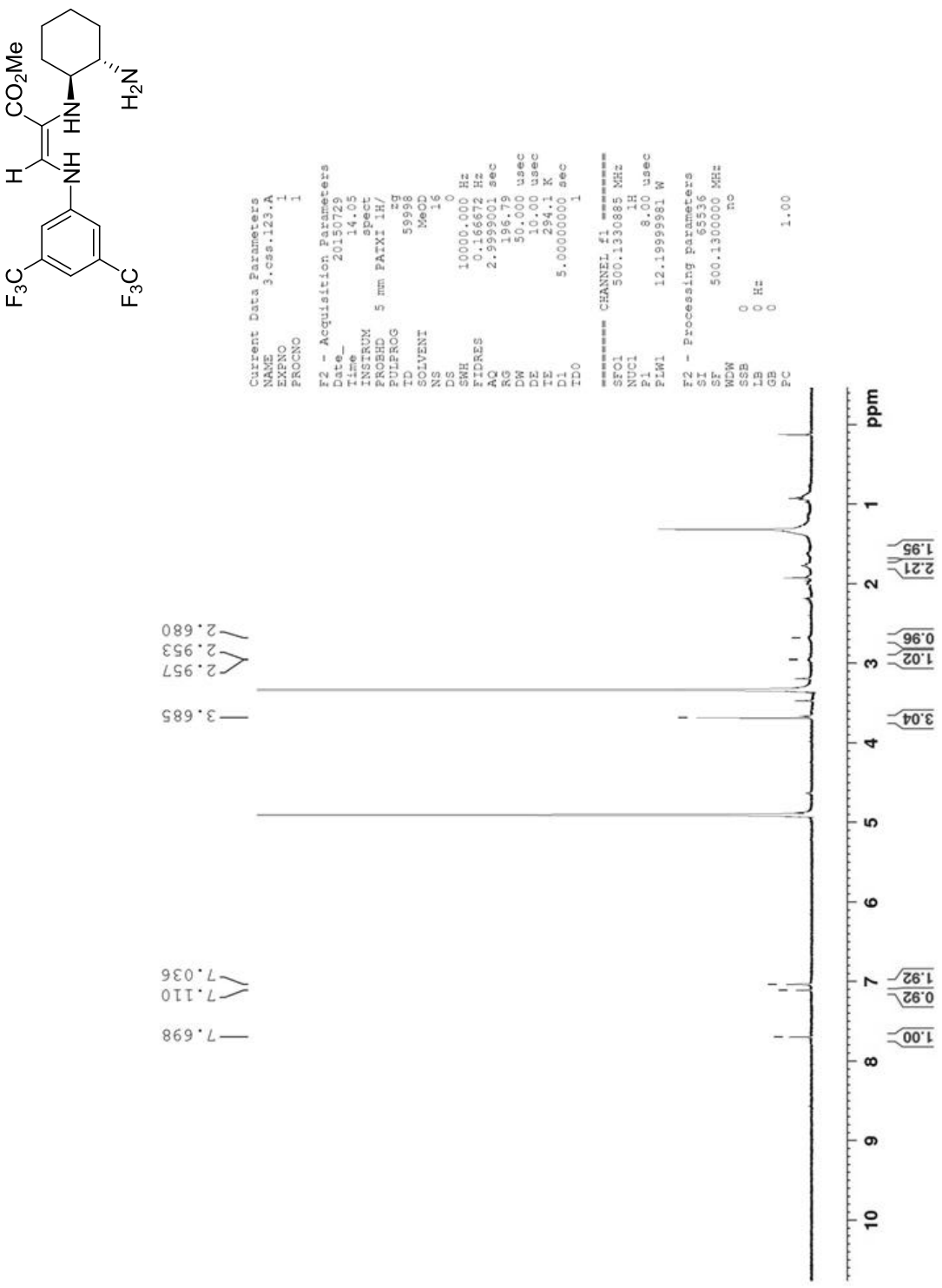

Figure 124: ^{1}H NMR Spectrum of 160 (500 MHz, CD_3OD, 298K)

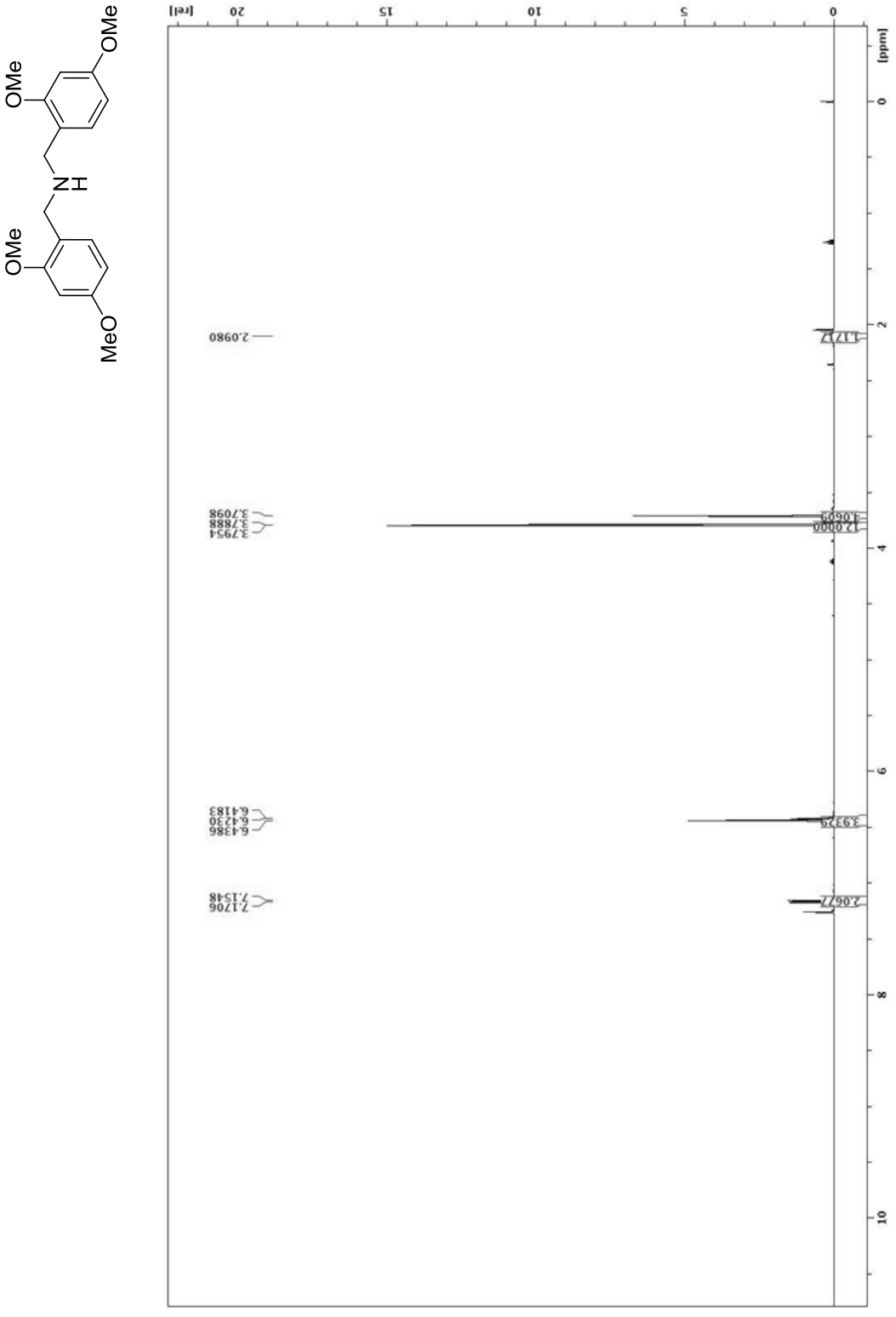

Figure 125: ^{1}H NMR Spectrum of 176 (500 MHz, $CDCl_3$, 298K)

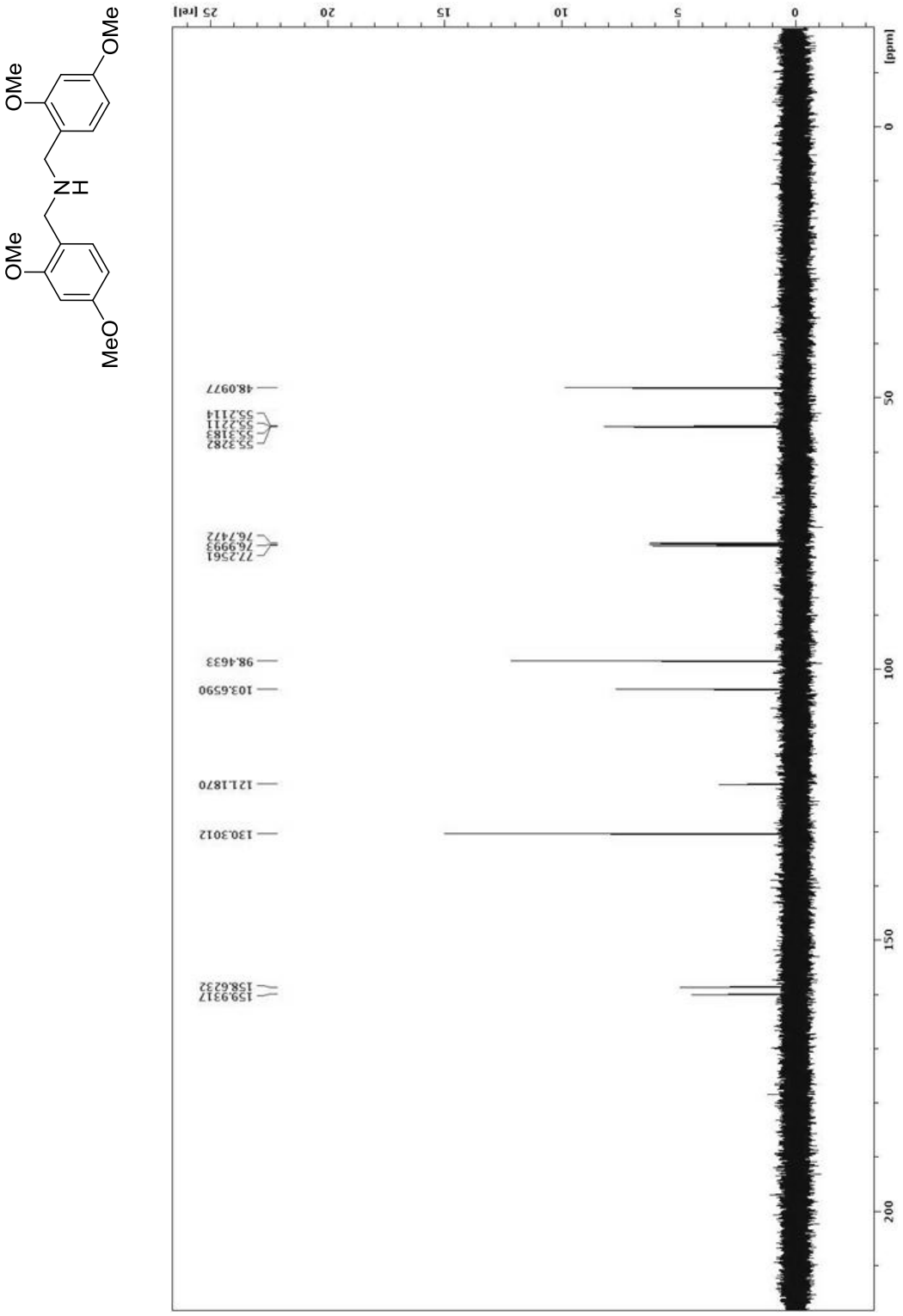

Figure 126: ^{13}C NMR Spectrum of 176 (125 MHz, $CDCl_3$, 298K)

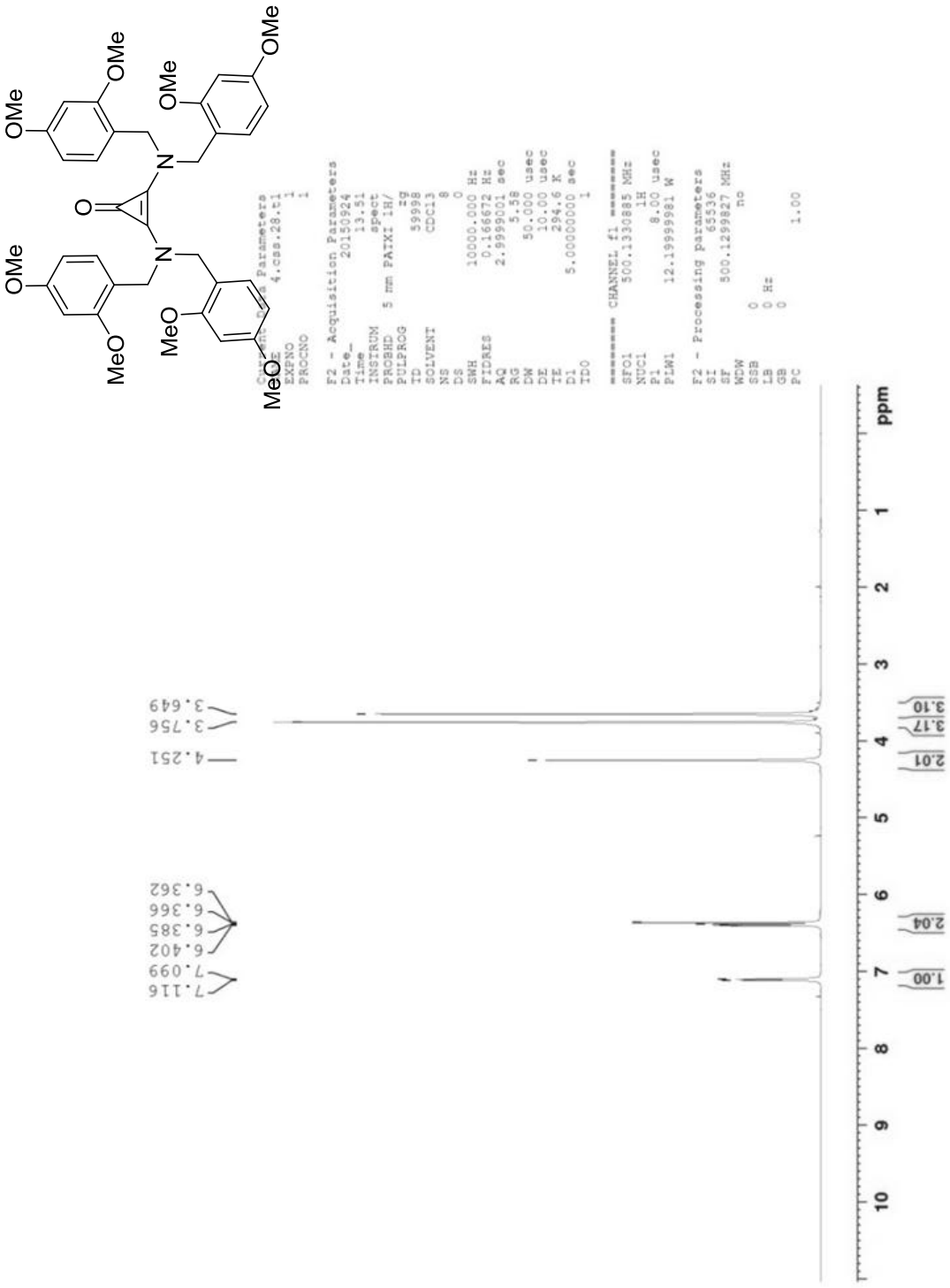

Figure 127: ^{1}H NMR Spectrum of 177 (500 MHz, $CDCl_3$, 298K)

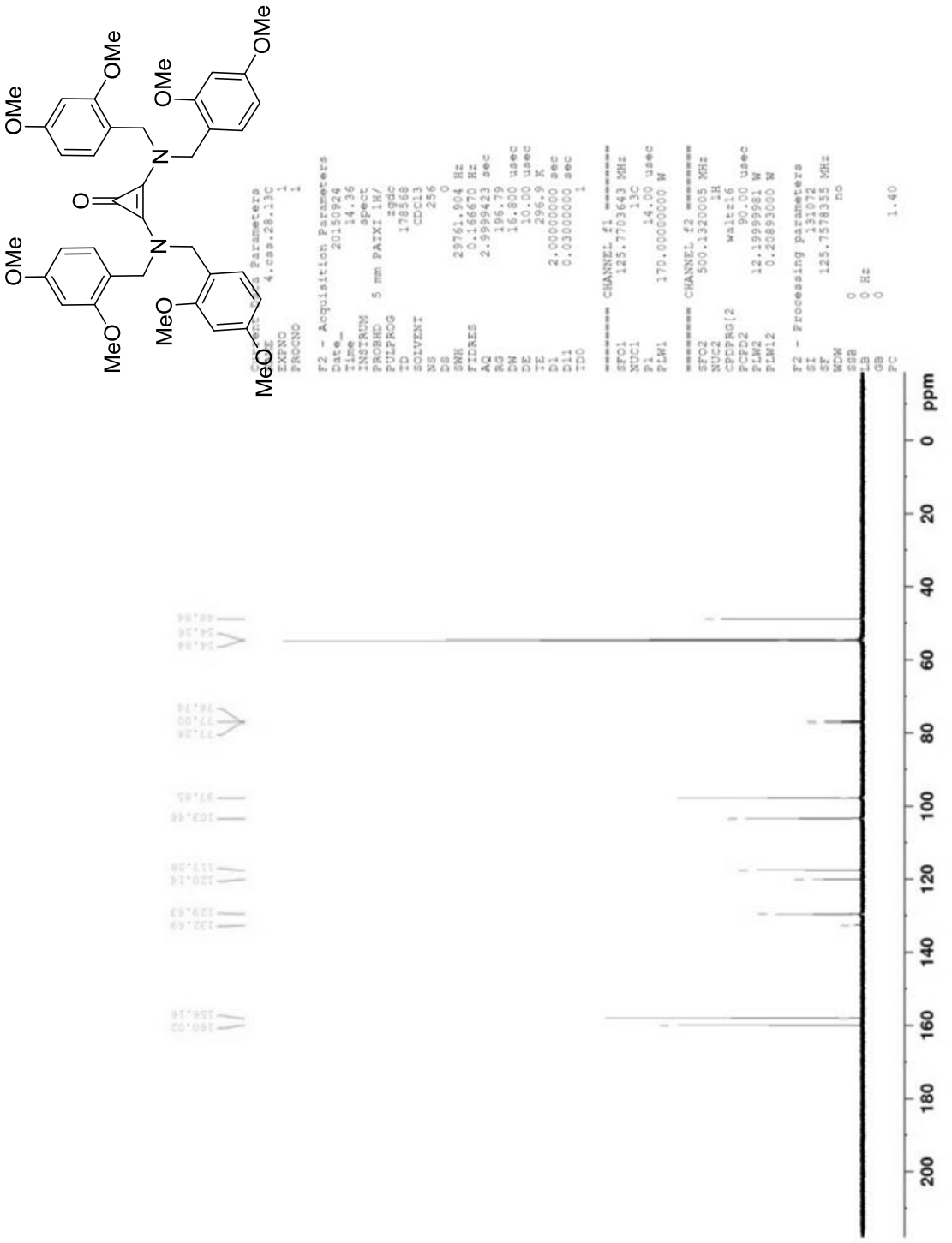

Figure 128: ^{13}C NMR Spectrum of 177 (125 MHz, $CDCl_3$, 298K)

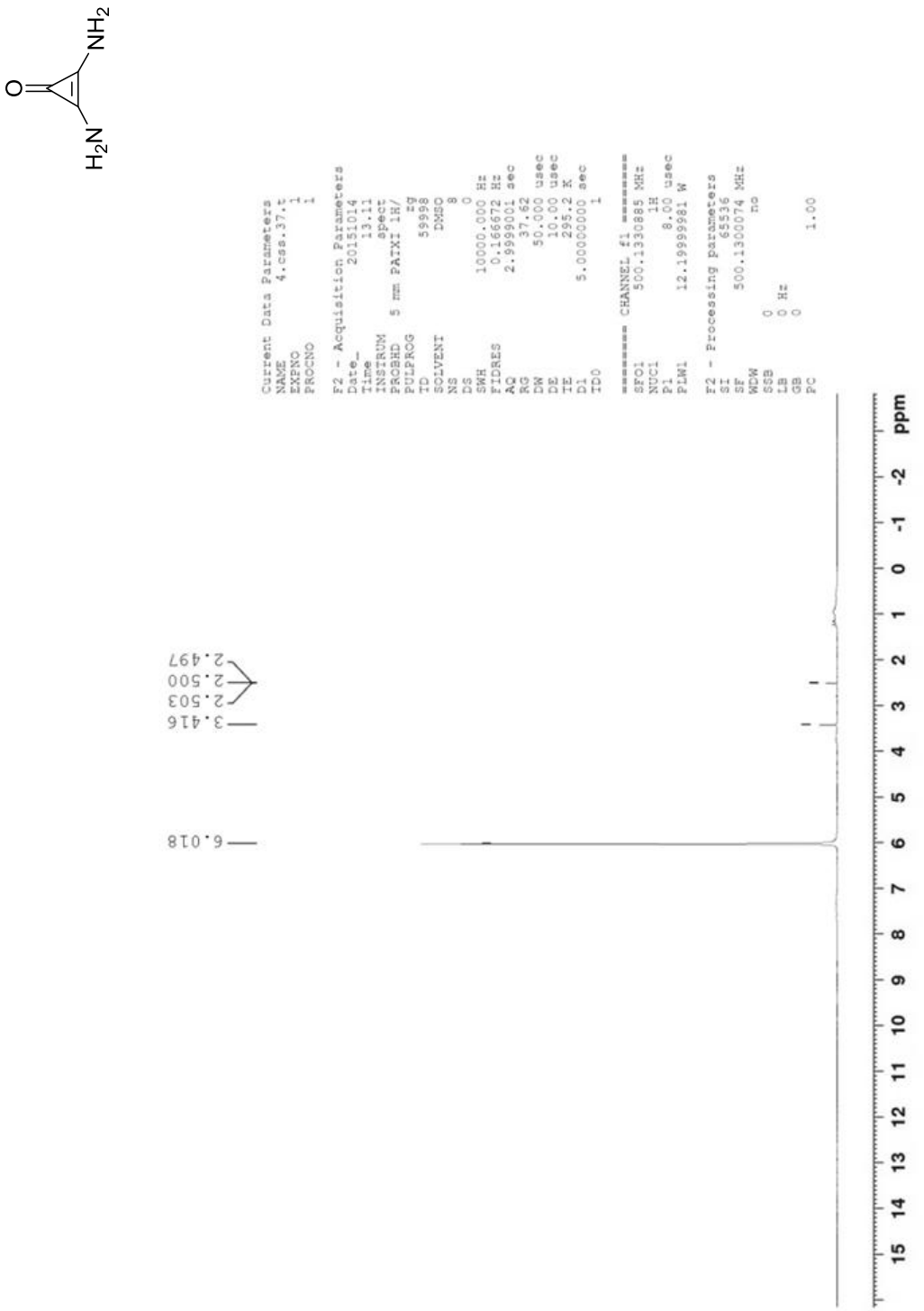

Figure 129: ^{1}H NMR Spectrum of 178 (500 MHz, d6-DMSO, 298K)

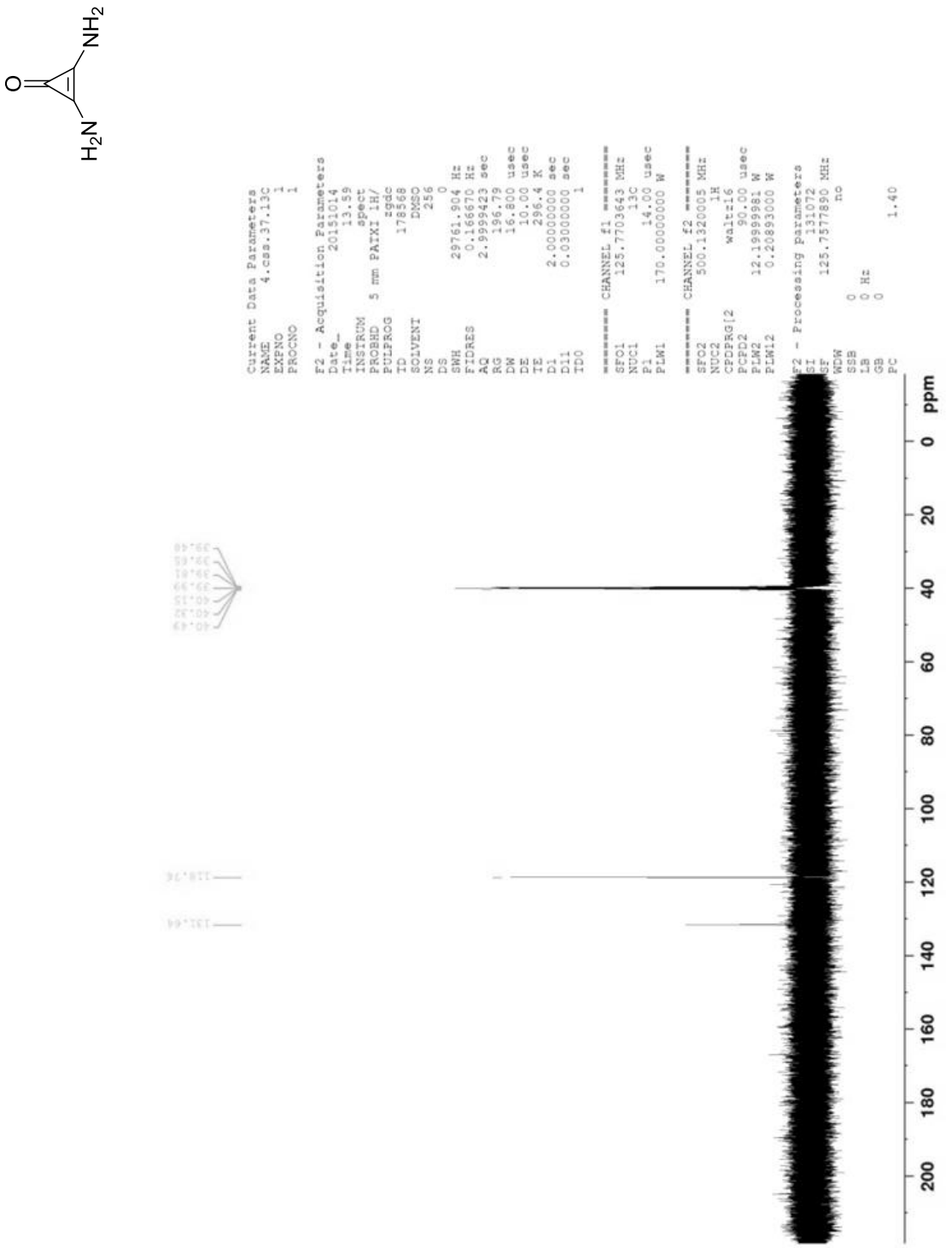

Figure 130: ^{13}C NMR Spectrum of 178 (125 MHz, d6-DMSO, 298K)

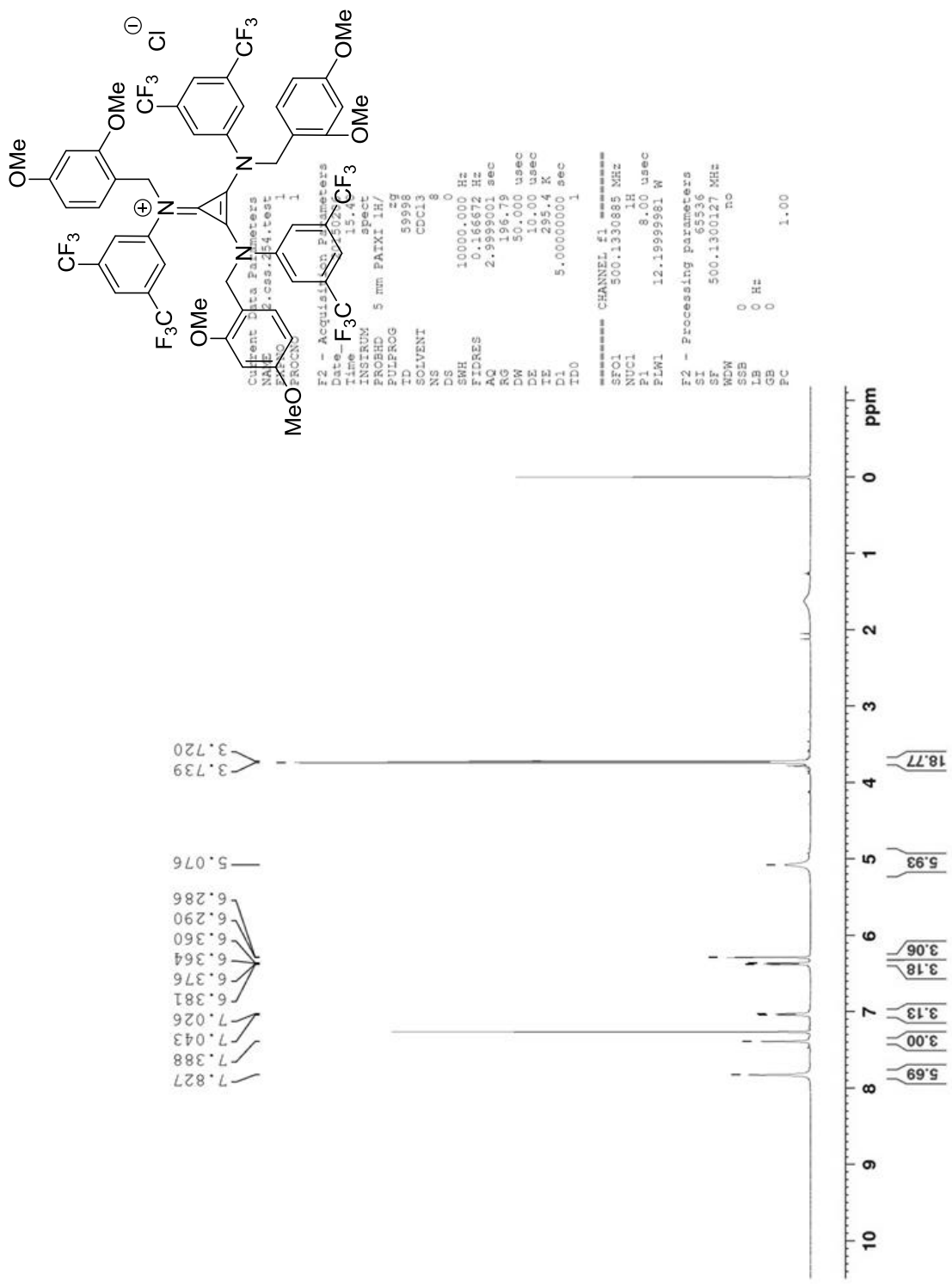

Figure 131: ^{1}H NMR Spectrum of 131 (500 MHz, $CDCl_3$, 298K)

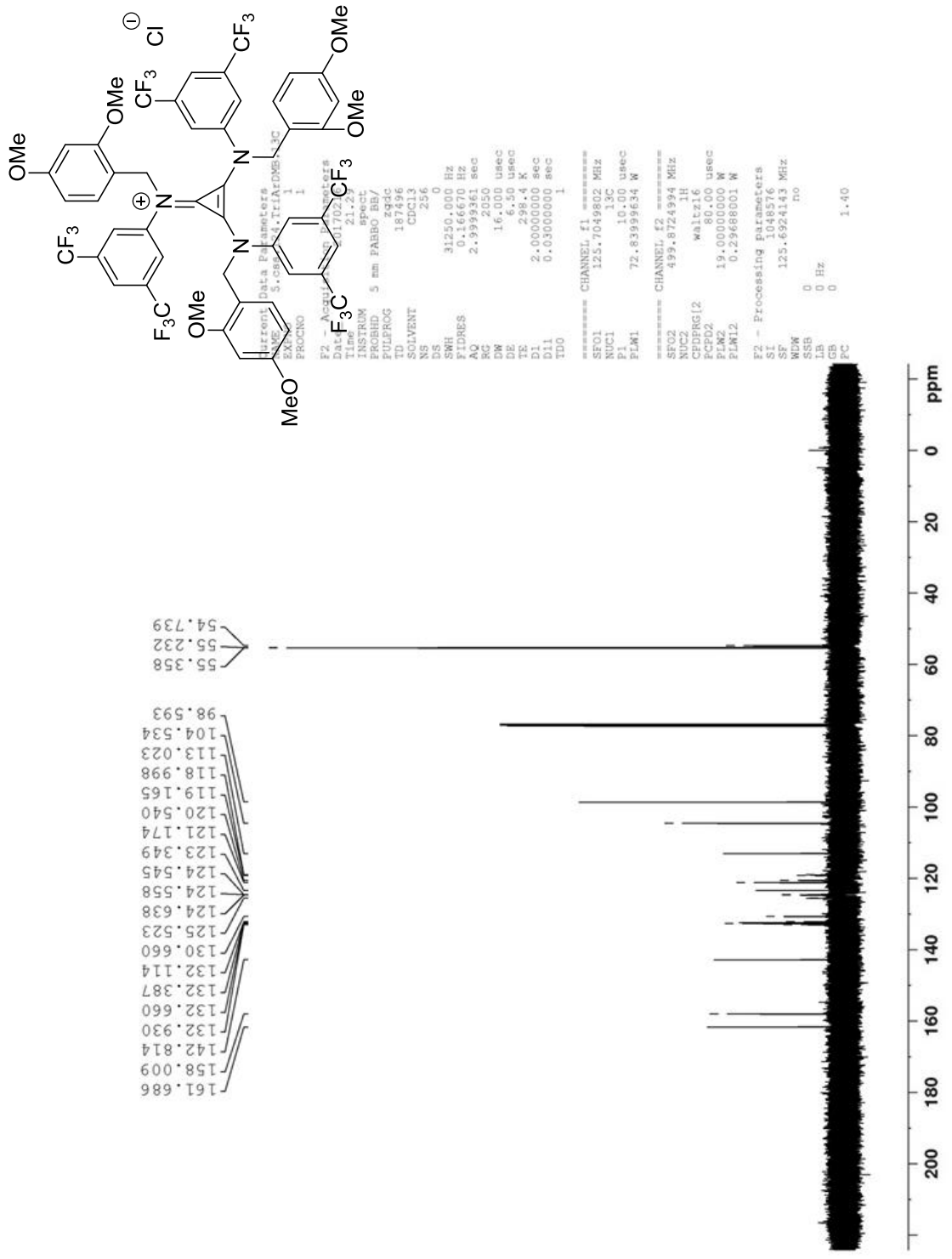

Figure 132: ^{13}C NMR Spectrum of 131 (125 MHz, $CDCl_3$, 298K)

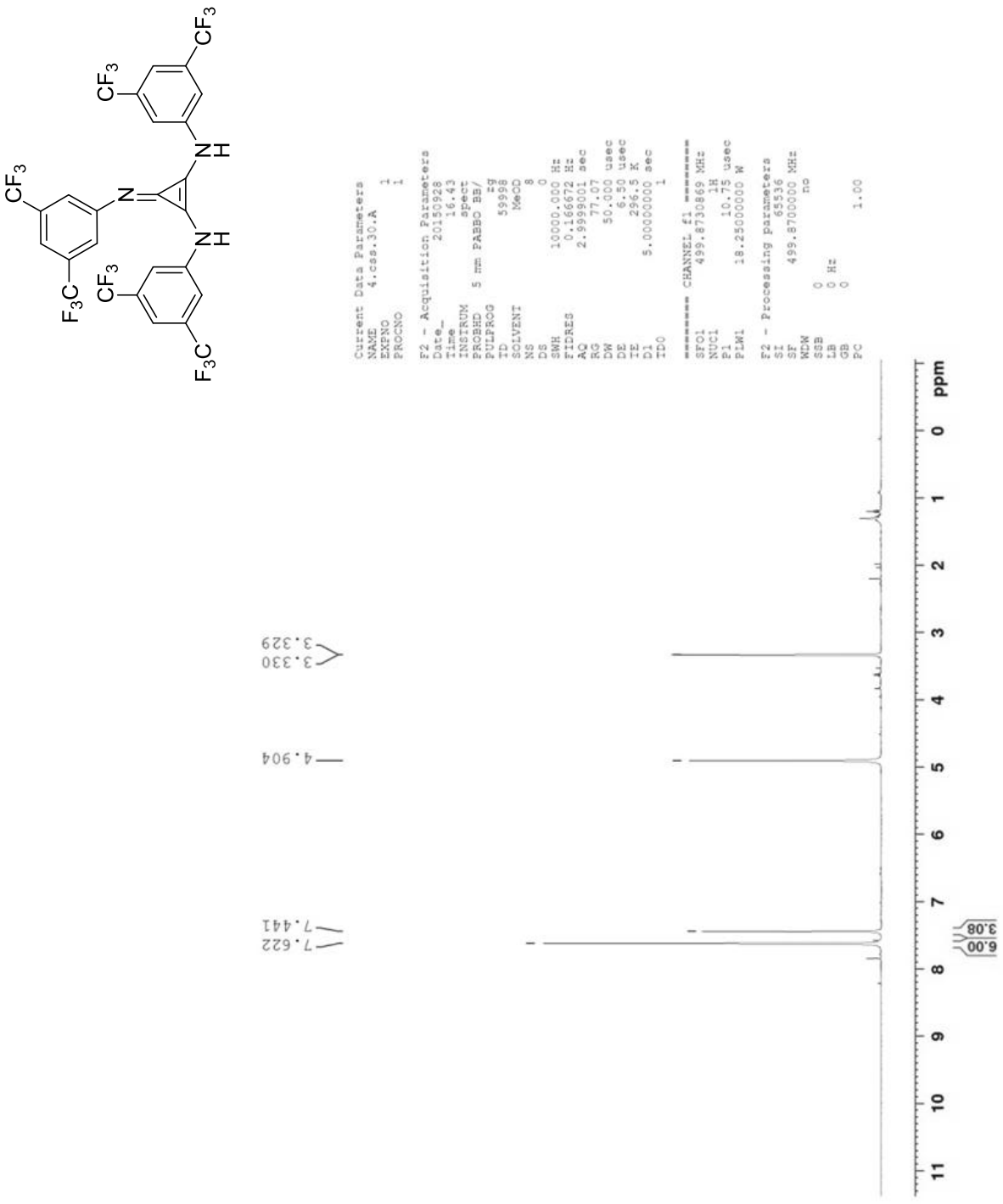

Figure 133: ^{1}H NMR Spectrum of 132 (500 MHz, CD_3OD, 298K)

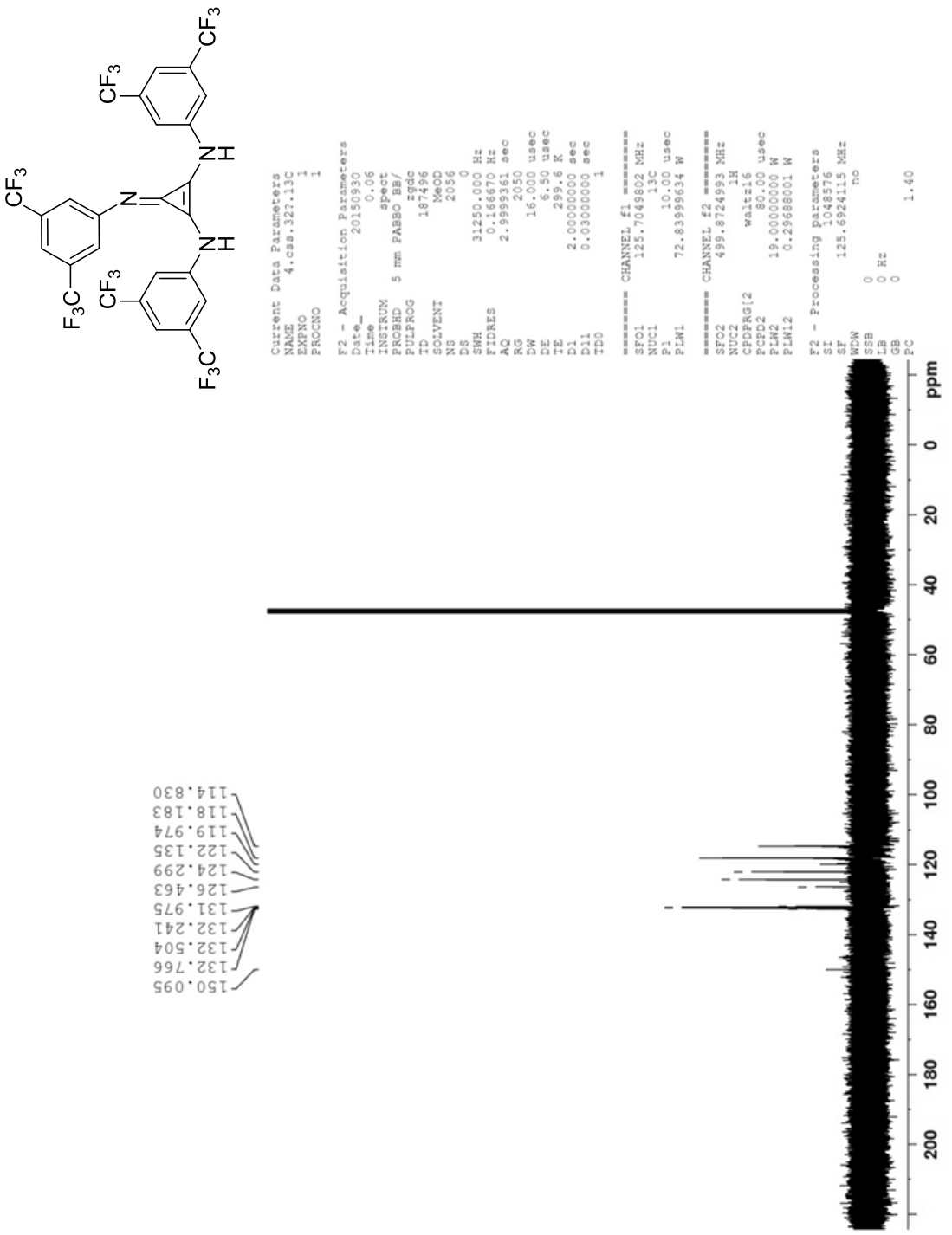

Figure 134: ^{13}C NMR Spectrum of 132 (125 MHz, CD_3OD, 298K)

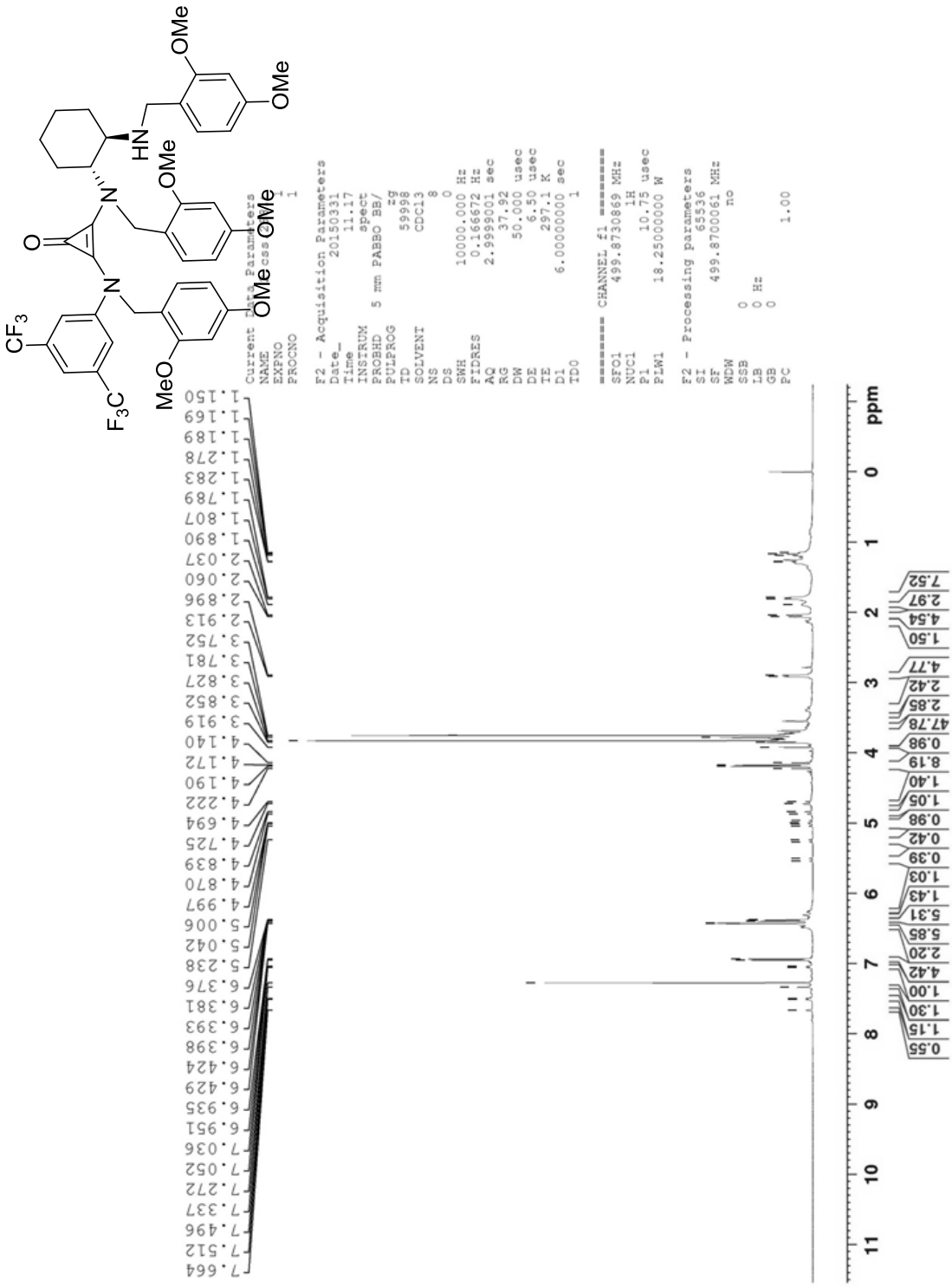

Figure 135: ^{1}H NMR Spectrum of 169 (500 MHz, $CDCl_3$, 298K)

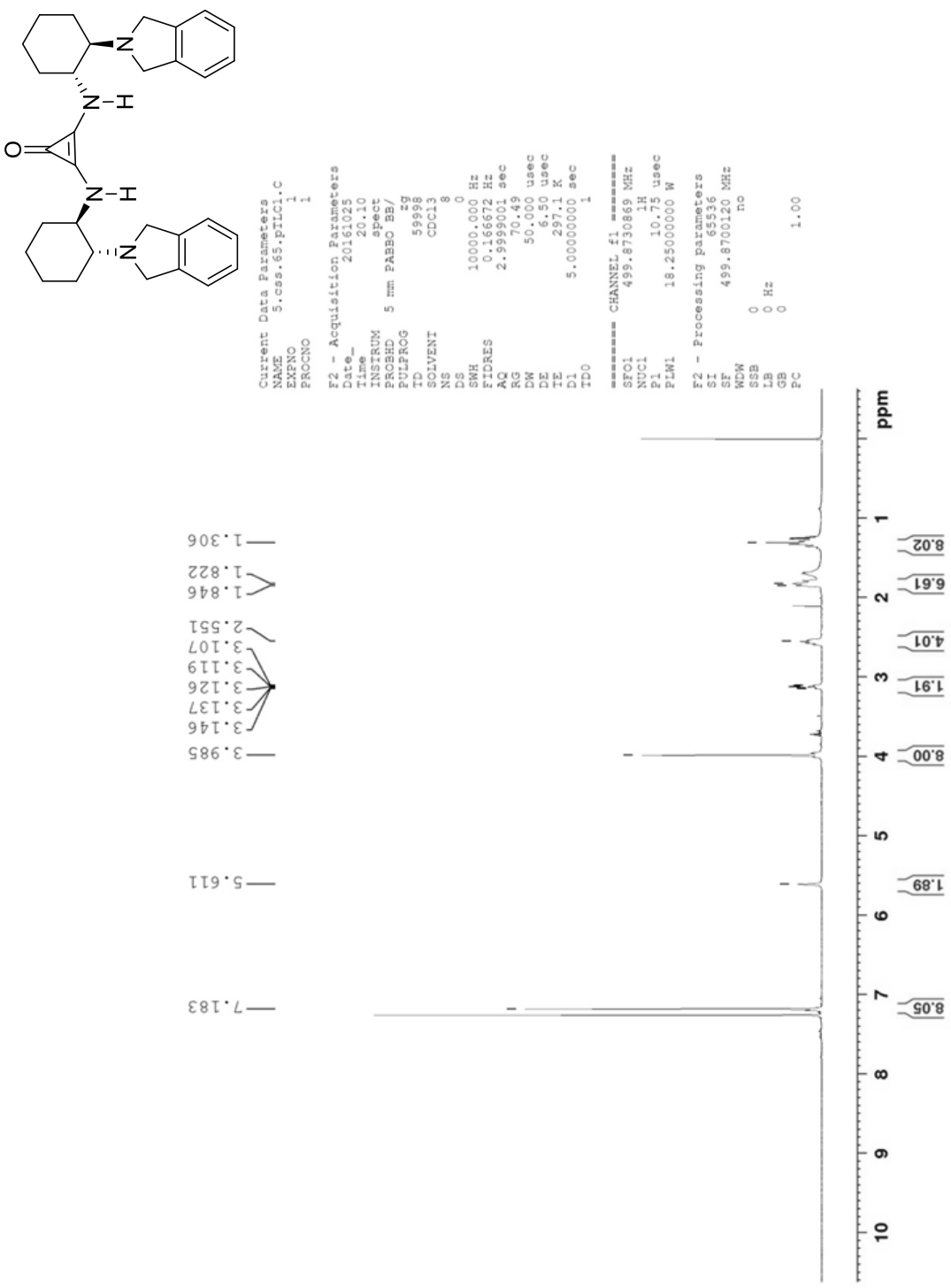

Figure 136: ^{1}H NMR Spectrum of 170 (500 MHz, $CDCl_3$, 298K)

0.3 mmol Et_3N + 0.3 mL CD_2Cl_2

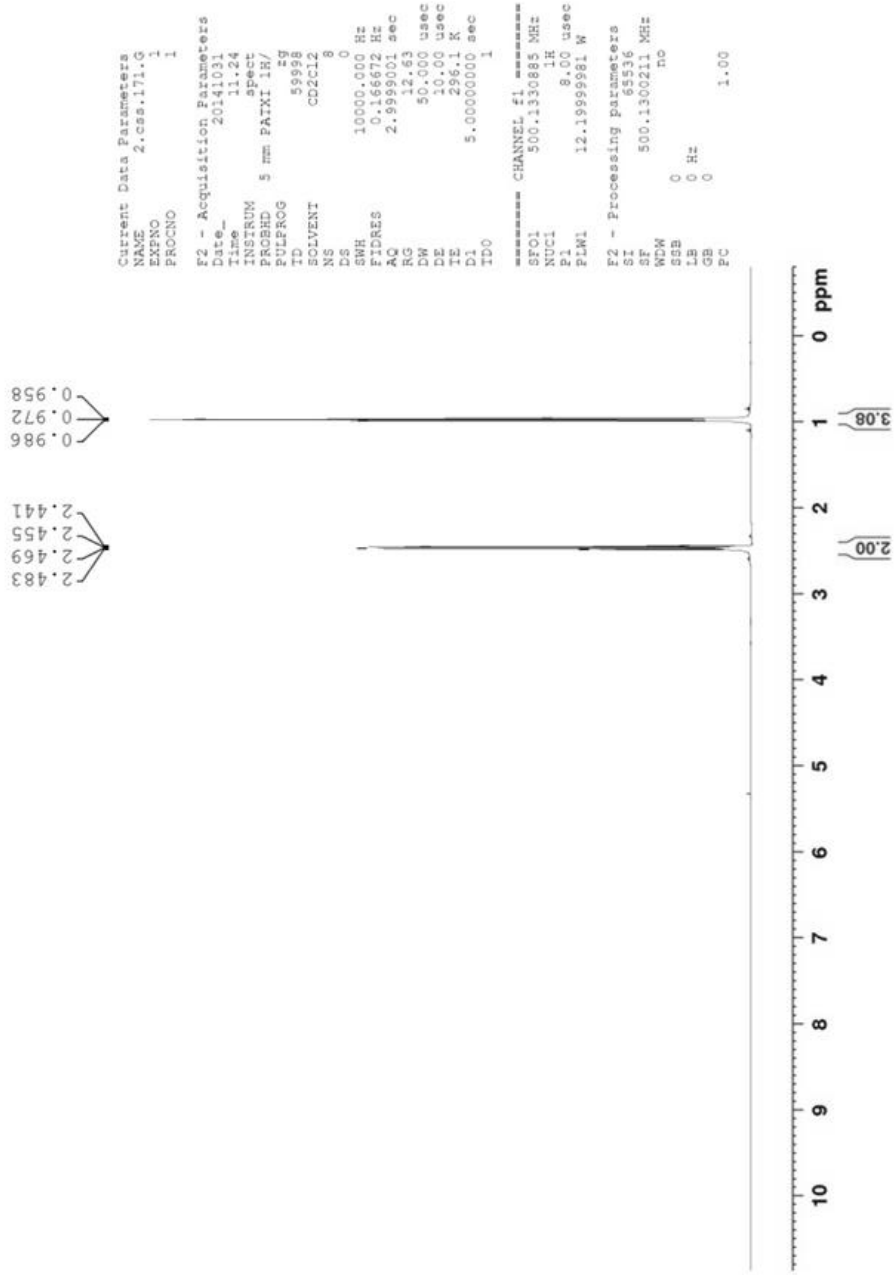

Figure 137: ^{1}H NMR Experiment 1a, Section II.7 (500 MHz, CD_2Cl_2, 298K)

0.3 mL CD_2Cl_2 + 0.3 mmol Et_3N + 0.3 mmol TCCP
(NMR recorded within 10 minutes)

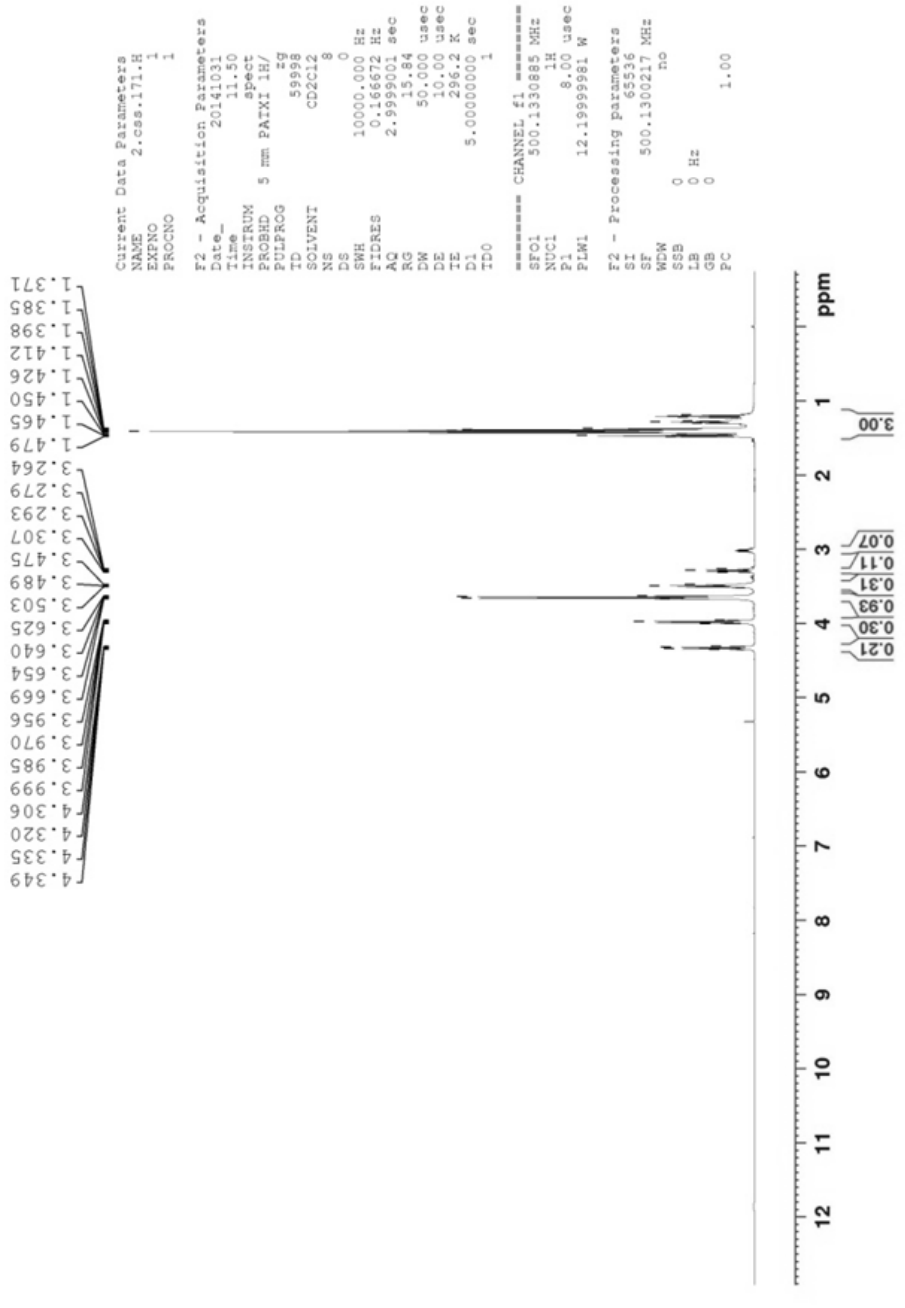

Figure 138: ^{1}H NMR Experiment 1b, Section II.7 (500 MHz, CD_2Cl_2, 298K)

0.3 mL CD_2Cl_2 + 0.3 mmol Et_3N + 0.3 mmol TCCP
(NMR recorded 3 hours after addition of TCCP)

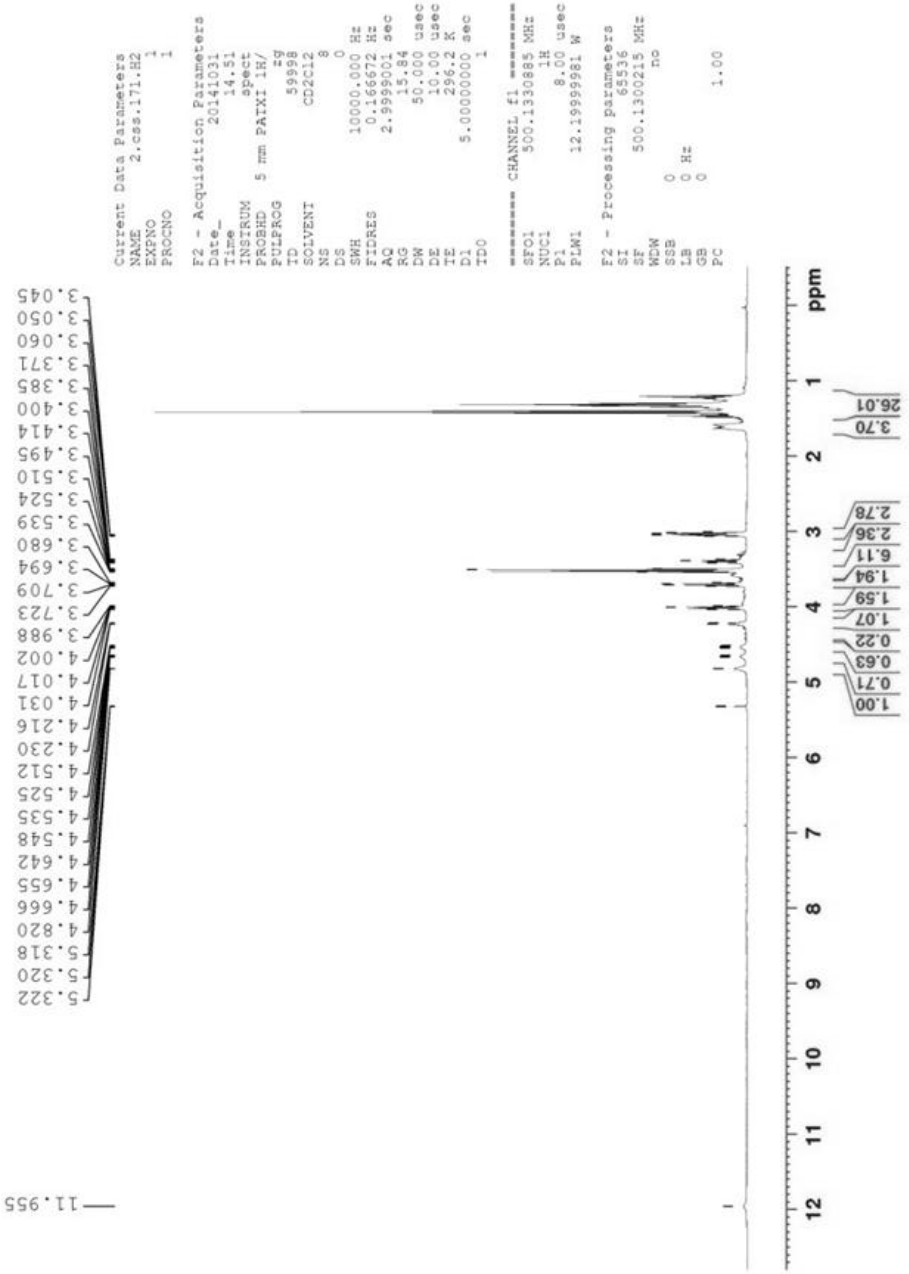

Figure 139: ^{1}H NMR Experiment 1c, Section II.7 (500 MHz, CD_2Cl_2, 298K)

0.3 mL CD_2Cl_2 + 0.3 mmol iPr_2NH

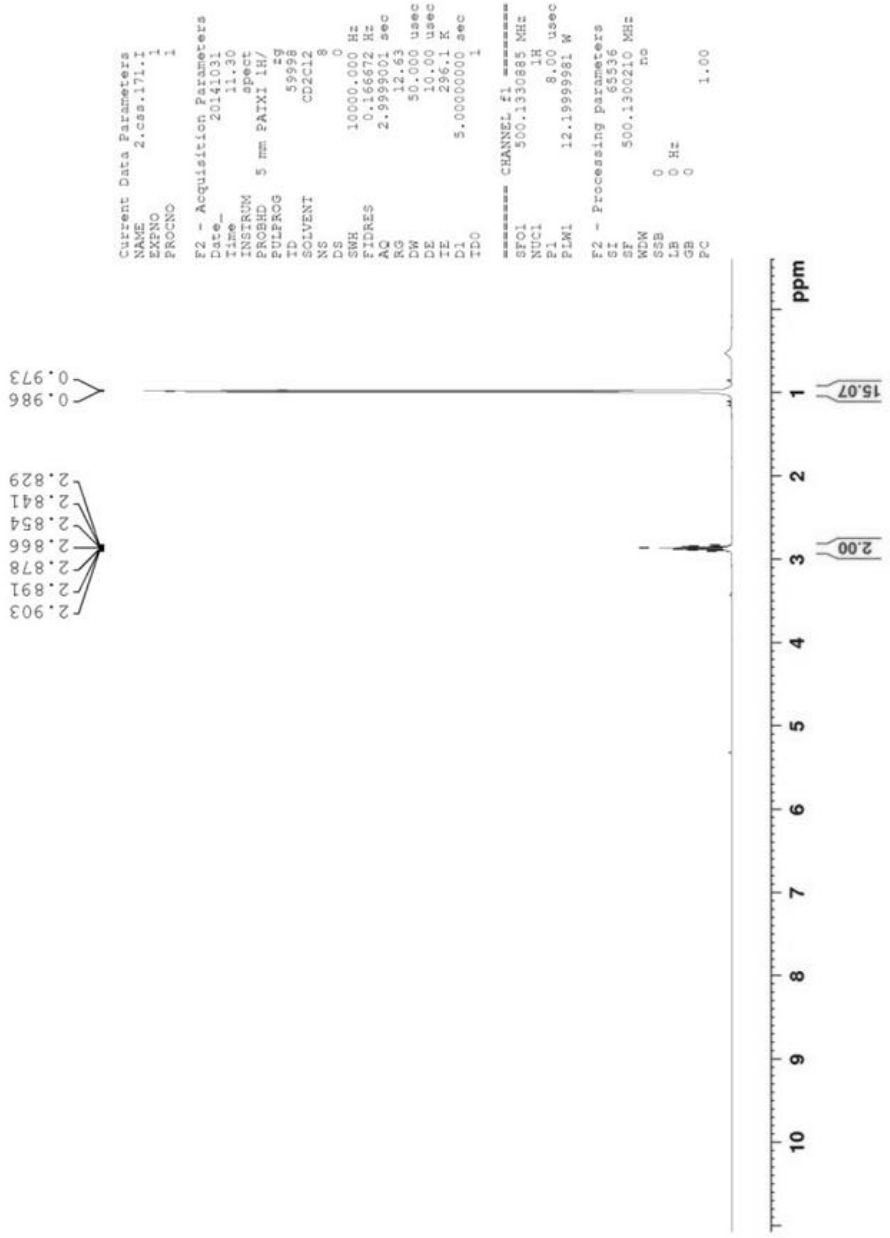

Figure 140: ^{1}H NMR Experiment 2a, Section II.7 (500 MHz, CD_2Cl_2, 298K)

0.3 mL CD_2Cl_2 + 0.3 mmol iPr_2NH + 0.3 mmol TCCP
(NMR recorded within 10 minutes of addition of TCCP)

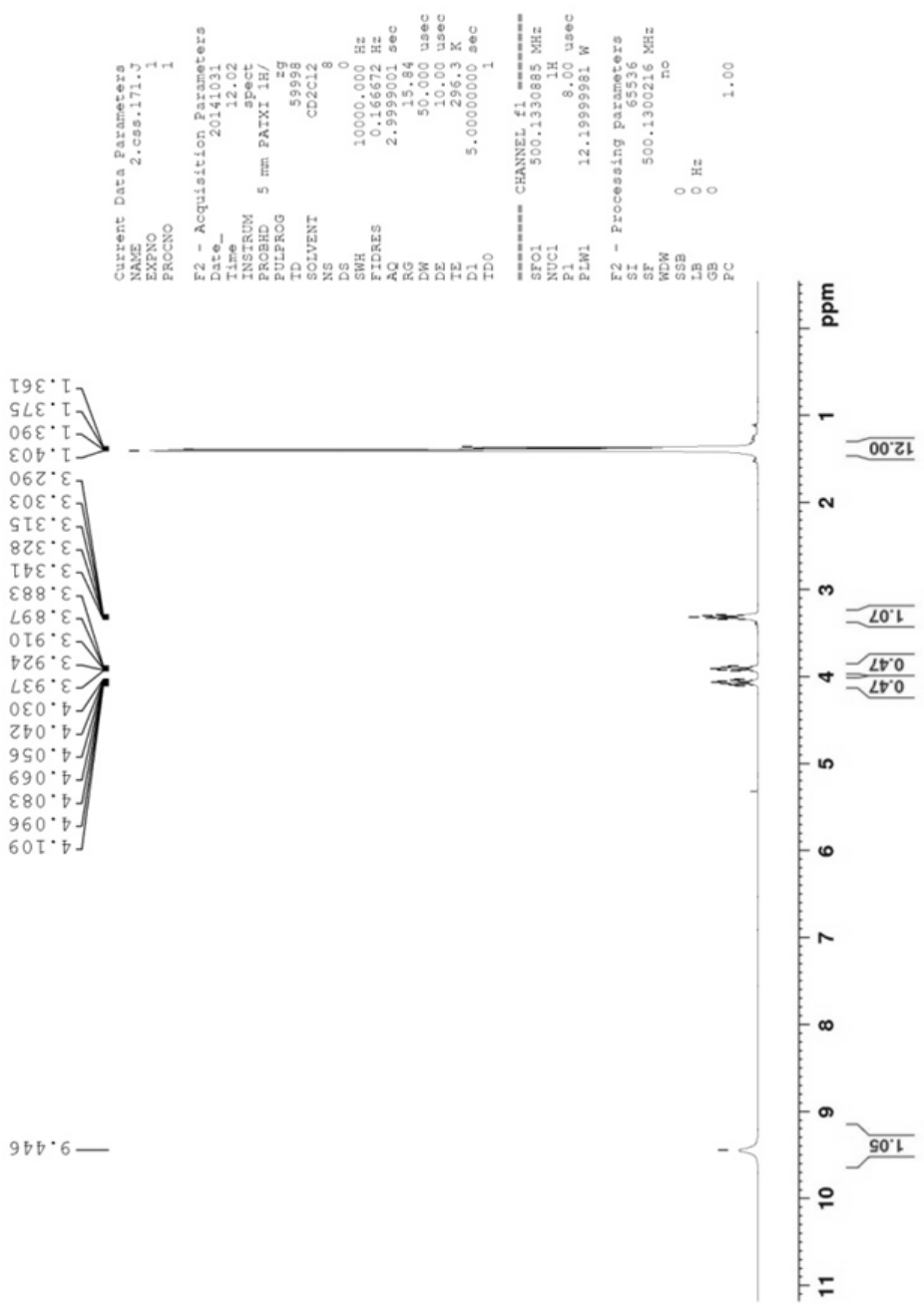

Figure 141: ^{1}H NMR Experiment 2b, Section II.7 (500 MHz, CD_2Cl_2, 298K)

0.3 mL CD_2Cl_2 + 0.3 mmol iPr_2NH + 0.3 mmol TCCP
(NMR recorded 3 hours after addition of TCCP)

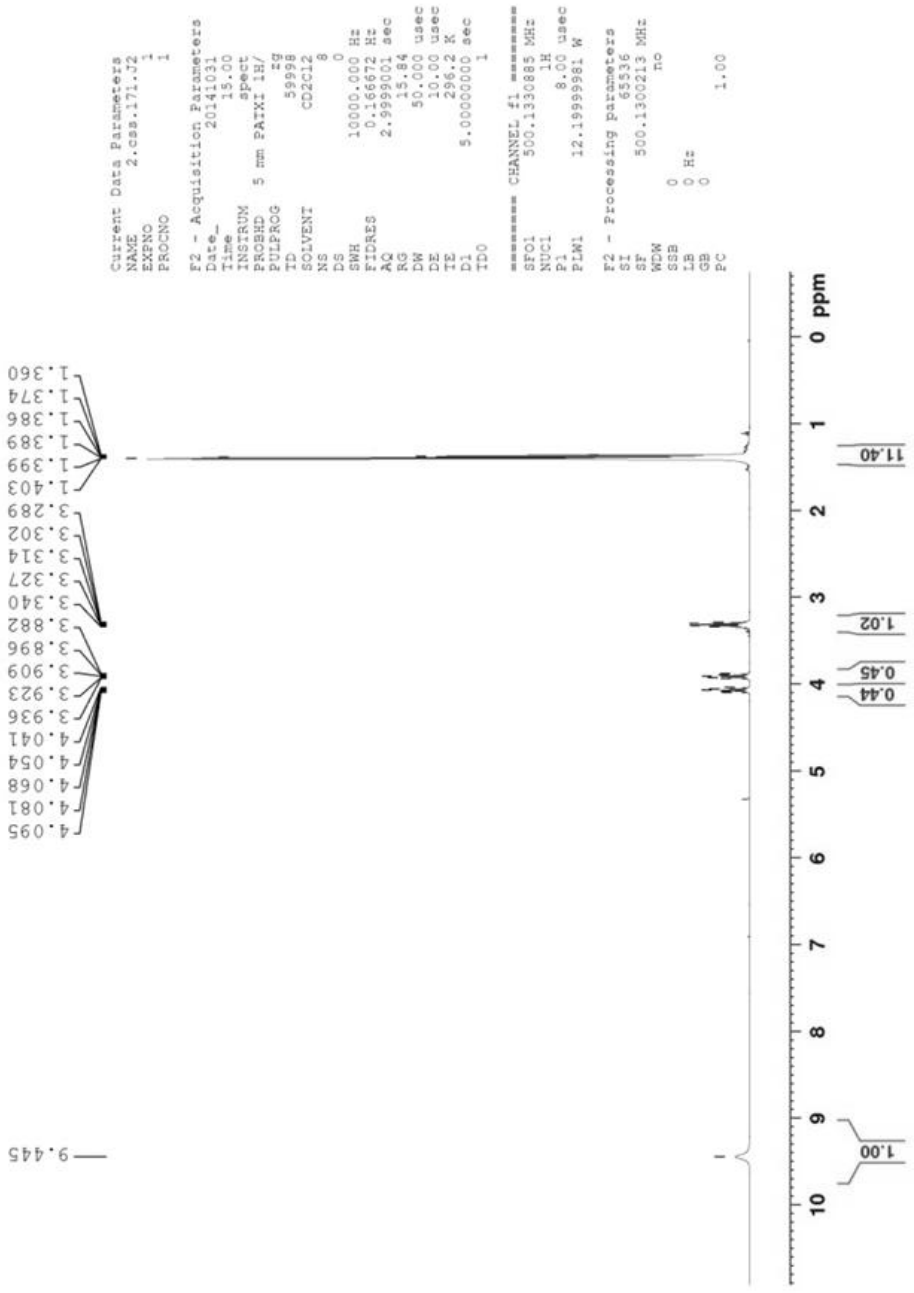

Figure 142: ^{1}H NMR Experiment 2c, Section II.7 (500 MHz, CD_2Cl_2, 298K)

0.3 mL CD_2Cl_2 + 0.3 mmol iPr_2NH + 0.3 mmol TCCP + 1.5 mmol Et_3N
(NMR recorded within 10 minutes of addition of Et_3N)

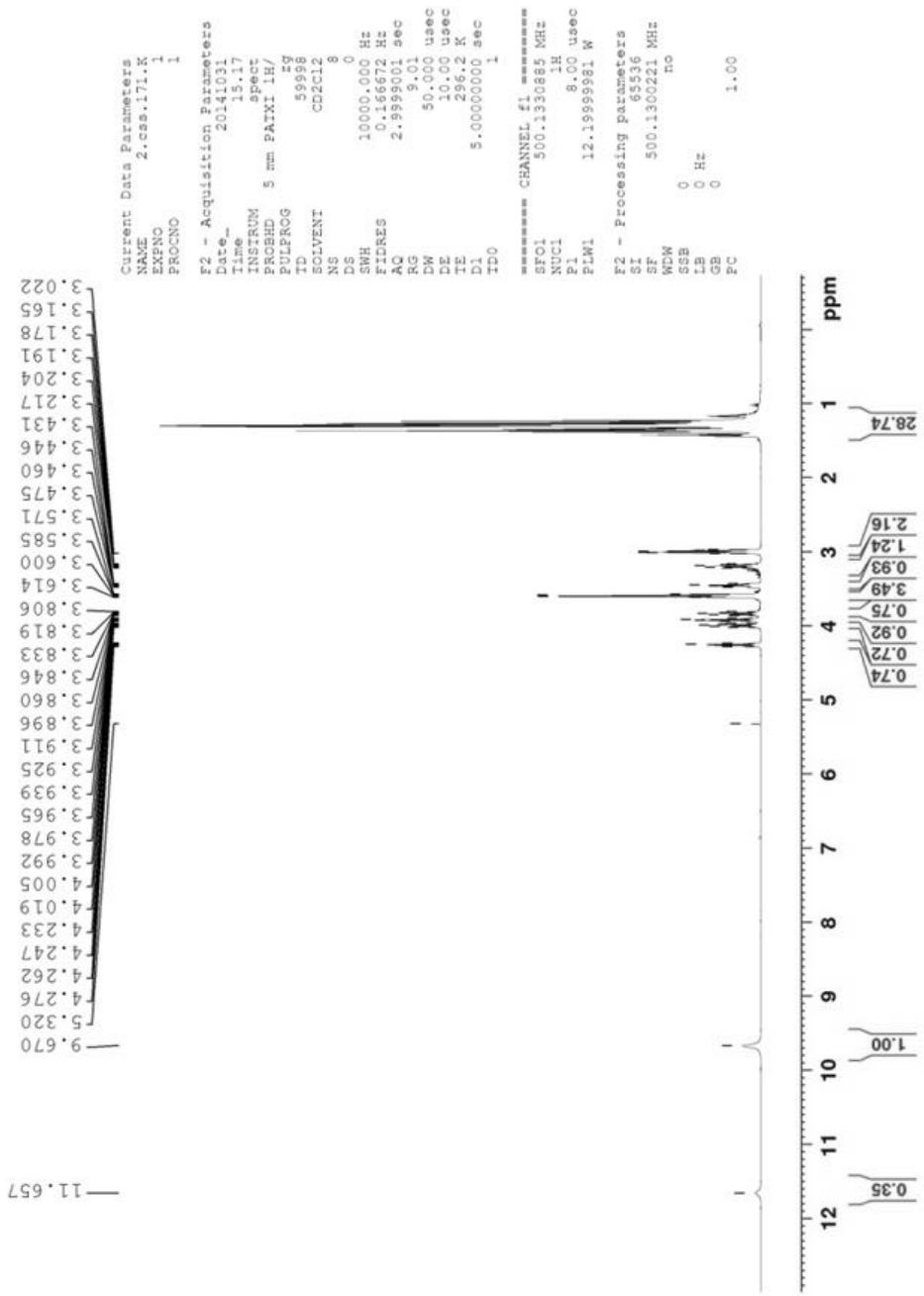

Figure 143: ^{1}H NMR Experiment 2d, Section II.7 (500 MHz, CD_2Cl_2, 298K)

0.3 mL CD_2Cl_2 + 0.3 mmol iPr_2NH + 0.3 mmol TCCP + 1.5 mmol Et_3N
(NMR recorded 2.5 hours after the addition of Et_3N)

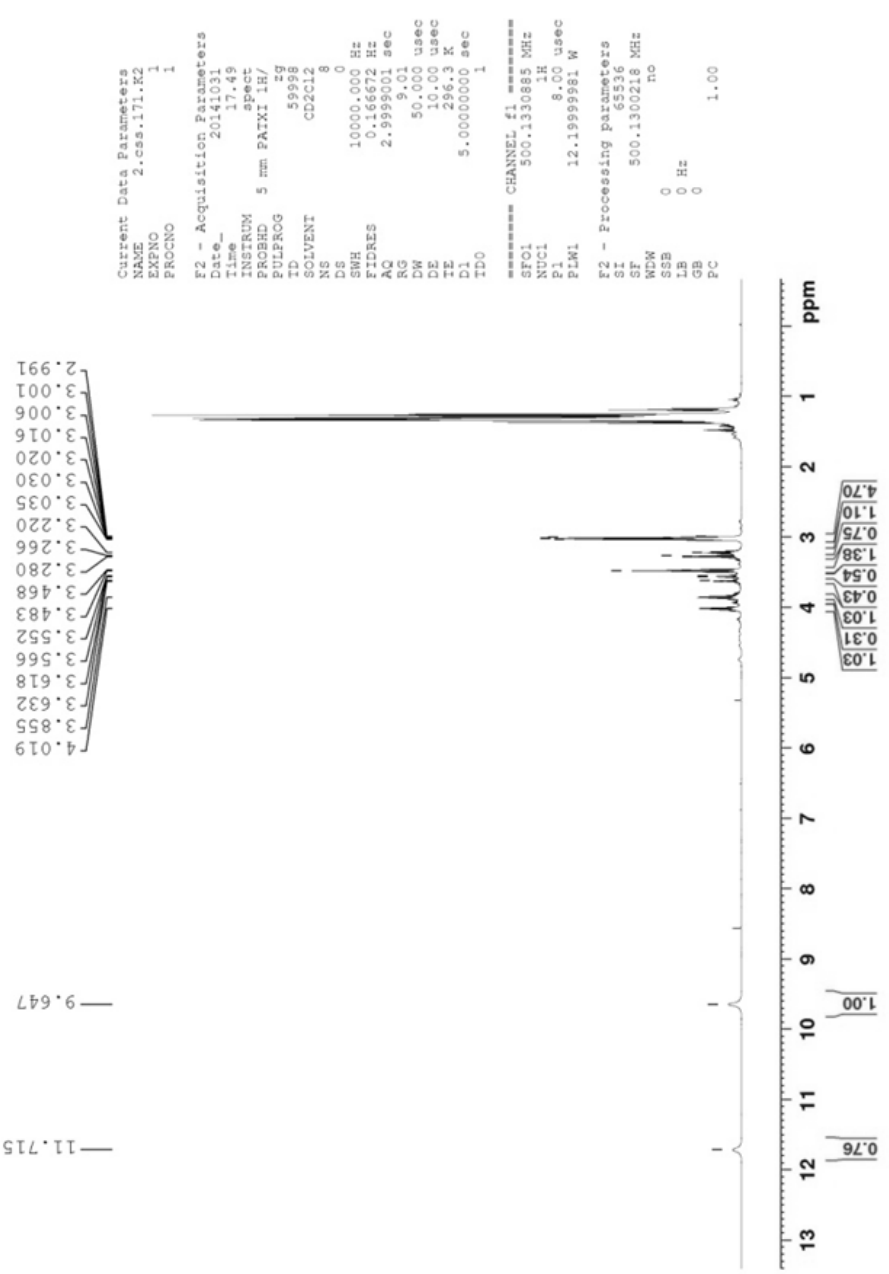

Figure 144: ^{1}H NMR Experiment 2e, Section II.7 (500 MHz, CD_2Cl_2, 298K)

0.3 mL CD_2Cl_2 + 0.3 mmol compound **136**

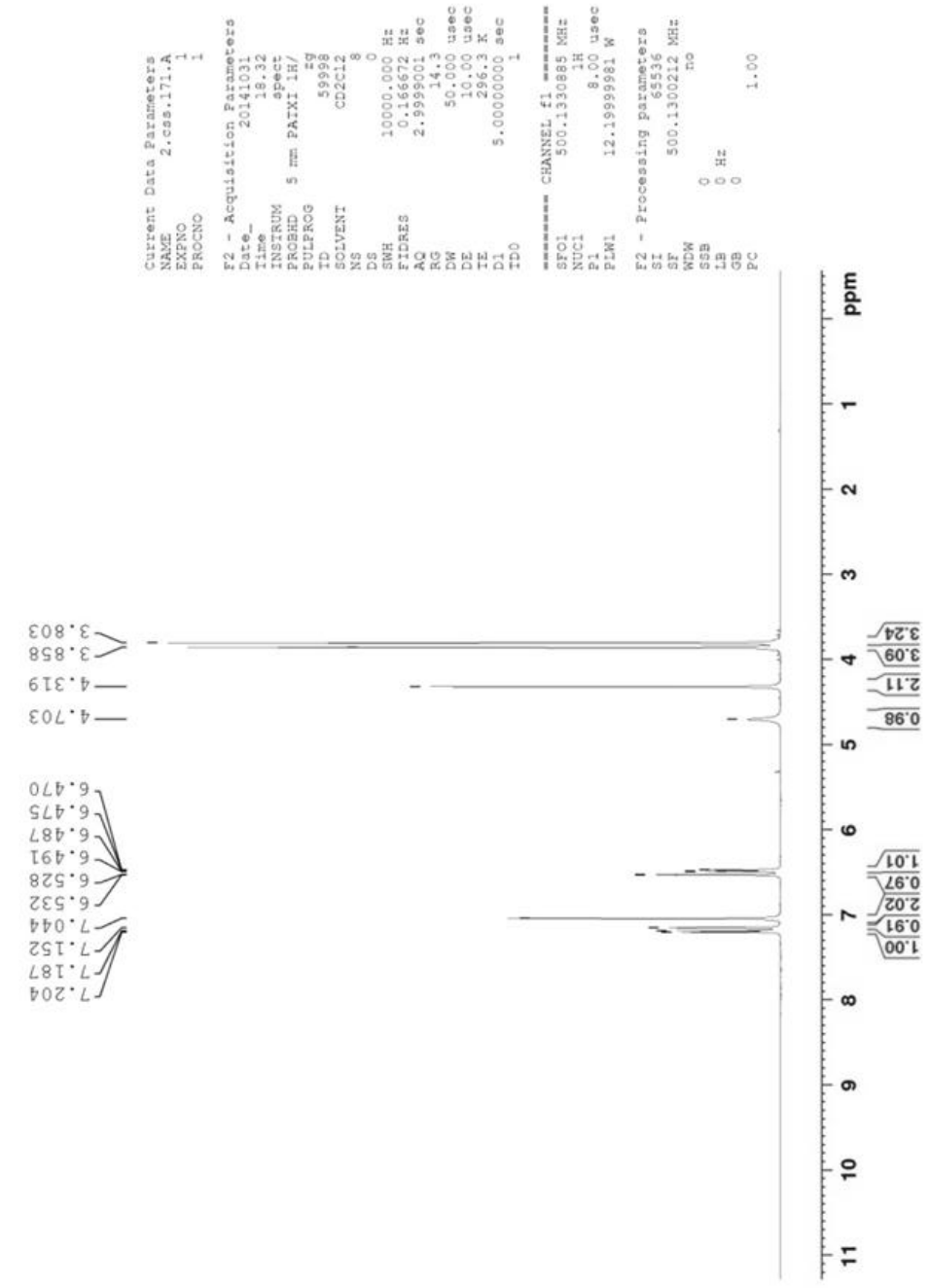

Figure 145: ^{1}H NMR Experiment 3a, Section II.7 (500 MHz, CD_2Cl_2, 298K)

0.3 mL CD_2Cl_2 + 0.3 mmol **136** + 0.3 mmol TCCP
(NMR recorded within 10 minutes of addition of TCCP)

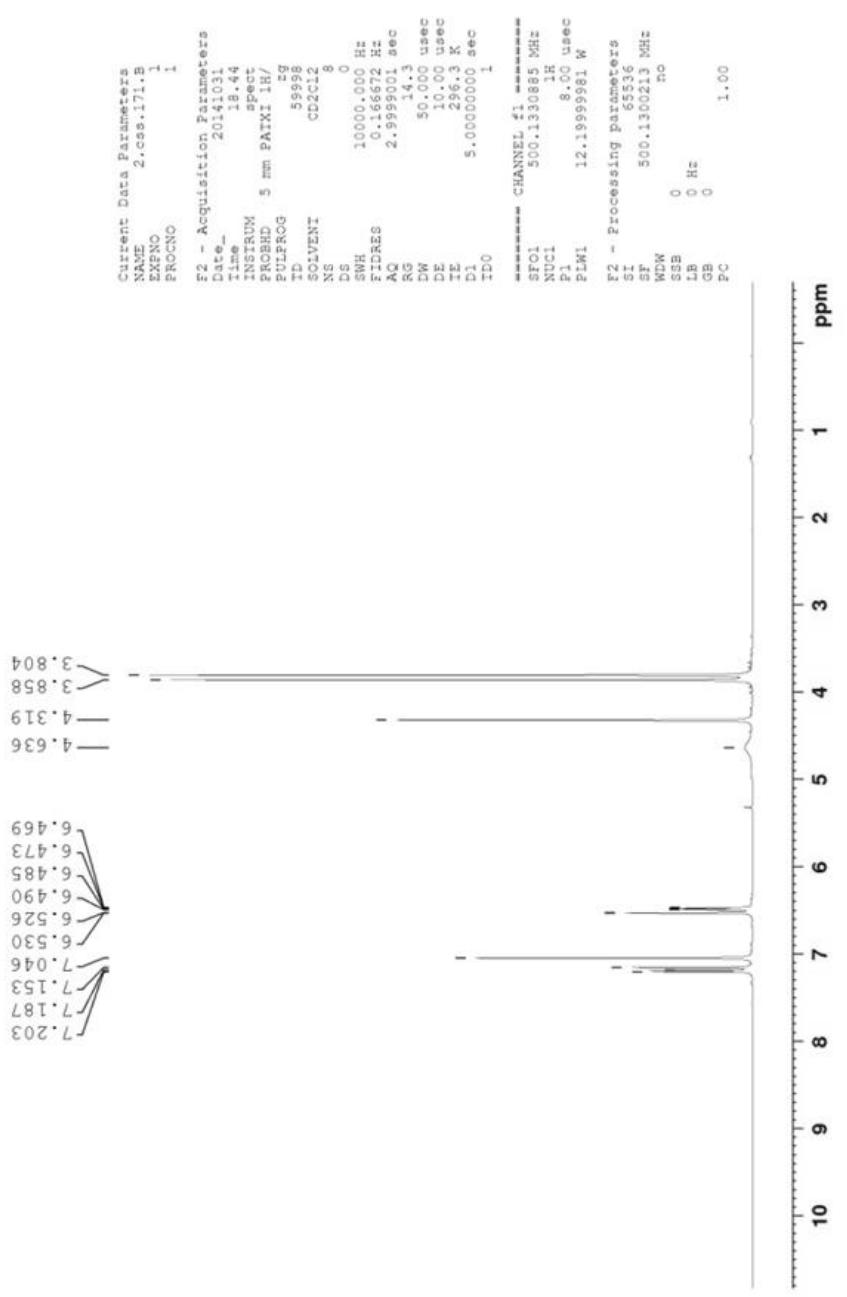

Figure 146: ^{1}H NMR Experiment 3b, Section II.7 (500 MHz, CD_2Cl_2, 298K)

0.3 mL CD_2Cl_2 + 0.3 mmol **136** + 0.3 mmol TCCP
(NMR recorded 64 hours after addition of TCCP)

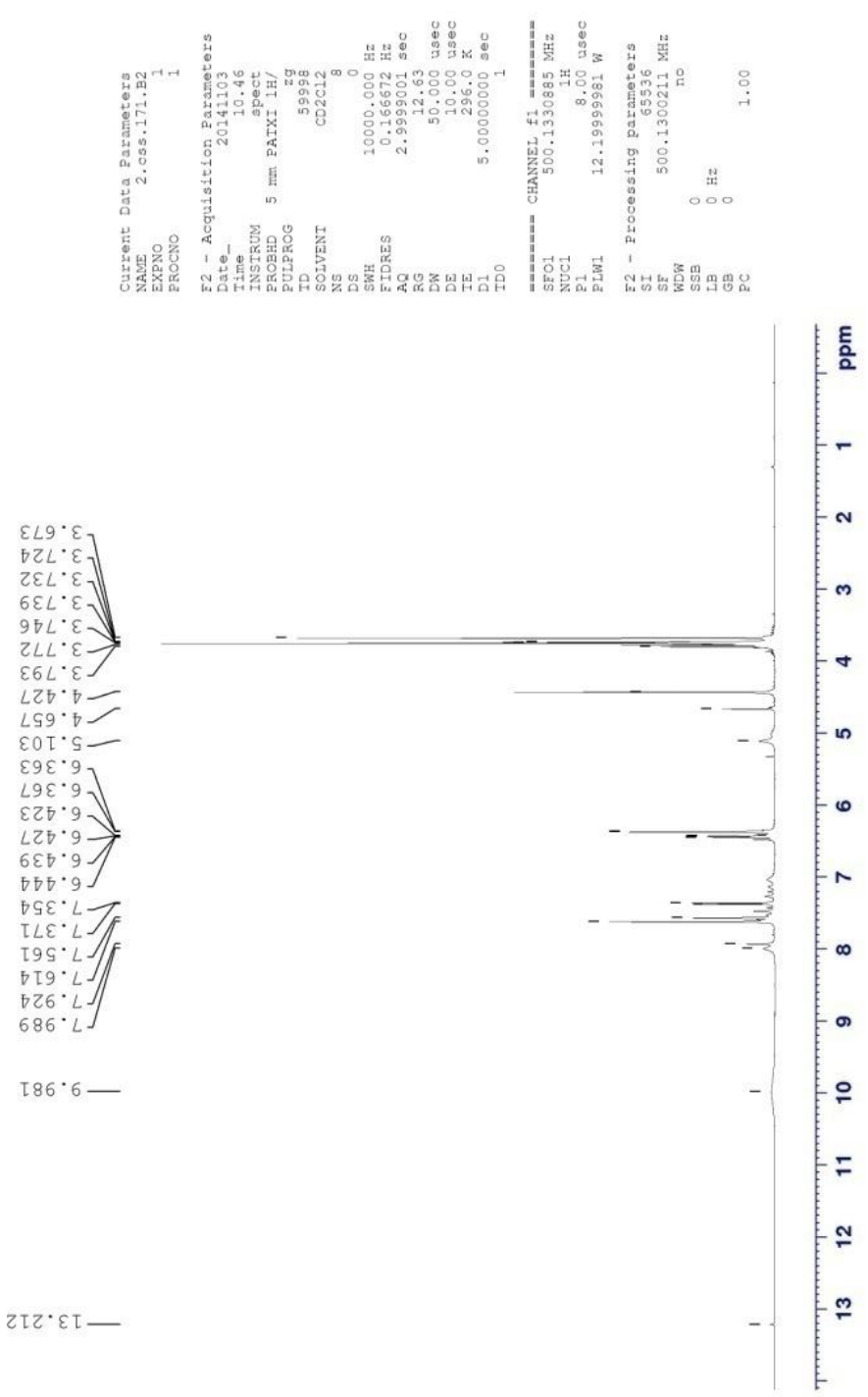

Figure 147: ^{1}H NMR Experiment 3c, Section II.7 (500 M Hz, CD_2Cl_2, 298K)

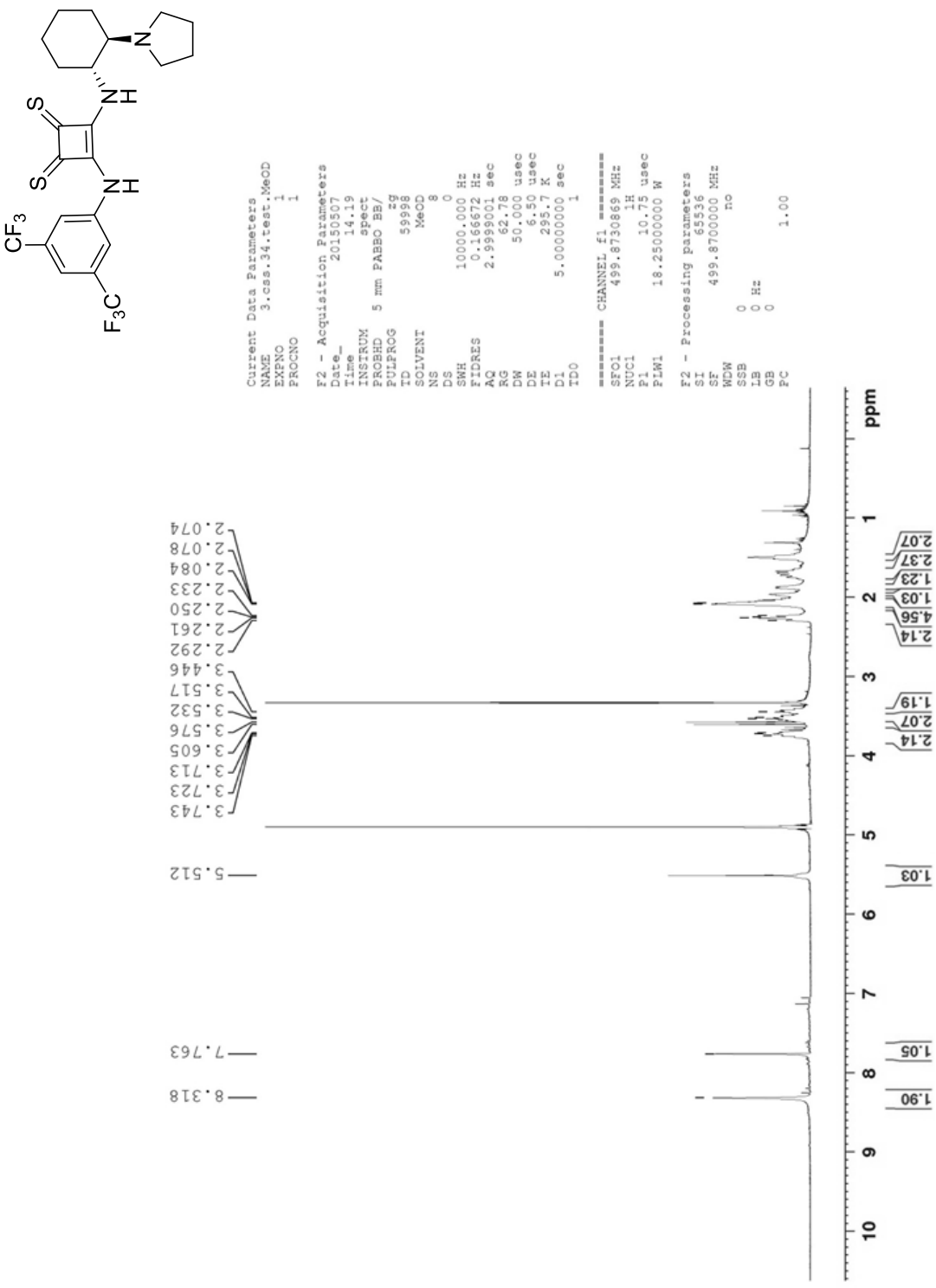

Figure 148: ^{1}H NMR Spectrum of 173 (500 MHz, CD_3OD, 298K)

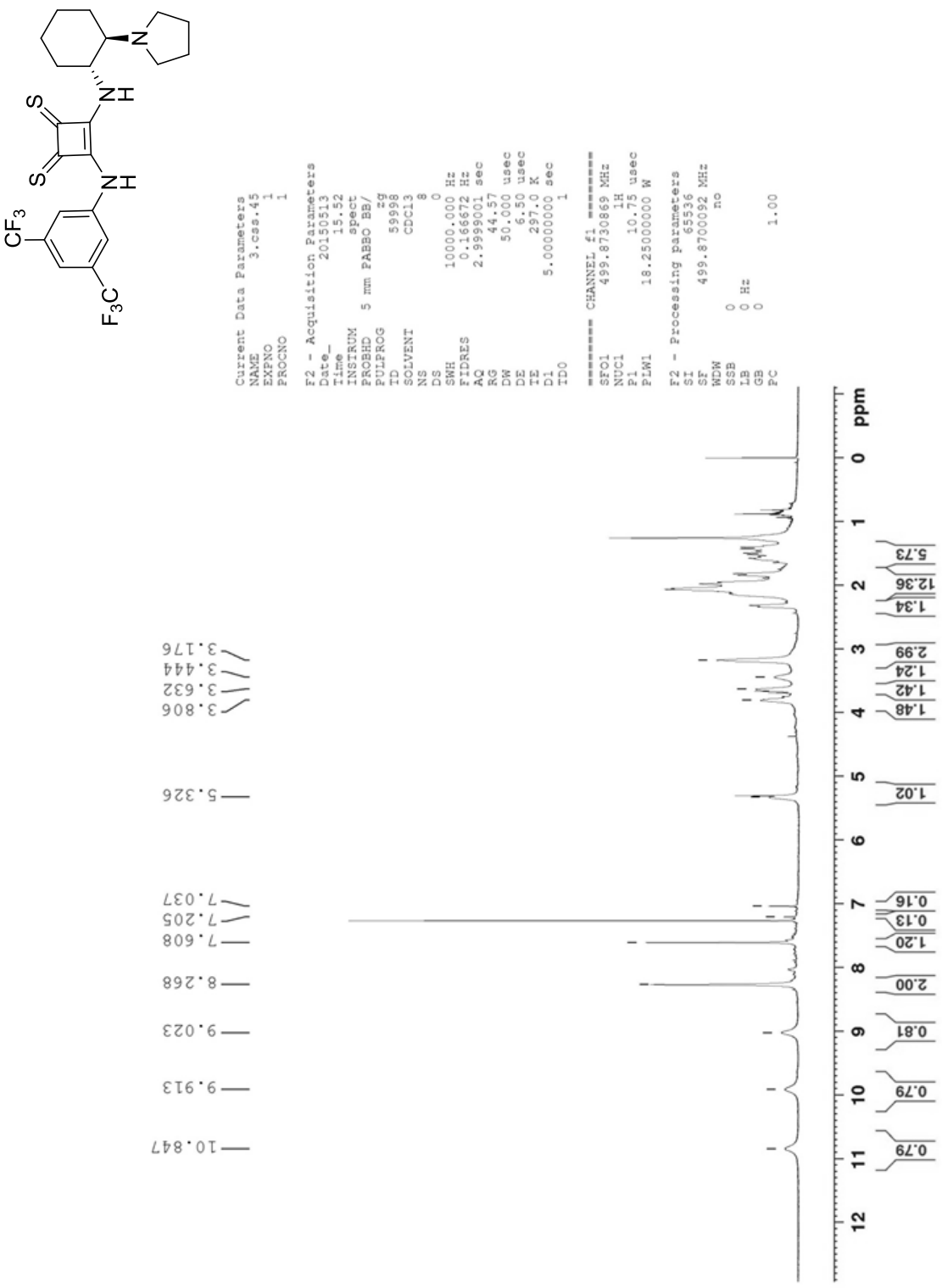

Figure 149: ^{1}H NMR Spectrum of 173 (500 MHz, $CDCl_3$, 298K)

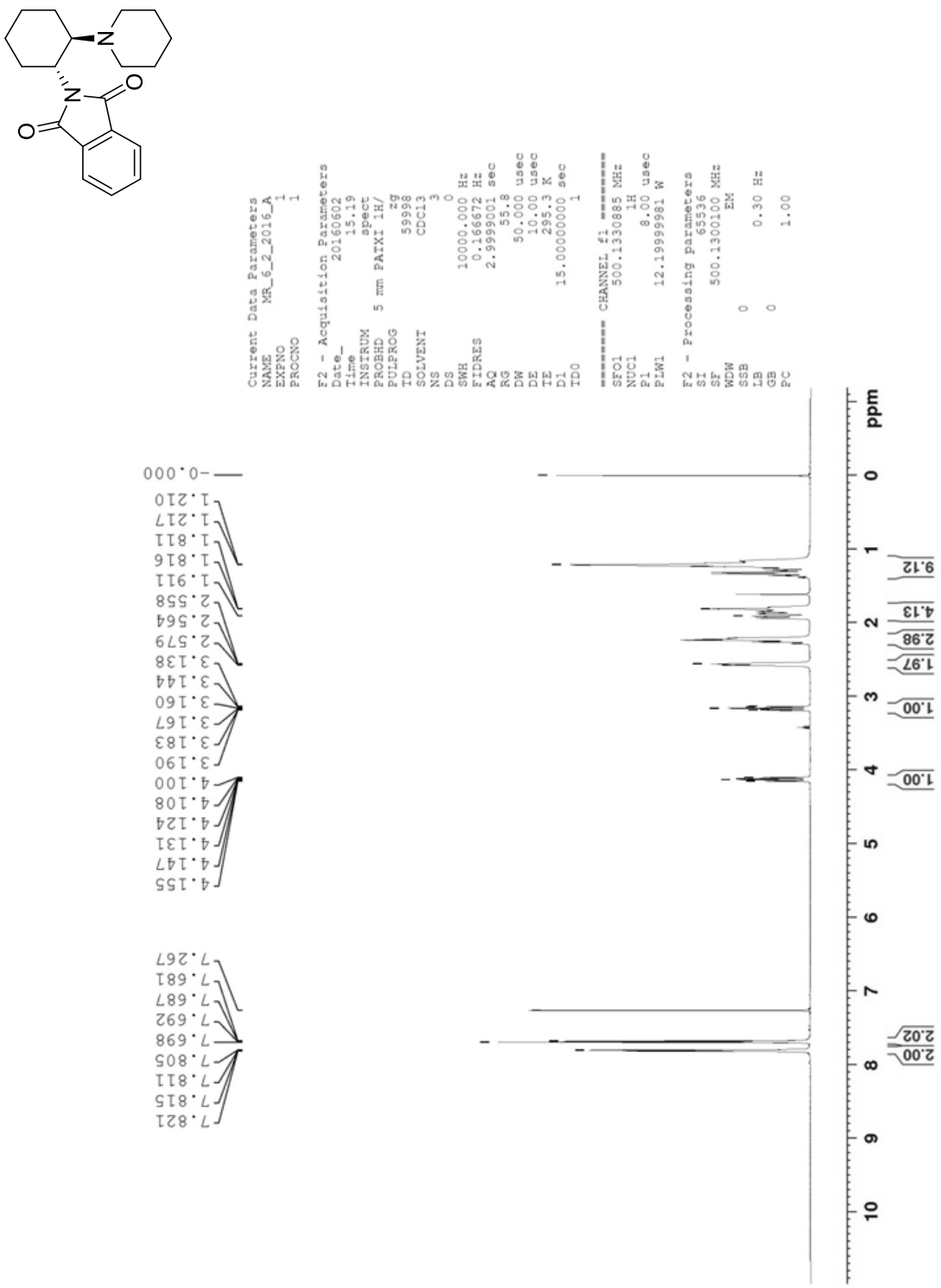

Figure 150: ^{1}H NMR Spectrum of 243 (500 MHz, $CDCl_3$, 298K)

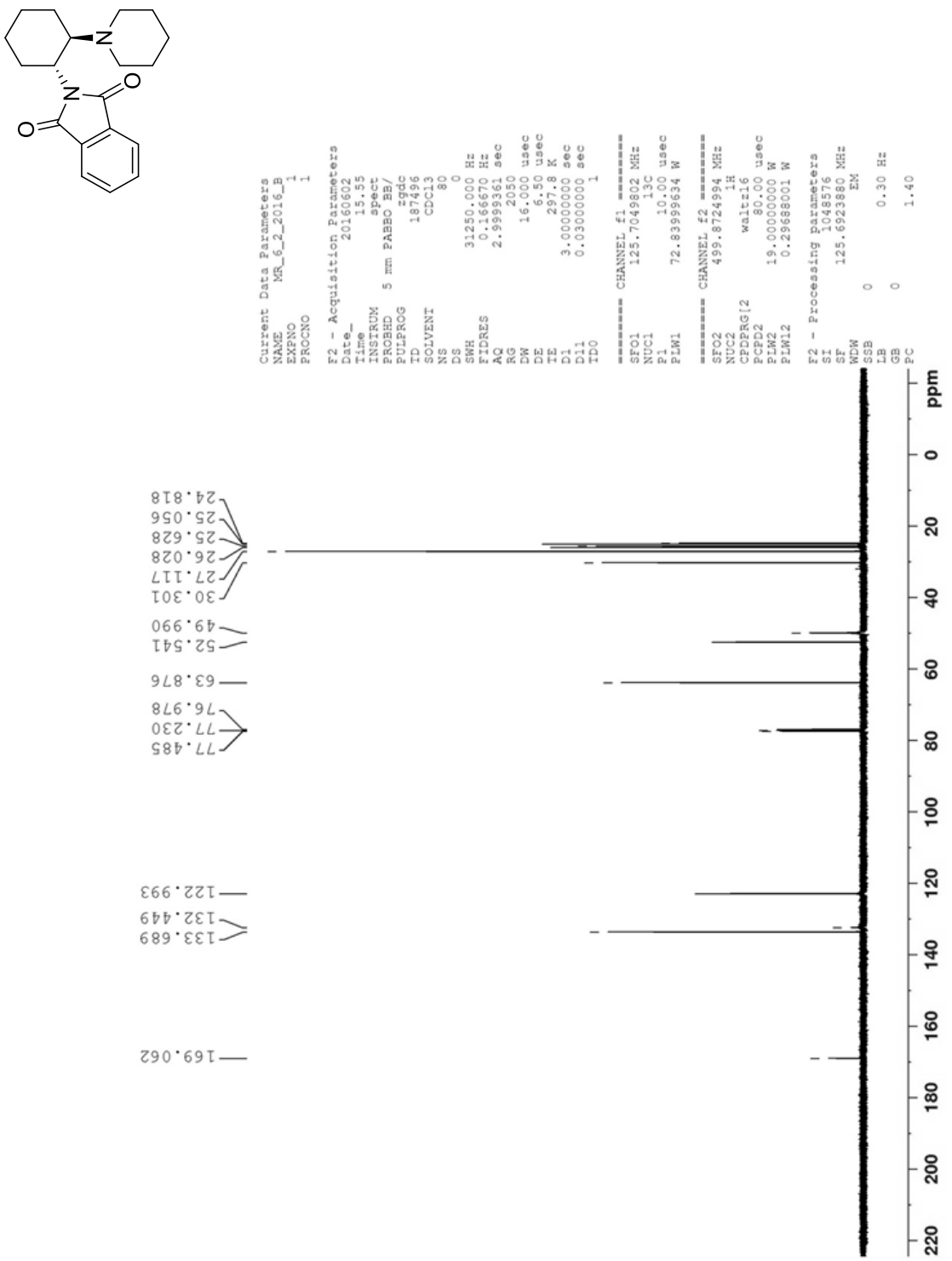

Figure 151: ^{13}C NMR Spectrum of 243 (125 MHz, $CDCl_3$, 298K)

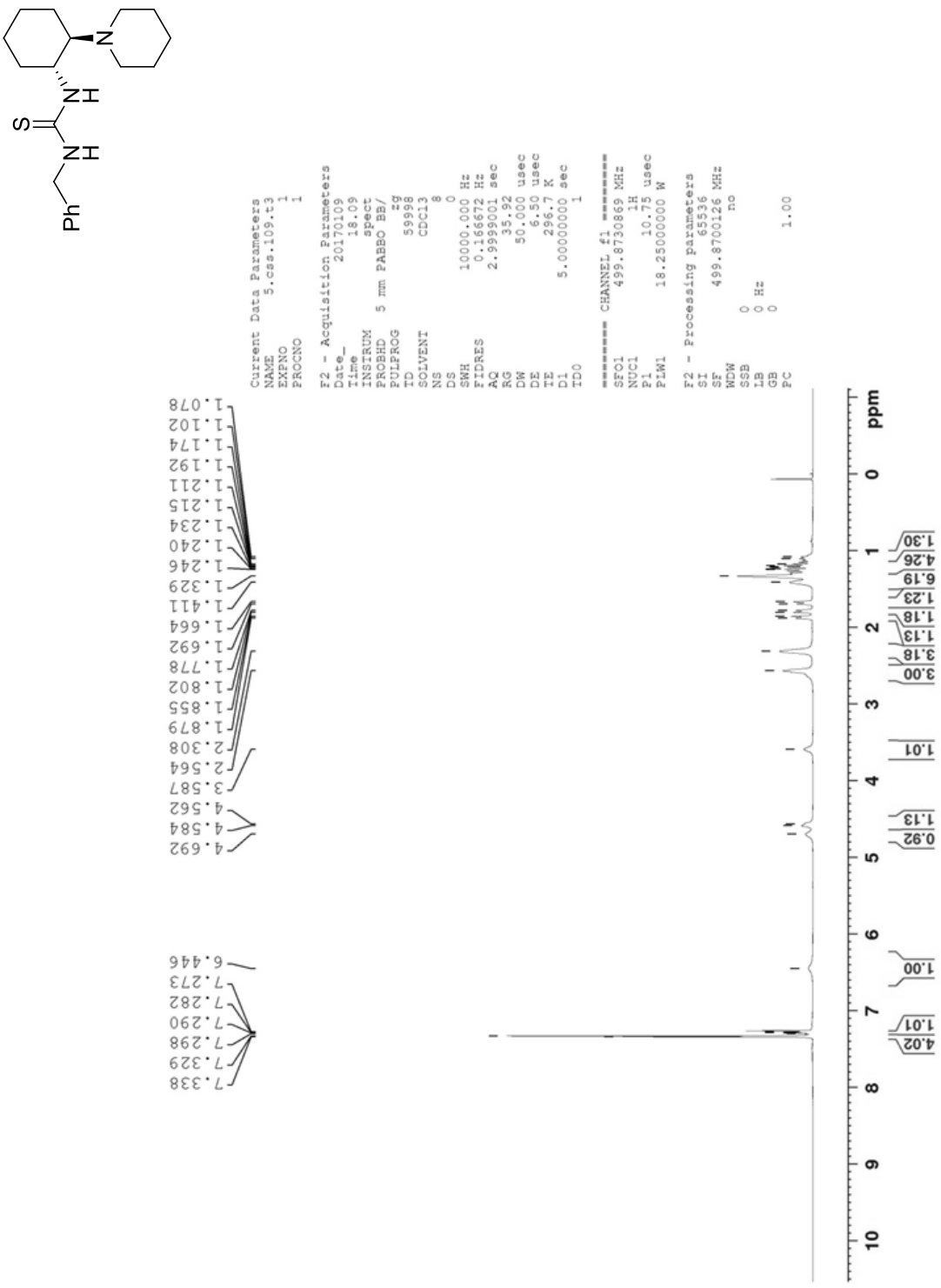

Figure 152: ^{1}H NMR Spectrum of 222 (500 MHz, $CDCl_3$, 298K)

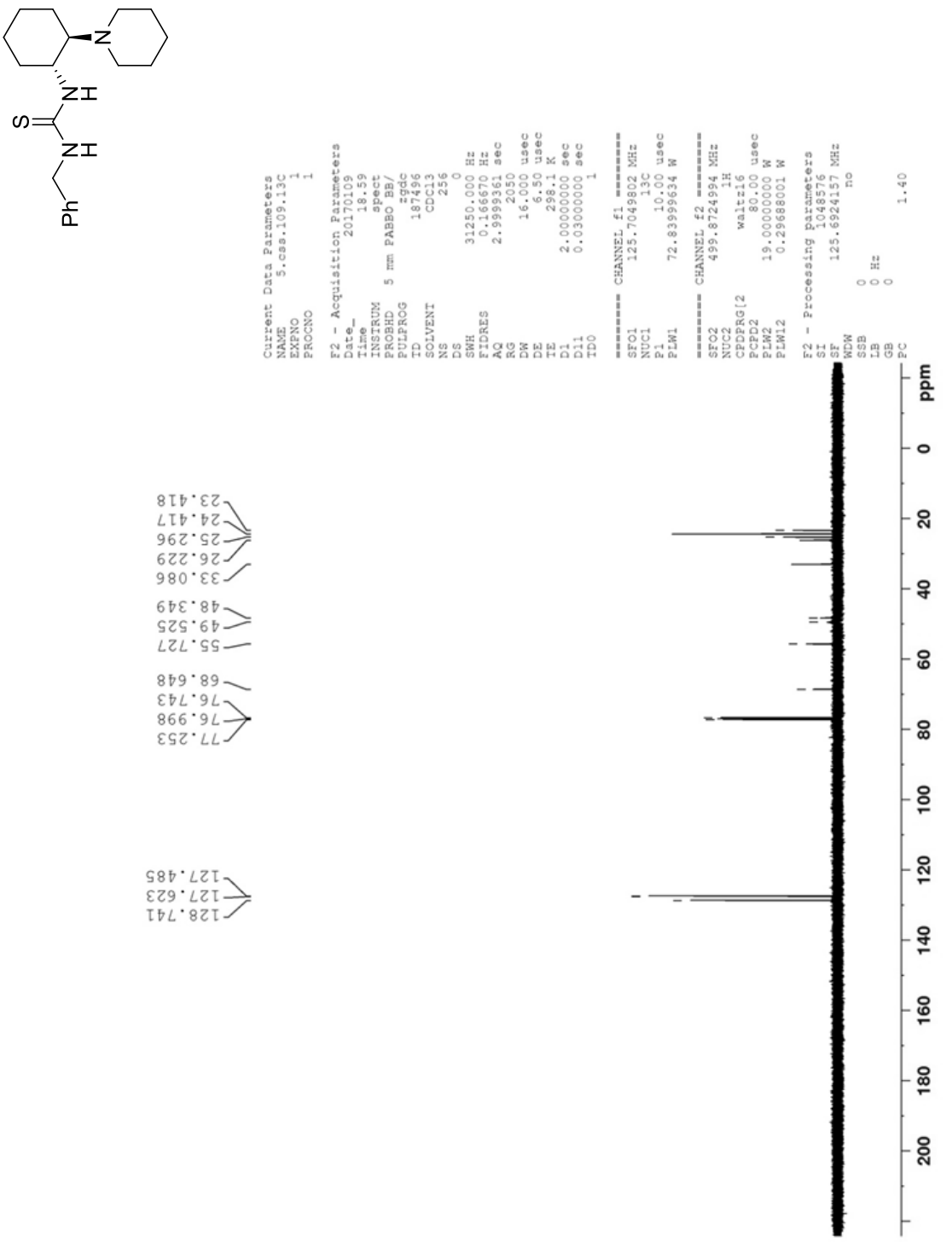

Figure 153: ^{13}C NMR Spectrum of 222 (125 MHz, $CDCl_3$, 298K)

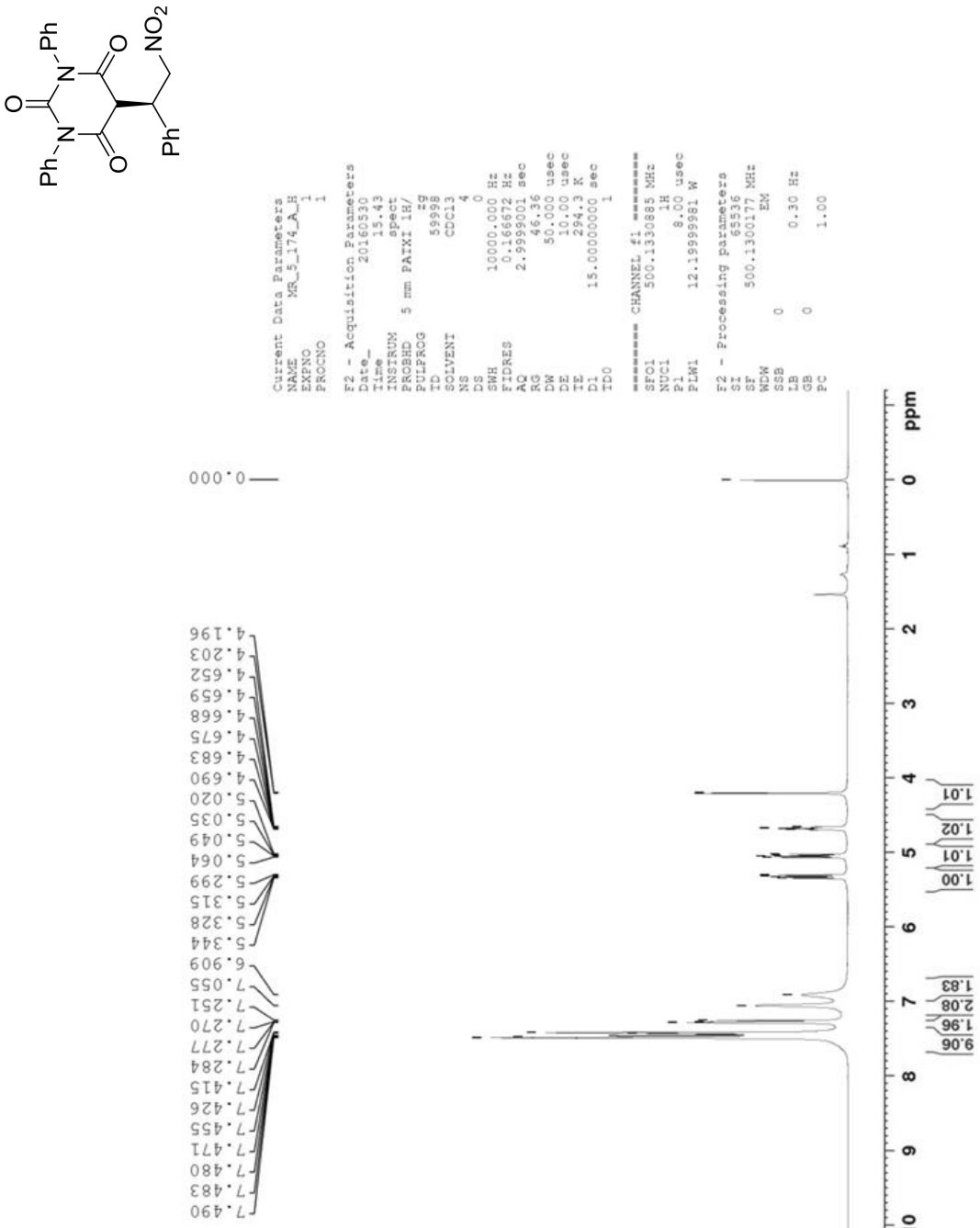

Figure 154: ^{1}H NMR Spectrum of 182 (500 MHz, $CDCl_3$, 298K)

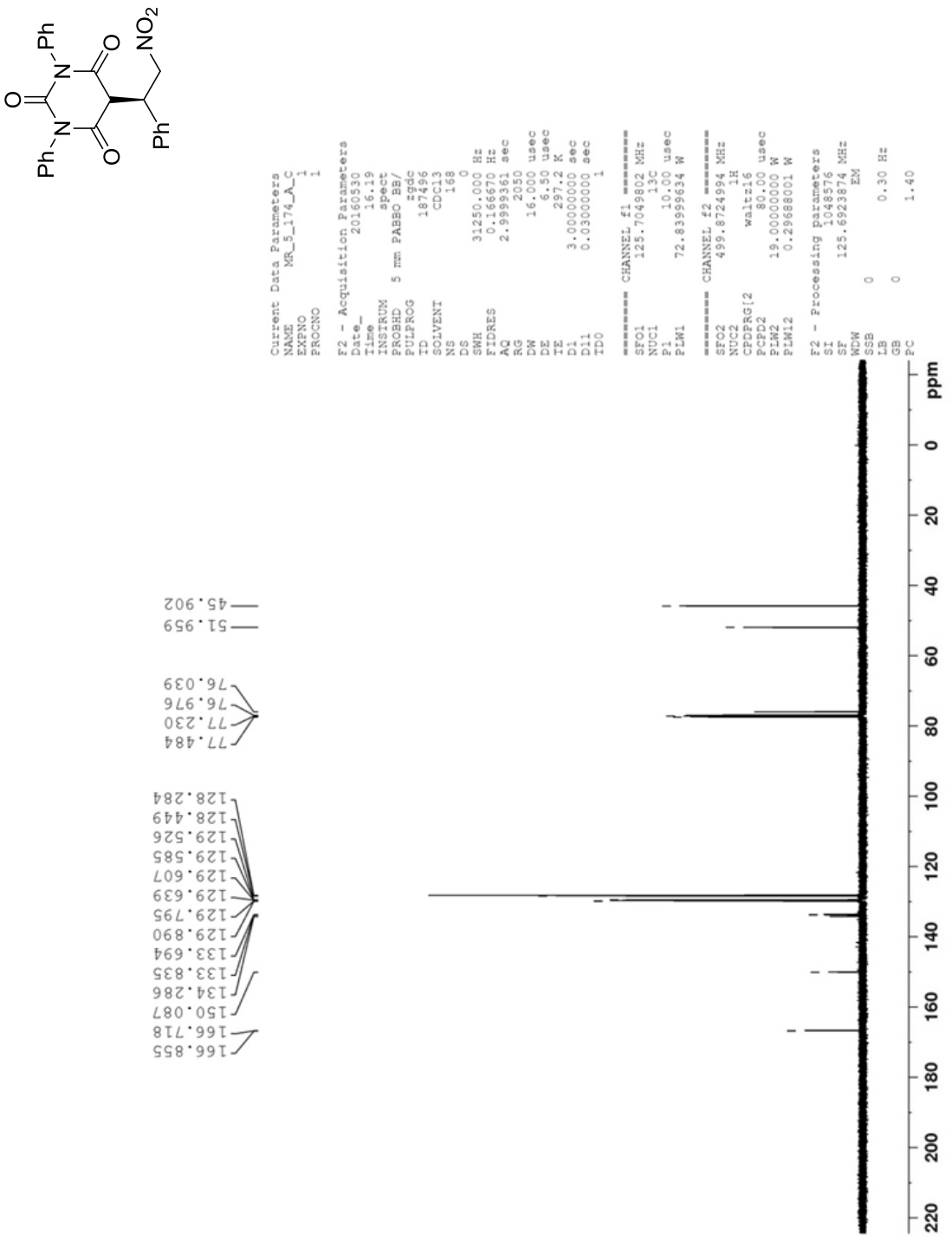

Figure 155: ^{13}C NMR Spectrum of 182 (125 MHz, $CDCl_3$, 298K)

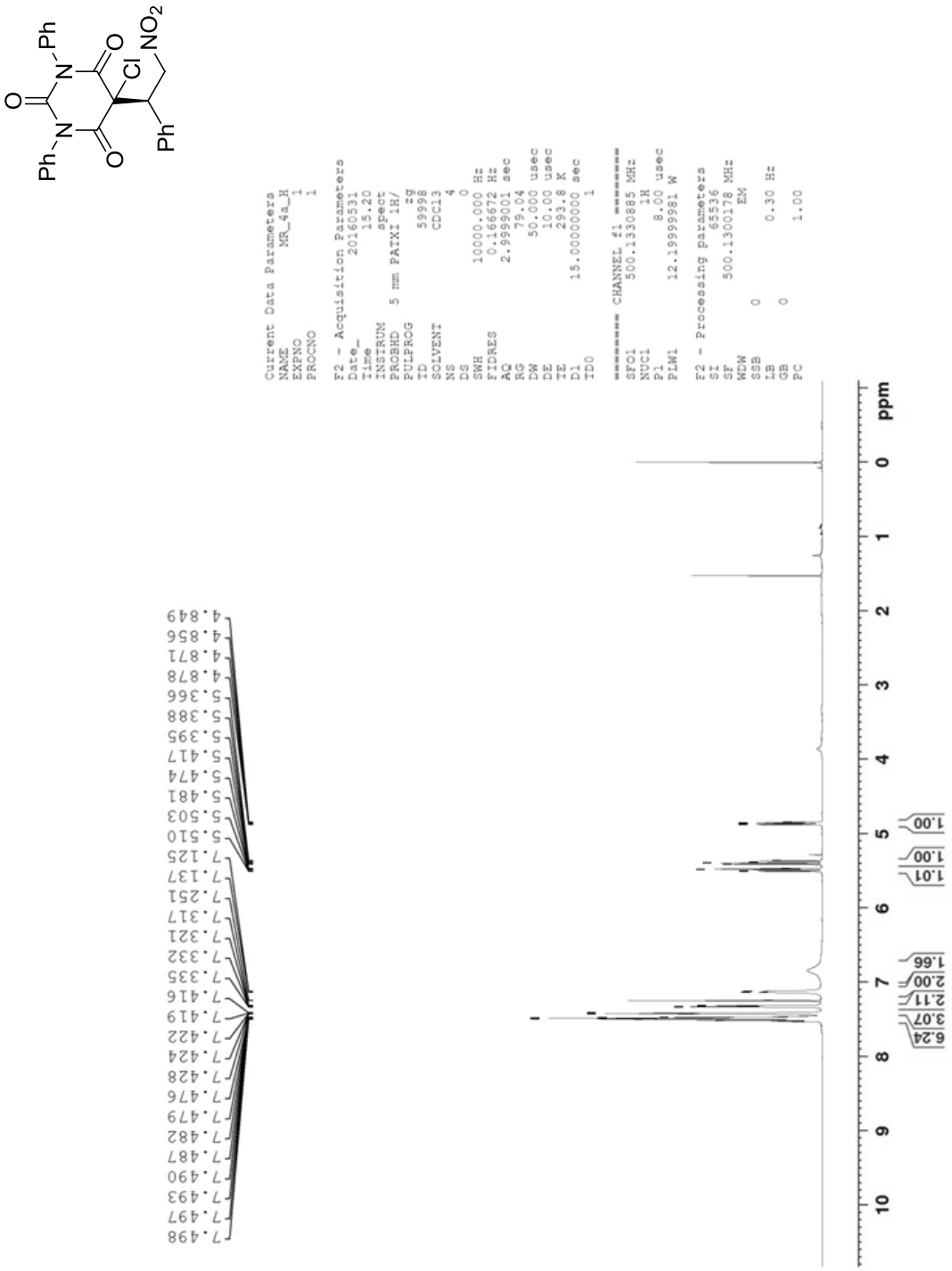

Figure 156: ^{1}H NMR Spectrum of 220 (500 MHz, $CDCl_3$, 298K)

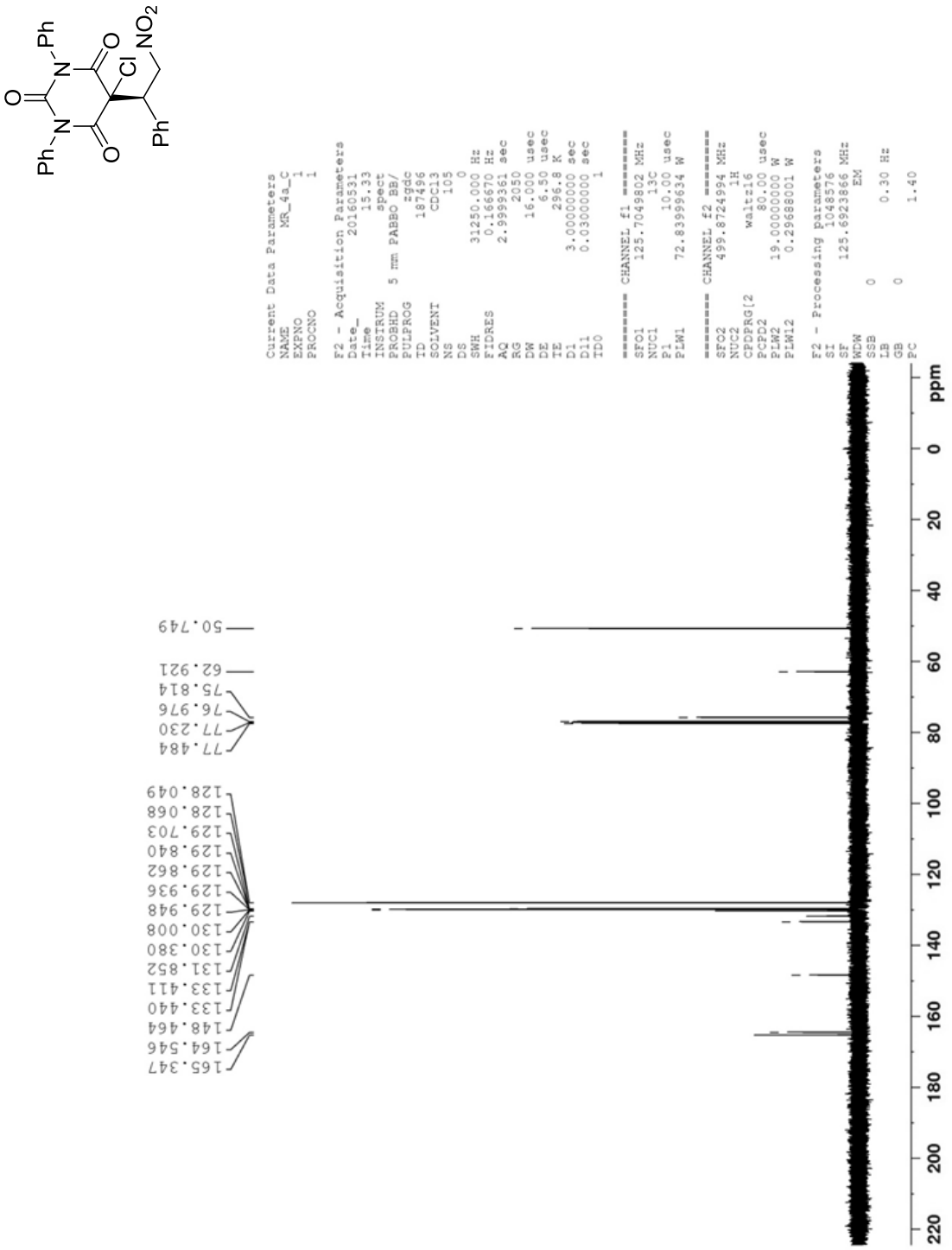

Figure 157: ^{13}C NMR Spectrum of 220 (125 MHz, $CDCl_3$, 298K)